ISWS/BUL-63/78
BULLETIN 63
ILLINOIS
ENT OF REGISTRATION AND EDUCATION

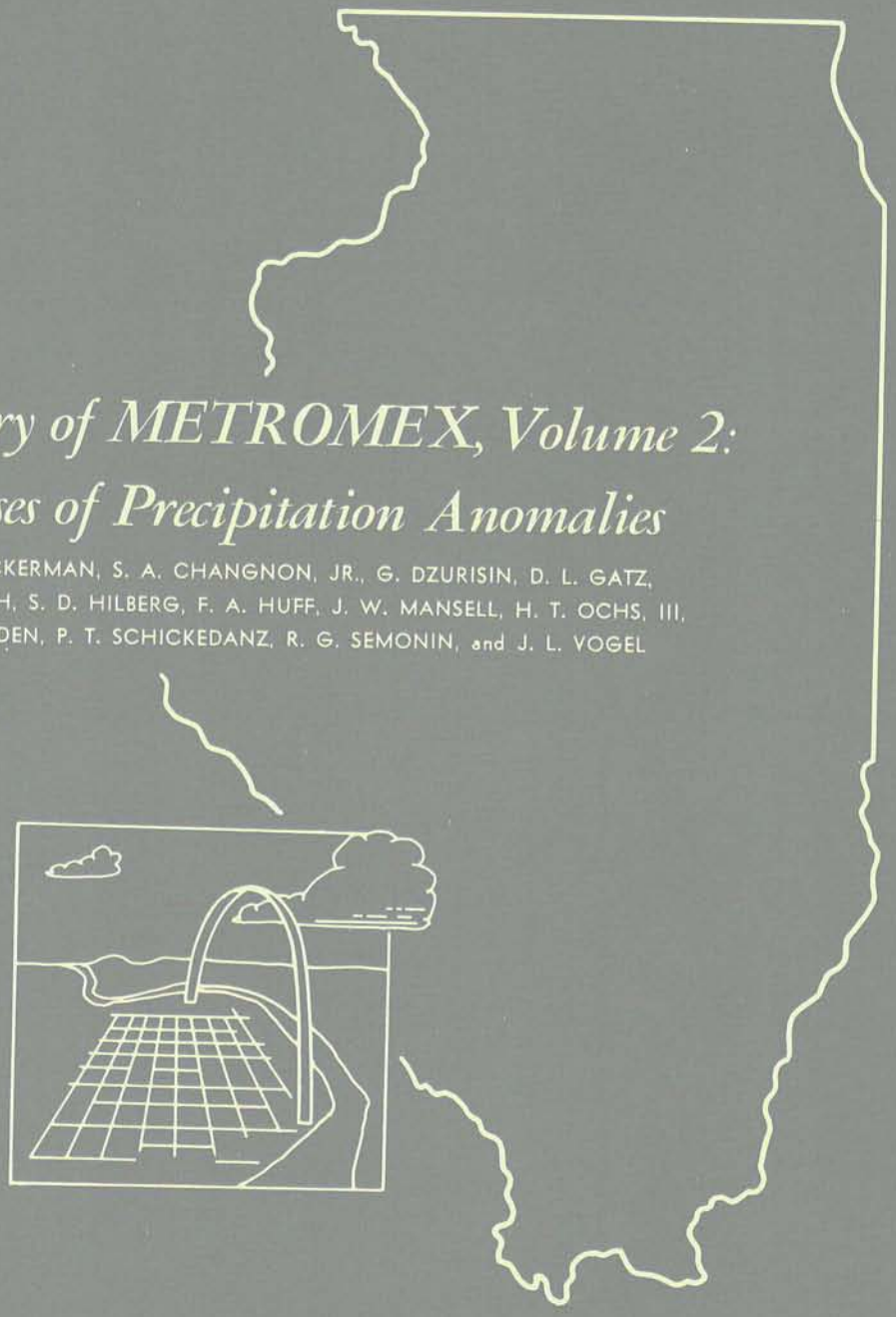

Summary of METROMEX, Volume 2: Causes of Precipitation Anomalies

by B. ACKERMAN, S. A. CHANGNON, JR., G. DZURISIN, D. L. GATZ, R. C. GROSH, S. D. HILBERG, F. A. HUFF, J. W. MANSELL, H. T. OCHS, III, M. E. PEDEN, P. T. SCHICKEDANZ, R. G. SEMONIN, and J. L. VOGEL

ILLINOIS STATE WATER SURVEY
URBANA
1978

BULLETIN 63

Summary of METROMEX, Volume 2: Causes of Precipitation Anomalies

by B. ACKERMAN, S. A. CHANGNON. JR., ©. DZURISIN, D. L GATZ,
R. C. GROSH, S. D. HILBERS, F. A. HUFF, J. W. MANSELL, H. T. OCHS. III,
M. E. PEDEN, P. T. SCHICKEDANZ, R. G. SEMONIN, and J. L. VOGEL

Title: Summary of METROMEX, Volume 2: Causes of Precipitation Anomalies.

Abstract: This is the last of two volumes presenting the major findings from the 1971-1975 METROMEX field operations at St. Louis. It presents climatological analyses of surface weather conditions, but primarily concerns those factors helping to describe the causes of the anomalies. Volume 1 covers spatial and temporal distributions of surface precipitation and severe storms, and impacts of urban-produced precipitation anomalies. Volume 2 describes relevant surface weather conditions including temperature, moisture, and winds, all influenced by the urban area. Urban influences extend well into the boundary layer affecting aerosol distributions, winds, and the thermodynamic structure, and often reach cloud base levels. Studies of modification of cloud and rain processes show urban-industrial influences on 1) initiation, local distribution, and characteristics of summer cumulus clouds; and 2) development of precipitation in clouds and the resulting surface rain entities.

Reference: Ackerman, B., S. A. Changnon, Jr., G. Dzurisin, D. L. Gatz, R. C. Grosh, S. D. Hilberg. F. A. Huff, J. W. Mansell, H. T. Ochs, HI, M. E. Peden, P. T. Schickedanz, R. G. Semohin, and J. L. Vogel. Summary of METROMEX, Volume 2: Causes of Precipitation Anomalies, Illinois State Water Survey, Urbana, Bulletin 63, 1978.

Indexing Terms: : Atmospheric chemistry, boundary layer, climatology, cloud physics, inadvertent weather and climate change, meteorology, model studies of cloud microphysics, pollution, rainfall, severe weather, urban climate, weather modification, weather radar.

STATE OF ILLINOIS
HON. JAMES R. THOMPSON, Governor

DEPARTMENT OF REGISTRATION AND EDUCATION
JOAN G. ANDERSON, B.S., Director

STATE WATER SURVEY DIVISION
WILLIAM C. ACKERMANN, D.Sc, Chief

URBANA
1978

(P.O. 6077-1500-5/78)

Printed by authority of the State of lllinois-Ch. 127, IRS, Par. 58.29
(7-78-1500)

CONTENTS

PART A CONTENTS

Part A. Introduction

Stanley A. Changnon, Jr. and Richard G. Semonin

Project Background

This report is the second of two volumes issued by the Illinois State Water Survey to summarize the METROMEX (Metropolitan Meteorological Experiment) activities and results obtained by the Survey staff during the 1971-1977 period. This second volume focuses on two of the major research areas of the Water Survey program in METROMEX: 1) the surface weather conditions, and 2) the urban factors related to the local anomalies in clouds, rainfall, and severe storms.

Volume 2 also serves as a progress report to the Department of Energy (DOE) on Contract EY-76-S-02-1199, and as part of the final report to the National Science Foundation on Grant ENV73-07796. This grant was the fourth in a series of NSF grants that began in March 1971; the DOE contract existed throughout METROMEX. Some of the research under the NSF grants pertained to the weather anomalies and their impacts, and these results are in volume 1 of this summary.

The Water Survey projects for METROMEX have major support from three sources including the National Science Foundation, the Department of Energy (ERDA and Atomic Energy Commission during the early years of METROMEX), and the State of Illinois. Some supplementary EPA funding for a minor portion of the field effort was also obtained. Most of the research reported here is a result of the *6V2* years of funding from the Department of Energy and National Science Foundation coupled with sizeable funding from the State of Illinois at a federal to state ratio of approximately 4:1.

Volume 1 essentially focuses on two of the four broad major METROMEX goals: 1) the dimensionalizing of the surface precipitation and severe weather anomalies, and 2) the resulting impacts. Volume 2 of this 2-volume summarization of Water Survey METROMEX activities focuses on a third major goal: the delineation and definition of the causes of the METROMEX precipitation anomalies.

It should be noted that, at this time, the research of the METROMEX data cannot totally delineate the causative mechanisms and that added research has been conducted by the Water Survey under NSF sponsorship in 1977-1978 for further studies of the METROMEX data. It should also be noted that a fourth major METROMEX goal, the translation and prediction of anomalies in other areas, has not been satisfied in existing Water Survey METROMEX research projects. Cloud modeling under NSF ENV73-07882, a 3-year grant, will be useful in the eventual translation process. However, a new research project launched by the Water Survey in 1977 is focusing on study of the past data in the Chicago area to develop comparisons with findings at St. Louis. This will test the transferability of the findings at St. Louis to another city with a different physical setting.

Goals of the Water Survey Projects

The general goals of the Illinois State Water Survey projects of METROMEX consisted of: 1) the delineation of any anomalies in the precipitation (quantity and quality) and in the severe weather frequencies in St. Louis and environs; 2) the definition of the causes for such anomalies;

3) investigations of the impacts of the weather anomalies on the local area and other urban-agricultural areas of Illinois; and 4) the transmission of all findings to potential users in the scientific community, the government, and the public.

These four broad goals of the. Water Survey projects in METROMEX actually consisted of 14 specific objectives involving field operations, data collection, analyses, and research. These objectives also included the application and transmission of the results to various user groups. The 14 specific objectives and activity areas of the Water Survey's METROMEX program appear in table A-1.

A flow chart depicting the 14 areas involved in the Survey's projects and how they inter-related appears in figure A-1. The means of information exchange and transmission of results indicated on this chart reflect how our METROMEX data and findings have been exchanged both with internal (other METROMEX groups) users and with external users.

The goals and activities addressed specifically by the DOE and NSF support coupled with state support can be followed by examining table A-l and figure A-l. This support addressed 9 of the 14 goal-activity areas:

- 2—Mapping of surface weather conditions
- 3—Study of the low-level airflow
- 4—Study of aerosol budgets
- 7—Identification of the causes for anomalies
- 8—Measurements for prediction
- 10—Planning information
- 11—Weather forecasting
- 12—Applications to planned weather modification
- 14—Transfer of knowledge

General Analytical Approach

Two basic approaches to the analyses of the METROMEX data were employed. The first of these is typified by the results on surface weather conditions presented here in volume 2. This approach is basically one that treats *all the data* from a particular source in a climatic-type evaluation. That is, total or very large data samples of a given event, say hourly temperatures, are treated for all months, seasons, or years of the METROMEX operations. The other basic research approach that has been employed and used extensively in this report has consisted of intensive meteorological analyses of individual periods exhibiting various precipitation conditions. This 'case study' approach has been pursued as part of the NSF, DOE, and related state support throughout METROMEX. Earlier results have appeared in separate publications (Changnon and Semonin, 1975).

Background and Adjustment to Emerging Findings

The major focus of the METROMEX effort was on summer (June-August) weather conditions. This focus was based on climatic research (Huff and Changnon, 1972) which had indicated the presence of major urban-related precipitation anomalies in this season. Much of the operational effort involving specialized field measurements was conducted during the summer months of the 1971-1975 period.

Other facets of this 5-year field program featured rapid data processing and a quick initial analysis to inspect the results of each summer. A primary reason for this approach was to

Table A-1. Specific Goals of METROMEX Program of the Illinois State Water Survey

Goals–Activity Areas	*Duration*	*Milestones**	*Application of findings and users*
FIELD ORIENTED PROJECTS			
1. Study of surface rainfall and severe weather at St. Louis to define their time-space distributions and the presence of any anomalies.	5 Years (±1)	A	Goals 6, 7, 9, 11
2. Study of surface weather conditions (temperature, humidity, and winds) at St. Louis to define their time-space patterns.	5 Years(±1)	A	Goals 6, 7, 9, 11
3. Study of the airflow, circulation, and turbulence over St. Louis.	5 Years(±1)	A	Goals 6, 7, 9, 10, 11
4. Study of aerosols including their general sources, their transport using airflow measurements to clouds, and their deposition, both wet and dry, on the ground in the St. Louis area.	5 Years(±1)	A	Goals 5, 6, 7, 9, 10
5. Study of changes in surface and groundwater quality downwind of St. Louis.	2 Years(±1)	B	Goal 9
INTERNAL APPLICATIONS - ANALYTICAL PROJECT			
6. Mesoscale analyses of the synoptic weather conditions and atmospheric structure with precipitation events to classify events and relate surface conditions to precipitation processes.	5 Years	C	Goals 7 and 12
7. Identification and quantitative definition of the causes for the precipitation anomalies.	Last 4 Years	C	Goals 8 and 13, and other METROMEX groups
8. Definition of the measurements critical to define urban anomalies and their causes in METROMEX and at other cities.	5 Years	C	Goals 1–4, 7 and 11, and other METROMEX groups
EXTERNAL APPLICATIONS			
9. Identification of scientific and business concerns in local St. Louis area where anomalies have relevance.	Last 4 Years	D	City engineers, consulting engineers, water supply superintendents, local farmers and farm associations, ecologists, and weather insurance companies; goal 13.
10. Utilization of pollution data derived from any deposition studies.	Last 3 Years	D	Illinois and federal EPA officials, air pollution studies (RAPS), and local pollution agencies.
11. Definitive information on weather-climatic changes, due to an urban-industrial area, available for local and regional planning.	Last 2 Years	D	City planners, engineers, and zoning boards.
12. Improvements in urban area forecasting of precipitation.	Last 3 Years	D	Meteorologists (forecasters) in government and private practice.
13. Planning for purposeful weather modification experiments in Illinois.	Last 3 Years	D	Water Survey scientists, other meteorologists contemplating rain and severe storm modification projects, and Illinois Advisory Board on Weather Modification Statute.
14. Transfer of knowledge gained and new technologies developed to other scientists and other disciplines.	5 Years	D	The scientific and engineering communities.

* *Milestones*

A. Goal-Activity Areas 1-4 are basically 5-year ongoing projects. They have annual (spring) milestones after data processing and initial analysis sufficient to detect measurement gaps. The final milestone involves summary, interpretation, and presentation of results to users.

B. Has an annual milestone involving review of first year results and re-design (if needed) of second year measurements. Final milestone is completion, summary, and translation of information to users.

C. These studies have 1-year milestones, each aimed at summarizing and reviewing all past results, and the final milestone is the summarization and conclusion of the studies.

D. These activities are basically continuous efforts largely related to user identification, communication of initial results to users, feedback of suggestions from users, and then final communication of findings and results. The only milestone is their completion.

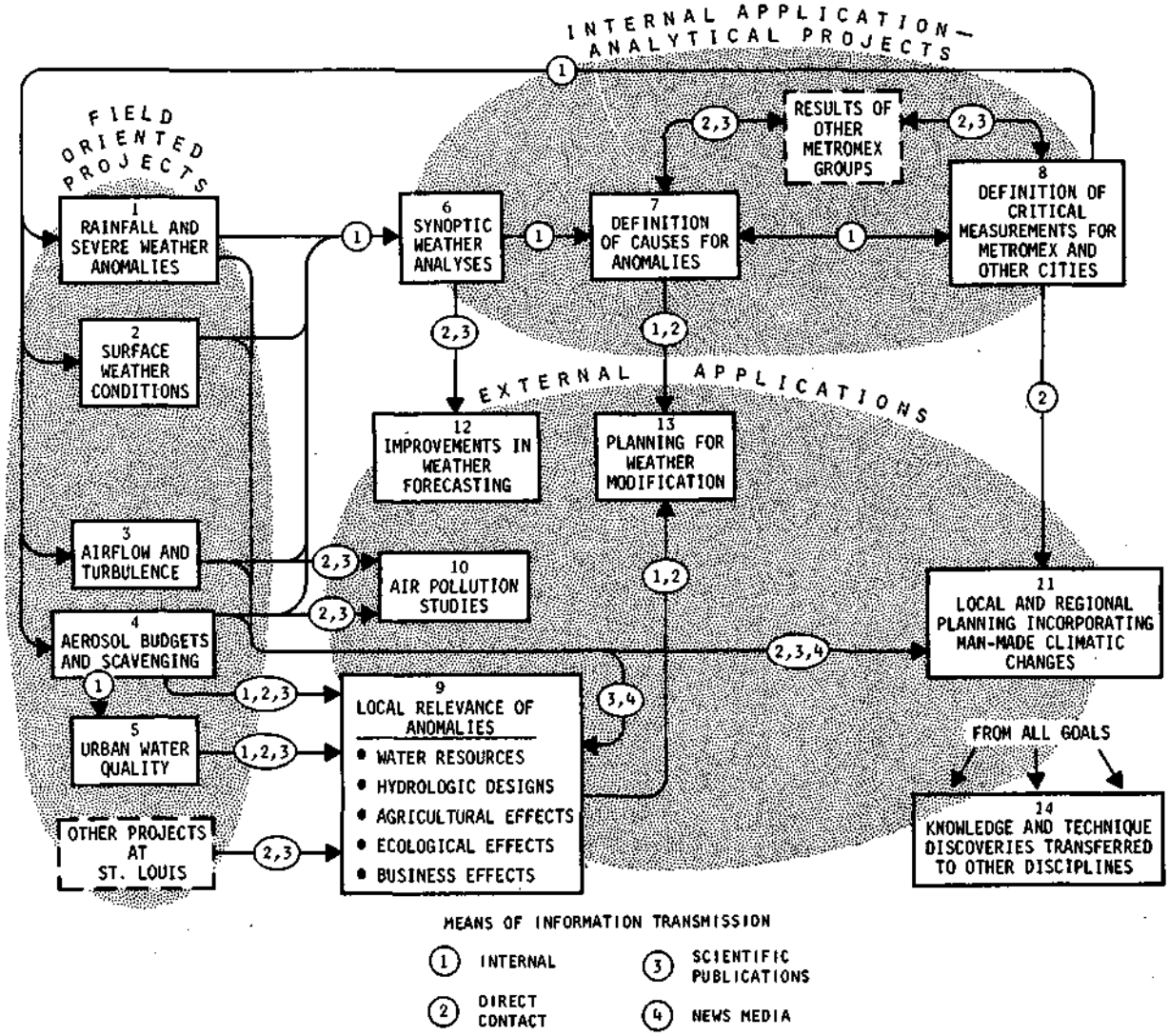

Figure A-1. Interaction of Water Survey METROMEX goal-oriented projects with their internal and external applications

continually refocus the field operations and analyses as new findings of interest developed. In other words, the experiment over five years was kept as flexible as possible to adapt data collection to new findings. Several major shifts in operational and research emphasis resulted from this approach, as described below.

After the analyses of 1971-1974 rainfall chemistry data, it became apparent that localized differences might be produced by the Alton-Wood River industrial area. Because of this possibility, the rainwater sampling network, which had been arrayed in and east of St. Louis, was relocated in 1975 to surround the Alton-Wood River area. The Alton-Wood River area field operations for 1975 also included a shift to that area in the tracer operations, both surface releases and airborne. The pibal and radiosonde network also was shifted from the St. Louis area to Alton-Wood River to cover the chemistry network for detailed study of rain scavenging. This area is essentially an industrial point source with a concentrated petroleum refinery area. It offered a test site to compare effects against those of the industrial area at St. Louis that was separated (south) by several miles.

A second change in focus resulting from the analyses of the early data of 1971-1972 concerned the rainfall findings. The climatological studies had suggested that the urban effect was related to an intensification of existing precipitation systems, but the METROMEX findings from the radar and the raingage network indicated that the urban areas also led to the initiation of precipitation under certain circumstances. Hence, radar operations beginning in 1973, and the ensuing analyses of radar and.raingage data, focused on the initiation of precipitation as well as on its intensification.

Another finding emerging from both the 'all-data' analyses and from early case studies was an indication that local rainfall initiation and intensification was related to warm, moist local surface areas. This finding, partially verified in the 1971 field data, led to an increase in the number of surface weather stations so as to better define the warm and humid areas.

The study of the urban effect on the boundary layer addressed several goals and the focus changed with time. As a consequence the field effort changed significantly between summers as it was modified to serve different objectives. The first of two approaches used was based on the implementation of special field experiments which were designed to investigate narrowly defined hypotheses concerning the potential effect of the urban area on the low level airflow. The second approach used routine daily measurements to delineate the mean summertime wind fields over the area for a range of mesoscale weather conditions. The first approach was used in 1971 and 1972, the second in 1973 and 1974, and both were used in 1975, the final field year for METROMEX.

The main element in the field experiments in 1971 and 1972 was a network of 8 or 9 wind stations from which pilot balloons were launched at 20 minute intervals, for periods of 3 to 4 hours. In 1972, in addition to the wind observations, radiosondes were launched periodically from three stations lying along a WNW-ESE line across the city.

In 1973 the pibal network plus 3 radiosondes was designed to delineate the kinematic fields and thermodynamic structure in the planetary boundary layer (PBL) over and around the metropolitan area, and extending northeastward to Alton-Wood River. In 1974 and 1975 the pibal and radiosonde networks were fashioned to support the air and rain chemistry project and were located in and around the Water Survey chemistry networks. The 1974 network extended from the city of St. Louis eastward some 30 km, and in 1975 it was centered around Alton-Wood River.

The field experiments in 1975 were quite extensive and were carried out for a short period during the winter as well as in summer. Three instrumental components utilized were 1) a network of five double theodolite pilot balloon stations, 2) two tethered-balloon stations for high resolution thermodynamic measurements in the boundary layer, and 3) an aircraft instrumented for measurement of air motions.

The search for means to transfer the METROMEX findings to other urban areas includes development of both prognostic and diagnostic models. Our emphasis on modeling shifted from a vertical plane 2-dimensional approach to the development of a sophisticated microphysical cloud model. This change of focus was in response to numerous observations relating urban-produced cloud condensation nuclei and the location of the rainfall anomaly.

The aforementioned revisions and shifts of operations and research during METROMEX were reflected in the equipment utilized under this project. Table A-2 lists the numbers and types of major project equipment employed during the first operational summer, 1971, and in the last operational summer, 1975. In every instance, there was an increase either in the frequency or the quality of the project equipment. All of these shifts were made in relation to findings revealed by the rapid data processing and early study of the results emerging from each summer. In 1972, 18 more surface weather stations consisting of standard weather shelters and recording hygrothermographs were purchased with state funds and installed to better describe the surface patterns of moisture and temperature throughout the network circle.

Table A-2. Shifts in Major Project Field Equipment during METROMEX Supported by NSF Grants, ERDA Contracts, and State Funding

	1971 (First summer)	*1975 (Last summer)*
Radar	Fixed antenna tilt scanning and photographic data	2-3 dimensional antenna scan computer controlled, and digital data
Number of surface temperature-humidity stations	7	25
Number of surface wind stations	6	8
Number of rawinsondes	0	3
Number of rain chemistry samplers	59	90
Number of raindrop spectrometers	2	12

Another important aspect of the projects within METROMEX concerned major developments of equipment and/or analytical techniques. These were important accomplishments needed to ensure the success of the projects, as described in volume 1.

Transmission of Results to Users

A major endeavor of these METROMEX projects has been to transmit project results to a wide variety of users (see figure A-l). A variety of means were used to accomplish transmission including these two summary volumes. The interactions with users occurred through a variety of media including 1) publications in scientific and technical journals, 2) talks at scientific meetings and seminars, and 3) oral presentations on radio and TV. A reflection of this effort can be gained by inspecting the project publications listed at the end of this volume.

The extensive user interactions that have occurred over *61/2* years of these projects are not reported in this volume though most of them, at least through 1976, have been reported in a variety of publications. Any one interested in user interactions of these projects should refer to the following publications. First is the *Interim Report of METROMEX Studies: 1971-1973,* edited by Floyd A. Huff (Huff, 1974). Another report itemizing user interactions is the *Study of Urban Effects on Precipitation and Severe Weather in St. Louis,* the Water Survey's annual report to the National Science Foundation (Changnon, 1973). A third source of information about the user aspects of the project is a publication entitled *RANN Utilization Experiment, Case Study No. 3 7; METROMEX.* This is an evaluation of METROMEX done by the Research Triangle Institute (1976).

Further information on user interactions of METROMEX can be found in volume 1 and in special reports prepared by the Water Survey at the request of NSF. Project results have appeared in a large variety of national magazines and on national TV. An estimated 70 million Americans had the opportunity to read about the METROMEX results by the end of 1973 (Changnon, 1974).

Scope of This Report

This report presents the major findings from analyses of data collected during the 1971-1975 METROMEX field operations supported by NSF and DOE (ERDA and AEC) grants and the State of Illinois. Information is provided on the various types of field measurements employed as well as on the analytical approaches used. A major focus is on the presentation of final interpretations and on the conclusions reached from the 5-year observational program. The report presents climatological-type analyses of surface weather conditions but primarily concerns those factors

helping to describe the causes of the anomalies. Volume 1 of this 2-volume series covers analyses of the spatial and temporal distribution characteristics of surface precipitation and severe storm events.

The text of this report has three major parts, each with several contributions from senior project researchers. Part B concerns a description of relevant surface weather conditions including temperature, moisture, and winds. Part C presents studies of the urban boundary layer including aerosol patterns, surface sources of aerosols, and thermodynamic and wind structures. Part D includes studies addressing the issue of modification of cloud and rain processes. This last section is followed by a general summary with conclusions addressing all parts of this volume. Also included is a list of published papers and reports generated by DOE-sponsored projects and by certain NSF sponsored projects and a listing of the abbreviations and acronyms found throughout the report.

Acknowledgments

The report was prepared under the general supervision of William C. Ackermann, Chief of the Illinois State Water Survey. The principal authors of this document were Bernice Ackerman, Stanley A. Changnon, Jr., Gregory Dzurisin, Donald L. Gatz, Ronald C. Grosh, Steven D. Hilberg, Floyd A. Huff, J. W. Mansell, Harry T. Ochs, III, Mark E. Peden, Paul T. Schickedanz, Richard G. Semonin, and John L. Vogel.

This report has resulted from the cooperation of all staff members involved in the METROMEX program. Each contribution and section of this volume indicates the author of that section, but it should be recognized that numerous staff members materially contributed to the work in all cases. Other past and present staff members who made major contributions in the field operations and analyses reported on herein include Donald Staggs, Douglas Jones, John Wilson, Robert Beebe, Mark Gardner, David Brunkow, Douglas Green, Marion Busch, Elmer Schlessman, Neil G. Towery, Connie Brunkow, and Griffith M. Morgan. The extensive graphic art was done by John W. Brother, Jr., William Motherway, Jr., June E. Blake, and Vidyadhar S. Patil. The final manuscript was edited by J. Loreena Ivens and Patricia A. Motherway, and camera copy was prepared by Marilyn J. Innes. It should be recognized that in addition to the above named contributors to the work in this report, many other sub-professional and student employees numbering more than 100 have worked on the project since 1971. The entire effort of this large team was needed to bring the project to a successful conclusion. Mr. Thomas J. Henderson and Mr. Donald Duckering of Atmospherics, Inc., Fresno, California, worked closely with Survey scientists throughout METROMEX, providing the project aircraft and acting as crew. Their contributions to the project have been invaluable and have helped resolve the causes of the precipitation anomaly.

This report is dedicated to Paul T. Schickedanz who died unexpectedly in 1977. Dr. Schickedanz made signal contributions to METROMEX and its rainfall analysis. His development of a semi-objective technique to delineate raincells was an innovative step forward in rainfall evaluation, and his work on the downwind rainfall was also a major contribution.

The advice and aid of the METROMEX advisory panel were of great help. These advisors included Horace R. Byers, Glenn Hilst, and James D. McQuigg.

The opinions, findings, conclusions, and recommendations expressed in this publication are those of the authors and do not necessarily reflect the views of the National Science Foundation or the Department of Energy.

REFERENCES IN PART A

Changnon, S. A. 1973. *Study of urban effects on precipitation and severe weather at St. Louis.* Annual Report NSF GI-33371, Illinois State Water Survey, Urbana, 34 p.

Changnon, S. A. 1974. *Translation of results and uses of project results. In* Interim Report of METROMEX Studies: 1971-1973, F. A. Huff, Editor, NSF GI-38317, Illinois State Water Survey, Urbana, 181 p.

Changnon, S. A., and R. G. Semonin, Editors. 1975. *Studies of selected precipitation cases from METROMEX.* Illinois State Water Survey Report of Investigation 81, Urbana, 329 p.

Huff, F. A., Editor. 1974. *Interim report of Metromex studies, 1971-1973.* NSF GI-38317, Illinois State Water Survey, Urbana, 181 p.

Huff, F. A., and S. A. Changnon. 1972. *Climatological assessment of urban effects on precipitation at St. Louis.* Journal Applied Meteorology v. 11:823-842.

Research Triangle Institute. 1976. *METROMEX, case study No. 37, RANN utilization experiment.* Contract C76-17165, Research Triangle Park, North Carolina, 27 p.

PART B CONTENTS

Part B. Description of Surface Weather Conditions

TEMPERATURE ANALYSIS

Steven D. Hilberg

A comprehensive program of acquisition of temperature and moisture data began in the summer of 1972, after the 1971 program had indicated that a large data base would be extremely valuable in helping to explain the temperature and moisture anomalies in the St. Louis urban area. By 1973, 29 hygrothermograph stations were in operation. The data from this network have been used for case studies of rain days and the identification of heat and moisture sources in and around the urban area. This section includes discussions of the characteristics of the temperature field-in the METROMEX research circle and its variations by month, time of day, wind speed and direction, and sky condition.

Sampling Network and Instrumentation

The temperature data were collected from the network of hygrothermographs in the METROMEX research circle (figure B-l). Hygrothermographs manufactured by the Bendix Corporation and Weather Measure, Inc., were used, with each type having a different method of measuring temperature and humidity. The WeatherMeasure hygrothermograph uses a bimetallic sensor for temperature and a bundle of human hairs for humidity, whereas the Bendix instrument uses a bourdon tube for temperature and a harp of human hairs for humidity. A further explanation of the principles of operation of the two instruments can be found in a discussion by Jones (1973). The hygrothermographs were placed in Cotton Region shelters. Accuracy of the instruments is given as ± 1.0° F for temperature and ± 5% for relative humidity (Jones and Schickedanz, 1974).

Processing of Data

Quality control of the temperature and humidity data began in the field. The field technician checked the readings by taking a sling psychrometer reading when the chart was changed. In 1973 an additional check on the data was made by the use of a calibrated minimum thermometer in each shelter. Minimum temperatures were compared with the lowest temperature on the chart. In 1975, aspirated psychrometers were used in the field, which more accurately represented the air conditions inside the shelter compared with the sling psychrometer readings outside the shelter.

Upon return for processing the charts were corrected if needed, and the temperature and humidity data were tabulated on forms from which cards were keypunched. As the data were processed on the IBM 360 computer system dew point values were calculated for each temperature-humidity pair, and cards were repunched containing the data, site number, temperature, humidity, and dew point.

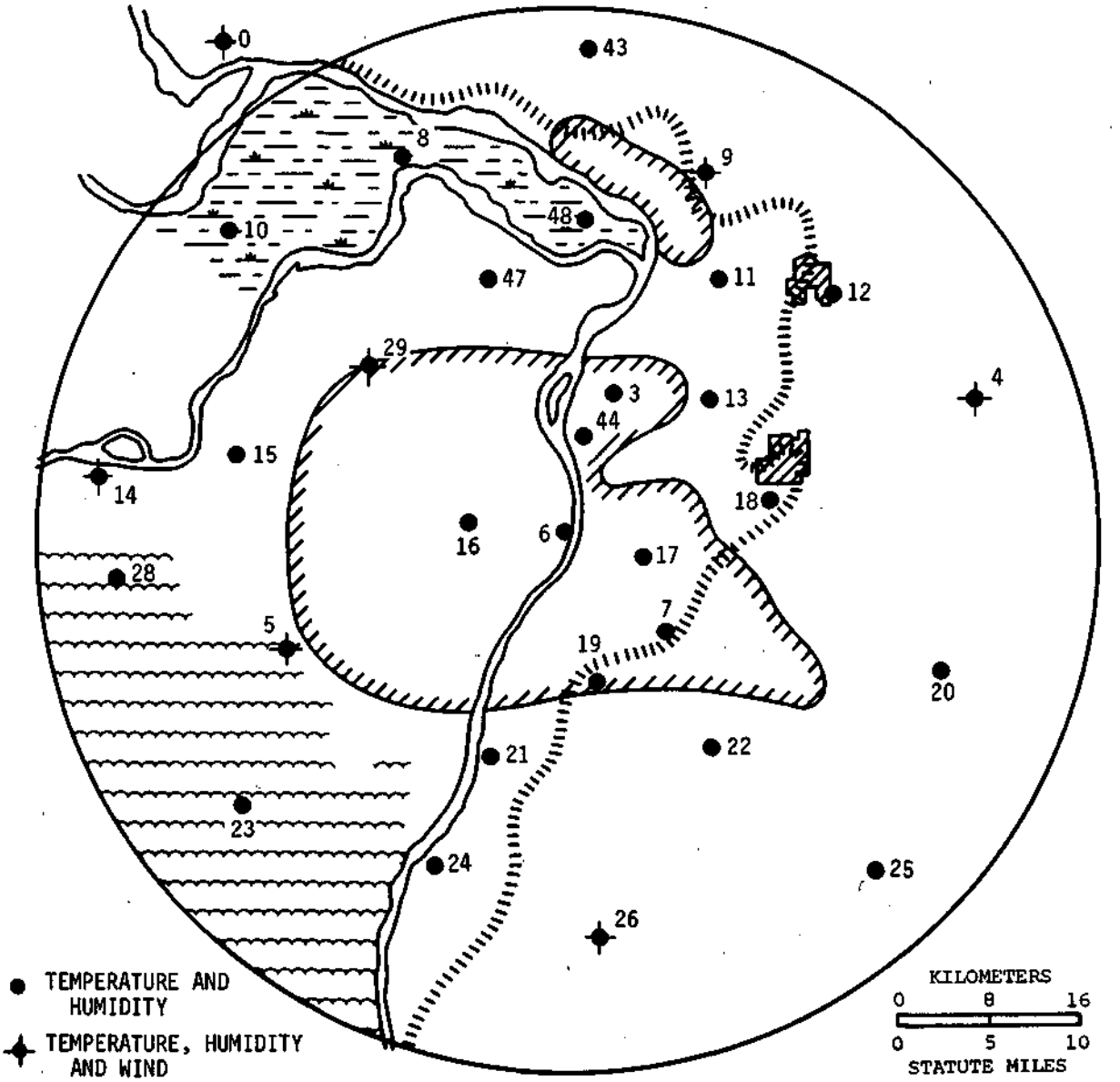

Figure B-1. Locations of hygrothermographs in METROMEX research circle

Analysis Procedure

Because differences between the urban and rural temperatures were of concern, the temperature field analyzed was the departure in degrees Celsius from the areal mean temperature for the network. The areal mean temperature for each map was calculated by summing the station temperature values and dividing by the number of sites. These departures were plotted and then analyzed. Thus, figures in this section indicate temperature departures from the network mean temperature, rather than absolute temperature values.

Average temperatures were calculated for a variety of times and conditions. Average temperature values at each station were calculated by month, year, wind speed, wind direction,

and three types of sky condition averages which were calculated for the hours 0000, 0300, 0600, 0900, 1200, 1500, 1800, and 2100 CDT.

Three categories of sky conditions were established for this study. *Fair* skies were defined as sky coverage from 0 to *0.3;partly cloudy* skies, from 0.4 to 0.7; and *cloudy* skies, from 0.8 to 1.0. The average sky condition for the METROMEX network was determined by averaging the hourly sky conditions for the period midnight to midnight at both Lambert International Airport in St. Louis (STL) and Scott Air Force Base near Belleville (BLV). The STL and BLV averages were in turn averaged to obtain one value of sky cover for the network.

In the period 1972-1975 six wind sets recording both wind speed and direction were in operation. Wind set locations were at sites 0, 4, 5, 9, 14, and 26 (figure B-l). Hourly wind data were also available from STL and BLV. The wind direction data were grouped into eight points of the compass, and a prevailing wind direction was assigned to each day that data were available. The prevailing direction at each site was determined by the frequency of direction during the period midnight to midnight, and the prevailing direction across the network was determined by the combined frequency of wind direction from all eight sites.

An examination of the diurnal trends of the urban heat island intensity indicated the heat island to be weakest about 1500 CDT and to attain maximum strength between 2100 and 0000 CDT. In order to examine the effect of wind speed on the heat island, areal averaged wind speed data were obtained for 1500 and 2100 CDT by averaging wind speeds from 1400 to 1600 CDT and 2000 to 2200 CDT at each site where wind data were available. These values were used to determine the effect of wind speed on the heat island when the heat island was weakest and when the strong formation was under way. Three categories of wind speed were chosen to examine the effect on the heat island; 0 to 1.5 m s^{-1}, 2.0 m s^{-1}, and >3.5 m s^{-1}. Upon examination of the data it was found that at the selected times there were very few days with wind speed >3.5 m s^{-1}, so that category was dropped from consideration.

Average Temperature for Individual Years

The average temperature departure fields for each of the 4 years appear in figure B-2. In all 4 years, the temperature pattern remained basically the same. The center of the urban heat island was located over the metropolitan area, generally from the center of St. Louis city into the East St. Louis area on the Illinois side of the river. The 1.0° C departure isotherm encompassed the city of St. Louis in all years except 1972. In 1972, a warm area was centered over the Arch, extending into the eastern metropolitan area. This dissimilarity with the other 3 years suggests that the quality control or the amount of data included in this analysis may be responsible for the difference. The effort to field check the data was increased during the last 3 years of the project. All sites in the research circle were not in operation at the start of the 1972 field program, and the lack of data at some sites may account for a slight bias in the data. In all years the urban heat island was oriented along the river.

The coolest areas in the research circle were the SW foothills and the area extending east from Collinsville. Both areas are cooler than the urban area by approximately 2.0° C. The NW and SE areas are also cooler, but slightly warmer than the SW and NE portions.

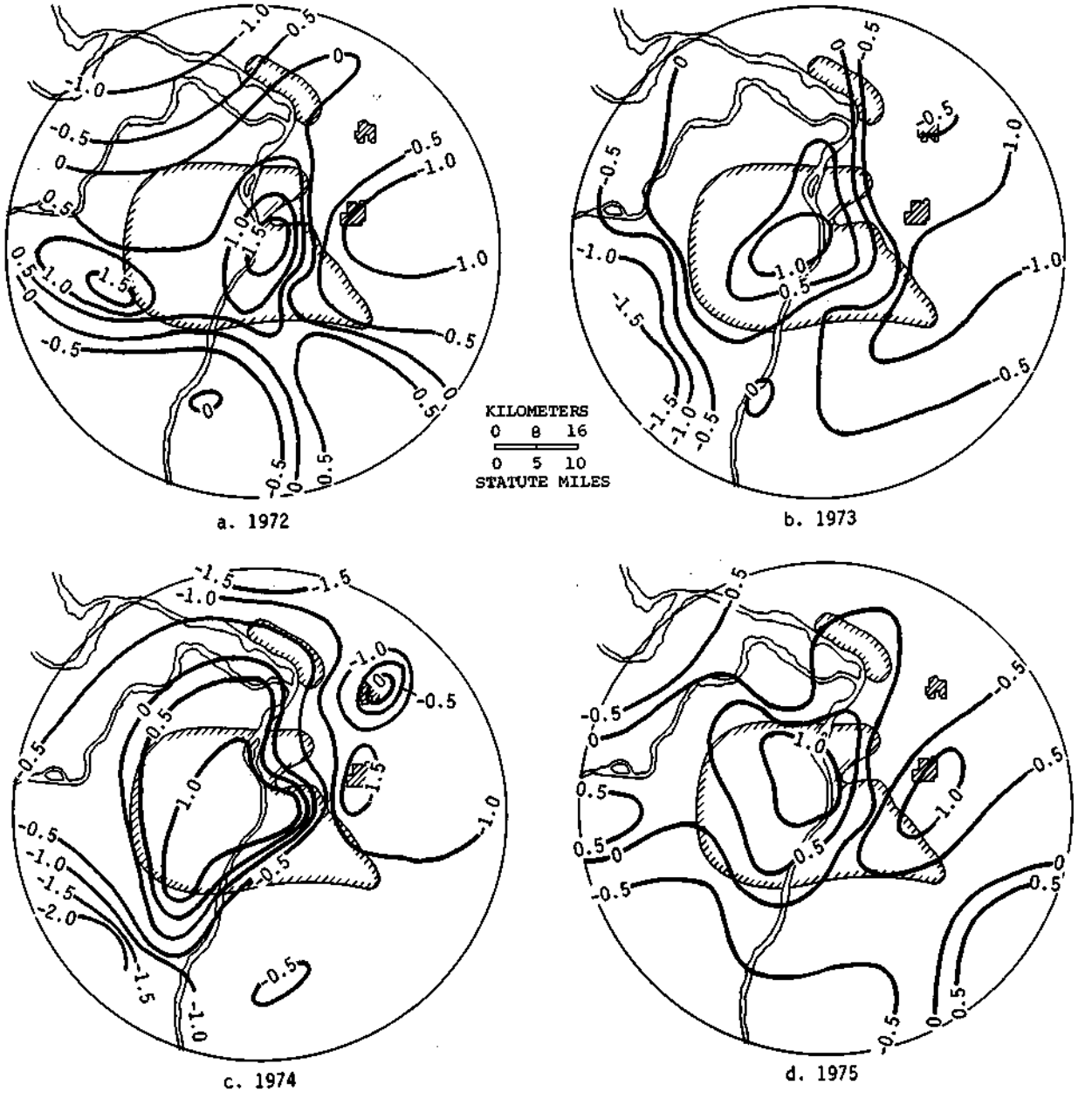

Figure B-2. Summer mean temperature departure fields, 1972-1975

Four-Year Monthly Averages

There was little change in the temperature patterns for the June, July, and August 4-year averages (figure B-3). The urban heat island maximized, as shown by the 1.0° C isotherm, over the center of the metropolitan area. The June and July temperature patterns were very similar. The heat island extended from the south near the confluence of the Meramec and Mississippi River north through the metropolitan area to the northern edge of the research circle. A warm area also extended westward from the city center to the edge of the network. The coolest areas were the E and SW portions of the circle.

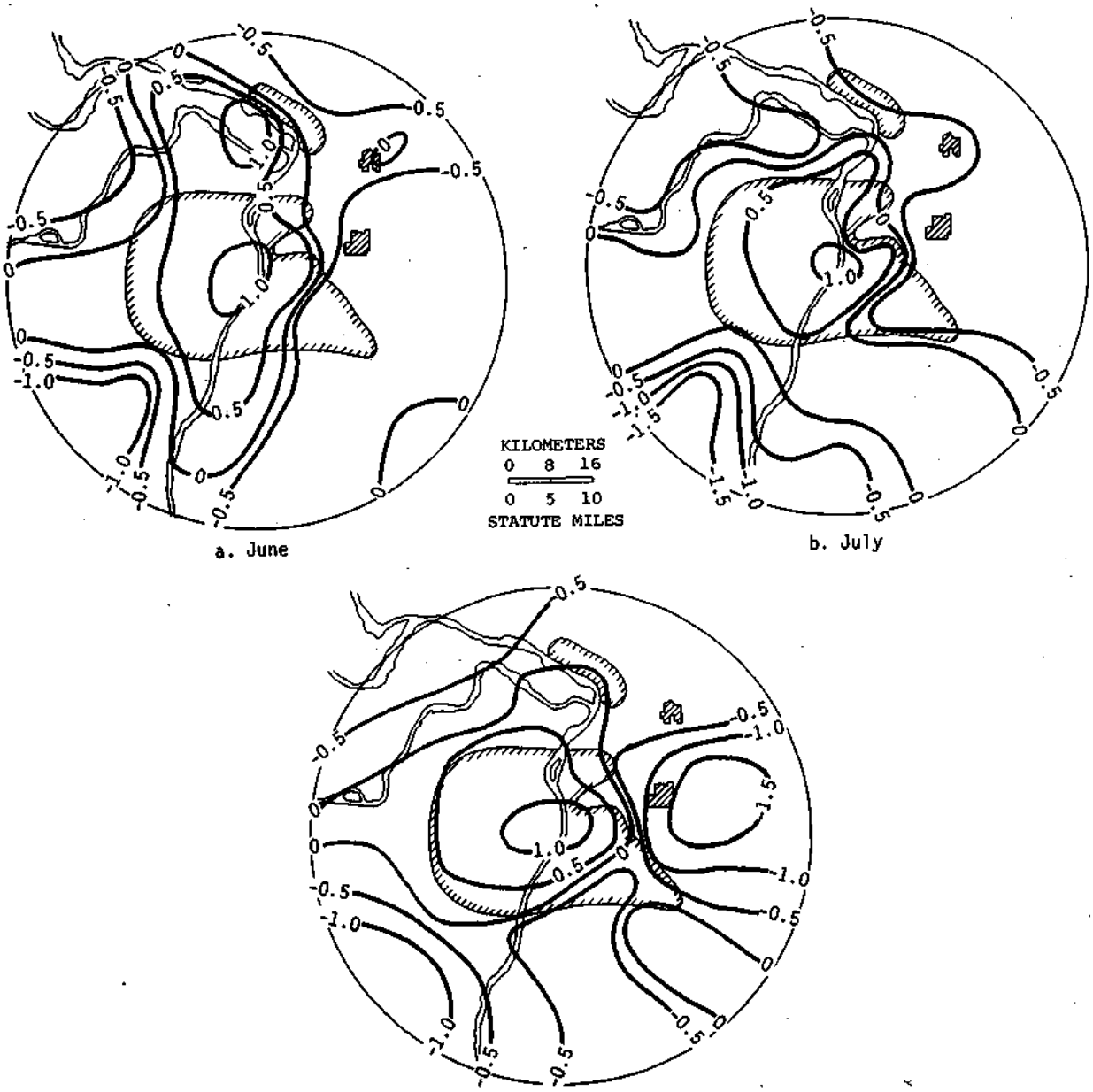

Figure B-3. June, July; and August mean temperature departure fields, 1972-1975

During August there were several notable differences. The heat island was less elongated, although it still extended to the west. From Collinsville eastward there was a strong cool pocket. This area was approximately 2.0° C cooler than the urban area in June and July, but was 2.5° C cooler in August. There was also a cool area extending from Waterloo (station 26) north along the bluff. This area was also evident in June and July, but it was weaker by 0.5° C.

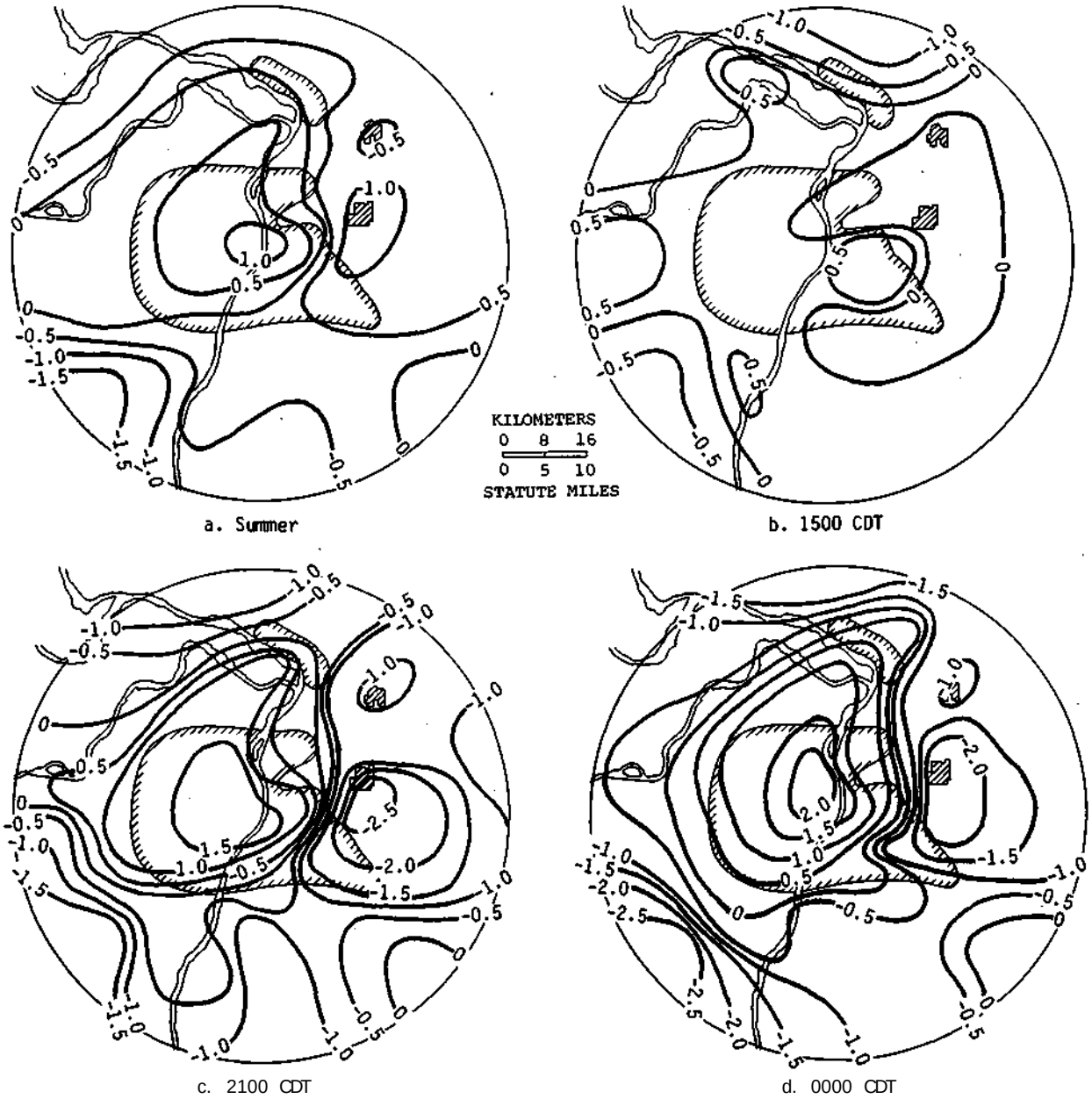

a. Summer

b. 1500 CDT

c. 2100 CDT

d. 0000 CDT

Figure B-4. Average temperature departure fields **for** summer and **1500,2100, and 0000 CDT, 1972-1975**

The 4-year summer average map displays essentially the same pattern as the monthly maps (figure B-4a). Relative warm temperatures were evident over most of the western part north of the Ozark foothills. One particularly cool spot (—1.0° C) was centered over Collinsville.

Variations in the Average Summer Pattern with Time of Day

It is generally well known that the urban heat island in the summer is weakest during the afternoon and strongest at night (Peterson, 1969). To investigate the patterns during the day, maps of the temperature field for 3-hour intervals from 0000 to 2100 CDT were analyzed. A diurnal study of the urban heat island showed that the heat island was weakest about 1500 CDT and attained its maximum strength in the period from 2100 to midnight CDT. Maps of the temperature pattern at 1500, 2100, and 0000 CDT appear in figure B-4. At 1500 CDT, the time at which most sites reached their maximum temperature, the urban heat island was still evident, although very weak. The warmest area of the heat island extended eastward from the city to over East St. Louis. The entire metropolitan area was warm compared with the SW, E, and NE areas. The largest temperature difference at this time between an urban and rural site was 1.5° C.

By 2100 CDT the urban heat island was well established but not yet at its maximum intensity. The strongest temperature gradient extended from the city center eastward to station 18, a distance of 16 km. There was also a strong temperature gradient to the SW of the metropolitan area. The heat island at this time extended from the southern edge of the research circle northward through the city, then slightly northeastward through the Alton-Wood River area. This warm area over Alton-Wood River became even stronger and extended farther NE three hours later at midnight. The gradient to the E had increased to 0.24° C km^{-1} since 2100 CDT and the gradient to the SW had also increased. Midnight was approximately the time that the urban heat island was at maximum intensity. It remained at that intensity for the rest of the early morning hours, and began to decrease just before sunrise. When the heat island was at maximum intensity, the urban area was 2.8 to 4.5° C warmer than the surrounding rural area.

Variations in Temperature Patterns with Sky Conditions

Temperature patterns for three different types of sky conditions were analyzed. The 4-year mean temperature patterns for fair, partly cloudy, and cloudy sky conditions appear in figure B-5. In general, there was little variation in the pattern configuration as a function of sky condition. The largest differences existed between the cloudy temperature pattern and the other two. Patterns for the fair and partly cloudy conditions were very similar with the major difference being somewhat stronger temperature gradients to the E and N with partly cloudy skies. Under cloudy skies, the temperature gradients from the urban to the rural areas were less, especially to the SW. The 1.0° C departure isotherm did not encompass the city as it did under fair and partly cloudy skies, but was confined to the eastern part of the city. The magnitude of the departures under cloudy skies was generally less than with either of the other two sky conditions. The departure at the Arch (station 6) was the same for all three conditions.

The formation of the urban heat island has been found to be largely dependent on the differential cooling between the urban and rural areas (Vukovich, 1973; Oke and Maxwell, 1975). Since cloud cover affects the amount of longwave radiation re-emitted to the atmosphere from the earth and thus the amount of nocturnal cooling, it also follows that it must in some way affect the urban heat island. Maps of the 4-year average temperature patterns for three types of sky conditions were analyzed for 1500 and midnight CDT, when the heat island is weakest and strongest,

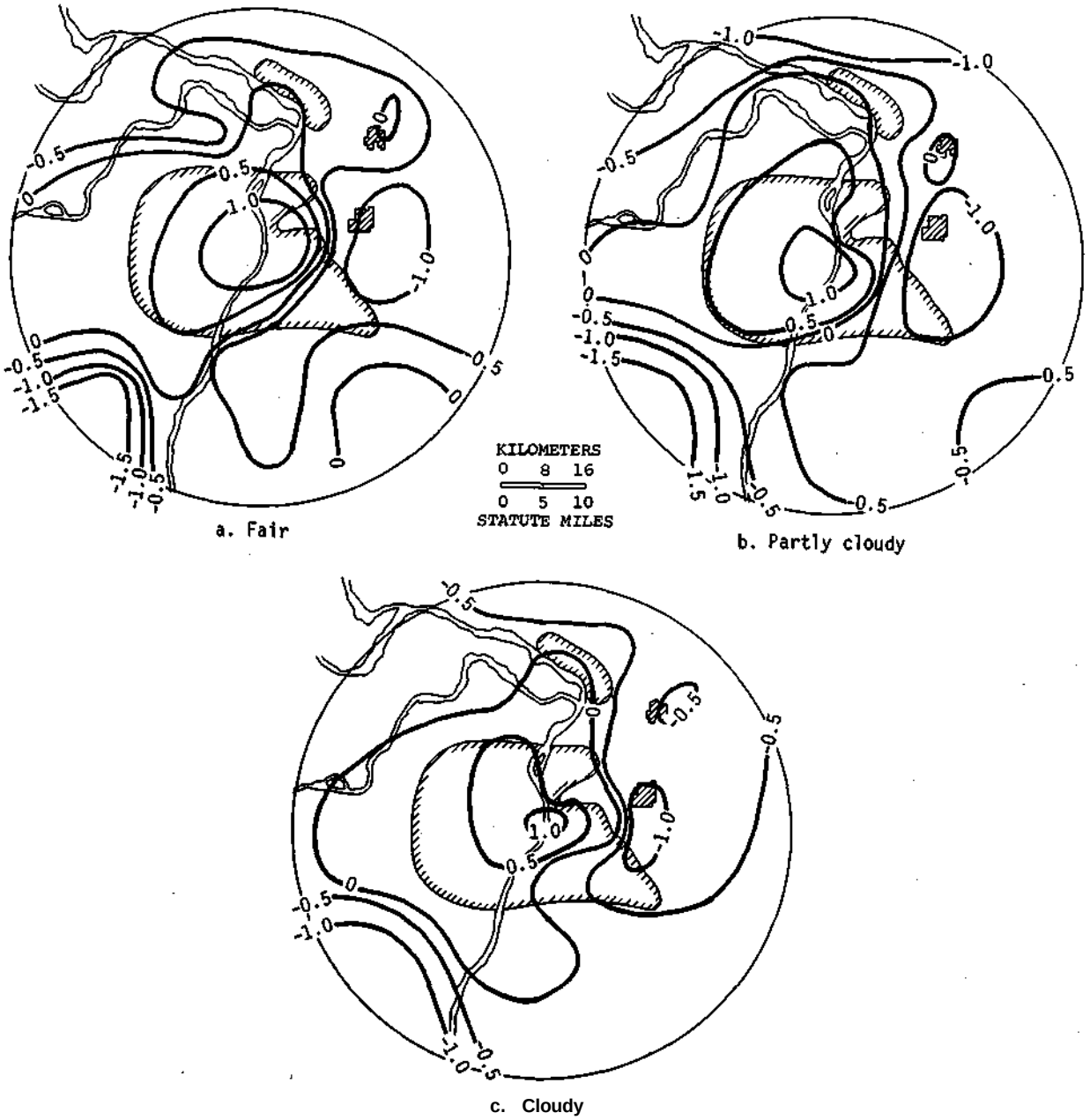

Figure B-5. Summer average temperature departure fields for fair, partly cloudy, and cloudy skies, 1972-1975

respectively. The temperature patterns analyzed (figure B-6) indicate that the intensity of the heat island generally decreased with increasing cloud cover at both times.

When skies were fair (figure B-6a) over the research circle, the heat island at 0000 CDT was the strongest. The urban area was as much as 5.0° C warmer than the surrounding rural area. The configuration of the heat island, noted previously as extending from the south through the city and then northeast, was evident for all three sky conditions at 0000 CDT. The intensity of

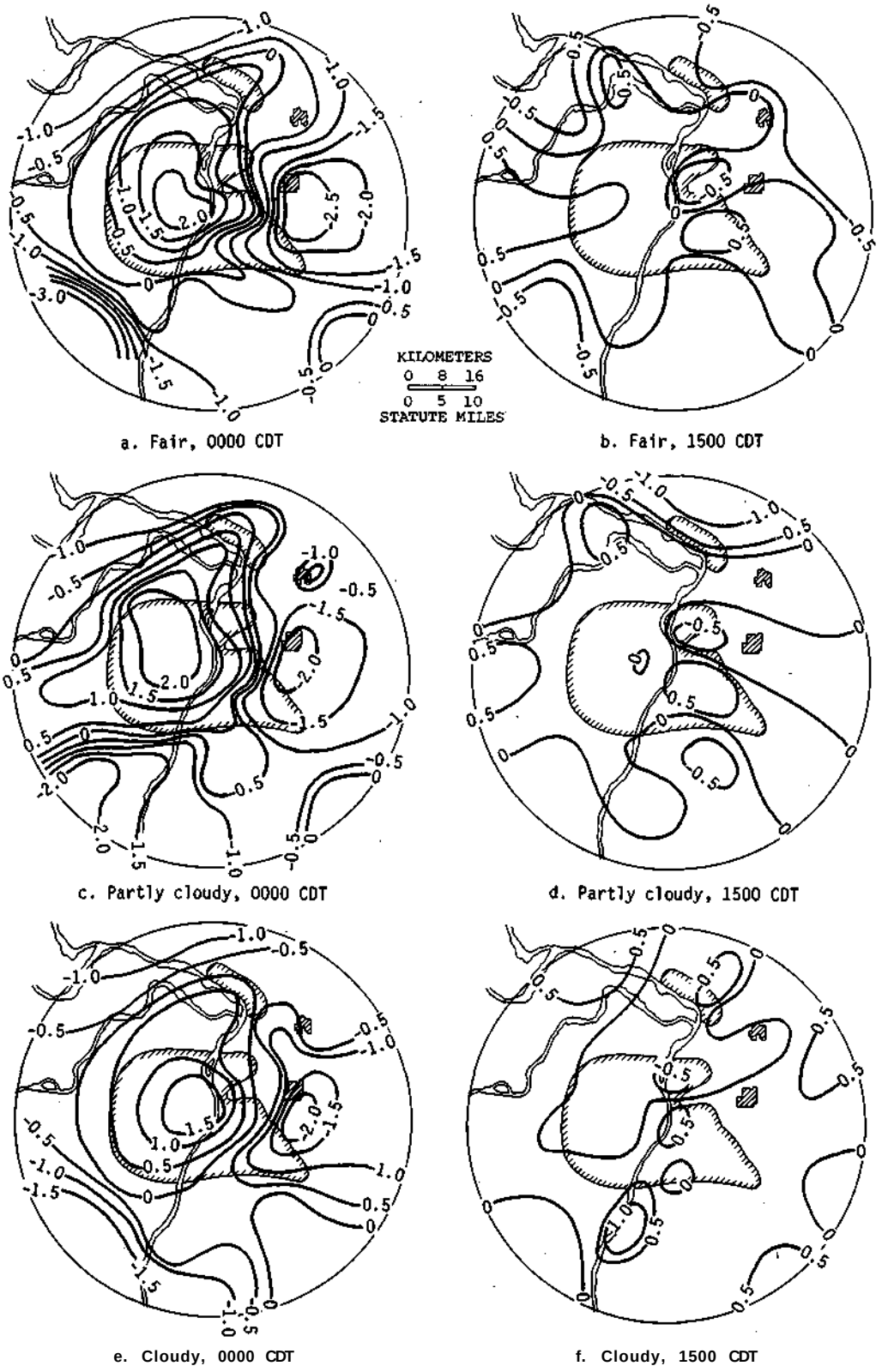

Figure B-6. Summer average temperature departure fields for three sky conditions at time of maximum and minimum intensity of urban heat island

the heat island decreased slightly with partly cloudy skies (figure B-6c). It was still well defined with cloudy skies (figure B-6e) although the temperature difference between the urban and rural areas had decreased to approximately 3.5° C. There was little change in the pattern configuration.

At 1500 CDT, the time when most maximum temperatures are reached and the heat island is the weakest, there was little or no variation in the heat island with cloud cover. The center of the heat island remained over the East St. Louis area. Cooler areas of the research circle remained essentially the same for fair (figure B-6b) and partly cloudy conditions (figure B-6d) but tended to smooth out with cloudy skies (figure B-6f). The largest difference noted between these three maps was the increase in uniformity of the temperature pattern with cloudy skies. Temperature gradients between the urban and rural areas were small, although there was an increase of isolated warm and cool spots. In all cases, the temperature anomaly at 1500 CDT was weaker than at 0000 CDT. This is in some contrast to results reported by Jones and Schickedanz (1974) where it was found that there was a tendency for the heat island to be stronger at 1500 CDT than at 0700 CDT with increasing cloud cover, when 0700 CDT was thought to be the hour for the most intense heat island. The results were thought to be possibly due to the small sample size. The results in this study indicate that this was probably the case, as no strong gradients were found at 1500 CDT compared with other times of the day.

Variations in Temperature Patterns with Wind Speed

The effect of wind speed on the urban heat island was investigated at 1500 and 2100 CDT for winds of 0 to 1.5 m s^{-1} and 2.0 to 3.5 m s^{-1}. Temperature fields for the above times and wind speeds appear in figure B-7. Wind speed appears to have only a slight effect on the temperature pattern at 1500 CDT. The center of the heat island was located over the East St. Louis area in both cases, with the intensity slightly greater with winds from 0 to 1.5 m s^{-1} (figure B-7a). The cool area extending from Edwardsville toward Granite City with winds of 0 to 1.5 m s^{-1} expanded to encompass a larger area NE of St. Louis when winds were between 2.0 and 3.5 m s^{-1} (figure B-7b).

Changes in the urban heat island were more apparent at 2100 CDT. The urban heat island was stronger by 0.5° C with stronger winds than with lighter winds (figure B-7c and 7d), contrary to previous studies of the urban heat island (Ackerman and Wormington, 1971; Nkemdirim, 1976). The greater intensity of the temperature anomaly with the stronger winds (figure B-7d) found in the METROMEX study can be explained by the amount of data included in the averages that make up the data for maps. Out of 338 possible days, only 41 had wind speeds of 2.0 to 3.5 m s^{-1} at 2100 CDT. This relatively low number of cases (12%) probably can account for the difference in heat island intensities. Despite these differences, the pattern configuration was nearly identical for both cases of wind at 2100 CDT. The temperature anomaly with winds of 2.0 to 3.5 m s^{-1} covered a smaller area than the one with winds of 0 to 1.5 m s^{-1}; it did not extend as far as to the SW and the NE.

Wind Direction and the Temperature Anomaly

Prevailing wind directions from the eight wind sites in the METROMEX network were used to stratify temperature data. The temperature anomaly as a function of wind direction is shown in figures B-8a-h. In general, most of the changes in the temperature pattern across the METROMEX research circle were minor. Because of the relatively small amounts of data available for some wind directions, only general conclusions can be reached on the associated temperature patterns.

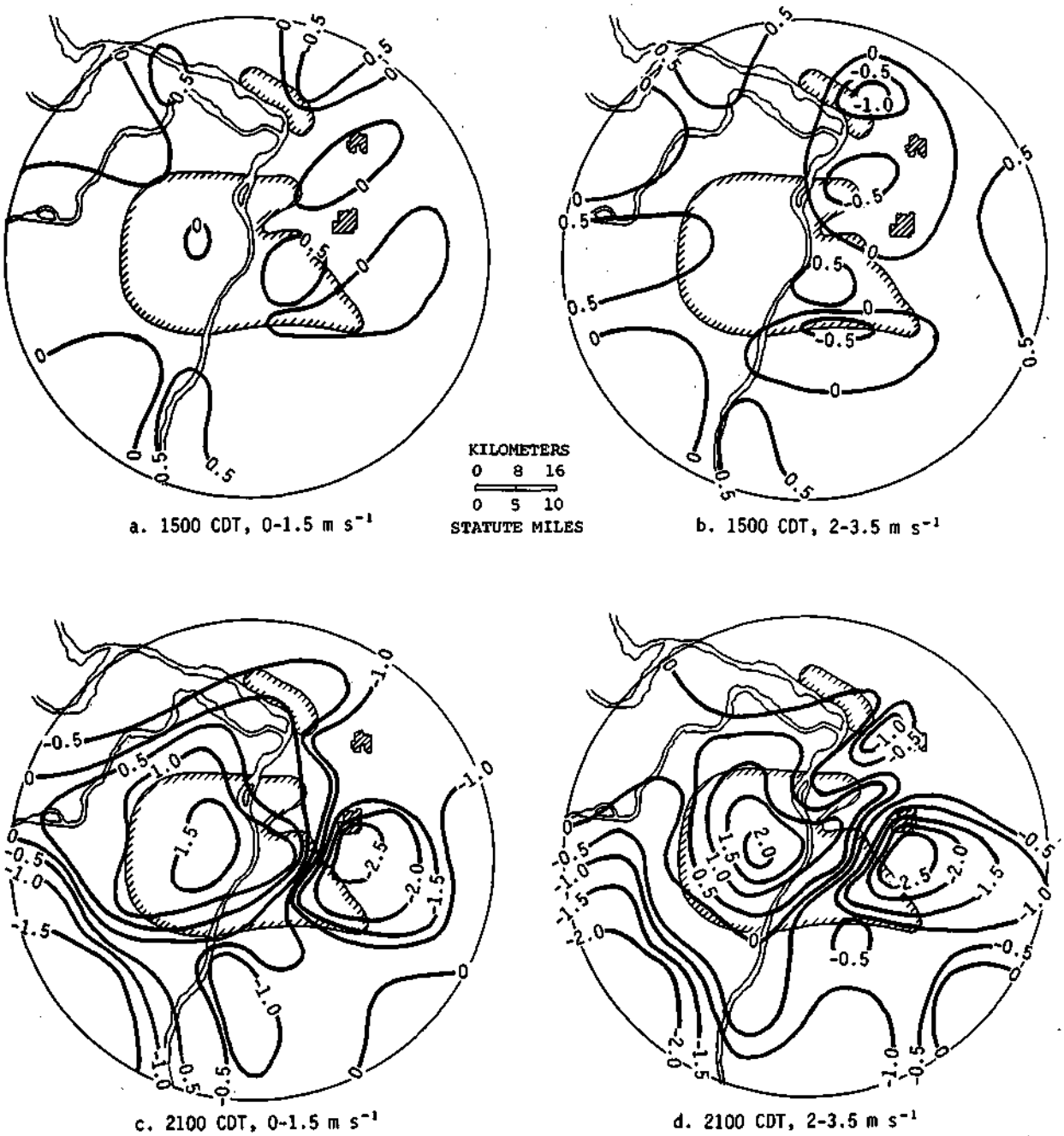

Figure B-7. Summer average temperature departure fields for two categories of wind speed

North winds occurred on 8% of the days included in this temperature study. The temperature pattern (figure B-8a) associated with this wind direction indicates some deviations from the 4-year mean pattern. Instead of an orientation along the Mississippi River, the anomaly had a more E to W alignment across the metropolitan area. The intensity of the heat island, however, deviates little from the 4-year mean pattern (figure B-4).

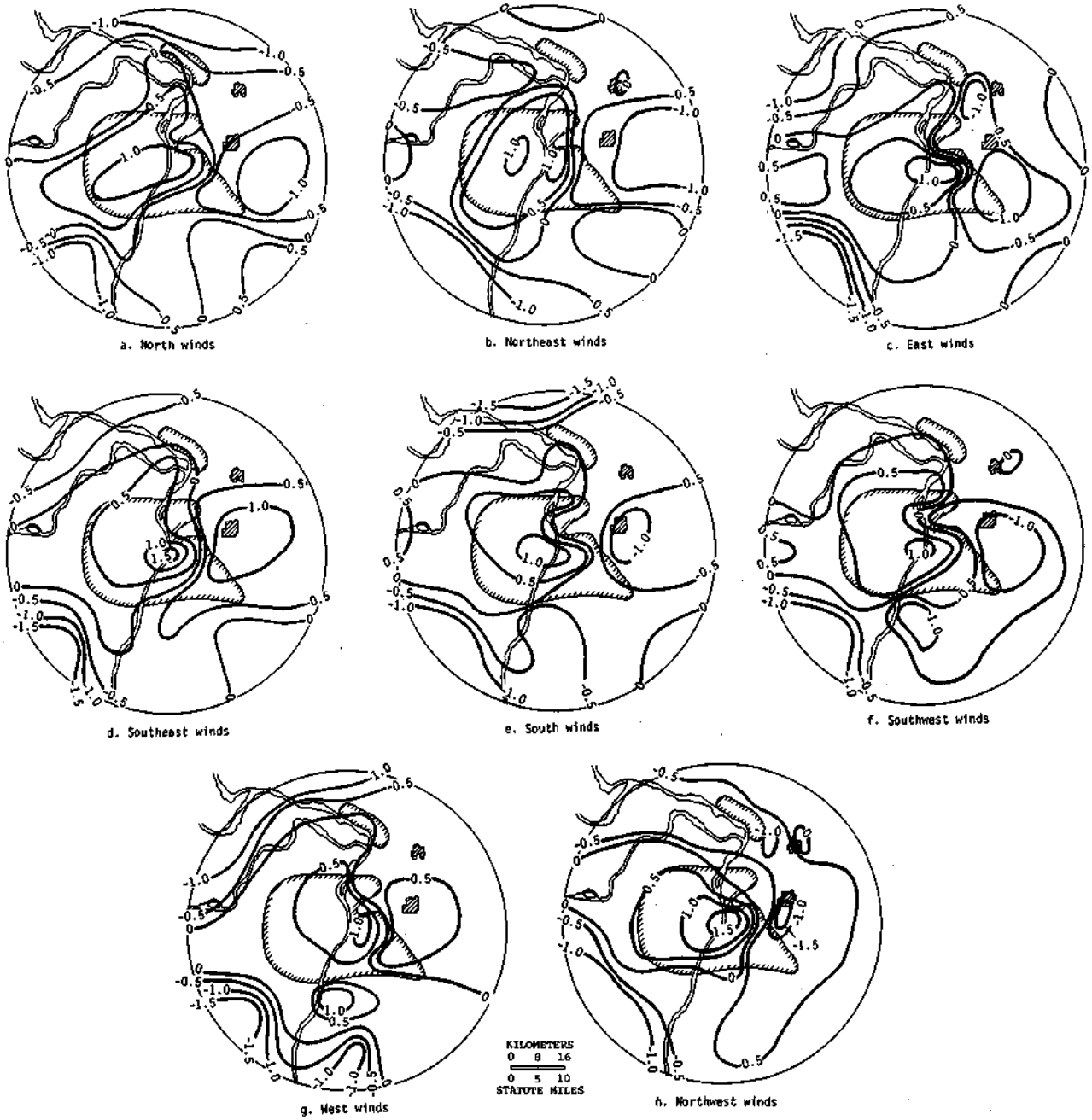

Figure B-8. Summer average temperature departure fields for given wind direction, 1972-1975

The frequency of NE winds was the same as N winds for the 4-year period (table B-1). The temperature pattern, though, was somewhat different from that with N winds (figure B-8b). Again, the intensity of the heat island had an orientation along the river, but it did not extend into the Alton-Wood River area as it did at other times. This could possibly be due to the advection of cooler air into the Alton-Wood River area from the rural area upwind, and the advection of warmer air from the area.

The heat island took on an E to W orientation with E winds (figure B-8c) although it did extend SW and NE of the city. There was a shift in the cool area normally centered over the Collinsville area S to over the Belleville area. Little change occurred in the intensity of the heat island.

The intensity of the urban temperature anomaly increased with SE winds to a value of 3.0° C (figure B-8d), approximately 0.5° C over the 4-year mean. This increase, however, was largely due to the analysis of one site, station 6 at the Arch. Most of the rural values remained about the same as the 4-year mean. The configuration of the temperature pattern was also very similar.

Table B-1. Frequency of Average Wind Direction in the METROMEX Research Circle, 1972-1975

Wind direction	*Number of days*	*Percent of total days*
North (337-21°)	26	8
Northeast (22-066°)	27	8
East (67-111°)	26	8
Southeast (112-156°)	53	16
South (157-201°)	85	25
Southwest (202-246°)	59	17
West (247-291°)	28	8
Northwest (292-336°)	34	10

South was the prevailing direction of the average winds during the period 1972-1975 in the research circle, occurring on 25% of the days included in this study. As with the patterns and the other directions, there was little change in the pattern configuration and in the intensity of the heat island (figure B-8e). This was also true for the pattern with SW winds (figure B-8f). However, with S and SW winds Granite City (station 44) was much cooler than the urban area, even though it is close to the St. Louis industrial area. This anomaly is probably due to the small number of days of data available for this site, which was in operation only in 1974.

The heat island changed little with W winds (figure B-8g), but it became much stronger when NW winds were observed (figure B-8h). The difference between the warmest and coolest location (stations 6 and 18, respectively) was 3.7° C, whereas the 4-year mean average difference was 2.4° C. The pattern was also different with NW winds. The heat island was smaller, and a cool area extended from NW of the city through the Alton-Wood River area and then S along and E of the bluffs. The increased intensity of the heat island may be due to the fact that NW winds normally are associated with the clockwise circulation around an approaching high pressure system. Clear skies and good visibilities often accompany such systems, and at night the lack of cloudiness would permit strong re-radiation of longwave energy into the atmosphere from the earth's surface. Since the rural areas by nature of their surface characteristics have lower heat capacities, they would lose the stored heat much faster than the urban area. The resultant differential cooling between the urban and rural area has been found to be the major factor in the development of the urban heat island (Oke and Maxwell, 1975).

Summary

The analysis of 4 years of temperature data collected as part of the METROMEX program has demonstrated the existence of the urban heat island in the St. Louis metropolitan area. The heat island existed at all times during the summer, although the strength of the heat island varied with time of day and with certain weather conditions. Temperature differences between the urban and rural areas were largest during the night, maximizing about midnight. The weakest stage in the urban heat island occurred during the mid-afternoon at approximately 1500 CDT.

There was little variation in either the strength or the configuration of the heat island during the summer months. With the exception of some cooler temperatures in the eastern portion of the network in August, the monthly patterns were the same. The 4-year mean surface

temperature pattern for the summer revealed that the urban area was, on the average, 2.0 to 2.5° C warmer than the surrounding rural areas. The heat island was centered over the center of the metropolitan area, from the St. Louis city center eastward into the East St. Louis area. The heat island extended from the western portions of the research circle to the eastern edge of the metropolitan area, and from the confluence of the Meramec and Mississippi Rivers north through the city and then northeastward to the Alton-Wood River area. Coolest areas in the research circle were found to be near the Collinsville area and in the SW Ozark foothills.

The effects of cloud cover, wind direction, and wind speed on the heat island were investigated. The urban heat island was found to be strongest with fair skies. With fair skies, and at midnight CDT, the urban area was as much as 5.0° C warmer than some surrounding rural sites. The intensity decreased slightly with partly cloudy skies, and the urban heat island was still well defined with cloudy skies, during which the urban area was 3.5° C warmer than the rural area. At the normal time of maximum heat island intensity, 0000 CDT, there was generally a decrease in intensity of the heat island with cloud cover. This tendency was not evident at 1500 CDT, the time when the heat island was characteristically the weakest. There was little change in the intensity or configuration of the heat island, although with cloudy conditions the temperature pattern became more uniform, that is, gradients between the urban and rural areas became less.

The temperature anomaly was found to be slightly greater when winds were at speeds from 0 to 1.5 m s^{-1} at 1500 CDT. At 2100 CDT, when maximum cooling is taking place in both the urban and rural areas, the heat island was weaker with light winds, and stronger with winds of 2.0 to 3.5 m s^{-1}. The stronger heat island with winds of 2.0 to 3.5 m s^{-1} is contrary to previous studies, and the results here are thought to be a problem of sample size, and not physical differences.

Only minor changes in the urban heat island were found as a function of wind direction. The largest changes occurred with winds from the NW. The area covered by the heat island was smaller, and the intensity was greater than the 4-year mean. A large area of cooler air was found to extend from NW of St. Louis through the Alton-Wood River area and then S along the east of the bluffs. Results of the variations in the heat island with wind direction are generally inconclusive because of the small amounts of data for certain wind directions.

DIURNAL TEMPERATURE AND MOISTURE CYCLES

Steven D. Hilberg

INTRODUCTION

Temperature and humidity data recorded from the large dense network of stations in the METROMEX research circle have been used to examine the hourly variations of temperature and moisture. Whereas previous studies were concerned with patterns of isotherm and isodrosotherms over the network, this study concerns the daily temporal distribution of temperature and moisture at specific sites. Data from 1972 through 1975 were used. Data were available for only a few sites in June of 1972, but the remainder of the 25 stations were added as the summer progressed. Data were generally available for most sites in 1973 and 1975, but only for July and August in 1974.

A large number of sites were available for this study but only two stations were selected for concentrated study of urban-rural characterization. The hygrothermograph stations were categorized as to whether they were urban influenced (urban) or non-urban influenced (rural). Comparisons were then made of the diurnal temperature and moisture (mixing ratio) cycles. Although this section will concentrate on the data at two specific stations, characteristics of the data at the remaining stations will be discussed where pertinent.

Sampling Network and Instrumentation

The data used in this study were collected from the network of hygrothermograph stations in the METROMEX research circle. Two types of hygrothermographs were used as described in the previous section. The hygrothermograph sites were spread out over the research circle (figure B-9) to represent as much of the research area as possible. Most of the stations were located in rural areas, but two were in the city of St. Louis proper, one at the Arch and the other in Forest Park. Others were located in the surrounding suburban metropolitan area. With only one or two exceptions, the hygrothermograph locations were suitable for accurate representation of the surrounding area. Because the location of these instruments was usually subject to permission from property owners and businesses and required some security, less than ideal locations had to be settled for on occasion. For example, the shelter in Forest Park, for security reasons, was located near a parking area for park equipment and vehicles. The proximity of the shelter to the concrete area and the vehicles may have had some less than obvious effect on the data. In general, the sites were located over grass whether in an urban or rural area.

Analysis Procedure

The hygrothermograph sites were stratified into two broad categories based on their geographical location, potentially urban and potentially rural. The areas enclosed by the hatched line in figure B-9 include those stations designated as urban. One station from each category was selected for the detailed comparative analyses of an urban or rural area with consideration given to the availability of data for the four summers. Station 6 (ARC) located on the riverfront in St. Louis near the Arch, was selected to represent the urban area, and station 20 (FRM), located

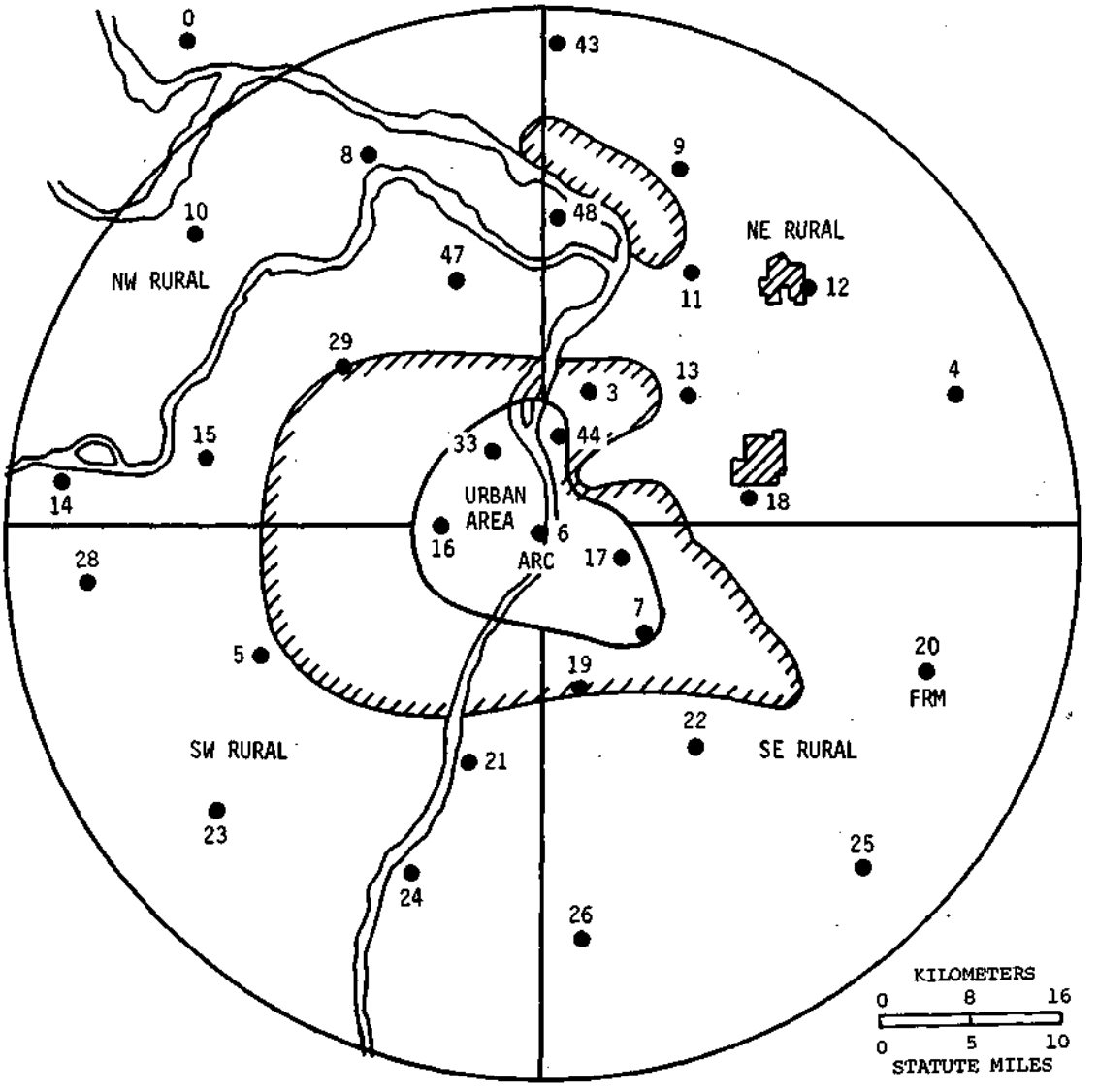

Figure B-9. Location of hygrothermograph sites in METROMEX research circle

on the SIU Experimental Farm east of Belleville, Illinois, was chosen to represent the rural area. Photographs of the two stations appear in figure B-10.

An averaging procedure was run on all the data from all stations for each year. The procedure averages a specified number of diurnal cycles and then normalizes the average curve to the mean temperature. For this study, a diurnal cycle was defined as the 24-hour period beginning at 0600 CDT. If more than three hourly values were missing in any one 24-hour cycle, that cycle was not used in the averaging process. An average temperature curve and mixing ratio curve for the 92-day summer period (62 days in 1974) were calculated for each station in the network. The average curves were then differentiated to yield the average rates of change of temperature and moisture.

The data were further stratified by sky condition: fair (0.03 coverage), partly cloudy (0.4 to 0.7 coverage), and cloudy (0.8 to 1.0 coverage) days which were tabulated for each summer

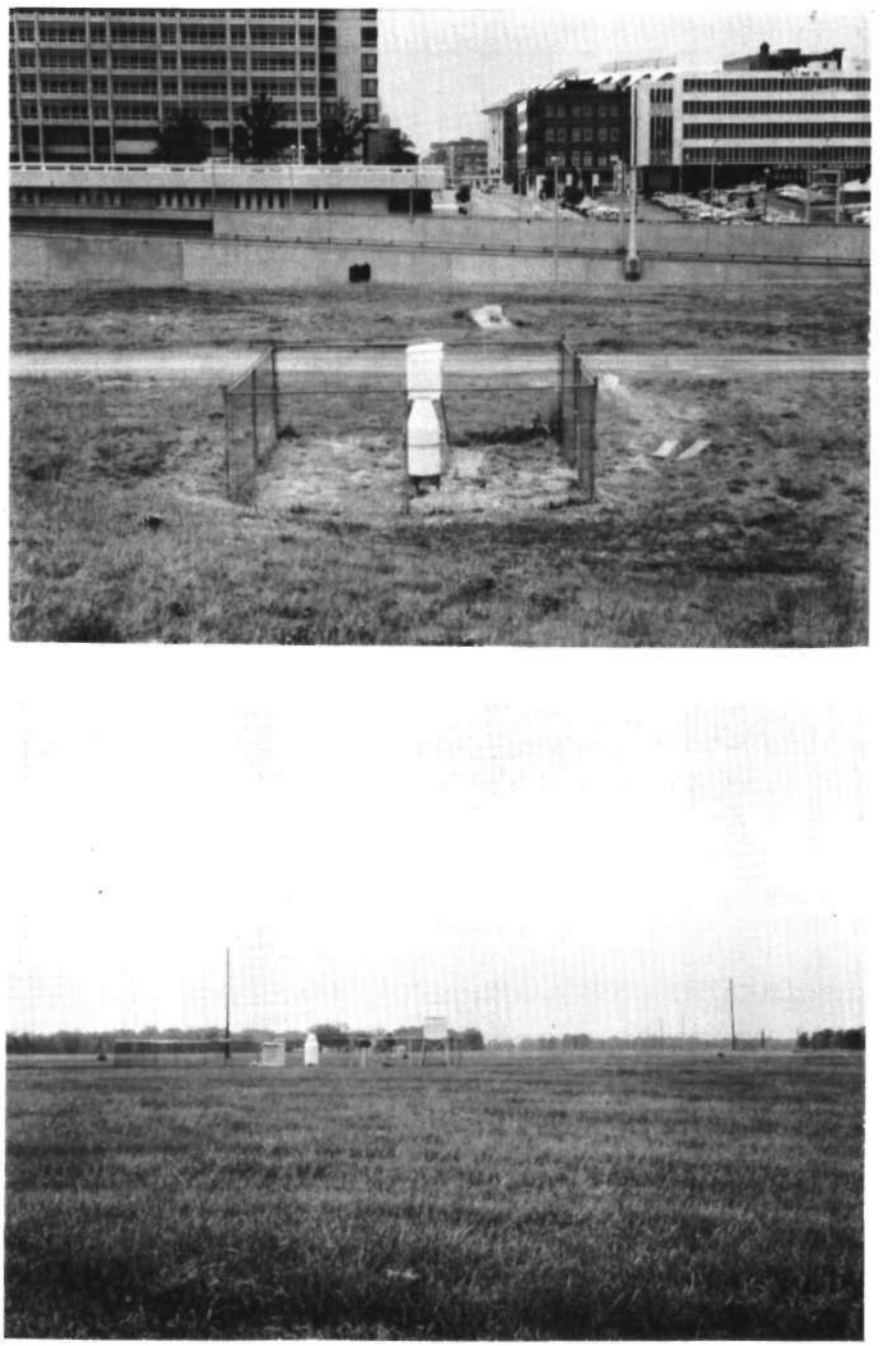

Figure B-10. (Above) Photograph of shelter located at Arch, looking west; (Below) Photograph of shelter at SIU Experimental Farm near Belleville, looking south

from the observations taken at STL and BLV. To insure that a sky condition persisted throughout a diurnal cycle, only periods in which a certain condition prevailed at least 2 consecutive days were used in the calculation of an average diurnal cycle.

Comparisons of urban and rural temperature change rates were made for the two representative stations. Station 20 (FRM) was located over a large, lush grass field at the SIU Farm.

The only obstruction in the area was a chain link fence 1.3 m high, approximately 1.3 m from the shelter. The urban site at the Arch in St. Louis was located in a sparse grassy area, with the river about 200 m to the east and a dirt access road about 10 m to the west. There are numerous buildings and paved roads as close as 200 m southwest and north of the site. Although on the eastern edge of the city, the site is about in the center of a metropolitan area divided by the Mississippi River which includes the East St. Louis area and St. Louis County, as well as the city of St. Louis.

DIURNAL TEMPERATURES

Comparison of Diurnal Temperature Cycles

The urban heat island is a well-documented phenomena (Peterson, 1969), but most studies to date examine the heat island as a spatial entity at some point in time, such as an hour of the day or a certain season. However, the heat island effect is discernable not only in a spatial analysis, but in a temporal one as well. Comparisons of urban and rural diurnal temperature cycles indicate significant differences which may provide insight into the dynamics of heat island formation.

The 4-year normalized diurnal temperature average curves for ARC and FRM are shown in figure B-l1. The FRM rural curve is markedly different from the urban curve (ARC) in several respects. It has a greater amplitude, and larger rates of heating in the morning and larger rates of cooling after 1930 CDT. Both stations reach their maximum temperatures about 1500 CDT, approximately 9 hours after local sunrise. Even though the urban site normalized maximum temperature value is 1.4° C less than the rural curve, the actual temperature is slightly greater than the rural area at the time of maximum temperature.

A comparison of the diurnal variation temperature change for these two curves (figure B-l2) indicates the point where the urban heat island is established. The maximum difference in the rate of cooling occurs between 1900 and 2000 CDT. At this point the rural area is cooling approximately 1.0° C hr"[1] faster than the urban area, and continues to do so until 2100-2200 CDT, when it decreases to approximately the same rate of cooling as the urban area. Both sites continue to cool at almost a linear rate (0.5° C hr^{-1}) until sunrise. This same trend has been noted by Oke and Maxwell (1975) for summer days with light winds and scattered clouds.

Most of the stations in the METROMEX research circle recorded their maximum cooling rate between 2000 and 2100 CDT. Approximately one-third of the stations attained the maximum rate of cooling between 1900 and 2000, with a slight decrease or no change between 2000 and 2100. Only one station, ARC, attained a maximum rate of cooling ($1^{o}C\ hr^{-1}$) between 1800 and 1900. This may be due to the sun setting behind the city buildings to the west. The cooling rate remains constant for the next 2 hours, then begins a slow decrease.

The time of occurrence of the maximum rate of cooling appears to be unrelated to the location of a site. Urban and rural stations both reached maximum cooling about 30 minutes after sunset. The magnitude of the cooling rates was, however, related to the location of the sites. In the rural area, maximum cooling rates were about 0.4° C hr^{-1} greater than the urban area on the average. The magnitudes, of course, are largely dependent on the land use in the area surrounding the site. The rural sites generally have a lower percentage of buildings and pavement as part of their land use. In some locations, topography plays a part in the magnitude of the cooling rates. Station 18, just south of Collinsville, is located at the base of a small hill, and has an average maximum cooling rate of 2.6° C hr^{-1}. Station 23 is located in a small valley in the

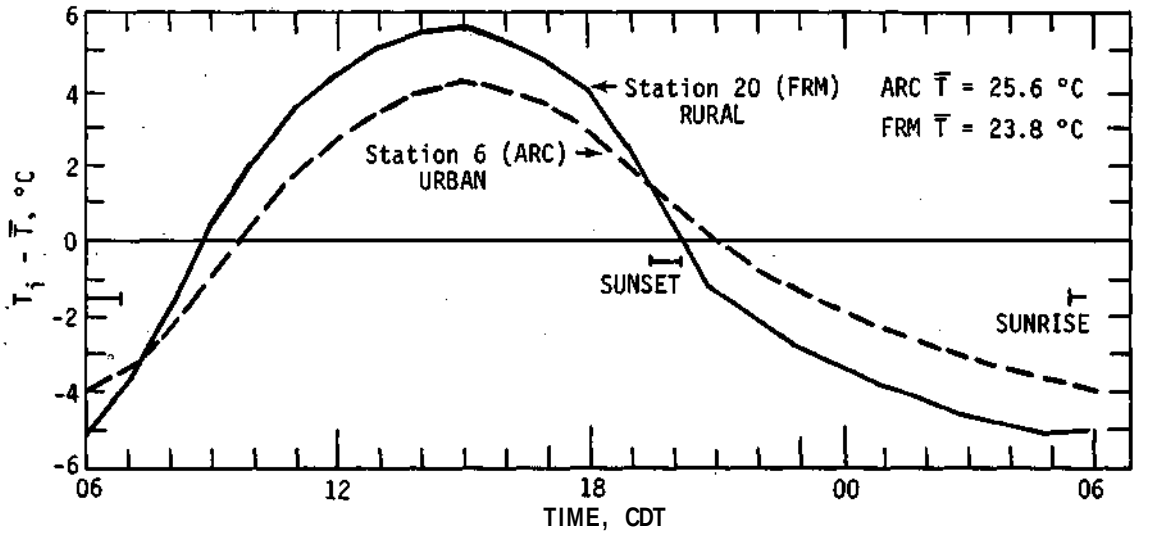

Figure B-11. Four-year average normalized diurnal temperature curves for a rural (FRM) and urban (ARC) station

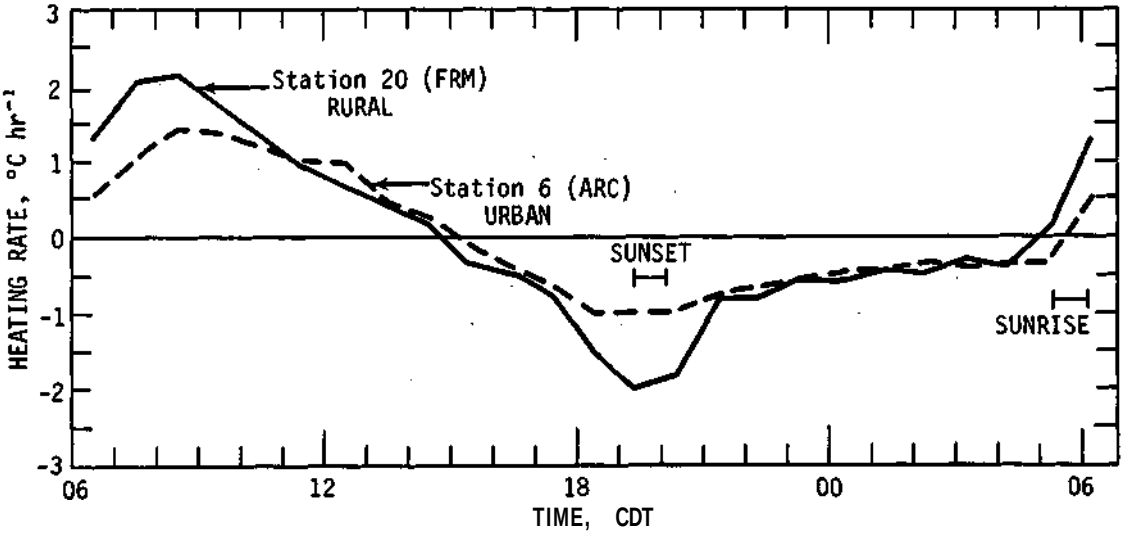

Figure B-12. Four-year average diurnal temperature rate curves for a rural (FRM) and urban (ARC) station

Ozark foothills, and cold air drainage into this valley after sunset produces an average maximum cooling rate of 2.0° C hr^{-1}, which is the highest value recorded in the network. Even though both of these stations are affected by the immediate topography, the rate curves for the stations are very similar to those of the other rural sites (figure B-l 3), the main difference being the magnitude of the maximum cooling rate.

Most studies of the urban heat island concentrate on the formation of the heat island and thus are concerned with nocturnal cooling. However, there are differences between urban and rural heating rates during the decrease in intensity of the heat island in the hours following sunrise.

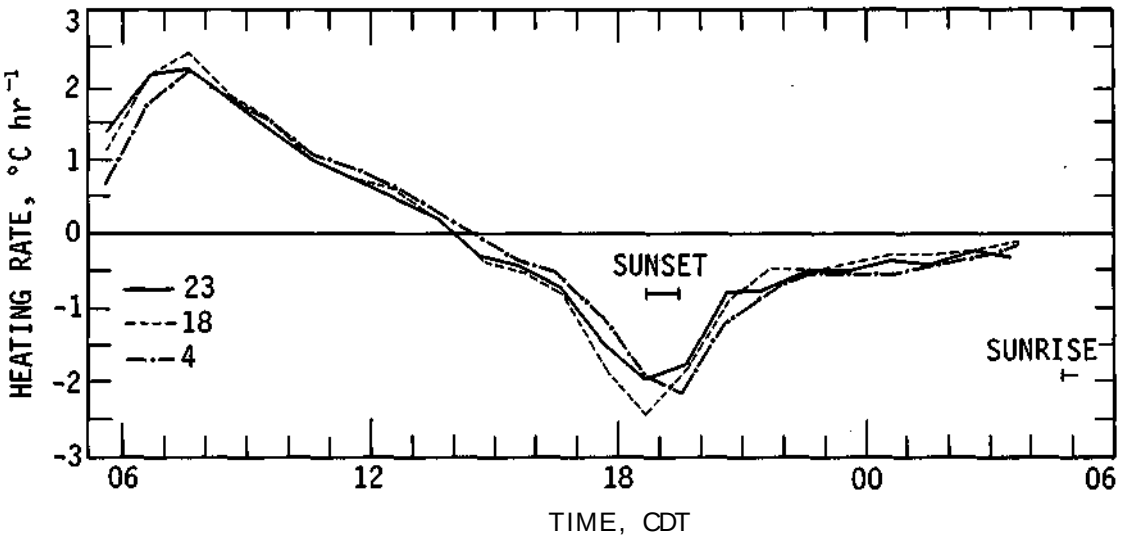

Figure B-13. Four-year average normalized heating rate curves for three rural locations

Not only do rural areas cool at a faster rate after sunset, but they heat at a faster rate following sunrise. The heating rate for both locations (figure B-12) is small in the first hour following sunrise. However, by the second and third hours after sunrise station 20 (rural) has attained a heating rate of 2.2° C hr^{-1}, while station 6 is heating at a rate of 1.4° C hr^{-1} . Note that while the rural site rises to its maximum heating rate quickly, there is almost a linear increase in the value of the urban heating rates. Whereas there were some differences in the time of occurrence of the maximum cooling rates between sites, all sites attained maximum heating rates between 0800 and 0900 CDT, 2 to 3 hours after sunrise. Rural sites on the average had maximum heating rates 0.3° C hr^{-1} greater than the urban areas. After 1100 CDT, the urban heating rates remain slightly greater than the rural heating rates.

Variations in Diurnal Cooling and Heating Rates with Sky Conditions

In addition to the average diurnal curves computed for the entire summer period, averages were computed for data stratified by sky condition. Three categories of sky condition (fair, partly cloudy, cloudy) were established, as previously described.

The criterion that a particular sky condition must have prevailed for a 2-day period to be included in any category did limit the data sample somewhat. There were very few cloudy days available for analysis, partly because a 24-hour period of overcast or near overcast skies is not typical summer weather in St. Louis. There were 59 fair, 75 partly cloudy, and 32 cloudy diurnal cycles available from the four summer periods.

Rural Variations. As expected, heating and cooling rates during days with cloudy skies were less than those during days with fair or partly cloudy skies at FRM (figure B-14a). The greatest differences between the cloudy, partly cloudy, and fair sky measurements occur in the first four hours after sunrise and from 1800 CDT through the nocturnal period. The maximum heating occurs about the same time as with fair and partly cloudy conditions, but the maximum cooling occurs approximately 3 hours earlier than with fair and partly cloudy conditions. The rate of cooling then decreases toward sunrise.

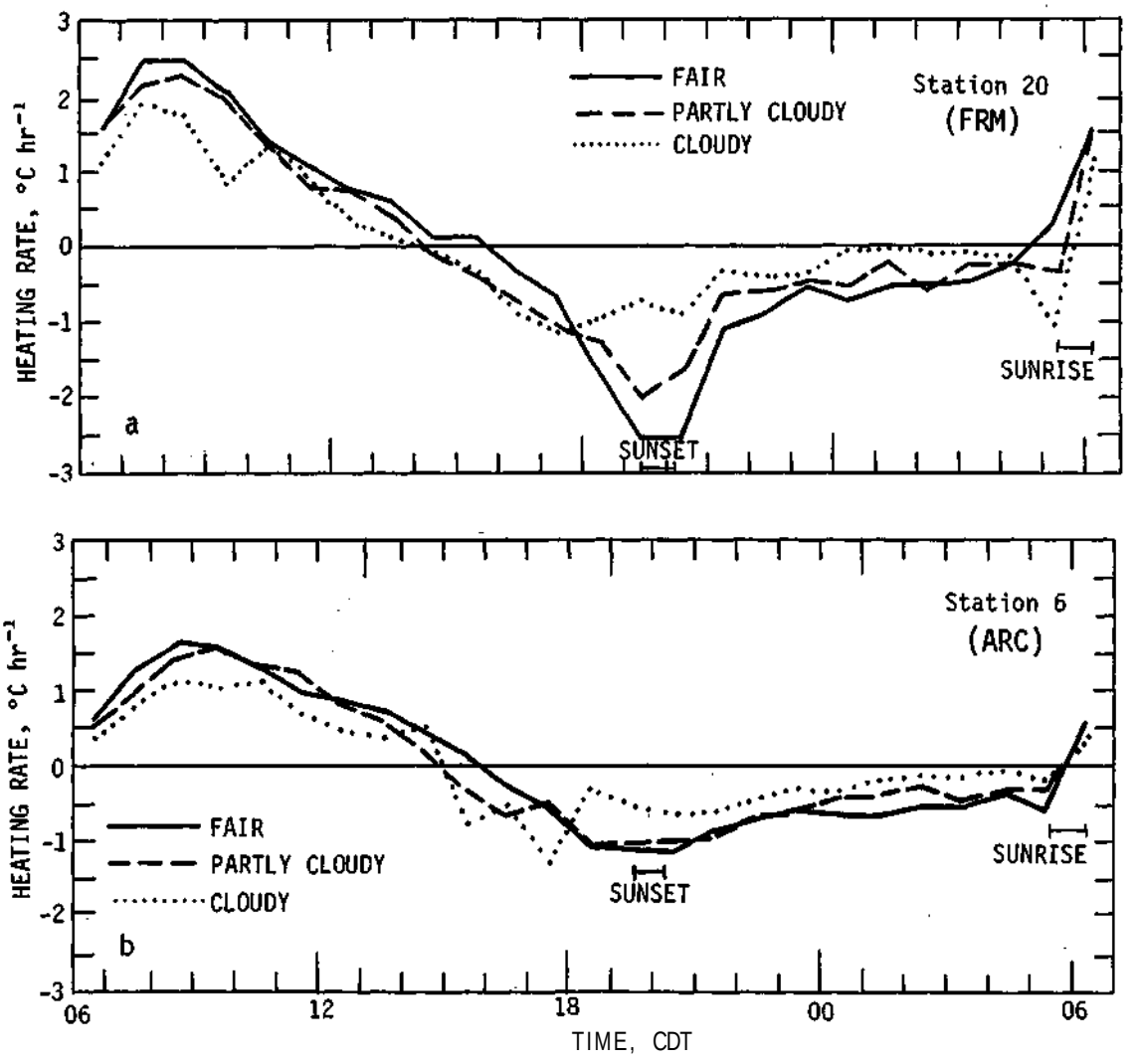

Figure B-14. FRM (rural) and ARC (urban) temperature rate curves for three sky conditions, 4-year average

The greatest heating and cooling occurs with fair skies. Maximum heating develops 1 to 3 hours after sunrise at which time the heating rate is 2.5° C hr^{-1}. With cloudy skies the maximum heating rate is 1.9° C hr^{-1}.

The largest differences, however, occur with the maximum cooling. Rates reach a maximum of *2.6° C* hr^{-1} under clear skies, decreasing to 2.1° C hr^{-1} under partly cloudy skies, and reaching a minimum of 1.2° C hr^{-1} under cloudy skies.

Urban Variations. The diurnal curves for ARC under various sky conditions do not follow the same trends evident in the rural area. Whereas there were distinct differences between each of the three diurnal curves in the rural area, the differences are much less obvious in the data for ARC (figure B-14b). There is very little difference between the diurnal curves for fair and partly cloudy skies. There is slightly less heating with partly cloudy skies than with fair skies in the first few hours after sunrise, and slightly less cooling after 0000 CDT. During the afternoon hours, when clouds

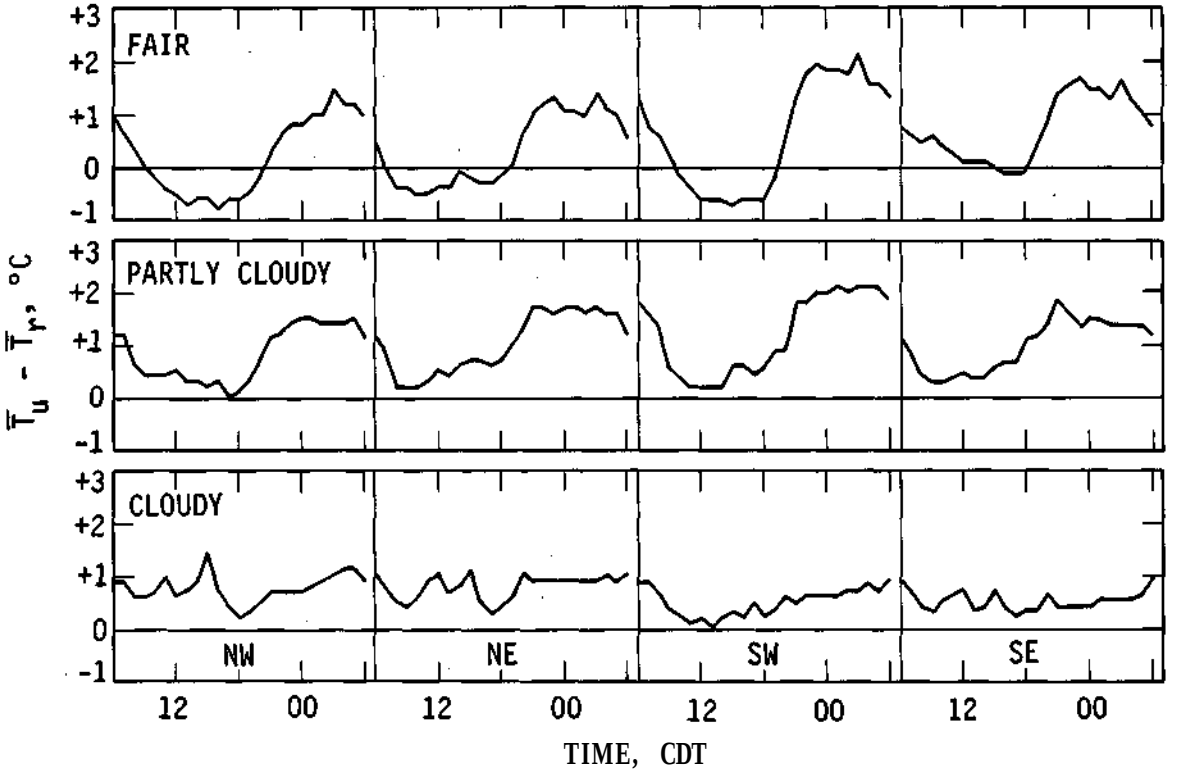

Figure B-15. Strength of urban heat island as a function of sky condition and four rural areas

would be forming, heating rates are less than with fair skies. However, the differences are small. The largest differences in the two rate curves, in fact, occur during the afternoon hours. At this time, the partly cloudy rates are approximately 0.3° Chr^{-1} less than the fair sky rates. About the same difference in rates occurs during nocturnal cooling from 0000 to 0300 CDT.

The more obvious difference is between the fair or partly cloudy and cloudy conditions. Here the rates for cloudy conditions remain smaller than the rates for either fair or partly cloudy. The largest difference in cooling rate attributable to cloudiness occurs between 1800 and 1900 CDT. Under cloudy skies, the cooling rate at ARC is about 0.7° C hr^{-1} less than for either fair or partly cloudy conditions.

There are variations in the cloudy urban diurnal curve between 1500 and 1800 CDT that are not evident in the other curves. These variations were caused by a combination of two factors. First, there were only two-thirds of the available cloudy sky data included in the ARC mean; the remainder was missing. Second, on 22 days that were included, rain fell in the area, and the proximity to the rain may have produced large changes in temperature.

Five areas (urban and the NW, NE, SW, and SE rural areas) were delineated in the METROMEX research circle as shown in figure B-9. Data from the stations within these areas were used to evaluate the strength of the urban heat island throughout the diurnal period. Areal mean temperatures for each hour were computed for the four rural areas and one urban area, and the difference, Tu-$T_{u,}$ was determined. These differences were then plotted as a function of time.

The strength of the heat island as a function of cloud cover and four rural quadrants is shown in figure B-15. With fair and partly cloudy skies the strength of the heat island is about

the same. There is, however, one major difference in the diurnal character. With fair skies the urban area actually is slightly cooler than the rural areas in the afternoon, on the average of 0.5° C. This is not the case with partly cloudy and cloudy conditions. With cloudy skies, the heat island loses its strong diurnal character, and there are smaller but more numerous variations. The strength of the heat island decreases from an average value of 1.7° C for fair skies to a value of *0.9° C* for cloudy skies.

Heat Island Dynamics and the Diurnal Cycle

Several questions about the formation of the urban heat island arise from the comparisons of the urban and rural diurnal curves. Primarily they concern the large differences in the heating and cooling rates in the 3 hours following sunrise and then again near sunset. Inherent in these differences are the various radiational properties of the urban and rural areas.

In the first 3 hours following sunrise, the rural area heats more rapidly than the urban area by 0.3° C hr^{-1}. After this time, both the rural and urban heating rates closely parallel each other. During the early morning heating, there must be some factor that either accelerates rural heating or dampens the urban heating. Since the rural area is generally considered to be a control area, and the urban area a modified area, the urban heating rates may be assumed to be dampened. Changes in an area undergoing urbanization have been documented for Columbia, Maryland (Landsberg and Maisel, 1972), providing further evidence that urbanization produces changes in meteorological variables.

The differences between urban and rural surface characteristics are well known. However, because of the varied surface material in the urban area, such as glass, wood, concrete, and asphalt, it is difficult to assign values to radiational parameters (Oke and Maxwell, 1975) since frequently the percentage of the materials in the urban area is unknown. It is known, though, that the urban area provides excellent sensible heat storage (Munn, 1966) and it is this factor, combined with other mechanisms, that helps to produce the urban heat island. Incoming shortwave radiation during the day is absorbed by the urban area, and then is released in the form of longwave radiation at night. Because of the greater heat capacity of the urban area, heat is released for a longer time . than in the rural area.

There could be several reasons for the lower heating rates in the urban area. In light of certain characteristics in the urban area, i.e., more particulate matter in the air and greater density of buildings, it is possible that less shortwave radiation is reaching the urban area. An inversion aloft in the urban area versus one from the ground in the rural area is one of the features attributed to urbanization. In ideal conditions, when a strong inversion forms aloft and winds are light, there will be a large buildup of pollutants in the levels below the inversion. Vukovich (1973) points out that, after sunrise, these pollutants prevent shortwave radiation from reaching the surface, and because of this the urban heating rates are less than in the rural area. Thus the nature of the inversion aloft and the radiation balance of the pollutant layer below have important implications in the nature of the heat island (Atwater, 1971).

The second major difference between the urban and rural diurnal cycle is in the period between 1830 and 2030 CDT. At this time the rural area is cooling 0.4° C hr^{-1} faster than the urban area. After this period, the rural cooling rate approaches the urban cooling rate and closely parallels it until sunrise. It is during this period of differential cooling that the heat island intensifies. Figure B-16 presents the urban-rural temperature difference for the four rural quadrants. This is similar to figure B-l5; positive departure values indicate the urban area is warmer. It is quite clear when the formation and decay of the heat island take place during the diurnal period. However,

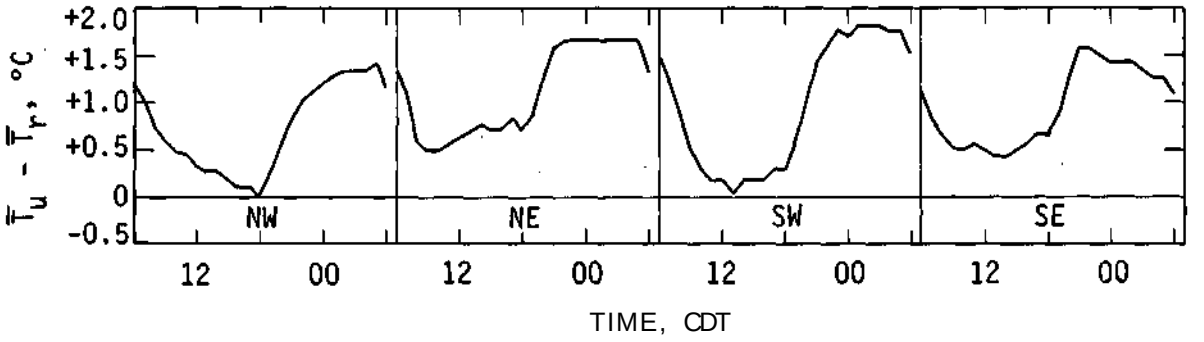

Figure B-16. Diurnal variation in the strength of the urban heat island with respect to four rural areas

the processes behind the heat island formation are less clear. Oke and Maxwell (1975) examined this problem with data obtained from nocturnal traverses in Montreal and Vancouver. They concluded that the processes behind the urban cooling are quite complex, and that the formation of the urban heat island is controlled largely by the amount of rural cooling with respect to the urban area. They also suggested that cooling described by an equation given by Brunt (1941) may be opposed in a mirror-image fashion by other processes in the urban area.

Much of the incoming shortwave radiation in the daytime is absorbed by the various surfaces. Some of this stored energy is radiated at night as longwave radiation. Although the rural areas also radiate longwave radiation, less energy is stored during the day because of the lower heat capacities of surface materials, and thus less energy can be released at night. In addition, because of the different surface materials in the urban area, there are different rates of the longwave radiation. The radiation of energy at different rates may account for part of the dampening of the urban cooling, but how much is difficult to say. Complicating this are the many tall buildings in the urban area. Much of the upward longwave radiation at night is not released to the atmosphere above the city, but rather is trapped in the lower levels because of exchanges between buildings (Munn, 1966).

A third possible reason for the lower cooling rates may be the release of anthropogenic heat. Although anthropogenic heat has been considered an important factor in the maintenance of the winter nocturnal heat island (Ackerman and Wormington, 1971), it has been thought to be relatively unimportant in summertime cases. During the summer months, however, there is considerable use of air conditioning, which produces heat as a by-product. It is conceivable that both residential and commercial air conditioning may make a small but significant contribution to the heat in a city. The warmer urban area is conducive to increased air conditioning use, especially at night. Rural residents may be more likely to turn their air conditioning down or off at night because of the rapid cooling of the rural area. The increased use of air conditioning combined with the greater density of buildings in the urban area may make a contribution to the low and relatively constant rate of urban cooling.

DIURNAL MIXING RATIO CYCLES

The relative humidity data collected were used to calculate mixing ratio values each hour at each station. These mixing ratio values were then processed in the same manner as the temperature data. Relative humidity values were not used because of their large dependence on temperature, and what is of interest is a parameter that describes the actual moisture content of the air. The large number of sites in the METROMEX network from which these data were collected permits not only a look at the diurnal variation of the mixing ratio but also a look at the different types of diurnal variations found in a relatively small area, and the diurnal variations of the urban-rural moisture difference.

Variations in Urban and Rural Mixing Ratio Cycles

Like the diurnal temperature cycles, there were distinct differences between the urban and rural mixing ratio cycles. However, there were more variations among the rural stations and among the urban stations than with the temperature cycles, and thus it was much more difficult to determine whether or not a mixing ratio cycle was rural or urban just by its characteristics.

The mixing ratio diurnal cycles for FRM (station 20) and ARC (station 6) are shown in figure B-17. As with the temperature, the variations about the mean of mixing ratio throughout the day is less in the urban area than in the rural area. The 4-year mean values for FRM and ARC are 14.5 g kg^{-1} and 14.0 g kg^{-1}, respectively. In the curves for FRM, there is a slight peak in the mixing ratio in the early afternoon hours, after which it decreases and then rises to a larger peak at 1900 CDT. The mixing ratio in the urban area, however, remains fairly constant from sunrise through the afternoon hours, beginning a slow rise around sunset. The increase continues for about 4 hours, after which the urban mixing ratio remains constant until just before sunrise. Because the curves in figure B-17 are normalized, they tell nothing about the absolute difference between mixing ratio values. Adding the difference in mean mixing ratios, 0.5 g kg^{-1}, to the FRM curve will show that ARC is drier at all times except for the period from midnight to 0600 CDT.

The maximum increase in mixing ratio at FRM occurs between 1800 and 1900 CDT. There is no corresponding maximum in the curve for ARC. Almost no increase or decrease in the urban mixing ratio takes place until after 1800 CDT, when it increases at a rate of approximately 0.2 g kg^{-1}, and then decreases just before sunrise.

Classification of Diurnal Mixing Ratio Curves

Hage (1975) found the diurnal trace of absolute humidity at a rural airport to exhibit a distinct double wave, with peaks occurring before sunset near the time of maximum cooling and following the maximum heating in the morning. The FRM curve did not exhibit a strong maximum after the early morning heating but did have a maximum near sunset. The curve for ARC did not have any maximum early in the day.

In order to find out if this lack of a double wave at the rural station was just a peculiarity of the site, criteria were set by which the diurnal mixing ratio curves could be classified. Three categories were established: a single wave, with a maximum departure from the mean ≥ 1 g kg^{-1} ; a single wave, with a maximum departure from the mean ≤ 1 g kg^{-1} ; and a double wave, with a difference between each maximum and the minimum ≥ 0.4 g kg^{-1}. The three types of diurnal curves are shown in figure B-18. Diurnal curves in the urban and rural areas were similar to these

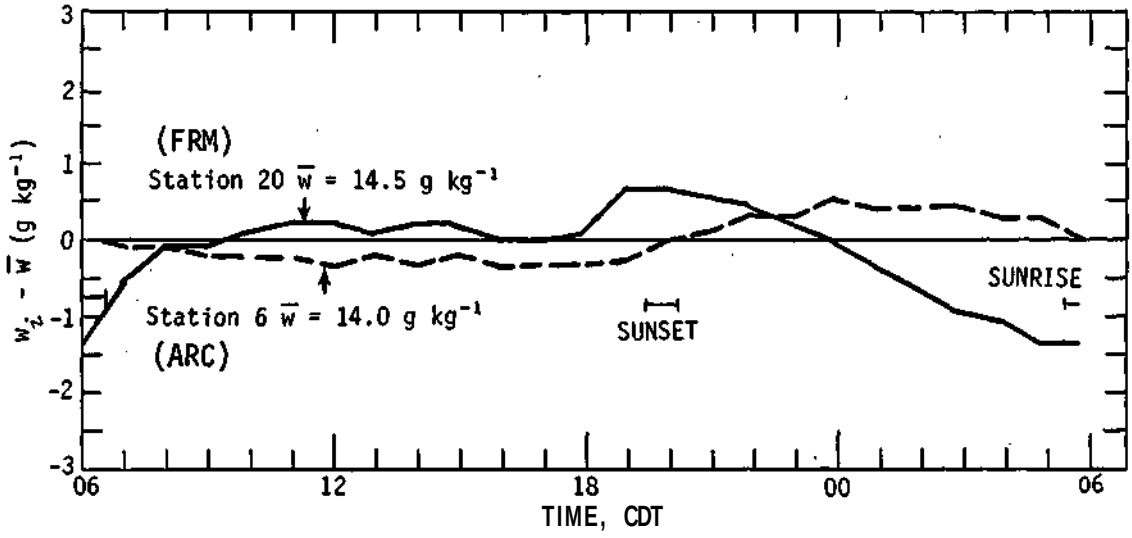

Figure B-17. Four-year average normalized diurnal mixing ratio curves for a rural (FRM) and urban (ARC) station

curves except for differences in the amplitude of the curves and the time of the occurrence of maximum mixing ratio. Table B-2 is a classification of the mixing ratio cycles based on the three patterns shown in figure B-18. Out of the 29 mixing ratio cycles examined, only seven were found to exhibit the 'double wave' pattern, and out of those seven, two were urban. The remainder of the curves were single wave patterns, similar to what Hage (1975) obtained for an urban airport location. Thirteen of the curves were single wave patterns of type 2. There appears to be no preference for an urban or rural area to exhibit a certain pattern. Within the individual categories, however, the urban mixing ratio cycles had lower amplitudes, and variations between the maximum and minimum values were generally less.

The differences in the types of mixing ratio curves in a relatively small area are probably due to local effects, such as advection and local moisture sources or sinks. Sisterson (1975) found that local moisture advection appeared to strongly affect the time rate of change of specific humidity in certain locations in the METROMEX area, and that local anthropogenic sources of moisture may contribute to the increase in moisture in the urban area at night. Another possible cause for the variations, especially in the rural areas, may be differences in type and amount of vegetative coverage. The type and amount of vegetative coverage would have an effect on evapotranspiration rates and thus the moisture rates. Ackerman (1971) found that variation in urban-rural differences in moisture in August may be at least partly attributable to reduced plant transpiration in the rural area.

Variation of Diurnal Mixing Ratio Cycles with Cloud Cover

The diurnal mixing ratio curves for FRM and ARC for three sky conditions described earlier appear in figure B-19. The general tendency for the curves at both sites is for increasing amplitude with decreasing sky cover. This trend of less variation about the mean with increasing cloud cover is similar to that noted in the temperature data.

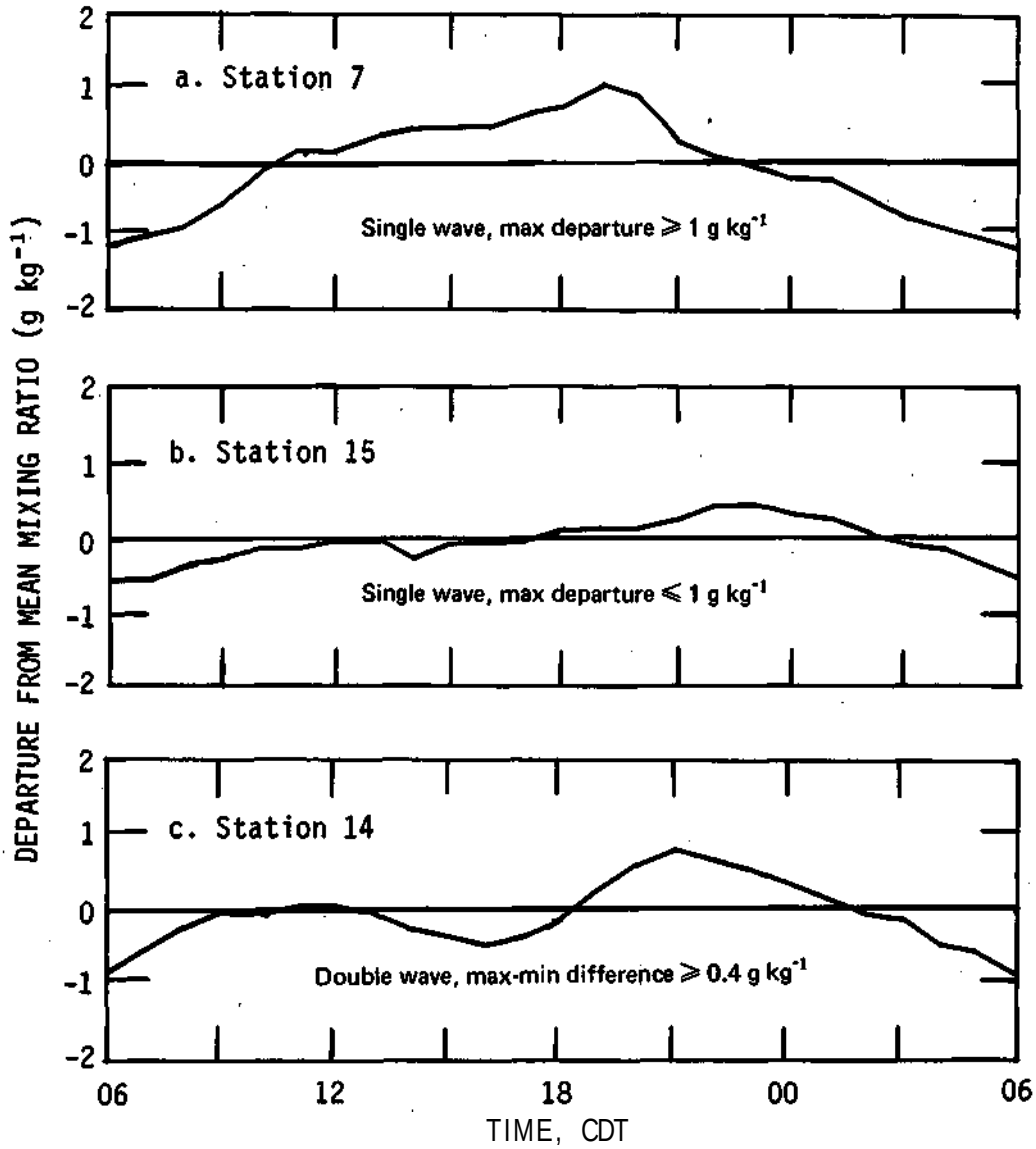

Figure B-18. Mixing ratio curves representative of three types of diurnal distributions

The diurnal mixing ratio curve for FRM (figure B-19a) for fair sky conditions is similar to the four mean curves for all conditions, but with larger amplitude. Lower mixing ratio values occur in the early morning and afternoon, and begin to increase approximately 2 hours before sunset. Maximum mixing ratio values occur about sunset, remaining fairly constant for 2 to 3 hours before decreasing at an average rate of 0.3 g kg^{-1} until sunrise, when the mixing ratio again increases.

Under partly cloudy and cloudy sky conditions, the FRM diurnal mixing ratio curves lose the characteristic shape of the mean diurnal curve for all conditions. The maximum mixing ratio values occur earlier in the day, decreasing during the nocturnal period. During the late morning and early afternoon, mixing ratio values with respect to the mean were approximately 1.0 g kg^{-1}

Table B-2. Hygrothermograph Sites According to Type of Diurnal Mixing Ratio Curve

Type 1	*Type 2*	*Type 3*
4	*6	*3
*7	9	5
8	10	12
18	11	14
21	13	*19
23	15	28
25	*16	48
43	*17	
47	20	
	22	
	24	
	26	
	*29	

** Denotes urban location*

Note: Type 1 = single wave with maximum departure ≥ 1.0 g kg^{-1}; type 2 = single wave with maximum departure ≤1.0 g kg^{-1}; and type 3 = double wave with difference between each maximum and minimum ≥ 0.4 g kg^{-1}.

greater than the values under fair sky conditions. The mean mixing ratio was also higher (15.3 g kg^{-1} versus 13.2 g kg^{-1} with fair skies), so in effect there is a very large difference in mixing ratios, on the order of 1.5 g kg^{-1}, between fair and partly cloudy sky conditions. This difference was also reflected in the remainder of the rural sites. On the average, the difference between the mean fair sky mixing ratio and the mean partly cloudy sky mixing ratio was 1.3 g kg^{-1}.

The differences are much less pronounced when a comparison of partly cloudy and cloudy conditions is made. Note in figure B-19a that the curves representing partly cloudy and cloudy conditions correspond closely, with the largest difference occurring from 1800 CDT to midnight. However, the average mixing ratio for cloudy sky conditions (16.1 g kg^{-1}) was greater than partly cloudy by 0.8 g kg^{-1} On the average, the mean mixing ratios for rural sites and partly cloudy skies were 0.4 g kg^{-1} greater than average mixing ratios for cloudy skies. On an areal average, the mean mixing ratio for the rural area was the same under both partly cloudy and cloudy sky conditions.

The same trends noted for FRM were also evident in the three ARC curves (figure B-19b). With fair skies, mixing ratio values with respect to the mean were less in the morning and afternoon hours, increasing to a maximum value around midnight after which it remains fairly steady until 1 to 2 hours before sunrise.

The curve for partly cloudy skies had less amplitude but still the same general configuration as the fair sky and 4-year summer mean curves. As with FRM, mean mixing ratio values increased to 15.3 g kg^{-1} under partly cloudy skies and to 15.6 g kg^{-1} under cloudy sky conditions from a value of 13.2 g kg^{-1} with fair skies. Whereas the mixing ratio decreases slightly from sunrise to mid-morning under fair skies, the mixing ratio under partly cloudy skies remains almost constant through the morning and afternoon. It begins a gradual rise about sunset until reaching a maximum at 0100 CDT. The mixing ratio then decreases until sunrise.

Mixing ratio values under cloudy skies are fairly constant throughout the day. The exception to this is at 1700 CDT, where there is a spike in the curve. Aside from this anomaly, the mixing ratio on cloudy days at ARC is 15.6 g kg^{-1}, 0.9 g kg^{-1} greater than on partly cloudy days.

The areal mean mixing ratio for the urban area and partly cloudy skies is 1.5 g kg^{-1} greater than the same mean for fair sky conditions. There is a negligible difference between the areal means for partly cloudy and cloudy sky conditions in the urban area.

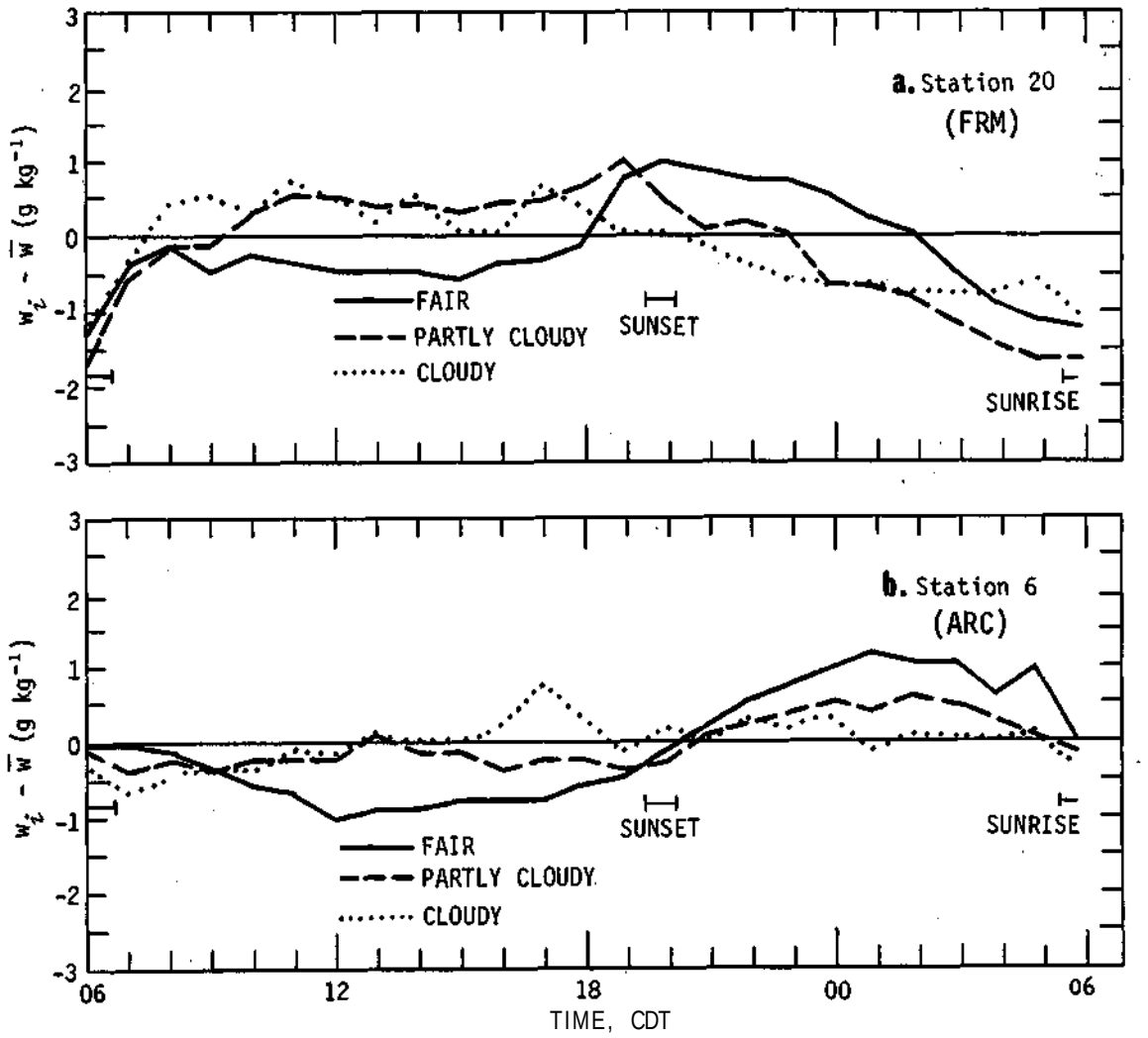

Figure B-19. FRM (rural) and ARC (urban) normalized diurnal mixing ratio curves for three sky conditions, 4-year average

Occurrence of the Urban Dry Island

Studies have indicated that the urban area is drier during the day and more moist at night relative to adjacent rural areas (Ackerman, 1971; Hage, 1975; Chandler, 1967). An investigation of this urban 'dry island' was included as part of this study. The mixing ratio data from the five areas in the research circle (see figure B-9) were used to calculate the strength of the urban dry island throughout the diurnal period. Areal means were computed in the same manner as for temperature. When an areal mean value was used to represent the urban and each of the four rural areas, the urban area displayed only a weak tendency to be drier than the rural areas. However, as Hage (1975) and others have reported, the largest and most important differences between the urban and rural areas occur on a diurnal basis.

The average diurnal mixing ratio difference wu - Wr for the 4-summer period appears in figure B-20. It can be seen from this figure that an urban dry island exists from approximately

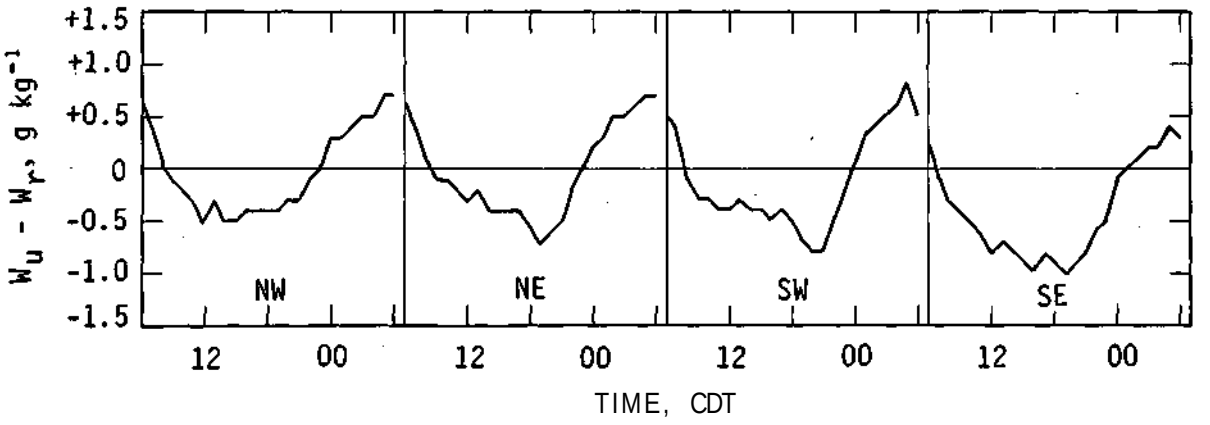

Figure B-20. Diurnal variation in the strength of the urban dry island with respect to four rural areas

0800 CDT until 0000 CDT. The dry island is strongest with respect to the SE rural quadrant, and weakest with respect to the NW rural quadrant. The dry island maintains its maximum strength (0.75 g kg^{-1}) just around sunset, and then weakens rapidly. Ackerman (1971) also reported that the urban-rural moisture difference decreases rapidly after sunrise. The difference then becomes negative but at a slightly slower rate about 1 hour past sunrise.

Variation in the Dry Island with Cloud Cover

The relationship between the intensity of the urban dry island and cloud cover is shown in figure B-21. It can be seen in this figure that the dry island decreases in intensity with increasing cloud cover. Cloud cover appears to have a strong effect on the intensity of the urban dry island, in contrast to the data presented by Ackerman (1971). However, it should be noted that the data used in this study were available from approximately 30 stations, whereas the comparison by Ackerman was made between two stations. Data presented previously in this section have shown that there can be wide variations in the moisture content even over a relatively small area. Under fair skies, the average maximum intensity of the urban dry island is 1.5 g kg^{-1}, decreasing to 0.9 g kg^{-1} under partly cloudy skies and to 0.5 g kg^{-1} under cloudy skies. Not only is the dry island much weaker under cloudy skies, but there are more variations in the intensity. Some of these variations may be due to rain in the area, and some may be due to the relatively small number of days (32) that were available for analysis.

SUMMARY AND CONCLUSIONS

An investigation of average urban and rural diurnal temperature cycles has shown that there are significant differences between the two. These differences also persist with various sky conditions, although to a lesser degree. The reasons behind these differences are not obvious, but there is strong evidence that the pollution layer over the city and the differences in the radiation balance between the urban and rural areas are important. Because it is the difference in the cooling rates at night that accounts for the formation of the urban heat island, the reasons behind

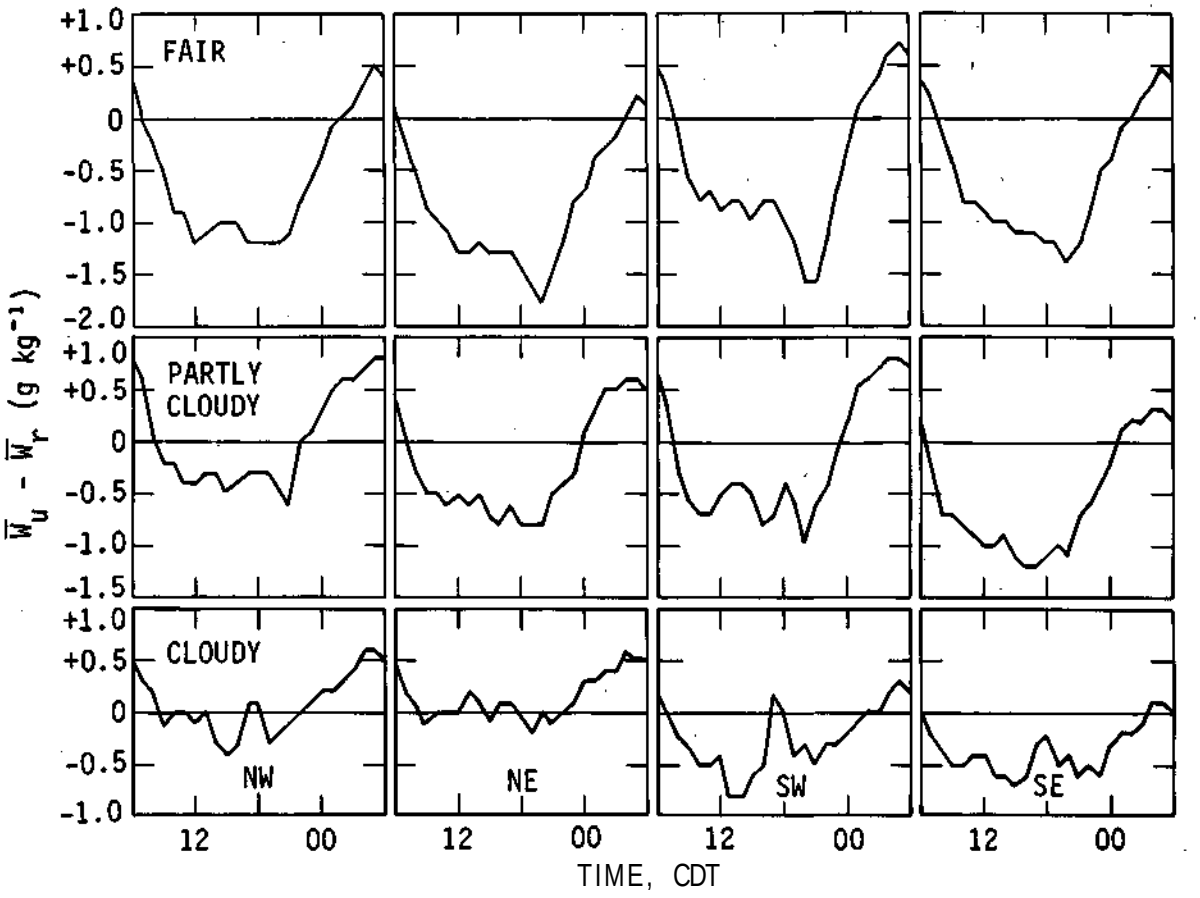

Figure B-21. Strength of urban dry island with respect to four rural quadrants as a function of time and sky condition

the diurnal heating and cooling rate differences are important to the understanding of the heat island dynamics. Comprehensive radiation measurements in both the urban and rural areas would contribute greatly to this understanding.

A study of the heat island as a function of the temperature difference between the urban area and four rural quadrants in the METROMEX research circle showed the urban heat island, on the average, persists throughout the entire day, although it is much weaker during the afternoon hours. The urban heat island was strongest with respect to the NW quadrant. During the afternoon hours, the heat island was weakest with respect to the SE and NE quadrants. The only time the urban area is cooler than the rural area is in the afternoon with fair skies. At this time the urban area is cooler by an average of 0.5° C. The strength of the heat island does not change substantially from days with fair skies to days with partly cloudy skies, but it does decrease about 0.9° C with cloudy skies from a value with fair skies of 1.7° C.

Although the moisture content of the air in the urban and rural areas varies more than the temperature, there are still definite patterns that can be discerned in the diurnal patterns of the mixing ratio. The urban mixing ratio curves vary less about the mean than the rural diurnal curves, but there is little else to distinguish between the two. Three types of diurnal mixing ratio curves were found, and the diurnal curves of the METROMEX data were classified according to these types.

The results indicated that the 'double wave' which had been previously reported to be characteristic of a rural airport in a dry continental climate is not predominant. Single wave patterns in which there is only one distinct maximum characterize most of the data in the METROMEX research area. There appears to be little correlation between the location of a site (urban or rural) and the diurnal pattern.

The daily variation in mixing ratio at a site is affected by cloud cover, the variations about the mean mixing ratio becoming less with increasing cloud cover. However, the mean mixing ratios increase by 1.5 g kg^{-1} from days with fair skies to days with partly cloudy skies in the urban area and 1.3 g kg^{-1} in the rural area. With cloudy skies, the diurnal curves at both locations lose the characteristic pattern of the 4-year mean curve.

An urban 'dry island' has been shown to exist for a large part of the day in the St. Louis area. It develops about 2 hours after sunrise, maximizing about sunset. The intensity of this dry island decreases with increasing cloud cover. However, considering that the dry island is still strong with partly cloudy sky conditions, it is likely that storms moving through St. Louis urban area would entrain air contributing to their weakening. The diurnal variations of mixing ratio in the urban and rural areas may be of assistance in determining what effect the temperature and moisture differences have on precipitation activity.

AVERAGE DEW POINTS

Greg Dzurisin

In an effort to help determine how possible urban conditions alter precipitation mechanisms, the mesoscale surface moisture field was investigated. Dew point temperature data from several weather stations in the METROMEX research circle were analyzed for the summer months of June, July, and August, 1972 through 1975. The urban heat island has been defined and recognized at many cities for many years, but only recently have there been attempts to measure the humidity field within urban regions (Ackerman, 1971; Dirks, 1974; Landsberg, 1975).

Ackerman (1971) found a slight increase in the relative humidity near the center of Chicago. Other researchers (Dirks, 1974; Landsberg, 1975; Sisterson, 1975) found urban relative humidity, especially in mid-afternoon, to be less than the relative humidity in surrounding rural regions. Dirks found the urban heat island in St. Louis, along with its corresponding reduced moisture content, to extend to heights exceeding 1 km (under certain conditions). This is indicative of no increase in moisture in the low levels of the atmosphere over the urban region due to moisture emissions from industrial sources. Sisterson (1975) concludes that the largest source of low level (or surface) water vapor in the summer is from evapotranspiration. He states that industrial emissions as a moisture source were insignificant when considered on the mesoscale (based on St. Louis data). He further states that precipitation is a significant water vapor sink, while absorption by hygroscopic aerosols and consumption in photo-chemical reactions are insignificant water vapor sinks.

This climatological analysis of the surface dew point data at St. Louis was done on a seasonal, monthly, and diurnal basis, with attention to varying weather conditions. Mesoscale analyses of various patterns were made for all dew point classifications because Kopec (1973) demonstrates that dew point patterns defined on the microscale do not follow the general mesoscale pattern. He suggests that eddy diffusion and frictional currents may ultimately affect dew points on the microscale.

Dew point temperatures (hereafter referred to as 'dew points') were calculated with the relative humidity from the hygrothermograph charts of the Water Survey weather stations in the METROMEX research circle plus the directly measured dew points from Lambert International Airport in St. Louis.

Analysis of primary patterns started with means calculated for each pattern. Then the station data were plotted as departures from the mean. A negative value at a data point (station) indicates the dew point there was below the mean, while a positive value indicates a departure above the mean. In such a pattern, negative values indicate a drier than average area condition, and a positive value indicates a moister than average area condition.

To show gradients more clearly, a table was compiled from each dew point pattern (table B-3). Station 6 (Arch) shown in figure B-22 was used as the reference station and all other stations were used as the variables. A positive value in table B-3 indicates a dew point departure that is higher than the Arch (thus indicating a moister environment), and a negative value indicates a dew point departure that is lower than the Arch (a drier environment). The stations were chosen to show variances from hills to bottomlands and urban to rural environments.

In order to illustrate the strength or weaknesses of the Arch to site gradients, the lowest and highest departures are listed in table B-3. The stations used were 6-17 East Metro, 6-16

Table B-3. 1972-1975 Dew Point Gradients and Means

	6-17 East Metro	6-9 Alton-Wood River	6-10 Northwest Bottomland	6-20 Southeast Rural	6-16 Forest Park	6-14 Far West Rural	6-23 Southwest Hills	Lowest departure	Highest departure
June 1972-1975	+0.6	+0.1	+0.2	+1.6	+0.1	-0.1	+0.2	-0.5	+1.2
Mean	17.1								
July 1972-1975	+0.2	-0.5	+0.2	+0.1	-1.2	-0.2	-0.7	-1.9	+0.9
Mean	19.2								
August 1972-1975	+0.5	+0.3	0.0	+0.2	-0.6	-0.1	+0.1	-1.4	+1.2
Mean	19.3								
Summer 1972-1975	+0.1	0.0	+0.2	+0.5	-0.5	-0.1	-0.2	-1.1	+1.1
Mean	18.8								
Summer 1972	+0.5	-0.4	-1.0	-0.2	-1.2	-0.6	-1.1	-1.1	+1.2
Mean	18.5								
Summer 1973	+0.7	-0.3	+1.0	+0.7	-0.1	+0.6	+0.1	-0.8	+0.7
Mean	18.8								
Summer 1974	+0.6	+0.5	+1.1	+0.8	-0.1	+0.2	-0.2	-0.9	+0.7
Mean	18.6								
Summer 1975	+0.1	+0.2	-0.5	+0.5	-0.7	-0.8	+0.2	-0.8	+0.6
Mean	19.2								
Summer 0300 CDT	+0.5	-0.4	-0.8	-0.6	-0.4	-0.6	-2.0	-0.9	+1.6
Mean	18.4								
Summer 0600 CDT	+0.4	-0.7	-1.2	-0.7	-0.3	-0.9	-2.1	-1.0	+1.1
Mean	18.0								
Summer 0900 CDT	+0.5	+0.2	+0.1	+0.6	-0.2	+0.1	+0.4	-0.8	+1.1
Mean	18.7								
Summer 1200 CDT	+0.3	+0.2	+0.8	+1.1	-0.3	+0.3	+0.5	-1.8	+1.0
Mean	18.8								
Summer 1500 CDT	+0.2	+0.2	+0.6	+0.9	-1.1	-0.2	+0.4	-1.7	+1.4
Mean	18.6								
Summer 1800 CDT	+0.1	+0.3	+0.7	+0.8	-1.0	-0.1	+0.6	-1.7	+1.4
Mean	18.8								
Summer 2100 CDT	+0.7	+0.5	+0.9	+1.0	-0.7	+0.6	+1.1	-1.4	+1.7
Mean	19.4								
Summer 2400 CDT	+0.7	-0.1	-0.1	+0.2	-0.5	-0.1	-0.8	-0.8	+1.2
Mean	19.1								
Clear 1972-1975	+0.4	-0.2	-0.2	+0.1	-0.6	-0.4	-0.3	-0.9	+1.6
Mean	17.7								
Partly cloudy 1972-1975	+0.4	+0.3	+0.1	+0.5	-0.6	+0.1	-0.3	-0.8	+1.1
Mean	19.1								
Cloudy 1972-1975	+0.4	0.0	+0.1	+0.6	-0.6	-0.1	-0.4	-0.8	+1.2
Mean	19.6								
North 1972-1975	0.0	-0.9	-0.7	-0.6	-0.9	-1.1	-0.6	-0.9	+1.2
Mean	18.9								
Northeast 1972-1975	+0.7	+0.1	-0.4	+0.4	-0.5	-0.3	-0.1	-1.1	+1.5
Mean	19.3								
East 1972-1975	-0.4	-0.3	-0.7	+0.4	-1.5	-0.4	-0.9	-1.2	+1.1
Mean	17.8								

Concluded on next page

Table B-3. Concluded

	6-17 East Metro	6-9 Alton-Wood River	6-10 North-west Bottom-land	6-20 South-east Rural	6-16 Forest Park	6-14 Far West Rural	6-23 South-west Hills	Lowest departure	Highest departure
Southeast 1972-1975	+0.6	-0.2	-0.1	+0.2	-0.9	-0.5	-0.3	-1.0	+1.6
Mean	18.4								
South 1972-1975	+0.1	-0.1	+0.6	+0.2	-0.8	-0.1	-0.5	-0.7	+0.8
Mean	19.3								
Southwest 1972-1975	+0.5	-0.1	+0.4	+0.6	-0.6	+0.1	0.0	-0.8	+1.1
Mean	19.4								
West 1972-1975	+2.4	+1.4	+1.1	+2.5	+0.9	+0.5	+1.3	-1.9	+1.1
Mean	18.4								
Northwest 1972-1975	0.0	-0.2	-0.2	-0.1	-1.2	-0.4	-0.8	-1.2	+1.7
Mean	17.4								
0-3 knots 1500 CDT 1972-1975	+0.1	+0.5	+0.6	+0.7	+0.1	-0.2	+0.8	-1.1	+1.8
Mean	18.6								
4-7 knots 1500 CDT 1972-1975	0.0	0.0	+1.2	+1.5	-0.9	0.0	+0.5	-1.5	+1.0
Mean	19.1								

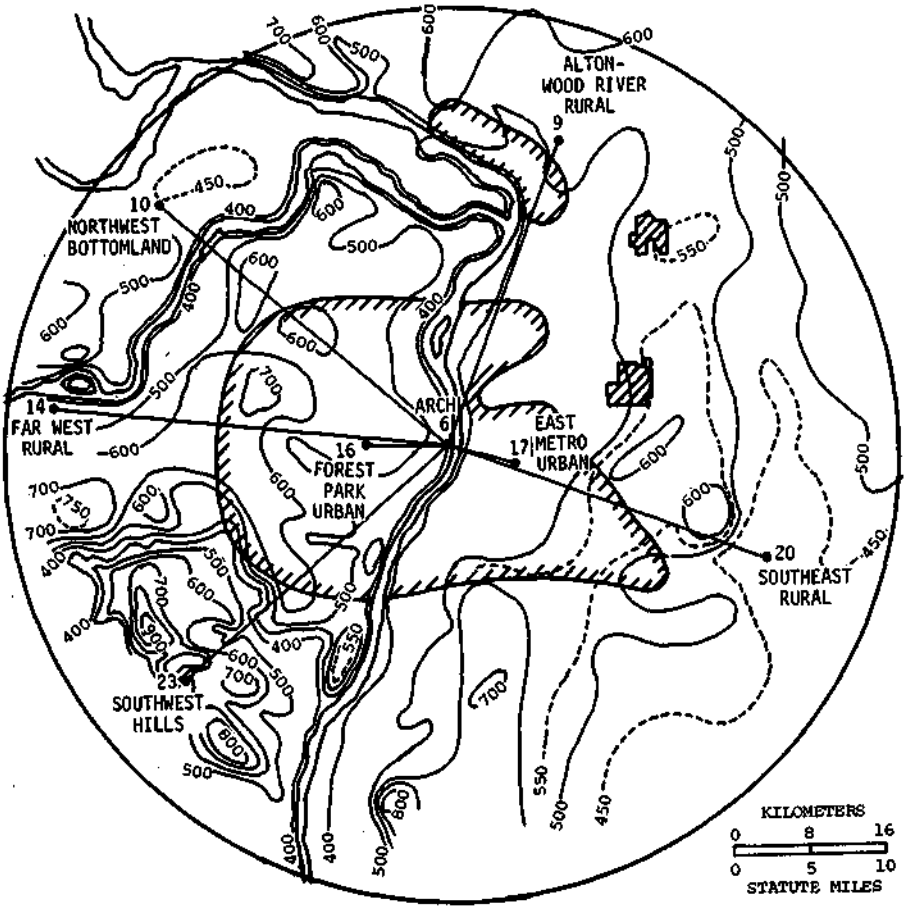

Figure B-22. Location of dew point gradient sites

Forest Park, 6-10 Northwest Bottomland, *6-9* Alton-Wood River, 6-20 Southeast Rural, 6-23 Southwest Hills, and 6-14 the Far West Rural. The dew point means also are listed in the table for each map that was plotted and analyzed.

Seasonal and Monthly Patterns

The summer patterns (June, July, August) for 1972 through 1975 were analyzed. The most encompassing use of data was the combination of the four summers. Comparisons were made between the mean 4-summer pattern and the patterns of the four June, July, and August months and the summer of each year.

The 4-summer pattern (figure B-23a) shows moist areas centered in the eastern part of the NW bottomlands, the southeast rural area, and slightly over the western edge of the circle. There was a general dry area over the metropolitan area.

The 3-year average dew point deviation pattern for June (data for June 1974 was missing) shown in figure B-23b was similar to the 4-summer pattern. There were no major differences in the centers of the moist and dry areas. The 4-year average July pattern (figure B-23c) was also similar to the summer pattern. However, the moist area in the bottomlands was weaker and was shifted to the west. The moist area in the southeast extended farther north to Collinsville, and a weak dry region appeared in the extreme south over Waterloo. The general dry area through the central urban region was now in a SW-NE orientation rather than E-W. The dry area centered in the metropolitan area was strengthened. The 4-year average August pattern (tigure B-23d) was almost identical to the summer pattern. The only difference was the disappearance of the small moist area in the far west part of the circle.

Since precipitation is an important water vapor sink, rainfall patterns corresponding to the dew point patterns were compared. The 4-year summer pattern of rainfall (figure B-24a) expressed as departures from the network mean, shows above mean rainfall amounts in the eastern half of the bottomlands and east of Waterloo which corresponds well with the moister dew point patterns. The below mean rainfall in the western urban area correlates well with the drier dew point values there. However, the relatively high rainfall amounts in other areas east of the Mississippi River are inversely related with the dry dew point values in these areas. The 4-year monthly patterns of rainfall (figure B-24b-d) were similar to the 4-year summer pattern of rainfall. Thus, these maps corresponded reasonably well with the 4-year monthly dew point patterns.

The summer dew point patterns (figure B-25) were quite different in some regions, from the 4-summer pattern (figure B-23a). The corresponding rainfall patterns also changed from year to year (figure B-26). In 1972 (figure B-25a) the biggest change from the 4-year pattern was the southward shift of the moist area over the eastern part of the bottomlands. The moist area was now centered between Wood River and Granite City and extended into the northeastern urban area. The eastern bottomlands were now close to the network mean. The 1972 rainfall pattern (figure B-26a) correlated well with the 1972 dew point pattern (figure B-25a). A lower than mean rainfall area was centered in the western urban area and higher than mean rainfall occurred in the Edwardsville-Collinsville-Belleville area. However, one area that did not correspond was that with lower than mean rainfall east of Waterloo where it was moist.

The 1973 summer dew point pattern (figure B-25b) did not resemble the 4-summer pattern. The only feature that remained the same was the dry area over the urban region. Otherwise, a dry area was centered east of Waterloo and another to the northeast of Edwardsville. A moist area occurred in the central bottomland area. The rest of the network area was slightly moist. The

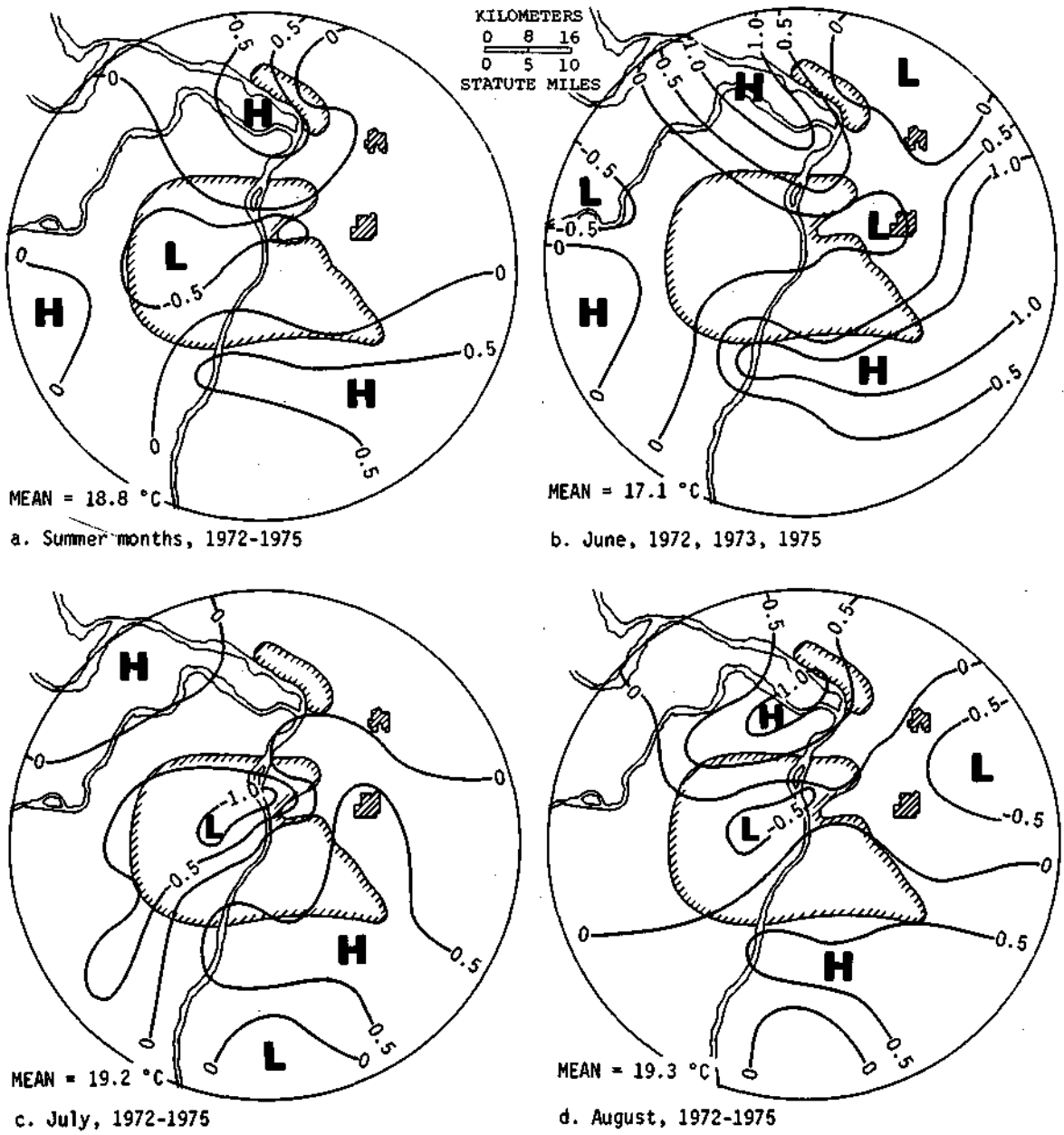

Figure B-23. Four-summer dew point patterns

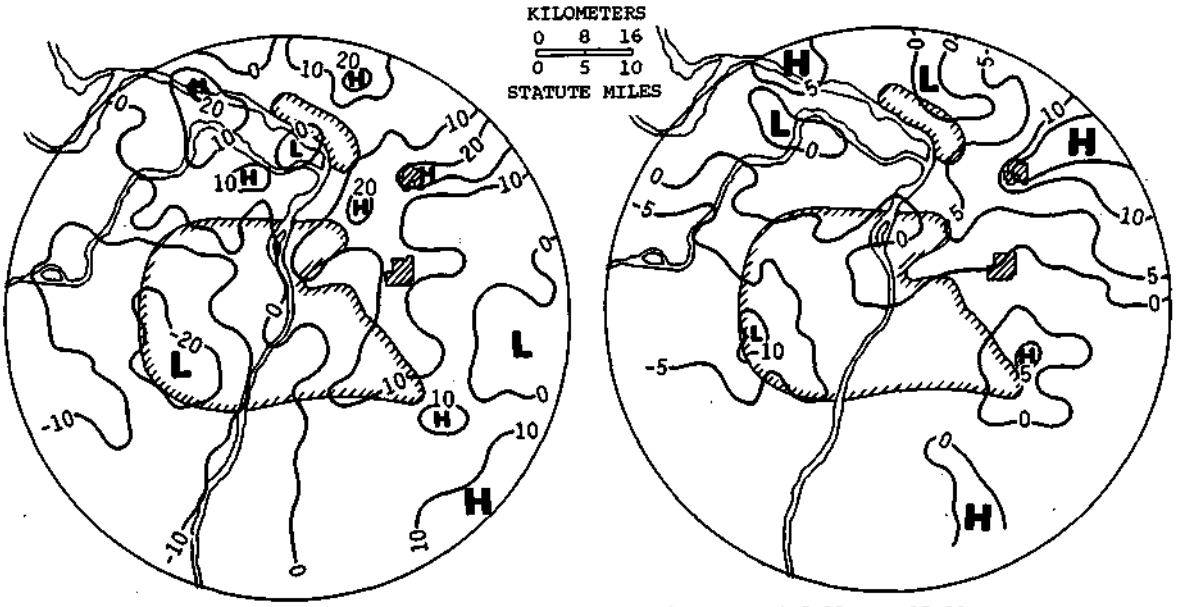

Network mean rainfall = 96.44 cm
Avg pos dev from mean = 2.99
Avg neg dev from mean = -3.65
Standard deviation = 11.07
Coefficient of variance = 11.50

a. Summer months, 1972-1975

Network mean rainfall = 25.30 cm
Avg pos dev from mean = 1.68
Avg neg dev from mean = -1.30
Standard deviation = 5.11
Coefficient of variance = 20.17

b. June, 1972-1975

Network mean rainfall = 29.18 cm
Avg pos dev from mean = 1.99
Avg neg dev from mean = -1.56
Standard deviation = 5.44
Coefficient of variance = 18.66

c. July, 1972-1975

Network mean rainfall = 41.99 cm
Avg pos dev from mean = 2.05
Avg neg dev from mean = -1.80
Standard deviation = 6.17
Coefficient of variance = 14.69

d. August, 1972-1975

Figure B-24. Four-summer rainfall patterns

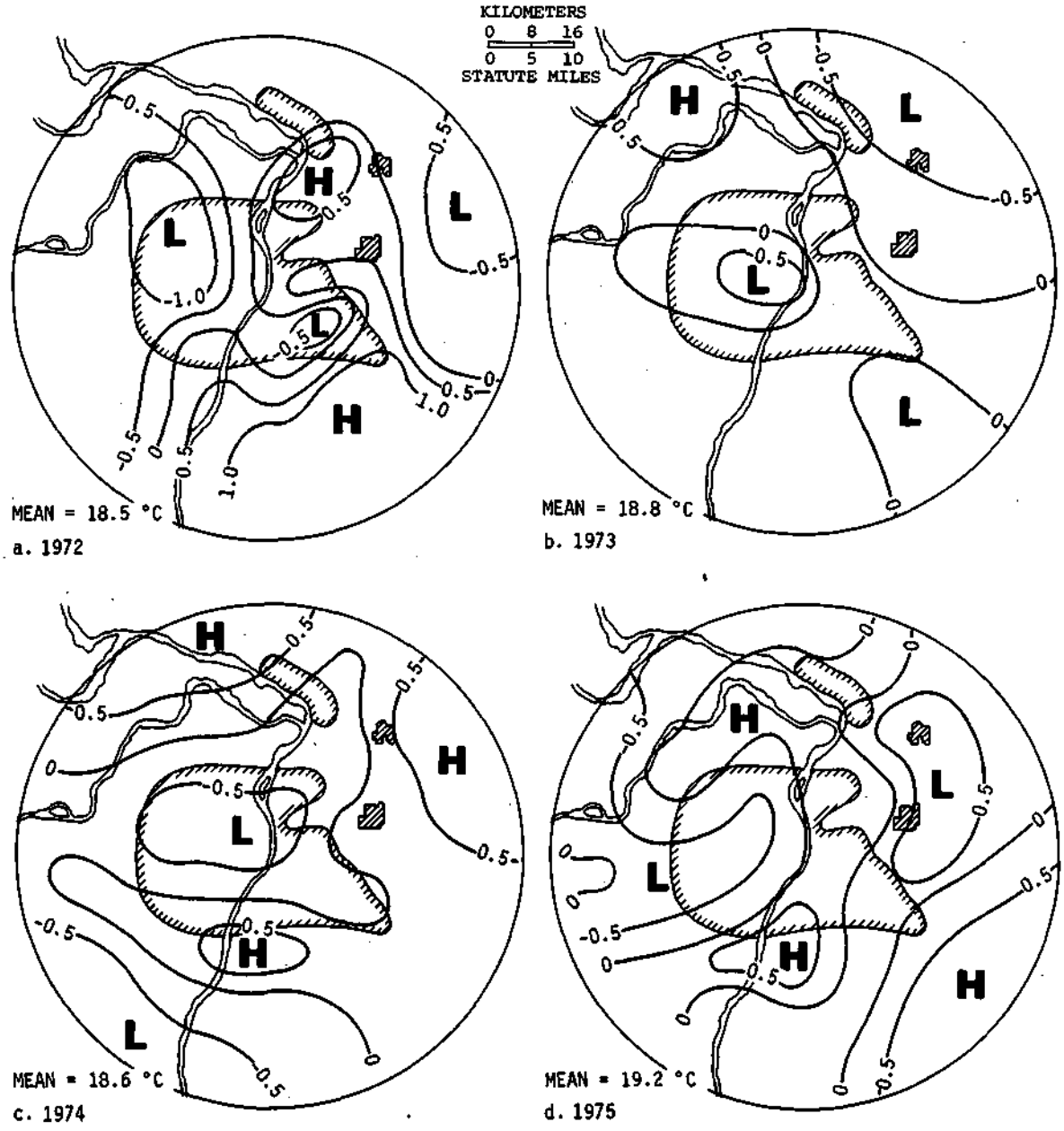

Figure B-25. Summer dew point patterns

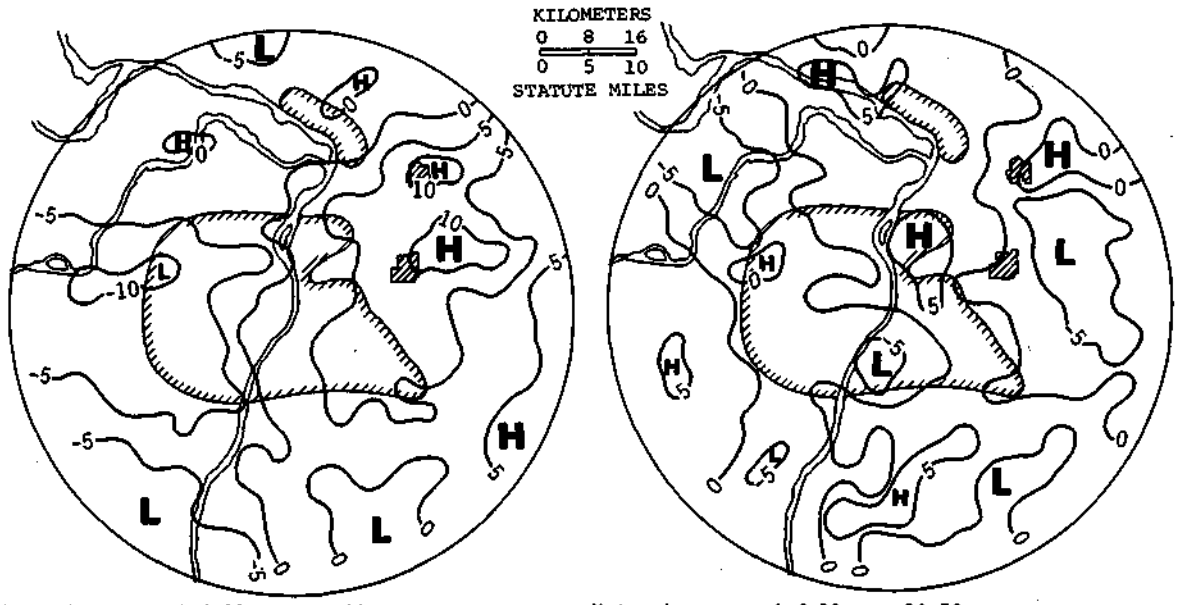

Network mean rainfall = 19.43 cm
Avg pos dev from mean = 2.15
Avg neg dev from mean = -1.06
Standard deviation = 5.59
Coefficient of variance = 28.73

a. 1972

Network mean rainfall = 24.59 cm
Avg pos dev from mean = 1.24
Avg neg dev from mean = -1.23
Standard deviation = 4.01
Coefficient of variance = 16.31

b. 1973

Network mean rainfall = 23.52 cm
Avg pos dev from mean = 1.85
Avg neg dev from mean = -1.67
Standard deviation = 5.31
Coefficient of variance = 22.56

c. 1974

Network mean rainfall = 28.91 cm
Avg pos dev from mean = 1.34
Avg neg dev from mean = -1.29
Standard deviation = 4.27
Coefficient of variance = 14.75

d. 1975

Figure B-26. Summer rainfall patterns

summer rainfall map of 1973 (figure B-26b) was also very dissimilar to the 4-summer rainfall pattern (figure B-24a) and did not correlate too well with the 1973 summer dew point pattern (figure B-25b). Above mean rainfall related to the slightly moist dew point areas, and lower than mean rainfall was located to the east of the Collinsville-Belleville area which corresponded to the drier area there. No relationship existed in the low dew point area west in the urban area where the rainfall was near the summer average, nor in the central bottomland area where the rainfall was below the summer mean.

The 1974 summer dew point pattern (figure B-25c) was not significantly different from the four-summer pattern. Moist air covered the entire bottomlands, not just the eastern half of the bottomlands as in the 4-year map. Also a moist area located north and east of Waterloo extended farther north to include Edwardsville and Collinsville. A dry area was more pronounced in the southwest hills and still enveloped the entire metropolitan area. The 1974 summer rainfall map (figure B-26c) had a good relationship to the dew point map. Above mean rainfall was observed over the Collinsville-Edwardsville area and the bottomlands where above mean dew points existed. Below mean rainfall was over the urban area and the southwest hills and low dew points existed there. However, below mean rainfall to the north and east of Waterloo did not correlate with the higher dew points there.

The 1975 dew point patterns (figure B-25d) were different from the 4-summer pattern. A slightly moist area was over the eastern urban area and extended southwest to the eastern part of the hills. The drier area over Collinsville and Edwardsville extended south to include Belleville and Waterloo. Features which remained the same were moist regions over the eastern part of the bottomlands and to the east of Waterloo, and a dry region over the western urban area. The 1975 summer rainfall pattern (figure B-26d) did not relate well with the 1975 summer dew point pattern. The only areas that related well were the below mean rainfall over the western urban region and hills and the above mean rainfall in the eastern half of the southwest hills and the eastern bottomlands. Otherwise, above mean rainfall was evident in most areas east of the Mississippi River.

Diurnal Variations

The 4-summer dew point patterns were developed for various times of the day. Values for every 3 hours were considered adequate and patterns for 0300, 0600, 0900, 1200, 1500, 1800, 2100, and 2400 CDT were drawn. An important feature revealed in these eight period patterns (figure B-27) was the change from negative dew point departures over the urban region (0900 through 2400) to positive values during the hours of 0300 and 0600 CDT. Also shown was the change from positive to negative values in the rural regions during those time periods. One cause of this reversal during the early morning hours is dewfall, according to Ackerman (1971). The condensation of water on vegetation in the rural areas permits the dew points to lower. There is relatively less dewfall in the city because of warmer temperatures and lesser vegetation. The 4-year patterns for 0300 and 0600 CDT show a north-south moist area extending along the river from Alton to the southern urban area. Another moist area was centered between Waterloo and Belleville. Also there was a slightly moist region extending westward to the edge of the research circle between the Meramec and Missouri Rivers. The dry areas were centered over Collinsville and east to the circle's edge, over the bottomlands, and over the southwest hills.

At 0900 CDT a dry area appeared over the western and northern urban areas extending northwest into the bottomlands, and a moist area was centered over Alton extending south to Granite City. Another moist region was over the southwest hills and still another was centered between Belleville and Waterloo.

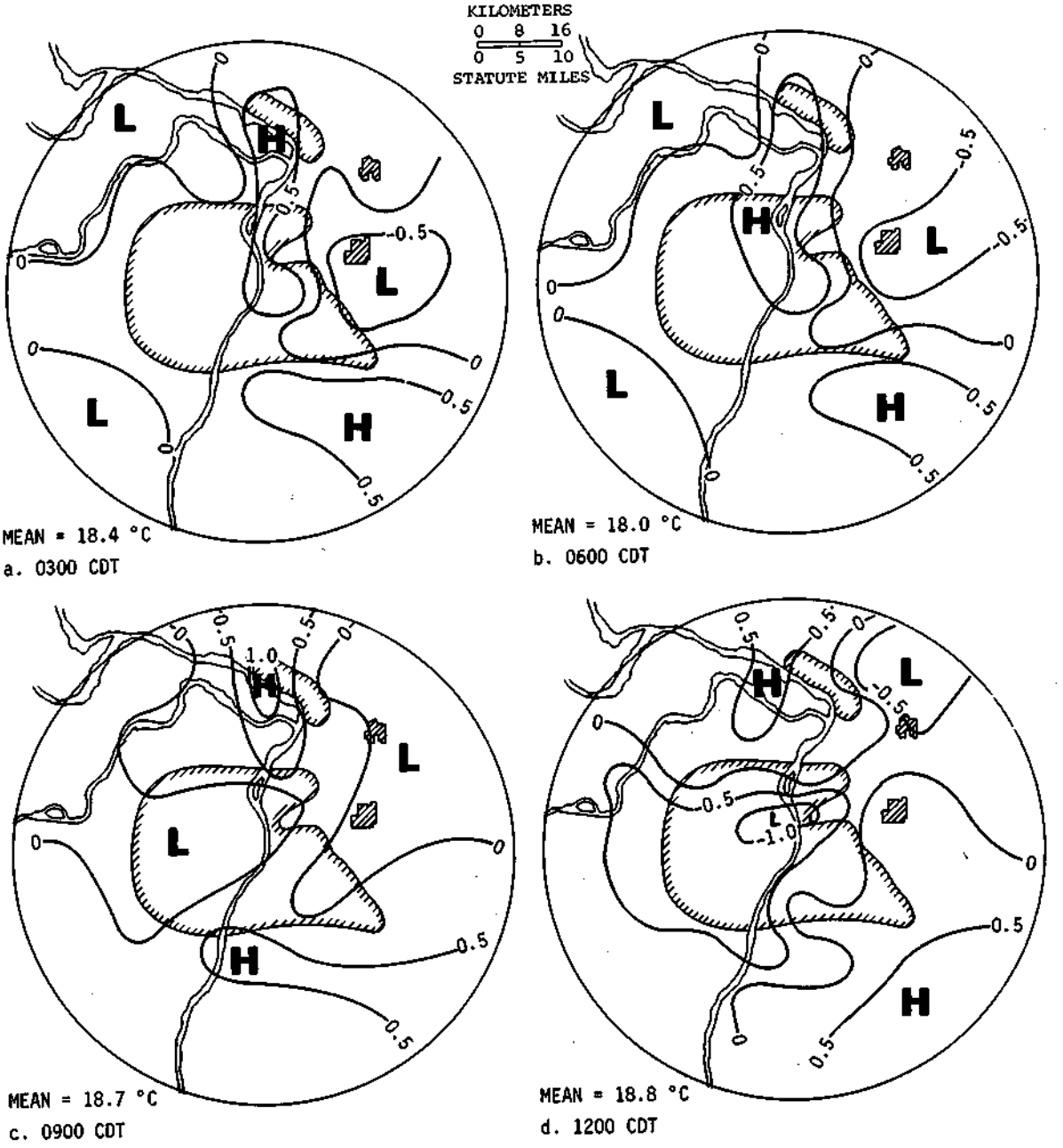

Figure B-27. Four-summer dew point patterns for selected hours

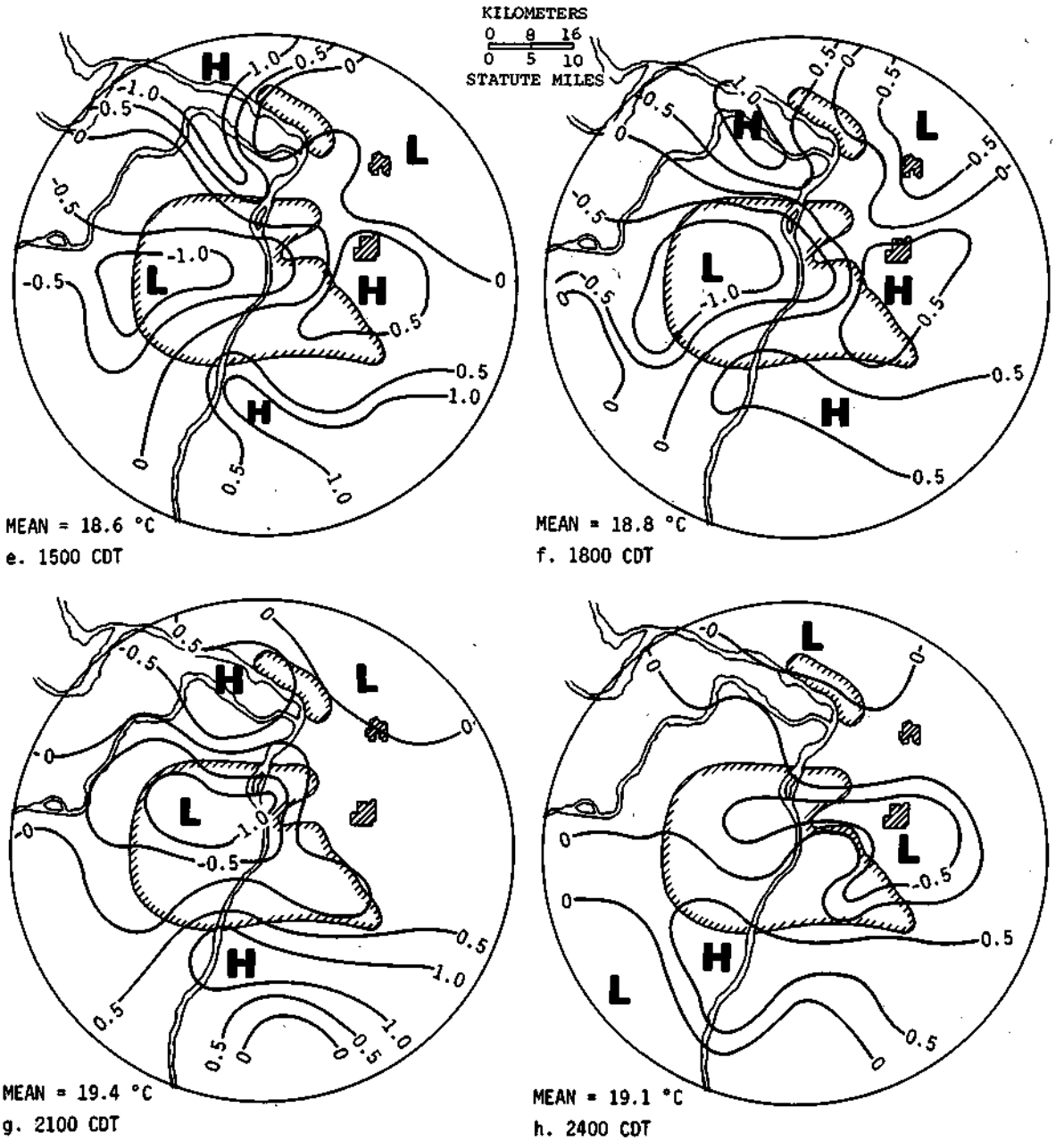

Figure B-27. Concluded

This midmorning pattern remained almost the same through the afternoon and evening hours (1200-2100 CDT). At 2400 CDT the transition of the moist and dry dew point areas began to reverse from the rural to the urban areas. A moist area was situated in the southeastern urban region and another between Belleville and Waterloo extending to the western edge of the circle. A slightly moist region existed in the eastern bottomlands through Edwardsville and east to the circle's edge. A dry area was centered over the Collinsville-Granite City area and west-northwest to the western half of the bottomlands.

Cloud Cover and Dew Points

Daily sky cover for the area was determined by averaging the hourly sky conditions measured at Lambert Field and Scott AFB (see figure B-22) for the entire day from midnight to midnight. The sky cover was given in tenths; 0 to 0.3 indicated a clear sky, 0.4 to 0.7 cover was a partly cloudy sky, and 0.8 to 1.0 indicated a cloudy sky. The two station values were then combined to get one area sky condition per day. The sky cover values sometimes varied greatly between the different localities. However, on most days the two reporting stations were similar.

The 4-summer dew point patterns for clear, partly cloudy, and cloudy days (figure B-28) were very similar in relation to one another and in relation to the 4-summer pattern. This suggests that cloud cover had little or no major effect on the general patterns of dew point. Table B-4 lists the percent of clear, partly cloudy, and cloudy days for each year and for the 4-summer period. Also listed for each year is the percentage of clear, partly cloudy, and cloudy days on which rain occurred in the METROMEX research circle. The 4-summer values reveal that 80% of all rain days occurred on cloudy and partly cloudy days. This illustrates the point that sky cover had little or no effect on the dew point patterns. Even though the majority of rain days occurred on cloudy and partly cloudy days, the dew point pattern on clear days was similar to that when it was cloudier. Thus, rain, a water vapor sink, did not show any difference on cloudy, partly cloudy, or clear days.

Wind Direction

There were six recording wind sets in use from 1972 through 1975 and these were located at stations 0, 4, 5, 9,14, and 26 (figure B-29). Data from these plus data from stations 29 and 30 (Lambert Field and Scott AFB) were used to study relationships between winds and dew points.

The wind directions were grouped into eight divisions (see figure B-29) north was 337 to 21° , northeast 22 to 66° , east 67 to 111^0, southeast 112 to 156° , south 157 to 201° , southwest 202 to 246° , west 247 to 291° , and northwest 292 to 3 36° . The north division included the Alton-Wood River area; the northeast division included Edwardsville and most of Granite City. Collinsville and most of East St. Louis were in the east division. Belleville and Centerville were in the southeast division and Waterloo in the south division. The northwest division included St. Charles. St. Louis spanned the entire westerly divisions.

A prevailing wind direction was assigned to each day of June, July, and August from 1972 through 1975. June 1974 data were missing. The daily prevailing wind direction was determined by the highest hourly frequency shown by all eight stations. Ties were broken by choosing the most frequent wind direction from each individual station. There was only one calm day.

Although a frontal passage at any given station may have meant the prevailing wind direction later in that day was somewhat unrepresentative, it must be remembered that the prevailing wind for the METROMEX research circle was the *average* wind direction for the *entire day*.

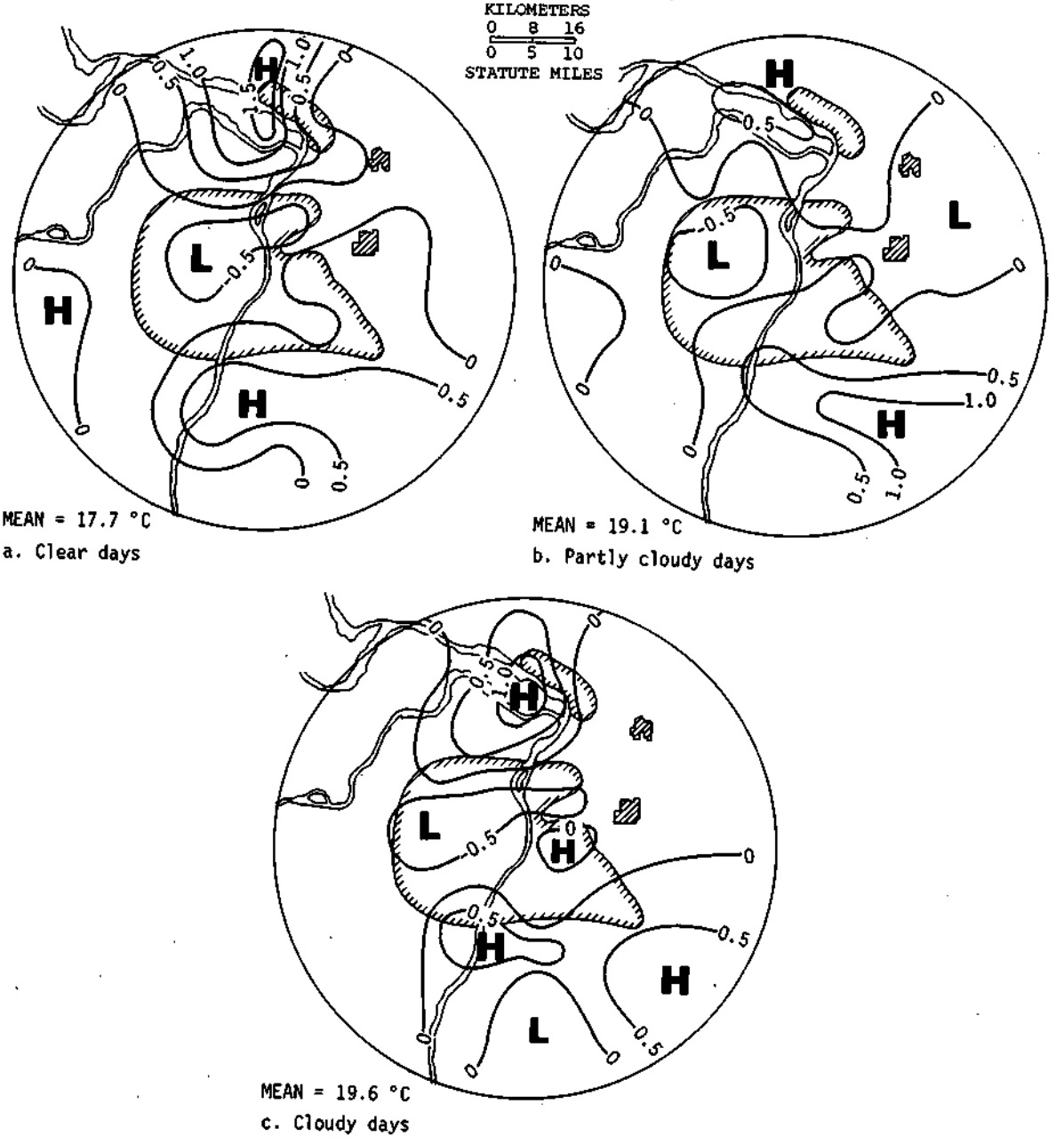

Figure B-28. Four-summer dew point patterns for clear, partly cloudy, and cloudy days

Table B-4. Percent of Clear, Partly Cloudy, and Cloudy Days

	Clear	*Partly cloudy*	*Cloudy*
1972 summer average	24	52	24
1972 MMX storms	11	46	43
1973 summer average	34	42	24
1973 MMX storms	10	45	45
1974 summer average	34	38	28
1974 MMX storms	13	40	47
1975 summer average	34	50	16
1975 MMX storms	05	65	30
1972-1975 summer average	31	46	23
1972-1975 MMX storms	10	48	42

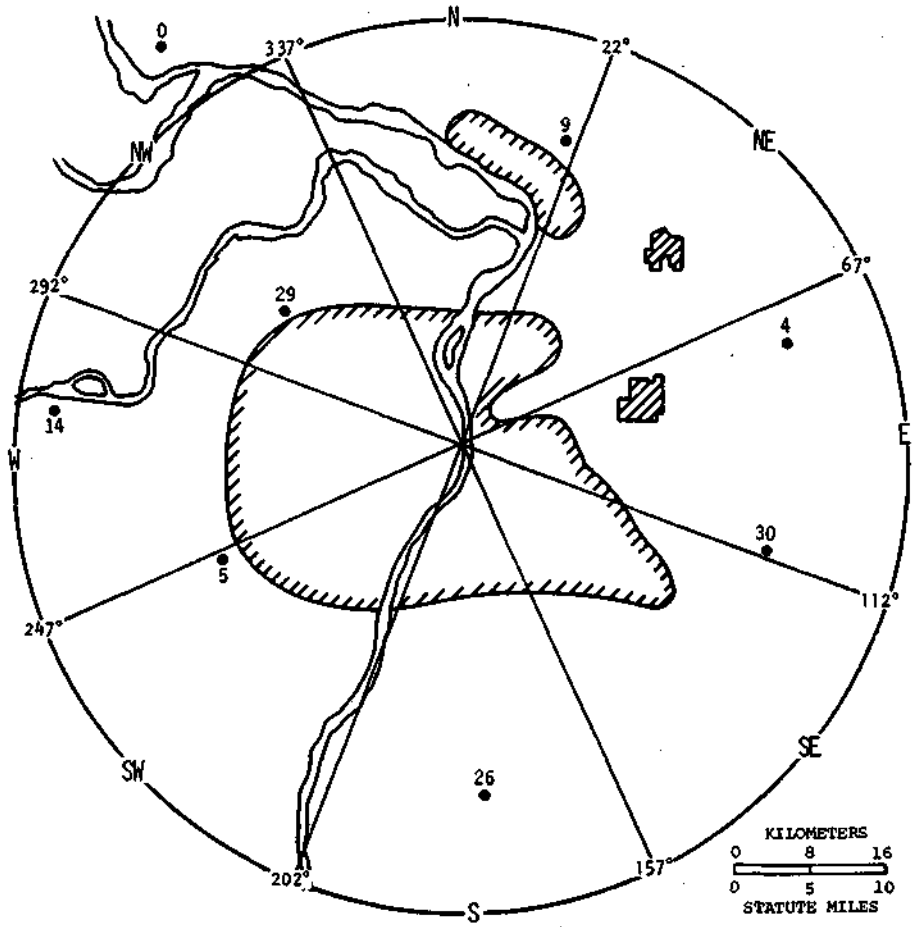

Figure B-29. Wind set locations and wind direction divisions

The 4-year patterns of dew point based on classification by the wind direction show some relationship at least in certain wind directions (figure B-30). Each direction map was referenced to the 4-summer dew point pattern (figure B-23a). The north wind pattern (figure B-30a) shows a wind influence on the dew point pattern. The moist area over the bottomlands extends southward to include the northeastern urban area. Thus, moist air was pushed south into the urban area. However, the remainder of the north pattern is the same as the 4-summer map. The northeast wind and dew point pattern (figure B-30b) shows a minor change from the 4-summer map. The moist area in the southeast near Waterloo extends farther north to cover the southeast urban area and Collinsville. However, this cannot be attributed to the northeast wind direction.

The east wind pattern (figure B-30c) shows some influence. The moist area in the eastern part of the bottomlands now extends southwest along the Missouri River to the other moist area located in the far west rural area. A moist area enlarged to cover the southern half of the area east of the Mississippi River. Moister air could have been moved into the eastern part of the research circle because of more evapotranspiration to the east of the research circle.

Like the northeast pattern, the southeast pattern (figure B-30d) shows little difference from the 4-summer pattern. A small change is the moist pocket extending into the southeast corner of the urban area, but this change does not reflect the southeast winds.

The south winds (figure B-30e) do show an influence on the dew point patterns because 25% of all 4-summer winds were from the south. The moist area in the southeast now reaches farther north to include the southeast half of the urban area. A moist area also covers the entire bottomland area. The southwest winds (figure B-3of) also show an influence on the dew point pattern. The dry region in the western urban area is pushed north to cover the eastern bottomlands. The moist area in the southeast is also pushed north to the Wood River area to include the eastern third of the urban area. The other features remained the same.

The west winds (figure B-30g) showed only a small influence on the dew point pattern. A dry area was squeezed between the moist area in the eastern part of the bottomlands. This is an extension of the dry area from the western bottomlands, possibly due to the west winds. The usual moist area in the far western rural area is absent on this map. The dew point pattern associated with the northwest winds (figure B-30h) shows some influence. The moist area in the eastern half of the bottomlands extends east and southeast to the edge of the research circle. This area includes the Edwardsville area and the southeast part of the urban area. The moist area also extends to the western half of the bottomlands. The remainder of the map is the same as the 4-summer map.

Table B-5 lists the percentage and frequency of winds from each direction and the average wind speed. Clearly, the southerly component (SW, S, SE) was dominant, accounting for 58% of the days. Table B-6 lists the number of rain storms that occurred within the METROMEX circle according to the prevailing wind direction for those days. These show that winds from the southerly component were evident on 73% of the days when rain occurred, and a south wind occurred on 30% of these days. Hence, mixing explains why the gradient of the dew point pattern associated with the south wind is so weak -0.7 to +0.8 (see table B-3).

The dew point temperature mean, when stratified according to wind direction, showed that moistest conditions existed when the winds were from the southwest and the driest conditions existed when the winds from the northwest, 19.4° C and a 17.4° C dew point mean, respectively (table B-3).

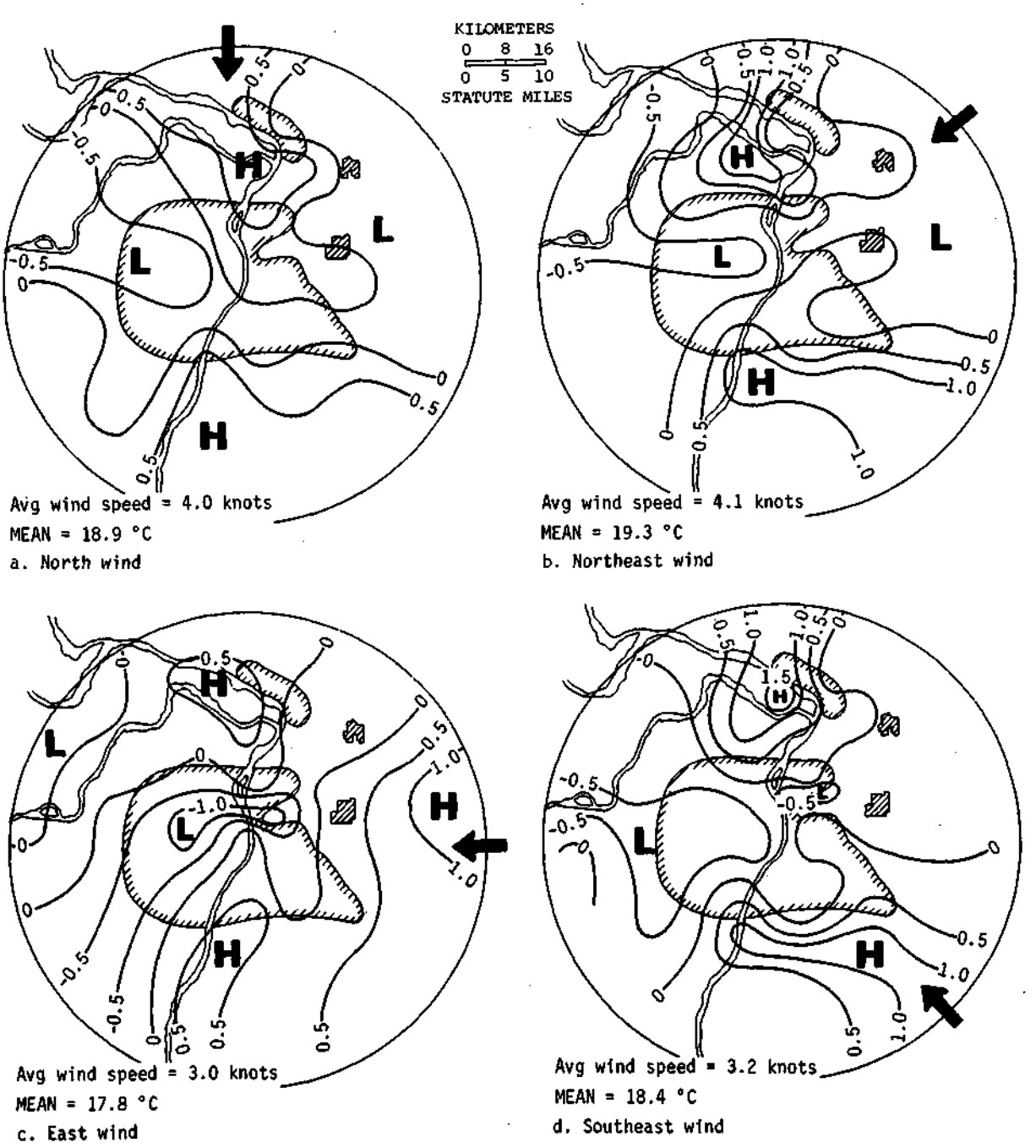

Figure B-30. Four-summer dew point patterns for each wind direction division

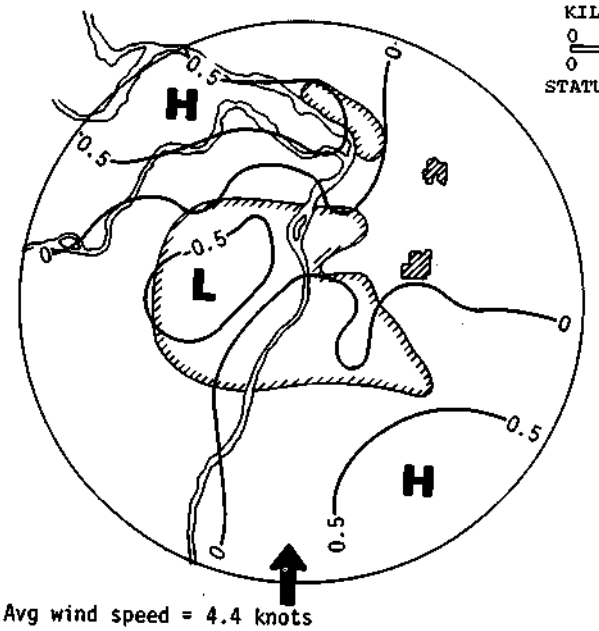

Avg wind speed = 4.4 knots
MEAN = 19.3 °C
e. South wind

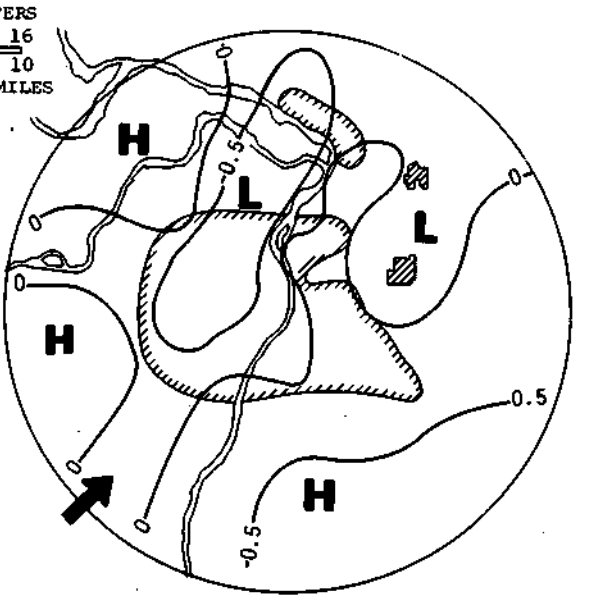

Avg wind speed = 5.3 knots
MEAN = 19.4 °C
f. Southwest wind

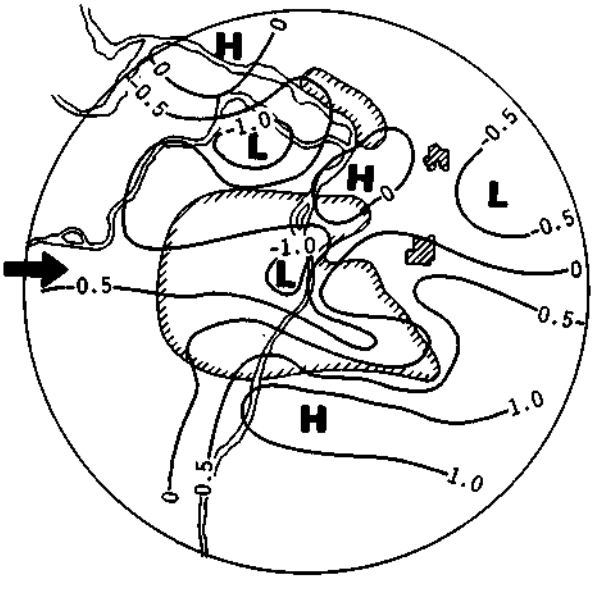

Avg wind speed = 4.5 knots
MEAN = 18.4 °C
g. West wind

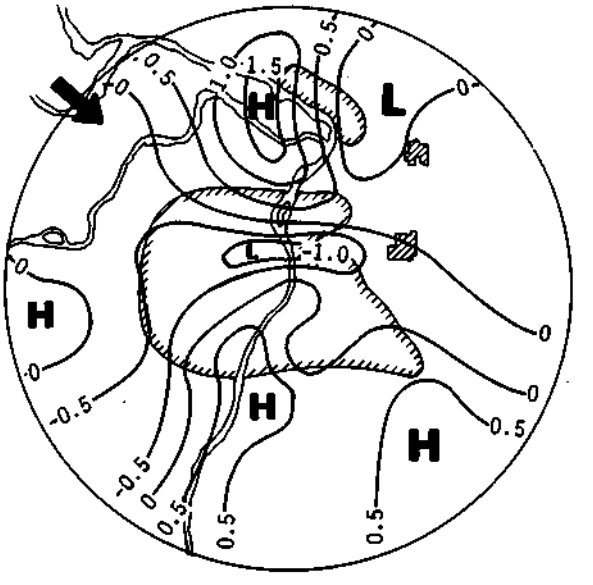

Avg wind speed = 4.4 knots
MEAN = 17.4 °C
h. Northwest wind

Figure B-30. Concluded

Table B-5. Percent of Wind from Each Direction and Average Wind Speed, 1972-1975

	Percent	Number of days	Average speed (knots)
N	08	26	4.0
NE	08	27	4.1
E	08	26	3.0
SE	16	53	3.2
S	25	85	4.4
SW	17	58	5.3
W	08	28	4.5
NW	10	34	4.4
Total		337	

Table B-6. Number of Storms and Rainfall versus Wind Direction, 1972-1975

	Number of storms	Percent of total	Precipitation (cm)	Percent of total
SE	46	18	32748	16
SW	65	25	51027	26
S	78	30	80567	41
N	19	7	17389	9
NW	22	8	5848	3
W	17	7	6410	3
NE	5	2	2537	1
E	7	3	1420	1
Total	259		197946	

Wind Speed

If wind speed had an effect on dew point, it should be evident at the time of maximum average wind speed. Maximum average wind speed occurred at 1500 CDT and was averaged from 1400-1600 CDT to get the 1500 value. An average wind speed was determined for each day in June, July, and August 1972 through 1975. June 1974 data were missing. Three categories of wind speed were chosen for study; 0 to 3 knots, 4 to 7 knots, and greater than 7 knots. A grand average was found for each time period by adding each station's wind speed and dividing by the total stations reporting for that time.

The average wind speeds that were determined are generally what the entire METROMEX area experienced for the times given since a 3-hour average smooths any local variations.

Because there was only a small amount of data for wind speeds greater than 7 knots for all years, no map was plotted. The 4-year dew point pattern when 0 to 3 knot winds existed at 1500 CDT (figure B-31a) was similar to the 4-summer pattern (figure B-23a). The only change was the moist area in the southeast which extended farther north to include the Collinsville area and the extreme southeast urban area.

The dew point pattern at 1500 CDT when 4 to 7 knot winds existed was drastically different from the 4-summer pattern. The only areas not different from the 4-summer map were the dry regions over the central urban area and the southwest hills. Table B-7 lists the prevailing wind direction versus the wind speed and shows that the southerly winds were dominant at all speed categories. In fact, 61% of the daily winds of 4-7 knots were from the south. Also the mean dew point temperature for wind speeds in the 4-7 knot range was higher than the 4-summer mean at 1500 CDT (18.6° C vs 19.1° C). The predominance of southerly winds and a 53% occurrence of rain on the days when these wind speeds occurred (table B-8) at least partly accounted for the high dew point mean temperature.

Although the wind speed has an effect on the dew point pattern, when compared against the 4-summer mean, no strong effect occurred. The maximizing of southerly moist winds, especially in the 4-7 knot range at 1500 CDT, did not overcome expected flattening of the dew point gradient due to mixing.

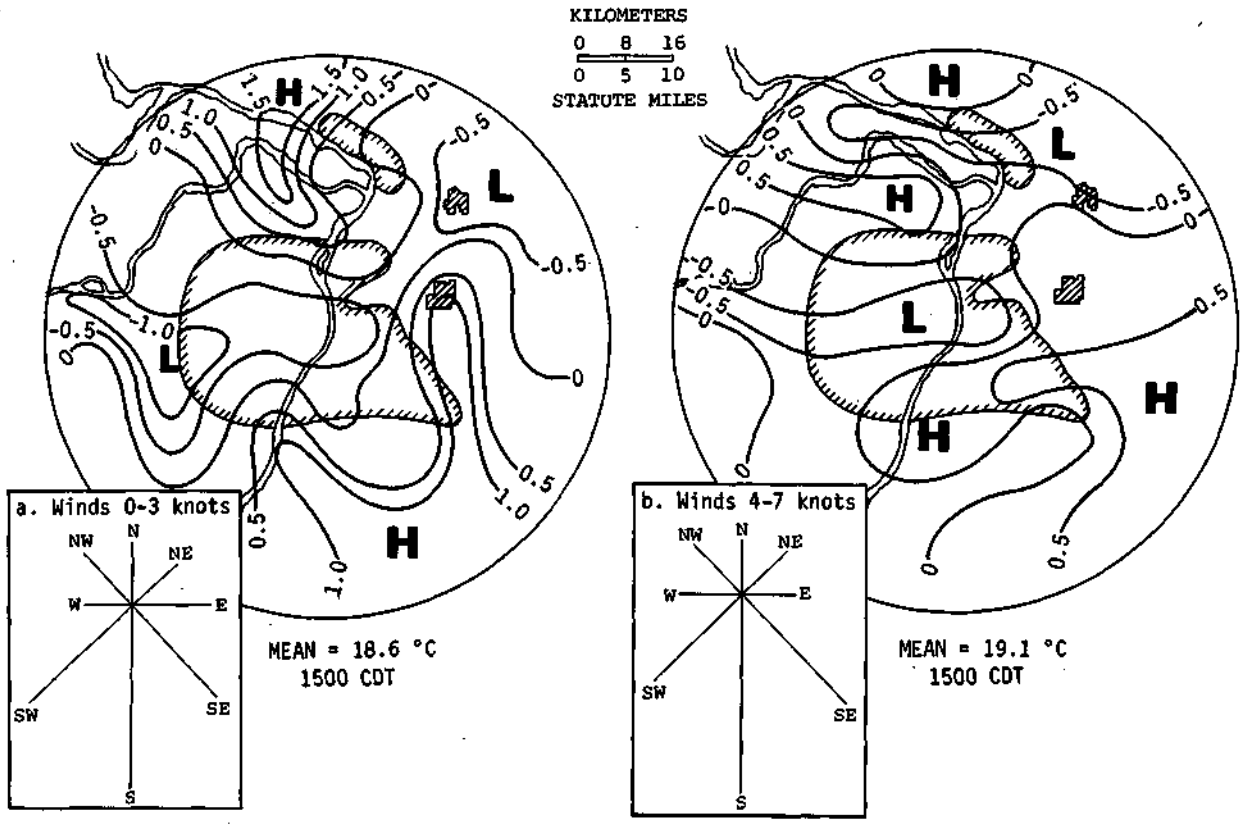

Figure B-31. Four-summer dew point patterns for winds 0-3 and 4-7 knots at 1500 CDT

Table B-7. Wind Direction versus Wind Speed at 1500 CDT, 1972-1975

	0-3 knots		*4-7 knots*		*>7 knots*	
	Days	*%*	*Days*	*%*	*Days*	*%*
N	13	8	10	7	3	8
NE	13	8	11	8	3	8
E	16	10	10	7	0	0
SE	26	16	26	19	1	3
S	38	24	35	26	12	30
SW	29	18	22	16	7	17
W	10	6	11	8	7	17
NW	15	9	12	9	7	17
Total	160		137		40	

Table B-8. METROMEX Rain Occurrence Days versus Wind Speed

0-3 knots	84/161	=	52%
4-7 knots	73/137	=	53%
>7 knots	18/40	=	45%

Summary

The surface dew point temperatures in St. Louis are lower (drier) than those in the surrounding rural areas. Highest dew points in the area existed in the southern, far western, and bottomland areas around St. Louis. Rural areas have much more evapotranspiration per unit area than urban areas which partly accounts for the moister rural conditions.

The dew point patterns of the monthly maps did not vary appreciably between years. The dew point patterns for the 1200 to 2400 CDT period were similar to the 4-summer pattern. In the early morning hours when dew was present, the city was relatively moister. Various weather conditions including sky cover, wind direction, and wind speed, had only minor effects on the average dew point patterns. There were places where the rainfall pattern related well with the surface dew point patterns and others where it did not. The results prove that the local rainfall does not have a strong dependence on low-level moisture variations.

EQUIVALENT POTENTIAL TEMPERATURE PATTERNS ASSOCIATED WITH RAINSTORMS

J. L. Vogel and G. Dzurisin

Introduction

Analyses were made to detect possible relationships of surface temperature and moisture distributions that existed prior to the initiation of rain events with land use features and with the resulting rainfall distributions. It is well known that cities exhibit an urban heat island effect (Landsberg, 1956; Sanderson et al., 1973; Jones and Schickedanz, 1974). Recent results also indicate that urban regions tend to be drier (Dirks, 1974; Landsberg, 1975; Sisterson, 1975). Thus, it is possible that locally induced surface or near-surface temperature and moisture anomalous conditions could lead to alterations in convective activity over the urban area and affect the resulting distribution of rainfall and severe weather. If warmer (or colder) and/or moister (or drier) surface or near-surface air is entrained into the updraft of a convective storm, the thunderstorm could become more (or less) vigorous because the air parcel being ingested would have more (or less) kinetic energy.

Boatman and Auer (1974a and 1974b) conducted several case studies and used equivalent potential temperature (EPT) as a tracer of air motions based on surface, upper air, and aircraft data. They concluded that:

1) The St. Louis urban complex is a source of drier air (lower EPT).
2) The ingestion of this lowered EPT air by thunderstorms passing over the urban complex decreases the intensity of the convective entities.
3) The weakened thunderstorms 'collapse' and the resulting release of their water load results in increased surface rainfall rates downstorm from the urban complex, thus being a possible cause for the climatic rainfall anomaly east of St.. Louis.

Jones and Schickedanz (1974) studied METROMEX surface temperature and moisture measurements prior to the initiation of rainfall for the summers of 1972 and 1973. They found that the areas of most frequent raincell initiation were in the general vicinity of warm, moist surface regions. There also appeared to be some relation between the prior moisture field and the subsequent development of precipitation. However, this relationship was not definitive.

With data from nine case studies, Changnon and Semonin (1975) also found that rain tended to initiate within zones that were relatively warm and moist at the surface. They were unable to find an intensification of rain within warm and/or moist zones.

Changnon et al. (1977) found that the major precipitation anomaly maximizes over the eastern part of the urban-industrial region of St. Louis from 1500 to 1800 CDT and downwind of the metropolitan region from 1800 to 2100 CDT. If the urban temperature and moisture distributions near the surface have an important effect upon this precipitation pattern, they should be most active just before this period. Others (Jones and Schickedanz, 1974; Sanderson et al., 1973) have found that on the average the urban heat island during this period is minimized, i.e., there is less temperature differential between the urban and rural regions than at night. Also during this afternoon-evening period the urban-industrial area is relatively drier than the surrounding rural regions. Since moisture has a greater impact than temperature upon the EPT at normal summer temperatures (75 to 85° F), the EPT over the city on the average can be expected to be lower than the EPT in the rural regions. If such surface or near-surface air is entrained into a

thunderstorm the intensity of the updraft can be expected to decrease; as a result, the updraft can no longer support as much total cloud water and a release of rain might be expected at the surface. An attempt was made to determine if the EPT pattern prior to the initiation of objectively defined rainstorms showed the expected lower EPT values over the urban-industrial region.

A sample of 45 objectively defined rainstorms (all thunderstorms) was chosen to test the hypothesis. This sample was derived from the 283 objective storms defined during the summers of 1972 through 1975. There were not enough stations measuring temperature and humidity during 1971 to define adequately the temperature and moisture patterns. Since the lower EPT occurs in the city during the day, all of the storms selected were among those that initiated over the network between the hours of 1000 to 1900 CDT, and 32 of the 45 storms initiated between 1200 to 1600 CDT. Usually the rainfall from these storms was most intense during the beginning phases of the storms. Since the major part of the precipitation anomaly has been found to be associated with the heavy rains and squall line storms (Changnon et al., 1977), there also was a deliberate attempt to choose storms with large rainfall amounts in squall line situations. Of the 45 storms selected, 34 had point rainfall amounts of ≥ 2.5 cm (1 inch), and 19 storms (42% of the sample) were produced by squall lines. The synoptic typing, percent distribution of the 45-storm sample, and the 4-summer distribution of the various synoptic types are shown in table B-9. Air mass storms made up 30% of the total storms, but only 14% of the EPT sample. Previous analyses (Changnon et al., 1977) showed that these storms had spotty coverage and were not of major importance in producing the summer rainfall anomaly. It was found that squall zone storms did not always reflect an urban influence, so a smaller storm sample was selected from this category. No pre- or post-frontal or low storms were selected because of the limited sampling of these storms (less than 9%) during the four summers.

Data Analysis

The equivalent potential temperature was calculated by the following formula

$$EPT = T\,(1000/P)^{0.286} \exp\,(LW/C_p\,T_c)$$

where T is the surface temperature (°K), P is the station pressure (mb), L is the latent heat of condensation, W is the mixing ratio, C_p is the specific heat of dry air, and T_c is the condensation temperature (°K). The station pressures were obtained from Lambert Field (STL) for each hour and an adjustment for the height at each weather station was made assuming a standard atmosphere. The condensation temperature, T_c, was obtained from the following equation for a lifting process (Inman, 1969).

$$T_c = 273.15 + T_c - (T-Td)(0.212 + 0.001571\,Td - 0.000436\,T)$$

where Td is the surface dew point. Both the temperature, T, and the dew point, Td, in this equation are given in °C.

Table B-9. Synoptic Distribution of Storms Chosen for EPT Study

	Squall zone	*Squall line*	*Air mass*	*Cold front*	*Warm front*	*Static front*
Number of storms	12	19	6	4	2	2
Percent of storm sample	27	42	14	9	4	4
Four-summer synoptic distribution	15	24	30	14	5	5

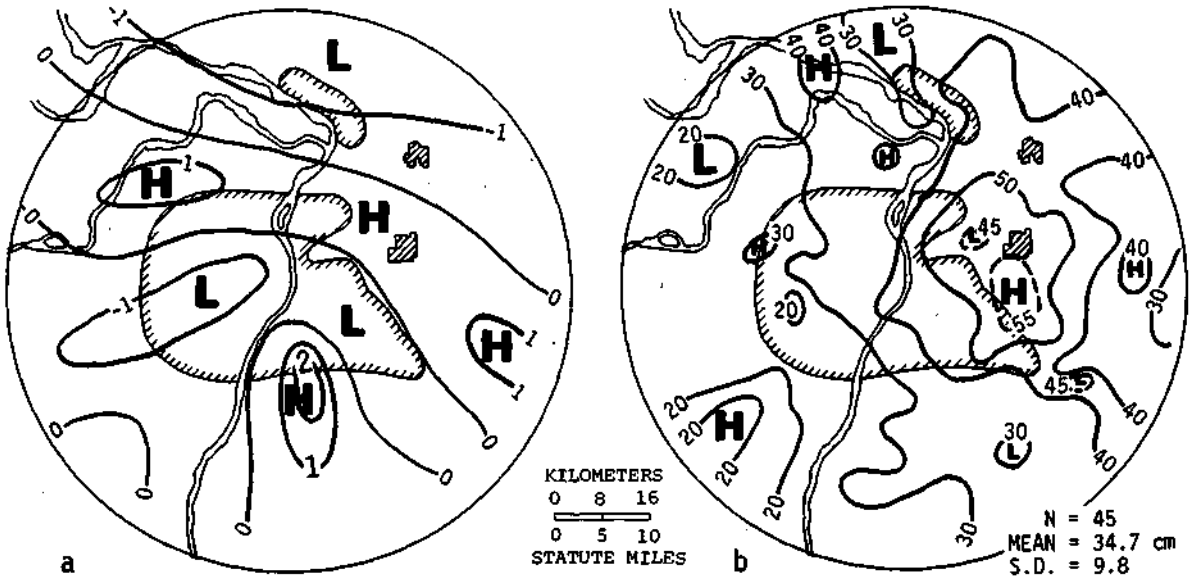

Figure B-32. EPT deviations (° K) for 45 selected storms and rainfall pattern for those storms

The EPT was calculated at each station, then each area, and averages for the 50-mile (80 km) diameter research circle were determined for each storm for time periods of 1 + 2, 2 + 3, and 1 + 2 + 3 hours prior to the initiation time of each of the 45 objective storms. The three time periods were chosen to determine if there was any difference due to the variation in EPT with time. Comparison of the EPT patterns for these three time periods revealed them to be similar. Hence, only the results for the 3-hour period prior to the initiation of each storm are discussed. The average area value for each of these storm periods was determined and the difference between this area average and each station's EPT was determined. If the EPT at a station was higher than the average, it was assigned a positive value (higher sensible and latent energies); if it was lower, it was assigned a negative value (lower sensible and latent energies). These deviations from the network average for each storm were then summed at each station to construct composite EPT maps for the 3-hour period prior to the initiation of the storms.

EPT and Rainfall

The mean EPT deviation pattern of 1972 through 1975 for the 3-hour period prior to the 45 selected storms is shown in figure B-32a. Below average EPT values were present in St. Louis, the rural areas west and southwest of St. Louis, and in the rural northern portions of the research circle. Positive EPT deviations were indicated in and just south of East St. Louis and along a general east-west axis which ran across rural areas as well as the northern urban area.

The lower EPT values observed in the rural north were caused by a combination of relatively (to network mean) below average temperatures and humidities; the lower EPT values in the rural west and the metropolitan region had generally above area average temperature and below average humidities. In the positive EPT deviation areas the surface temperatures were both above and below the area average, whereas above average humidities were generally observed. Importantly, the resulting pattern does not appear to be related to any land uses, urban effects, or

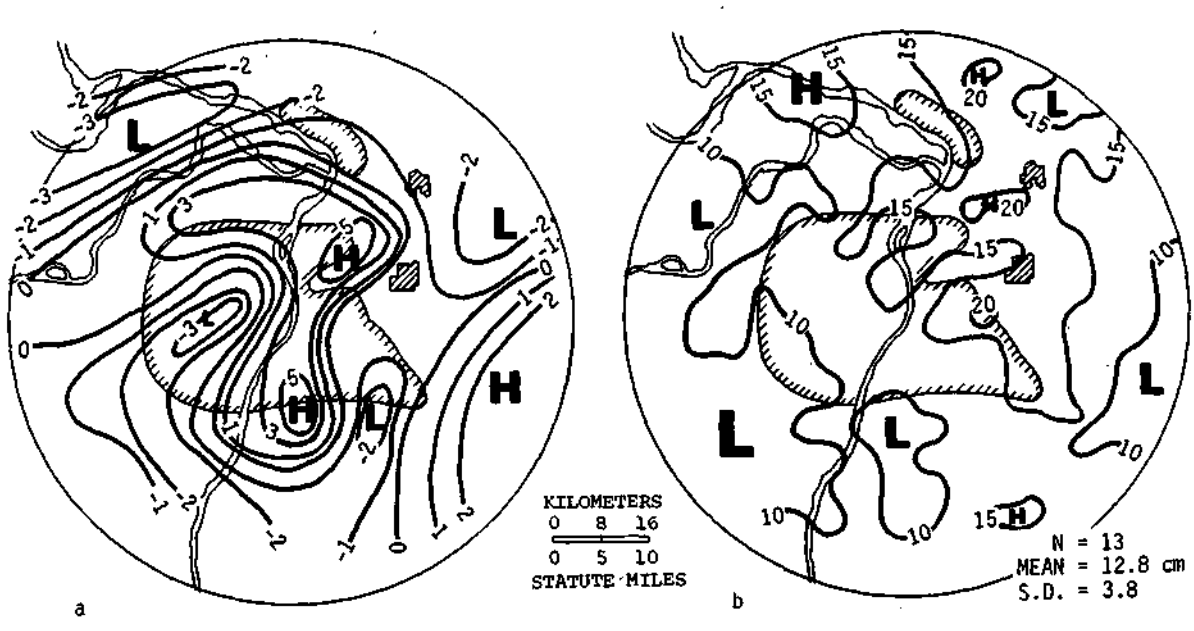

Figure B-33. EPT deviations in 1975 storms and rainfall pattern

orographic effects. Furthermore, it does not support the general hypothesis that the urban areas should have daytime EPT values lower than rural values.

The. corresponding rainfall pattern associated with the selected storms (figure B-32b) shows a high east of St. Louis, and a general rainfall minimum west of the Mississippi River. This rainfall pattern is similar to the rainfall pattern found for the periods from 1500 to 1800 CDT and 1800 to 2100 CDT for the five summers (1971-1975), i.e., a rainfall maximum over the eastern part and east of the urban region (Changnon, et al., 1977). If lower EPT air reduced the intensity of the convective entity updrafts and then released surplus cloud water, the EPT pattern of figure B-32a would suggest a general rainfall maximum could be expected over the southwest quadrant and extreme northern part of the network. Figure B-32b does not show a rainfall maximum in the north and shows below network average rainfall in the southwest, indicating little direct relationship between surface EPT and the total rainfall pattern for the sample.

The EPT patterns for each of the summers of 1972, 1973, and 1974 showed a minimum in St. Louis and the rural area west of St. Louis. However, in 1975 the EPT pattern maximized over the city (figure B-33a) which should not have produced maximum rain in the area. Yet the precipitation which fell within the 13 selected storms in 1975 exhibited a maximum in and just east of St. Louis (figure B-33b). In general, all these results indicate a rejection of the initial hypothesis for this total storm sample.

EPT Relations by Storm Types

Squall Line Storms. The EPT deviation pattern associated with the 19 squall line storms (figure B-34a) showed positive deviations over the southern rural area and over the northern portions of the metropolitan area and the rural river bottomlands to the northwest. Negative deviations were located over and west of St. Louis and in the northeast rural area. Thus, lower EPT values were observed over much of the central and southern parts of the urban-industrial region,

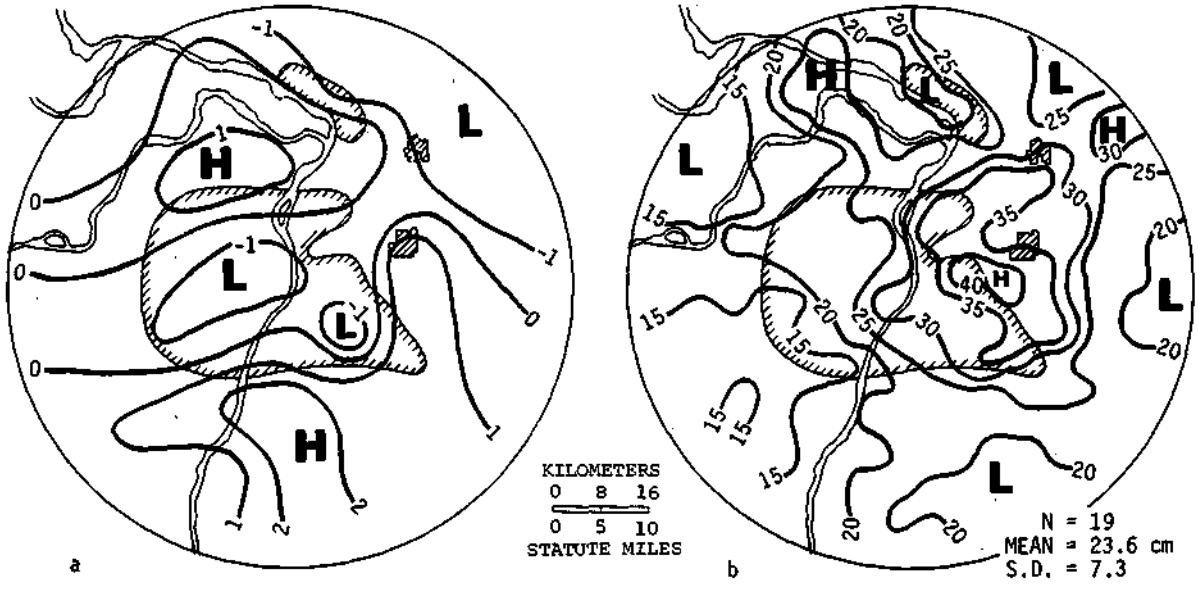

Figure B-34. EPT deviations (° K) for squall line storms and rainfall pattern

but elevated EPT values were also present over the northern third of the urban-industrial region. The corresponding rainfall pattern (figure B-34b) indicates a general rainfall maximum in and just east of St. Louis, with a secondary high over the northwest bottomlands. Thus, the primary rainfall maximum was just downstorm from a negative EPT anomaly centered over St. Louis, suggesting a cause and effect relationship between EPT and rainfall during squall line conditions.

Squall Zone Storms. The EPT deviation pattern for the 12 squall zone storms (figure B-35a) in the sample showed negative deviations over the urban and rural southwest quadrant, and the northern rural and urban areas. Both high and low EPT values were found in the metropolitan region. The rainfall pattern associated with these storms (figure B-35b) indicated maximums in St. Louis, to the southeast and northeast of the city, and in the northwest bottomlands. Once again the primary rainfall maximum was over and east of St. Louis with its mixture of high and low EPT values. No evidence for EPT-rain relationship is reflected for squall zone storms or for the other synoptic types.

West-Southwest Storms. Figure B-36a shows the EPT deviation pattern associated with the 11 storms which moved from the west-southwest. Negative deviations are indicated as a strip from the rural south edge of the circle curving northeastward across St. Louis, and broadening to encompass most of the rural northeast. Generally low EPT values existed in the metropolitan region. The associated rainfall pattern (figure B-36b) shows maximums of rainfall over and downstorm of these low urban EPT values indicating some support of the hypothesis. However, a rainfall maximum existed in the NW which was not a low EPT region. Clearly, EPT is not a major factor controlling the rainfall quantities and their distribution.

West-Northwest Storms. Negative EPT deviations (figure B-37a) were present near Alton-Wood River, the west rural area, in portions of the eastern urban area, and in the western and southern rural areas prior to the eight storms which moved from the west-northwest. The rainfall from the storms which moved from the west-northwest (figure B-37b) showed maximums from Granite City to Edwardsville and some isolated maximums over St. Louis and Belleville. Thus,

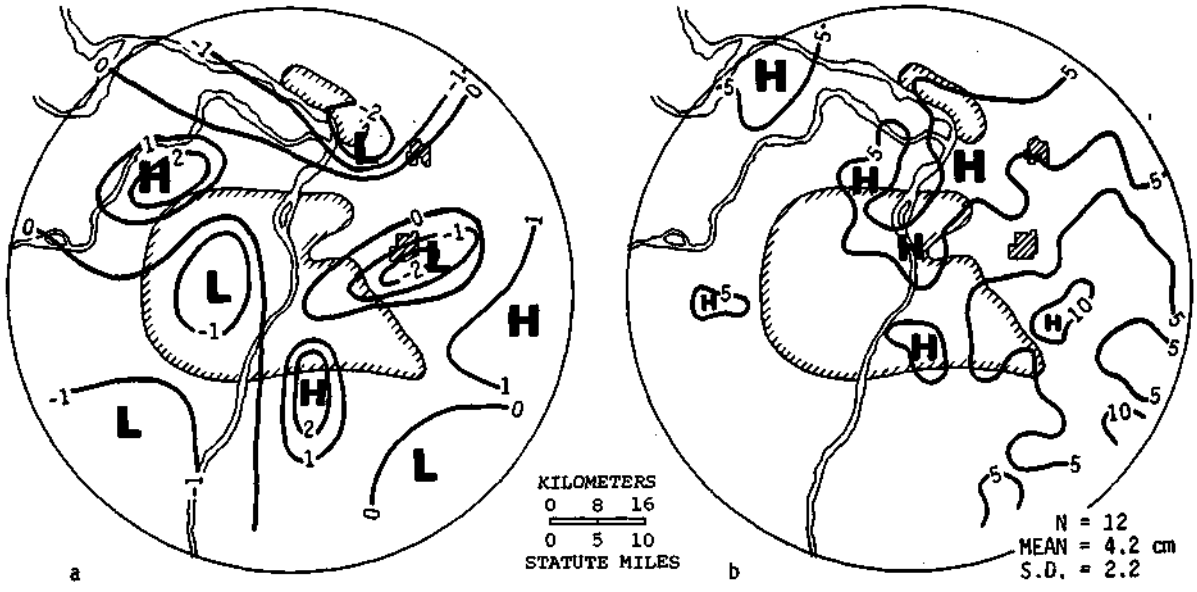

Figure B-35. EPT deviations (° K) for squall zone storms and rainfall pattern

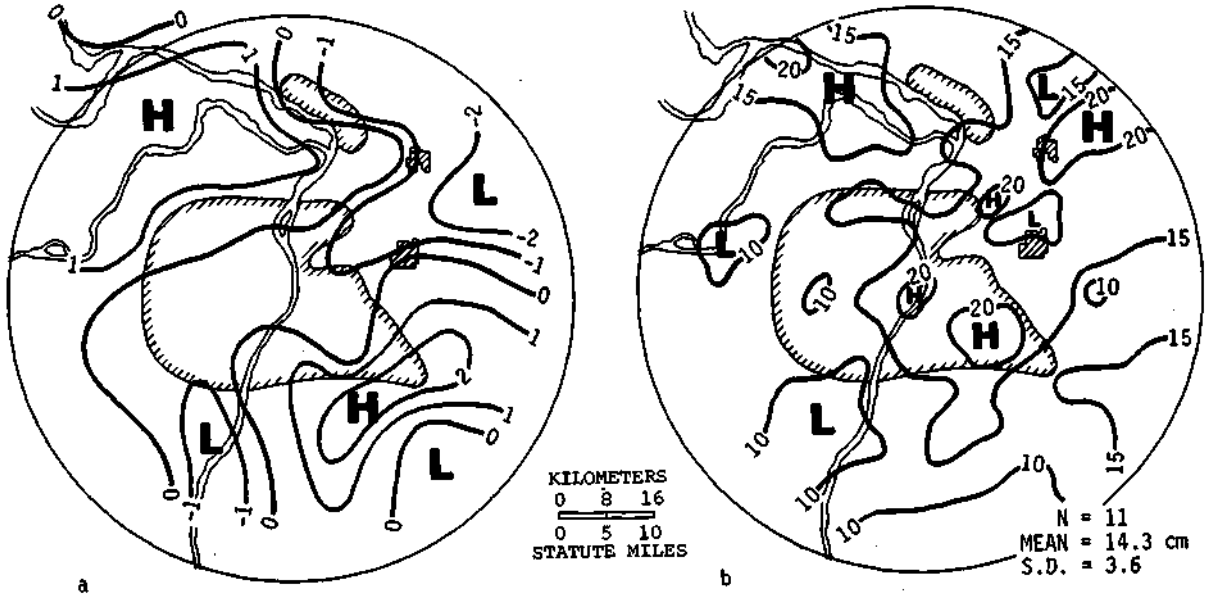

Figure B-36. EPT deviations (° K) for storms from the west-southwest and rainfall patterns

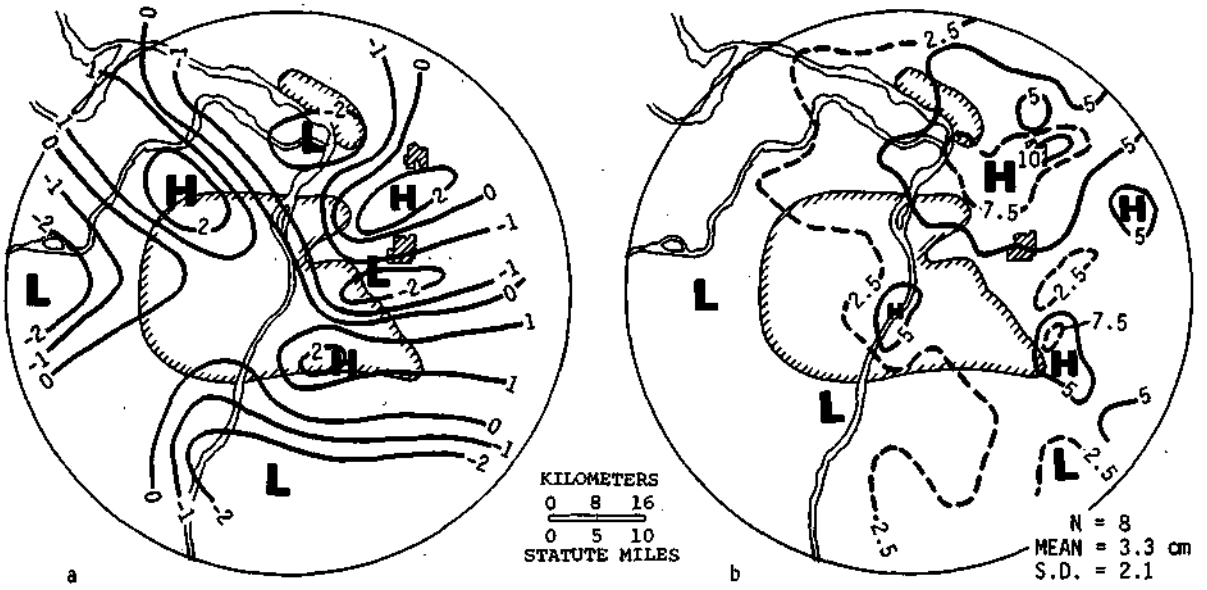

Figure B-37. EPT deviations (° K) for storms from the west-northwest and rainfall pattern

a rain-EPT relationship is indicated downstorm of the Alton and northwest rural area, but none is found with lower EPT values elsewhere.

Other Storm Movements. The EPT patterns for the storms which moved from the southwest or northwest also exhibited both positive and negative regions of EPT over the St. Louis urban-industrial region. The rainfall pattern for both types with mean maximums downstorm from the urban region did not show a strong relationship with the EPT patterns.

Summary and Conclusions

An attempt was made to determine whether there was a relation between the surface distribution of EPT prior to rain and the resulting rainfall pattern. The network average EPT and the point deviations were calculated for the 3-hour period prior to the initiation of 45 rainstorms. These EPT patterns were developed and then compared with the resulting rainfall patterns for the total sample and for various synoptic types, different summers, and storm motions.

The predicted relationship between low EPT air at the surface and land use types (urban areas) was not found. Typically, both the metropolitan and rural areas had regions of relatively high and low EPT values before rain started. This suggests that daytime EPT values do not have a unique relationship with land use. Hence, one would predict that the urban effect on precipitation processes is not strongly related to the daytime EPT. As in previous rain analyses, the main precipitation highs in the 45-storm sample (and its sub-samples) were downstorm from the urban-industrial region. In other network regions there were both rainfall maximums and minimums where EPT values were frequently a mixture of plus and minus departures from the average value.

Furthermore, the ensuing spatial comparative analysis of the EPT patterns and their rain patterns did not reveal a strong relationship.

Some evidence supporting an EPT-rain relationship was found for squall line storms and for storms moving from the WSW. In both cases much of the urban area had relatively low EPT

values and a major rain maximum occurred in and just east of the area. However, the lack of low EPT values in the urban area in other storm stratifications, and the lack of low EPT-high rainfall relationships in other network areas in the squall line and WSW storms (plus in all other storm stratifications) augers against declaring that a meaningful EPT-rain relationship exists in most situations. Comparisons made between individual yearly EPT values and the associated rain patterns also showed no relationship.

The precipitation may be affected by less than average or greater than average surface EPT values on some occasions, but the effect does not appear to be a major factor for explaining the precipitation anomaly downstorm (east) of the urban region. If the raised or lowered EPT air is ingested in storms, the effect is apparently being offset.

SURFACE WIND CLIMATOLOGY

Stanley A. Changnon, Jr.

Recognition of the importance of wind measurements in helping to understand how urban factors affect clouds and rainfall led to the collection and study of surface wind data, as well as that in the boundary layer. The Water Survey, as part of its state-supported METROMEX effort, chose to develop, within its limited resources, the best possible mesoscale surface wind network within the circular study area.

Survey scientists first inventoried existing recording wind systems in the St. Louis area in 1971. Some 18 systems were found, many concentrated in the industrial region. Many had poor exposures and/or questionable quality control and hence poor data. Following this inventory, which indicated 11 apparently good quality stations with most within the urban area, the Survey installed its seven recording wind stations distributed in a circle surrounding St. Louis at a radius of about 20 miles (36 km). This installation and calibration effort was completed in August 1971. Collection of summer data began in June 1972 and continued each summer through the end of METROMEX in August 1975.

These wind data have been analyzed and studied to present a general climatological description of the surface wind fields in summer (all days and by 6-hour periods). The data have also been compared for all-rain, pre-rain, and no-rain periods to discern any climatic differences during these conditions.

In this section, first the data and then the analyses performed are described. Results are then presented for the 4-summer (1972-1975) data set 1) for all days, 2) for each of the four 6-hour periods of the day, 3) for winds in all 3-hour periods preceding rainfall initiation in the circular raingage network, 4) for winds occurring on all no-rain days, and 5) those winds during all-rain periods.

Data and Analyses

The wind data obtained for the study of surface winds in the METROMEX study area came from 19 stations. Seven stations were installed and operated during each summer of the 1972-1975 period by the Illinois State Water Survey (ISWS). The recorded wind data of the NOAA station at Lambert International Airport and that of the U.S. Air Force at Scott AFB (near Belleville) were obtained for these four summers. Summer wind data were also obtained for the nine automatic wind stations of the St. Louis Air Pollution Control District (APCD) and one station of the Illinois EPA.

Two types of wind equipment were used at these 19 stations. The stations at Lambert, Scott AFB, and Pere Marquette (PMQ) had aerovane systems. The PMQ anemometer was at an elevation of 15 feet above ground, that at Scott was at 15 feet, and that at Lambert was at 20 feet. The other 16 stations had standard 3-cup type anemometers and vanes. These had varying heights, but all were at heights above ground in the 10 to 15 feet (~4 to 5 meters) range. Analysis of the average speed values was done with consideration of these height differences and their impact (higher speeds at the sites with taller sensors). The major adjustment was made for the Lambert station values which generally were 30% higher than those from other nearby stations with sensors closer to the ground.

The seven ISWS stations were installed at sites with very open exposures (three were at airports) in rural areas. Visual inspection of the other 12 stations suggested some questionable exposures, particularly with respect to blockage in certain sectors by nearby buildings.

Awareness of possible site problems and equipment differences led to a comparative evaluation of the data from these 19 stations. This was based on an inspection of the processed speed and direction values. Stations with questionable appearing data at sites judged earlier to be questionable were eliminated from further study and from the presentation of surface wind results.

This evaluation indicated that the 1972-1975 data (summers) at the Scott AFB site and at the APCD sites Bellfontaine, Camp Site, Lindberg , and Ladue were faulty. These were not used and the study was pursued with the data for the 14 stations shown in figure B-38. Unfortunately, their distribution is not perfectly uniform, throughout either the urban area or the rural area. The directional data at Cahokia were found satisfactory but the speeds were considered unusable (too high).

The basic data used in the study were 'hourly' values. These were actually mean wind speeds and preferred directions determined from the 10-minute periods just prior to each hour (i.e., 0950 to 1000 CDT, 1050 to 1100, etc.). These 10-minute values for each hour were the data used in this study.

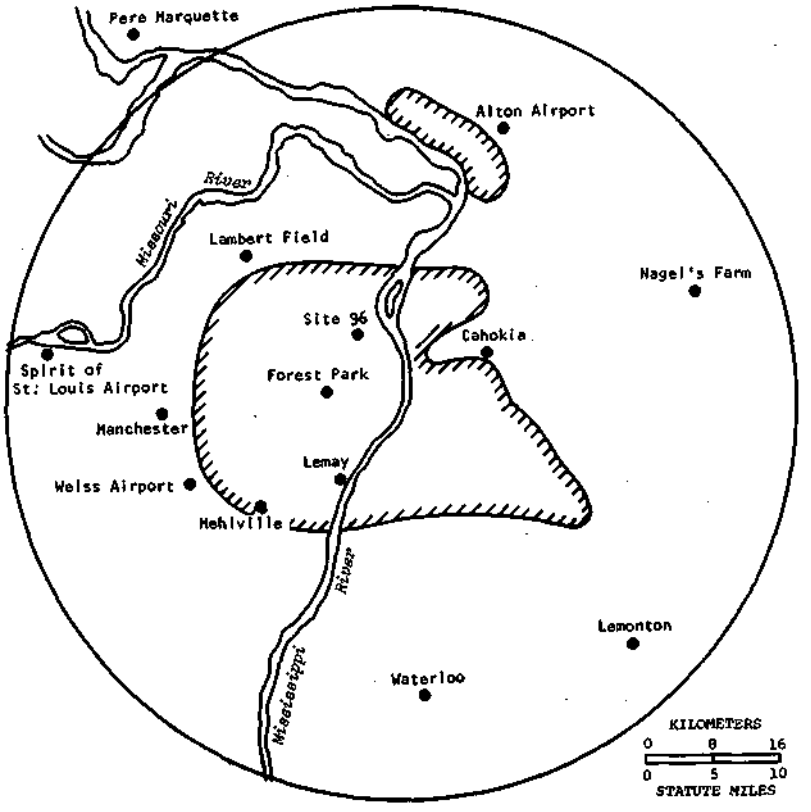

Figure B-38. Surface wind data stations, 1972-1975

The direction analyses were performed initially on the basis of 16 directions of the compass (every 221/2 degrees: N, NNE, NE, ENE, etc. and calm). Speeds (in mph) were sorted and classed into groups including 0,1 to 3 mph, 4 to 6 mph, 7 to 9 mph, and other 3-mph classes up to 30 with all winds > 30 mph in one class. For certain analyses, the data were studied on the basis of a classification of directions into north (316 to 45°), east (46 to 135°), south (136 to 225°), and west (226 to 315°). Average wind speed values were calculated for all possible stations and regional combinations of stations. [To convert miles per hour to meters per second multiply by 0.44704.]

The wind values of the stations were further sorted according to various types of weather conditions. Results are presented in the above directional and speed formats. First, all data (all hours for all four summers) were processed. Then, all the data for each of the four 6-hour periods of the day (0001-0600 CDT, 0601-1200, etc.) were sorted for analysis. The winds under three specific weather conditions, including those during 1) all-rain periods on the network, 2) no-rain days, and 3) those for the 3 hours prior to the onset of rain, were separated and analyzed as three distinct data sets.

Summer Wind Conditions

The climatological study of the summer surface winds included an extensive analysis of the winds on all days and hours, or the total sample of the data. The frequency of winds in all speed and direction classes for 13 stations appears in table B-10. No data are presented for the station at Cahokia (see figure B-38) because its speed values were considered erroneous.

The directional wind roses appear in figure B-39. Most stations show strong southerly frequencies, but differences in the directional distributions are noticeable. Note, for example, the rather marked tendency for more SE and E winds at stations east of St. Louis (Cahokia, Nagels Farm, and Lemonton) than at stations elsewhere. In contrast, note that several stations (Forest Park, Spirit of St. Louis, Mehlville, Weiss Airport, and Manchester) in and to the west of St. Louis show a greater distinct tendency for W and SW flows than stations elsewhere. These two observations suggest a tendency for convergent low-level flow over St. Louis, and more important, a regional-scale influence by the metropolitan area on the low-level flow.

Figure B-40 presents the pattern based on the average wind speed for all summer days in 1972-1975. A general south-to-north increase is noticeable with averages in the south of 4.1 to 4.4 mph, as opposed to 5.2 to 5.4 mph in the north, a regional difference of about 20%. Implanted on this regional gradation are apparent urban influences. Included is a high in the central part of the metropolitan area (Forest Park with 5.3 mph) which is 15 to 20% above the expected speed. Chandler (1965) noted surface wind increases in London when there was a well-developed heat island. Two small lows, one to the north and one to the south of the metropolitan area, appear to be urban-generated features reflecting 10% decreases in expected speeds.

Average speeds were calculated for three major land use areas: urban, suburban, and rural. There were seven stations classed as rural (Pere Marquette, Alton, Nagels Farm, Lemonton, Waterloo, Weiss Airport, and Spirit of St. Louis Airport); three classed as suburban stations (Manchester, Lambert Field, and Mehlville); and three urban stations (Lemay, Forest Park, and site 96). The three regional land use averages were 4.73 mph for the urban area, 4.37 mph for the suburban, and 4.63 mph for the rural area. These indicate the urban wind speed is, on the average, the highest in the entire region, whereas the suburban is the lowest. The urban-rural difference, 0.10 mph, reflects a 2% increase in the city; and the suburban-rural difference, —0.26 mph, is a 5% decrease in the suburbs. If the urban and suburban values are combined, the metropolitan average is 4.55 mph which is only slightly lower, by 0.08 mph, than the rural value. In essence, they are equal.

Table B-10. Frequency of Wind in All Speed and Direction Classes for 13 Stations, 1972-1975

Percent of total hours

Class (mph)	NNE	NE	ENE	E	ESE	SE	SSE	S	SSW	SW	WSW	W	WNW	NW	NNW	N	Var	Totals
Pere Marquette (Total hours = 7047)																		
Zero	*	*	*	*	0	*	*	*	*	*	*	0	*	*	0	0	*	2
1-3	1	*	1	1	2	2	2	2	2	2	1	1	*	1	1	1	1	21
4-6	3	1	2	2	2	2	5	6	6	3	4	3	2	2	2	2	*	48
7-9	2	2	2	1	1	*	1	1	3	1	2	1	1	*	1	1	*	21
10-12	1	*	*	*	*	*	*	*	1	*	*	*	*	1	*	1	0	6
⩾13	0	*	0	*	0	*	*	*	0	*	*	0	*	0	0	*	0	2
Totals	7	4	5	5	5	5	9	10	12	6	8	5	4	4	4	5	2	100%
Nagel's Farm (Total hours = 6517)																		
Zero	*	*	*	2	2	1	1	2	1	*	1	*	1	1	2	*	*	16
1-3	2	2	4	4	5	2	4	4	5	2	2	1	1	2	2	*	3	46
4-6	2	1	2	2	3	1	1	1	3	2	1	1	2	1	1	*	1	26
7-9	1	*	1	*	1	*	1	1	0	*	1	*	*	*	*	*	*	8
10-12	*	*	*	*	*	0	*	*	*	0	*	*	*	*	*	*	*	2
⩾13	*	0	0	*	0	0	*	0	1	*	0	*	*	*	0	0	0	2
Totals	6	4	7	9	11	4	8	8	10	4	5	3	5	5	5	1	5	100%
Weiss Airport (Total hours = 5266)																		
Zero	*	*	*	*	1	3	3	1	*	*	1	*	*	1	1	1	*	15
1-3	1	1	1	1	5	7	7	2	2	1	3	4	3	1	3	1	3	46
4-6	1	*	*	*	2	3	5	2	2	1	2	1	2	1	2	1	*	27
7-9	*	0	*	*	*	*	2	1	1	*	1	*	1	*	*	*	*	8
10-12	*	0	0	0	0	*	*	*	*	*	*	*	*	*	*	0	0	2
⩾13	*	0	0	0	0	*	*	*	*	*	*	*	*	0	*	0	0	2
Totals	3	1	1	2	8	14	17	7	6	3	8	6	7	4	6	3	4	100%
Alton Airport (Total hours = 6663)																		
Zero	0	*	0	0	*	0	*	*	0	0	0	*	*	*	*	0	*	2
1-3	2	1	2	1	3	2	3	2	3	2	2	*	2	2	2	1	1	32
4-6	2	1	2	1	3	2	4	4	6	2	3	1	2	2	3	2	*	41
7-9	1	*	*	*	*	*	2	2	2	*	1	1	1	*	2	*	*	16
10-12	*	*	0	*	1	*	1	*	1	1	0	*	*	*	*	*	0	6
⩾13	*	*	0	*	*	*	*	*	*	0	0	0	*	*	*	*	0	3
Totals	6	3	4	3	8	5	11	9	12	5	6	3	6	5	8	4	2	100%
Spirit of St. Louis Airport (Total hours = 5815)																		
Zero	*	*	*	1	*	*	*	1	2	2	*	*	1	1	*	1	*	11
1-3	2	*	2	2	3	3	3	3	4	4	4	1	2	*	2	*	3	41
4-6	1	*	1	1	2	3	2	2	2	3	3	1	1	1	1	1	*	28
7-9	1	1	*	*	2	1	1	1	1	2	1	*	1	*	*	*	*	14
10-12	1	*	*	*	*	*	*	*	1	*	*	*	*	*	*	0	0	4
⩾13	0	0	0	*	*	*	*	*	*	*	*	*	*	0	0	*	*	2
Totals	5	2	4	5	8	8	7	8	10	11	9	3	6	3	4	3	4	100%

Continued on next page

Table B-10. Continued

Percent of total hours

Class (mph)	NNE	NE	ENE	E	ESE	SE	SSE	S	SSW	SW	WSW	W	WNW	NW	NNW	N	Var	Totals
Waterloo (Total hours = 4486)																		
Zero	0	1	*	*	*	*	*	0	*	*	*	1	*	1	*	*	*	6
1-3	2	1	4	3	5	2	4	1	5	2	2	1	2	1	1	1	3	40
4-6	3	1	3	1	2	1	2	3	7	3	3	2	2	*	2	*	*	36
7-9	1	*	*	*	*	*	*	1	3	1	1	*	*	1	*	1	1	12
10-12	0	*	0	*	*	*	*	1	1	*	*	0	*	0	*	*	0	4
⩾13	*	*	*	0	0	0	0	*	*	*	*	*	*	0	*	*	*	2
Totals	6	4	7	5	8	4	7	6	16	7	7	4	5	3	4	3	4	100%
Lemonton (Total hours = 1002)																		
Zero	0	0	0	0	0	1	*	1	1	1	*	*	0	0	0	0	0	5
1-3	2	1	1	2	6	4	7	3	2	1	2	1	3	2	3	1	2	43
4-6	*	1	1	4	5	6	6	3	1	*	*	1	*	3	4	1	*	38
7-9	*	*	1	1	1	1	2	1	*	1	0	*	*	*	1	*	*	10
10-12	*	0	0	*	*	*	*	*	1	*	*	0	0	*	*	0	0	3
⩾13	0	*	0	0	0	0	0	0	*	0	0	0	*	*	0	0	0	1
Totals	3	3	3	7	12	12	15	8	6	3	3	3	4	6	8	2	2	100%
Site 96 (Total hours = 3321)																		
Zero	*	*	*	1	*	*	*	1	*	1	*	*	*	*	*	*	0	5
1-3	*	2	3	2	3	3	5	4	5	4	3	2	*	1	1	2	1	42
4-6	1	1	*	*	3	3	4	3	3	4	3	3	3	2	1	2	*	38
7-9	1	*	*	*	*	*	1	1	1	2	1	1	1	1	*	*	0	11
10-12	0	0	*	*	0	1	*	0	*	0	*	*	*	*	*	*	0	2
⩾13	0	0	0	0	0	0	1	*	0	0	*	*	*	*	0	0	0	2
Totals	3	3	4	4	6	8	10	9	9	11	8	6	5	5	3	5	1	100%
Forest Park (Total hours = 3290)																		
Zero	*	*	1	*	*	0	0	0	*	*	0	*	*	*	*	*	0	3
1-3	*	1	*	1	1	2	2	2	2	3	4	5	2	1	*	1	*	28
4-6	1	1	1	1	1	3	3	4	5	5	4	4	2	1	1	1	1	38
7-9	1	*	*	1	1	1	2	3	3	2	2	2	2	1	*	*	0	23
10-12	*	0	0	*	*	*	*	*	1	1	*	*	*	*	1	*	0	5
⩾13	0	1	0	0	0	0	0	*	1	*	0	*	*	*	*	0	0	3
Totals	3	3	2	3	3	6	7	9	12	12	10	12	7	4	3	3	1	100%
Mehlville (Total hours = 2611)																		
Zero	*	*	*	*	*	*	*	*	1	1	*	*	*	*	1	1	0	8
1-3	1	1	1	2	2	2	2	5	14	8	3	2	2	1	*	*	0	47
4-6	*	*	*	*	1	2	2	4	6	4	3	3	3	2	*	*	0	32
7-9	*	*	*	*	*	*	*	1	1	1	*	*	1	*	1	*	*	8
10-12	*	1	0	0	*	*	0	*	*	0	*	*	*	*	*	1	0	3
⩾13	1	*	*	0	0	0	0	*	0	0	*	*	0	0	0	0	0	2
Totals	3	3	2	3	4	4	5	11	22	14	7	6	6	4	3	3	0	100%

Concluded on next page

Table B-10. Concluded

Percent of total hours

Class (mph)	NNE	NE	ENE	E	ESE	SE	SSE	S	SSW	SW	WSW	W	WNW	NW	NNW	N	Var	Totals
Lemay (Total hours = 2959)																		
Zero	1	1	2	1	1	1	1	2	2	*	*	1	*	*	*	*	*	15
1-3	2	1	2	3	3	5	5	5	2	2	2	1	2	1	*	1	*	37
4-6	*	2	1	1	1	2	3	5	2	2	2	2	2	1	1	*	*	28
7-9	*	1	*	1	*	*	2	3	1	*	*	*	1	1	*	1	*	13
10-12	*	*	*	*	*	*	*	1	*	1	*	*	*	*	*	0	*	5
⩾13	*	*	*	0	0	*	*	*	*	*	*	0	0	0	0	*	0	2
Totals	3	6	6	6	6	9	12	16	7	5	5	4	5	3	2	3	2	100%
Manchester (Total hours = 3343)																		
Zero	*	*	0	0	0	*	2	2	2	1	*	*	*	*	*	*	0	8
1-3	2	2	2	2	2	3	5	10	6	4	4	4	3	2	2	2	1	56
4-6	*	1	*	1	*	*	3	3	2	3	3	3	2	1	*	*	1	25
7-9	*	0	*	*	*	*	*	1	2	2	1	*	1	*	*	0	0	8
10-12	0	0	0	0	*	0	1	*	0	*	0	0	*	*	0	0	0	2
⩾13	0	0	0	0	0	*	0	*	0	0	*	0	0	0	0	0	0	1
Totals	3	3	2	3	3	4	11	17	12	10	8	7	6	4	3	2	2	100%
Lambert Field (Total hours = 6983)																		
Zero																		
1-3	*	*	*	*	*	*	*	*	*	*	*	*	*	*	*	*	N	5
4-6	2	1	2	4	4	2	2	4	2	2	3	4	2	1	1	1	O	37
7-9	1	*	1	2	2	3	3	7	3	2	3	3	2	1	1	2	D	36
10-12	*	*	*	*	*	*	2	4	1	1	1	1	1	*	*	*	A	15
⩾13	*	*	*	*	*	*	*	1	*	*	*	*	*	*	*	*	T	7
Totals	4	2	4	7	7	6	8	16	7	6	8	8	6	3	4	4	A**	100%

*=<1%

** No data because values were taken from WBAN hourly records which do not show variable or 0 winds.

This indication that the average winds are reduced in the suburban ring and then increased in the central city was supported by a cross-sectional analysis of the upwind and downwind speeds, regardless of wind orientation. Average speeds at stations aligned along four orientations, such as north-to-south, were calculated and combined according to mean wind direction through a common point in the city. For example, with northerly flow, the mean values at the stations along a line from the north (Pere Marquette) to the south (Lemonton) were listed by their distance upwind and downwind from Forest Park, the common point. These were combined with similar west-to-cast averages (for west winds), east-to-west (for east winds), and south-to-north (for south winds).

The resulting averages presented a cross section of average winds across St. Louis, regardless of the wind direction (figure B-41). This shows a slight acceleration between 30 and 20 miles upwind, a sharp decrease in speed between 10 and 5 miles upwind of the metropolitan area center (Forest Park), followed by a major increase reaching the maximum 5 miles downwind where the average is 5.5 mph compared with 4.6 mph 30 miles upwind. The difference (0.9 mph) represents

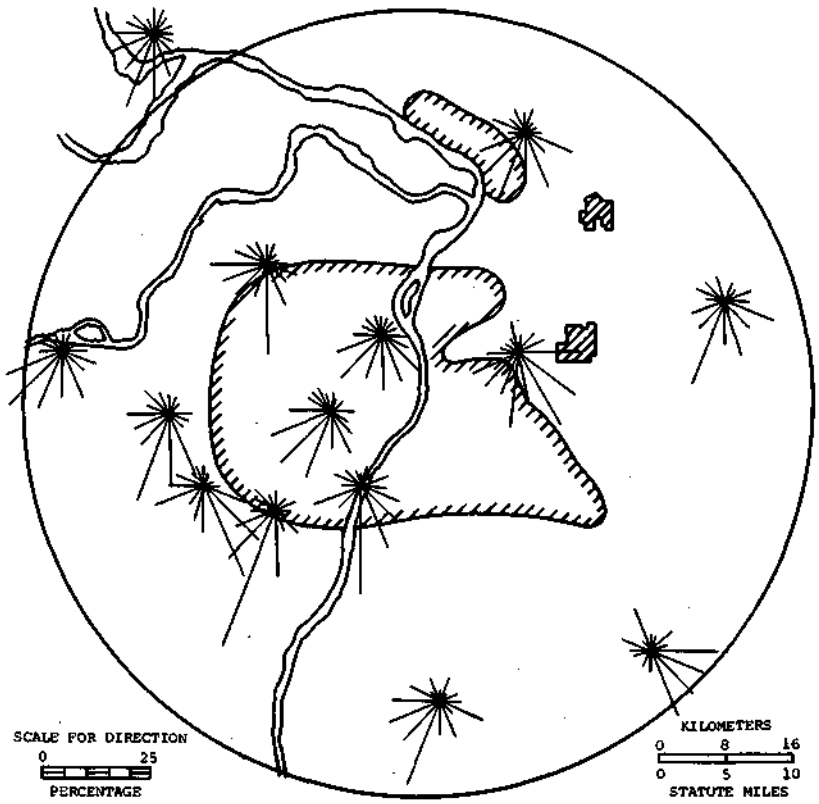

Figure B-39. Wind direction frequencies, all hours and all days, 1972-1975

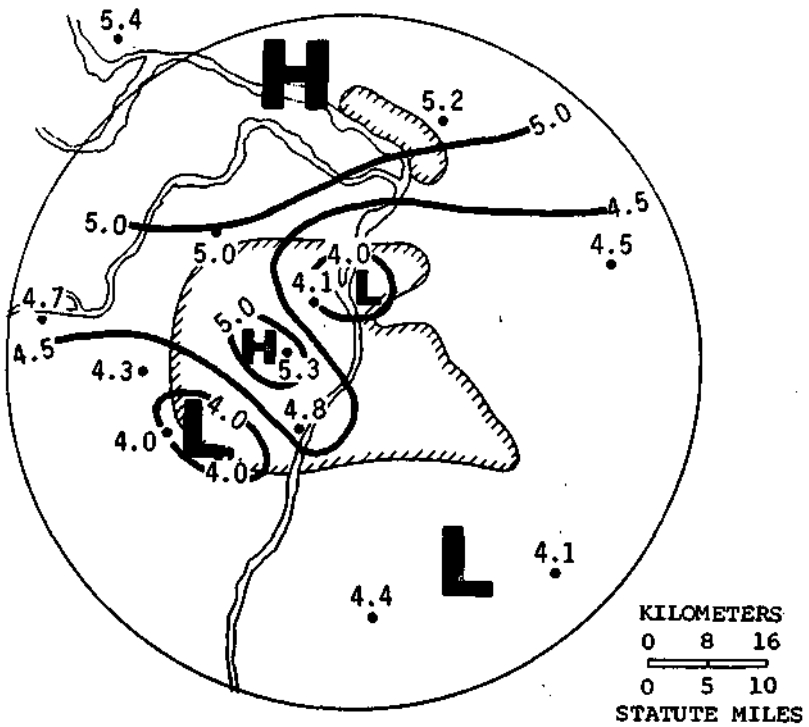

Figure B-40. Average wind speed (mph) for all summer days, 1972-1975

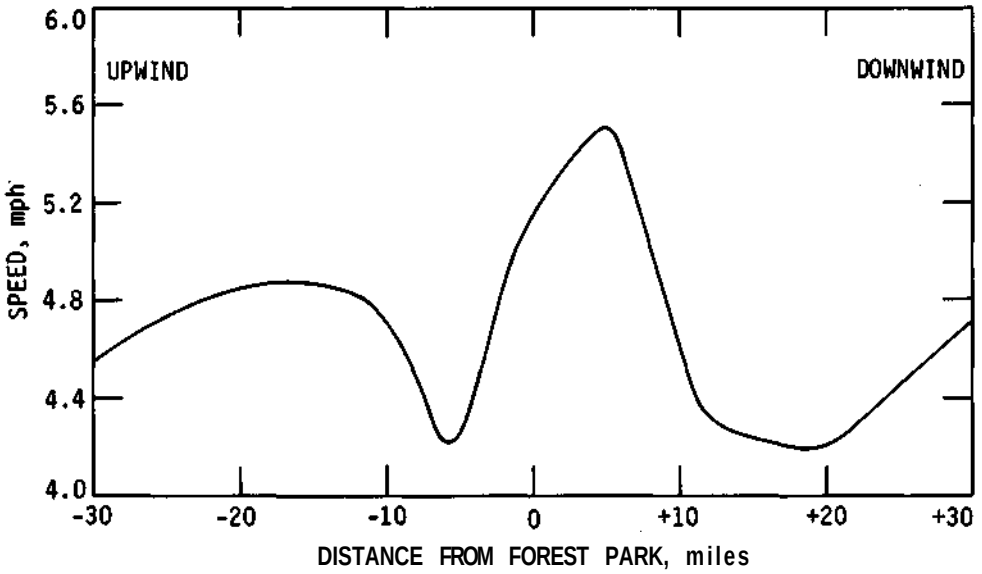

Figure B-41. Profile of average summer wind speeds across St. Louis, based on all wind directions

a 20% increase in the downwind portion of the urban area. This high is followed by a sizeable decrease, to 4.3 mph, 11 miles downwind. This downwind 'low' extends to about 20 miles beyond the urban center and then speeds 'to recover' to match the 30-mile upwind value at about 30 miles downwind of the city center.

Inspection of the profile on figure B-41 supports the land use analysis showing the suburban speeds to be lower than the urban and rural values. As winds approach the city they apparently are decreased by increasing surface roughness in the suburbs (Oke, 1973). Thermodynamic factors act to increase winds in and just beyond the center of the metropolitan area.

Figures B-42 and B-43 are based on the frequency of wind directions and average speeds of winds sorted according to four principal wind directions. North winds show a regional or background (north area) frequency of about 20% (figure B-42), reduced over St. Louis to become 13%. The shadow effect of the city extends southward at least 20 miles with northerly winds being 16% of the total at Waterloo. Examination of the easterly flow pattern (figure B-42) also shows an urban decrease, going from 30% east of St. Louis to 15% in the city.

The west wind pattern is different, showing an increase in the urban area but also showing a shadow extending well beyond (east of) St. Louis where only 15 to 20% of the winds were westerly as compared with 25 to 30% in and west of St. Louis. The south wind frequency pattern (figure B-42) has different features than the other three directional patterns. The frequency is increased in the southern half of the city, possibly reflecting an influence on flow (to become southerly in this area) when north or east winds predominate elsewhere. Otherwise the southerly frequency pattern is flat with all rural values between 35 and 38%. No urban shadow appears north of St. Louis.

Figure B-43 presents the average wind speed patterns for northerly easterly, southerly, and westerly winds. The north pattern shows a north-to-south decrease suggesting, as did the north wind frequency pattern, an urban reduction and shadowing (slowing) to the south of St. Louis. Rural values to the north were 5.0 to 5.4 mph, compared with 4.1 to 4.3 mph at Waterloo, Weiss Airport, and Lemonton. This N-to-S shadowing of the strong northerly winds (highest mean

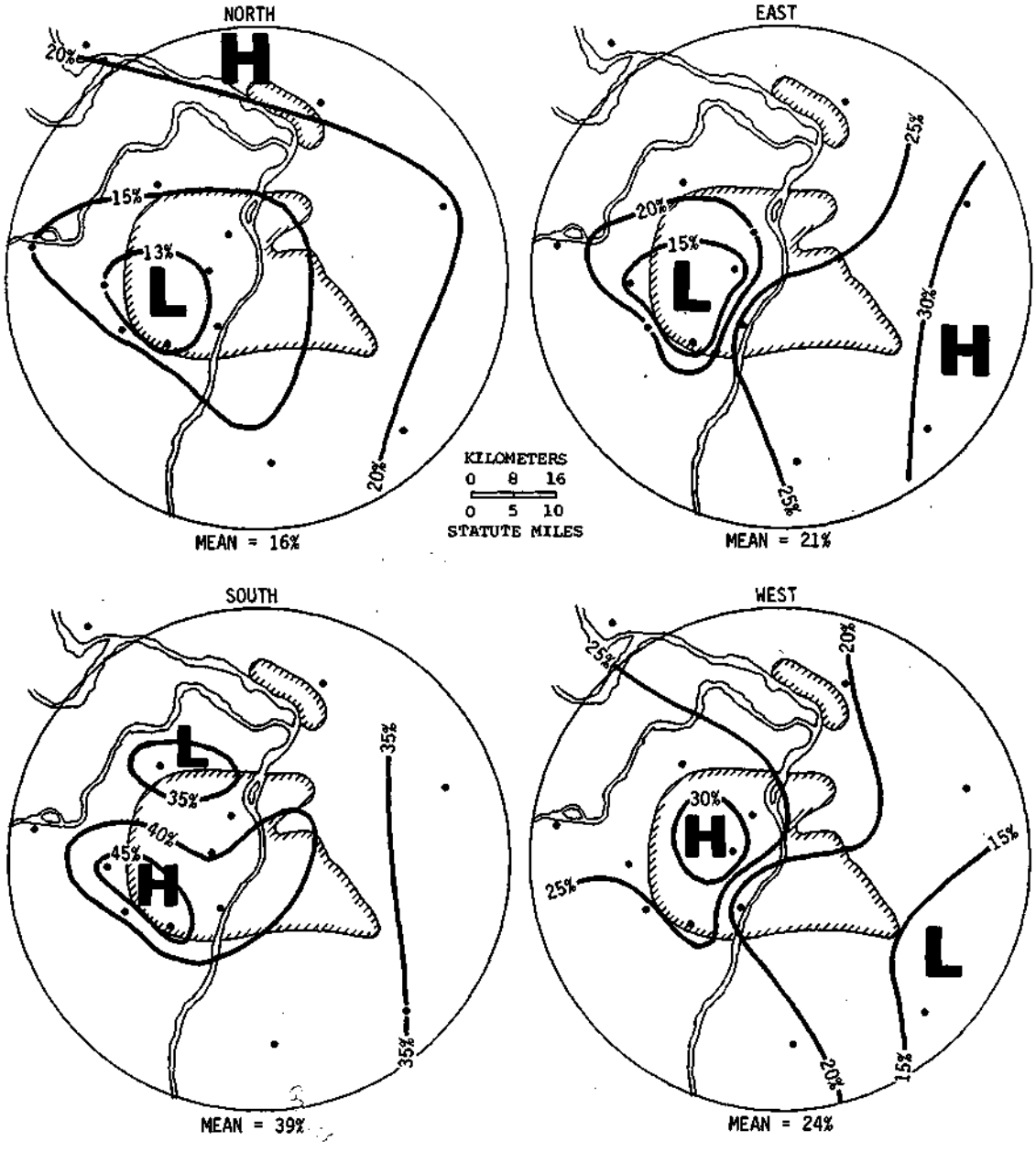

Figure B-42. Patterns based on the frequency of wind directions in four major directions

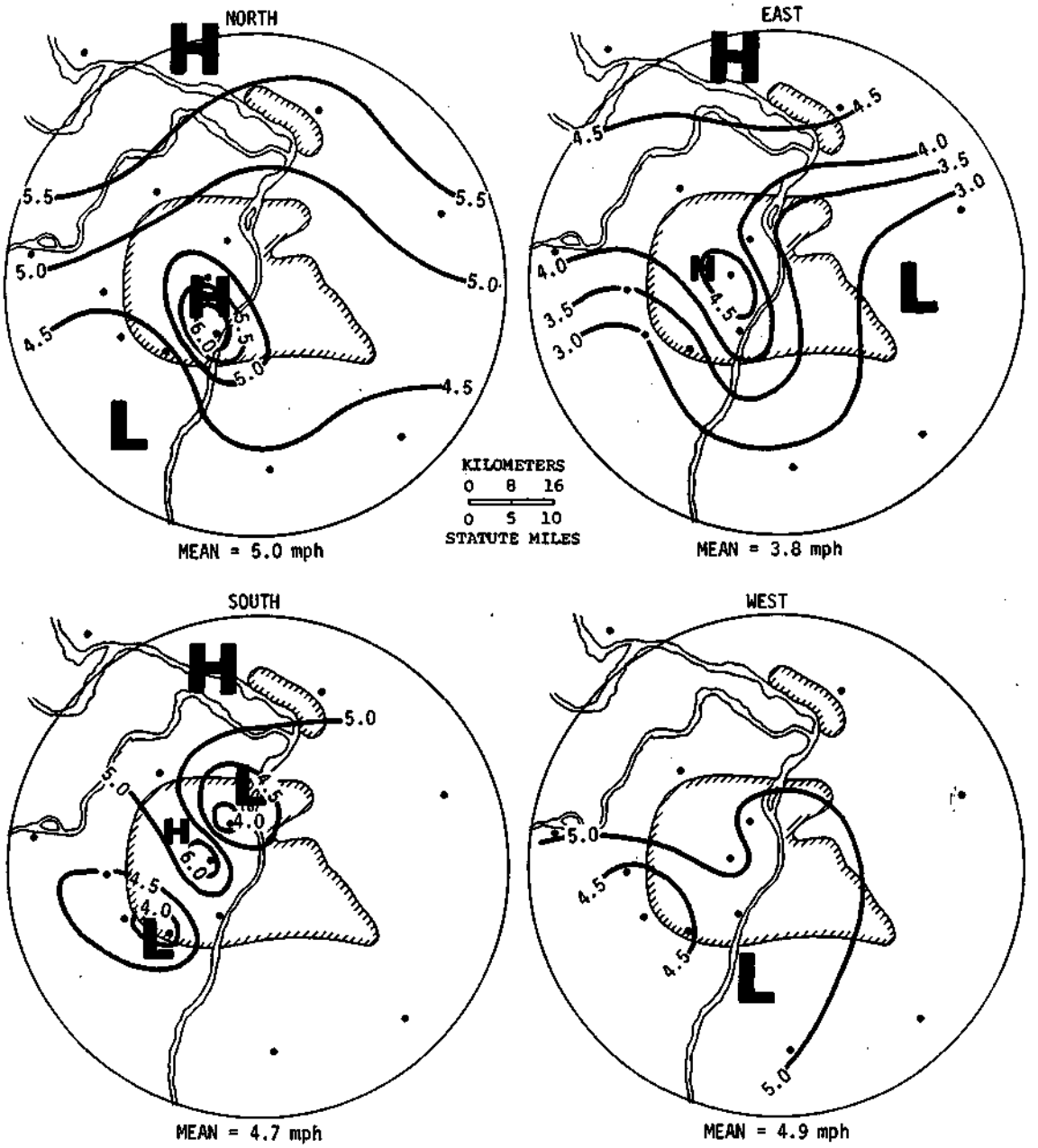

Figure B-43. Patterns of average speed (mph) for various prevailing wind directions

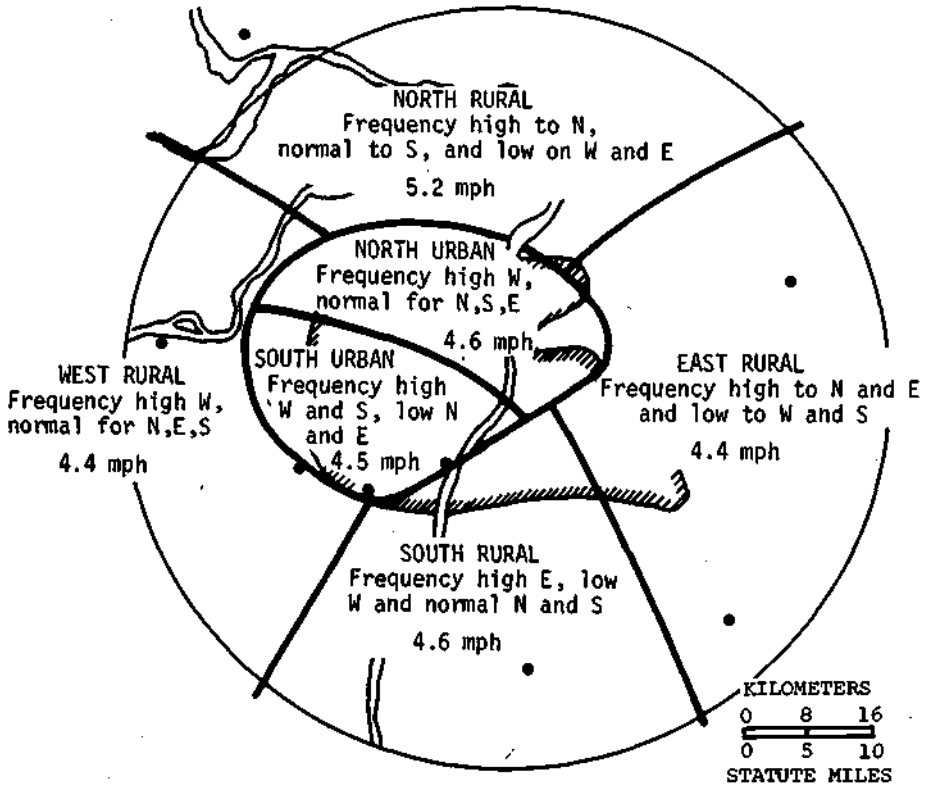

Figure B-44. Distinct areas of wind regimes

value of the four shown on figure B-43) is a major factor in producing the N-S gradient in the 4-summer speed pattern (figure B-40). Also shown for the north speed pattern is an area of acceleration in and to the south of the city center. This is typical of the cross section shown in figure B-41. The frequency of north winds is reduced in this area but the average is increased.

Average speeds with easterly winds (figure B-43) show an increase in and beyond the city. The urban shadowing of easterly wind frequencies (figure B-42) is not evident and, as with the northerly speed pattern, an urban center high is apparent.

The speed pattern with southerly winds also shows higher average speeds beyond St. Louis than south (upwind) of the city. They are 4.7 to 4.8 mph in the south and 5.1 to 5.5 mph north. This apparent S-to-N acceleration helps produce the 4-summer pattern (figure B-40), and may be somehow urban related or just a sampling vagary. Three other features of the south pattern deserve mention. Again, as in the north and east patterns, a high in speed is found in the city center. Also found are two small lows in the suburbs SW and NE of the city. The westerly speed pattern is generally flat except for a trough in the SW area. No acceleration or shadowing is evident.

Examination of the 4-summer directional values (figures B-39 and B-42) indicated six distinctly different regions. These wind regime regions appear on figure B-44 along with their basic characteristics and a region average speed. The rural regions are generally distinguished by their high upwind frequencies; that is, the west rural has a high west frequency. The two urban regions differ considerably with flow in the northerly area less disturbed than in the southerly area which has fewer N and E winds and more S and W winds than the undisturbed flows would predict.

Table B-11. Average Summer Wind Speeds for Major Land Use Areas for 6-hr Periods in the St. Louis Area

Period (CDT)	Speeds, mph			
	Rural	Suburban	Urban	Urban-rural
0001-0600	3.6	3.5	3.7	+0.1
0600-1200	5.0	4.7	5.1	+0.1
1201-1800	5.4	5.2	5.7	+0.3
1801-2400	3.8	3.5	4.0	+0.2

Diurnal Distribution of Summer Wind Conditions

Diurnal differences generally exist in surface winds because of the influence of daytime heating and nocturnal cooling. These factors, plus expected urban influences, led to an investigation of the characteristics of winds for the four 6-hour periods (0001-0600 CDT, 0601-1200 CDT, etc.) of the day.

Figure B-45 presents the patterns of average speeds for these four periods. All four periods show S-to-N increases in average speeds, although it is less in the daytime hours (0601-1800) than found at night. The S-N gradients at night are 3.5 to 4.5 mph (0001-0600 and 1801-2400), but are 4.9 to 5.3 mph for 0601-1200 and 5.3 to 5.8 mph for 1201-1800. All four patterns also reveal a maximum in the city center, although the daytime values are relatively higher than expected values (by typically > 1.0 mph) and higher than the nocturnal highs (by 0.5 to 1.0 mph). The two nocturnal patterns have twin low speed areas in the SW and NE urban areas. These are not evident in the daytime when higher overall speeds exist.

Table B-11 presents the diurnal distribution of the average wind speeds for three land use areas. The urban averages are the highest in all four periods and the suburban values are the lowest throughout the day. The urban-rural differences are greatest in the 1201-2400 period (time of greatest rainfall), being about 5% higher in the urban area.

Figures B-46a and B-46b present the wind direction frequency and speed patterns, by four major directions, for the 0001-0600 period. Under northerly flow there is an urban reduction in frequency and speed, except for a small maximum in the center of St. Louis. Shadowing in frequencies and speeds also occurs in the east and west patterns. South shows an up-city frequency maximum and the typical nocturnal low-high-low speed pattern.

The patterns for 0601-1200 CDT (figures B-47a and B-47b) are generally similar to those in 0001-0600. However, the west speed pattern for 0601-1200 CDT has high values in the city where a low existed at 0001-0600. The east speed pattern for 0601-1200 shows a SE-to-NW increase, whereas the 0001-0600 easterly pattern showed a downwind (west side) decrease.

The frequency and speed patterns for 1201-1800 CDT (figures B-48a and B-48b) are similar to those for 0601-1200 CDT. The frequency pattern for 1801-2400 (figure B-49a) also resembles that for all three earlier 6-hour periods. However, the wind speed pattern for 1801-2400 (figure B-49b) differs. The east speed pattern for 1801-2400 CDT shows an urban high, but with shadowing (decreases) in and west of the city. This resembles the 0001-0600 east pattern (figure B-46b) but not the two daytime patterns. The 1801-2400 CDT westerly speed pattern (figure B-49b) shows no urban high, whereas the daytime westerly speed patterns had a marked high.

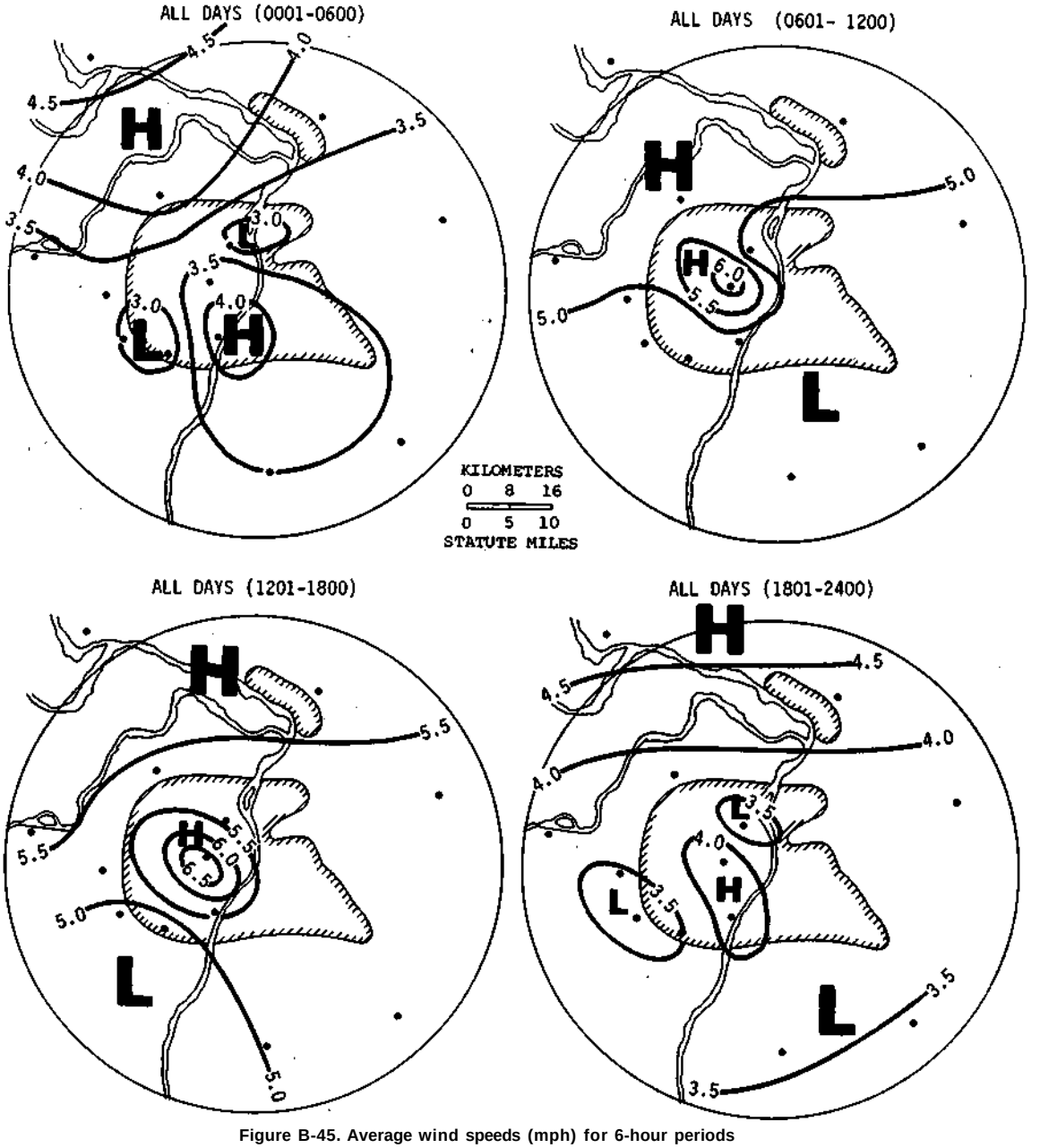

Figure B-45. Average wind speeds (mph) for 6-hour periods

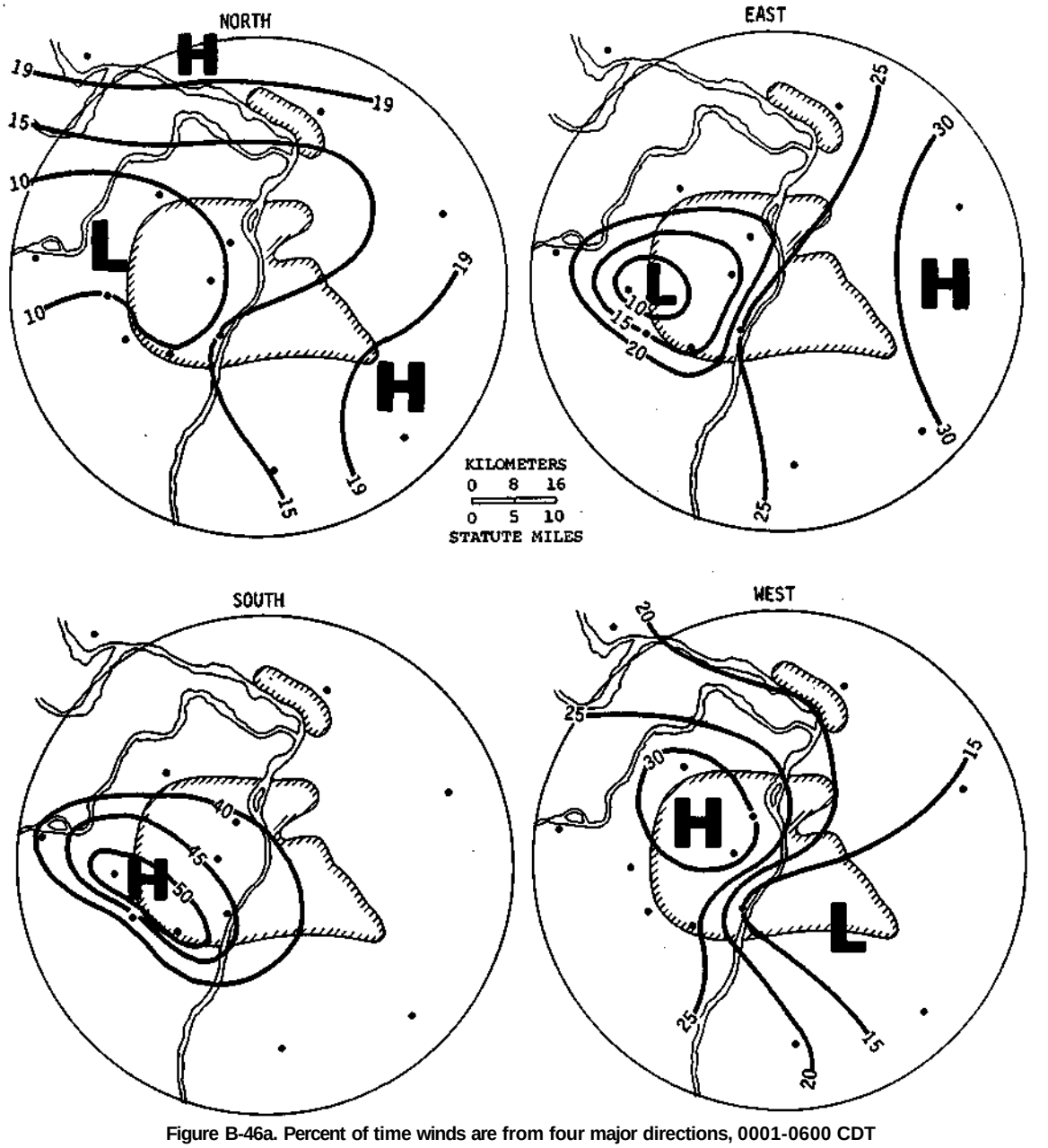

Figure B-46a. Percent of time winds are from four major directions, 0001-0600 CDT

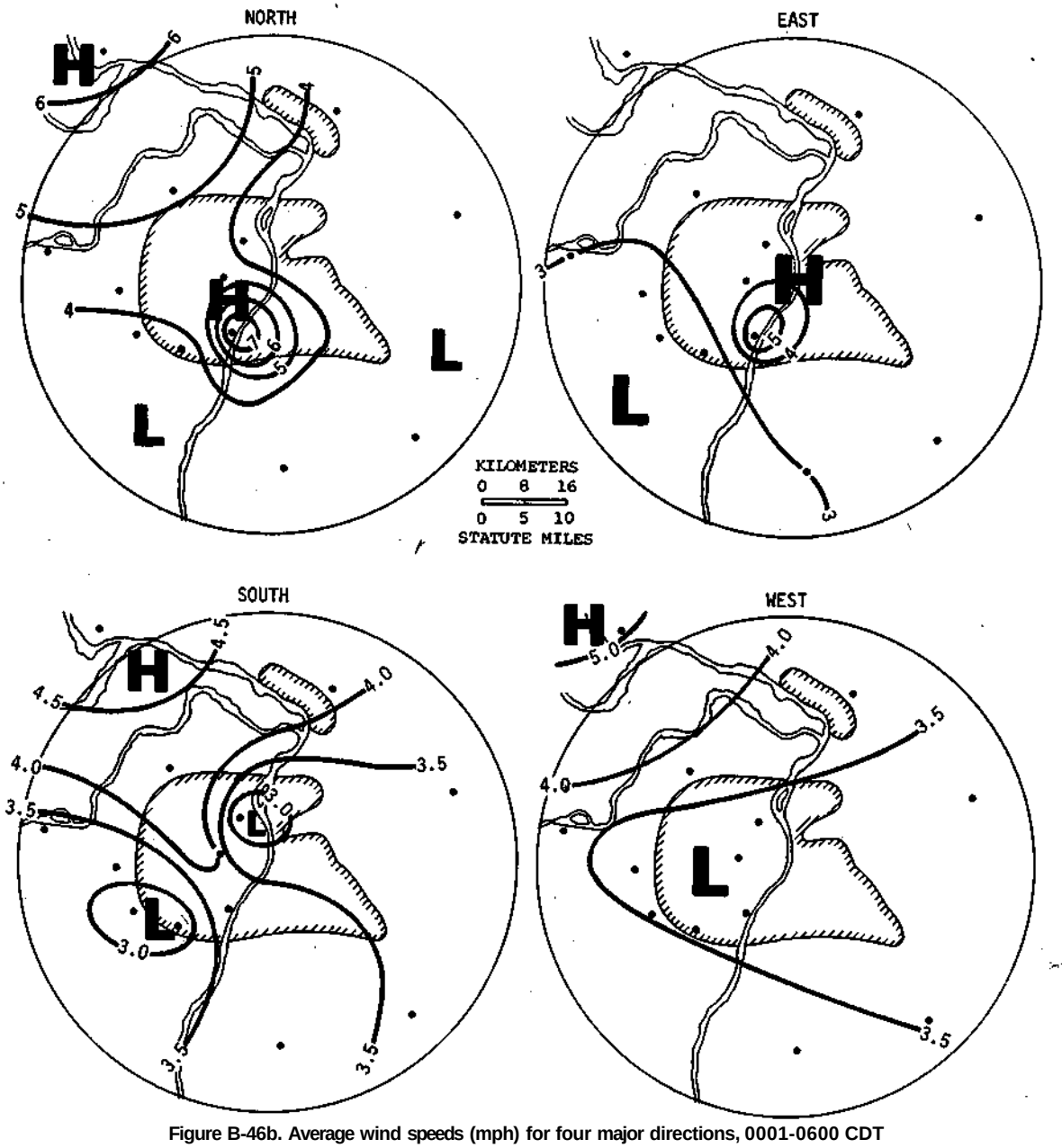

Figure B-46b. Average wind speeds (mph) for four major directions, 0001-0600 CDT

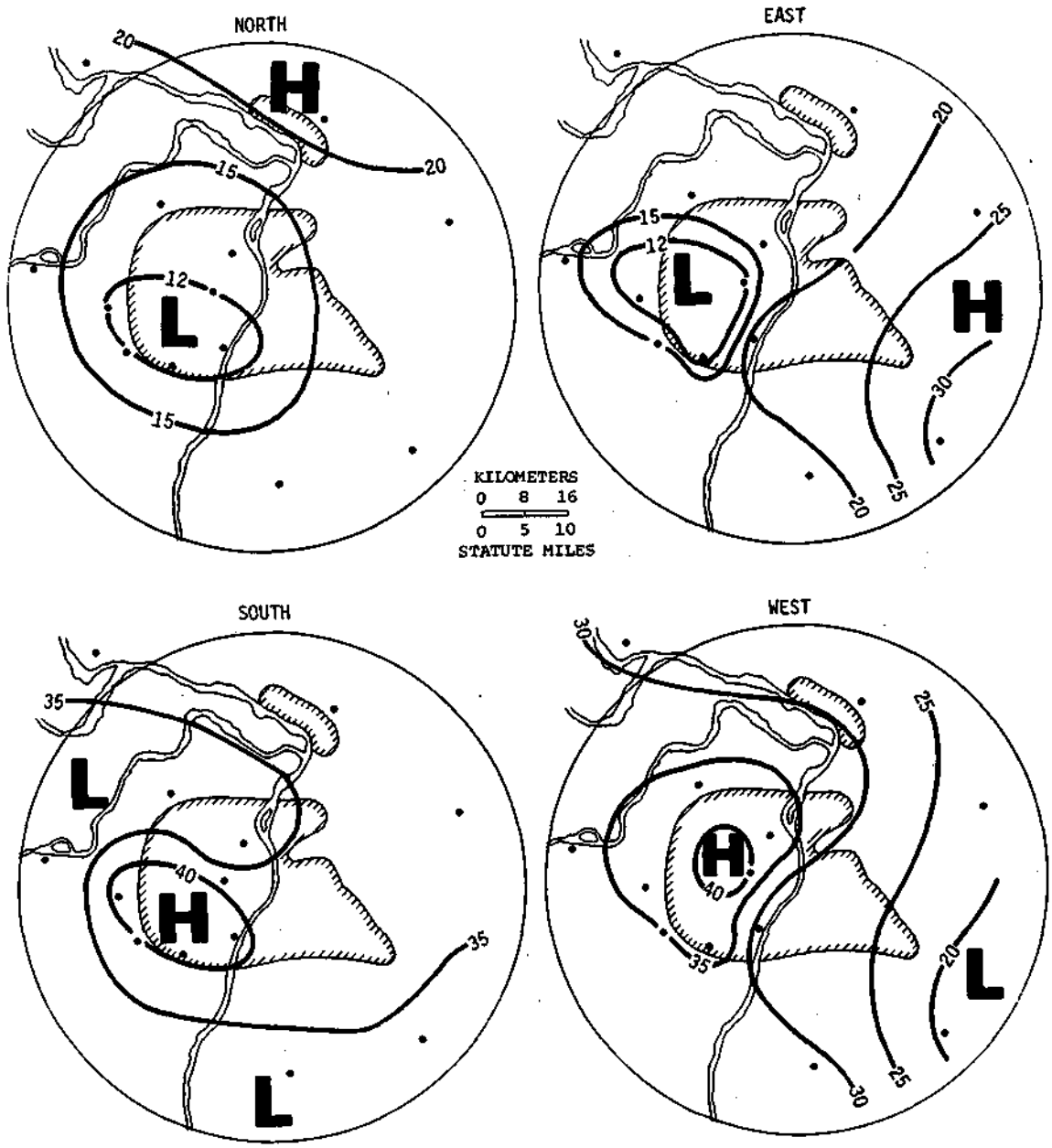

Figure B-47a. Percent of time winds are from four major directions, 0601-1200 CDT

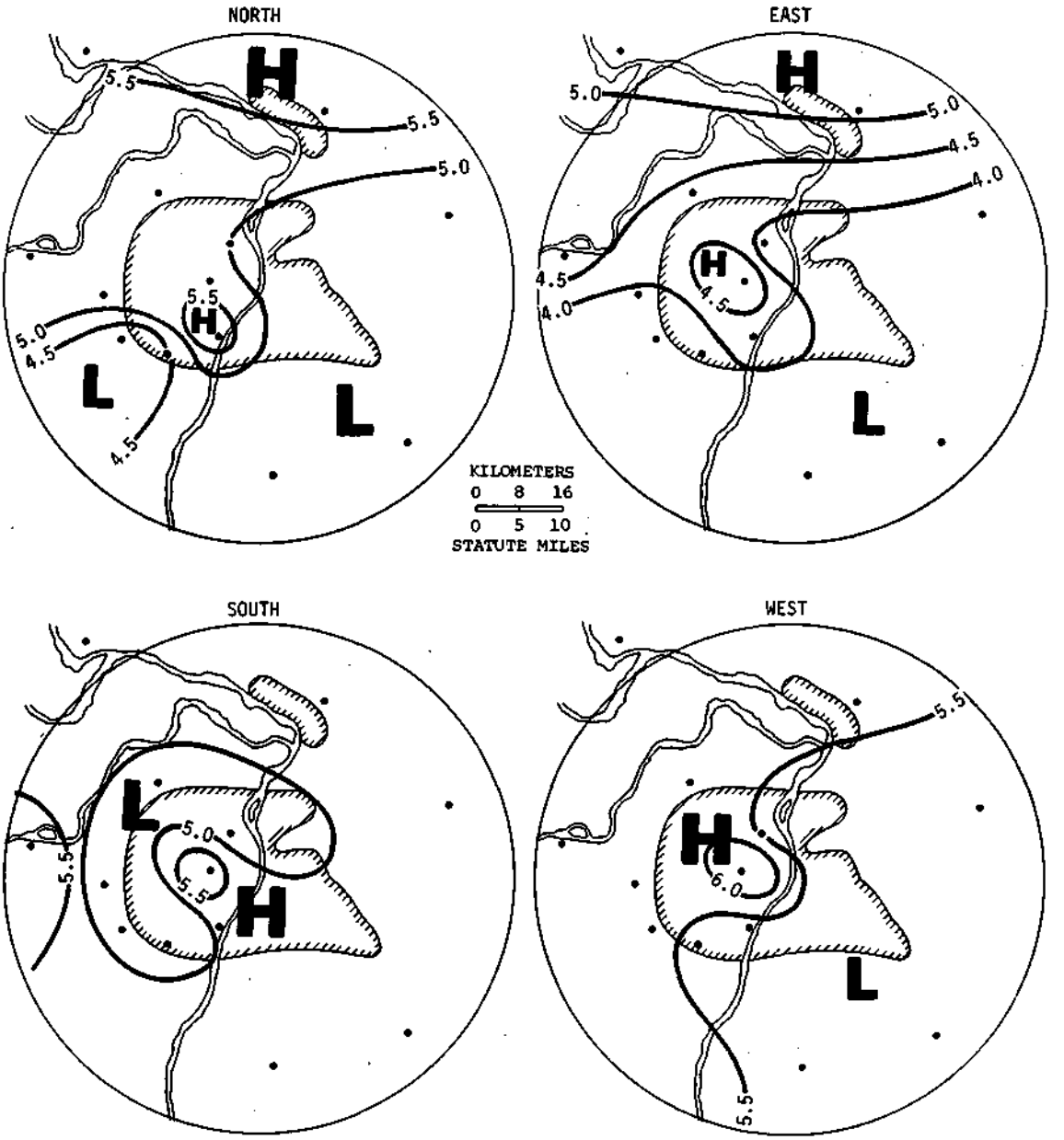

Figure B-47b. Average wind speeds (mph) for four major directions, 0601-1200 CDT

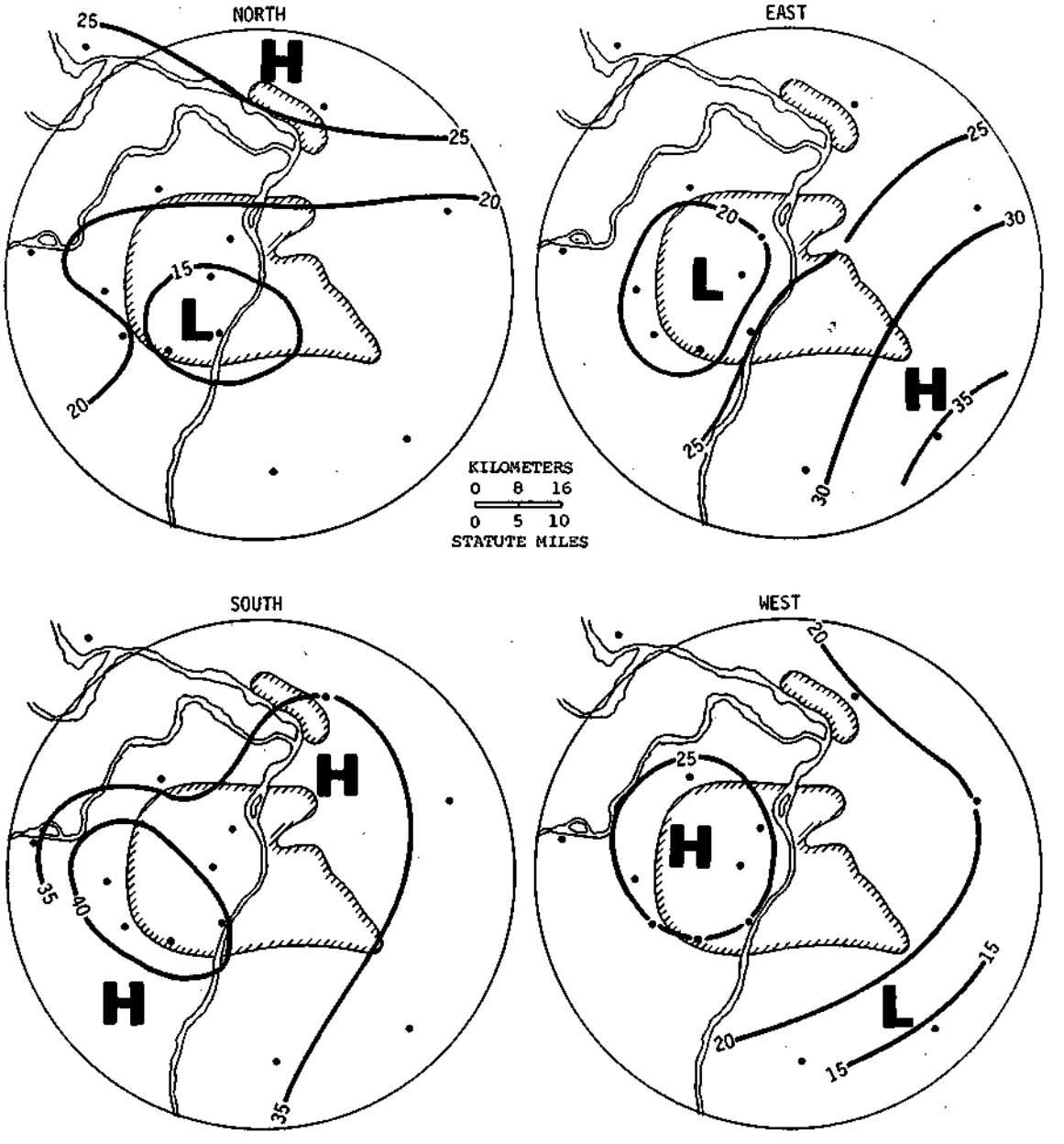

Figure B-48a. Percent of time winds are from four major directions, 1201-1800 CDT

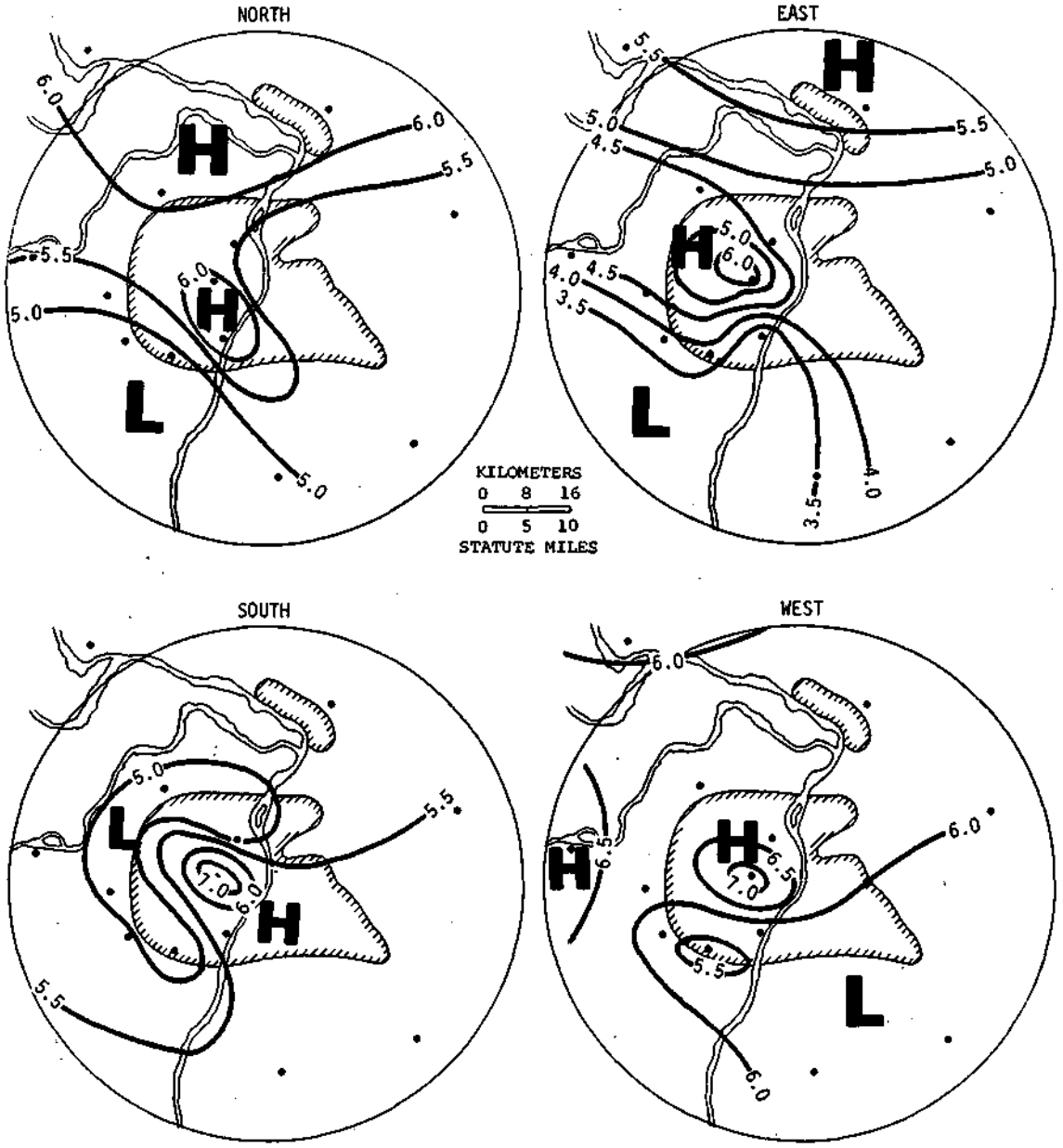

Figure B-48b. Average wind speeds (mph) for four major directions, 1201-1800 CDT

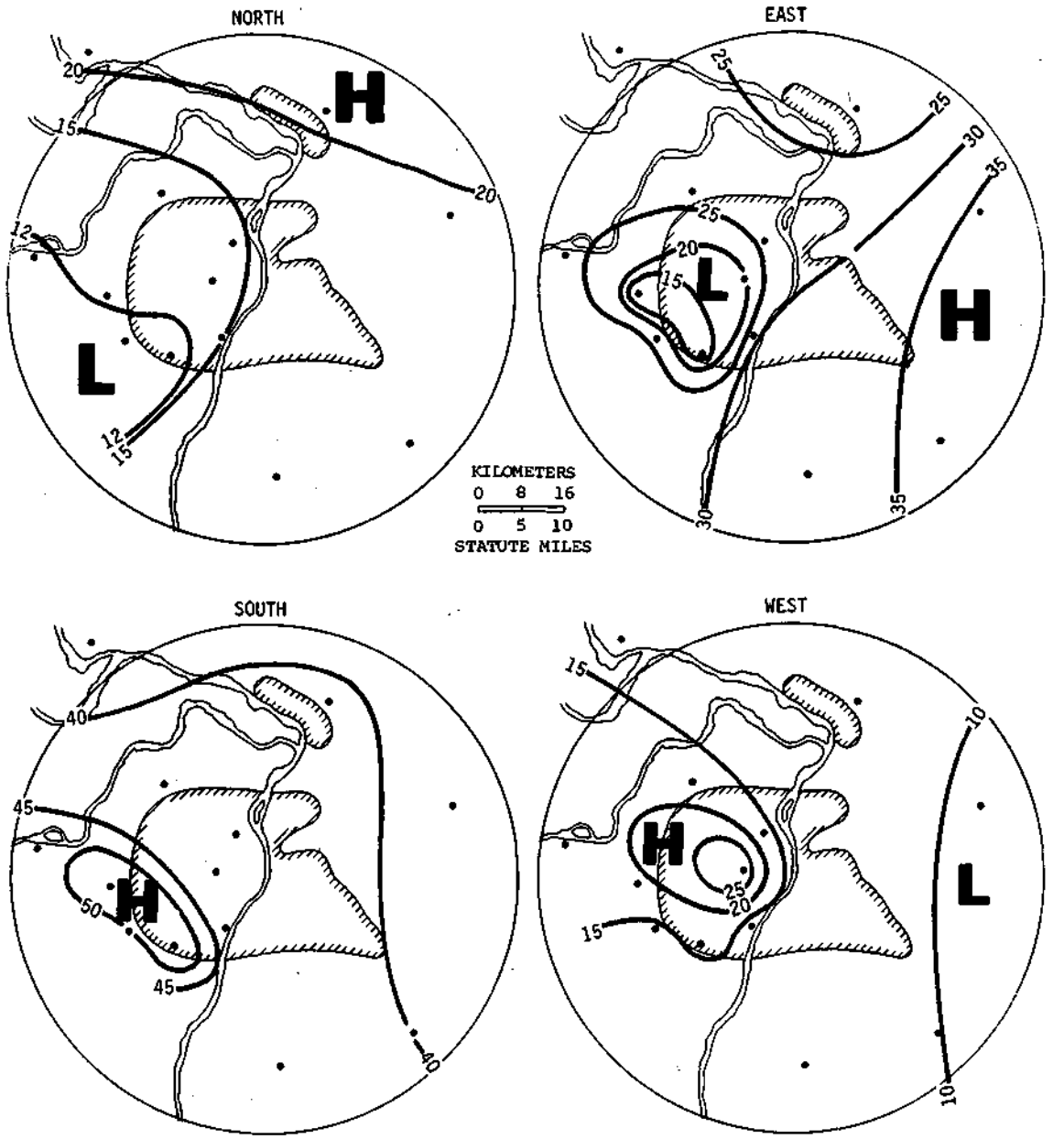

Figure B-49a. Percent of time winds are from four major directions, 1801-2400 CDT

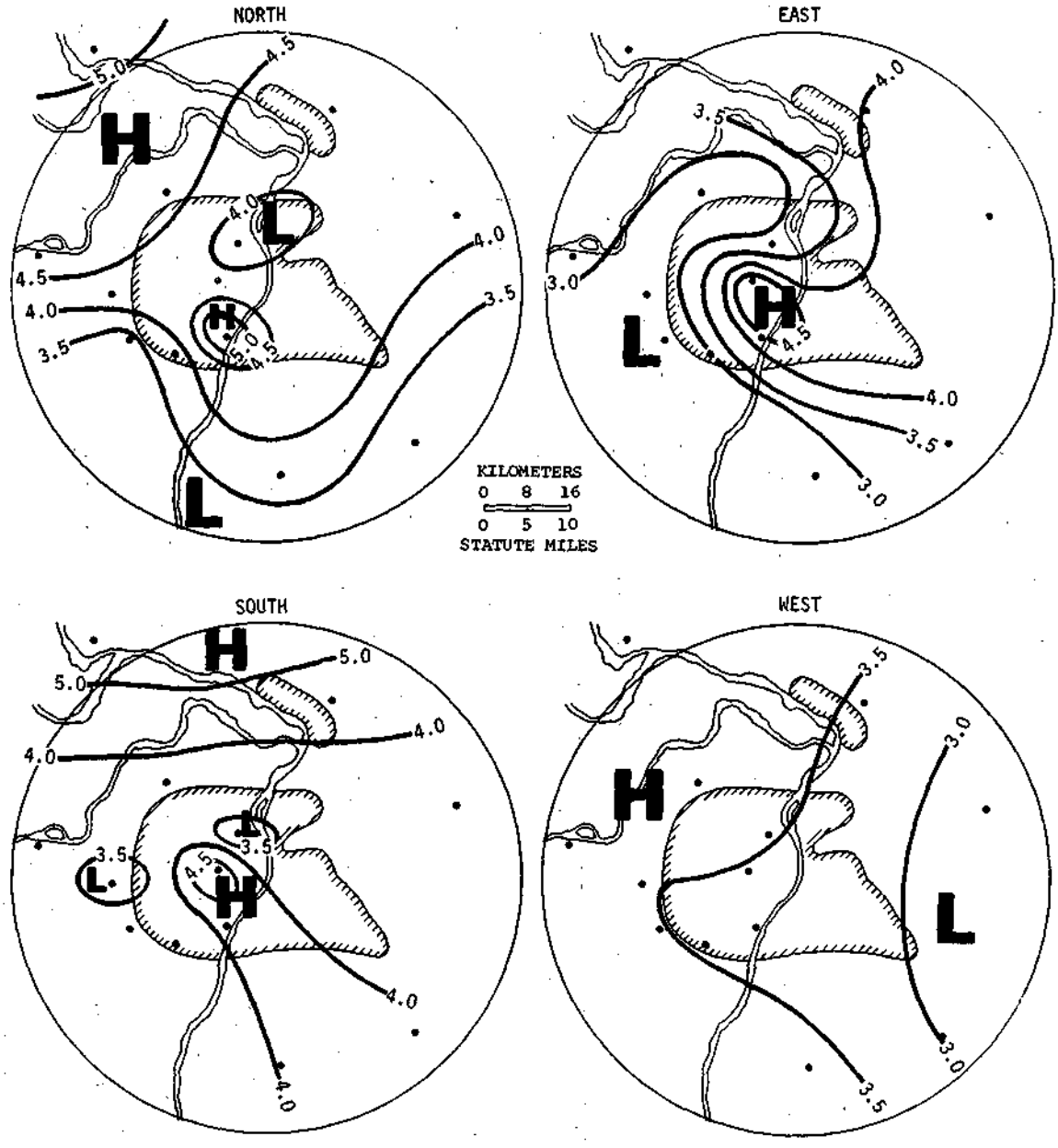

Figure B-49b. Average wind speeds (mph) for four major directions, 1801-2400 CDT

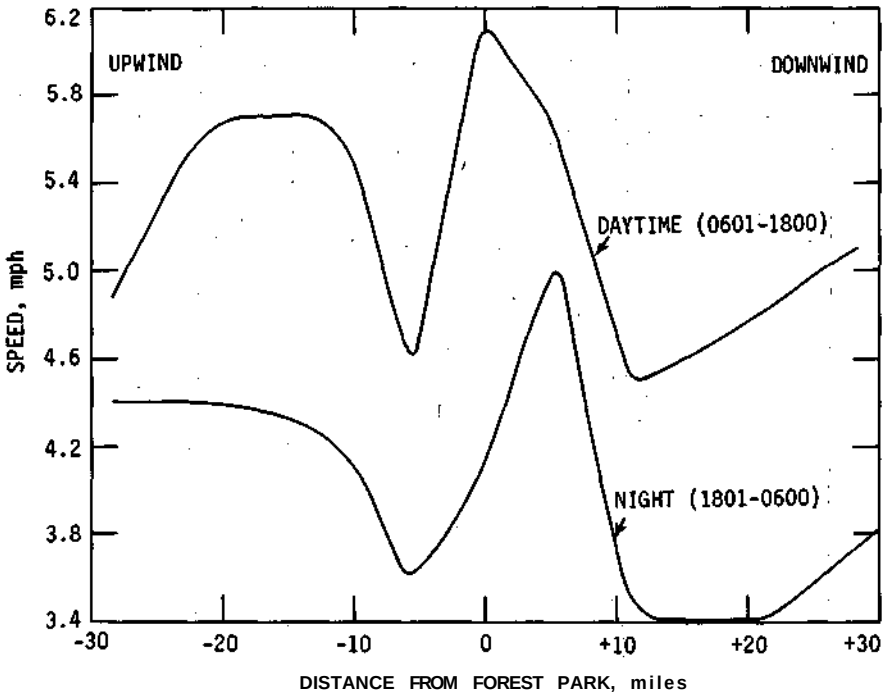

Figure B-50. Profiles of mean day and night wind speeds across St. Louis, based on all directions

In summary, the four 6-hour wind frequency patterns are very consistent throughout the day showing continuous features like 1) urban lows with north and east winds; 2) urban highs with south and west winds (particularly on the upwind half of the metropolitan area); and 3) shadowing beyond the city in the north, east, and west (but not south) patterns. The speed patterns for north and south show general consistency throughout the day. However, the east and west speed patterns in the day differ from their counterparts in the nocturnal hours.

An upwind-downwind cross-sectional analysis of average wind speeds through St. Louis was done for the daytime hours (0601-1800 CDT) and the nocturnal (1801-0600 CDT) hours. The resulting profiles (figure B-50) reveal certain interesting differences. Both show an urban maximum and the two 'suburban' minimums at about 5 miles upwind and 12 to 15 miles downwind. The speeds are lower at night and the nocturnal downwind effect (decrease) appears to extend beyond 30 miles. Speeds in the daytime indicate recovery to upwind unaffected speeds by 25 to 30 miles downwind of the city center. The urban maximums differ also, that at night being farther downwind.

In many respects the average wind profiles (figure B-50) at St. Louis resemble those for New York (Bornstein and Johnson, 1977). The New York nocturnal profile showed a maximum at 9 to 10 miles from the city center (5 to 7 miles at St. Louis). The New York daytime curve for light winds (<7 mph) showed a maximum at about 5 miles, similar to that at St. Louis. However, the New York profiles did not reveal the double minimums, between the rural area and the urban maximum, found at St. Louis. The New York wind observations differed. They were based on more stations; the night data were all 0000-0200 LST and the day data were all 1200 to 1400 LST, and they came from all seasons. Thus, some differences could be expected.

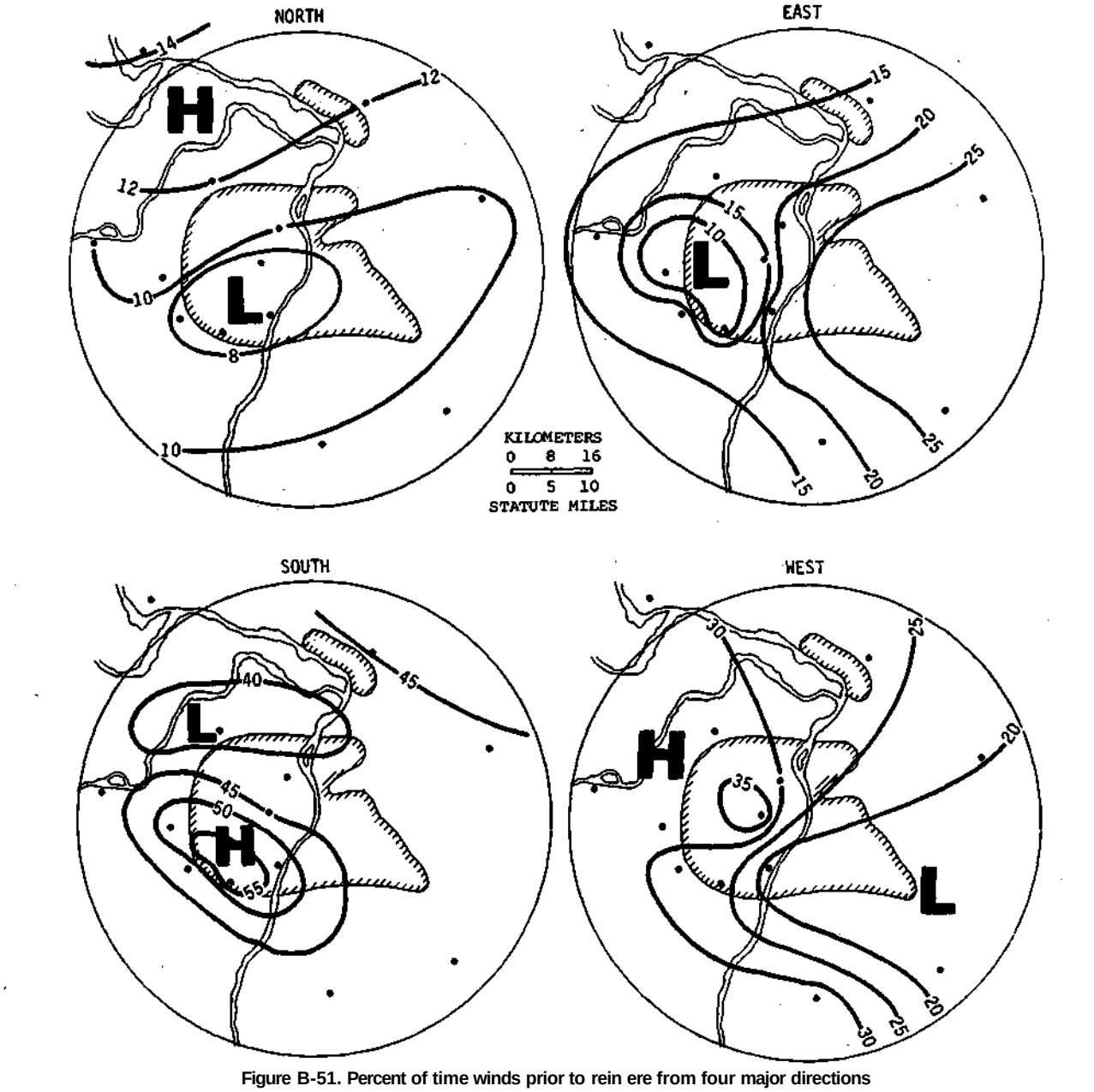

Figure B-51. Percent of time winds prior to rein ere from four major directions

Characteristics of Winds Prior to Rain

The wind direction and speed prior to the onset of rainfall in the St. Louis area are considered important in ascertaining the placement of the urban plume, and where and when convective elements might be under the influence of the urban area. The winds during the 3 hours prior to the onset of a rain period, as defined by rain anywhere within the circular raingage.network, were determined. This represented wind conditions prior to 183 network rain periods in the 1972-1975 period.

The frequency of winds from the four basic directions appears in patterns in figure B-51. Basically, the patterns resemble those for all days (figure B-42) with highs over the city with S and W

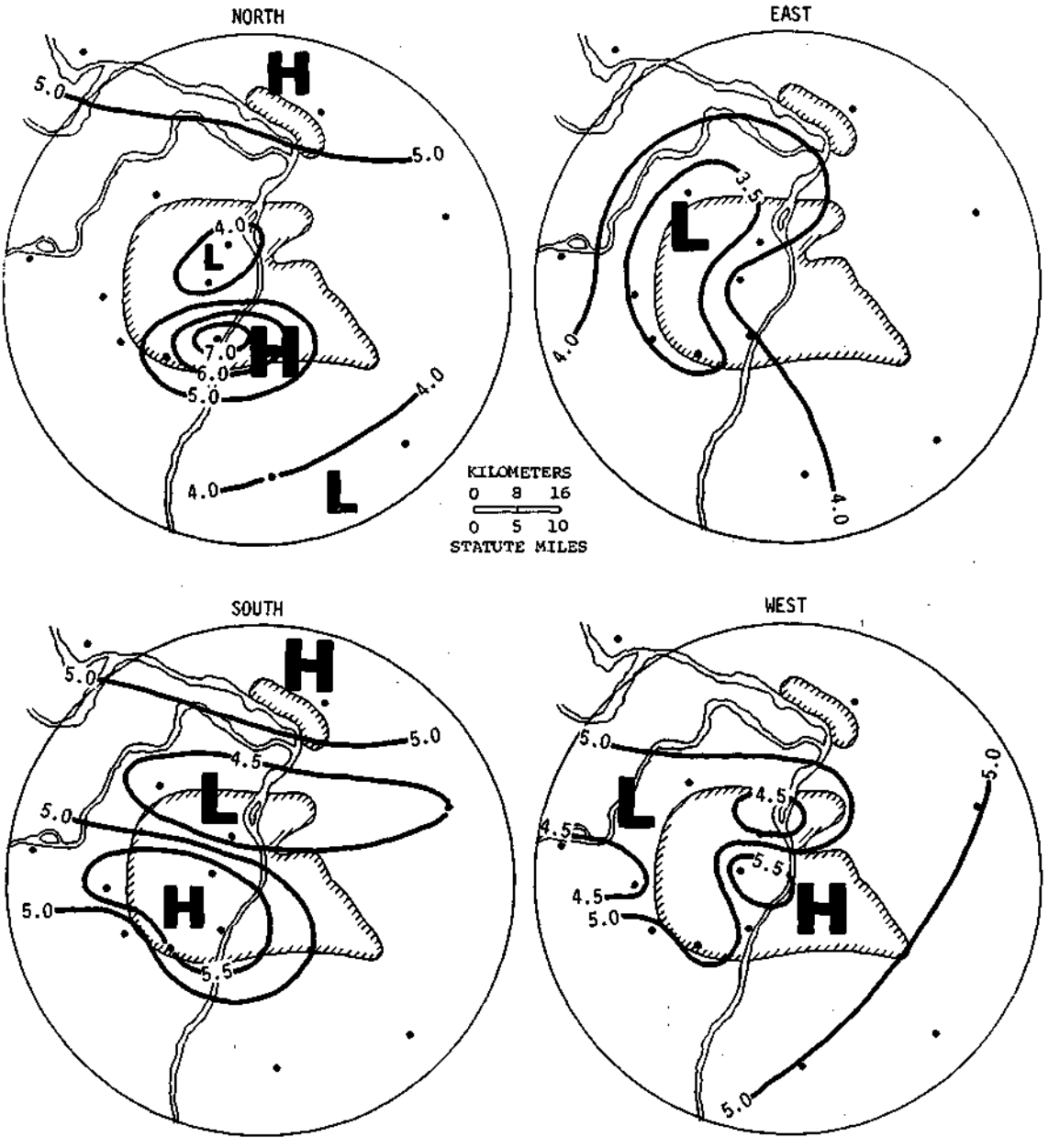

Figure B-52. Average wind speeds (mph) prior to rain for four major directions

winds. However, the frequency of S and W winds prior to rains is higher by 3 to 5%. The south wind pattern (figure B-51) has a major high in the south urban area (59% at the Mehlville station in SW St. Louis). Immediately north of this high, a low frequency area occurs, suggesting possible convergence in the northern part of the urban area.

Figure B-52 presents the average wind speed patterns for the four major directions and the 3 hours prior to rain. The north flow pattern shows a major speed maximum in and just south of St. Louis, and this maximum is much greater than that found for all winds (see figure B-43). East wind speeds are diminished over the western urban area, as are their frequencies (figure B-51).

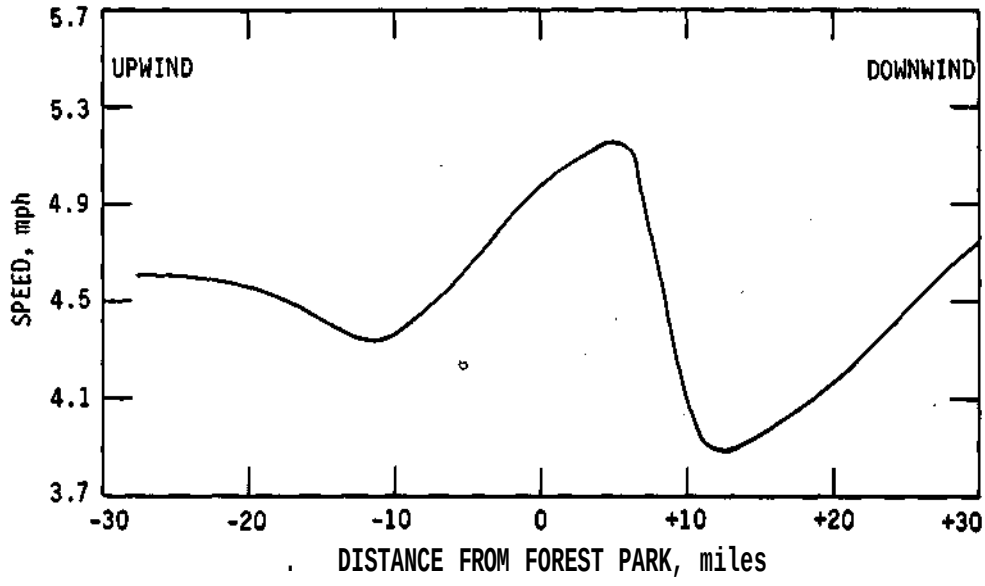

Figure B-53. Profile of average speeds across St. Louis for the 3-hour periods prior to rain based on all directions

The south wind speed pattern prior to rain (figure B-52) is quite different from the summer average (figure B-43). The pre-rain speed pattern is like the south frequency pattern with a high over the south urban area and a low beyond (north) of it, helping to suggest urban induced wind convergence. The west speed pattern indicates low values west of St. Louis with a maximum at Forest Park where there is also a frequency maximum (figure B-51).

A cross section based on average pre-rain wind speeds, and for all wind directions, done by. combining profiles passing through the city center, appears in figure B-53. This suggests a major maximum over and up to 6 miles beyond the city center, followed by a major decrease, from 5.2 to 3.9 mph, at 12 to 15 miles downwind. This should be a zone of convergence.

The six distinct wind regions, as defined on figure B-44, were studied for the pre-rain situation. Table B-12 presents the area mean speeds and their differences from the all hours summer sample. In general, the pre-rain speeds are higher by 0.1 mph, but over the north urban and

Table B-12. Mean Wind Speeds Prior to Rain in Wind Regions

*Regions**	*Mean speed (mph)*	*Difference between 3-hrs prior and all hours*
South urban (3)	4.6	+0.1
North urban (2)	4.8	+0.2
West rural (2)	4.5	+0.1
South rural (2)	4.7	+0.1
North rural (2)	5.7	+0.4
East rural (2)	4.5	+0.1

• *Number of stations given in parentheses*

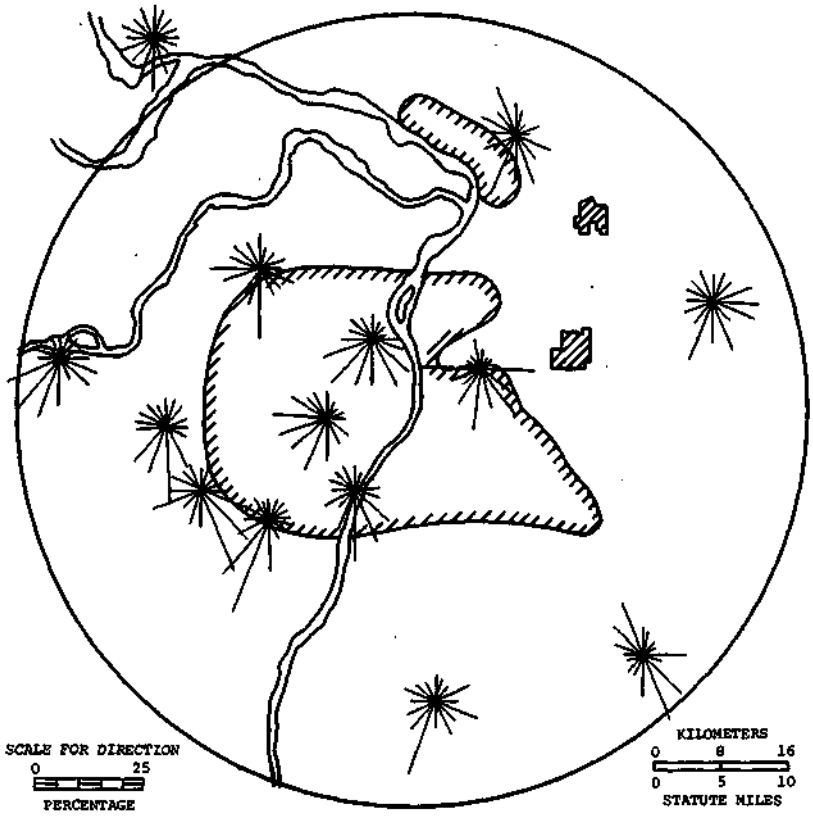

Figure B-54. Wind direction frequencies for the 3 hours prior to rein, 1972-1975

north rural area, they are even higher. The mean pre-rain speeds for the three major land use areas were 4.8 mph for the rural area, 4.7 mph for the suburbs, and 4.8 mph for the urban area. This indicated little regional difference in speeds.

The pre-rain wind direction frequencies for 16 directions appear as frequency roses in figure B-54. Most rural stations (Pere Marquette, Alton, Nagels Farm, Waterloo, and Spirit of St. Louis) show a predominance of southwesterly flows prior to rain, all with prevailing directions of SSW. However, two stations to the east (Cahokia and Lemonton) show SE as the prevailing direction. Lemay and Mehlville (south urban area) show south to be most frequent. Several suburban and urban stations show SW to be the prevailing direction. These prevailing directions (from SE at stations to the SE of St. Louis, S to the south, and SW at stations to the SW of St. Louis) collectively indicate a net convergence of pre-rain winds over and north of the city.

Winds in Rain and No-Rain Periods

Differences, if any, in surface wind characteristics between network rain periods and no-rain periods were examined for the summer seasons of 1972 through 1975. Figure B-55 presents the average wind speed pattern for rain periods. In general, the pattern closely resembles the summer average pattern (figure B-40). However, the rain values are faster. The point differences between the rain winds and all-hour winds, as shown in figure B-55, are generally 0.1 to 0.4 mph faster.

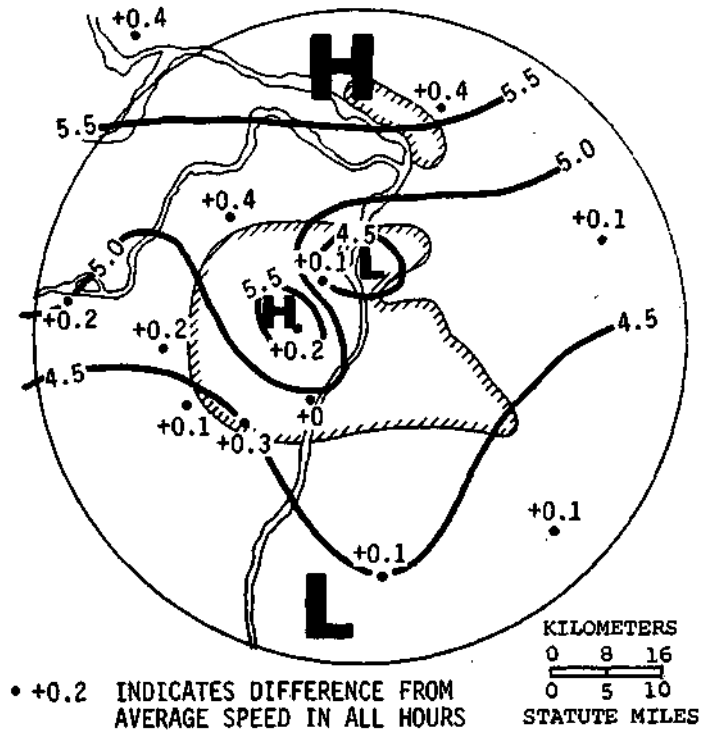

Figure B-55. Average wind speed pattern tor rain periods, 1972-1975

Patterns of average wind speeds for the four principal wind directions were developed for the rain cases and for the no-rain cases. They were compared and their differences appear in figure B-56. The north wind differences show that winds in rain periods are higher than no-rain winds in the rural north, but north winds in rain are lower in the urban area. East winds in rain (figure B-56) are higher than no-rain speeds throughout the area with an urban center maximum.

The southerly flow differences show an increase in rain winds in the southern urban area, followed by slower speeds or less difference in the northern part of the urban area. This indicates a relative acceleration of winds during rain due to urban factors, followed by deceleration (less difference) in the downwind portions of the urban area. The differences with westerly winds show an increase, or relative acceleration, in winds during rain over the urban area. This is followed by a relative decrease in differences such as rain winds becoming slower than no-rain winds east of St. Louis.

Summary

This climatic-type investigation of the summer surface winds has dimensionalized the regional wind characteristics and the influence of the metropolitan area on the winds. Although the urban effect varies with wind direction, in general the urban effect perturbs the surface winds, both in direction and speed, out to about 30 miles downwind of the urban center (Forest Park). Winds inside the metropolitan area are different, under most circumstances, from rural winds, both as to direction frequency and speed.

There is a general south-to-north increase of 20% across the network in wind speeds in all hours, in pre-rain hours, and in rain hours. This appears to occur because the city buffers or

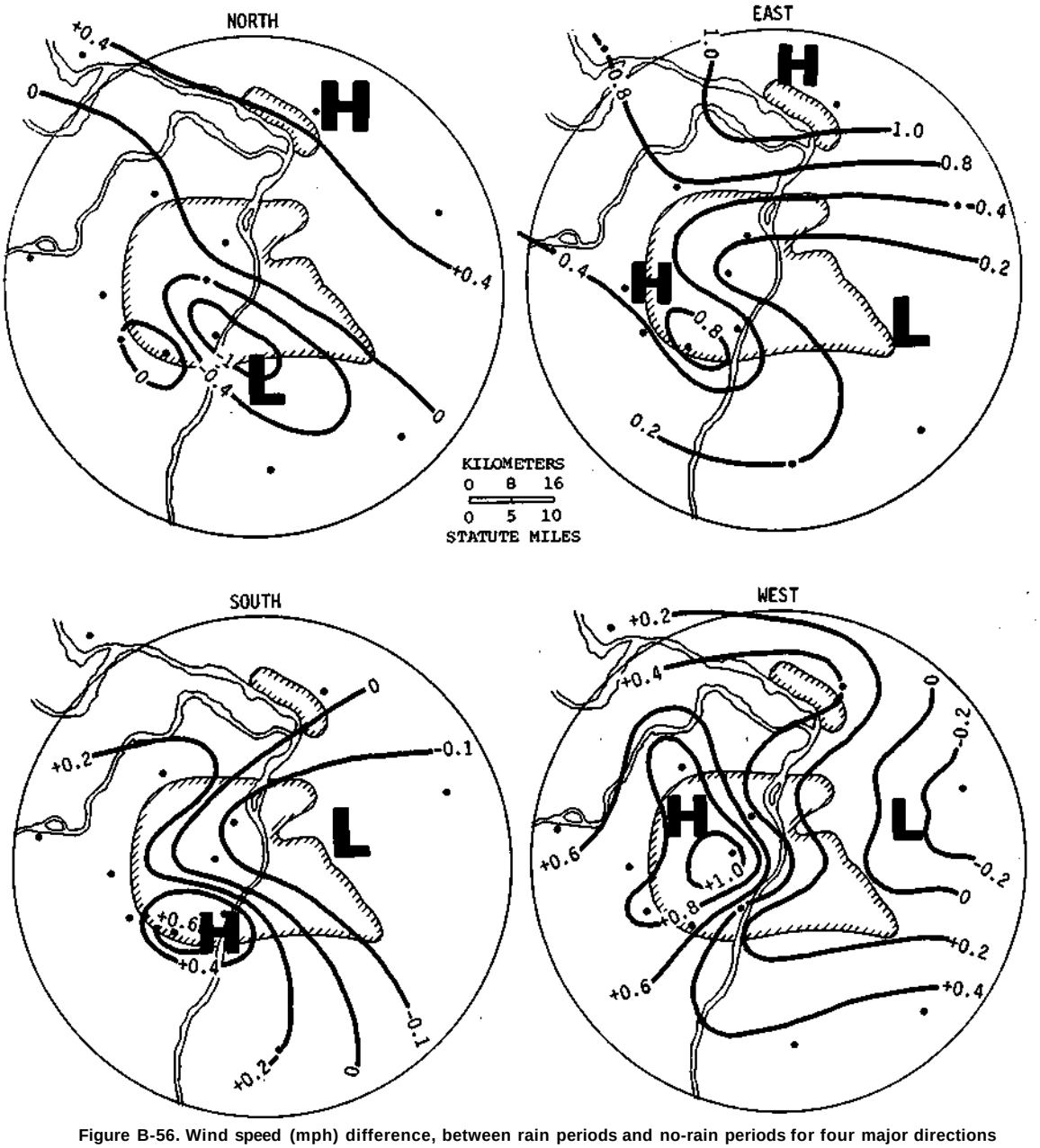

Figure B-56. Wind speed (mph) difference, between rain periods and no-rain periods for four major directions

shields the north winds, decreasing them in the city and well to the south (~20 miles), whereas the city does not buffer the south and east winds which are as high or higher beyond the city.

Basically, the city reduces the frequency of winds in and well beyond it when the winds are from the north, east, or west. The frequency of southerly winds is increased over the southern metropolitan area but is otherwise unaffected.

Wind roses for all hours and for pre-rain conditions both show that prevailing winds at stations to the E of the St. Louis area are SE, those to the south are southerly, and those to the SW and W of St. Louis are from the SW. Thus, convergence of the prevailing flow over the city is indicated.

Patterns of average wind speeds most often display:

1) The highest network speed (+15 to 20%) over or just beyond the urban center
2) Areas of low speeds (—10%) in the SW and NE urban areas
3) A decrease beyond the city with north or west winds
4) An increase beyond the city with south and east winds

Profiles of wind speeds show decreases, on the average, over the suburban areas. Urban average wind speeds, on the average, were slightly higher (+2%) than rural speeds, and suburban area averages were lowest, being 5% less than rural speeds.

The wind direction distributions do not change very much on a diurnal basis. The urban area has increases in the number of S and W winds in all hours and has decreases in N and E winds at all times. The major diurnal differences, other than the fact that winds at night are lower than those in the daytime, relate to the fact that:

1) The city center wind maximum in the day is relatively greater than it is at night
2) Speeds with west winds have an urban high in the day and an urban low at night
3) Speeds with east winds at night are decreased over the city and beyond, but are increased in and beyond the city in the daytime

Winds in the 3 hours prior to summer rain periods have patterns, in both direction frequencies and average speeds, much like those for all summer hours. However, the frequency of S and W winds over the city is relatively higher (3 to 5%) in the pre-rain cases with a low, in both wind frequency and speed, in the downwind urban-suburban areas. This suggests 1) acceleration, 2) deceleration, and then 3) convergence over the downwind urban area. Pre-rain winds and winds during rains are faster on the average than no-rain winds.

The St. Louis metropolitan area, through mechanical and thermodynamic effects, affects wind speeds and directions in the city and at least 10 miles beyond its border. Urban wind directions are altered with more southerly and westerly winds and fewer easterly and northerly. Urban wind speeds are increased in some circumstances and decreased in others but generally the center of the urban area has the area's highest speeds. There is a suggestion of greater low-level convergence due to the city during pre-rain periods. The metropolitan area has two distinctly different regions of wind regimes. The southwestern two-thirds, approximately, has high frequencies of S and W winds plus a suburban area of low speeds and a center area of high speeds. The other part of the urban area, generally the northeastern third, has more northerly winds with fewer southerly winds and is an area of relatively low wind speeds.

REFERENCES IN PART B

Ackerman, B. 1971a. *Moisture content of city and country air.* Preprints Conference on Air Pollution Meteorology, AMS, Boston, pp. 154-158.

Ackerman, Bernice. 1971b. *An urban-rural comparison of humidity.* Argonne National Laboratory Radiological Physics Division Annual Report ANL 7860 Part III, pp. 193-205.

Ackerman, Bernice, and Brian Wormington. 1971. *Some features of the urban heat island.* Argonne National Laboratory Radiological Physics Division Annual Report ANL 7860 Part III, pp. 183-191.

Atwater, Marshall A. 1971. *The radiation budget for polluted layers of the urban environment.* Journal of Applied Meteorology v. 10(4):205-214.

Boatman, J. F., and A. H. Auer, Jr. 1974a. *Inadvertent thunderstorm modification by an urban area.* Fifth Conference on Weather Forecasting and Analysis, AMS, Boston, pp. 183-188.

Boatman, J. F., and A. H. Auer, Jr. 1974b. *Inadvertent thunderstorm modification by an urban area.* Fourth Conference on Weather Modification, AMS, Boston, pp. 366-373.

Bornstein, R. D., and D. S. Johnson. 1977. *Urban-rural wind velocity differences.* Atmospheric Environment v. 11:597-604.

Brunt, D. 1941. *Physical and dynamical meteorology.* Cambridge University Press, London, 428 pp.

Chandler, T. J. 1965. *Climate of London.* Heffner & Sons, Ltd., Cambridge, England.

Chandler, T. J. 1967. *Absolute and relative humidities in towns.* Bulletin American Meteorological Society v. 48(6):394-399.

Changnon, S. A., Jr., F. A. Huff, P. T. Schickedanz, and J. L. Vogel. 1977. *Summary of METROMEX, Volume 1: Weather anomalies and impacts.* Illinois State Water Survey Bulletin 62, 260 p.

Changnon, S. A., Jr., and R. G. Semonin. 1975. *Studies of selected precipitation cases from METROMEX.* Illinois State Water Survey Report of Investigation 81, 329 p.

Dirks, R. A. 1974. *Urban atmosphere: Warm dry envelope over St. Louis.* Journal of Geophysical Research v. 79(24):3473-3475.

Hage, K. D. 1975. *Urban-rural humidity differences.* Journal of Applied Meteorology v. 14(10):1277-1283.

Inman, R. L. 1969. *Computation of temperature at the lifted condensation level.* Journal Applied Meteorology v. 8:155-158.

Jones, Douglas M. A. 1973. *Network surface temperature and humidity. In* Summary Report of METROMEX Studies, 1971-1972, Floyd A. Huff, editor, Illinois State Water Survey Report of Investigation 74, pp. 95-97.

Jones, Douglas M. A., and Paul T. Schickedanz. 1974. *Surface temperature, moisture, and wind studies. In* Interim Report of METROMEX Studies: 1971-1973, Floyd A. Huff, editor, NSF Grant GI-38317, pp. 98-120.

Kopec, R. J. 1973. *Daily spatial and secular variations of atmospheric humidity in a small city.* Journal of Applied Meteorology v. 12(4):639-648.

Landsberg, H. E. 1956. *The climate of towns. In* Man's Role in Changing the Face of the Earth. University of Chicago Press, pp. 584-606.

Landsberg, H. E. 1975. *Atmospheric changes in a growing community. (The Columbia, Maryland, Experience.)* Technical Note BN 823. Institute for Fluid Dynamics and Applied Mathematics, University of Maryland, College Park, 54 p

Landsberg, H. E., and T. N. Maisel. 1972. *Micrometeorological observations in an area of urban growth.* Boundary Layer Meteorology v. 2:365-370.

Munn, R. E. 1966. *Descriptive micrometeorology.* Academic Press, Inc., New York, 245 p.

Nkemdirim, Lawrence C. 1976. *Dynamics of an urban temperature field, A case study.* Journal of Applied Meteorology v. 15(8):818-828.

Oke, T. R. 1973. *Review of Urban Climatology 1968-1973.* World Meteorological Organization Report 383, Geneva, 133 p.

Oke, T. R., and G. B. Maxwell. 1975. *Urban heat island dynamics in Montreal and Vancouver,* Atmospheric Environment v. 9:191-200.

Peterson, James T. 1969. *The climate of cities: A survey of recent literature.* National Air Pollution Control Administration Publication No. AP-59, Raleigh, North Carolina.

Sanderson, M., I. Kumanan, T. Tanquay, and W. Schertzer. 1973. *Three aspects of the urban climate of Detroit-Windsor.* Journal Applied Meteorology v: 12:629-638.

Sisterson, Douglas L. 1975. *Studies on the urban moisture budget.* Department of Atmospheric Science, College of Engineering, University of Wyoming, Laramie, Report No. AS 114, 52 pp.

Vukovich, Fred M. 1973. *A study of the atmospheric response to a diurnal heating function characteristic of an urban complex.* Monthly Weather Review v. 101(6):467-474.

PART C CONTENTS

Part C. Urban Boundary Layer

AEROSOL PATTERNS

Richard G. Semonin

Introduction

Various measurements of condensation nuclei, ice nuclei, and certain cloud properties were made by project aircraft during the five summers (1971-1975) of METROMEX. These data provide insight into local sources and concentrations of nuclei that can affect the microphysical properties of clouds. These data resulted from an aircraft used throughout the field program to assist in studies of scavenging of chemical pollutants by convective precipitation.

The flight program evolved during METROMEX to include a variety of studies and measurements of atmospheric composition and structure, largely within the research circle. In addition to the equipment required for the release of tracer chemicals into clouds, the aircraft also carried instrumentation for the measurements of condensation nuclei (CN), ice nuclei (IN), small particles, temperature, wet bulb temperature, and liquid water content (LWC).

The flight priorities were changed nearly each year to reflect and accommodate the changing needs dictated by the findings from the previous year's field program. For example, the first year emphasized the release of tracer material into convective storm updrafts with simultaneous measurements of the meteorological variables to depict the subcloud atmospheric structure. Consequently, the aircraft was used only during periods of precipitation. Desires to obtain measurements of the atmospheric state during non-precipitation intervals led to precipitation-free flight programs in 1972. These were designed to map the thermodynamic structure in the boundary layer and to acquire routine measurements of condensation and freezing nuclei.

A subsequent requirement in later years led to measurements of these phenomena in the boundary layer and near convective cloud tops to assess the transport of boundary layer material to upper levels. Further aircraft instrumentation was introduced in 1974 and 1975 to obtain air filter samples for chemical analyses of the urban aerosol in addition to the measurement of particle number concentration by the various on-board particle counters.

The results of the CN measurements obtained at 600 m MSL along the flight tracks extending N and S through the Arch and WSW-ENE crossing at the Arch were also reported by Semonin and Changnon (1974). These measurements indicated an average increase of number concentration by a factor of three to four between upwind samples and those acquired downwind of the urban area source. Nearly 60% of the aircraft sampling missions were carried out between 1300 and 1600 CDT with very few flights conducted during nighttime hours. Therefore, the results relate only to observations obtained in the typically well-mixed lower atmosphere of the afternoon.

Results of additional analyses based on the observations of CN and IN are the focus of this section.

Condensation Nuclei Measurements

Aircraft measurements of CN were obtained by two instruments. A hand-operated Gardner Small Particle Detector (GC) was used in all five years by the flight meteorologist. A second counter, the Environment-One Continuous Particle Detector (E-l), was installed in 1972 and the measurements were recorded on an oscillograph along with other aircraft-observed variables. These measurements, along with flight notes, form the basis for characterizing the aerosol concentration in the boundary layer, at or near convective cloud bases, and inside small convective clouds.

The GC is operated by flushing with ambient air a sample tube lined with wet blotting paper. A second chamber of variable volume is then brought to a desired partial vacuum by means of a hand pump. A photocell is located at one end of the sample tube and a collimated beam of light is transmitted through the long-axis of the tube. A brief period is allowed between admitting the ambient air and the release of the partial vacuum to permit the sample to attain vapor saturation and thermal equilibrium. The partial vacuum is suddenly released and the resultant expansion and cooling produces a supersaturated condition resulting in fog formation in the sample tube. The extinction of the light intensity as detected by the photocell is a measure of the fog density which is dependent on the number of CN present in the sample.

A range of supersaturations in the GC can be achieved by varying the partial vacuum for successive samples. In this way a spectrum of particle number density can be acquired. The supersaturations range between 4 and 200% or more and is dependent not only on the partial vacuum but also on the altitude and ambient temperature. These problems were discussed and correction techniques for observations were presented by Auer (1965). The E-l operates similarly except that the manual operation of the pump is accomplished by an automatic mechanical means. The supersaturation is approximately 250% and is relatively constant.

A comparison between the two methods is shown in figure C-l. The data were compiled by comparing a 3-minute average of the E-l values and the discrete GC observations. A correlation analysis of the data indicates that the GC values are approximately one-half the values obtained by the E-l. The E-l values were empirically changed to conform to the GC by the statistically derived relationship GC = 0.528 (E-l) 0.9937 to provide a uniform set of data.

Condensation Nuclei Point Sources

The upwind CN concentrations in the boundary layer W of St. Louis are approximately 1.6×10^4 cm^{-3} increasing to 7.5×10^4 cm^{-3} in the downwind region (Semonin, 1974). This increase of 4.7 times for particle concentration is in direct response to the variety of sources available in the St. Louis metropolitan area, as described by Auer (1975). The number concentration ratio of downwind to upwind values obtained by the E-l and GC reported by Semonin (1974), and the independent observations of Auer (1975), agree quite closely. There is no doubt that the city, industry, and other human activities supply a copious quantity of particles to the atmosphere.

The important fraction of the nuclei generated in St. Louis which becomes involved in cloud processes has been measured by Auer (1975) and Fitzgerald and Spyers-Duran (1973). These cloud condensation nuclei (CCN) represent a very small fraction of the total particle concentration with typical values of 1000 cm^{-3}. The qualitative implications of such a local increase in CCN on precipitation enhancement mechanisms appear to contradict the concept of precipitation efficiency related to the number concentration of CCN.

In the simplest categorization of cumulus clouds, one finds maritime and continental types. The maritime type is characterized by relatively small number concentration with a broad size

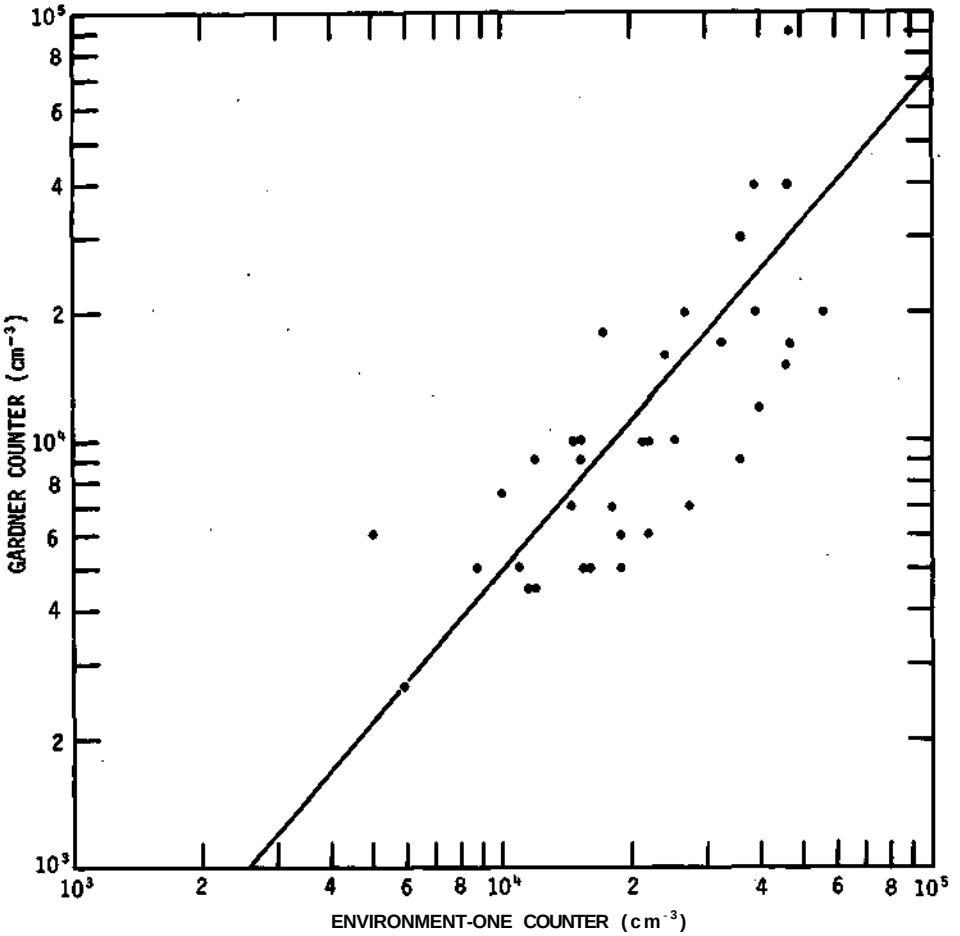

Figure C-1. Relationship between the hand-operated GC detector and the E-1 detector (E-1 data represent 3-minute averages centered on the time of the GC observation)

distribution, and the continental by a large number concentration in a narrow size distribution. Observations show that maritime clouds develop precipitation earlier relative to cloud lifetime than do continental clouds. The tendency toward increasing continentality of a cloud is linked to increased numbers of available CCN, resulting in large number concentrations and narrowing of the size distribution. This leads generally to less efficient precipitation production within a cloud. Unless the size distribution is further altered in the direction of giant and ultra-giant particles, a mere increase in number concentration would lead to greater competition for available water vapor with less growth of individual droplets and less rain.

The suggestion that the precipitation anomaly east of St. Louis is possibly linked to the presence of giant and ultra-giant CCN was first expressed by Semonin and Changnon (1974), Semonin (1974), and Braham (1974). This spurred additional work in cloud model development (Ochs, 1974) and field measurements (Dytch, 1974). The final outcome of this effort was that, indeed, the urban-generated particles in the ultra-giant size range are present (Dytch, 1974) but the model results described in a later text show the in-cloud processes are insensitive to their presence (Ochs and Semonin, 1976; Ochs and Semonin, 1977).

Consequently, the role of urban-produced CCN in contributing to the precipitation anomaly appears less than a major effect. This conclusion is based largely upon the currently available cloud model results. This model does not include all features of continental clouds. For example, the ice phase is not incorporated and this could dramatically affect the development of precipitation. As will be seen later, observed high CN concentrations qualitatively correlate with the placement of the rainfall anomaly. Even though the relationship of urban-produced CCN to the summer rainfall anomaly cannot be totally determined at this time, their importance to other aspects of inadvertent weather modification is well recognized. For example, the continuing problem of haze in urban centers can be partially attributed to increased aerosol production. In turn, the aerosol loading affects solar radiation with direct effects on the planetary boundary layer structure including the surface heat island.

Even more important is the fact that some fraction of the urban-generated aerosols is removed by clouds and precipitation, thereby altering the quality of precipitation (Gatz, 1974; Semonin, 1976). Individual particles provide catalytic sites for chemical transformations providing a sink for one chemical species and a source for another. For these reasons it is important to identify the sources, measure downwind concentrations, and determine the area of influence of an urban source region.

The strong individual sources of CN identified by measurements from the Survey's leased aircraft are shown in figure C-2. In close proximity (~ 1 km) to these point sources, the CN concentration is increased above background by at least a factor of three. Surprisingly, many of these point sources retain their identity many kilometers downwind under certain flow conditions, with ratios of in-plume/background aerosol concentrations of greater than 2 persisting frequently at 50 km beyond the source.

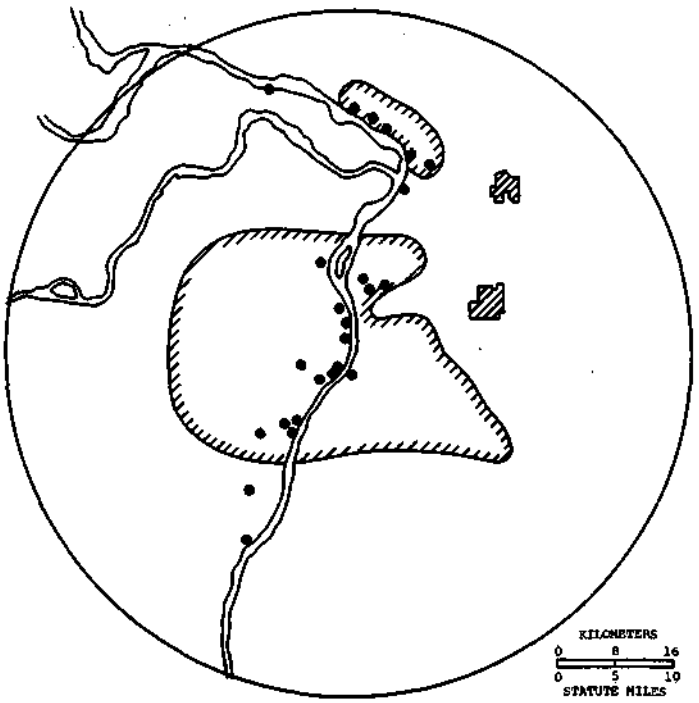

Figure C-2. Location of strong condensation nuclei sources as determined by aircraft measurements, 1971-1975

The general background CN concentration at low altitudes is on the order of 10^3 cm^{-3} (Semonin and Changnon, 1974; Braham, 1977). The CN reach well into the inversion layer and usually maximize at the inversion top. It is clear that convective clouds which penetrate the inversion transport CN to higher levels. These particles were frequently observed by project aircraft personnel in upper-level strata after the cessation of cloud activity, with gradual dimunition of the concentration over 24 hours. However, particulate strata were also observed unrelated to local convective mixing, and may result from convectively active regions upwind of the METROMEX research area.

Areal Distribution of CN

The CN observations acquired during the entire 5-year flight support period were obtained over much of the area of the 80-km diameter research circle. In any one year, the distribution of observations did not cover all the area, but the 5-year collection provided a sufficient number of observations to depict well the areal distribution of CN. The pattern based on all CN measurements at 300 m AGL is shown in figure C-3. The day-to-day and year-to-year differences in a given area where many measurements were taken were sufficiently small to allow development of a meaningful composite pattern.

Relatively high values of concentration parallel the Mississippi River valley with isolated concentrations W and NW of the urban center. Many of the isolated maxima can be identified with either major stack sources of isolated power plants or a closely located group of individual

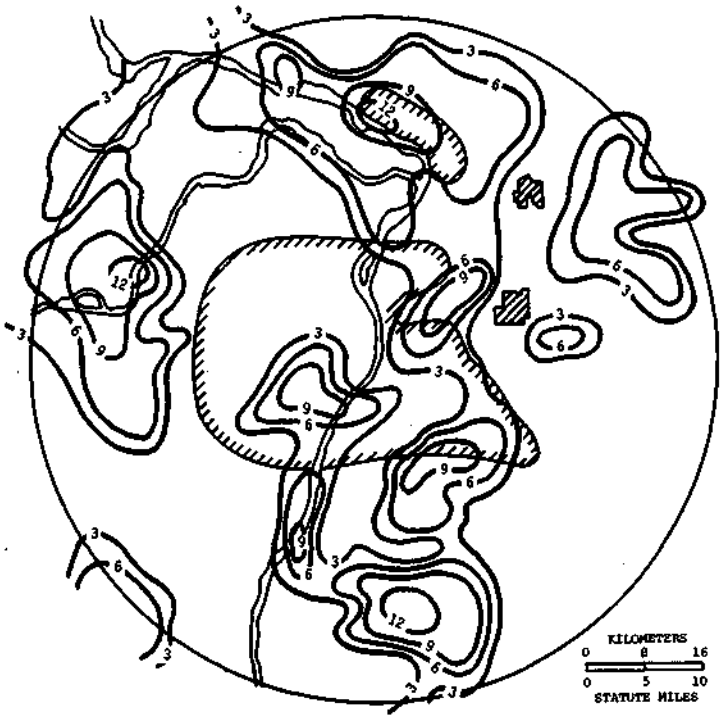

Figure C-3. Composite distribution of CN concentration at 600 m MSL derived from all flights, 1971-1975. (Contour values are units of 10^4 cm^{-3} number concentration)

sources. For example, the maximum value of 12 X 10^4 cm^{-3} along the western edge of the research circle on the Missouri River can readily be traced to its source at the Labadie Power Plant located a few kilometers further west. The maximum of > 12 X 10^4 cm^{-3} observed over the extreme southern area of the circle is more difficult to rationalize in relation to the point sources shown in figure C-2. This maximum may be a reflection of the confluence of aerosol from sources in south St. Louis and the prolific source from a large coal-burning power plant near Baldwin, Illinois, located 30 km SE of the observed high.

The general features of the distribution of CN correspond qualitatively to the total summer rainfall pattern (Changnon et al., 1977). More striking, however, is the comparison between observed CN and the rainfall pattern over the research circle from the three driest months during 1971-1975 (see figure B-12, Changnon et al., 1977). The position of high and low values for both aerosol concentration and rainfall closely coincide. The 5-year total air mass storm precipitation (Vogel, 1977) is also very similar to the CN distribution. Under relatively dry conditions, it is likely that the rain-producing cloud systems may become more responsive to the addition of CN, or more precisely, the addition of the CCN fraction of the total aerosol. The most frequent synoptic event during the three driest months was the air mass storm (17) followed by the squall zone (10). The air mass storm is typified as a small-area, slow-moving convective storm, which would respond to microphysical alterations very close to the source involved. This concept necessitates a physical link between the CN and alteration of the precipitation mechanism through cloud microphysics. If the observations are not mere coincidence, then additional research is suggested to explain the similarity between the patterns of nuclei concentrations and precipitation during dry periods.

In support of this qualitative implication between CN, cloud microphysics modification, and precipitation, the typical mixing height is frequently very high when air mass storms occur. Thus, the CN released near the surface are well-mixed to heights equal to or greater than the cloud base heights. In other words, the cloud bases during air mass storm events are embedded in air presumably containing high CCN concentrations. The in-cloud measurements of CN clearly show the greater difference between urban-affected and rural clouds.

Observations of the effects of aerosol on the radiation budget in urban areas are very scarce although several models espousing different theories are available. One such model presented by Atwater (1975) produced simulations of the effects of elevated pollution concentrations on the surface and vertical temperature distribution. While Atwater concluded the effects of pollutants are generally smaller than that for other urban factors, such as changes in surface characteristics, the presence of radiatively active aerosol increases vertical stability during daylight hours leading to increased near-surface concentrations. Unfortunately, insufficient radiation data were collected in METROMEX to allow a comparison between CN concentration distribution and radiation flux.

Ice Nuclei

The concentrations of ice nuclei (IN) were estimated by the portable cold box technique. Samples were collected during many flights throughout the project duration. The portable cold box consists of a 2-liter chamber maintained at a prescribed temperature by circulating isopropyl alcohol cooled by dry ice. A collimated light beam passes through the chamber illuminating a cross-sectional area of 1 cm^2. A lens with a focused grid is placed at a right angle to the light beam to view a volume of 50 cm^3. Outside air is admitted to the chamber, after flushing the previous sample, and the number of ice crystals observed by scintillation in the light beam are counted and recorded as a number per cubic centimeter. The chamber was maintained at —20° C for the observations discussed below.

Although this system for IN measurement is not as sophisticated as some of the latest continuous monitoring instruments, it has been used extensively over many years with consistent results. It will not be argued here as to the absolute value of the measurements, but, rather, that the relative differences in concentrations are valuable in defining regional patterns and in detecting source areas. The measurement of IN is certainly one of the serious instrumentation problems still confronting weather modification research after more than 30 years. Until such time that instrumentation to observe IN reaches the current capabilities of equipment for CN and CCN measurements, the field of weather modification will continue to suffer from lack of knowledge of the dispersion and mixing of ice nucleating agents in the atmosphere.

Czys (1977) summarized the measurements obtained by the University of Chicago during 25 constant level flights on which filters were exposed at 460 m MSL. The filters were analyzed in a chamber of similar design to that described by Langer and Rodgers (1975). The results presented by Czys (1977) indicated an overall decrease of IN during the summer months compared with winter, but the 1975 flights gave strong evidence for local sources along the Mississippi River valley N and S of the city center.

The IN measurements obtained by our leased aircraft during the summer flight programs of 1971-1975 were combined to study areal patterns. Those measurements acquired at the level of 600 m MSL are shown in figure C-4. More than 200 data points scattered throughout the area were used to obtain the pattern. Contours are shown for those areas with repeated observed concentrations greater than 25 per liter. These results show high concentrations extending south from central St. Louis, but these are confined to a narrow band along the river where heavy industry is located. Three isolated areas of high IN concentration were observed near Waterloo, Belleville, and Collinsville. A large area of high concentration encompassed the Alton-Wood River industrial center and along the floodplain between the Missouri and Mississippi Rivers west of Alton.

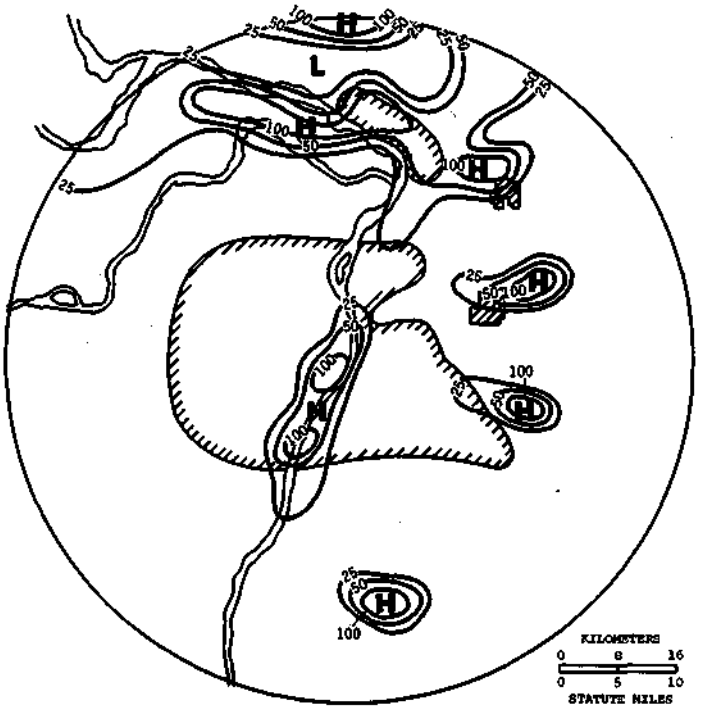

Figure C-4. Distribution of high ice nuclei number concentration (per liter) derived from a composite of all flights during 1971-1975 at 600 m MSL

In a qualitative sense, this composite distribution of IN agrees with the findings of Czys (1977) although the magnitude of the concentration values differ by a factor of about 100. However, it is not clear as to exactly what types of nuclei are measured by each instrument. At least four processes are considered responsible for ice crystal formation in clouds. These are: 1) nuclei contact with sub-cooled water particles; 2) direct deposition of water vapor to crystal form on a suitable nucleus; 3) condensation of water vapor on a nucleus with subsequent freezing; and 4) the incorporation of a nucleating particle into a water particle at above freezing temperature with subsequent freezing as the water is transported to below freezing temperatures.

The filter technique used by Czys (1977) is probably biased toward those nuclei involved in the condensation-freezing process of ice crystal development. The portable cold box probably produces ice crystals from all modes of crystal formation by varying degrees. The different instrumentation may account for part of the difference in number concentrations. In addition, the filter data were obtained at temperatures warmer than —20° C which may also contribute to the lack of correspondence between the observed IN concentrations by the cold box and filter methods. Of course, possibly overriding both of these factors is that the samples were not taken simultaneously and are subject to natural variability, in both space and time.

In relation to the observed precipitation anomaly northeast of St. Louis the locations of high IN concentrations are such that the opportunity for the IN to interact in the convective clouds precipitation process is certainly present. As with the CN described previously, the air mass type storm is that most likely affected, although the possible influence on more transitory storms should not be dismissed.

A comparison between the CN (figure C-3) and IN (figure C-4) patterns shows some interesting similarities and a few disparities. First, the IN maximum near the center of St. Louis and extending south coincides with a similar CN maximum. This observation suggests, perhaps, a common source for both the IN and CN. A similar relationship of IN and CN maxima can be seen in the Alton-Wood River area, the Waterloo area, and near Collinsville.

The obvious disparity is the absence of a high IN concentration in the same area as the CN maximum west of the urban area. The CN maximum is very likely associated with the large fossil fuel electric generating plant nearby, as mentioned previously, leading to the hypothesis that not all such plants alone are prolific sources of IN. The various observed IN maxima along the Mississippi River and east, therefore, are likely due either to sources independent of power plants or to complex chemical interactions of several types of effluents including those from coal-fired sources.

AEROSOL SOURCE IDENTIFICATION

Donald F. Gatz

Investigations of urban aerosols generally seek to answer one or more of the following questions:

1) What elements or molecules are present?
2) What are the sources of the aerosols?
3) How much does each source contribute to the total aerosol?

Analytical techniques have advanced to the point where it is possible to detect 20 to 30 elements in urban filter samples of reasonable duration (one day or less). In addition, statistical techniques are available whereby multielement analytical data can be used to identify major sources. If observed aerosol concentrations, measured near ground level, are used in these analyses, they will identify sources of aerosols in the air that people breathe. Usually, both natural and man-made sources can be identified.

EXPERIMENTAL METHODS

Field Methods

Elemental concentrations in air were measured during the METROMEX summer field seasons of 1973, 1974, and 1975 with Nuclepore filters. Figure C-5 shows the sampling sites, along with their years of operation and sampler heights (near ground level, or on a roof).

Aerosol samples were collected on pre-weighed 37-mm or 47-mm diameter Nuclepore polycarbonate membranes with 0.8 μm diameter pores. Each filter was exposed face down under an inverted polyethylene funnel rain shield at 1 m above grass or a flat roof.

The filters collect at 100% efficiency for all particles larger than 0.8 μm, up to the size where particle inertia causes imperfect sampling, perhaps 20 μm. Below 0.8 μm, theoretical efficiencies drop to a minimum of about 20% at a particle diameter of 0.04 *μm* for our sampling conditions (Spumy and Lodge, 1972). For the data used here, collection efficiencies were determined separately for each element using pairs of identical filters in series. Adjustment of the measurements for imperfect sampling is necessary to determine absolute concentrations, but the factor analysis techniques used in this work depend only on relative values, since the data are standardized before use.

Airflow through the filters was provided by 1/6 hp vacuum pumps. Sample volumes were estimated from sample durations and the mean of flow rates measured at the beginning and end of each sample. Rates were measured with a rotameter and vacuum gauge, calibrated against a dry gas meter known to be accurate to 0.5%. Concentrations are expressed in units of mass per standard (21°C, 76 mm Hg) cubic meter. Sample duration was measured by recording times when samples were started or ended manually, or by automatic timer verified with an electric clock.

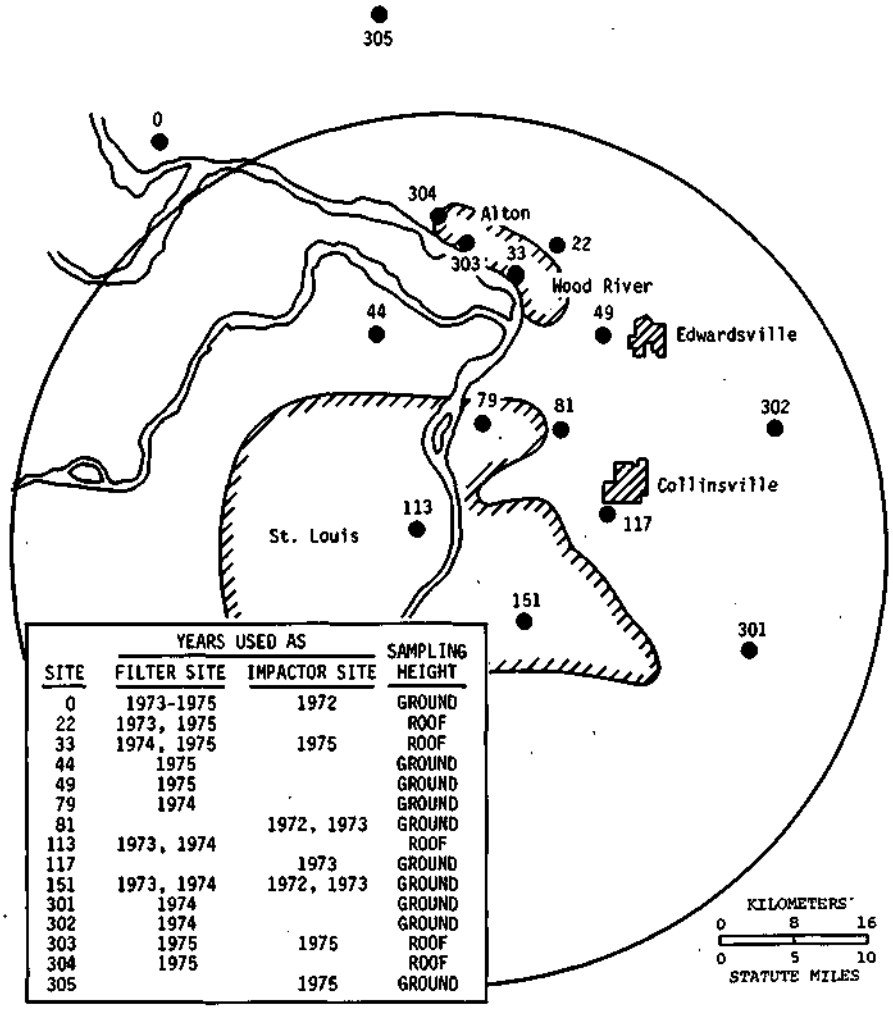

SITE	YEARS USED AS FILTER SITE	YEARS USED AS IMPACTOR SITE	SAMPLING HEIGHT
0	1973-1975	1972	GROUND
22	1973, 1975		ROOF
33	1974, 1975	1975	ROOF
44	1975		GROUND
49	1975		GROUND
79	1974		GROUND
81		1972, 1973	GROUND
113	1973, 1974		ROOF
117		1973	GROUND
151	1973, 1974	1972, 1973	GROUND
301	1974		GROUND
302	1974		GROUND
303	1975	1975	ROOF
304	1975		ROOF
305		1975	GROUND

Figure C-5. Aerosol sampling network, 1973-1975

Laboratory Methods

Filters were weighed to the nearest hundredth of a milligram on a microbalance, under a radioactive source to dissipate static charge. No humidity conditioning was necessary during pre-weighing since the polycarbonate membranes do not absorb moisture. After sample collection, the filters were conditioned for at least 24 hours at 47% relative humidity to allow moisture absorbed on the collected particulate matter to come to equilibrium. Filters were then reweighed under the radioactive source.

Elemental analysis on the filters was carried out at the Crocker Nuclear Laboratory, University of California at Davis, by ion-excited X-ray fluorescence (Flocchini et al., 1972; Flocchini et al., 1976). These authors quote absolute error limits of ± 10% in most cases to as high as ± 30% near detection limits. The analyses reported here were only rarely near detection limits. When not detected, elemental concentrations were assumed to have been half the detection limit. The following elements were detected regularly and make up most of the data set considered here: Al, Si, S, K, Ca, Ti, Mn, Fe, Zn, Br, and Pb.

Statistical Methods

The multivariate statistical technique of factor analysis (Harman, 1967) was used for source identification. Factor analysis is a tool for explaining observed relationships between numerous variables in terms of fewer variables, where the new variables are linear combinations of the original ones. The input data are in the form of a matrix with each column being a measured variable and each row a separate entity. In this case the variables are element concentrations in air and the entities are separate filter samples.

This technique has previously been described in the literature and applied to source identification in the Boston area by Hopke et al. (1976) and in the Tucson area by Garenstroom et al. (1977). The analysis performed on the present data was very similiar to that described by Hopke et al. (1976) except that a principal components model was used instead of the factor model they described. The principal components model describes the original variables completely in terms of common factors, and the unique factors of the factor model are not included. Comparison of both methods on the same data showed only minor differences in results for selected sets of our data.

Computations were carried out with the factor analysis program from the BMDP Biomedical Computer Programs (Dixon, 1975). With this program, after standardizing the data, a matrix of correlation coefficients between all variables is computed. Initial factors are then extracted. The first factor is that linear combination of original variables that explains more of the variance in the data than any other possible combination. The second factor explains more of the remaining variance than any other possible combination, and is independent of the first factor, that is, the correlation coefficient between factors is zero. Factor extraction continues until the number of factors equals the number of variables, but since the first few factors usually explain nearly all of the variance, only a few factors are kept for rotation to a final solution.

Rotation of the initial factors to final factors is possible because the factor structure is not unique. One solution can be rotated to another without violating the basic assumptions. One may choose a rotational method to yield a final solution that best meets the practical needs of the research problem.

In the present case, several methods of rotation were compared; only minor differences in the results were found for the several rotational methods, but all differed significantly from the unrotated solution. Furthermore, the rotated factors always appeared to be interpretable in terms of known sources of aerosols.

For this work, a matrix of correlation coefficients between variables was calculated from standardized data. Initial factors were extracted by a principal components solution. Factors having eigenvalues ≥ 0.6 were kept and rotated to a final solution with a Varimax rotation. The final factors have been interpreted in terms of aerosol sources.

RESULTS AND DISCUSSION

Several exploratory analyses were carried out with the elements listed earlier as variables, plus a number of meteorological and miscellaneous parameters. The non-chemical parameters included in the exploratory analyses were:

1) Day of the week
2) Mean wind speed

3) Maximum wind speed
4) Percent of time with wind from NE, SE, SW, or NW quadrants, or variable winds
5) Ventilation rate
6) Rain amount
7) Rain duration

These analyses showed that only the wind direction parameters (including variable winds) showed significant correlations with element concentrations. Therefore, all other meteorological parameters were omitted from subsequent analyses.

Single Site Analysis

Factor analyses were performed separately for each filter site shown in figure C-5. The factor loadings (or correlation coefficients between variables and factors) for a typical analysis are shown in table C-3. Values less than 0.50 explain less than 25% of the variance of an element and are generally not included. Some values have been included (in parentheses) for Pb and Br, however, because they aid interpretation. Site 79 is the sampling location closest to the extensive industrial area of Granite City, Illinois.

The five factors shown in the table account for 80% of the total variance. Two other factors had eigenvalues of 0.6 or more and were included in the rotation to a final solution. They are not shown in the table, however, because their high loadings occurred only on a single meteorological variable, adding no information for identification of sources.

Interpretation of factors as sources was made from the particular combination of elements and wind directions that have high loadings on the same factor. Variables that are highly correlated

Table C-1. Factor Analysis of 21 Samples for Site 79,1974

	Factor 1	2	3	4	5
Variance explained	31%	20%	12%	10%	7%
Al	0.97				
Ti	0.96				
Si	0.94				
K	0.83				
Br		0.84	(0.44)		
S		-0.82			
Zn			0.92		
Pb		(0.43)	0.69		
Ca				0.66	
Mn					0.84
Fe					0.76
Variable					
NE					
SE		-0.68		-0.56	
SW		0.76			
NW				0.94	

with the same factor are, of course, also highly correlated with each other. Factor 1, explaining 31% of the total variance, has high loadings for Al, Ti, Si, and K. These elements are very abundant in soil, but also in coal flyash. Since it is difficult to separate these two sources on the basis of the composition of their emissions, this factor, which was found at all sites,, is referred as to the 'soil and flyash' factor. However, the lack of a high loading for S and the lack of association with a particular wind direction suggest that no large point sources of coal flyash were involved.

The second factor, which accounts for 20% of the total variance, shows moderately high positive loadings for Br and SW winds and similar negative loadings for S and SE winds. This means that Br concentrations are high and S low with SW winds, and S is high and Br low with SE winds. A positive loading of 0.43 for Pb indicates that the Br is associated to some degree with Pb, suggesting an auto exhaust source from St. Louis. At other filter sites, the auto exhaust factor typically has a high Br loading and a high to low Pb loading, depending on the strength of non-auto sources of Pb. Sulfur from the SE is reasonable because the St. Louis Air Quality Control Region's largest SO_2 source is a steel mill in Granite City.

Factor 3, at 12% of total variance, has moderate to high loadings for Zn and Pb and a Br loading of 0.44, but is not associated with any particular wind direction. The lack of a directional association is somewhat puzzling because, with factor 2 representing auto exhaust, the main Pb source in factor 3 is almost certainly a secondary Pb smelter in Granite City. The Br loading, although low, shows that a portion of the Pb is still automotive, and indeed, air from the direction of the smelter also crosses a 4-lane expressway shortly before arriving at site 79. The high Zn loading also indicates Zn sources in the same direction, and several are known to be located in the area indicated. The Zn may even come from the secondary Pb source, although measurements of others (Winchester, 1977) suggest not.

Factor 4 shows a Ca source NW of site 79. This matches the location of a Portland cement plant in the northern portion of St. Louis.

Factor 5 has moderately high loadings for Mn and Fe. Although there is no associated wind direction, this source would appear to be the large steel mill in Granite City, since iron, steel, and ferroalloy production account for about 80% of Mn emissions in the U. S. (U.S. Environmental Protection Agency, 1975).

Element concentration data from each of the filter sites shown in figure C-5 were analyzed by factor analysis in the same way as at site 79. Further discussion of results from individual sites is not presented here. Rather, those factors found to be common to all sites will be discussed, and unique sources will be mentioned.

Common Factors

Most factors found at any given site were quite similar to others found at sites throughout the research area. For example, table C-2 compares soil and flyash factor loadings at all 12 locations. In each case, this was the first factor extracted, with the variance explained ranging from 29 to 49%. In this discussion, high loadings are defined as those ≥ 0.87, moderate loadings are between 0.50 and 0.86, and low loadings are below 0.50. Loadings of 0.87 and 0.59 explain 75% and 25% of an element's variance, respectively.

Variance explained and loadings for site 302 shown in table C-2 are median values of six separate factor analyses using different (arbitrarily chosen) combinations of elements. This unusual procedure was used because of the small number of samples at this site. It is impossible to perform the usual R-mode factor analysis on data having more variables than observations. A Q-mode factor

Table C-2. Summary of Four Factor Loadings at Twelve Sites

Site	Number of samples	Factor	Variance explained (%)	Loadings Al	Si	S	K	Ca	Ti	Mn	Fe	Zn	Br	Pb	Wind direction**
Soil and flyash factor															
0	61	1	46	0.94	0.91		0.90	0.67	0.90		0.90				
22	48	1	37	0.88	0.86		0.71	0.52							
33	48	1	32	0.96	0.88		0.62		0.94	0.57	0.94				
44	29	1	49	0.92	0.87		0.95	0.92	0.76		0.90				NW: −0.32
49	29	1	43	0.89	0.86		0.78	0.95	0.67		0.78				SW: 0.28
79	21	1	31	0.97	0.94		0.83		0.96		0.53				
113	39	1	33	0.84	0.89		0.94	0.79	0.55		0.85				
151	29	1	29	0.80	0.88		0.87				0.64				SW: 0.34
301	20	1	36	0.94	0.93		0.96	0.65	0.64	0.62	0.92				
302	15	*	41*	0.76	0.92		0.93	0.62	0.94		0.68				
303	29	1	46	0.89	0.96		0.90	0.95	0.80		0.77				SE: 0.30
304	30	1	47	0.90	0.94		0.96	0.92	0.79		0.88				
Sulfur and metal factor															
0	61	7	5			0.88									
22	48	2	15			0.61					0.50	0.88			
33	48	2	16			0.81	0.59	0.69							
44	29	6	4			0.83									
49	29	4	8			0.88				0.70					
79	21	2††	20			0.82							−0.84		SE: 0.68
113	39	3	10			0.73									SE: 0.41
151	29	4	8			0.82									NE: 0.47
301	20	3	12			0.51				0.62					SW: 0.93
302	15	*	12			0.89				0.68		0.73			SE: −0.37
303	29	6	5			0.84									
304	30	6	5			0.87									
Auto exhaust factor															
0	61	5	6										0.96		
22	48	3	10										0.88	0.68	NW: 0.84
33	48	3	12										0.92	0.76	
44	29	2†	17							0.74		0.90	0.97	0.92	SE: 0.33
49	29	5	7										0.95		
79	21	2††	20			−0.82							0.84		SW: 0.76
															SE: −0.68
113	39	2	17										0.79	0.89	SW: 0.37
151	29	2	18						0.89				0.92	0.84	SW: 0.34
301	20	2§	25					0.51				0.86	0.85	0.82	NW: 0.81
302	15	*	16*										0.87	0.87	NW: 0.66
303	29	3	8										0.83	0.87	
304	30	3	10										0.93	0.59	Var: 0.61
Metals without sulfur factor															
0	61	2	11					0.58		0.85		0.79		0.55	
22	48	4	9					0.72		0.82					
33	48	5	7									0.90		0.51	
44	29	2†	17							0.74		0.90	0.97	0.92	SE: 0.33
49	29	2	13						0.57		0.52	0.81		0.76	SW: 0.87
79	21	3	13									0.92		0.69	
		5	7							0.84	0.76				
113	39	4	10							0.62		0.90			SW: −0.26
151	29	3	16									0.81			NW: 0.93

Concluded on next page

Table C-2. Concluded

Site	Number of samples	Factor	Variance explained (%)	Loadings Al	Si	S	K	Ca	Ti	Mn	Fe	Zn	Br	Pb	Wind direction**	
301	20	2§	25					0.51				0.86	0.85	0.82	NW:	0.81
302	15	(none)														
303	29	2	14									0.72			SE:	0.87
304	30	2	13							0.68		0.51			SE:	0.74

*Variance explained and loadings for site 302 used different factors as explained in the text
**All wind direction loadings having absolute values >0.25 are shown, except if positive loading (direct correlation) is present, negative loadings (inverse correlation) are omitted
+Same factor listed under auto exhaust and metals without sulfur
++Same factor listed under sulfur and metal and auto exhaust
§Same factor listed under auto exhaust and metals without sulfur

analysis was performed on a transposed data matrix, but the results cannot be compared directly with those from other sites. These loadings are very similar (except for K and Ca) to those obtained for this factor by performing a factor analysis omitting the K and Ca data so that observations exceeded variables.

Al, Si, and K had moderate or high loadings at all sites, with mean loadings of 0.89, 0.90, and 0.86, respectively. Fe had similar loadings at all but one site, with a lower mean loading of 0.77. Ti and Ca fell below the moderate range at two and three sites, respectively, with respective mean loadings of 0.70 and 0.62. The only other element with any moderate loadings was Mn, appearing at two sites. Only very weak wind direction loadings were observed.

It is apparent from comparing loadings of the various elements that these factors were the same or very similar at all sites. In fact, they are so similar that the occurrence of a low loading for one of the usual elements of this factor is a signal of a significant non-soil source of that element. For example, the absence of moderate loadings for Ti at site 151 reflects the presence of a nearby Ti pigment plant. Similarly, the low Ca loading at site 151 probably reflects several nearby limestone quarries.

The sulfur and metals factor (table C-2) explained between 4 and 20% of the total variance of the data at the 12 sampling sites. Particulate sulfur is the only constituent having loadings ≥ 0.50 at all sites. Its loadings range from 0.51 to 0.88, with a mean of 0.63. Zn with two sites, and Mn with three, are the only other two elements with more than one site having loadings of 0.50 or above.

One might suspect that high loadings for these elements would suggest specific sources for the associated sulfur. However, examination of the four sites involved gave mixed results. The 0.70 loading for Mn at site 49 suggests that its source might be the large steel mill in nearby Granite City, since Mn is commonly used in steel making. Also, the high Zn loading at site 22 suggests known sources in the Alton-Wood River area. However, the other two sites, 301 and 302 are quite distant from likely sources. Still, one wonders whether the moderate loadings for Mn at these sites are connected with the known catalytic action of Mn in converting SO_2 to sulfate in aqueous solution. The strong loading of SW winds at site 301 would argue against the steel mill in Granite City as the source of sulfur. On the other hand, the steel mill *is* suggested as the source of sulfur at site 79 by the moderate loading of SE winds at that site.

In general, however, wind direction loadings are low, suggesting that most of the sulfur detected in this factor is not from local sources, but rather is secondary sulfate from distant sources throughout the region.

No explanation is apparent for the moderate K and Ca loadings on this factor at site 33.

The auto exhaust factor summarized in table C-2 explained between 6 and 25% of the variance at the several sampling sites. It is characterized by moderate or high loadings on both Br and Pb, and frequently has a high wind direction loading. At three of the 12 sites, Br alone defines the factor; the Pb loading is less than 0.50. This shows the presence of a significant non-automobile Pb source, to be discussed later in connection with another factor.

The frequent wind direction loadings in the moderate range show the importance of local sources. The direction of the high loading usually points to a nearby road or intersection, although in at least one case (site 44) the source to the SE may be the entire central city area. The occasional high loadings of other elements on this factor would appear to be caused by separate sources in the same direction as the automobile exhaust source. Examples of this such as the high Ti loading at site 151 will be discussed later.

The metals without sulfur factor, summarized in table C-2 explained between 7 and 25% of the variance at the various sampling sites. At one site (79), two different factors appear, involving different sets of metals. At another (site 302), none of the factors appeared to fit into this general category.

Zn appears with loadings greater than 0.50 at 10 of the 12 sites. Mn and Pb both have loadings in the same range at six sites. Wind direction loadings in the moderate and high ranges occur at five of these sites.

Note that the factors given for sites 44 and 301 were also included in the auto exhaust factor (table C-2). This was done because of their high loadings for Br, in addition to those of other metals, such as Zn and Mn. Note also that Pb occurs with moderate loading *without* Br at four sites. This signals the presence of a secondary Pb smelter, to be discussed in greater depth later in this report.

Table C-2 shows that Mn and Zn may exhibit high loadings singly, or in various combinations with each other and with Pb. The fact that these three elements do not *always* occur together at the various sites suggests that they do not have a common source, but rather have separate sources in the same general area. This is confirmed by figure C-6, which shows the locations of known or suspected sources of Zn, Mn, and non-auto Pb. These elements all have some sources in the St. Louis-East St. Louis industrial area, with additional scattered sources elsewhere in the region.

Site 79 is of interest because of its two separate factors in the 'metals' category. The question arises whether the large steel mill in Granite City might be the source of the nearby maximum in Zn deposition by rainfall (Gatz, 1976). These results suggest not. The steel mill is the obvious source of the Fe-Mn factors, while Zn is found together with Pb on the other metals factor. The Pb is quite likely from a secondary Pb smelter in Granite City. Whether the Zn and Pb are emitted by that same source, or merely by separate sources in the same direction from the sampling site, is not clear. The data are inconclusive, but others (Winchester, 1977) have suggested that the secondary Pb smelter is *not* the source of the Zn. As seen in figure C-6, any of several separate Zn sources in the East St. Louis area could have contributed to this factor.

The preceding paragraphs have demonstrated a marked *visual* similarity of the major factors found at each of the 12 sampling sites. The coefficient of congruence (Rummel, 1970) is a *quantitative* measure of the similarity of two factors. The coefficient of congruence, 5 , varies between

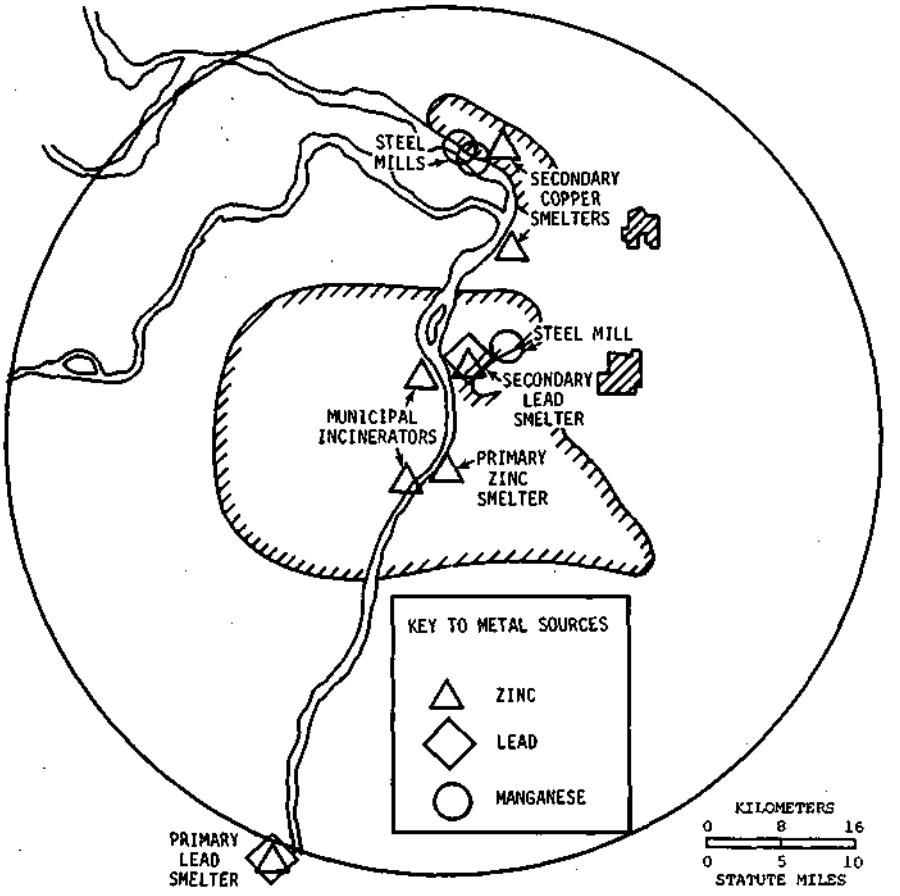

Figure C-6. Known or suspected sources of Zn, Mn, and non-auto Pb

−1.00 and +1.00, and is defined by

$$\delta_{lq} = \left(\sum_{j=1}^{m} a_{jl}\, a_{jq}\right) \Big/ \left[\left(\sum_{j=1}^{m} a_{jl}^2\right)\left(\sum_{j=1}^{m} a_{jq}^2\right)\right]^{1/2}$$

where

a_{jl} = loading of variable x. on factor S, at one site

a_{jq} = loading of variable x. on factor S at another site

m = the number of variables common to both sites

This provides a comparison of factor 1 at one site with factor q at another. The coefficient of congruence provides a quantitative measure of the similarity of visually similar factors at different locations. For example, the matrix of congruence coefficients for the soil and flyash factor is shown in table C-3. It shows uniformly high values, indicating that this source is the same or very similar over the whole area.

Other visually similar factors are compared in table C-4, which gives mean values and standard deviations of coefficient of congruence for each site. The soil and flyash factor, as mentioned earlier, has quite uniformly high values, with an overall mean of 0.94. The factor interpreted as auto exhaust is somewhat lower at an overall mean of 0.77, but still indicates considerable

Table C-3. Matrix of Congruence Coefficients for Soil and Flyash Factor

Site	0	22	33	44	49	79	113	151	301	302	303	304
22	0.93											
33	0.94	0.84										
44	0.98	0.94	0.89									
49	0.98	0.91	0.87	0.97								
79	0.95	0.89	0.92	0.91	0.91							
113	0.96	0.93	0.89	0.98	0.95	0.90						
151	0.92	0.98	0.86	0.94	0.91	0.88	0.96					
301	0.96	0.93	0.92	0.98	0.94	0.90	0.98	0.95				
302	0.98	0.88	0.92	0.96	0.97	0.94	0.94	0.90	0.95			
303	0.98	0.93	0.88	0.99	0.98	0.92	0.97	0.93	0.97	0.98		
304	0.98	0.93	0.87	0.97	0.98	0.90	0.94	0.91	0.95	0.97	0.98	
Mean	0.96	0.92	0.89	0.96	0.94	0.91	0.95	0.92	0.95	0.95	0.96	0.94
Standard deviation	0.02	0.04	0.03	0.03	0.04	0.02	0.03	0.04	0.03	0.03	0.04	0.04
Standard error	0.01	0.01	0.01	0.01	0.01	0.01	0.01	0.01	0.01	0.01	0.01	0.01

Table C-4. Summary of Mean Coefficients of Congruence for Four Visually Similar Factors

	Factor			
Site	Soil and flyash	Sulfur and metals	Metals without sulfur	Auto exhaust
0	0.96(0.02)	0.72(0.13)	0.74(0.09)	0.80(0.06)
22	0.92(0.04)	0.53(0.19)	0.46(0.22)	0.79(0.09)
33	0.89(0.03)	0.62(0.13)	0.60(0.23)	0.80(0.08)
44	0.96(0.03)	0.73(0.14)	0.68(0.18)	0.73(0.14)
49	0.94(0.04)	0.68(0.14)	0.67(0.12)	0.73(0.11)
79	0.91(0.02)	0.50(0.16)	0.69(0.18)	0.61(0.11)
113	0.95(0.03)	0.57(0.15)	0.64(0.16)	0.79(0.12)
151	0.92(0.04)	0.74(0.11)	0.61(0.21)	0.74(0.09)
301	0.95(0.03)	0.62(0.16)	0.61(0.22)	0.77(0.10)
302	0.95(0.03)	0.69(0.13)	0.47(0.22)	0.84(0.07)
303	0.96(0.04)	0.74(0.12)	0.64(0.11)	0.82(0.09)
304	0.94(0.04)	0.63(0.17)	0.71(0.10)	0.80(0.08)
Overall mean	0.94	0.65	0.63	0.77
Single site maximum	0.99	0.93	0.95	0.94
Single site minimum	0.84	0.22	0.10	0.42
Ratio	1.2	4.2	9.5	2.2

Note: Standard deviations are given in parentheses

similarity among sites. Standard deviations for this factor are generally larger than for the first two mentioned, which indicates greater variation in congruence between individual sites.

This is also revealed in the differences between maximum and minimum individual values, and the ratio of these two. The ratio is 1.2 for the soil and flyash factor and 2.2 for the auto exhaust factor, but 4.2 for the sulfur and metals factor. The ratio is still larger, at 9.5, for the metals without sulfur factor, which also has the smallest overall congruence, 0.63. This is still high enough to indicate considerable area-wide similarity between sites, but the greater variability is apparent.

To summarize, the coefficient of congruence is relatively high for all four factors shown in table C-4. The coefficient decreases from an overall mean of 0.94 to 0.63 in the order: soil and flyash, auto exhaust, sulfur and metals, metals without sulfur. The *variability* of values for individual pairs *increases* in the same order.

The factors discussed so far have identified sources whose influence is felt to a greater or lesser extent at all sampling sites. In addition, factor analysis of the data has identified several local sources, which were detected at only a few sites. These are discussed in the next section.

Local Sources

Factor 4 at site 79 (table C-l) shows a loading above 0.50 for only one element, Ca, with a high loading on winds from the NW. A cement plant located just across the Mississippi River to the NW of site 79 is the obvious source associated with this factor, which accounts for 10% of the total variance at that site. This factor was not detected at any other sampling sites.

It may be noted from table C-2 that Ca usually appears with a moderate or high loading on the soil and flyash factor, but this is not the case at site 79. Because loadings of an individual element, squared and summed across factors at a given site, must total to 1.00, it is clear that a high loading on one factor precludes significant loadings on others. Conversely, the absence of high loadings for a given element on a factor where it usually appears signals an uncommon source for that element at the site in question.

This clue to local sources is also illustrated by the detection of a strong Ti source. As shown in table C-2, Ti is usually associated with the soil and flyash factor. However, a plot (figure C-7a) of Ti loadings on the soil and flyash factor shows very.low values at sites 151, 301, and 22, and a value of 0.55 at site 113. Figure C-7b shows maximum Ti loadings on any non-soil factor at the same sites, along with other moderate or high-loading elements on the respective factors. At site 113, almost-equal Ti loadings appeared on two separate factors, both associated with SW winds. One of these factors also included moderate or high loadings for Br and Pb, caused by strong vehicle traffic sources in the same direction. [Note that, contrary to customary usage, wind directions are indicated by arrows pointing *into* the wind. This shows the direction of the source from the point of observation.]

High loadings for Pb and Br also occurred on the same factor with Ti at site 151, also caused by nearby road traffic in the same direction as the Ti source.

The remaining two sites having high Ti on non-soil factors, sites 22 and 301, are not so clearly linked to the known Ti source. At site 22, Ti occurred with S and Zn, without a strong association with any wind direction. If the known industrial source is responsible for the Ti on a non-soil factor at site 22, it is difficult to explain why similar factors were not observed at sites like 44 and 79, which are closer to the source than 22. At site 301, the interpretation of the factor with the high Ti loading is uncertain. Since it has moderate Al and Fe loadings, it might just as well have been identified as the soil and flyash factor as the one actually chosen (see table C-2). Still, however, the evidence of Ti on non-soil factors at sites 113 and 151, and the added weight of associated wind directions pointing to the source, is convincing; a local industrial Ti source is clearly indicated and is consistent with the location of a known source.

In a similar fashion, a non-auto Pb source apparent at sites 79, 49, 303, 304, and 0 was identified as a secondary Pb smelter in Granite City.

To summarize, factor analyses of multielement aerosol concentrations at 12 filter sites in the St. Louis area have identified four area-wide sources and several local industrial point sources. Because the list of elements measured routinely was limited to 11, it is expected that other signifi-

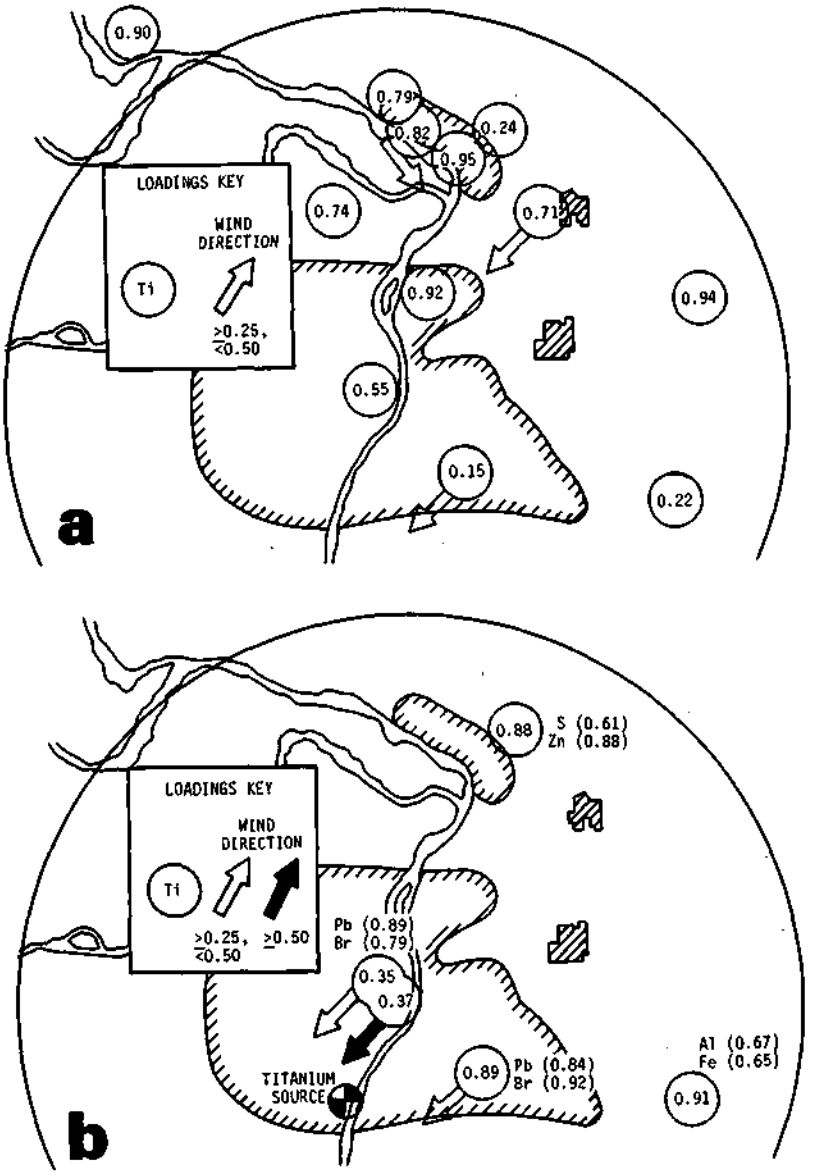

Figure C-7. Ti loadings; a) soil and flyash factor, b) other factors

cant sources also exist. Increasing the number of elements should allow additional sources to be identified.

Multielement analyses of element concentrations followed by factor analysis can answer, at least partially, the first two questions identified in the introduction as major goals of urban aerosol chemistry studies. Identification of sources is the first step in the assessment of the relative contributions of all sources to the ambient aerosol burden at any location. Appropriate techniques are also available for these estimates (Friedlander, 1973; Gatz, 1975; Mayrsohn and Crabtree, 1976). They require information on the chemical composition of emissions from the major sources, as well as ambient airborne element concentrations.

SUMMARY OF AEROSOLS

Richard G. Semonin

The spatial relationship between the average condensation and ice nuclei concentrations and the precipitation anomaly east of St. Louis suggests a possible influence by the urban aerosol in the modification of cloud processes. However, little direct evidence is available to establish a physical explanation.

The results show that urban aerosols do affect clouds. The vertical profiles show that high concentrations of urban-industrial derived CN and IN reach cloud base levels at St. Louis. In-cloud measurements show much higher CN values in urban clouds than in rural non-affected clouds. Other observations show these urban aerosols are processed by the clouds including exhaling them out of their tops into higher levels in the atmosphere. Cloud models (which cannot handle the IN effects) indicate, however, that the added CCN influence on local precipitation development is negligible. At this time, the evidence suggests that direct microphysical effects due to urban aerosols is much less important than other effects in producing the rainfall anomaly.

It is apparent that the observed high concentrations of both CN and IN are not solely due to fossil fuel used for electrical power generation. The general distribution of CN and IN maxima cannot be uniquely related to individual plants butrather to high concentrated areas of industrial activity.

The factor analyses of multielement aerosol concentrations at 12 filter sites in the St. Louis area identified four area-wide sources and several local industrial point sources. Because the list of elements measured was limited to 11, it is expected that by increasing the number of elements additional sources would be identified. Identification of sources is the first step in the assessment of the relative contributions of all sources to the ambient aerosol burden at any location.

Future research, not requiring the extensive effort put forth in METROMEX, is recommended to study in depth the effects of urban-related CN, IN, andtheir chemical composition on cloud microphysics. Such a measurement program would provide additional guidance for model development of urban-modified clouds allowing greater predictive capability to assess the magnitude of inadvertent weather modification in other locales.

INTRODUCTION TO PHYSICAL STRUCTURE OF THE PBL

Bernice Ackerman and Richard G. Semonin

An urban area has the capability of modifying weather and climate by virtue of 1) its anthropogenic effluents and 2) the replacement of natural surfaces with surfaces having distinctly different thermal and physical characteristics. The anthropogenic effluents include not only solid and liquid aerosols, but also heat and water vapor. They impact on air quality, atmospheric radiation balance, atmospheric buoyancy, and the atmospheric capacity for water vapor. The thermal properties of man-made surfaces and their relative impermeability for water, plus the obstacles to air flow represented by the vertical walls of urban structures, influence the surface radiation balance, the winds and turbulence, and through these the transfer of energy (latent, thermal, and kinetic) between the surface and the atmosphere.

The impact of the urban area would be restricted to only local surface weather such as temperature, humidity, and fog if its impact was not transferred upward and outward. That the impact is more than local has been demonstrated in the first volume of this report (Changnon et al., 1977) in which the precipitation anomaly associated with St. Louis has been extensively documented, as well as in a number of other reports in which weather and air quality are traced back to other urban sources (e.g., Hall et al., 1973; Kocmond and Mack, 1972; Angell et al., 1971). The dissemination of the effect of the urban area on weather, and particularly on clouds and precipitation, must involve atmospheric processes in the planetary boundary layer (PBL), which must in turn be reflected in its thermodynamic and kinematic structure.

The possibility that the structure and processes of the PBL might be altered by an urban area and the potential consequences of the alteration for inadvertent modification of weather was recognized early in METROMEX. As a consequence the measurement of wind, temperature, and moisture in the first two or three kilometers above the surface was an integral part of the program from the time of its inception.

Goals and Objectives

The boundary layer studies carried out by the Water Survey have addressed several goals with funding from NSF, ERDA(AEC), and EPA. As a consequence, the field effort changed significantly between summers as it was modified to serve different objectives. Two approaches were used. One was based on the implementation of special field experiments which were designed to investigate narrowly defined hypotheses concerning the potential effect of the urban area on the low level airflow. The second approach used routine daily measurements to delineate the mean summertime wind fields over the area for a range of mesoscale weather conditions. The first approach was used in 1972, and also in 1971 as part of the Argonne National Laboratory effort. The second approach was used in 1973 and 1974, and both were used in 1975, the final field year for METROMEX. The operational dates and other general information for each of the five years may be found in the annual METROMEX operational reports (Ackerman, 1971a; Semonin and Changnon, 1972; Staff, Atmospheric Sciences Section, ISWS, 1973, 1974, 1975).

The 1971 boundary layer field project was designed and carried out by the first author while she was on the staff of the Argonne National Laboratory. It is incorporated in this report because, after she joined the Water Survey staff in 1972, similar efforts were carried out by ISWS and the 1971 data are archived with the data from subsequent years at the Water Survey.

The specialized field experiments were designed to investigate four objectives, based on hypothesized modifications of the boundary layer by the urban surface.

- The first was to determine whether the nocturnal urban heat island induced a sufficiently strong pressure perturbation to initiate and maintain a local heat island circulation (investigated in 1971, 1972, and 1975)
- The second was to define the alterations, if any, in the wind profile as air moved from a rural surface over an urban surface having significantly different surface roughness (done in 1971)
- The third was concerned with the evolution of the subcloud airflow as convective cloud systems developed and moved through the metropolitan and adjoining areas (the 1972 program)
- The last was to determine if the intensity and scale of the turbulence and the vertical fluxes of heat, moisture, and momentum in the PBL differed significantly over city and country surfaces (done in 1975)

Field Operations and Data Collection

The field experiments in 1971 and 1972 featured a network of wind stations from which pilot balloons were launched at 20-minute intervals, for periods of 3 to 4 hours. The network was composed of 8 or 9 stations. On any given day the stations were selected from at least twice that number of pre-established sites to form an array which would best serve the objectives of the particular experiment. The pilot balloons were tracked to about 2 km with two theodolites spaced 500 to 600 m apart at each site. Balloon sightings were made every 20 seconds, giving 50 to 60 m vertical resolution in balloon location. In 1972, in addition to the wind observations, radiosondes were launched periodically from three stations lying along a WNW-ESE line across the city.

The field experiments in 1975 were much more extensive and were carried out for a short period during the winter as well as during the summer. Three instrumental components were utilized for studies of the turbulence and turbulent fluxes and of the development of the mixed layer over urban and rural surfaces. These components were 1) a network of five double theodolite pilot balloon stations (the number limited by available resources), 2) two tethered-balloon stations for high resolution thermodynamic measurements in the boundary layer, and 3) an aircraft instrumented for measurement of air motion and state parameters. Again each field experiment was of 3 to 4 hours duration, with each component operated in a mode to best address the experimental objectives. These data were supplemented by rather extensive PBL measurements made by the Regional Air Pollution Study (RAPS) of the U.S. Environmental Protection Agency (USEPA) as well as the routine daily ISWS pibal observations from 11 stations and radiosonde from 3 stations, in summer.

The program to delineate the mean summertime wind fields in the planetary boundary layer over the complex METROMEX meso-region carried out in 1973, 1974, and 1975 was based on pilot balloon measurements made regularly 6 days a week, from a fixed network of 11 stations. Although double theodolite measurements would have been preferred, funding limitations permitted only single theodolite tracking of the balloons. Balloons were launched at approximately 30-minute intervals between 1100 and 1600 CDT (continuing to a later hour if rains were in the area) and were tracked to about 3 km with about 100 m vertical resolution in sightings. PBL thermodynamic structure was monitored by radiosonde observations at three stations in the area, twice daily in 1973, every 2 hours in 1975, and every 60 or 90 minutes when rains were forecast.

In 1973 the pibal and radiosonde network was designed to delineate the kinematic fields and thermodynamic structure in the PBL over and around the metropolitan area, and extending northeastward to the industrial complex of Alton-Wood River (figure C-8a). In 1974 and 1975 the

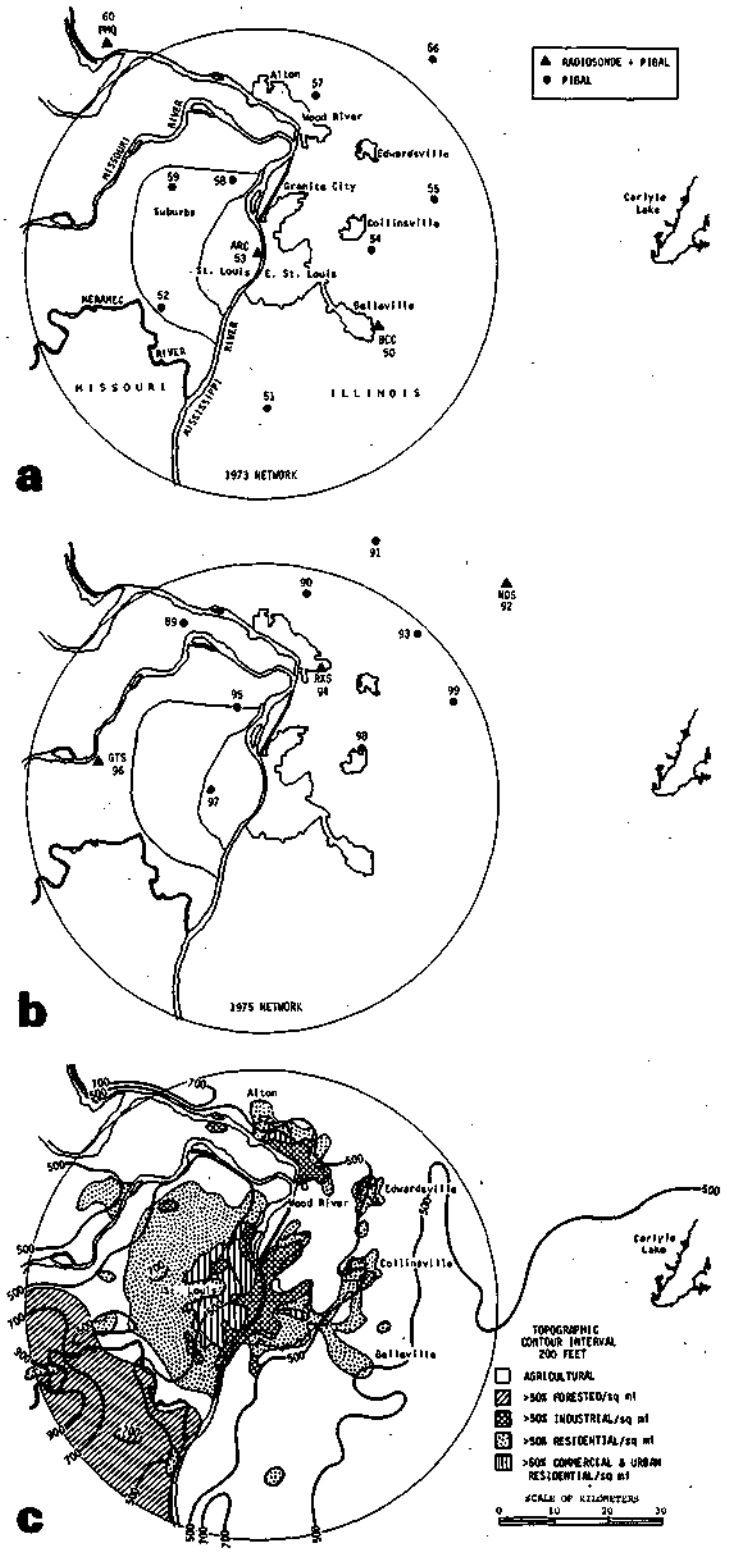

Figure C-8. Network of stations from which routine radiosonde and pilot balloon measurements were made in a) 1973, b) 1975, and c) the topography and land use in the METROMEX area

Table C-5. Operations Information for ISWS Boundary Layer Project

Year	*Dates*	*Number of days*
1971	June 14-29	12
	August 2-31	21
1972	July 17–August 10	18
1973	July 10–August 23	42
1974	July 13–August 18	18
1975 Routine	July 7–August 15	33
1975 Experiment	February 19-28	7
	July 3-31	22

networks were fashioned to support the air and rain chemistry project. The 1974 network extended from the city of St. Louis eastward some 30 km, and in 1975 it was centered around Alton-Wood River extending southwestward 45 km to the western suburbs of St. Louis and northeastward about 40 km (figure C-8b).

In table C-5 are shown the annual periods during which the PBL project operated and the numbers of days each year on which observations were taken. Information on observational methods and data processing may be found in Ackerman (1971b, 1973a) and Ackerman and Appleman (1974).

Personnel and equipment for double theodolite observations in 1971, 1972, and 1975 and for radiosondes in 1972 were provided by the Air Weather Service of the U. S. Air Force, with per diem and travel expenses provided by the AEC under Grant AEC-1199 in the first two years and by the USEPA under Grant EPA-R-80362-01 in 1975. Support for the other boundary layer measurements were provided by NSF-RANN Grants NSF GI 39213 and GI 38317 and by ERDA Grant 1199. In addition, the National Center for Atmospheric Research (NCAR) which is supported by NSF, provided airplane and crew and other field equipment in 1971 and 1975.

In the course of the five years an enormous data bank has been compiled consisting of over 12,000 wind profiles (including 1600 archived at Argonne National Laboratory) and 900 thermodynamic profiles. This data bank has been used in a number of studies investigating the alterations of the PBL by the urban-industrial area and has been utilized as well for a number of studies focused on the urban precipitation anomaly and on air chemistry and rain scavenging (Ackerman, 1972; 1973a; 1974a, b, c, d; 1975a, b; 1977; Changnon and Semonin, 1975; Grosh and Semonin, 1973;Murray et al., 1978).

The next two sections emphasize the results of studies of the midday kinematic fields over the St. Louis metropolitan area based on the routine measurements made in 1973, and studies of the average midday thermodynamic structure over urban and rural sites based on the 1973 and 1975 routine radiosonde observations. The station locations and the general topography and land use in the area are shown in figure C-8c.

All days for which sufficient valid and representative data were available were included in the analysis. Because of the difficulty of getting representative measurements during precipitation, only non-rain or pre-rain conditions were analyzed. Fair weather conditions were defined as existing if no rain fell anywhere in the METROMEX raingage network within 6 hours of the observations; pre-rain conditions were defined as those existing when rain was recorded in any amount in at least one raingage in the ISWS network within 6 hours following the observations. The full range of summer synoptic conditions usually found in the Midwest are represented in the samples used in the studies of the PBL structure over the METROMEX region, described in the two sections

Table C-6. Number of Cases for Indicated Surface and 500 mb Synoptic Patterns in Fair Weather Samples

	500 mb				
			Zonal flow		
Surface	*Trough*	*Ridge*	*Weak*	*Strong*	*Col*
1973 Samples					
1) Post-frontal	3				1
2) Ridge between 2 fronts	1	3	1		
3) Pre-frontal		1		1	
4) Major trough		2			
5) High pressure	7	1			
1975 Samples					
1) Post-frontal	3		1	1	
2) Ridge between 2 fronts	1	1			
3) Pre-frontal	2	1			
4) Major trough					
5) High pressure	3	3	1		1

Table C-7. Number of Synoptic Storm Types for Pre-Rain Samples Used in Wind and Sounding Analyses

		Sounding Analyses				
	Wind analyses	*ARC*	*PMQ*	*BCC*	*ARC/PMQ**	*ARC/BCC**
1973 Samples						
1) Squall line	4	4	3	4	3	4
2) Squall zone	3	2	2	2	2	2
3) Cold front	1	1	1		1	
4) Warm front						
5) Static front						
6) Pre- and post-front	1	1	1		1	
7) Air mass	5	4	2	4	2	4
8) Low pressure						
1975 Samples		*RXS*	*NDS*	*GTS*	*RXS/NDS**	*RXS/GTS**
1) Squall line		1		1		1
2) Squall zone		3	3	2	3	2
3) Cold front		1	1	1	1	1
4) Warm front						
5) Static front						
6) Pre- and post-front						
7) Air mass		2		1		1
8) Low pressure						

** Cases with simultaneous soundings at both stations*

that follow. Table C-6 shows the distributions of the surface and 500 mb synoptic patterns over St. Louis in the fair weather samples in 1973 and 1975. Table C-7 shows the frequencies of the synoptic storm types (Vogel, 1977) for the pre-rain samples in the two years.

THERMODYNAMIC STRUCTURE OF THE PBL AT MIDDAY

B. Ackerman and J. W. Mansell

BACKGROUND

The thermodynamic structure of the planetary boundary layer (here used to include both temperature and moisture) is the product of complex energy transfers between the surface and the free atmosphere. It is highly dependent on the nature of the underlying surface, the air chemistry, and the mean and turbulent air motions. The physical characteristics of urban surfaces are so different from those of most rural surfaces that the surface heat balance and resultant temperature are most assuredly different. Indeed, the elevated temperature of the urban surface air has been documented for many cities, and has become known as the 'urban heat island.' Although the urban surface-air heat island maximizes shortly after sunset and is very small during the afternoon (usually less than 1° C), infra-red urban *surface* temperatures measured during the special field experiments in 1975 were higher by several degrees than the surrounding rural surface temperatures during the afternoon as well as at night.

However, the thermal structure of the PBL is only partly dependent on the surface temperature. Radiation, eddy fluxes, flux divergences, and anthropogenic heat all play critical roles. The interactions are very complex, and it is not at all clear what the net effects of changes in paniculate loading, air chemistry (e.g., carbon dioxide and moisture contents), and turbulence might be.

Similarly the amount of moisture and its stratification in the PBL is the product of a number of complex processes. The urban surface with less evapotranspiration is a poorer source of moisture than vegetative surfaces and even of most soils, at least during the summer. However, anthropogenic moisture partially offsets this deficit —and during the winter when most vegetation is dormant, the urban area may be a better source of atmospheric moisture than rural areas.

Despite the complexities and the unknowns, there has been evidence that the urban heat island and an urban moisture deficit extends several hundred meters into the PBL above St. Louis (Braham, 1974; Auer and Dirks, 1974; Dirks, 1974). In addition, there have been several reports of greater mixing depths over the urban area. This suggests lesser stability over the city although this is poorly documented.

The routine radiosonde measurements made at midday in 1973 and 1975 have been used to study the average thermodynamic stratification in the PBL across the METROMEX area, and to determine a number of physical quantities for urban and rural sites which are important to the dispersion of pollutants and to the development of precipitation. The emphasis in this section is on the early to mid-afternoon thermodynamic structure in the PBL. A wide range of summertime synoptic conditions is represented in the sample cases (tables C-6 and C-7).

ANALYSIS APPROACH

Radiosonde measurements were made routinely at least twice a day, and often more frequently, from three locations during most of July and August in 1973 and 1975. The schedules

Table C-8. Times (CDT) of Radiosonde Launches, 1973 and 1975

	Predicted weather conditions	
	No rain	*Rain*
1973	0700,1330	0700, 1330, plus hourly thereafter to 1800
1975	1200, 1400, 1600	1130 to 1800, hourly

Table C-9. Characteristics of the Radiosonde Stations, 1973 and 1975

Site number, letters	*Elevation (m)*	*Location and characteristics*
1973 Stations		
50, BCC	155	At Belleville Community College in a rural area about 4.2 km east of the small city of Belleville; near surroundings flat, agricultural
53, ARC	139	Next to the Memorial Arch in downtown St. Louis. Grassy surface; immediate surroundings, central city
60, PMQ	273	In Pere Marquette State Park, Illinois, about 27 km to the nearest significant urban area; immediate surroundings, hilly and wooded
1975 Stations		
92, NDS	186	In a rural area about 38 km NE of Alton; flat, agricultural
94, RXS	134	Near an industrial complex in the small city of Roxana, Illinois; high density, low rise residential
96, GTS	182	On the fringe of the St. Louis metropolitan area 6 km west of the interstate highway loop; rolling, low density suburban

varied from year to year, but one sounding was always made at about the time of high sun (1300-1400 CDT), as shown in table C-8. The station locations also varied, but differed in the two years. In 1973 they were situated approximately in a line oriented parallel to the mean PBL wind and crossing the city (figure C-8a). In 1975 the three stations were in a line parallel to the mean steering winds and crossing the Alton-Wood River complex (figure C-8b).

The geographic characteristics and land use of the sites varied considerably. The 1973 network (figure C-8a, table C-9) provided the best data source for comparison of the PBL overriding a large city with the surrounding rural PBL. Station ARC was in downtown St. Louis, PMQ was in a natural setting of forested, rolling hills, and BCC, although relatively close to a small city, was surrounded by flat cultivated fields.

The stations in the 1975 network were not so distinct. The urban station, RXS, was in a residential section of a small city incorporating major industrial complexes. Although locally urban, the areal extent of the urbanization was limited. Station 92, NDS, although on the edge of a small town, was actually rural and surrounded by flat, agricultural land. Station 94, GTS, had mixed characteristics, locally suburban, surrounded partly by open country and partly by new suburban development. In the discussion that follows GTS is referred to as a 'suburban' station.

The observations were made with over-inflated 100-gram balloons which rose at rates of 3 to 4 m s^{-1} and usually reached 500 mb or higher. Relative humidity and temperature readings were evaluated manually for every pressure contact (roughly every 10 to 15 mb). These were

corrected for electronic drift, and were scaled by preflight checks of the relative humidity and temperature sensors. Additional thermodynamic parameters also were calculated (e.g., dew point, potential temperature, equivalent and wet bulb potential temperatures, etc.). Processing was by computer; the processed data were carefully edited and recorded on magnetic tape for archiving.

A wide range of weather conditions were included in the data sample. Since a major interest was the inadvertent modification of precipitation, and 50% of that rain occurs in the afternoon and evening in the area, emphasis has been placed on midday rather than morning soundings.

A fair fraction of the scheduled launches were aborted or the data had to be discarded because of equipment problems or poor radiosonde packages. In addition, some soundings were not included in the analysis because it was obvious that the profiles were strongly affected by rain at or near the station during or just prior to the launch. In order to maximize the information available for analysis, the data from each station have been subdivided in various ways. There are two basic sets —one containing all available valid soundings and a second set (matched data) for which simultaneous data were available from the urban station and from at least one of the rural stations. The data were then stratified according to rain conditions —'fair' if no rain occurred anywhere in the METROMEX area within 6 hours of the sounding and 'pre-rain' if rain occurred within 6 hours immediately following the radiosonde launch.

The data from the rural stations were classified as being potentially 'affected' (A) by urbanization if the-low level air came from the direction of the urban area, or 'unaffected' (U) if the low level air came from a rural area. Stations 50 (BCC) in 1973 and 94 (GTS) in 1975 were both fairly close to the metropolitan area: BCC data were classed 'A' if the mean PBL winds were the WSW through the NW, and GTS data were classed 'A' if the winds were from the NNE through the SSE. Despite their distance to the nearest urban areas, PMQ (1973) was classed 'A' if the winds were from ESE to SE and NDS (1975) if the winds were from WSW to SW. Unless otherwise indicated only unaffected soundings from PMQ, BCC, and GTS were used in the analyses discussed below. Since NDS was so removed from sizeable urban areas, all soundings, U and A, were included for this station. Of the fair weather cases, all NDS soundings had been classified as U; of the pre-rain cases, which totaled only 5, two have been classified as A.

The following discussion is based on the characteristics of the vertical profiles, and a number of derived thermodynamic parameters (e.g., mixing height, stability indices, convective condensation level, etc.). The results are first presented with very little interpretation; they are summarized and discussed in the final section.

A number of factors should be kept in mind in reading the following presentation:

- The accuracy of radiosonde measurements (1 C in temperature, 10% in relative humidity under the best of circumstances)
- The characteristics of the various stations in the two networks
- The relatively small sample sizes, particularly in the pre-rain categories, and particularly in 1975 [Note. Sample sizes can differ in the various analyses because missing data within a sounding may preclude calculation of some of the thermodynamic parameters but not others.]

AVERAGE PROFILES

The profiles of a number of variables were averaged, level for level, over the full fair weather and pre-rain samples for each station as well as for the various stratifications. The most informative of these average profiles are presented. The profiles of differences in the urban and

rural values of a number of variables, averaged level for level for each pair of stations, are also presented. It was essential to base the analysis of urban anomalies on simultaneous soundings at pairs of stations because the sample was small and the synoptic pressure patterns and air mass histories varied.

It is reasonable to expect that the effect of the city is not likely to be detectable at heights above 4 km or so and that synoptic gradients across the networks were likely to be minimal in the averages. Thus the expected value of urban-rural differences at the upper altitudes (above 4 km or so) is zero and any deviation from this may be taken as an average error or bias which should not be considered in evaluating the profiles. In most cases, the average profiles of station differences indicate that there was some residual error of this type. This 'bias' is indicated in the figures and has been taken into consideration in the discussions of the urban-rural differences in the various parameters.

Although the primary interest is in the lower 2 to 3 km, the PBL, the profiles have been shown to 5 or 6 km. In a few instances, one or two of the soundings may have terminated for one reason or other, below 5 km. These early terminations were usually above the PBL, and caused no noticeable discontinuity in the average profile. Average profiles of the data sets with and without these cases of low termination differed very little.

Temperature Stratification and the Urban Heat Island

. Average midday (1330-1400 CDT) profiles of temperature and potential temperature for all fair case soundings in 1973 and 1975 are shown in figures C-9 and C-10. Only the unaffected soundings at the rural stations are included in the averages. The 1973 station samples contained seven days in common and the 1975 station samples contained 6 days in common. The uncertainties in the mean temperature profiles are indicated by the range of +1 standard errors of the mean potential temperatures in figure C-10.

The average temperature profiles have many of the characteristics to be expected on fair afternoons in the Midwest when the convection is limited in depth. A shallow unstable layer often occurred near the surface but the temperature stratification in the lower half of the PBL (roughly 600 to 800 m) was near neutral, the upper PBL was conditionally unstable, overlain (at 1.5 to 2 km) by more stable conditions of synoptic-scale origin which acted as an effective lid to the convection.

There were some interesting station-to-station differences in the fair cases. At BCC, the 1973 'near urban' rural station, a shallow inversion at about 900 m MSL topped a slightly unstable layer below (figure C-9c), a feature not found at the other rural station or at the urban station. At PMQ, the other rural station, and at ARC, the city station, the average temperature stratification was neutral in the lowest 700 m or so with an increase in stability above that height, but no inversion or isothermal layer. Also in 1973, the urban atmosphere tended to be less stable than the rural atmosphere in the lower 2 to 3 km. These station-to-station differences are found also in the average profiles for matched data samples. In the matched sets, as in the full samples, the PBL at ARC was significantly warmer than the PBL at the rural stations. Moreover, the neutral layer in the lower PBL was deeper at the city station, particularly when ARC and PMQ profiles are compared and the upper half of the urban PBL was less stable. The height above sea level of the synoptic 'lid' at ARC was about 150 to 200 m higher than at PMQ; in view of the differences in station elevations, this means that the depth of the PBL was about 300 m greater at ARC.

As has already been mentioned, the land use characteristics of the 1975 stations were less distinctive than they were in 1973. Nevertheless, comparison of the average profile at the urban-industrial location (RXS) with those at the other more rural stations, gave indications similar to

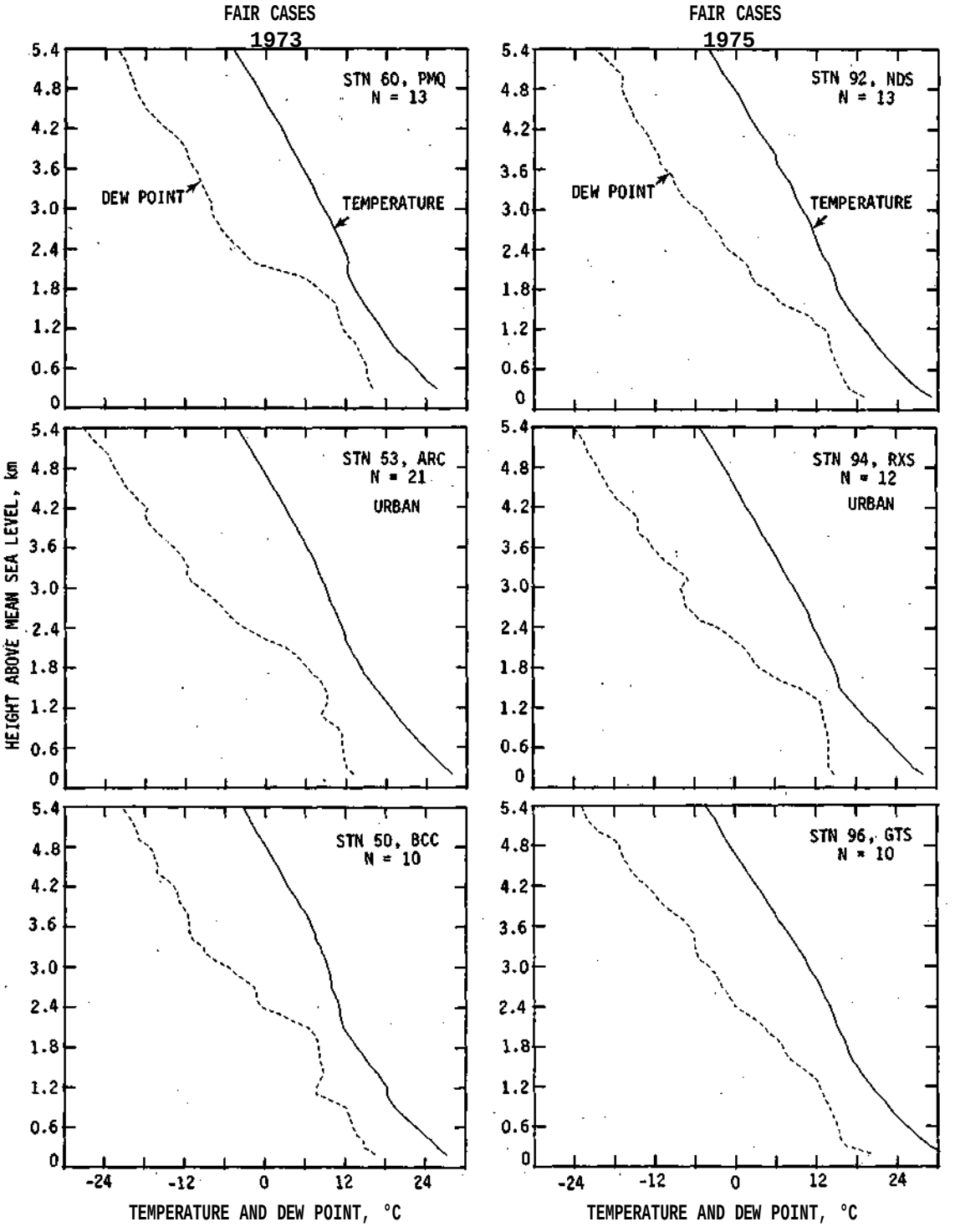

Figure C-9. Average profiles of temperature and dew point in fair weather
(Only unaffected (U) soundings at the rural stations are included in the average)

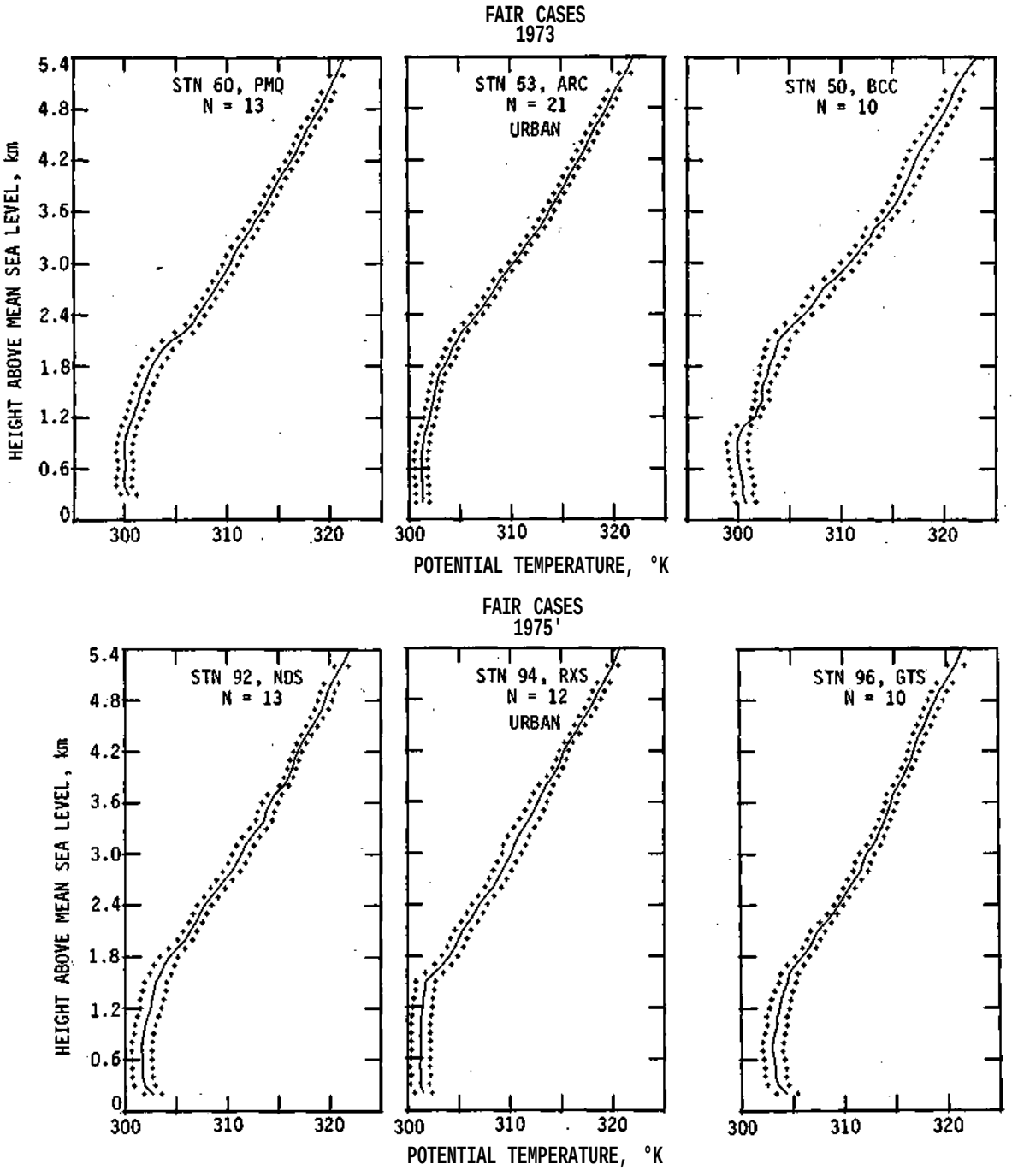

Figure C-10. Average profiles of potential temperature in fair weather (Only unaffected (U) rural soundings included. Number of soundings in the average is given by N. The plus signs indicate the spread for ± 1 standard error)

those found in 1973. The thermal stratification in the average fair-case profiles at NDS and GTS were very similar (figure C-10), despite their diverse physical characteristics, while the thermal stratification at RXS, the urban station, was significantly different. At RXS a deep neutral layer extended from the surface to 1.5 km MSL, whereas the average temperature lapse at the other two stations was neutral or slightly unstable only to about 700 m, and conditionally unstable to the top of the PBL at 1.5 or 1.6 km.

The average temperature profiles for the pre-rain cases are shown in figures C-ll and C-12. The temperature stratification within 6 hours of precipitation was similar to that in fair weather, with but one very important exception: the PBL was not topped with a stable layer; rather, there was a gradual transition from the unstable or neutral lapse rate in the lowest 600 or 800 m, to conditional instability in the next kilometer, and to an approximately moist-adiabatic lapse rate above about 3.5 km MSL.

The 1973 network differences for pre-rain conditions were similar to those found in fair weather. Both of the rural stations, PMQ and BCC, had shallow unstable layers, even in the average profiles, but the lapse rates became slightly stable (for dry ascent) above 400 to 500 m MSL. Conversely neutral, and therefore probably well-mixed conditions, extended to 900 m MSL in downtown St. Louis.

Station-to-station differences are not as apparent in the 1975 network. Differences between the rural-suburban station of GTS and the city station were minimal. Comparison of the average profiles at RXS and the rural station NDS, however, shows that, similar to fair conditions, there was greater stability at the country site throughout the PBL. This is even more strongly indicated in the average profiles of the 4-day matched RXS-NDS subsets: the neutral layer at RXS extended to 1.1 km and there was less stability at RXS than at NDS for a kilometer above that.

Although the urban-rural temperature difference at the surface is known to be at a minimum, and sometimes non-existent, at midday (see Hilberg, page 25 of this report), aircraft measurements have shown urban-rural temperature differences of 0.5 to 1.0° C at 300 to 800 m over St. Louis on some days (Dirks, 1974; Braham, 1974). The profiles in figures C-9 through C-12 suggest that the urban sites were on the average probably warmer than the rural ones for the first kilometer or so. A truer representation of the urban temperature 'anomaly' is provided by the average profiles of urban-rural temperature differences shown in figure C-l3.

In 1973 the city site ARC was warmer than the rural stations to at least 1.5 km in both pre-rain and fair conditions. The average urban-rural temperature difference reached a maximum of about 1° C in the lower part of the PBL —at about 1 km in fair weather and at about 500 m in pre-rain periods. The city site ARC was cooler than PMQ in the upper part of the PBL on fair days (figure C-l3a). However, for all other urban-rural combinations on fair days, and for all pairs (including ARC-PMQ) on rain days, the city station was, on the average, warmer than the rural station up to nearly 3 km (figures C-l 3b-d).

As mentioned earlier, in the 1975 network the urban site RXS was on the south side of a small sized industrial area and, as one might suspect, the urban heat island is not as apparent in the analysis as it is for the 1973 data. Only differences between the RXS and NDS temperatures for pre-rain cases are large enough to be considered out of the noise level (figure C-13g). These indicate that RXS was warmer than the rural site through the lower km at least, by a maximum of about 1° C at about 500 m. Although the sample is extremely small, this result agrees with the urban-rural comparisons for the 1973 network.

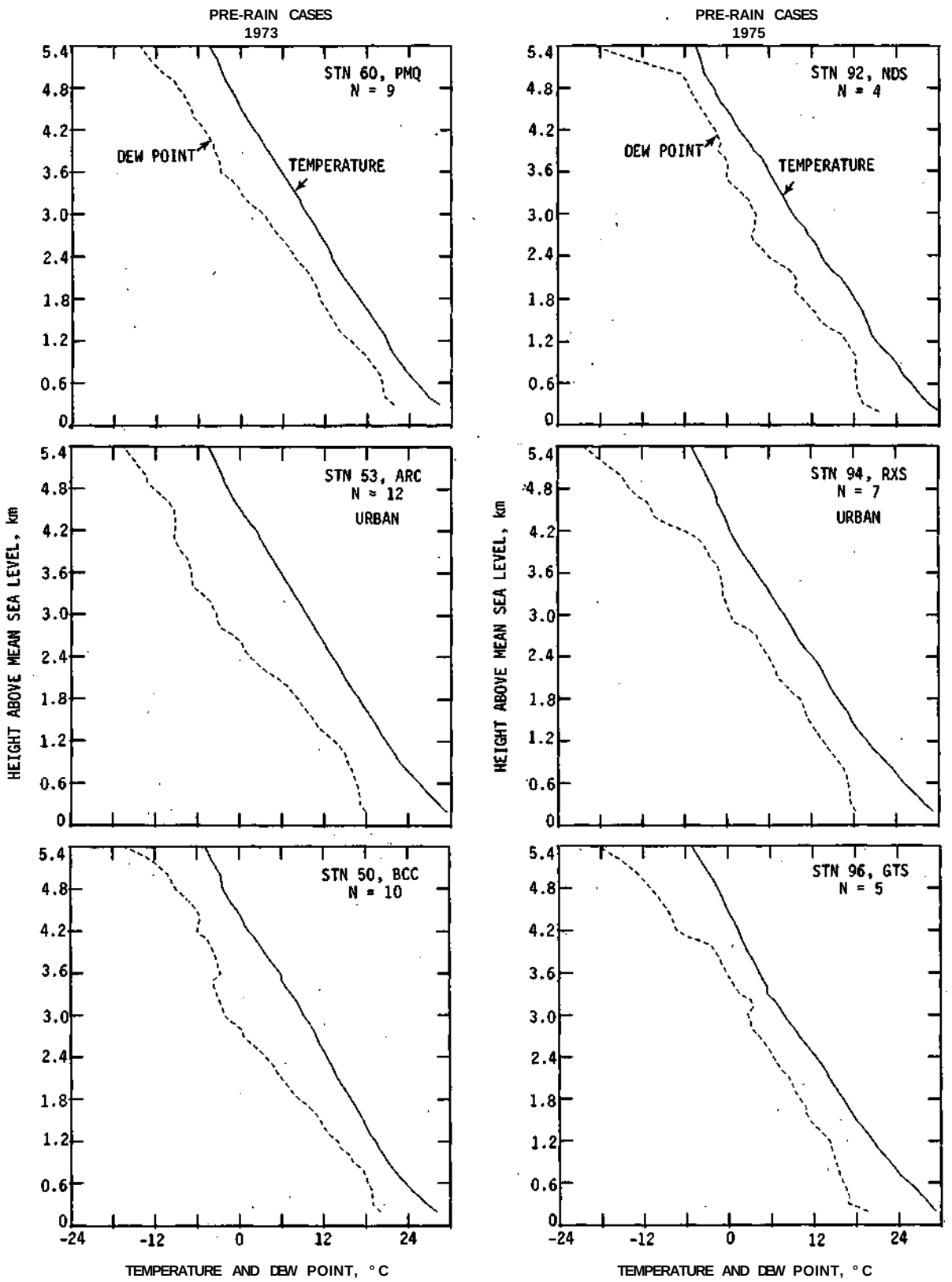

Figure C-11. Average profiles of temperature and dew point in pre-rain cases (notes as in figure C-9)

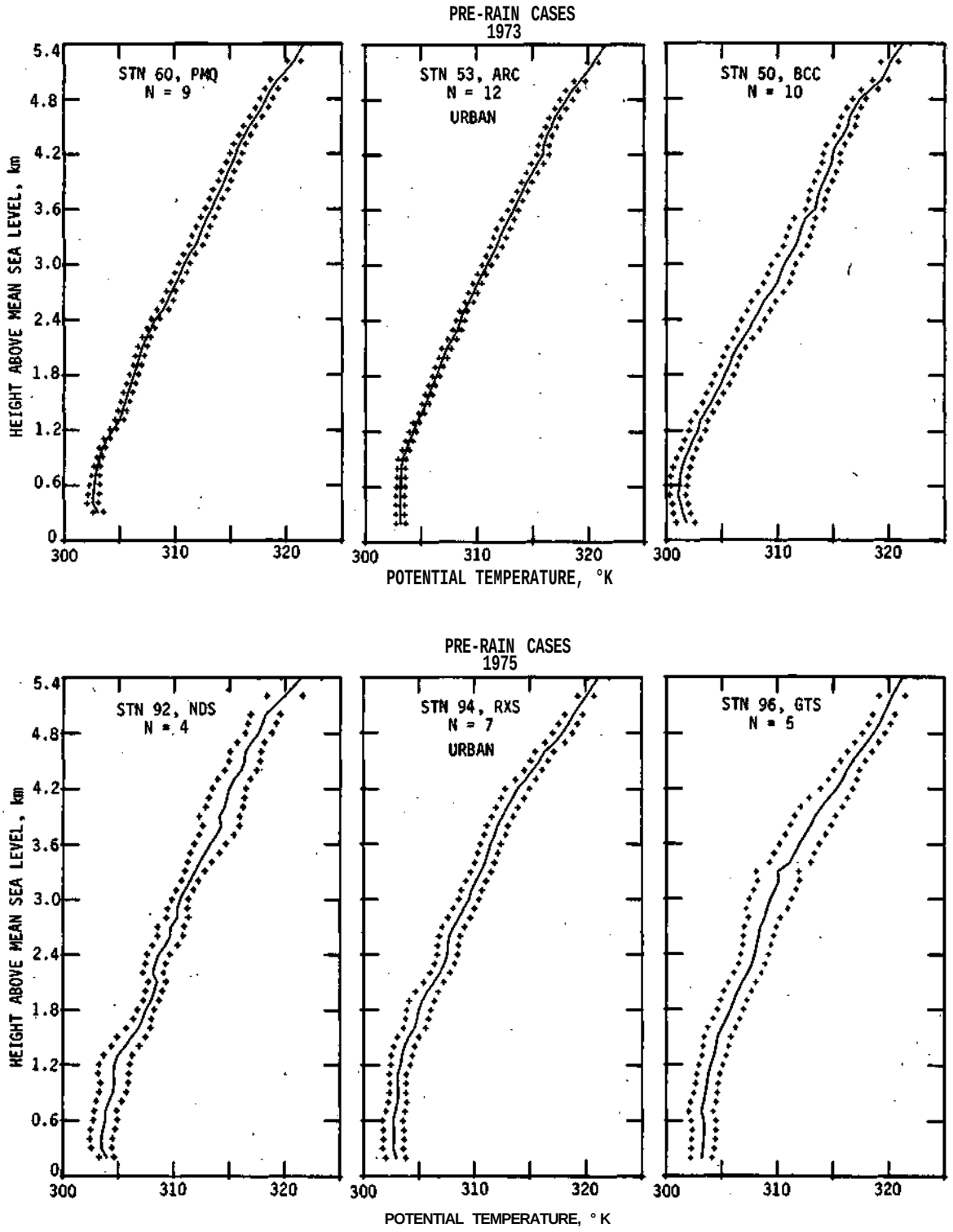

Figure C-12. Average profiles of potential temperature in pre-rain cases (notes as in figure C-10)

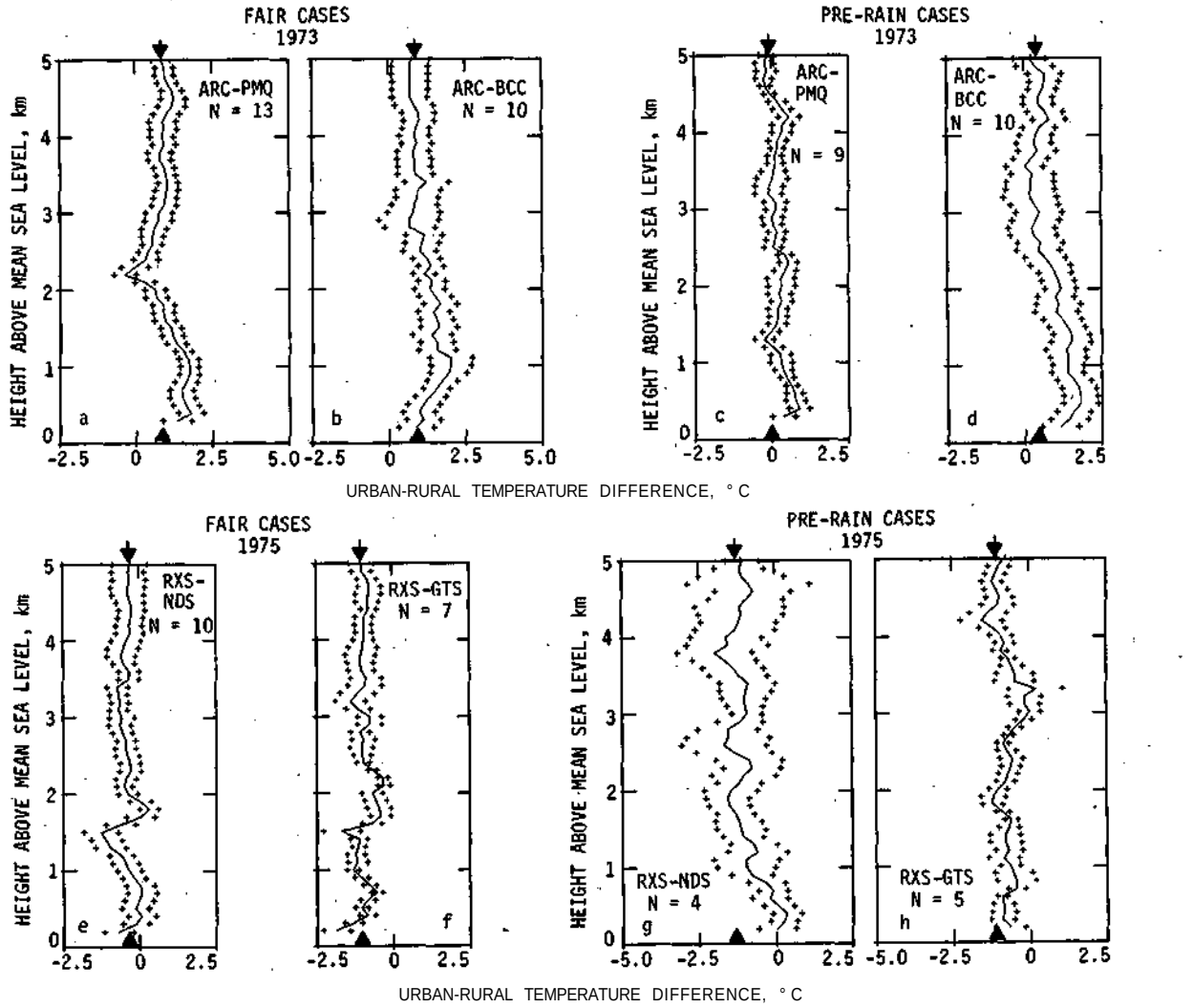

Figure C-13. Average profiles of urban-rural differences in temperature in fair weather and pre-rain conditions (Only unaffected rural soundings were included in the average. The arrow head along the abscissa indicates the 'adjusted' zero, based on the suspected bias in the data from one of the stations in the pair. N gives the size of the sample for each matched pair.)

Moisture Distribution

The lower troposphere on fair days was, on the average, fairly humid up to about 1.5 to 2 km at all stations (figure C-9). Above 2 km, and associated with the synoptic stable layer mentioned above, the moisture decreased fairly rapidly to much drier conditions aloft. Among the 1973 stations, PMQ, in a heavily wooded area, had the smallest dew point depressions (highest relative humidities); in the 1975 network, NDS, the remote rural site, had the smallest dew point depressions.

In fair conditions, the vapor content decreased very gradually up to about 1.5 to 2 km at the rural stations, while at the urban stations (ARC and RXS) it was almost constant throughout this depth (figure C-14). The top of the mixing depth occurred at about 2 km where the moisture decreased sharply, even in the average profile, often a symptom of upper level subsidence. This

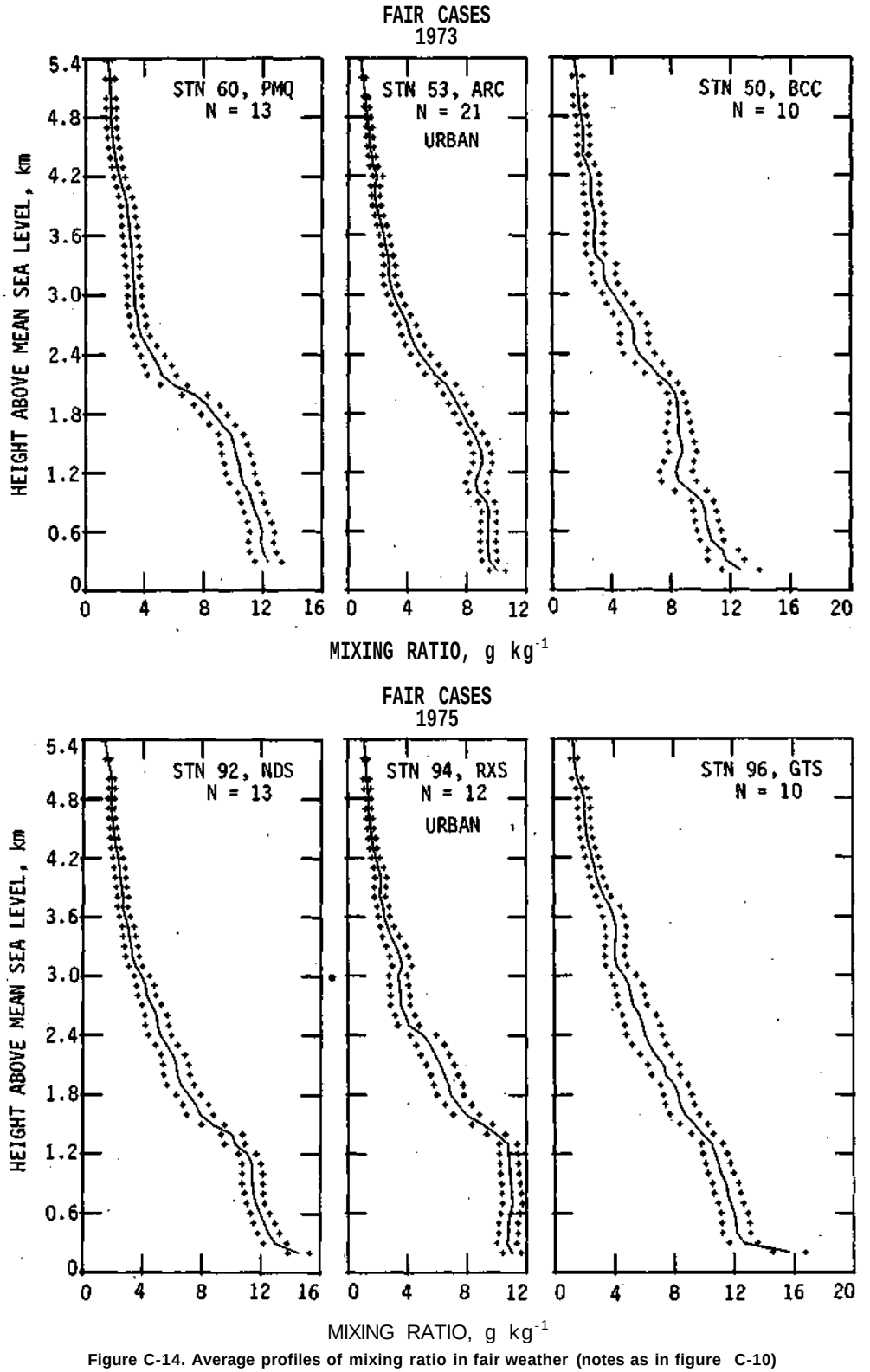

Figure C-14. Average profiles of mixing ratio in fair weather (notes as in figure C-10)

is less well-defined in the 1975 average profiles than in the 1973 data set, possibly because of greater day-to-day variation in the height at which it occurred. The suggestion of deeper mixing at BCC than at the other 1973 stations is a consequence of sampling. The average profiles for matched samples show the mixed moist layer at BCC no deeper than at the other stations, and in fact suggest that the urban stations had slightly deeper moist layers (by about 100 to 200 m) than the rural stations.

As one would predict, the humidity in the pre-rain cases was, on the average, higher than in the fair cases, and there was no drying aloft (figure C-l1). However, the depth of nearly constant mixing ratio was generally less than on fair days, with a more-or-less steady decrease of moisture to 3 or 4 km (figure C-l5). In the 1973 network, only the city station showed a layer of constant vapor content in the lower boundary layer. As was true for the fair days, the average profiles for 1973 matched data sets verify that the layer of near-constant mixing ratio was deeper at the city station than at the rural stations. This was not the case in 1975, however, but the samples were very small (4 and 5 cases for NDS and GTS, respectively)..

The urban moisture deficit is apparent in the 1973 average profiles of urban-rural differences in mixing ratio for both fair and pre-rain cases (figure C-l6). However, if the differences are reduced by the suspected bias, it can be seen that this deficit was primarily a low-level phenomenon, particularly in fair weather. For fair cases, the low level urban moisture deficit was from 500 m to over 1 km deep, and deepest when the city PBL is compared to that over a heavily wooded location (figure C-l6a). However, in the *upper* PBL there were layers 800 m to 1.5 km deep which tended to be more moist over the urban site than over the rural areas.

The lower-level region of urban moisture deficit was deeper, on the average, for pre-rain cases, on the order of 1 to 2 km in depth, and urban moisture excess did not occur over layers of significant depth. The extreme depth of the urban deficit indicated in the ARC-PMQ profile in figure C-l6c, is probably due to meteorological (or instrumental) bias. The profile of differences between the moisture content at the agricultural site of BCC and at PMQ (not shown) indicates a similarly deep layer in which BCC was relatively dry, with the BCC-PMQ deficit about the same magnitude as that of the ARC-PMQ deficit above 1.6 km.

Equivalent Potential Temperature (EPT)

The equivalent potential temperature (EPT) is one of the few parameters which is conserved in parcel ascent both before and after saturation. Thus it has sometimes been used as a 'tracer' to identify the source of cloud air. The average profiles of urban-rural differences in EPT (figure C-l7) indicate lower equivalent potential temperatures in the urban PBL than in the rural PBL at least below 1 km in most instances. This suggests that although the temperatures in the lower PBL were higher over urbanized areas than over the country, the lower mositure content apparently more than compensated for the higher sensible heat content. The magnitude of the standard errors indicate that the urban-rural differences in EPT had much greater interdiurnal variability than did the other parameters and their urban-rural differences.

On fair days in both years, the EPT was usually lower over the urban areas than over the country, primarily in the lower layers below 1 km (figure C-17a-d). The one exception is the comparison of downtown ARC with the remote forested site, PMQ. In the middle and/or upper part of the PBL, the urban air tended to have higher, rather than lower, equivalent potential temperature than country air on fair days.

In cases when rains were in the offing, the indications from these small samples are not as straightforward. For the 1973 network, the central city again had low EPT only in the lower PBL,

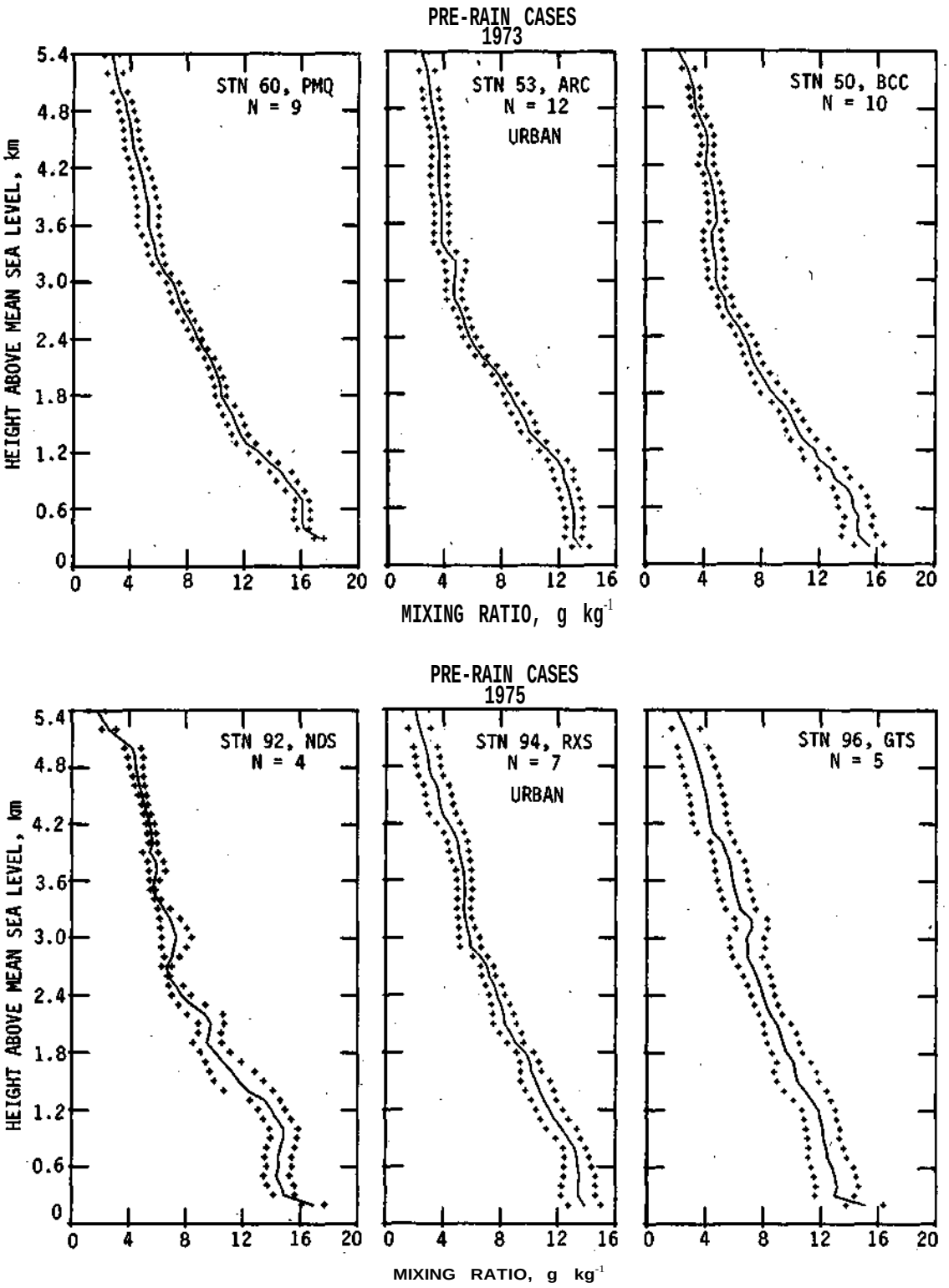

Figure C-15. Average profiles of mixing ratio in pre-rain cases (notes as in figure C-10)

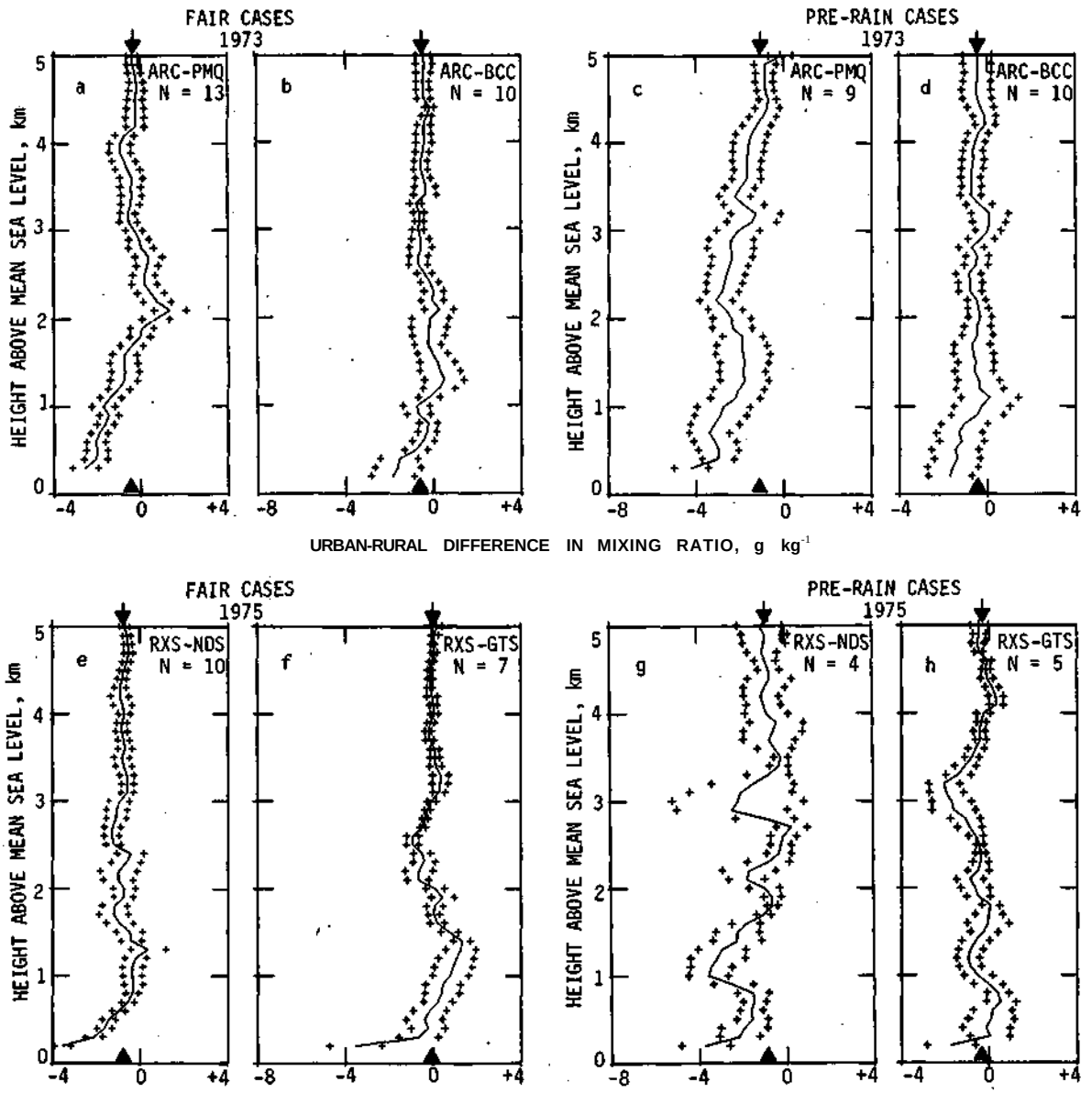

Figure C-16. Average profiles of urban-rural differences in mixing ratio in fair weather and pre-rain conditions (notes as in figure C-13)

when compared to a near-urban agricultural site (BCC). However, in the upper PBL where the urban-rural difference in EPT was positive (urban high) on fair days, the deviation in pre-rain cases was not much above the noise level (figure C-17f). The average profiles of ARC-PMQ differences in EPT indicate lower EPT at the city location all the way to 3 or 4 km. However, as mentioned in the discussion of the mixing ratio, there appears to have been synoptic or instrumental bias, since the EPT at BCC, the other rural site, was also considerably below the EPT at PMQ through most of the profile.

In the 1975 network in pre-rain cases, the urban PBL at RXS, when compared to the agricultural PBL at NDS had comparatively low EPT in a shallow layer near the surface, a second layer of low EPT between 1 and 1.5 km, and relatively high EPT near the top of the PBL (figure C-17g). Similarly, two low-level layers of comparatively low EPT are found in the comparison of RXS with suburban GTS, but a layer of comparatively high EPT near the top of the PBL did not occur (figure C-17h).

In summary, the air in the lowest kilometer tends to have significantly lower EPT over the city than over the surrounding countryside. In fair weather the air of the upper PBL over the city tends to have higher EPT than over the agricultural regions around it.

THERMODYNAMIC PARAMETERS

A number of parameters derivable from temperature and humidity profiles have been found to be indicative of the potential for the development of shower clouds and the severity of precipitation, as well as of the potential for upward transport of heat and moisture from the surface. These parameters are of the following types: 1) heights (or associated temperatures) at which certain processes are likely to occur (e.g., convective condensation level), 2) vertical integrations (e.g., precipitable water), and 3) 'stability indices' which have been found to have some predictability for severity of weather.

The general characteristics of the vertical profiles have been discussed in the previous section, particularly those relating to stability and mixing in the PBL. Comparisons between derived thermodynamic parameters for urban and rural PBLs are presented below.

Mixing Height

The mixing height, as used here, indicates the height to which mixing, by free or forced convection, could have occurred before the rising air experienced a strongly stable 'lid.' Thus it gives the *potential* for mixing of low level air, but does *not necessarily* give the height to which mixing actually occurred. The depth through which thorough mixing of the lower atmosphere had taken place (the mixed depth) at the time of an observation is more appropriately indicated by the depth of near-neutral temperature lapse rate and near-constant mixing ratio. This is most easily detected in the average profiles and also has been discussed.

The mixing height was determined from the temperature profile as the height of the lowest isothermal or inversion layer with a minimum depth of 10 mb. [This is a minor modification of the method used by the environmental support units (EMSU) of the National Weather Service (Wuerch et al., 1972).] When such a layer did not occur in the lowest 3 km, the mixing height was undefined but was assigned a value of 3.001 km for convenience. Potentially deep mixing, which such undefined mixing heights indicate, could be due to generally unstable conditions in

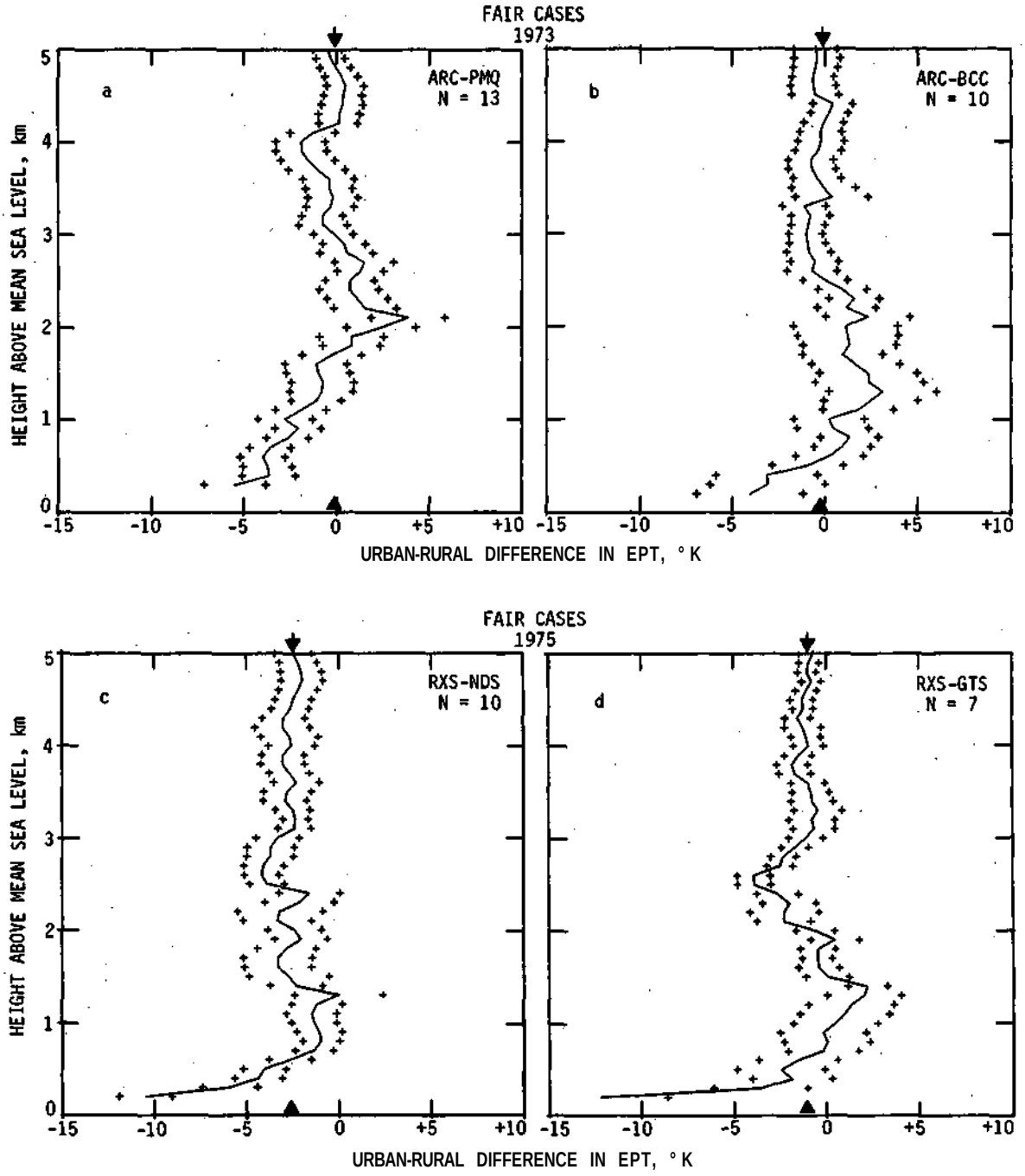

Figure C-17. Average profiles of urban-rural differences in equivalent potential temperature (notes as in figure C-13)

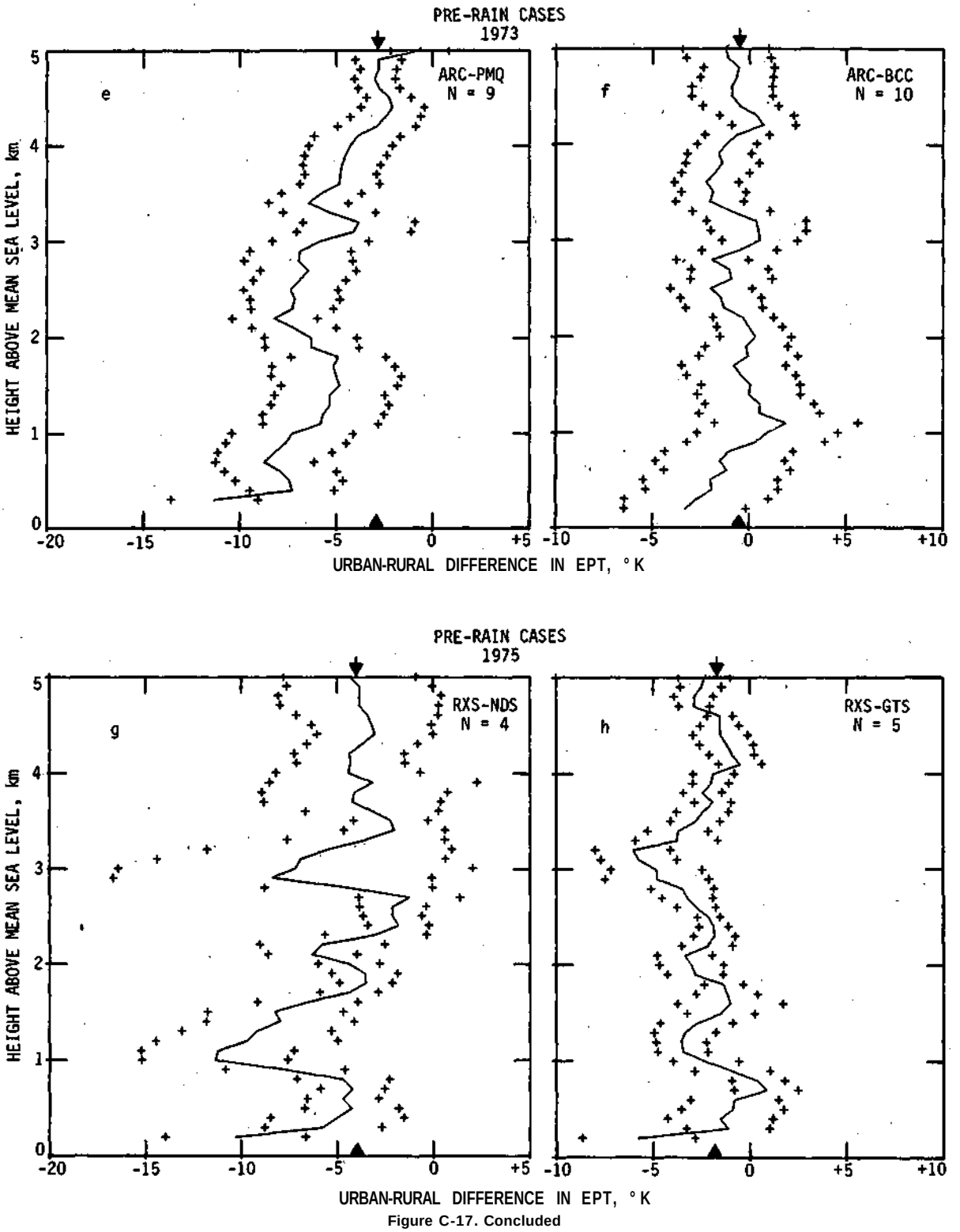

Figure C-17. Concluded

the troposphere or could be the result of locally enhanced mixing which eroded a low-level stable layer. The former was probably the case when both the urban and rural mixing heights exceeded 3 km. In the following discussion the mixing height is given as mean sea level (MSL) elevation, unless otherwise indicated.

Matched sets of urban and rural mixing heights, determined from nearly simultaneous soundings taken around 1330 CDT, are shown in the scatter diagrams in figure C-18. The symbols identify the rural station, and the probability that the sounding had been affected (A) by urbanization, as described earlier. There were very few instances in which the rural sounding might have been affected by passage over the metropolitan area. Moreover, the urban-rural differences for affected and unaffected soundings were similar. Thus, in order to enlarge the sample all available cases, affected and unaffected, were used in the analysis of mixing heights.

In general, the mixing height was below 3 km in fair weather. Undefined mixing heights occurred at two stations or more on only two occasions out of 15 in 1973, but they were relatively more frequent in 1975 (3 cases out of 9). The mixing heights tended to be higher over downtown St. Louis than over the adjacent countryside in both fair weather and pre-rain conditions (figure C-18).

On fair days in 1973, the mixing height was greater in downtown St. Louis than at the rural station, PMQ, 62% of the time, whereas the reverse was true only 8% of the time (table C-l0). Similarly, the mixing height at the Arch was greater by 100 m or more than at BCC six times as compared to twice when BCC > ARC. The mixing heights at RXS, in a small urban-industrial area, were higher than at rural NDS twice as often as the reverse was true. On the other hand, there seems to have been no consistent difference between the mixing heights at RXS and the suburban station of GTS.

In pre-rain conditions in both 1973 and 1975, the urban location tended to have higher mixing heights than did the rural stations 55 to 75% of the time, whereas the urban mixing height was lower than rural less than 10% of the time. Again there was no consistent difference between the urban (RXS) and suburban (GTS) locations in the 1975 network.

The average mixing heights and the potential depth of mixing (i.e., mixing height MSL elevation minus station MSL elevation) are given in table C-l1, based on simultaneous soundings for which both urban and rural mixing heights could be defined. Over all, potential depth of mixing averaged between 1.3 and 2 km. The 1975 pre-rain averages are not shown because of the small number of cases.

Of all the stations in the two networks, the wooded site at PMQ had the lowest mixing heights and potentially shallowest depth of mixing, and downtown St. Louis (ARC) the deepest.

Table C-10. Fraction of Cases in Which the Mixing Height at the Urban Site Was Higher or Lower, by at Least 100 m. Than That at the Other Two Stations

	FAIR		PRE-RAIN	
Rural site	*Higher*	*Lower*	*Higher*	*Lower*
1973 — ARC, urban station				
PMQ	8/13	1/13	6/11	1/11
BCC	6/13	2/13	7/11	1/11
1975 — RXS, urban station				
NDS	4/9	2/9	3/4	0/4
GTS	3/9	3/9	1/6	2/6

Note. The denominator gives the total number of cases

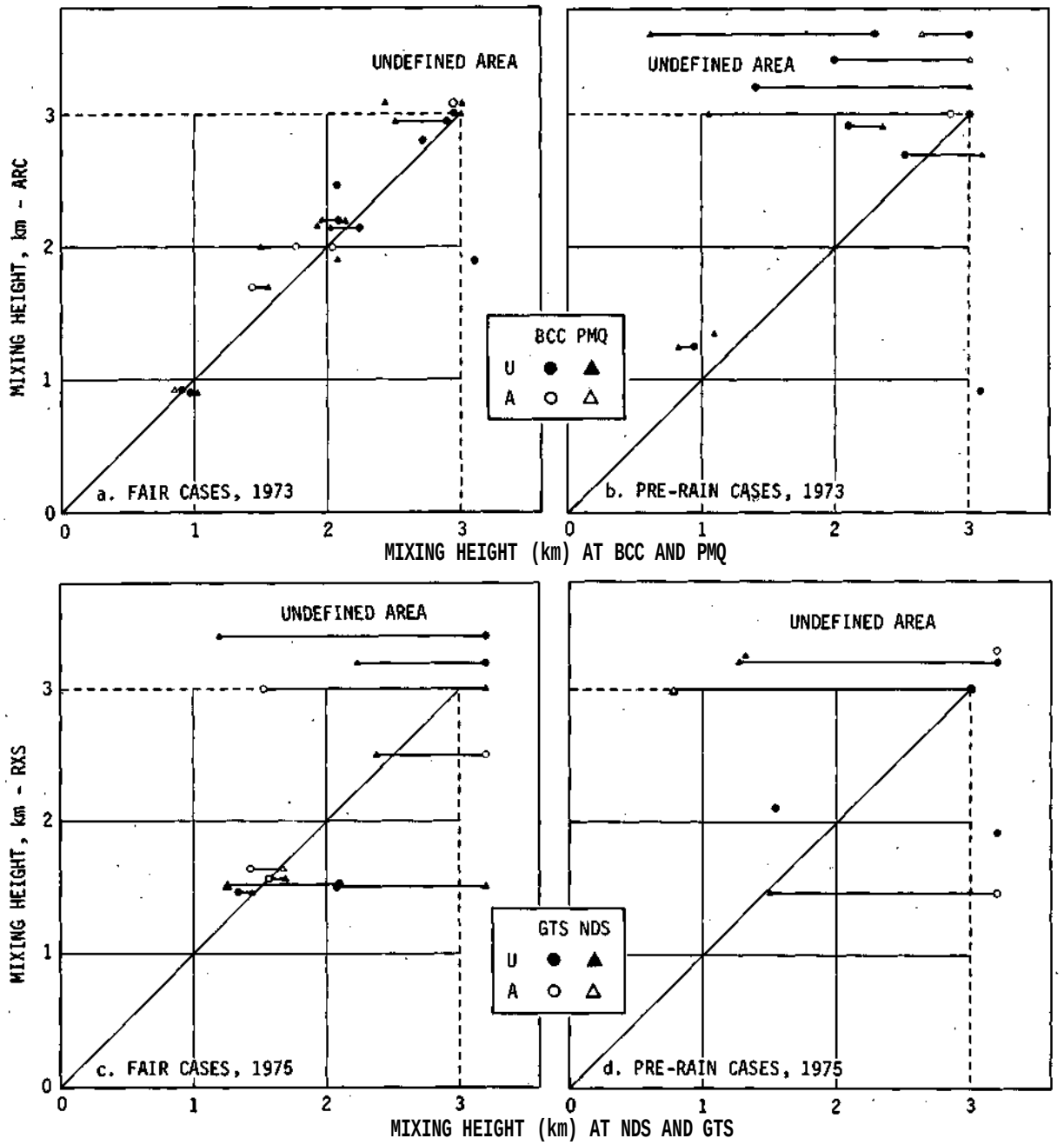

Figure C-18. Plot of mixing height at the urban station against the mixing height at one of the non-urban stations (Points plotted in the undefined area indicate mixing height greater than 3 km)

Table C-11. Average Elevation (m, MSL) of Mixing Heights, and Urban-Rural Differences

1973 Fair	*PMQ*	*ARC*	*ARC-PMQ difference*	*BCC*	*ARC*	*ARC-BCC difference*
Mean	1755(1482)	1909(1707)	154(288)	1917(1762)	2007(1868)	90(106)
SE	162	195	66	218	209	51
N	10	10	10	10	10	10
1973 Pre-Rain						
Mean	1425(1152)	1833(1964)	408(542)	1855(1700)	2280(2141)	425(441)
SE	471	537	85	467	521	197
N	3	3	3	3	3	3

1975 Fair	*NDS*	*RXS*	*RXS-NDS difference*	*GTS*	*RXS*	*RXS-GTS difference*
Mean	1687(1501)	1743(1600)	47(99)	1702(1520)	1537(1403)	-165(-99)
SE	191	190	68	160	30	167
N	5	5	5	5	5	5

SE = standard error, N = sample size
Note. Values in parentheses give potential depth of mixing. (See text for definitions and details of samples used in calculations)

The differences in potential depth for mixing between these two stations were sizeable in both fair and pre-rain conditions, being several times the standard errors. The Wilcoxon signed-rank and Fisher sign tests based on all matched data indicated that the hypothesis that the ARC mixing height was greater than the PMQ mixing height may be accepted at a significance level of 0.03 for fair weather and 0.06 for pre-rain cases, despite the small sample sizes.

The potential mixing depth at ARC was higher than at the agricultural site (BCC) by amounts averaging over 100 m. The differences are only twice their standard errors but the Wilcoxon and Fisher tests give significance levels of around 0.10 to 0.15 for an acceptance of the hypothesis that the mixing heights were greater at ARC than at BCC. Clearly there is a very strong indication that the mixing heights over downtown St. Louis were higher than those over the surrounding rural areas.

As has been noted in the frequency counts, there is no significant difference between the mixing heights at the smaller city and at a suburban location (RXS and GTS). Although the data suggest that the mixing height was greater at RXS than at the agricultural site of NDS, the high variability and small sample size do not permit any conclusion as to the validity of this finding.

Condensation Levels and Related Temperatures

The lifting condensation level (LCL) and the convective condensation level (CCL) are estimates of the height at which an air parcel, rising dry adiabatically from the surface layer would first become saturated. They differ in the assumed initial parcel characreristics: the LCL is the saturation level for a parcel having surface temperature and moisture content; the CCL is the saturation level for a parcel having the moisture content of a mixed boundary layer and a predicted 'convective' temperature.

Because of potentially large errors in the surface measurement and the variability in the physical properties of the surface, the LCL was determined for a parcel of air originating at the

height of the first pressure contact of the sounding above the surface, rather than at the surface itself. The first pressure contact of the sounding was within 100 m of the surface in all cases, and within 30 m in most. The computed LCL, based as it was on midday soundings, was probably within the limits of error of the surface LCL. Standard methods were used in calculating the LCL (e.g., Huschke, 1959). Computation of the CCL, which was based on the average mixing ratio in the layer of air below 100 mb, was also by standard methods.

The heights of the CCL for the fair cases ranged from about 1.4 to nearly 5 km MSL and the temperature at the CCL ranged between -2 and +17° C. The CCLs tended to be lower, and, warmer, in the pre-rain cases, ranging from 1.2 to 3.5 km in height and +8 to +20° C in temperature (figure C-19). Although there appears to be a semblance of a linear relationship between the urban and rural CCL on fair days (figure C-19a, e) there is virtually none in pre-rain conditions (figure C-19b, g). However, it is evident from these scattergrams that the distributions of the CCL height and temperature at PMQ (and to a lesser extent at BCC) were different from those in downtown St. Louis, particularly in pre-rain conditions. In general, the width of the distribution at the Arch was considerably greater than at the rural stations, indicating greater variability.

The 1973 data set indicates that on fair days the CCL in downtown St. Louis was on the average higher (cooler) than in the surrounding countryside. The urban-rural difference was nearly 1 km (4° C) when the urban value was compared with that of a rolling and wooded rural site, PMQ (table C-12), and it was over 400 m (1° C) when the city CCL was compared with that of the near-urban agricultural site of BCC. There was considerable scatter in the magnitude of the urban-rural differences, but good consistency in the signs of the difference. The CCL at ARC was higher and colder than at PMQ in all fair cases and higher and colder than at BCC in over three-fourths of the cases in which the rural sounding was classed as unaffected by the urban area (table C-13). Although the average urban-rural difference was about the same for fair and pre-rain conditions, there was less consistency in the signs of the differences between ARC and the rural station PMQ, and a near-even split between positive and negative differences between ARC and BCC.

In the 1975 network, the CCL over the smaller urban-industrial community (RXS) tended to be higher and colder than the agricultural site (NDS) more often than the reverse, in both fair and pre-rain conditions (table C-13). However, the average urban-rural differences tended to be smaller than they were in 1973 when the comparison was based on the St. Louis site (table C-12). There was very little difference between RXS and the suburban location of GTS, with nearly an even split in the number of positive and negative urban-rural differences. The average urban-suburban differences suggest that the CCL at GTS may have been higher (colder) than at RXS, but this did not prove to be statistically significant.

Several statistical analyses were applied to the data to determine which, if any, of the observed urban-rural differences in CCL heights and temperatures were statistically significant. The tests used were as follows: the two-sample T test using all available unaffected soundings, the one-sample T test for matched samples (test for zero mean), the Kruskal-Wallace H and the Mann-Whitney U tests for both total data and matched sets, and the sign and Wilcoxon signed-rank tests for matched pairs. In all cases the null hypothesis, H_o, was that there was no difference between the CCLs at the urban site and the other station.

It is not surprising, in view of the consistency of sign and the magnitude of the differences, that the null hypothesis could be rejected when the CCL heights and temperatures at ARC and PMQ are considered, with significance level of better than 0.01 for fair weather cases and 0.05 for pre-rain conditions. On the other hand the null hypothesis could not be rejected (at the 0.10 level) in comparisons of either CCL heights or temperatures between the downtown St. Louis station and the near-urban rural station of BCC on rain days. In fair conditions H_o could be rejected, at the 0.10 level, for ARC and BCC CCL *heights* (but not temperatures) in matched data sets.

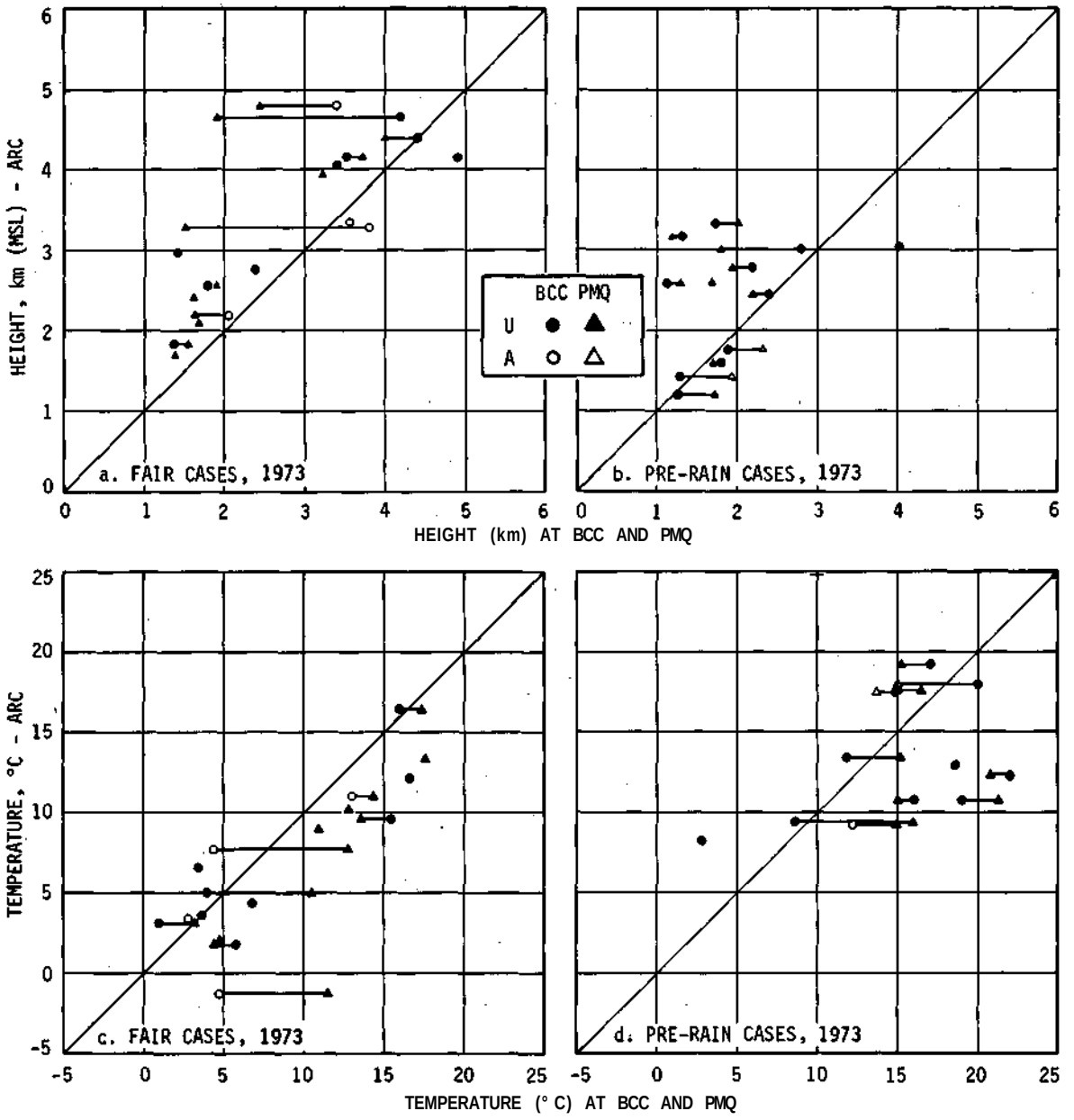

Figure C-19. Plot of the height and temperature of the CCL at the urban station against the height temperature of the CCL at one of the non-urban stations

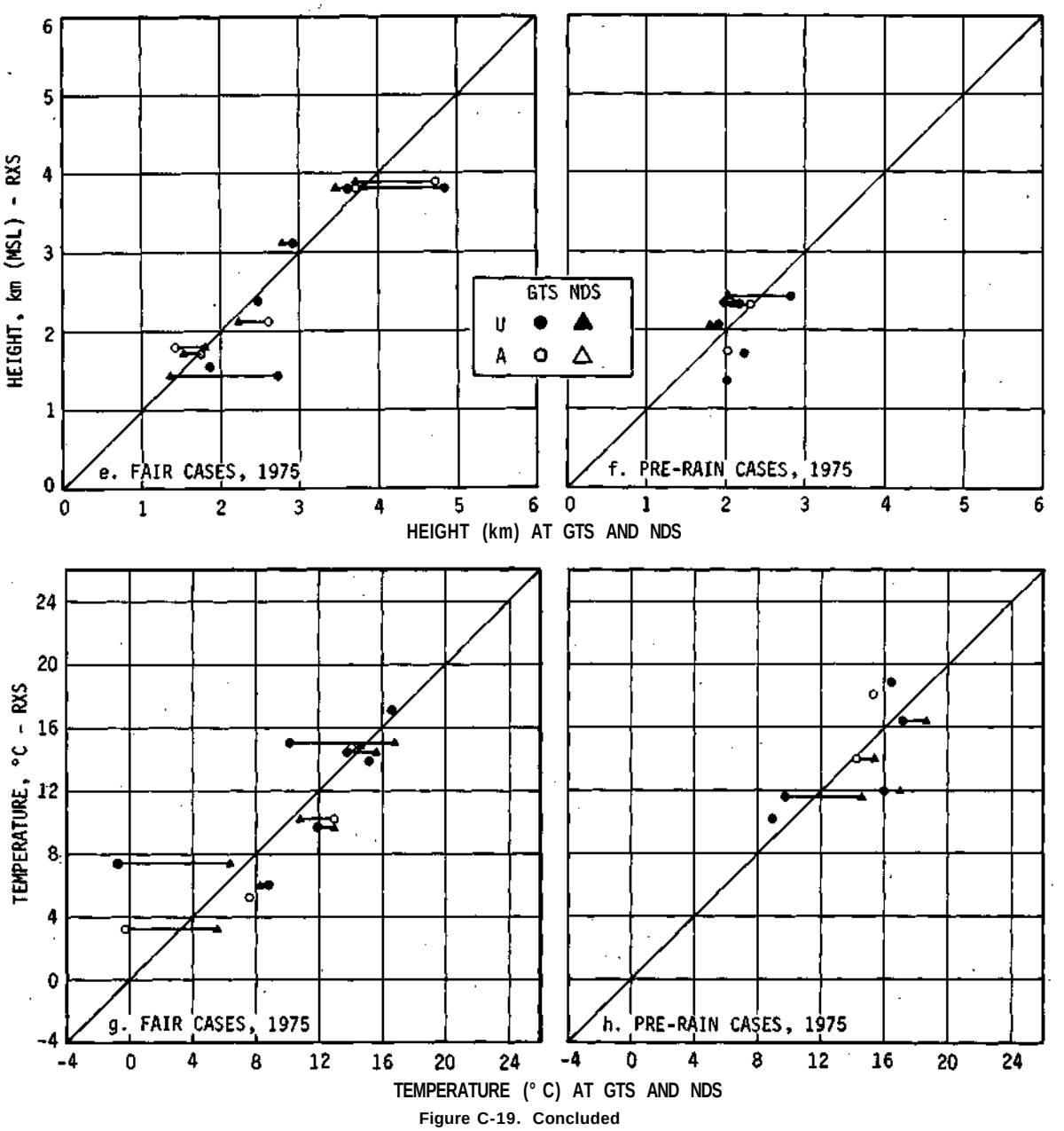

Figure C-19. Concluded

Table C-12. Average Heights and Temperatures of the CCL and Urban-Rural (or Urban-Suburban) Differences

	1973					1975				
	All soundings			Avg diff matched pairs, ARC minus		All soundings			Avg diff matched pairs, RXS minus	
	ARC	PMQ	BCC	PMQ	BCC	RXS	NDS	GTS	NDS	GTS
FAIR										
Height, m										
Mean	3257	2206	3044	967	456	2663	2633	2767	117	-388
SE	219	266	446	244	205	280	285	339	57	224
N	20	12	9	12	9	12	11	10	8	7
Temperature, °C										
Mean	6.9	11.2	8.1	-3.8	-1.1	10.5	11.6		-1.3	+1.1
SE	1.1	1.4	2.1	0.9	1.1	1.3	1.2		0.5	1.5
N	20	12	9	12	9	12	11		8	7
PRE-RAIN										
Height, m										
Mean	2409	1737	1964	786	389	2020	2031	2174	293	-160
SE	212	107	285	263	291	153	74	172	57	209
N	12	9	10	9	10	7	4	5	4	5
Temperature, °C										
Mean	13.2	17.0	14.7	-4.2	-1.0	14.5	16.4	13.6	-2.9	+0.2
SE	1.1	2.6	1.8	1.5	1.6	1.3	0.9	1.8	0.8	1.2
N	12	9	10	9	10	7	4	5	4	5

SE = standard error of the mean, N = number of cases
Note. Only unaffected rural and suburban soundings included

Table C-13. Fraction of Cases for Which CCL at the Urban Site Was a) Higher or Lower by at Least 100 m and b) Colder or Warmer by at Least 0.6° C Than the CCL at the Other Two Stations

	a) Elevation		b) Temperature	
	Higher	Lower	Colder	Wanner
1973 — ARC CCL				
FAIR				
PMQ	12/12	0/12	11/12	0/12
BCC	7/9	1/9	4/9	3/9
PRE-RAIN				
PMQ	7/9	2/9	7/9	2/9
BCC	5/10	3/10	4/10	5/10
1975 — RXS CCL				
FAIR				
NDS	5/8	1/8	6/8	1/8
GTS	2/7	3/7	3/7	3/7
PRE-RAIN				
NDS	4/4	0/4	4/4	0/4
GTS	2/5	3/5	2/5	3/5

Note. The denominator gives the total number of cases
Only unaffected rural and suburban soundings included

Differences between the CCLs at the urban and suburban sites in 1975 are not significant, even for an alternate hypothesis that the GTS CCL is higher (colder) than that at RXS. The indicated differences between CCLs at RXS and the rural site NDS on rain days are significant at the 0.05 level (for an extremely small sample). The results of the tests for fair cases were mixed. Only the one-sample T and the signed-rank tests indicate statistical significance at the 0.10 level (with $P < 0.05$ for both height and temperature), whereas the other tests did not permit.the rejection of the null hypothesis.

The average profiles discussed earlier indicate that the lower boundary layer was fairly well mixed at midday at all radiosonde stations. Nevertheless, the moisture frequently decreased with height and the LCL was (as it customarily is) considerably lower and warmer than the CCL. Although the differences between LCL and CCL were not always the same at every station on every day, the relationship between urban and rural LCLs was similar to that of urban and rural CCLs. In fact, there was greater consistency in the sign of the urban-rural differences in LCL than in the sign of the urban-rural difference in CCL.

The LCL over downtown St. Louis (ARC) was, in fair and pre-rain conditions, higher than at either of the rural stations in most cases in 1973 (table C-14). There was also a preponderance of cases in which the city LCL was colder than the rural sites, particularly when the latter was remote from the metropolitan area. Similarly in 1975 the LCL over the small city RXS was without exception higher and colder than the rural area (NDS). As in the case of CCLs, there appears to be no obvious difference in LCLs at RXS and GTS. In fact, the data weakly suggest that in pre-rain conditions, a suburban location adjoining a massive urbanized area may tend to be even more 'urban,' at least as far as LCL is concerned, than a small industrial city.

Although the signs of the urban-rural difference in LCL were a little more consistent than they were for the CCL, the average magnitudes, and the variability, were usually smaller (table C-15), at least in the 1973 network. The LCL at ARC averaged around 500 m higher and 3.5 to 4° C colder than at PMQ, and around 300 to 350 m higher and 1.5 to 2° C colder than at BCC. The

Table C-14. Fraction of Cases for Which the LCL at the Urban Site Was a) Higher or Lower by at Least 100 m and b) Colder or Warmer by at Least 0.6° C Than the LCL at the Other Two Stations

	a) Elevation		*b) Temperature*	
	Higher	*Lower*	*Colder*	*Warmer*
1973 – ARC LCL				
FAIR				
PMQ	12/12	0/12	11/12	0/12
BCC	7/9	0/9	5/9	2/9
PRE-RAIN				
PMQ	8/9	0/9	8/9	1/9
BCC	7/10	0/10	5/10	3/10
1975 – RXS LCL				
FAIR				
NDS	9/10	0/10	9/10	0/10
GTS	3/7	3/7	4/7	3/7
PRE-RAIN				
NDS	4/4	0/4	4/4	0/4
GTS	1/5	4/5	1/5	2/5

Note. The denominator gives the total number of cases
Only unaffected rural and suburban soundings included

Table C-15. Average Heights and Temperatures of the LCL and Urban-Rural (or Urban-Suburban) Differences

	1973					1975				
	All soundings			Avg diff matched pairs, ARC minus		All soundings			Avg diff matched pairs, RXS minus	
	ARC	PMQ	BCC	PMQ	BCC	RXS	NDS	GTS	NDS	GTS
FAIR										
Height, m										
Mean	2072	1560	1768	505	261	1814	1587	1830	276	-108
SE	98	83	143	102	77	99	82	167	55	148
N	21	12	9	12	9	12	13	10	10	7
Temperature, °C										
Mean	9.5	13.1	11.9	-3.4	-1.5	12.2	14.7	13.8	-2.5	+0.0
SE	0.9	1.1	1.5	0.9	0.9	0.9	0.9	1.4	0.5	1.4
N	21	12	9	12	9	12	13	10	10	7
PRE-RAIN										
Height, m										
Mean	1678	1204	1230	508	393	1553	1474	1658	286	-90
SE	111	59	97	106	114	159	66	205	46	184
N	12	9	10	9	10	7	4	5	4	5
Temperature, °C										
Mean	15.0	19.2		-4.2	-2.2	15.9	17.4	15.1	-2.5	0.1
SE	3.1	1.7		1.1	1.3	1.5	0.8	2.0	1.0	1.5
N	12	9		9	10	7	4	5	4	5

SE = standard error of the mean, N = number of cases
Note. Only unaffected rural and suburban soundings included

average difference between LCL heights at RXS and NDS were slightly less, around 250 to 300 m, but the average temperature difference was slightly higher than in 1973. The average urban-suburban (RXS-GTS) differences in LCL temperatures and heights are well within their standard errors.

The results of the statistical tests were also similar to those for the CCL for most of the significance tests. The null hypothesis that there was no difference between the heights of the LCLs at urban and rural locations was rejected at the 0.05 level in every test and for both fair and pre-rain conditions. The null hypothesis that the condensation temperatures (i.e., temperatures at the LCL) were the same at urban and rural sites was rejected at the 0.10 or better level when the rural site was remote from the urban area but not when it was close to the urban area (i.e., BCC). There was no evidence of any significant differences one way or the other between LCLs over a small city and over a suburb on the periphery of a large metropolitan area.

Columnar Moisture Content: Precipitable Water

The moisture contained in the lower troposphere is very important to the production of precipitation since it is the main source of water vapor. The mean mixing ratio profiles presented earlier indicate that the moisture content of the lowest layers above the surface is less over the city than over the country. However, the moisture remained nearly constant over a considerable depth above the city, whereas it decreased rather rapidly over the country. Thus, it is not obvious that the total moisture content of the subcloud layers was less over the city than over the country.

The precipitable water (PW) is an expression of the total moisture content of a column of air in terms of the depth of water that would be produced if all of the vapor were condensed and precipitated. Thus, it is a direct measure of the integrated moisture content in a column extending through any depth that may be selected.

The precipitable water was calculated for all soundings for 1) the layer from the surface to 850 mb, which is, on the average, close to the depth of the well mixed subcloud layer, and 2) for the layer from the surface to the convective condensation level. In considering these calculated quantities, it must be kept in mind that the depth of the layer affects the result. The major difference in the depth of the column from surface to 850 mb arises from the difference in the surface elevations of the radiosonde stations. Since the maximum variation in station elevation was in the neighborhood of 100 m, and the 850 mb level is commonly around 1.5 km, the error introduced will be about 7%. The differences in the depths of the column from the surface to the CCL, however, is considerably greater, since it was shown previously that the CCL may occur several hundred meters higher over the city than over the countryside. However, if one accepts the CCL as being a predictor of the height at which clouds will form, then the precipitable water calculated for the layer from the surface to CCL represents the low-level moisture source for the cloud. Thus, this PW value is highly relevant to the study of the formation of an urban precipitation anomaly.

There was very little difference between the average precipitable water from surface to 850 mb for the city and country sites on fair days. Although the PW was slightly smaller over the urban area, the average urban-rural differences were less than 0.05 cm for both the 1973 and 1975 network (table C-16). The average difference in PW between the urban and suburban sites (RXS-GTS) in 1975 was about a millimeter, with the urban being high. The difference is roughly the magnitude of the standard error of the mean. Not only was the average urban-rural difference close to zero, but there were about equal numbers of cases in which the city site had higher precipitable water values than the country and vice versa (table C-17). Comparison of the urban site with distant rural site, PMQ in 1973 and NDS in 1975, shows that in one-fourth to one-third of the cases the urban-rural difference was less than 0.5 mm.

The data are not as consistent in pre-rain conditions. There is an indication that in pre-rain conditions the downtown site, ARC, may indeed have had lower PW below 850 mb than did the country sites. The average differences were 1 to 1.5 mm, about equivalent to the standard

Table C-16. Average Precipitable Water (cm) from Surface to 850 mb and Urban-Rural (or Urban-Suburban) Differences

	1973					*1975*				
	All soundings			*Avg diff matched pairs, ARC minus*		*All soundings*			*Avg diff matched pairs, RXS minus*	
	ARC	*PMQ*	*BCC*	*PMQ*	*BCC*	*RXS*	*NDS*	*GTS*	*NDS*	*GTS*
FAIR										
Mean	1.42	1.47	1.45	-0.01	-0.00	1.66	1.66	1.68	-0.04	0.12
SE	0.08	0.09	0.15	0.06	0.10	0.09	0.08	0.12	0.04	0.09
N	21	12	9	12	9	12	12	10	9	7
PRE-RAIN										
Mean	1.85	1.97	1.98	-0.15	-0.13	1.91	1.84	1.66	-0.31	0.07
SE	0.09	0.08	0.12	0.13	0.13	0.16	0.26	0.20	0.10	0.08
N	12	9	11	9	11	6	5	6	3	6

Note. Only unaffected non-urban soundings included

Table C-17. Fraction of Cases in Which the Precipitable Water (PW) from the Surface to 850 mb or from Surface to CCL at the Urban Station Was More or Less Than That at the Rural (Suburban) Station

	Surface to 850 mb		*Surface to CCL*	
	More	*Less*	*More*	*Less*
1973 — ARC Precipitable Water				
FAIR				
PMQ	5/12	4/12	9/11	1/11
BCC	4/9	5/9	5/8	3/8
PRE-RAIN				
PMQ	2/9	7/9	4/9	4/9
BCC	4/10	6/10	8/10	2/10
1975 — RXS Precipitable Water				
FAIR				
NDS	2/9	4/9	2/7	3/7
GTS	4/7	3/7	3/6	2/6
PRE-RAIN				
NDS	0/3	3/3	0/3	3/3
GTS	3/15	1/5	0/4	3/4

Note. The denominator gives the total number of cases

error for this group of data. However, the PW below 850 mb (lower 150 mb of the atmosphere) at the urban site was more often less than that at the rural site than vice versa (table C-17). The ARC PW was less than the PMQ PW almost 70% of the time, and less than the BCC PW 60% of the time. The same is true when RXS is compared with the rural site in the 1975 network. Hampered as always by the small sample size, the three cases in the matched data set uniformly showed greater precipitable water over NDS than over the city, averaging almost 3 mm, or three times the standard error. There was virtually no difference between the urban and suburban site for pre-rain cases, though the frequency count (table C-17) suggests that the RXS site had greater precipitable water values than the suburban site more frequently than the reverse was true.

The precipitable water from the surface to CCL was about 0.5 to 1 mm greater than that from the surface to 850 mb because of the greater depth over which the water vapor was typically integrated. The CCL PW were about 2 to 2.5 cm (see table C-18) compared with 1.5 to 2 cm for the 850 mb PW (table C-16). Both precipitable waters were about 10 to 30% larger in pre-rain cases than in fair cases.

On fair days in 1973, the CCL PW had a consistent tendency (90% of the cases) to be greater over the city than over PMQ (the wooded site to the northwest), averaging about 3 mm more over the city (table C-18). The difference between the CCL PW at the Arch and BCC, however, was of the same order as the standard error of the mean, and there was a more or less even distribution of cases in which the urban site had more or less precipitable water than the rural site. There are no urban-rural differences in CCL PW of any significance in 1975 fair cases, either in the magnitude of the average difference or in the frequency of positive or negative values (tables C-17 and C-18).

The urban-rural differences under pre-rain conditions in 1973 were not significant either in frequency or in magnitude of the average difference. There is, however, an indication in the 1975 data, primarily in consistency, of a negative urban-rural difference in precipitable water up to the CCL. However, once again the sample size is so small as to leave the results in question.

Table C-18. Average Precipitable Water (cm) from Surface to CCL and Urban-Rural (or Urban-Suburban) Differences

	1973					1975				
	All soundings			Avg diff matched pairs, ARC minus		All soundings			Avg diff matched pairs, RXS minus	
	ARC	PMQ	BCC	PMQ	BCC	RXS	NDS	GTS	NDS	GTS
FAIR										
Mean	2.36	2.06	2.43	0.28	0.16	2.38	2.46	2.50	-0.14	0.03
SE	0.13	0.10	0.09	0.11	0.18	0.14	0.13	0.21	0.11	0.15
N	19	12	8	11	8	11	10	8	7	6
PRE-RAIN										
Mean	2.65	2.58	2.51	0.05	0.14	2.67	2.62	2.66	-0.21	-0.15
SE	0.06	0.08	0.18	0.12	0.16	0.21	0.34	0.31	0.18	0.05
N	12	9	10	9	10	6	5	5	3	4

Note. Only unaffected non-urban sounding included

Not surprisingly there were no statistically significant differences between the urban and rural precipitable water values. Thus, one must conclude that there is no difference in the availability of moisture for the precipitation process for the urban and rural sites considered in this analysis. Although the precipitable water in the lower 150 mb under pre-rain conditions tended to be slightly smaller over the city, indicating a lower average mixing ratio, the precipitable water up to the CCL tended to be very similar over city and country under pre-rain conditions. To the extent that the CCL is representative of cloud base, a cloud over the city may be required to process more air than a cloud over the country in order to have available the same amount of moisture for precipitation.

Stability Indices

A large number of atmospheric indices have been proposed for use as predictors of the probability and severity of convective storms. Virtually all of these are derivable solely from the radiosonde measurements, although more recently these have been used in conjunction with dynamic predictors or have been modified to include dynamic factors. The thermodynamic predictors are commonly referred to as stability indices.

A large number of stability indices, some commonly used and others which were derived during the course of the research, have been computed for the afternoon soundings at each site for both the pre-rain and fair weather data groups. By and large this study was not very productive as far as identifying significant differences between urban and rural locations. The results of the calculation of a few of these indices, primarily those in more general use, are described below. These are as follows:

1) The Showalter Stability Index (SSI)
2) The Lifted Index (LI)
3) The K Index
4) The cross total (CT), vertical total (VT), and total total (TT)

The Showalter Stability Index is the difference between the temperature of a saturated parcel originating at the 850 mb LCL and the temperature of its environment when it reaches 500 mb, with the difference taken as environment minus parcel temperature (Showalter, 1953).

The SSI gives a measure of the buoyancy of a cloud parcel at 500 mb, assuming that the 850 mb LCL is the cloud base. A value of +4 has been identified as critical: SSI less than +4 is indicative of significant instability, leading to showers or thunderstorms; an SSI greater than +4 indicates minor or no convective instability. It can be seen from figure C-20 that the SSI is a fairly good indicator of rain conditions, but tends to over predict the probability of showers, as indicated by the sizeable fraction (30 to 35%) of the fair weather cases for which the SSI was less than +4. In 1973, the SSI for downtown St. Louis was greater than the rural SSI slightly more frequently than the reverse, on fair days when the SSI was less than +4, and in all pre-rain cases, suggesting less convective instability over the city. There was virtually no difference in SSI at urban and rural sites when the observation was made in a relatively small urban area as it was in 1975.

The Lifted Index is similar to the SSI except that the saturated parcel is assumed to originate at the LCL for a well mixed boundary layer 100 mb thick (Winston, 1956). A critical value of the LI has not been identified, However, it is obvious that large positive values would indicate suppressed convective activity and negative values strong convective activity since the latter indicate significant buoyant energy available for cloud development at 500 mb. The results for the Lifted Index were very similar to those for the SSI. Table C-19 shows the frequency of cases in which the Lifted Index at the urban station was greater or less than that at the rural stations for both fair and rain days. Except when comparing the Arch and PMQ there was virtually no difference between stations. The urban LI was greater than or less than the rural LI with almost equal frequency, and there was a high incidence of cases in which the difference between the two stations was less than 0.5° C. However, the LIs indicate that there was less thermal energy available at 500 mb at a downtown urban station (ARC) than at a forested location (PMQ), in both fair weather and pre-rain conditions.

The K Index was developed by J. J. George (1960) to provide a predictor for air mass thunderstorms when there was no frontal or cyclonic influence in the vicinity. George pointed out that the K values are sensitive to synoptic divergence or convergence and that a suitable adjustment should be made to the K value as used for purely air mass thunderstorms. The K Index tries to take in consideration the lapse rate in the cloud layer, low level moisture, and the moisture deficit in the midcloud layer. This is done by combining the following three terms: the difference, 850 mb temperature less the 500 mb temperature (lapse rate), is added to the 850 mb dew point *(low level moisture),* and from this sum is substracted the 700 mb dew point depression *(the moisture deficit at midcloud level).* K values greater than +20 indicate thunderstorm activity with increasing areal frequency as the index increases in magnitude. The critical values indicating increasing areal frequency are shown in figure C-21, a scattergram of urban-rural K values. To the extent the K Index is a good predictor of the ability of the atmosphere to induce thunderstorm activity, it is

Table C-19. The Fraction of Cases in Which the Lifted Index (LI) at the Urban Site was Less Than or Greater Than at a Rural (or Suburban) Site by at Least 0.5° C

	1973			*1975*	
	ARC LI			*RXS LI*	
	Less	*More*		*Less*	*More*
FAIR					
PMQ	0/12	9/12	NDS	0/8	3/8
BCC	2/9	4/9	GTS	3/7	3/7
PRE-RAIN					
PMQ	1/8	7/8	NDS	0/3	2/3
BCC	4/10	5/10	GTS	1/5	1/5

Note. The denominator gives the total sample size
Only unaffected rural and suburban data included

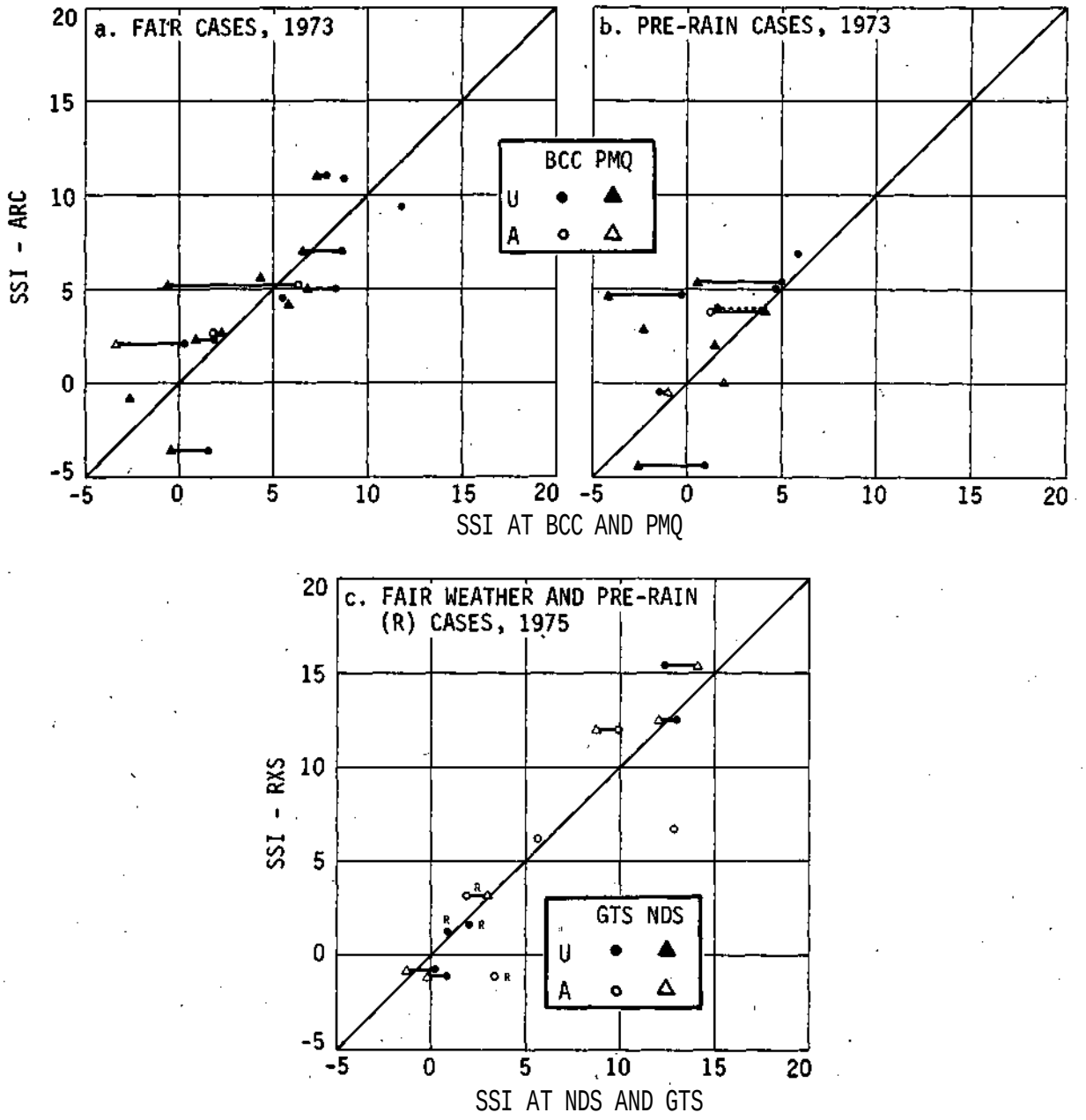

Figure C-20. Plot of the Showalter Stability Index (SSI) at the urban station against the SSI at one of the non-urban stations

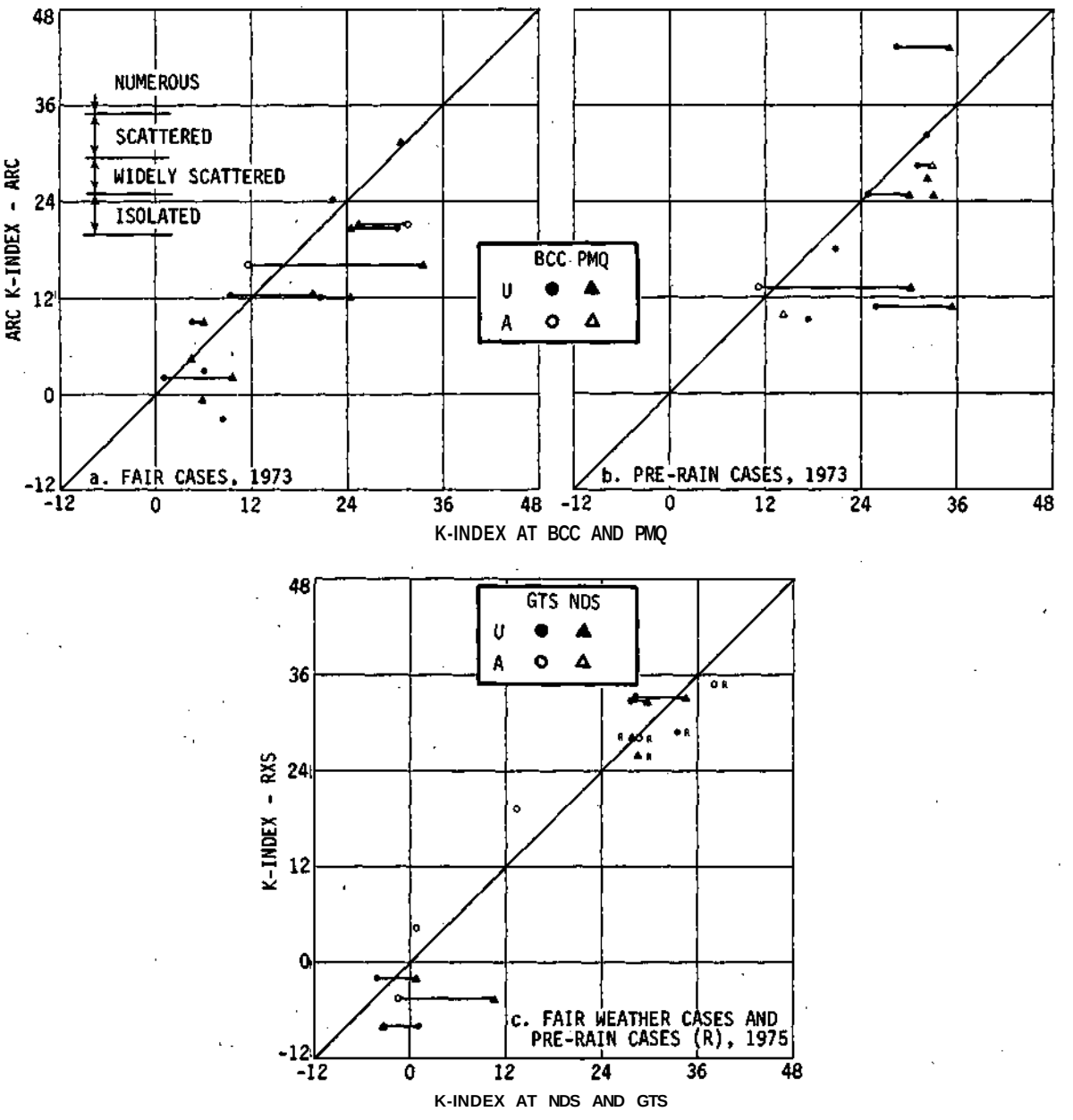

Figure C-21. Plot of the K Index et the urben station against the K Index at one of the non-urban stations

Table C-20. Number of Cases for Which the Cross Total (CT), Vertical Total (VT), and Total Total (TT) Indices Would Predict Thunderstorms at the Rural Station and Not at the Urban Station and, in Parentheses, Predict Thunderstorms over the City But Not over the Country

Rural station	Fair weather				Pre-rain conditions			
	N	CT	VT	TT	N	CT	VT	TT
1973 – ARC								
PMQ	10	1(0)	0(1)	2(0)	6	3(0)	0(2)	3(0)
BCC	8	0(0)	0(0)	1(1)	7	2(0)	0(2)	2(0)
1975 – RXS								
NDS	5	0(0)	0(0)	0(0)	1	0(0)	0(0)	0(0)
GTS	4	0(0)	0(0)	9(0)	2	0(0)	0(0)	1(1)

N - Total number of cases

obvious from figure C-21 that less thunderstorm activity (though not necessarily less intense thunderstorm) would be expected over an urban area than over a rural one. This is true for pre-rain days in particular, but it also true in fair weather when the K Index would predict scattered to widely scattered thundershowers which did not (in 1973) materialize. The differences in the K Index over city and country sites in 1975 were minimal. For K less than 20, the data may suggest more suppression of convection over the city than over the country.

The cross total, vertical total, and total total were developed as indices which could be computed easily and quickly for use in short range forecasting of thunderstorms. As with the other parameters, they are crude estimates of the humidity and temperature structure of the atmosphere between 850 and 500 mb. The cross total (CT) is the difference between the dew point at 850 mb and the temperature at 500 mb; the vertical total (VT) is the difference between the 850 mb temperature and the 500 mb temperature and the total total (TT) is the sum of CT and VT. Thunderstorms become probable when CT > 18, VT > 26, TT > 44. It can be seen from table C-20 that insofar as these critical values of the CT, VT, and TT are valid predictors, thunderstorms over the city are no more probable than over the rural areas. In most cases the indices would have indicated either no thunderstorm activity at either the urban or rural site, or thunderstorm activity at both locations. The one weak exception was at PMQ, where thunderstorms would be predicted to develop more frequently than at ARC when the TT and CT are used as predictors. However, thunderstorms would have been predicted to occur at PMQ more frequently than at ARC on non-rain as well as rain days suggesting a major failing in these indices as predictors.

In summary, it is obvious these thermodynamic indices do not indicate any strong difference between urban and rural locations. There is some very slight suggestion that, if anything, the urban atmosphere might be slightly less favorable for thunderstorm development than the rural atmosphere.

SUMMARY

The thermodynamic profiles do not, in general, indicate that more favorable thermodynamics over the city are a major direct cause of the precipitation anomaly. Many of the urban modifications

of the low level (PBL) thermal and humidity stratifications have important implications for the upward transport of heat and moisture and for the diffusion of materials from the surface. In the presence of favorable meso-scale dynamics, they may also influence cloud development.

On fair days the lower atmosphere in the region around St. Louis tended to have near-neutral thermal stratification up to about the middle of the PBL (approximately 700 or 800 m), and then be conditionally unstable above, up to a stable layer, probably synoptically induced, at heights ranging up to 2 km. On such days the city locations tended to be less stable overall in the lower 2 km, except for a shallow layer close to the surface where the rural atmosphere was unstable, and the urban atmosphere was more likely to be neutral. The overall lesser stability stemmed from the fact that the neutral layer commonly found in the PBL was much deeper over the city, frequently extending up to the synoptic inversion, whereas over the country the upper half of the PBL usually became conditionally unstable. In addition, the stable layer was, on the average, 150 to 200 m higher over the city than over the country.

Thermal stratification in pre-rain cases was similar to that on fair days except that there was no well-defined stable layer capping the PBL. Instead, there was a gradual transition from neutral to conditionally unstable stratification to a nearly moist adiabatic lapse rate near the upper PBL, which was maintained to 5 or 6 km. The PBL temperature profiles over the city and over the country differed in pre-rain conditions in the same way as they did in fair weather with the urban atmosphere characterized by a deeper neutral layer than the country atmosphere.

There was strong evidence that an elevated urban heat island exists over St. Louis which has extensive and intensive urban land use. The atmosphere was, on the average, warmer over St. Louis than over the surrounding country up to 1.5 km or more. The maximum temperature difference averaged 1° C, and occurred at about 1 km on fair days and somewhat lower (500 m) on pre-rain days. There were indications that there may have been compensation in the upper PBL, at least in fair conditions, with slightly cooler temperatures over the city than over the country.

St. Louis is usually humid during the summer. In fair weather, the high humidity was usually confined to the PBL; above the synoptically induced inversion the mixing ratio decreased rapidly, a symptom of upper level subsidence. On rain days, however, the relative humidity remained high up to at least 5 or 6 km. The rural, wooded location (PMQ) tended to have the highest relative humidity, in both fair and pre-rain conditions, and the agricultural sites in both 1973 and 1975 the next highest.

On fair days the average vertical distribution of moisture over the country was constant through a very shallow layer of 100 or 200 m, then the mixing ratio decreased gradually to the subsidence-induced dryness. On the other hand, the urban mixing ratio tended to be nearly constant from the surface up to the inversion. In pre-rain conditions, the moisture decreased more rapidly in the PBL than on fair days, in both country and city. Although a layer of constant water vapor was missing in the country, in the city such a layer extended through the lower half of the boundary layer.

The constancy of the water vapor in the boundary layer over the city could be indicative of a loss of moisture to the surface, or enhanced mixing. The former is not likely, since the urban surface is warm. Thus, the deeper layer of constant mixing ratio suggests enhanced vertical mixing in the boundary layer over the city, and increased transport of moisture to the free atmosphere. The occurrence of a neutral thermal stratification through a deeper layer over the city than over the country also indicates enhanced and deeper vertical mixing through thermally or mechanically driven eddies.

A moisture deficit in the low-level urban air has been reported by several researchers. The average moisture profiles indicate that this probably occurred through a significant depth. On fair

days the urban atmosphere contained, on the average, less moisture than did the country atmosphere through the lower several hundred meters. However, the upper PBL tended to be more humid over the city than over the country, again suggesting a vertical exchange rather than a loss of moisture to the surface. In pre-rain conditions this was not the case. The layer of moisture deficit over the city tended to be much deeper (1 to 2 km) with urban moisture excess occurring only in shallow elevated layers.

The precipitable water (PW) calculations also indicate that mixing was the cause of low level moisture deficit over the city. The PW in the lower 150 mb (1.5 km) was about the same for city and country air in fair weather. In pre-rain conditions, the PW in the lower 150 mb was slightly less over the city than over the country, but in the layer from surface to CCL, it was the same in both locations. Thus the total vapor available to urban and rural clouds for processing was about the same, although more air would have to be processed in urban convection because the CCL was higher.

The equivalent potential temperature, EPT is a conservative parameter based on both the sensible and latent heat content of the air. The EPT was on the average lower in the urban atmosphere through the lowest several hundred meters. On fair days, the layer of low EPT over the city was usually confined to 600 m to 1 km; in the middle and upper parts of the PBL the EPT was higher over the urban area than over the country. In pre-rain cases, low EPT was found over the city in the lower PBL as on fair days, but the EPT over the city was not significantly different from that over the country in the upper PBL.

Mixing heights (potential mixing depths) were lowest over PMQ, a hilly, forested area, and were highest over the two urban locations. The urban-rural differences in mixing height were greater in pre-rain than in fair conditions. The differences in potential mixing depth over the urban area in fair (and rain) cases were 100 (400) m greater than over a rural agricultural site and 250 (500) m greater than over a rural forested site. There was virtually no difference in the mixing height between a small urban site and a suburban location on the edge of a large city.

The convective condensation levels were lower and warmer on rain than non-rain days, as one would expect. The CCL was almost always higher, and therefore cooler, over the city than over the rural sites with the differences being greater between central city and natural forested locations. The CCL over a downtown location in St. Louis averaged 1 km higher and 4° C cooler than the forested site and 400 m higher and 1° C cooler than an agricultural location in fair weather. In similar weather, the CCL over a small urban area averaged about 100 to 200 m and about 1° C cooler than an agricultural site, but there was virtually no difference between the CCLs over a small urban site and a suburban site. The average urban-rural difference in CCLs in pre-rain conditions was about the same as in fair weather, but the interdiurnal variability was greater on rain days. The *difference* in the lifting condensation levels over urban and rural surfaces was essentially the same as in CCL except that the difference in LCLs tended to be smaller in magnitude.

Taken in concert these results show that mixing is deeper over the urban area than over the surrounding rural areas. In addition, conditions favorable for transport by thermal and mechanical eddies extend over greater depths in the city than in the country. Thus, on summer afternoons, surface effluents, including heat and moisture, are likely to be dispersed through a deeper layer over the city than over the country.

In speculating on the effect that the observed urban-rural differences in PBL thermodynamic structure may have on the rainfall, it should be kept in mind that the soundings used in these analyses were taken early in the afternoon, whereas the major rain anomalies occurred in late afternoon and at night. Moreover, only a little over half the pre-rain cases were on 'effect' days, that is, days on which the rainfall analysis indicated an urban effect, and all of these were in the squall

line, squall zone, and cold front storms. Nevertheless, some of the urban thermodynamic conditions could influence the development of clouds and precipitation over an urban area.

First of all, the urban-rural differences in CCL and LCL indicate that cloud bases are likely to be higher over the city. Aircraft observations have verified that this is the case (Cataneo, 1973). Secondly, the greater depth of neutral stability over the city means that thermal and mechanical eddies would encounter less resistance between the surface and cloud base, and low level heat and moisture are more likely to reach the cloud. Thirdly, if the temperature and vapor content differentials in the upper parts of the PBL persist, conditions would be more favorable over the city than over the country for initiation or enhancement of cloud development in late evening and at night when, because of surface layer stability, the cloud roots are less likely to be at the surface.

Further interpretation of the findings concerning PBL thermodynamics are deferred until the end of the next section in which the kinematics in the PBL over the region are discussed, because of the feedback between dynamical and thermodynamical processes.

REGIONAL KINEMATIC FIELDS

Bernice Ackerman

BACKGROUND

The boundary layer wind fields are apt to be perturbed over an urbanized area because the unique character of the urban surface can alter the forces which govern the air flow. The movement of air is governed by the pressure gradient force, P, the friction force, F, and an 'apparent' force, the Coriolis force, C, which enters because the coordinate system is fixed to a rotating earth. Winds will change in response to changes in P and F, with the acceleration given by

$$\frac{dV}{dt} = P + F + C$$

for forces given per unit mass and V, P, F, and C are all vector quantities.

The urban heat island imposes a deformation on the ambient pressure field, resulting in a pressure gradient over the city different from that in the surrounding region. Although the strength of the heat island is at a minimum during midday (e.g., Hilberg, page 25 of this report; Ackerman and Wormington, 1971) it has been observed to extend through considerable depth in St. Louis (see previous section; also Braham, 1974; Auer and Dirks, 1974) so that the perturbation can influence the pressure force P and consequently the velocity of an air parcel V.

The density and characteristics (e.g., solid vertical walls) of man-made structures represent a significant change in the roughness elements from those found in rural areas. This results in an increase in frictional drag and may alter the eddy stresses. Thus the frictional force F over a city should also be different from that over the surrounding rural area.

As a consequence of these potential urban-produced alterations in P and F, the mean winds may change as air moves from country to city and again as the air moves from the city to the country. Since the urban fabric is not homogeneous and these perturbation forces are directional, their effects may vary over the urban 'island'. Thus the perturbation in the wind field may be very complicated close to the surface, but should smooth out with height as the smaller perturbations decay.

There have been investigations of surface winds and of winds in the lower boundary layer over urban and rural areas. These studies have established that the winds over the city do indeed differ from that over the surrounding countryside (see reviews by Oke, 1974, 1977; and Chandler, 1976). However, they also verify that the urban effect is not simple and may differ under different general atmospheric conditions. Most of the investigations have been based on comparisons of urban and rural wind profiles, or of winds along air trajectories or streamlines. The few studies of the wind fields over a region containing an urban complex and of the dynamic consequences of the urban-induced alterations in the wind velocity, have been, principally, investigations into the nocturnal heat island circulation. Results from urban boundary layer simulations indicate that an urban area can induce a local circulation with significant mean vertical motions arising from zones of horizontal divergence and convergence (e.g., Bornstein, 1975; Vukovich et al., 1976) but these too have been concerned principally with the urban heat island.

The five-year climatology of surface winds (in Part B of this volume) indicate considerable local deformations in wind speed and direction in and well beyond St. Louis during most conditions. The objectives of the studies which are discussed in this section were to describe the 3-dimentional wind field over the METROMEX experimental area and to determine the strength,

depth, and characteristics of the urban-induced perturbations and their kinematic consequences. A major goal was to try to determine if the modification of the boundary layer flow could be a factor contributing to the modification of the cloud and precipitation processes and thus to the observed precipitation anomaly.

In order to provide information for a wide range of summertime conditions (table C-6 and C-7), the analysis was based on the data collected on a routine basis in 1973, rather than on data from the specialized field experiments, because the latter were limited as to the kinds of weather conditions they included. The presentation in this section emphasizes the 3-dimensional analysis of the wind fields in the lower 1.5 km over the area and of the kinematic fields of the transport (i.e., average) winds in the subcloud portion of the mixed layer.

ANALYSIS METHODS

The study of the wind field was based on measurements in the lower 1.5 km over the St. Louis metropolitan area and its rural surroundings on 35 of the 42 operational days in 1973. Two criteria were used in the selection of days. One was that data be available from a suitable network to delineate the wind field over the whole area. The second was that there be no rain in the network at the observation time and that on rain days, there be no rain in the network for at least 3 hours prior to the observation.

The measurements were made from 11 stations within 40 km of downtown St. Louis (see figure C-8a) by single theodolite tracking of pilot balloons. The geographic and land use characteristics of the stations varied widely from central city to natural forest (table C-21, figure C-8).

Paired balloon releases, separated by 30 minutes and centered in time at 1200, 1400, and 1600 CDT were made from each site. Balloon positions were calculated from angular readings at 30-second intervals, but the winds were computed for 60 seconds (approximately 200 m) overlapping layers to smooth the profiles. The sounding pairs were averaged in an effort to diminish the influence of transients which, from previous studies, were known to occur in the afternoon PBL (Ackerman, 1973b, 1974b). These averaging procedures appear to have been successful since the resulting wind fields tended to be consistent with time and remained stable during tests in which stations were omitted and the wind field re-analyzed.

The wind measurements from the 11 stations were objectively analyzed with a modification of the technique described by Barnes (1964) and Ackerman et al. (1978). The analysis yielded the wind components at grid points with 5 km spacing over a rectangular area 70 by 80 km, with . the St. Louis Arch approximately at the center. The fields of divergence and vorticity were derived from the grid point values of the wind components by finite differencing.

In addition, a 'perturbation' wind field was determined by objective analysis of the perturbation wind, defined as the deviation of the station wind velocity from the average network wind velocity. That is, if V_i is the wind at the ith station, then the perturbation wind at the ith station, ΔV_i, is given by

$$\Delta V_i = V_i - \sum_{i=1}^{n} V_i$$

where n is the number of stations in the network, and all winds are at a common altitude.

The kinematic fields were analyzed for 7 levels: 250, 350, 500, 700, 900, 1200, and 1600 m MSL. The vertical velocity was calculated at each level by a stepwise integration through

Table C-21. Characteristics of the Pilot Balloon Stations, 1973

Site	Elevation (m)	Station location and characteristics
50	155	Rural, 4.2 km east of small city of Belleville, IL; flat, agricultural
51	210	Rural, 1 km north of town limits of Waterloo, IL; gently rolling, agricultural
52	193	Suburban, southwest edge of metropolitan area; rolling, low density residential
53	139	Central city; at the Memorial Arch in downtown St. Louis
54	171	Rural, 6 km southeast of Collinsville, IL; gently rolling, agricultural
55	143	Rural; flat, agricultural
56	174	Rural; flat, agricultural
57	165	Rural, 5 km east of Alton city limits; flat, open, very low density commerical
58	160	Suburban, north side of metropolitan area; rolling, low density residential
59	184	Suburban, northwest corner of metropolitan area, at St. Louis airport; flat, open east and southeast, gently rolling, low density commercial other directions
60	273	Rural, Pere Marquette State Park, 27 km WNW of Alton; locally hilly, wooded

depth, according to the equation

$$w_z = w_{z-\Delta z} + \frac{1}{2}(D_z + D_{z-\Delta z})\,\Delta z$$

where w is vertical velocity, z is the height of interest, Δz is the height difference between successive levels, and D is divergence. The divergence at 250 m MSL was assumed to be the average for the layer between the surface and 250 m MSL and the vertical velocity at the surface was assumed to be zero. The density was neglected because it changes very little over the lowest 1.5 km and inclusion had a negligible effect on the calculated vertical velocity.

Similarly the kinematic fields were analyzed for the transport wind (vector-averaged wind) for 5 layers: the subcloud layer, the first kilometer, and the layers from the surface to the lifted condensation level, the convective condensation level, and the mixing height, with the last three heights calculated according to the procedures described in the preceding section on thermodynamics. The discussion below is limited to the wind fields at the standard levels and to the transport wind field for the subcloud layer. Because of the well-mixed nature of the subcloud layer, particularly at 1400 and 1600 CDT, there is great similarity between the patterns of the wind, and its derivatives at all levels below the top of the layer, and the patterns for the transport wind. The gradients, maxima, and minima, however, do differ, with the values in the transport wind field approaching the average for the layer.

The 35 operational days were categorized as being pre-rain cases or fair cases. Rain fell in the network on 20 operational days. However, on 3 of these the rain ended more than 6 hours before the first balloon release, and on one day it started more than 6 hours after the observations ended. It was believed that the wind fields were not affected by the cloud systems in these cases and they were included in the fair weather category. On two of the rain days the rain fell during,

or ended less than 3 hours prior to, the observations. Thus the final sample sizes were 21 fair cases and 14 pre-rain cases. Although the two categories were treated similarly during the analysis, the results were not pooled and the two data sets are discussed separately. The synoptic weather characteristics for the fair and rain days were given earlier, in tables C-6 and C-7.

WIND FIELDS IN FAIR WEATHER CASES

Although the local atmosphere was generally undisturbed by convective showers or major weather systems in these fair cases, the weather conditions varied considerably. Cloud cover ranged from clear to overcast and low-level winds were from all four quadrants, at speeds varying between 2 and 10 m s^{-1}. The mesoscale wind field over the entire area was disturbed at all three observation times and on every one of the 21 days. In view of the variability of the ambient conditions on these 21 days, it is not surprising that the nature and strength of the perturbation varied also. Sometimes the disturbance was manifested primarily in the wind direction; at other times it was reflected more subtly, as relatively small variations in both direction and speed.

When the direction of the flow was disturbed, the streamlines were wavelike, with amplitudes that varied from case to case and usually decreased with height. Within 200 or 300 m of the surface most of the stronger disturbances in wind direction (over 80%) occurred at 1400 and 1600 CDT, around the time of 1) maximum temperature, 2) maximum depth of the mixed layer, and 3) greatest instability (table C-22). Moreover, it can be seen from table C-22 that with but two exceptions, the strongest perturbations occurred with very light winds, while in two-thirds of the cases when the wind direction changed only slightly across the city, the wind speeds on the upwind side of the region were strong. Conversely, in 70% of the cases when the winds were very light, the streamlines were strongly affected, whereas when the winds were strong, the direction field tended to be only weakly disturbed. Obviously the urban perturbation is more weakly manifested in wind direction as the wind speed increases.

Although the exact nature of the urban-induced disturbance in the air flow may have differed, the dynamic consequences on days with light winds could, at least in some instances, be remarkably similar to those on days with strong winds. This is demonstrated in the two case studies presented below, one for a day with low regional flow and the other with strong regional flow.

Table C-22. Number of Fair Cases in Which Streamlines at 350 m MSL Were Strongly (S), Moderately (M), or Weakly (W) Perturbed, as a Function of the Strength of the Upwind Speed and Time

Speed	*1200*			*1400*			*1600*			*All times*		
(m s^{-1})	*S*	*M*	*W*	*S*	*M*	*W*	*S*	*M*	*W*	*S*	*M*	*W*
≤3	3	4	2	7	1	0	6	0	0	16	5	2
4-5	0	2	3	0	5	1	1	4	2	1	11	6
≥5	0	3	4	0	2	5	1	1	6	1	6	15
All speeds	3	9	9	7	8	6	8	5	8	18	22	23

4 August 1973. On 4 August the METROMEX area was under the influence of a deep high pressure area. The airflow in the lowest kilometer was generally from the west and very light —about 2 m s^{-1}. The winds veered rather sharply with height, primarily above 800 m or 1 km, MSL,but the zone of veering was shallower and occurred at a higher level later in the day as the well-mixed lower layer deepened. Scattered cumuli, with increasing coverage during the afternoon, had bases at about 1.6 km.

In figure C-22a are shown the wind fields at about 1200 CDT at four levels from 250 m to 1.6 km MSL (surface elevation averaged about 170 m MSL). A strong disturbance in streamlines, obvious at the low levels, damped with height. At 250 m the flow was complicated, with strong cyclonic turning of the streamlines over and south of the city and anticyclonic turning downwind, but cyclonic turning to the left (north) of the zone of confluence. The confluence shifted southeastward with height, in the direction of the vertical wind shear. The shift from westerly to northerly flow occurred around 1 to 1.2 km; a disturbance in the flow was noticeable up through 1.2 km —and to some extent even the 1.6 km winds were disturbed.

The relationship of the disturbance to the city is more clearly seen when the network mean wind velocity is removed (figure C-22b). The streamlines of the perturbation wind at 250 m clearly show relative flow into metropolitan St. Louis, directly inward from all directions at low levels but changing with height to a zone of confluence oriented NNE-SSW over the metropolis. By 900 m MSL the perturbation flow over the area was anticyclonic and became one large clockwise whirl with its center over East St. Louis by 1.2 km MSL.

As the daytime heating and low-level mixing continued and the mixed layer deepened, the flow over the region was disturbed to greater heights. Direct inflow into the city was evident in the observed wind fields at 250 and 350 m MSL by 1400 CDT (figure C-23a) and up through 500 m by 1600 CDT (figure C-23b), with a disturbance obvious in the flow up through 1.2 km at the latter time. The perturbation-wind streamline patterns are similar to the observed streamlines at both 1400 and 1600 CDT, at least up to 500 m (figure C-24). The anticyclonic perturbation found as low as 900 m at 1200 CDT, was pushed upward, not occurring until 1.4 or 1.6 km at 1400 CDT. Late in the afternoon, outflow from the city appears in the perturbation wind at 1.6 km MSL, but not below.

These wind fields resulted in convergence through most of the urban PBL but primarily over the Missouri metropolitan area (figure C-25). The magnitude of the convergence was greatest at the lowest level (250 m MSL) and the latest time, reaching 2.5 X 10^{-4} s^{-1} at both 1200 and 1400 CDT and 4 X 10^{-1} s^{-1} at 1600 CDT. The divergence patterns were similar at all three times. The area of convergence over metropolitan St. Louis (which extended through 350 m) sloped southward with height, in the direction of the vertical wind shear vector and the upper level winds, particularly later in the day. Upper-level divergence occurred above low-level convergence in the metropolitan area, whereas convergence occurred above the major center of low-level divergence over the Mississippi-Missouri bottoms in the northwest. The transition from convergence to divergence occurred higher later in the day; at noon it took place below 900 m and by 1400 CDT the low-level pattern was maintained to 1.2 km MSL.

The major areas of upward motion were, of course, in the areas of converging flow. At noon the strongest upward velocity over metropolitan St. Louis was about 15 cm s^{-1} at 900 m MSL. By 1600 CDT, the highest vertical velocity over St. Louis was about 18 cm s^{-1} at heights from 900 m to 1.6 km MSL, but it reached 25 cm s^{-1} at 1.6 km in the country southeast of the city.

8 August 1973. The synoptic weather conditions on 8 August were quite different from those on 4 August. The METROMEX area was lying in a region of strong southerwesterly flow.

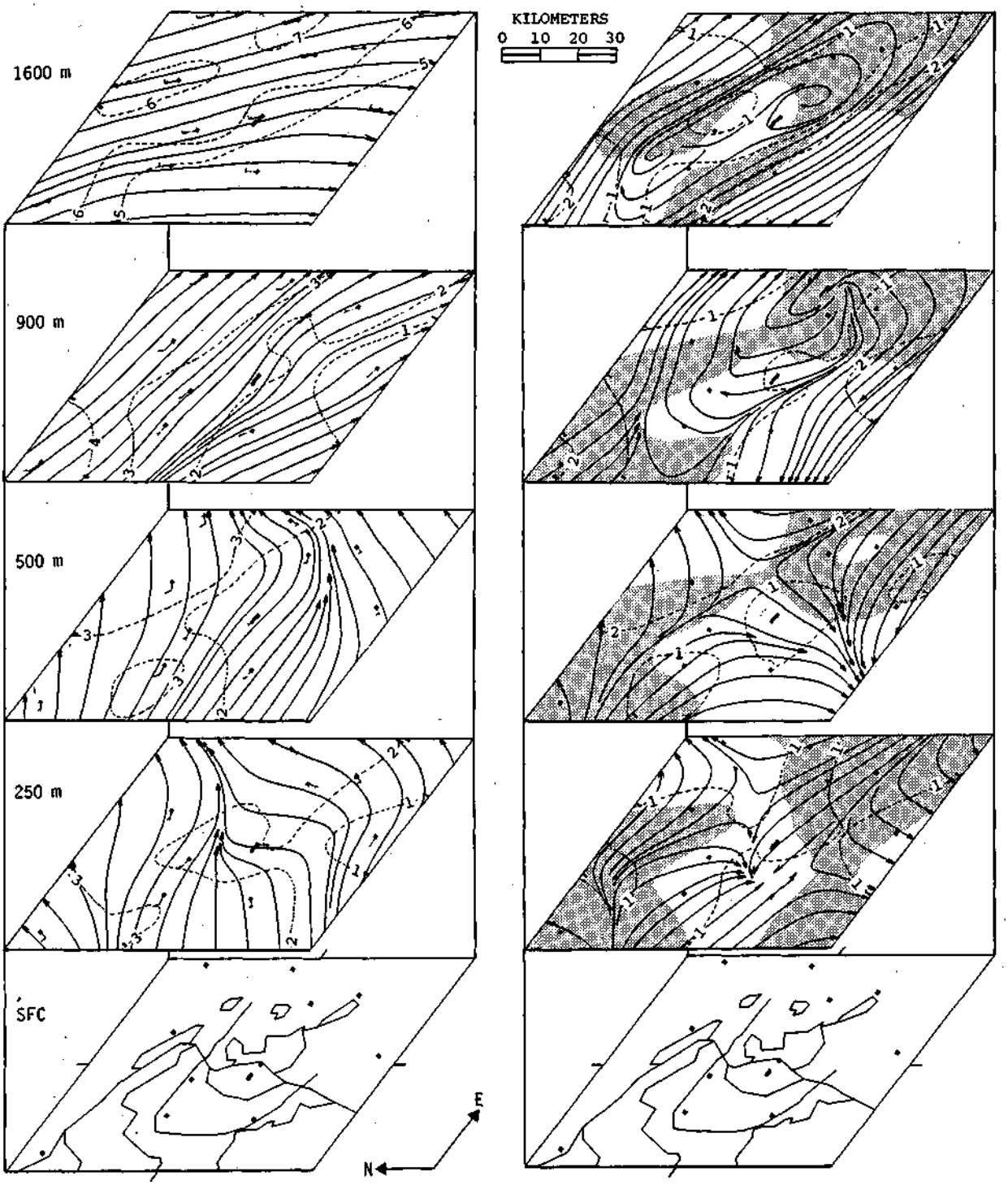

a. Observed wind field

b. Perturbation wind field

Figure C-22. Streamlines and isotachs (dashed) of the observed and perturbation fields at 1200 CDT on 4 August (Unshaded areas upward motion, shaded downward motion)

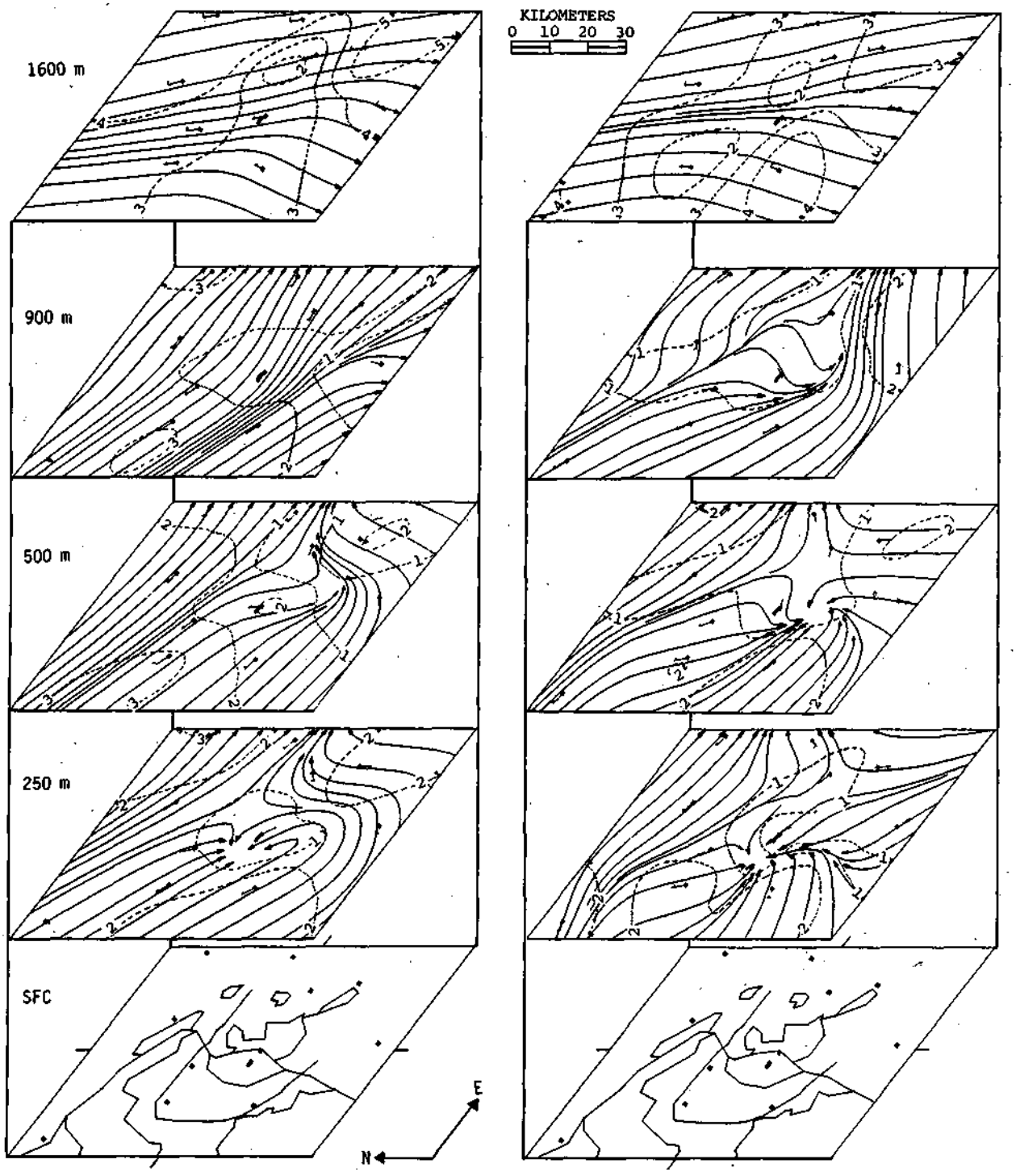

a. 1400 CDT b. 1600 CDT

Figure C-23. Streamlines and isotachs (dashed) of the observed winds on 4 August at 1400 and 1600 CDT

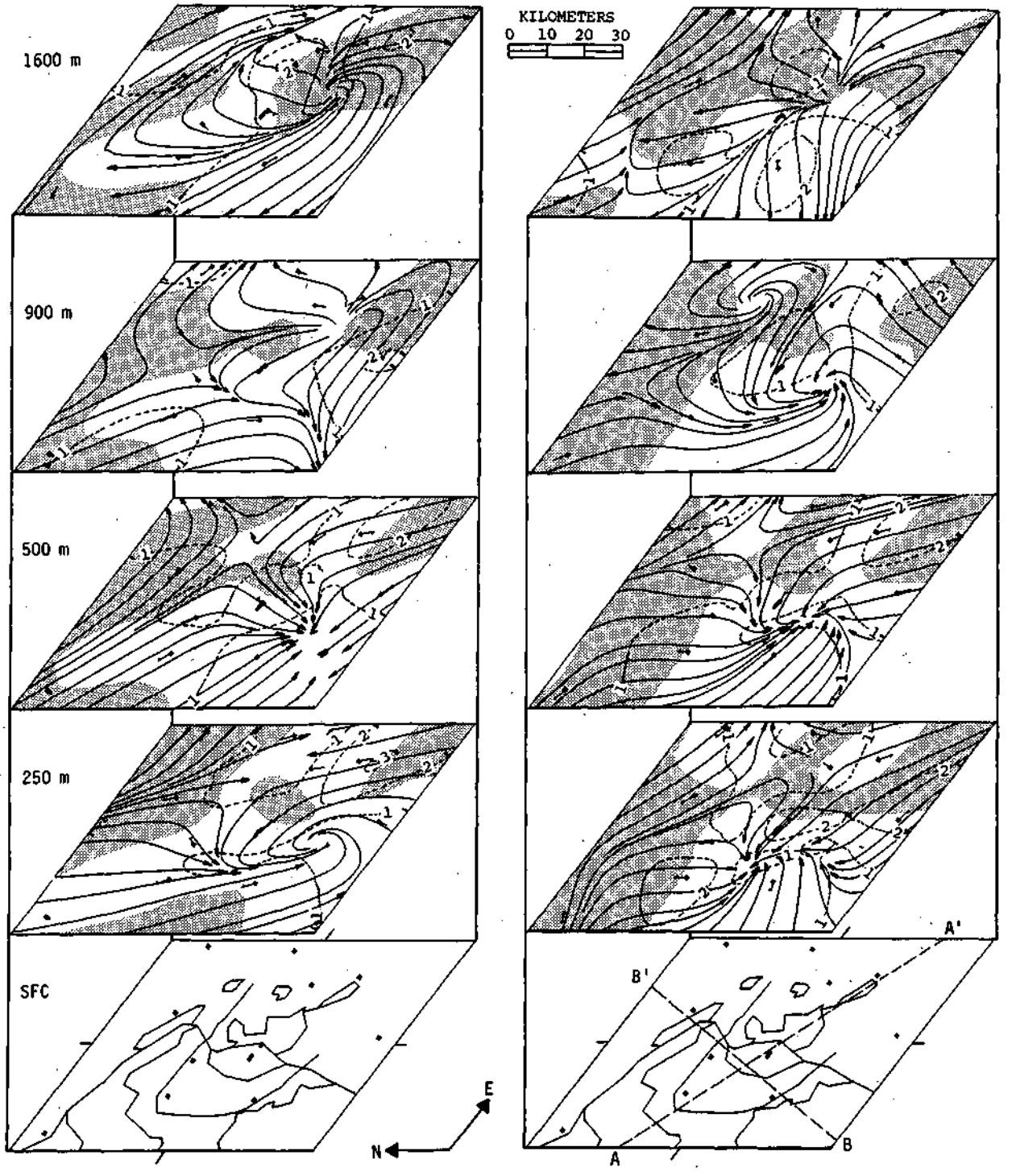

a. 1400 CDT b. 1600 CDT

Figure C-24. Streamlines and isotachs (dashed) of the perturbation wind field at **1400** and **1600 CDT** (Unshaded areas upward motion, shaded downward motion; see figure C-30 for vertical cross sections A-A and B-B')

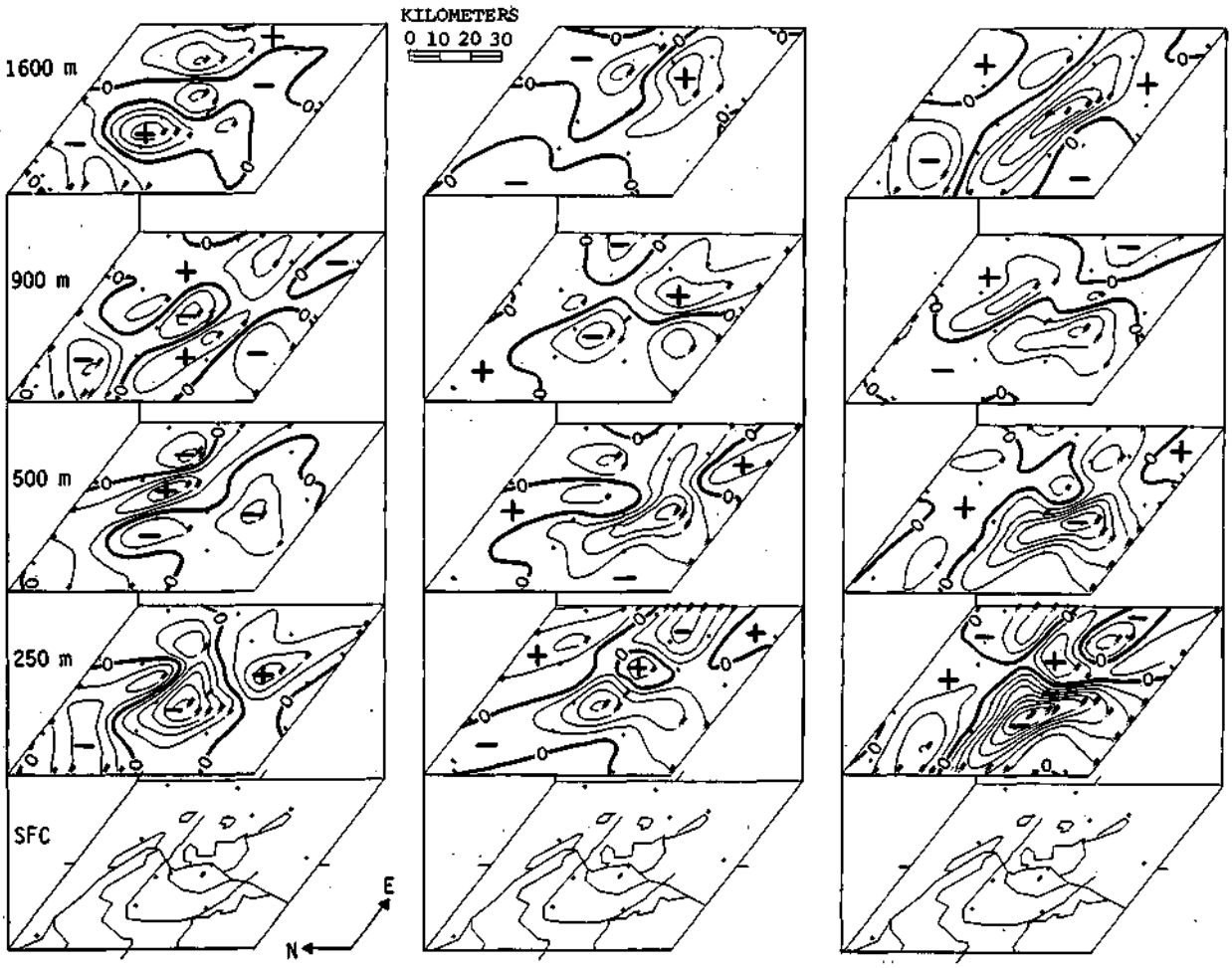

a. 1200 CDT b. 1400 CDT c. 1600 COT

Figure C-25. Fields of divergence on 4 August (Plus signs indicate areas of divergent flow, minus signs convergent flow; contour interval 50 X 10^{-6} s^{-1})

The cloud cover was scattered to broken with cumulus clouds having bases at about 1.4 km. The winds were 8 to 10 m s^{-1} and gusty throughout the mixed layer. The direction of the flow veered gradually above about 1 km, shifting from SSW to about WSW at 3 km.

The wind direction varied relatively little across the area, or with time during the afternoon. The streamlines in the lower levels indicate slight cyclonic turning upwind and over the city and some anticyclonic turning downwind, while in the upper levels the reverse turning occurred (figure C-26). The wind speed, on the other hand, varied significantly with time and space, despite the smoothing that is a byproduct of the analysis. There was a tendency for speeds to be lower on the north side and downwind of the city, at least in the lower kilometer or so.

Although the total flow did not at all resemble that on 4 August, removal of the network mean wind shows that the disturbance in the wind field over the network on this day of strong winds was similar to that on the day with weak winds. The perturbation wind field indicates converging flow into the urban-industrial area throughout the lowest 1.5 km, at all three times (figure C-27).

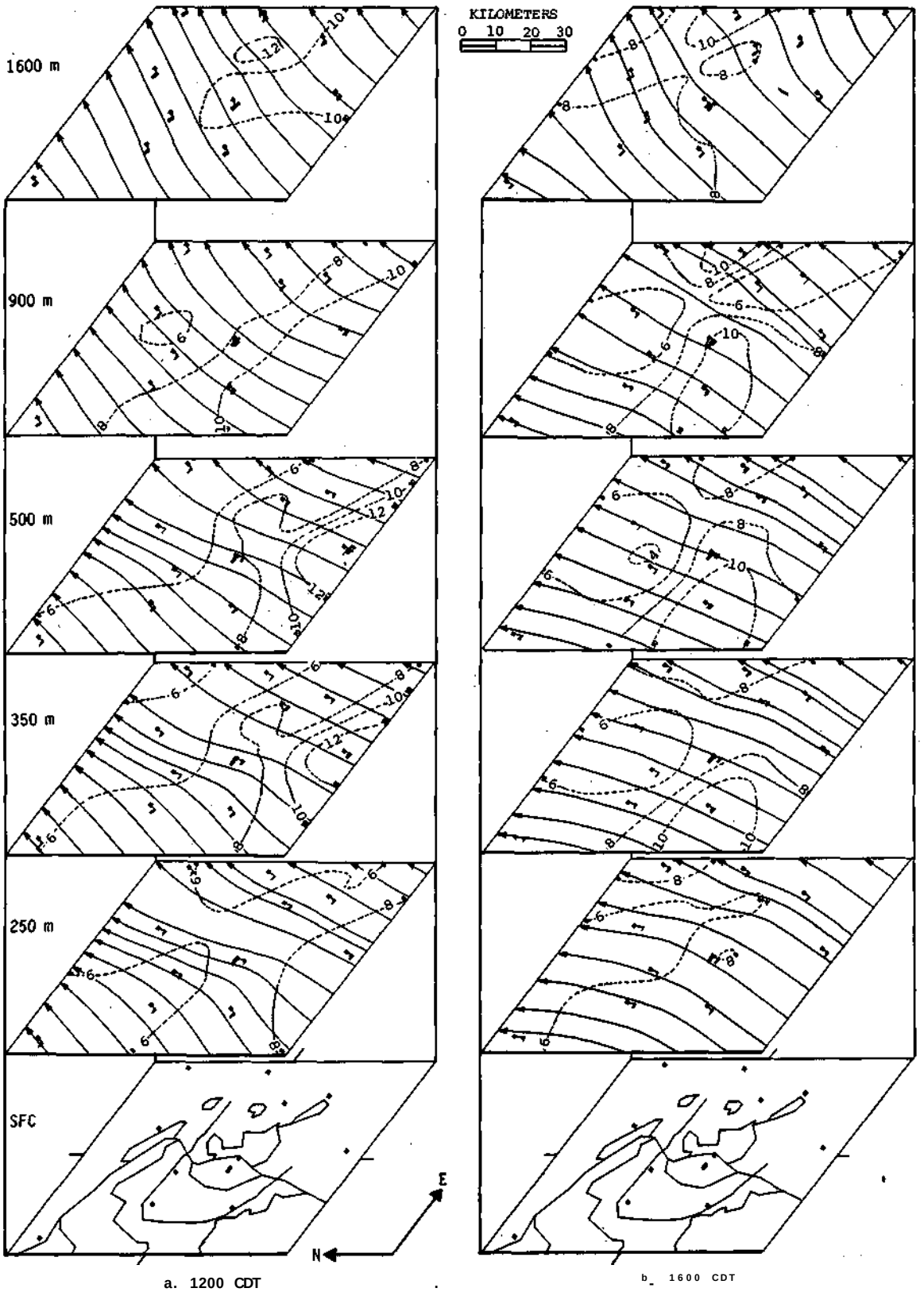

a. 1200 CDT

b. 1600 CDT

Figure C-26. Streamlines and isotachs (dashed) of observed wind field on 8 August

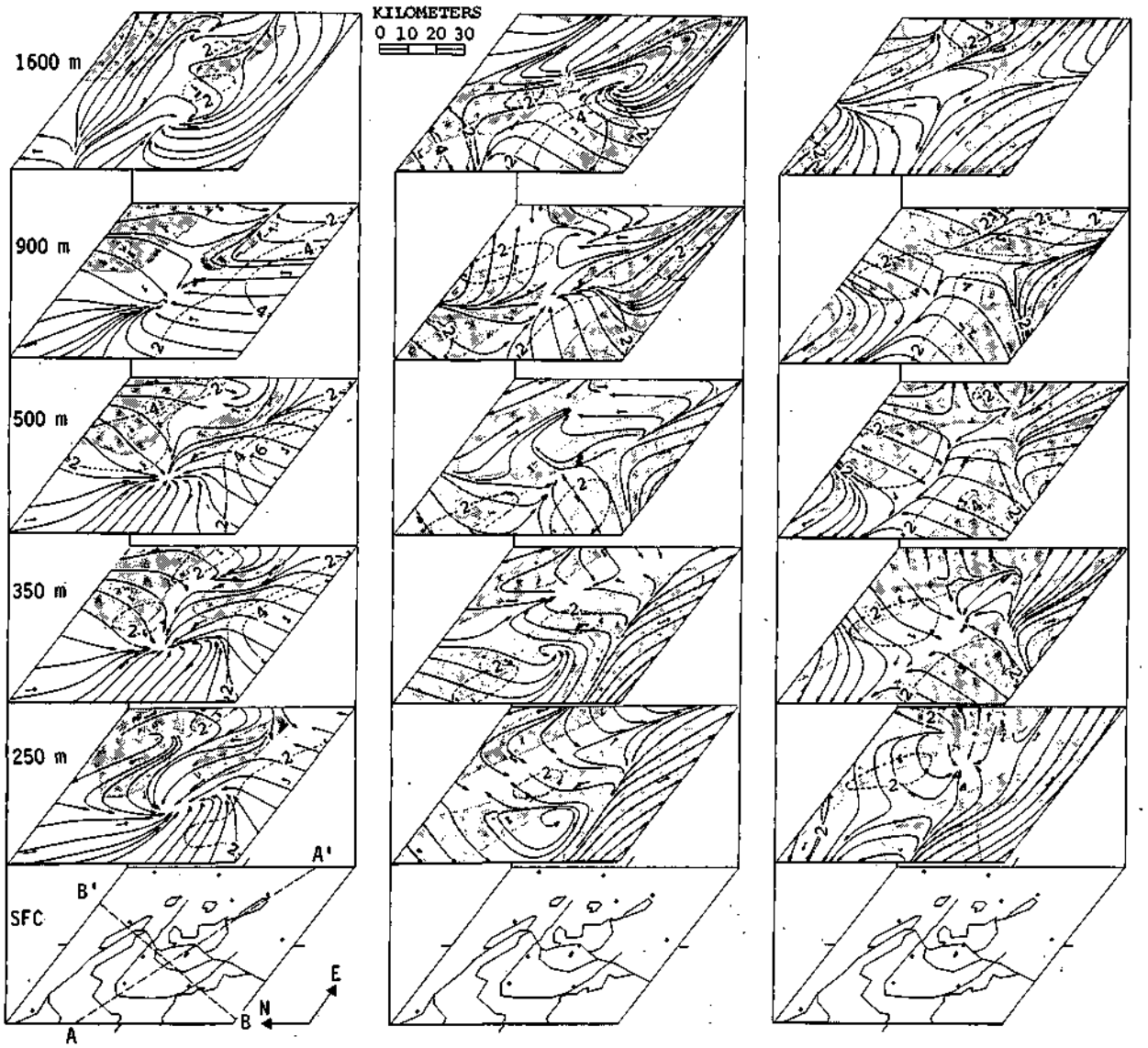

a. 1200 CDT b. 1400 CDT c. 1600 CDT

Figure C-27. Streamlines and isotachs (dashed) of perturbation wind field on 8 August (Unshaded areas upward motion, shaded downward motion; see figure C-30 for vertical cross sections A-A' and B-B')

At noon the perturbation wind below 1 km MSL was directed toward the center of the metropolitan area from all directions, and with very little horizontal displacement of the center of the inflow in the vertical (figure C-27a). By 1400 CDT the disturbance at 250 m MSL had changed to cyclonic perturbation flow over the city and a major zone of convergence downwind (NE) of the city. A hundred meters above (350 m MSL), the zone of confluence reappeared on the north (downwind) side of the metropolitan area, which persisted with height at both 1400 and 1600 CDT (figure C-27b,c). This confluent zone is evident in the perturbation flow, with very little horizontal displacement in the vertical-, up through 2 km MSL at 1600 CDT.

The converging flow was stronger on 8 August than on 4 August particularly earlier in the day. At noon, areas of convergence occurred over the downwind (north) side of the city, in the rural area just south (upwind) of the city, and in the Collinsville area (figure C-28a). These persisted up through 1.6 km, although with some minor change in shape and location in the lower 1.2 km. Maxima in convergence of 3 to 5 X 10^{-4} s^{-1} were reached in the lower third of the PBL. Vertical velocities calculated from the divergence field reached about 20 cm s^{-1} over the city by 900 m MSL and 35 cm s^{-1} on the south edge of the metropolitan area at 1.6 km.

By 1400 CDT the convergence south of St. Louis and in the Collinsville area had disappeared and convergence over metropolitan St. Louis and Granite City dominated the region. Two hours later the flow over the metropolitan area proper was divergent at 250 m, but it became convergent at 350 m MSL (figure C-28c). This area of convergence dominated the pattern up through 2 km, although the location of the center shifted downwind with height. The convergence reached 3 X 10^{-4} s^{-1} over much of the lower half of the PBL. Upward motions due to this converging flow were 35 cm s^{-1} at 1.6 km over Granite City and the downwind (north) half of the St. Louis metropolitan area at 1600 CDT.

Discussion. The effect of the disturbance in the PBL winds over the region and the similarities and differences between two days are well illustrated by the perturbation wind field and horizontal convergence of the transport wind for the layer in which the atmosphere was both well mixed and below cloud base (1 km and 1.4 km for 4 and 8 August, respectively). [The well-mixed layer was defined for this study as the layer in which potential temperature and moisture content was near constant. This was usually accompanied by near uniformity in wind velocity. On 4 August the well-mixed layer extended to 1 km MSL, on 8 August it extended to 2 or 2.5 km.]

Clearly on both days the vertically integrated disturbance resulted in flow into the Missouri metropolitan area (figure C-29). Sometimes the perturbation wind was directed inward toward the city from all directions, but more often there was confluence in the perturbation flow. When the latter was the case, the zone of confluence was oriented normal to the direction of the ambient upwind winds. With low wind speeds (4 August) the PBL airflow was convergent over the urban area and also in the rural area south of the city throughout the afternoon (figure C-29a-c). When the winds were strong (8 August), there was convergent flow in the rural areas south and southeast only early in the day; after noon that rural area was divergent (figure C-29d-f). On both days the flow was divergent to the east and north of St. Louis. Usually the flow occurred as a narrow band oriented NNW-SSE across the region to the east of the main urban area.

Not only the disturbances in the horizontal but also the imposed disturbance in the vertical were similar on the two days. Figure C-30 shows the horizontal divergence, and arrows indicate 30-minute displacements estimated from the perturbation wind and the vertical motion due to the divergence, for two vertical planes cutting across the city (A-A, B-B in figures C-24b and C-27a). The WNW-ESE and SSW-NNE planes were parallel and perpendicular to the upwind ambient flow on 4 August. The orientation of these planes to the ambient flow was reversed on 8 August. Despite this reversal in orientation, the characteristics of each of the cross sections on the two days were remarkably similar.

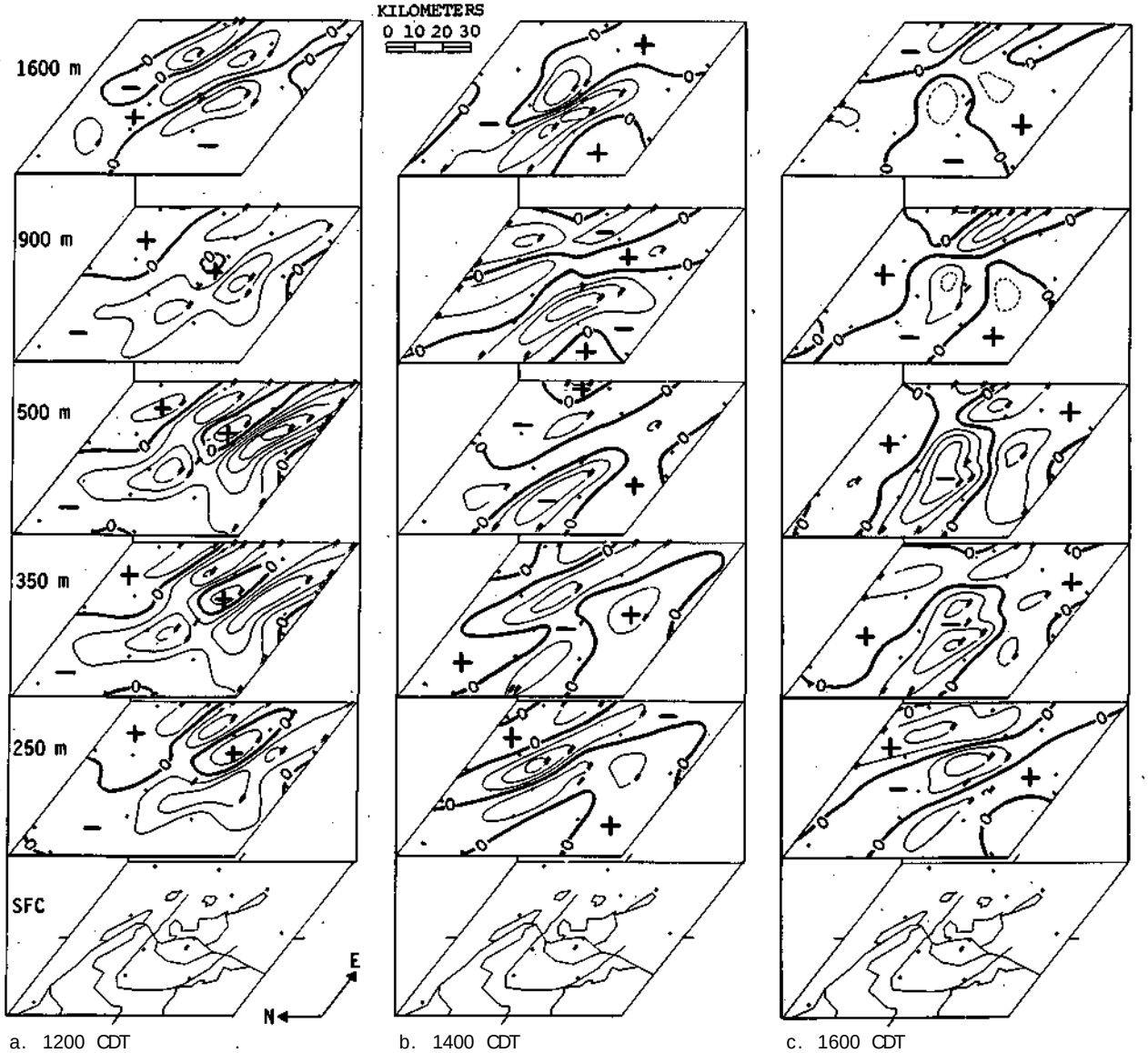

a. 1200 CDT b. 1400 CDT c. 1600 CDT

Figure C-28. Fields of divergence on 8 August (Plus signs indicate areas of divergent flow, minus signs convergent flow; contour interval **100** X 10^{-6} s^{-1} except for **900** and **1600** m levels at **1600 CDT** which is **200** X 10^{-6} s^{-1})

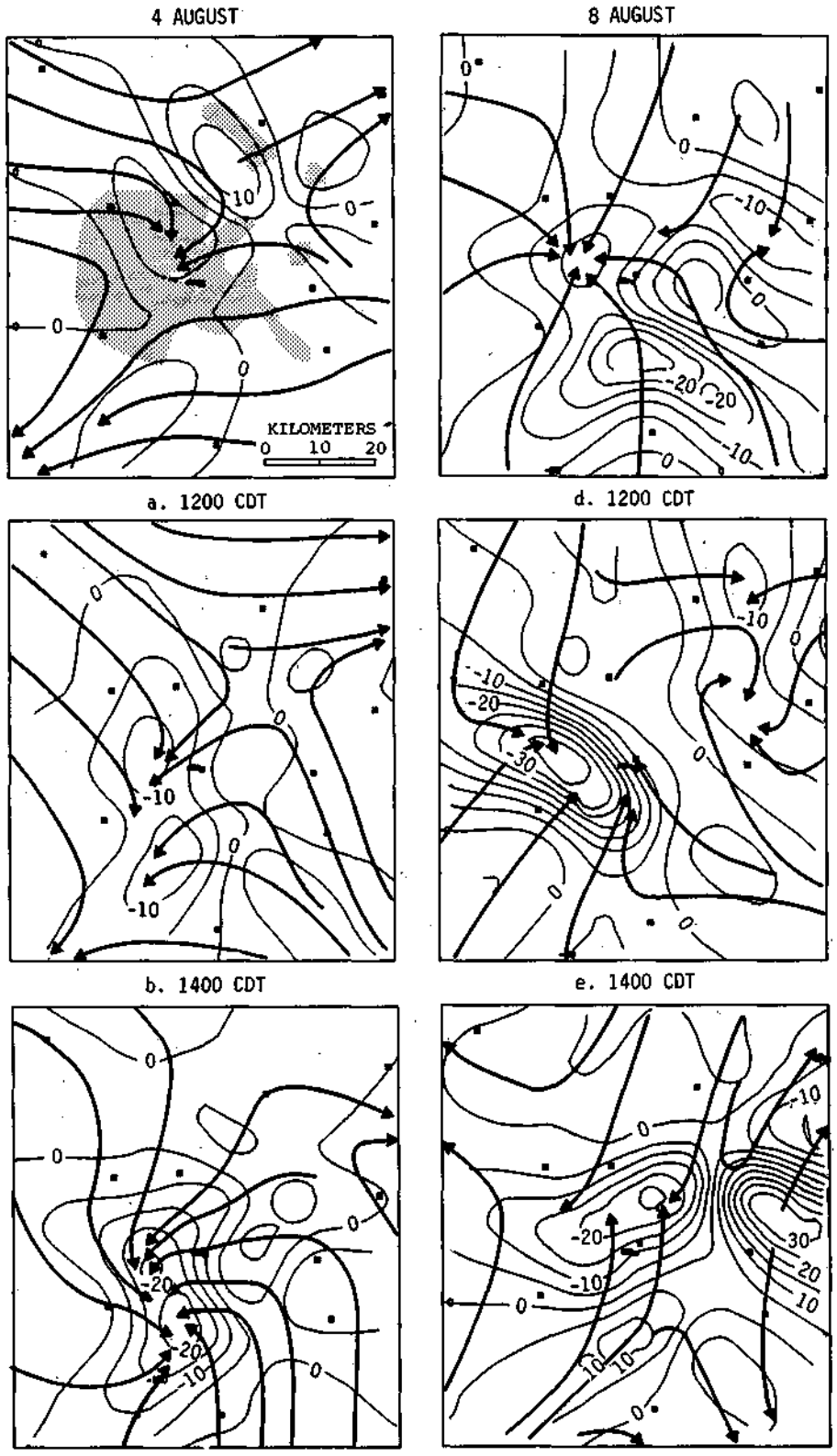

Figure C-29. Perturbation streamlines and divergence contours for transport wind in the subcloud layer on 4 and 8 August (divergence contour interval 5 X 10^{-5} s^{-1})

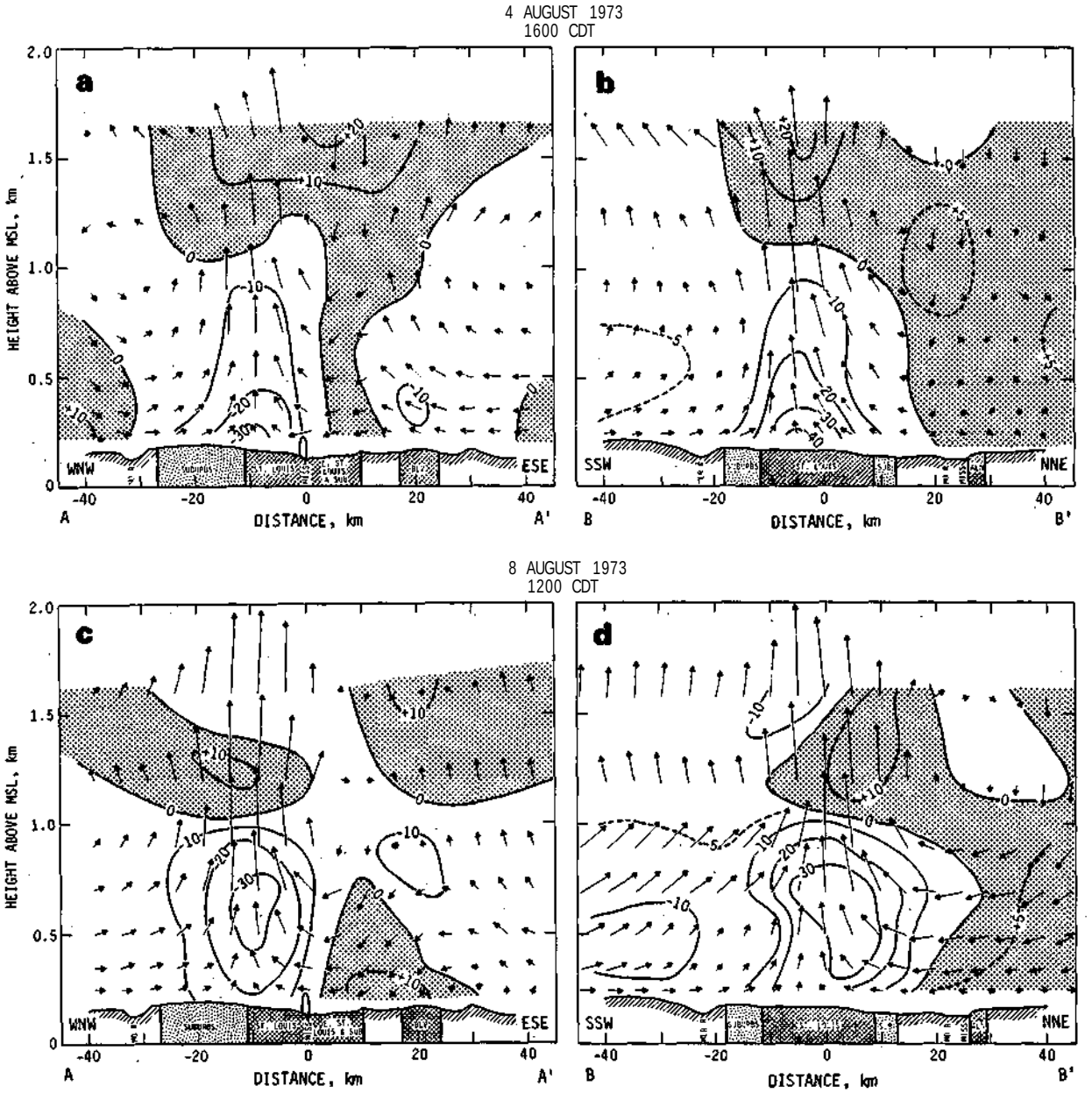

Figure C-30. Vertical cross sections along lines A-A' and B-B' in figures C-24 and C-27 (Shaded and unshaded areas indicate divergent and convergent, respectively, flow in the horizontal; divergence contour units, 10^{-5} s^{-1}; arrows give 30-minute displacements)

A 'dome' of convergent flow was located over St. Louis and its Missouri suburbs from the surface to about 1 km, with divergent flow above. The convergence was fairly symmetric over the metropolitan area in the cross sections normal to the winds, but was displaced downwind in the vertical plane parallel to the ambient wind (figure C-30a,d). The magnitude of the maximum convergence in these planes was approximately the same on both days, but the level of the strongest convergence was near the surface when the winds were light and elevated on the day with strong winds. Vortical rolls with opposing rotation and axis around 1 km are indicated

above and on either side of the centers of the convergence on cross sections parallel to the winds, particularly on 4 August. Although poorly defined, a similar structure is suggested in the vertical planes perpendicular to the winds.

In both of these cases —one having low ambient wind speed and the other high wind speed, the perturbation flow resulted in more convergence over metropolitan St. Louis, at least below 1 km. Moreover, on both days the perturbation flow suggests a direct urban circulation with flow inward and upward over the urbanized areas.

Ensemble Analysis, All Fair Weather Cases

In view of the variety of synoptic weather patterns, local cloudiness, wind velocity, etc., that occurred on the 21 fair weather days, diversity in the strength and characteristics of the disturbance over the region must be expected. However, in every case, a perturbation existed in the horizontal wind field which occurred over the meso-region. The centers of divergence and convergence varied in location and magnitude from day to day, and to some degree also with time. However, as this analysis shows, they were in the mean usually associated with the metropolitan area.

The fields of divergence for several layers in the PBL, averaged over all 21 fair weather cases appear in figure C-31. [Average fields of all parameters were calculated by averaging grid point values of the parameter over the specified group of times or days.] There are striking similarities between these average fields and those for 4 and 8 August, although the reduction in the magnitudes of the divergences is indicative of the considerable interdiurnal variability in the strength and locations of the main areas of divergence and convergence. Nevertheless, there is striking evidence of inflow into the metropolitan area in the mean, with converging airflow in the lower part of the PBL over St. Louis and suburbs overlain above 1 km by diverging flow.

At noon the average convergence pattern was very similar to the convergence pattern on 4 August, particularly in the lowest and topmost levels. A line of confluence in the perturbation wind field extended N to S across the city from near surface up to 900 m, where the pattern weakened (figure C-31a). At 1.2 km and above, the disturbance over the region was a single large anticyclonic outflow from the city. Two hours later (figure C-31b) the mean perturbation winds indicated direct inflow into the urban area up to 1.2 km, at many levels in the form of a cyclonic vortex. The inflow and convergence were deeper than, and twice as intense as, they were earlier, with the anticyclonic outflow first appearing at 1.6 km MSL.

The low-level convergence south and southeast of the urban area earlier in the day decreased by 1400 CDT and was replaced by divergent flow at 1600 CDT. Again there was cyclonic inflow into the urban area (figure C-31c) through the first kilometer although it dimished by 1 km. The main area of convergence at 250 m MSL was over Granite City and to the northeast but, as was the case at the later times on 8 August, by 350 m MSL the convergent zone extended back over St. Louis and its suburbs. At 500 m MSL the most intense convergence coincided fairly well with the main metropolitan area. Through much of the lower kilometer the average divergence field suggests a convergent center with a divergent ring around it. As at the earlier times, there was at 1600 CDT cyclonic outflow from the Missouri metropolitan area at 1.6 km, but the mean winds were still convergent over Granite City and to the northeast.

The main features of the average divergence fields and perturbation flow are also seen in the average kinematic fields for the transport (integrated) wind in the well-mixed and subcloud layer (figure C-32). These mean fields were obtained by averaging the kinematic fields of the transport winds analyzed for each day and time. The use of transport wind for this purpose represents, to some extent, a 'scaling' in the vertical.

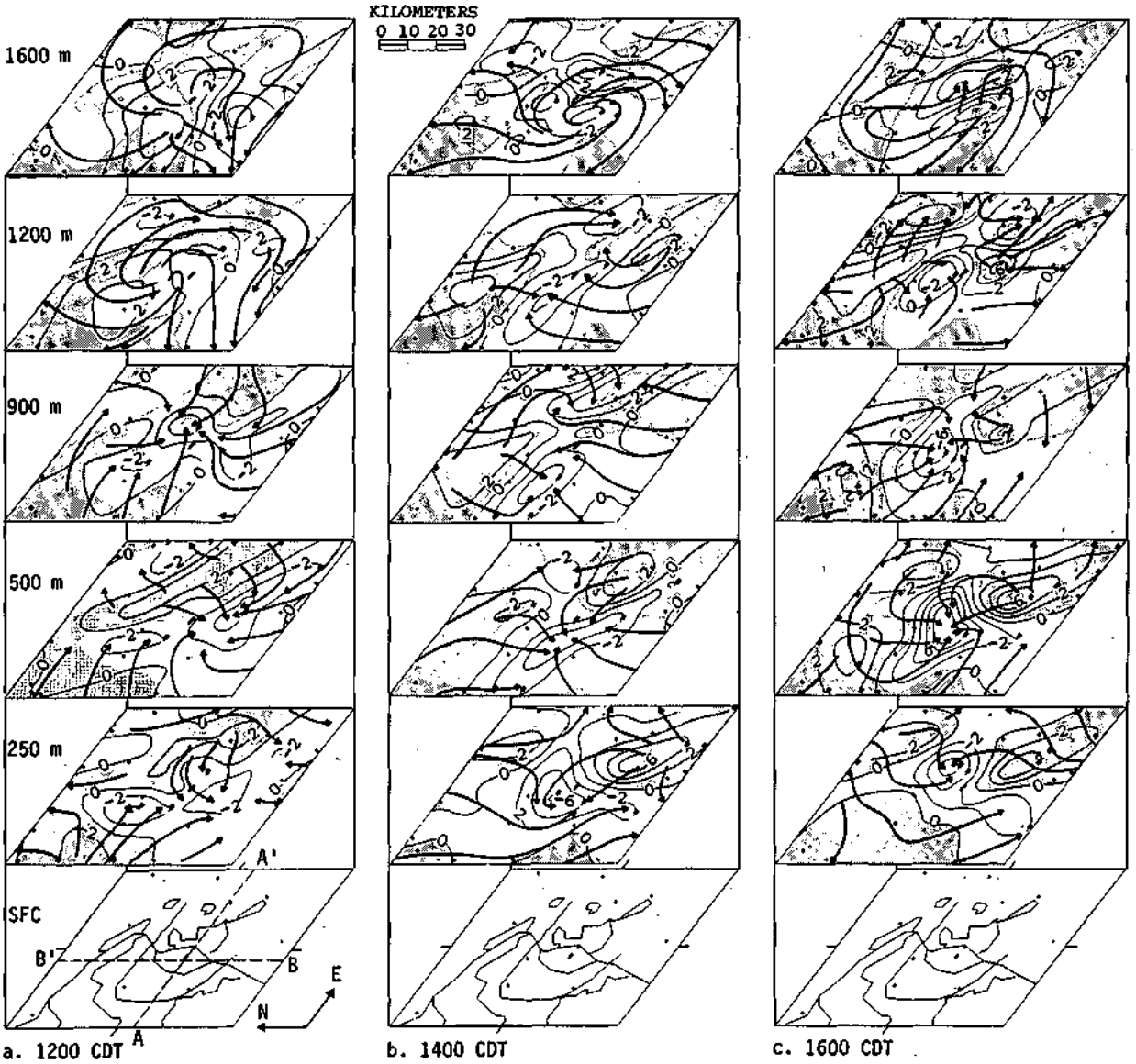

Figure C-31. Streamlines of the perturbation wind and divergent fields averaged over 21 fair weather cases (Unshaded areas upward motion, shaded downward motion; contour interval 2 X 10^{-5} s^{-1}; see figure C-33 for vertical cross sections A-A' and B-B')

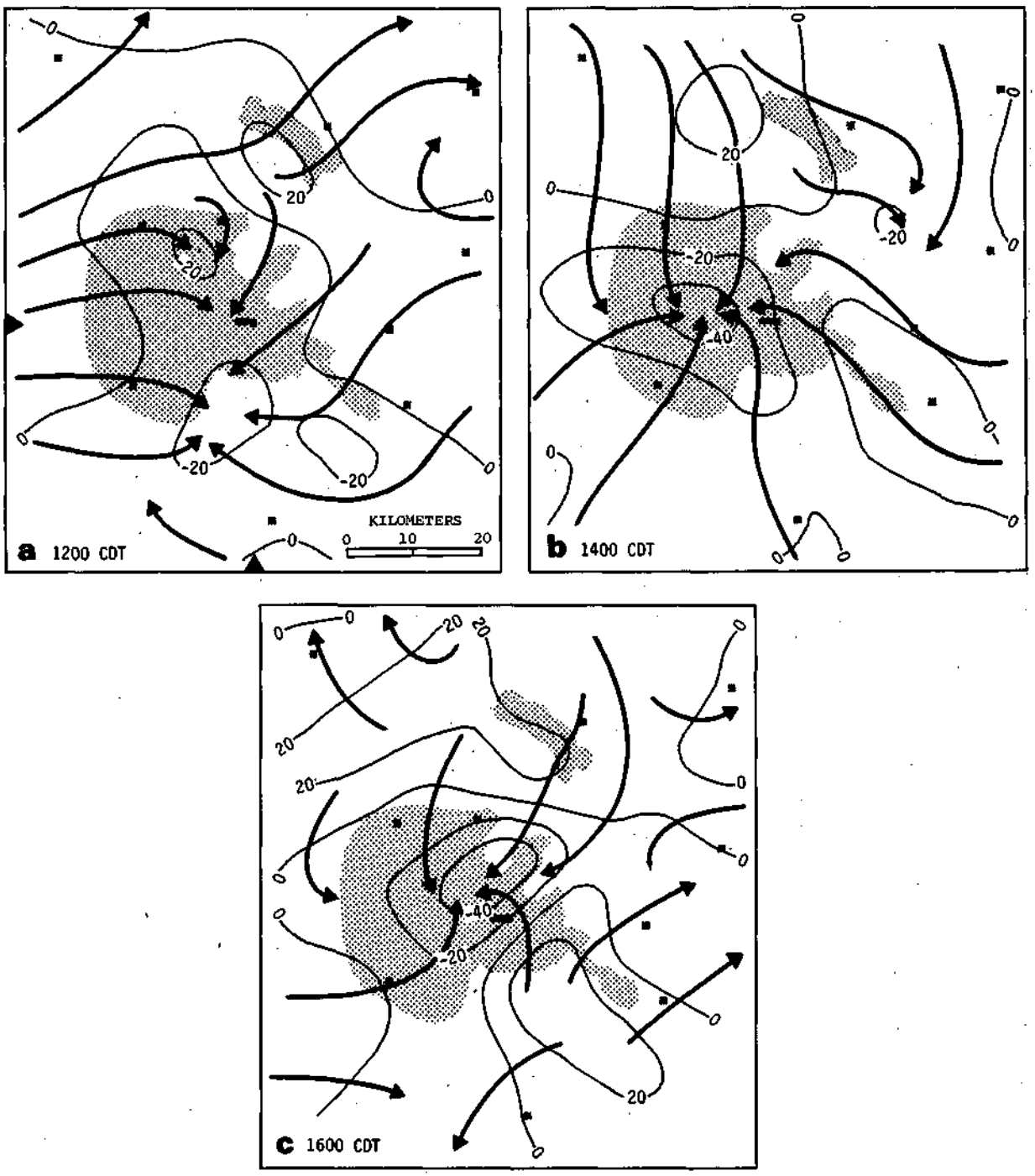

Figure C-32. Perturbation streamlines and divergence contours (10^{-6} s^{-1}) averaged over 21 fair weather cases

The relative inflow and convergence in the mixed layer over the metropolitan area throughout the afternoon is clearly indicated. Converging flow in the subcloud layer south of the metropolitan area evident at 1200 CDT was minimal by 1400 CDT and, at least in the southeast, was replaced by divergent flow by 1600 CDT. At 1200 CDT the flow over the metropolitan area was convergent. By 1400 the magnitude of the convergence had doubled and the area of convergence had expanded northeast. A second, smaller center of convergence occurred just to the west of Edwardsville, where a positive precipitation anomaly has been found between the hours of 1500 and 0200 CDT (Huff, 1977). The center of the convergent flow had shifted northeast at 1600 CDT and was in good agreement with the area of the highest average rainfall for the period from 1500 to 1800 CDT.

The distribution of the mean hbrizontal divergence in E-W and N-S vertical planes across the center of the city (figure C-33) indicates that the convergence over the metropolitan area seen in figure C-32 was actually a dome of convergent flow. At 1200 CDT the deepest and most intense convergence was over the river bottoms to the south of the city, but it shifted to the Missouri metropolitan area later in the day. These cross sections also show divergent outflow above the low-level convergent flow and vice versa, except in situations where the convergence extended to the upper limit of the section.

The arrows, showing 2-hour displacements due to the mean perturbation wind and divergence-induced vertical motion, indicate mass inflow at low levels into the urban area, ascent over the city, and mass outflow aloft. They also show descent at the upper levels north of the city all afternoon, and west of the city only early in the afternoon. A cyclonic vortex with axis at about 1 km appears in the perturbation flow west and north at noon, and there is some suggestion of it at a higher altitude north of the city at 1400 CDT. If there was such a vortex in the disturbance over the region later in the day, it was beyond the boundaries of the cross sections.

The convergent flow was deepest over East St. Louis and the rural area to the south of the city only at 1200 CDT; it was very shallow in these areas later in the day. The depth of the convergence over the main metropolitan area in Missouri increased from about 700 or 800 m at noon to over a kilometer at 1600 CDT, as the level of maximum convergence increased in height by about 200 m and its magnitude more than doubled from 2 or 3 X 10^{-5} s^{-1} to over 8 X 10^{-5} s^{-1}.

The vertical profiles of divergence averaged over two urban and three rural areas for the 21 fair weather cases are shown in figure C-34. These areas were chosen on the basis of approximately homogeneous land use and good delineation by the pibal station network. Average profiles of divergence were also calculated for subdivisions which were based partly on land use but mostly on dominant features of the divergence patterns. These subdivisions are not, in most cases, well defined by the pibal network. Thus the magnitude of the calculated divergences may be in part a reflection of the objective analysis scheme that was used to interpolate between the stations.

The areas shown in figure C-34 coincide approximately with some of the areas used by Huff and Vogel (1977) in their study of urban and topographic effects on precipitation. Area A is a combination of their Suburban West and St. Louis Urban, B is their St. Louis Industrial East plus a small section of Collinsville-Belleville, C coincides to a great extent with their East Bluffs, D is nearly equivalent to their SE Hills-Bluffs, and E is an extension of their ALN-WDR Bottomlands.

The average flow was more convergent over the city of St. Louis than over the suburbs to the west —by a factor of two in the lower levels, somewhat less aloft. However, the profiles were very much alike. For the St. Louis metropolitan area the average horizontal inflow in the lowest 1.5 km must have increased significantly between 1200 and 1400 CDT, due to the increase in both magnitude and depth of the convergence, and then probably decreased by 1600 CDT as the convergence

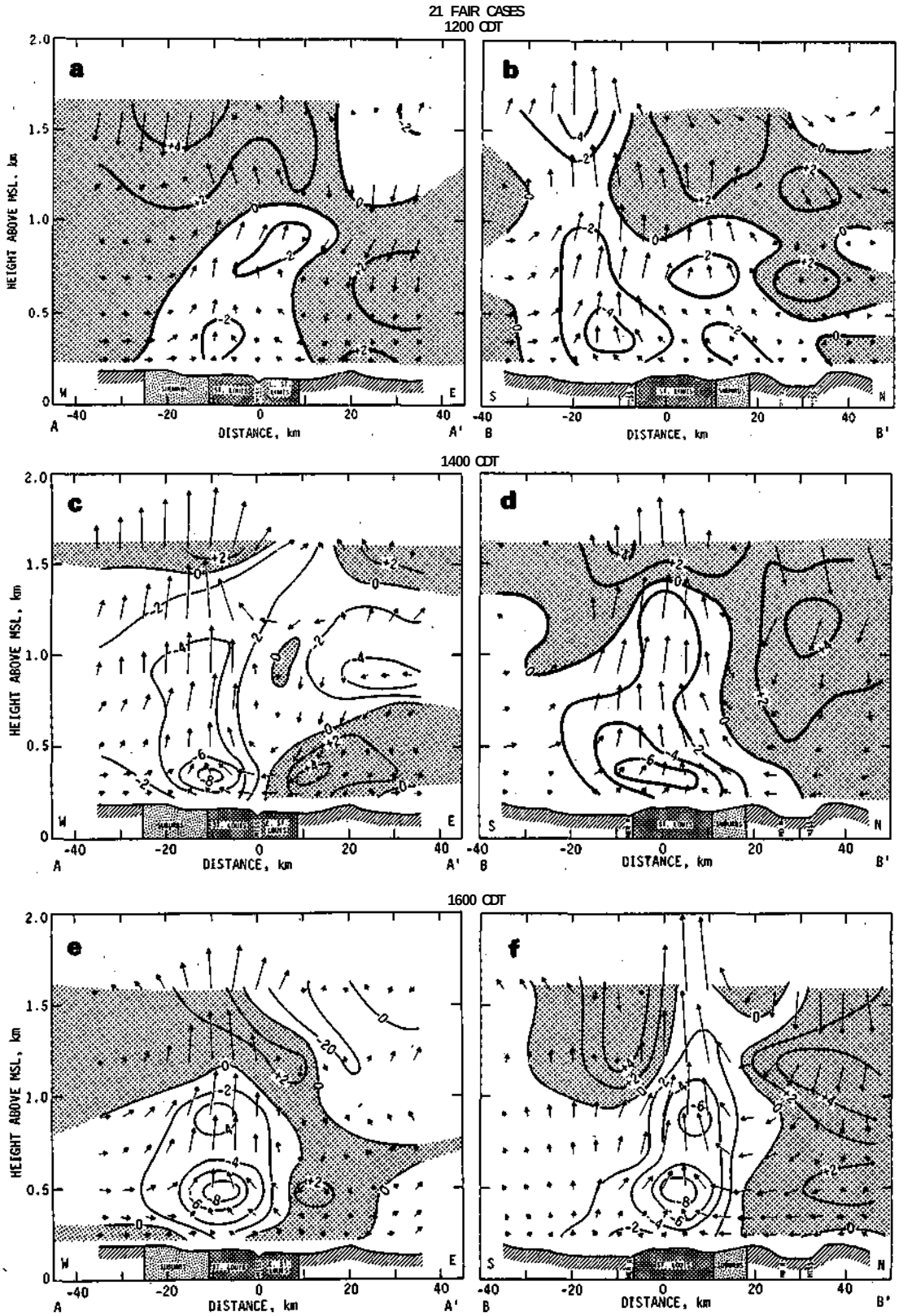

Figure C-33. West-to-east and north-to-south vertical cross sections (see figure C-31) across the city, showing average divergence (10^{-5} s^{-1}) and 2-hour displacement arrows

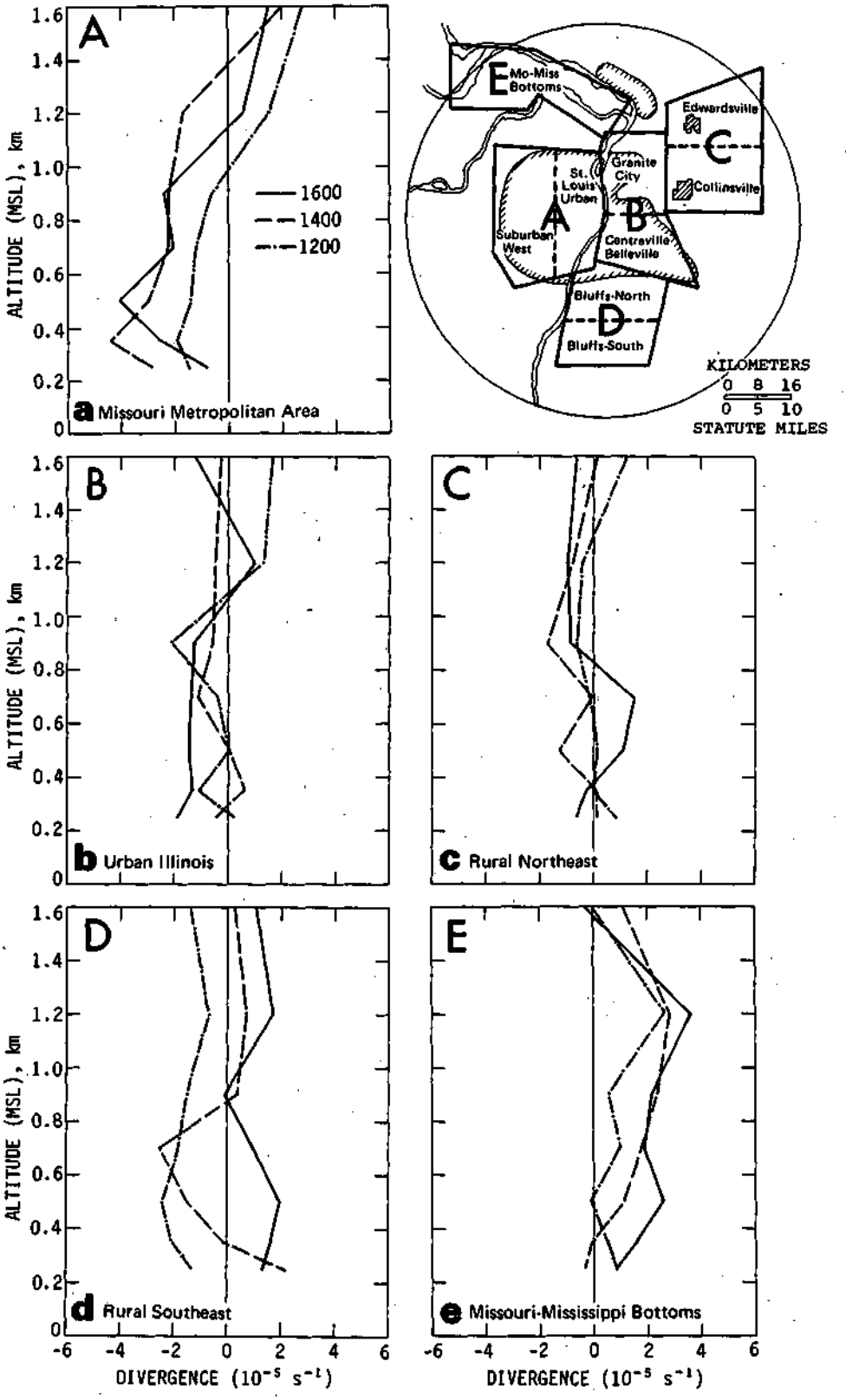

Figure C-34. Vertical profiles of areal-averaged divergence for five areas, mean of 21 fair weather cases

subsided (figure C-34a). The Illinois urban area (area B), on the other hand, was close to non-divergent (horizontal flow) on the average, except at 1600 CDT (figure C-34b). However, the convergence indicated at 1600 CDT was due solely to the airflow in the Granite City subdivision which was convergent at 1400 CDT as well, albeit not as strong. Conversely, at 1200 CDT the flow over the Centreville-Belleville subdivision was convergent below 1 km whereas it was divergent over Granite City.

Similarly, in Area C, the rural area to the northeast, convergent flow in the lowest kilometer in the Edwardsville subdivision was largely balanced by divergent flow in the Collinsville subdivision, at both 1200 and 1400 CDT, resulting in non-divergence on the average for the total area (figure C-34c). The airflow over both sections was divergent at 1600 CDT. Of the three rural areas, only Area D, south of the urban industrial complex, showed significant convergence when compared to that over the city (figure C-34d). However, as has been noted several times already, this was characteristic only of the flow in early afternoon. The flow over the rural bottoms between the Mississippi and Missouri Rivers in the northwest (Area E) was non-divergent early in the day, but became divergent as the day progressed —in opposition to the trend over the metropolitan area.

Horizontal convergence (divergence) must be accompanied by vertical stretching (shrinking) of the air mass. Vertical velocities calculated from the horizontal divergence are generally much smaller than those associated with thermals of relatively small diameter, but are important nevertheless since they indicate the rate at which the boundary layer may deepen (and destabilize) due to converging air. The 21-day means of the area-averaged vertical velocities at the top of the sub-cloud layer for the areas in figure C-34 are given in table C-23, with values given for subdivisions where it is instructive. The mean vertical velocity varied from around +4 cm s^{-1} in the city to -2.6 cm s^{-1} in the rural area to the north. In line with the divergence pattern, the vertical motion was upward over the Missouri metropolitan area and was downward over the bottoms to the north at all three times. These values are modest, due in part to large variability. However, it must be borne in mind not only that 21 days are involved but also that the values represent averages over areas of 300 to 400 km^2 . On individual days the average vertical velocity over these areas may be much larger —and the maxima still larger. The case studies described earlier illustrate this. The average vertical velocities at the top of the mixed layer over the city were 13 cm s^{-1} at 1600 CDT on 4 August and 25 cm s^{-1} at 1400 CDT on 8 August.

The representativeness of the average quantities cited above are important since there is evidence of considerable diversity in the sample. The statistical significance of the mean patterns has not been determined. However, the frequencies with which sub-areas of the meso-region were the location of centers of divergence and convergence, which are shown in table C-24, allow inferences as to the features likely to be significant. (There was usually more than one center of negative and positive divergence at each time, and in the case of Area 6, which was very large, there were also occasions where two centers were in the area). The high average convergence over the metropolitan area is probably real since despite the fact that it represents only 3% of the total area, the city (Area 1) was the site of centers of convergence in one-third of the 63 times for which wind fields were analyzed, and convergence centers were located in the combined city and suburbs of St. Louis, Missouri (Area 2) in 44% of the cases. Moreover, a center of convergence occurred 2 to 7 times more frequently than a center of divergence in the city, and up to 5 times more frequently for the whole metropolitan area. This 'preference' for convergence in the city seems most dominant at midday, when the mixed layer is at its deepest. The small convergent center in the Edwardsville area at 1400 CDT (figure C-32) is probably representative also, since convergent centers occurred in this region (Area 4) almost 3 times more often than did centers of

Table C-23. Area-Average Vertical Motion (cm s^{-1}) at the Top of the Subcloud Layer Mean for 21 Fair Weather Cases

Area	1200	1400	1600
A Missouri, metropolitan			
St. Louis, Urban	2.21	4.27	3.58
Suburban, West	1.14	3.26	1.67
B Urban, Illinois			
Granite City	-0.27	0.59	3.82
Centreville-Belleville	0.73	-0.33	-1.65
C Rural, NE			
Edwardsville	1.49	0.85	0.97
Collinsville	-0.90	0.58	0.19
D Rural, SE			
Bluffs, north	2.30	1.70	-2.41
Bluffs, south	1.30	0.13	0.59
E Missouri-Mississippi River Bottoms	-1.34	-1.26	-2.64

Note. Positive values indicate upward motion, negative values downward motion
See figure C-34 for location of areas

Table C-24. Number of Occurrences of Maxima in Convergence (C) and of Divergence (D) in the Transport Wind Field as a Function of Location and Time

	1200		1400		1600		All times	
Area	C	D	C	D	C	D	C	D
1	6	4	7	1	8	4	21	9
2	6	7	10	2	12	5	28	14
3	5	2	3	6	6	4	14	12
4	5	5	11	4	3	5	19	14
5	4	4	1	3	1	1	6	8
6	9	8	9	13	6	12	24	33
7	2	4	3	4	2	3	7	11
8	4	4	1	5	3	7	8	16

Note. 1, City; 2, City and suburbs, MO; 3, Urban, IL; 4, Granite City-Edwardsville-Collinsville Triangle; 5, Missouri hills around metropolitan area; 6, Rural SE; 7, Rural NE; 8, Missouri-Mississippi bottoms N of urban area

divergent flow. However, the high average convergence in the rural SE at 1200 CDT (figure C-32) may have been due to a few very large values, since the frequencies of centers of divergence and convergence in this region (Area 6) were about the same at 1200 CDT, and convergent centers were less frequent than divergent centers at 1400 and 1600 CDT.

Possible sources of diversity in the wind pattern were mentioned earlier in this section. The sample is not large enough to examine the influence of all potential factors, short of individual case studies, and in some instances (e.g., distribution of cloudiness) the appropriate measurements are not available. Since the ambient wind direction and strength is expected to influence the pattern, the data were stratified by these two variables. The resulting samples are small but, as will be seen, the results are illuminating.

Fair Days Stratified by Wind Direction and Speed

The perturbation over the area is expected to vary as a function of the wind direction because of the non-symmetrical distribution of terrain and land use. It might also be expected to vary as a function of the strength of the wind since local effects, particularly those associated with the urban heat island, are more likely to be well developed in strength and depth with light ambient winds than with strong winds.

Of the 21 fair weather cases, 4 fell into each of the two quadrants centered on NE and SE, 8 in the quadrant centered on SW, and 5 in the NW quadrant. With winds from the NE and SE, the average wind speed in the subcloud layer was always less than 5 m s^{-1}. However, wind speeds were greater than 5 m s^{-1} in 60% of the cases with NW or SW winds.

The individually analyzed kinematic fields were averaged for the cases falling into each of these four quadrants. They were also averaged over two categories of wind speed, S, one for $S \leq 5$ m s^{-1} and the other for $S > 5$ m s^{-1}. Since all of the cases with $S > 5$ m s^{-1} fell in the NW and SW quardrants, a second analysis was carried out for cases with speeds less than 5 m s^{-1} and directions in those two quadrants.

The discussion below is based on the averaged divergence patterns for the transport wind in the subcloud layer. It is possible to infer from these the direction and relative magnitude of the vertical motion near the top of the layer. Convergence in the transport wind implies upward motion near the top of the layer and vertical stretching of the layer; divergence in the transport wind implies downward motion near the top and vertical shrinking of the layer. The larger the value of the convergence (or divergence), the greater is the magnitude of the vertical motion.

NE and SE Flow. The fair weather cases in which the planetary boundary layer winds were from the NE and SE quadrants were characterized by light winds, generally averaging less than 5 m s^{-1} in the PBL. In almost all of these cases the METROMEX study area had experienced a cold frontal passage within the previous 24 to 48 hours and was usually on the south side of a cool high pressure area centered to the north or northeast. When the planetary boundary layer winds were northeasterly, the area generally was east of the surface ridge. In almost all instances the ridge was very shallow so that aloft the METROMEX area was on the backside of the upper level trough. Thus, the winds backed from NE in the lower troposphere to NW aloft. The St. Louis area was farther into the cold air when the planetary boundary layer winds were southeasterly, and was on the leading edge of the upper level ridge. The winds were SE or SSE veering to the W or NW aloft.

The large scale pressure distribution in the middle troposphere on days with NE and SE winds caused widespread subsidence, so that the St. Louis area was experiencing synoptic scale divergence. The depth of the subcloud layer averaged about 1.23 km at noon, deepening during the afternoon to 1.35 km at 1400 CDT and 1.45 km at 1600 CDT.

On three of the four cases with northeasterly winds, divergence dominated the METROMEX area early in the day, although the magnitudes of the divergence were only 10^{-5} s^{-1}. Weak convergence frequently developed later in the afternoon. Figure C-35 shows the average fields of divergence for the transport wind in the subcloud layer, for the four cases with northeast winds.

At noon the dominant feature was divergence over the metropolitan area, extending east-northeast (upwind) of the city, to the vicinity of the topographic ridge extending from Collinsville to Edwardsville (figure C-35a). Although the PBL flow over practically the whole metropolitan area was divergent, the divergence was strongest over the northern half. The divergence reached 5×10^{-5} s^{-1} over both the northern urban area and the rural area to the northeast. The pattern over the rest of the region is quite weak, a reflection of the fact that to the northwest and southeast of the urbanized area, convergence and divergence were equally frequent in the sample.

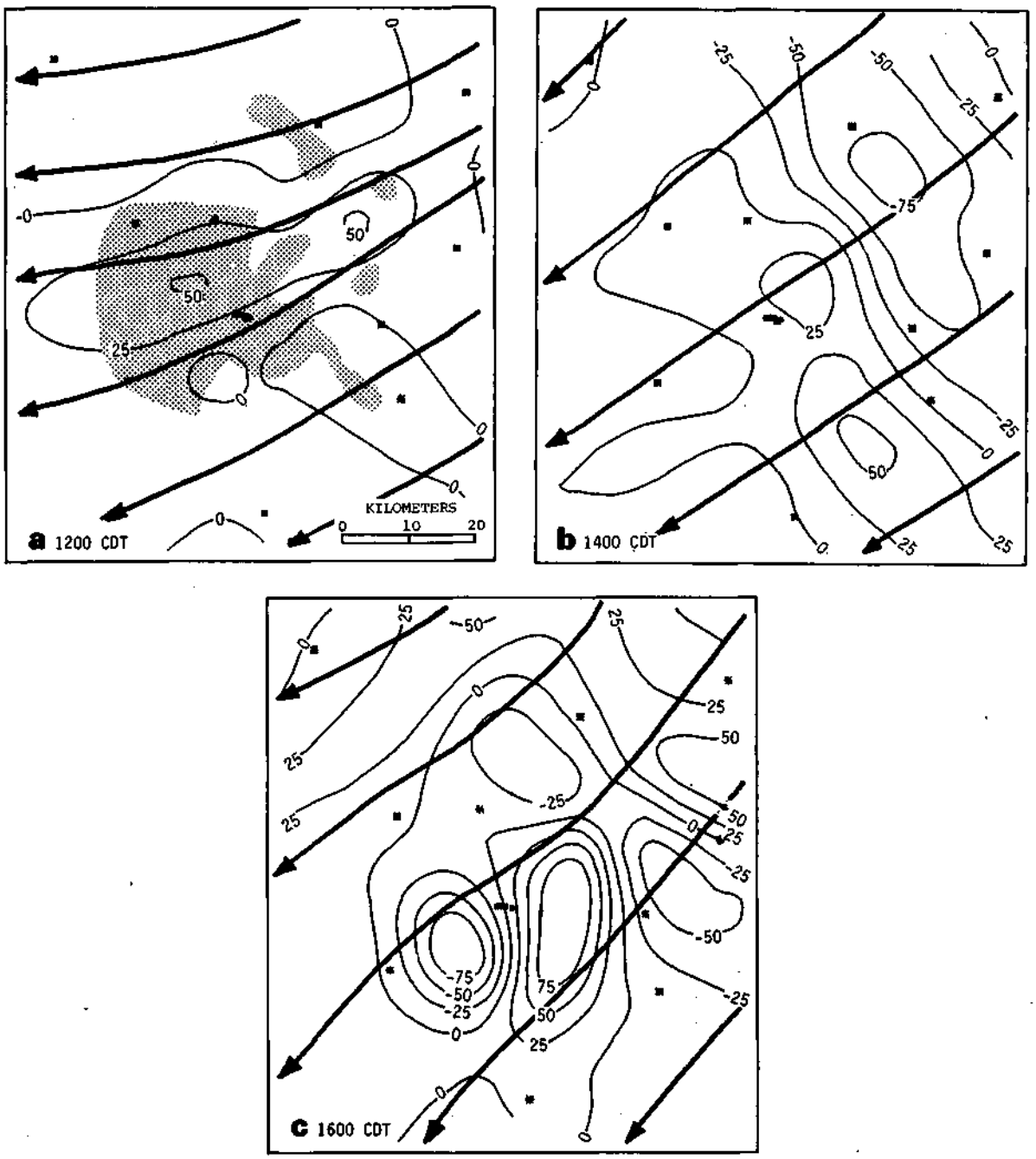

Figure C-35. Streamlines and divergence (10^{-6} s^{-1}) of the subcloud transport wind averaged over fair weather days with northeast winds

The divergence pattern changed significantly in the 2 hours between noon and 1400 CDT (figure C-35b). The divergence over the urban area decreased significantly in magnitude and was confined to the northern part of the metropolitan area, and to East St. Louis and Granite City. The weak divergence over the rural area to the southeast of the city at 1200 CDT increased five-fold and was a principal feature of the pattern at 1400 CDT. The other dominant feature was a relatively strong average field of convergence centered in the area of Wood River and Edwardsville, upwind of the urban area where earlier the flow was divergent. The average convergence in this area reached 8×10^{-5} s^{-1}.

There was an even greater change in the pattern between 1400 and 1600 CDT (figure C-35c) when the flow over the Missouri metropolitan area became convergent, with a maximum of nearly 10^{-4} s^{-1} located to the SSW (downwind) of the center of the city. Compensating divergence, equal in magnitude to that of the convergence, occurred over the Illinois urbanized area and slightly to the east. The flow over the rural areas just upwind of the urbanized area was also convergent. The average divergence field at 1600 CDT was very representative of the four cases. The flow over the main metropolitan area in Missouri was convergent in all four cases and the other features which have been mentioned were repeated in at least three.

Many of the features of the average divergence fields for the northeasterly wind cases are also found in the average fields for the southeast winds, if allowance is made for the difference in the orientation of the topography to the general air flow. Similar to the general situation with northeast winds, the METROMEX area was dominated by divergent flow early in the day in three of the four southeast cases.

At noon (figure C-36a), the SE flow over the metropolitan area was, as in the northeast cases, divergent, most particularly over the northern half. The divergence extended to the ENE. However, unlike the situation with northeast winds, strongly convergent flow reaching 7×10^{-5} s^{-1} occurred over the rural regions to the south (upwind) of the metropolitan area.

By 1400 CDT the pattern (figure C-36b) had reversed, with the divergence over the metropolis and to the north replaced by convergence (maximum 4×10^{-5} s^{-1}), and divergence replacing convergence on the upwind side of the metropolitan area and in the rural areas to the south. In addition divergent flow was developing east and northeast of the metropolitan area.

The basic divergence pattern changed very little between 1400 and 1600 CDT (figure C-36c), although the intensities increased significantly. Divergent flow ringed a zone of convergence which was shifted slightly downwind from the main urban area, with particularly strong compensating flow in the rural areas to the northeast and south.

In summary, the air flow over the metropolitan area on fair weather days dominated by synoptic-scale subsidence and with light winds from the north through east to south was divergent over at least the northern half of the metropolitan area during the late morning and very early afternoon. With southeast winds, the rural areas upwind of the city at the early hour tended to be convergent. Later in the afternoon, however, the flow over the metropolitan area was convergent, with the greatest convergence taking place slightly downwind from the central portion of the city. Compensating divergence produces a 'ring' in the average pattern when the winds were from the SE, but with NE winds, the compensating flow was primarily over the urbanized area of Illinois and to the east.

The divergence fields presented above indicate, on the average, mesoscale lifting (upward motion) in the upper part of the mixed subcloud layer, displaced slightly downwind of the metropolitan area on afternoons with light winds from the NE-SE, in the mid and late afternoon.

NW Flow. The five fair weather cases with winds in the NW quadrant were on consecutive days starting within 8 hours after a cold frontal passage, and continuing as a large cool air mass

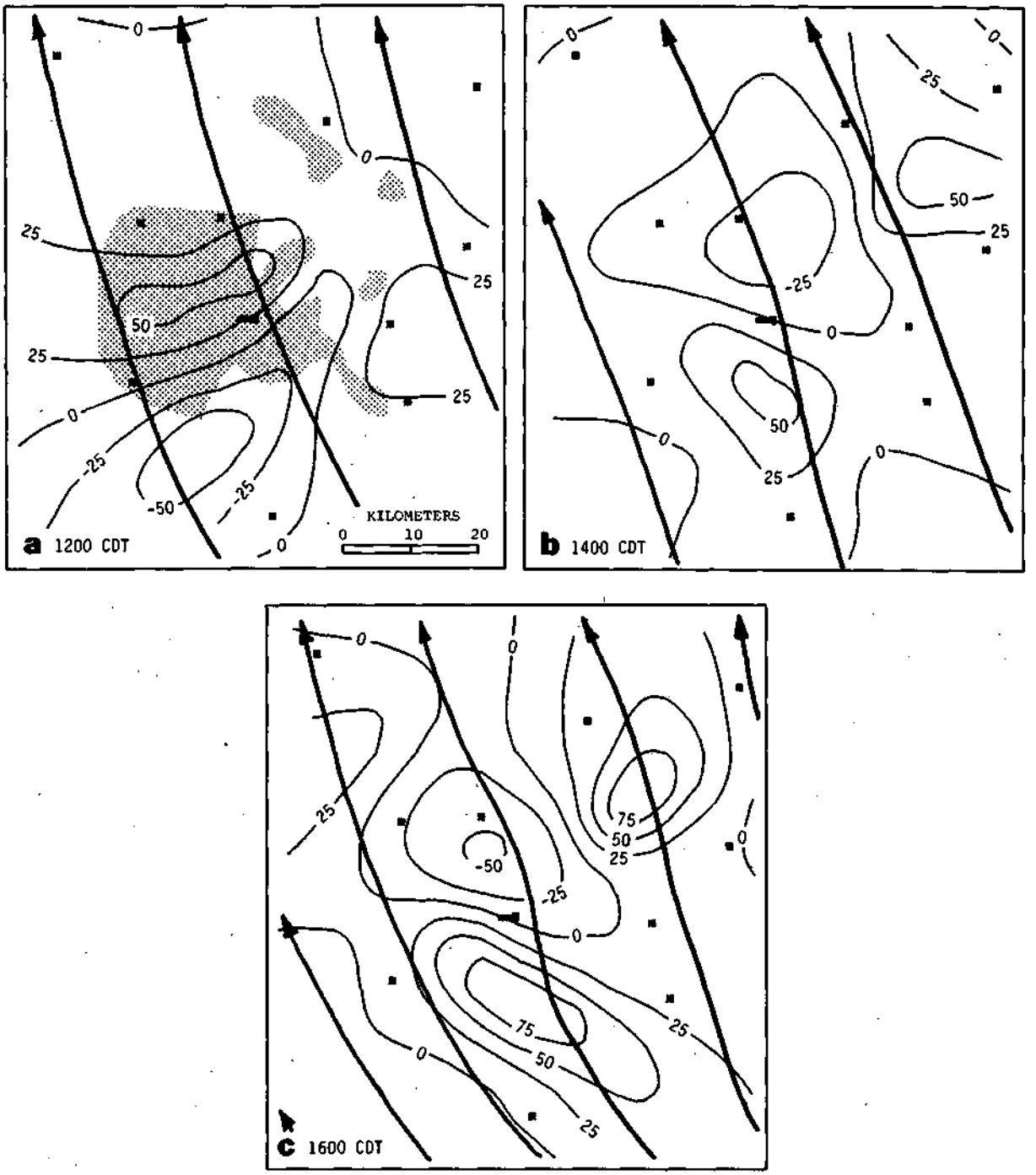

Figure C-36. Streamlines and divergence (10^{-6} s^{-1}) of the subcloud transport wind averaged over fair weather days with southeast winds

moved over the central U.S., eventually covering almost 50% of the country. The winds were strong on the first three days, when St. Louis was just ahead of and in the major upper air trough. On these days the winds backed from northwesterly at the surface to west-southwest aloft. On the last two days of the sequence, the high pressure stagnated and St. Louis was near the central axis of the surface ridge and in the major high pressure area aloft. The PBL winds were 2 m s^{-1} or less and the general flow veered from west-northwest at the surface to northwest aloft. The chief difference between the synoptic conditions in the light wind cases with northwesterly winds and the light wind NE cases lay in the upper level pressure pattern. The major waves were generally farther north in the NE cases, the cold Canadian air masses did not move as far south when they entered the U.S., and consequently the METROMEX area was generally on the southeast edge of the high rather than being in the center, as they were when the PBL winds were weak and from the NW.

The depths of the subcloud layer on days with NW winds were not very different from those when the winds were from the easterly quadrants. However, when the winds were from the NW, the subcloud layer did not deepen during the day as much as it did when the winds were from NE and SE. The depth at 1600 CDT averaged about 1.35 km with NW flow.

The average divergence pattern for northwest subcloud layer winds was significantly different from that for the cases with winds from the northeasterly quadrant. Whereas with NE flow divergence tended to dominate the area, with NW winds there was always a zone of significant convergence, usually associated with the metropolitan area. At noon (figure C-37a) the main zone of convergence occurred east and southeast of the city, with the central axis oriented across the wind and located just downwind from the Missouri metropolitan area. Strongest convergent flow was over Granite City. The winds over the Mississippi-Missouri River bottoms upwind (NW) of the city were also convergent. The zones of convergence alternated with regions of divergence so that the general pattern suggests a wave-like perturbation, oriented roughly 60° to the direction of the mean wind in the subcloud layer.

Alternating zones of divergence and convergence also occurred in the mean patterns at 1400 CDT but the bands were broader, and more nearly perpendicular to the mean flow than earlier. The flow in the Missouri-Mississippi bottoms had become divergent but the region of convergence had broadened to cover the whole urbanized area. The central convergence in the mean pattern increased by 50% (5×10^{-5} s^{-1} to 7.5×10^{-5} s^{-1}) in the two hours and had shifted northeastward to the Collinsville-Edwardsville-Wood River area. Rural areas to the southeast were divergent as they had been earlier.

At 1600 CDT the mean perturbation flow appears to have been in the process of reverting to that of the late morning. Again the flow was convergent over the downwind half of the urban area and over the rural area to the southeast, with central axis of the region of convergence downwind of the city. Upwind of the city the flow was divergent, particularly in the rural areas near the confluence of the Missouri and Mississippi Rivers.

Most of the features of the mean divergence pattern were found in the individual wind fields, regardless of wind speed, with variations more in magnitude than in sign. For instance, the convergent flow in the rural areas to the south and southeast of the urbanized area was much stronger on days with weak winds than on days with strong winds. On the other hand, the convergence northeast of the urban area in the average field at 1400 CDT was a more dominant feature in strong wind cases than in weak winds. Moreover, with weak winds the flow was divergent over most of the metropolitan area at noon, and became convergent later in the afternoon, as it had been with the easterly weak wind cases. In strong winds the flow was convergent over the metropolitan area early in the day and the convergent region tended to shift downwind as the day progressed.

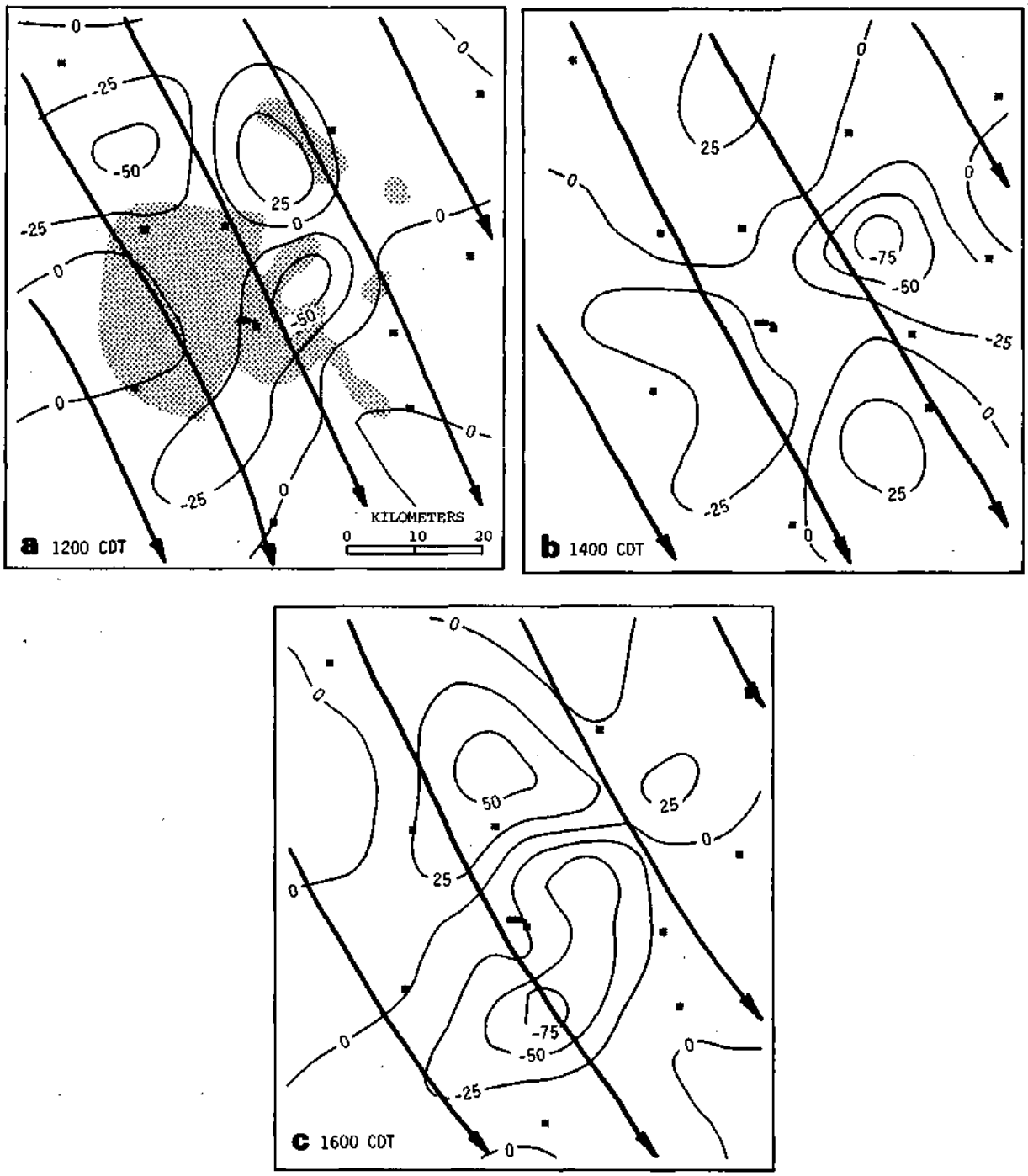

Figure C-37. Streamlines and divergence (10^{-6} s^{-1}) of the subcloud transport wind averaged over fair weather days with northwest winds

SW Flow. The largest subsample of days was with southwest winds. On five of the eight days in this group, the wind speeds were greater than 5 m s^{-1}. The synoptic conditions varied considerably even when the sample was divided into strong and weak wind subsamples. For the three light wind cases, on one day the METROMEX area was ahead of a cold front, on a second day it was behind a stationary front, and on the third it was between a major and secondary front. In general, however, the pressure gradients were very flat throughout the troposphere in all three light wind cases.

Synoptic conditions in the METROMEX area also varied on days with strong southwesterly winds although on all five days there was deep westerly or southwesterly flow. On one day the area was post cold frontal, on another it was in the warm sector of a wave cyclone close to the low pressure center, and on the remaining three days (all consecutive), the area was on the leading side of a nearly stationary major long wave trough reaching from the surface to 500 mb that extended from the Canadian border to the Mexican border.

The subcloud layer tended to be deeper on days with southwesterly winds than on days with flow from other directions. It was deeper by about 100 m on the average for strong winds, and by 300 to 400 m when the winds were light.

At 1200 CDT the southwesterly flow was, on the average, convergent over the Missouri urban area and over the country to the south and southeast, with the central axis of the region of convergence roughly perpendicular to the mean wind (figure C-38a). The flow was divergent over the Missouri-Mississippi bottoms to the north of the urban area and over the Illinois urban area. The mean pattern was dominated by the strong wind cases, with the magnitudes of the convergence (divergence) reduced by about 35% from the values with strong winds. The flow on the low wind days was divergent over the south side of the metropolis and the country to the south (maximum 4×10^{-5} s^{-1}) with weak convergence only over the north side of the urban area. The divergent flow over the Missouri-Mississippi River bottoms was characteristic of both weak and strong ambient flows.

The characteristics of the mean divergence pattern at 1400 CDT (figure C-38b) were very similar to that 2 hours earlier. However, with the disappearance of the pocket of divergence over the Illinois urban area, the pattern takes on a 'banded' appearance. The band of convergence, with central axis over the main metropolitan area and extending southeast, and the band of divergence downwind of the metropolis are nearly perpendicular to the mean wind. The patterns were very similar in the means for both strong and weak wind subsets, although in the latter the central axis of the convergence was shifted downwind of the metropolitan area and was about half the strength of that in the mean pattern for the strong wind cases. On the other hand, the divergence zone on strong wind days was not as far downwind from the city and was considerably weaker than on the weak wind days.

There was a significant change in the pattern between 1400 and 1600 CDT (figure C-38c). Although the flow was still convergent over the metropolitan area and divergent over the rural area to the north, it was strongly divergent southeast of the metropolis also, rather than convergent as it had been earlier. In addition, a new center of convergence appeared downwind of Granite City. Again the pattern has the appearance of alternating bands of convergent and divergent flow which at this time were parallel to the mean flow rather than perpendicular. The average patterns for light and strong wind cases were virtually identical, even to the magnitudes of the divergence and convergence. There was but one exception: the center of convergence downwind of Granite City and near Edwardsville where the convergence was quite weak on the days with light winds, and very pronounced on days with strong winds.

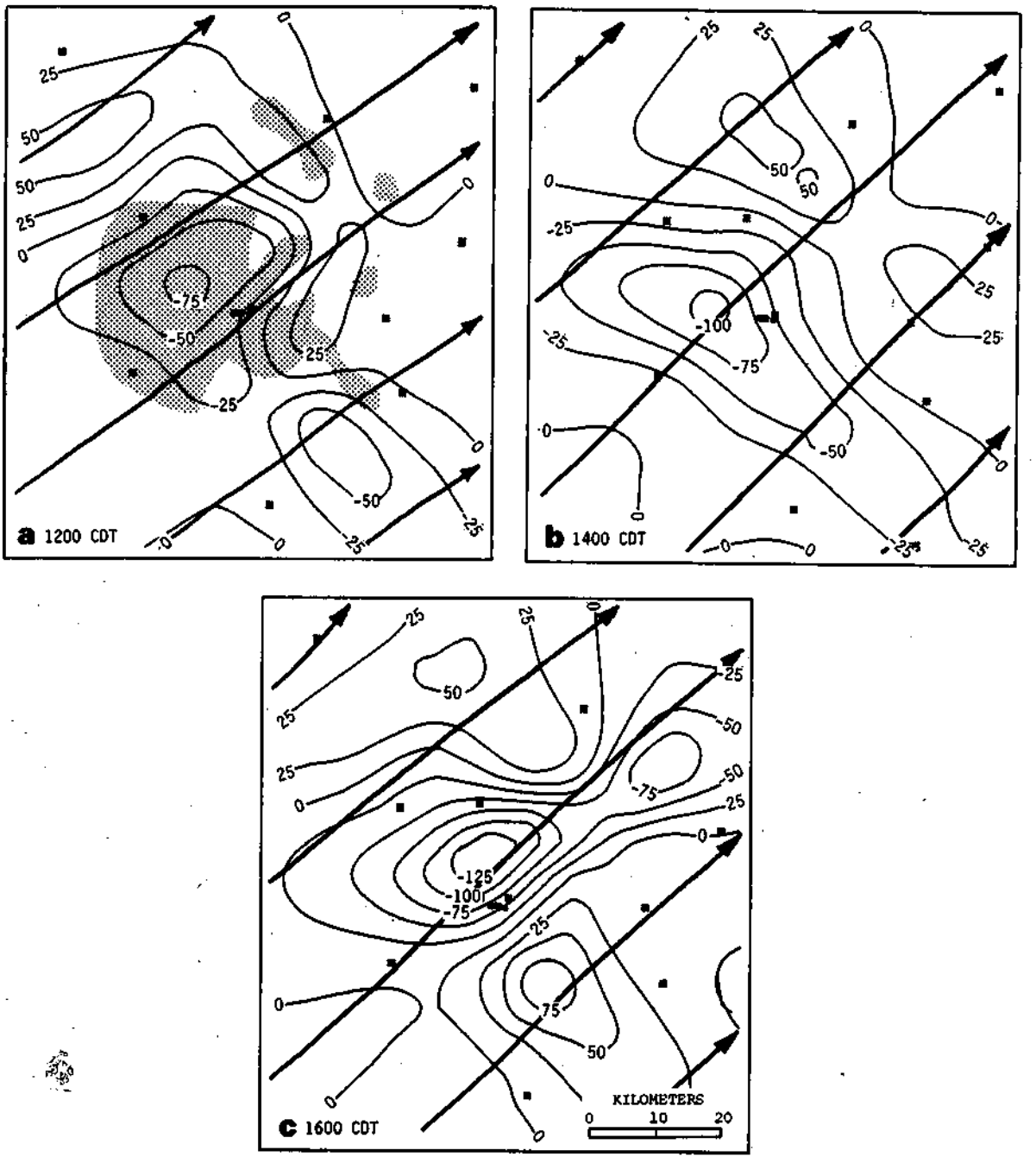

Figure C-38. Streamlines and divergence (10^{-6} s^{-1}) of the subcloud transport wind averaged over fair weather days with southwest winds

Summary. It is evident from the discussion above that except with easterly winds in late morning or early afternoon, convergent flow is associated with the metropolitan area. The dominant characteristics of the flow in the region considered may be summarized as follows:

1200 CDT

1) Metropolitan area: Weakly divergent airflow, except with southwest winds when flow was convergent
2) Rural areas upwind of metropolitan area: Convergent flow with centers of convergence sometimes displaced to right of flow
3) Rural areas downwind of metropolitan area: Variable, sometimes divergent, sometimes convergent, and sometimes close to non-divergent (horizontal flow)

1400 CDT (More diversity in pattern)

1) Metropolitan area: Convergent flow with westerly winds, extended to form band perpendicular to mean flow; with SE winds convergence was shifted downwind from city center, and with northeast winds airflow was weakly divergent
2) Rural areas upwind of city: Divergent flow with NW and SE winds; with NE winds, divergence was confined to band near urban area, with convergence farther upwind
3) Rural areas downwind of metropolis: Divergent flow with westerly winds but generally non-divergent with easterly winds

1600 CDT

1) Metropolitan area: Convergent flow with maximum convergence shifted downwind from the center of the city; with NW winds, convergent flow extended downwind to rural area southeast of the urbanized area
2) Rural area upwind: Divergent except with southwest winds
3) Rural area downwind: Convergent with westerly winds, non-divergent with easterly winds

Wind Strength. Differences have been noted between the mean divergence patterns for light and strong wind speeds in the discussion of westerly wind cases, primarily to indicate representativeness of the overall mean fields. Figure C-39a and b shows the mean patterns of divergence for two wind categories, with the breakpoint at 5 m s^{-1} regardless of wind direction. Since all of the strong winds occurred with winds from the NW and SW quadrants, the average divergence for a subset of light wind cases in these quadrants is also shown (figure C-39c).

At 1200 CDT the flow over the metropolitan area was divergent when the winds were light, particularly when the winds were from the NE and SE quadrants. When the winds were from the NW and SW quadrants and weak, the airflow was convergent over the east (downwind) side of the urban area. The airflow over rural areas to the south and southwest was, in the average, convergent, and over rural areas to the north was divergent. With strong winds, the airflow over the metropolitan area was strongly convergent, with convergent flow extending to the southeast. In common with the light wind cases, to the north of the metropolitan area the winds were divergent, while to the south they were convergent.

By 1400 CDT the airflow over most of the urban area was convergent in both light and strong wind conditions although the mass convergence was greater when the wind speeds were higher than 5 m s^{-1}. To the north of the metropolitan area, the air was divergent, as it had been earlier, although with strong winds a pocket of convergent flow occurred around Edwardsville. The rural area south of the city was largely non-divergent for both categories of wind speeds from the NW and SW quadrants, but were probably divergent with light winds from the other quadrants. This was a major change from the situation two hours earlier when, with light winds, the flow was convergent in this area.

At 1600 CDT the air was definitely converging over the metropolitan area for both light and strong winds, again more strongly with the latter. Extension of the convergence to the east or

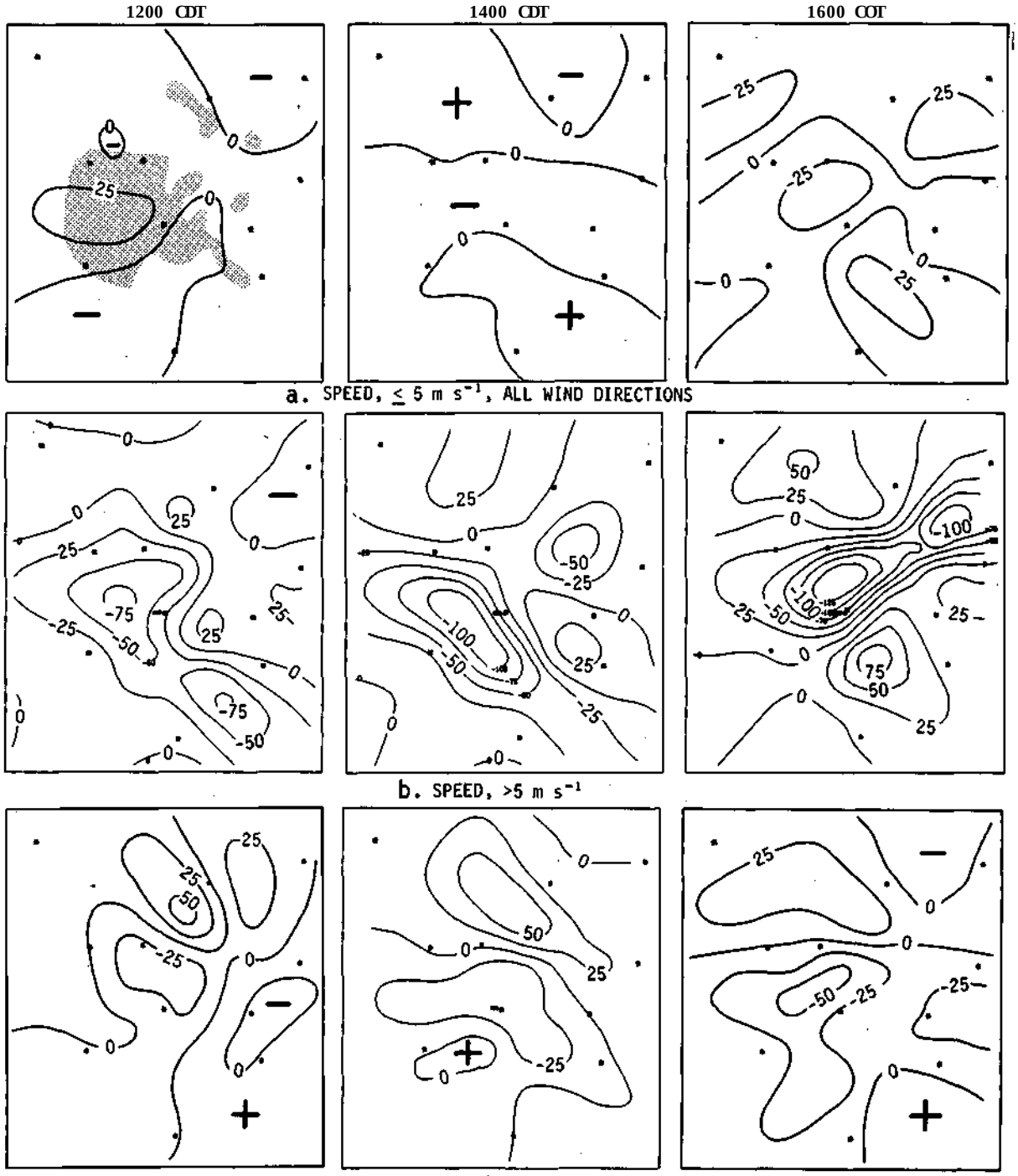

Figure C-39. Perturbation streamlines and divergence (10^{-6} s^{-1},) stratified by wind speed

northeast also occurred with both weak and strong winds. The diverging flow over the rural areas to the north persisted for both speed categories, and diverging flow was also occurring over the country to the southeast. With light winds from the NW and SW quadrants, however, strong convergence also occurred along the river south of the city.

The question was raised earlier in this section as to the representativeness of the 21-day average pattern. The results indicate significant interdiurnal variability. The general features of the divergence pattern were more sensitive to wind direction than to wind speed, whereas the magnitude of the divergence and convergence was more sensitive to wind speed. The divergence pattern was more consistent at 1400 and 1600 CDT when, for all stratifications, the flow was convergent over the metropolitan area, with greater mass inflow when the winds were strong and when they were from the NW and SW quadrants. To the north of the urban area the winds were divergent, and to the south they were either divergent or non-divergent. The divergence pattern appeared to be more dependent on wind direction and wind speed at 1200 CDT than at the later times. With SE and NE winds (all light winds) the flow over the metropolitan area was divergent, whereas with winds from NW and SW it was convergent over the whole area for strong winds, but only over the downwind regions for weak winds.

KINEMATIC FIELDS IN PRE-RAIN CONDITIONS

Low-level wind patterns become more complex in the presence of rain systems because shower clouds produce their own local disturbances. These can mask or alter urban-induced disturbances so that it becomes difficult to sort out the urban- and cloud-produced perturbations in the wind field. The wind patterns prior to the onset of the rain should, however, reflect the urban effect on the wind field although it may be affected by other processes also if the showers are being triggered by larger-scale systems.

In all but 2 of the 16 rain cases observations were available before the onset of rain in the network. In the remaining two, rain was in the network during most or all of the afternoon observation period and all the wind fields were obviously disturbed by the shower clouds. Since the rain started at various times in the afternoon, and on a few occasions two precipitation periods occurred, the size and composition of the samples at the three observation times varied.

All but warm frontal rains are represented in the sample of pre-rain cases (table C-25). Non-frontal rains dominated the sample with air mass showers being the most common. As in the fair weather sample, SW and NW winds were the most common, and particularly the former (table C-26). The transport winds were less than 5 m s^{-1} in 65 to 70% of the cases, except at 1600 CDT when they were greater than 5 m s^{-1} in 4 of the 5 cases.

With the same techniques that were used for the fair weather ensemble analysis, all pre-rain cases were averaged for each of the three observation times. The rain started within 2 hours in 3 of the 9 cases in the 1200 CDT sample, and within 3 to 4 hours in the remaining 6 cases. In the 1400 CDT sample, the onset of rain was within 2 hours in 7 cases and within 3 or 4 hours in the remaining 4. Rain started within 1 hour for all of the cases in the 1600 CDT sample.

The average divergence fields and the perturbation streamlines for the transport wind in the subcloud layer in pre-rain condition are shown in figure C-40. The similarities between these average divergence patterns and the fair weather patterns (figure C-32) are obvious, particularly with regard to the convergence over the metropolitan area.

At 1200 CDT confluence in the perturbation streamlines was associated with converging airflow over the Missouri metropolitan area. The greatest mass convergence was in the northeast

Table C-25. Number of Pre-Rain Cases in Each Synoptic Classification

Synoptic class	*1200*	*1400*	*1600*
Cold front	0	1	1
Post cold front	1	1	1
Air mass	4	4	2
Squall zone	2	1	0
Squall line	2	4	1
Total	9	11	5

Table C-26. Distribution of Transport Wind Speeds and Direction in Pre-Rain Cases

	Number of cases at given speed, m s^{-1}					
	1200		*1400*		*1600*	
Direction	*≤5*	*>5*	*≤5*	*>5*	*≤5*	*>5*
NE	0	0	0	0	0	0
SE	0	1	3	1	0	0
SW	4	2	3	2	1	3
NW	2	0	1	1	0	1

quadrant of the metropolitan area, perhaps a reflection of the preponderance of southwest winds. The flow over most of the Illinois urban area, on the other hand, was divergent.

There was little difference between the divergence fields at 1200 and 1400 CDT except that by 1400 CDT the center of converging air had shifted southward and was centered over the metropolitan area. The divergent flow decreased in intensity but increased greatly in size. The area of divergence also was more to the southeast so that flow over East St. Louis and Granite City was convergent.

Between 1400 and 1600 CDT the average mass convergence doubled, from 5 X 10^{-5} to over 10 X 10^{-5} s^{-1} and covered all of the Missouri metropolitan area as well as most of the Illinois urban area. A small pocket of divergent flow occurred over the extreme eastern part of the urbanized area and over the rural area just to the east, but significant convergence was occurring over the rural areas in the southeast. The perturbation streamlines indicate cyclonic inflow into the center of St. Louis.

The convergence over the Missouri metropolitan area was a highly persistent feature, occurring in all cases at 1200 and 1600 CDT, and in all but two of the cases at 1400 CDT. The divergence over or east of the Illinois urban area was also very persistent, occurring in all cases at 1200 CDT and in 80% of the cases at the other two times. The flow south and southeast of the urbanized area was, however, much more variable, with a nearly even split between convergence and divergence at 1200 CDT, and divergent flow in 7 of the 11 cases at 1400 CDT. At 1600 CDT, the flow was convergent in the southeast in 4 of the 5 cases making up the average.

Figure C-41 shows the profiles of the average divergence over five land use areas, averaged over all of the pre-rain cases available at the three observation times. The convergence over the Missouri metropolitan area was largely confined to the lower 600 to 800 m at 1200 and 1400 CDT (figure C-41a). Between 1400 and 1600 CDT the mass inflow not only increased in magnitude but also increased in depth, with convergence greater than 3 X 10^{-5} s^{-1} up through at least 1.5 km.

The flow over the Illinois urban area (figure C-41b) was, on the average, divergent through most of the first kilometer at 1200 CDT, but low-level convergence appeared at 1400 CDT. The depth of the convergence increased and extended through the lowest kilometer by 1600 CDT.

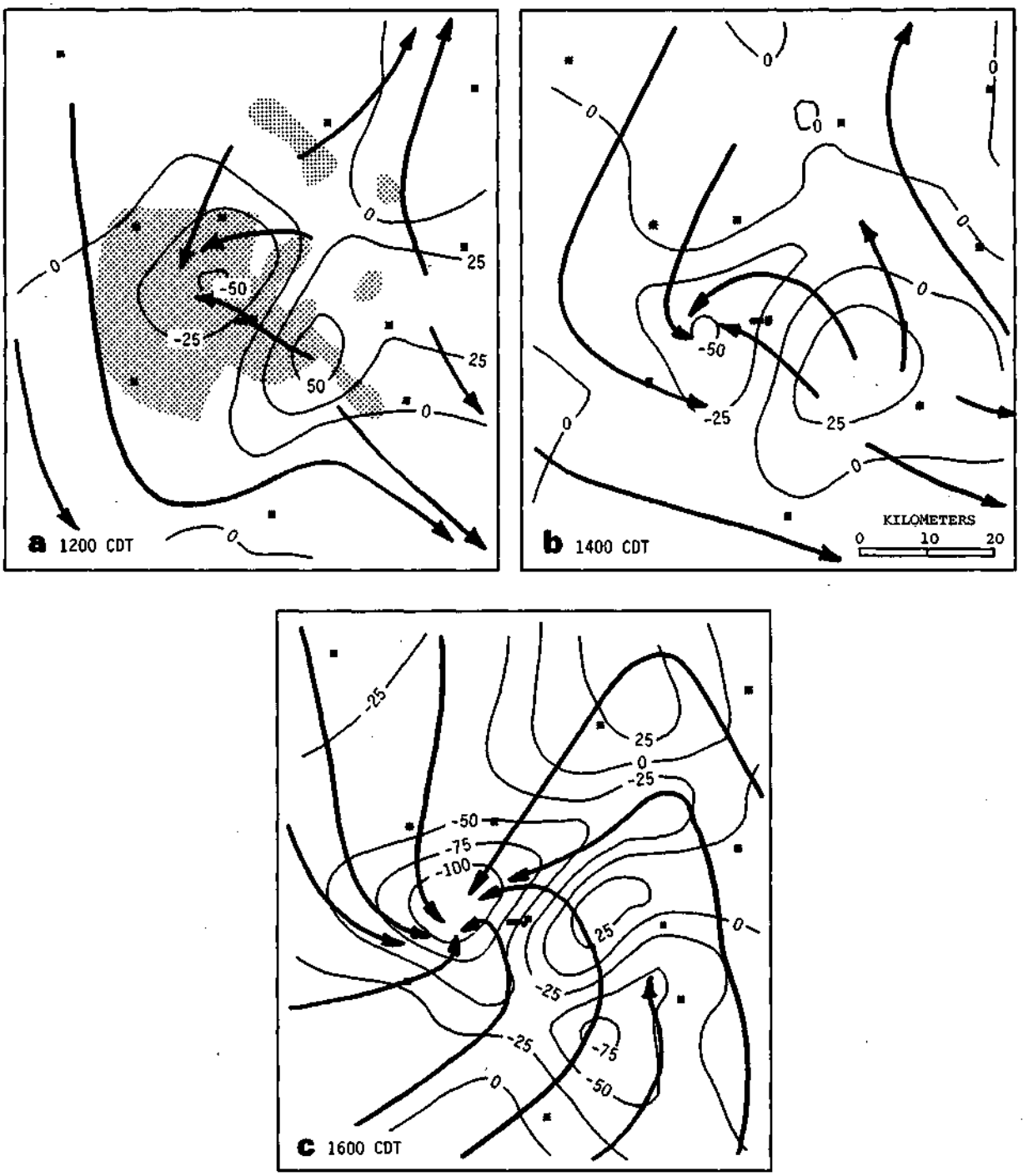

Figure C-40. Perturbation streamlines and divergence (10^{-6} s^{-1}) for pre-rain conditions

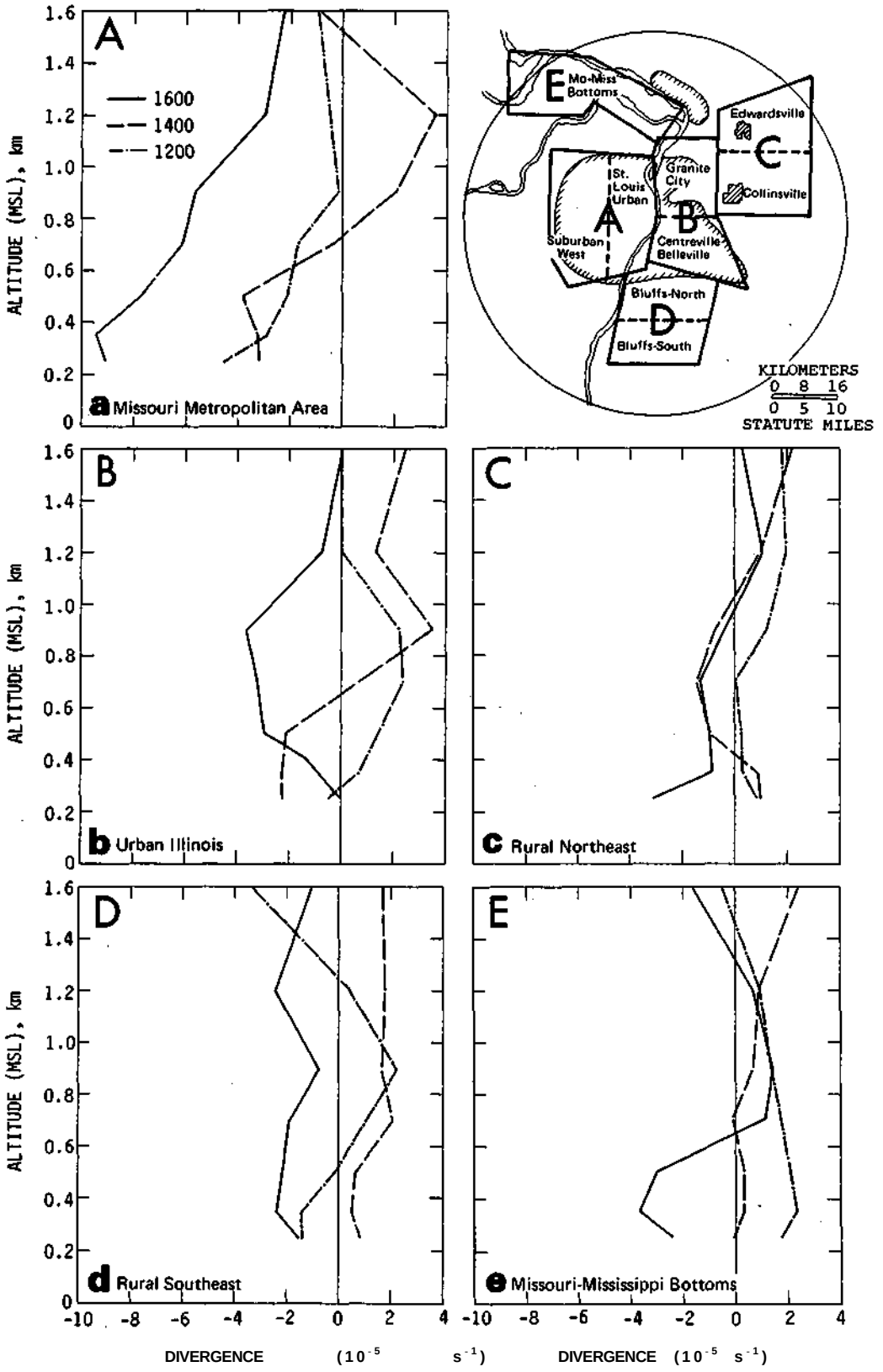

Figure C-41. Vertical profiles of areal-averaged divergence of five areas, for pre-rain conditions

The flow over the rural area to the northeast (which included Edwardsville and Collinsville) was non-divergent in the lower PBL, and divergent above, early in the day (figure C-41c). Converging flow appeared in the middle PBL from 500 to 900 m MSL at 1400 and then propogated downward so that at 1600 CDT the lower kilometer was characterized by relatively weak converging flow.

The flow over the Mississippi-Missouri bottoms was divergent at noon but by 1400 CDT had become non-divergent and by 1600, convergent in the lower 500 m, with compensating divergence above. Over the rural area south of the city the flow at noon was divergent through most of the PBL with convergence at the bottom and the top. The low-level convergence was replaced by deep (but relatively weak) divergence at 1400 CDT. Deep but moderate (2×10^{-5} s^{-1}) convergence occurred in this area at 1600 CDT.

In general there appears to have been convergence over most of the region at low levels for the 5 cases in the 1600 CDT sample, with the convergent flow deepest and strongest over the metropolitan area, and shallowest in the Missouri-Mississippi bottoms to the north.

Because of the limited sample it is not possible to do a complete analysis by synoptic type. However, at 1400 CDT data are available for 4 squall line and 4 air mass cases. The average divergence fields for these two groups (figure C-42) are similar to the average for the whole sample. Both show convergence over the metropolitan area, although the magnitude of the convergence in squall line cases is double that for the air mass cases. In addition, in the squall line cases a second center of convergent flow, equal in magnitude to that of the main one, occurred just northeast of Granite City, and a matching zone of divergence occurred just north of the city. In both subsamples divergent flow occurred over East St. Louis and the ESE rural sector.

The 5-year rainfall patterns for squall line storms (Changnon et al., 1977, page 93) had maxima just east of St. Louis and over Edwardsville. Although it is precarious to extrapolate from a 4-day wind sample to a 5-year rainfall pattern, the agreement between the two patterns is striking, with the maximum rainfall occurring just downwind (for steering level winds) of the convergent centers.

The squall line rainfalls on the four days included in the wind sample were fairly widespread, with maxima in excess of 25.4 mm (1 inch) in every case. The air mass rainfalls on the other hand were isolated, scattered, and very light. Rainfall of any consequence fell on only one of the four air mass cases; in this case the shower was over the city with a maximum rainfall of about 7.62 mm (0.3 inch).

Although there may be some instances in which the perturbation in the wind field may determine cloud development, it is more likely that its impact is more in modifying the storm history, particularly in view of the fact that the precipitation anomalies are associated primarily with the heavier rain storms. Thus the role of the urban-induced modifications in airflow within the context of the urban modification of the precipitation can be seen better in individual case studies.

An example of the potential role of the wind field in the modification of rainfall is illustrated by a storm which passed through the southern part of the network on 14 July 1973 (Semonin, 1975). The divergence field of the transport wind shortly before rain started in the network on 14 July is shown in figure C-43a. The storm of interest entered the network in the extreme west edge about 1600 CDT and rapidly propogated eastward (figure C-43b). The coincidence between the rain band and the pre-existing convergence zone is striking. The rate at which the rain propogated eastward increased significantly when the leading edge of the storm reached the convergence zone over the Missouri metropolitan area. In fact, the rains on the eastern edge of the 1630-1700 CDT rain area actually started some 15 minutes before any surface rain occurred immediately to the west. Moreover, the rain accumulations were greater from the rain clouds in the convergence

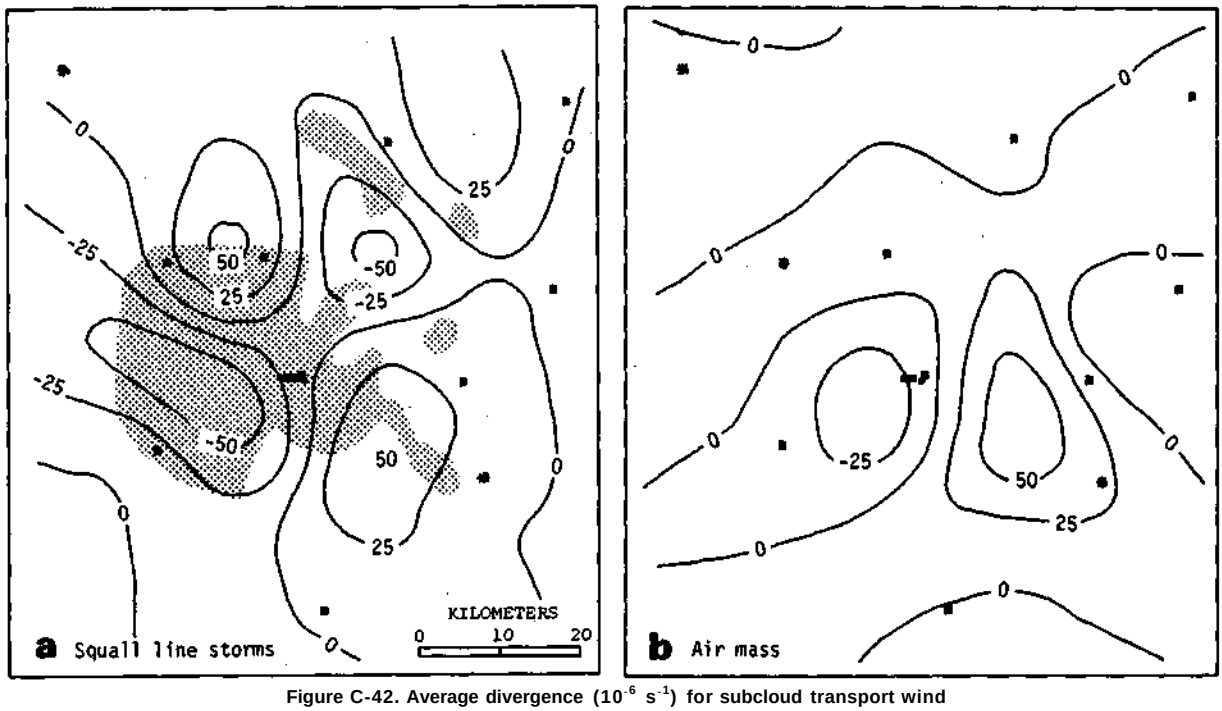

Figure C-42. Average divergence (10^{-6} s^{-1}) for subcloud transport wind preceding squall line storms (a) and air mass showers (b)

area downwind from the city, with the largest accumulation just downwind of the center of the pre-existing convergence zone in the southeast quadrant. The largest vertical velocities calculated at the top of the subcloud layer were +35 cm s^{-1} in the southeast quadrant, and +30 cm s^{-1} over the city.

The PBL winds on 14 July were from the northwest. The low level air, in passing over the city, was being destabilized, at least in the upper PBL, due to the convergence and it was also picking up the urban effluents. Therefore, the low-level air feeding the storm as it moved ESE would be relatively warm, and probably would have neutral stratification. Moreover, the low-level mass inflow would also be enhanced by virtue of the convergence so that despite possibly reduced vapor density in the subcloud layer, the total moisture fed into the storm may actually have been increased.

SUMMARY AND DISCUSSION

The analysis of wind measurements in the PBL on 37 summer afternoons in 1973 clearly demonstrates that the airflow was disturbed in the mesoscale region including the metropolitan area of St. Louis. This occurred in both fair weather and pre-rain conditions. The exact nature of the disturbance is obviously a function of a number of factors, but in almost all instances, the disturbance was associated with metropolitan St. Louis.

The disturbance was most obvious in the observed wind field when winds were light because it was manifested in the wind direction, whereas when the winds were relatively strong, the wind direction was only slightly affected. However, the amount of perturbation in the wind fields, obtained by subtracting the area mean value, was very similar in both strong and weak winds.

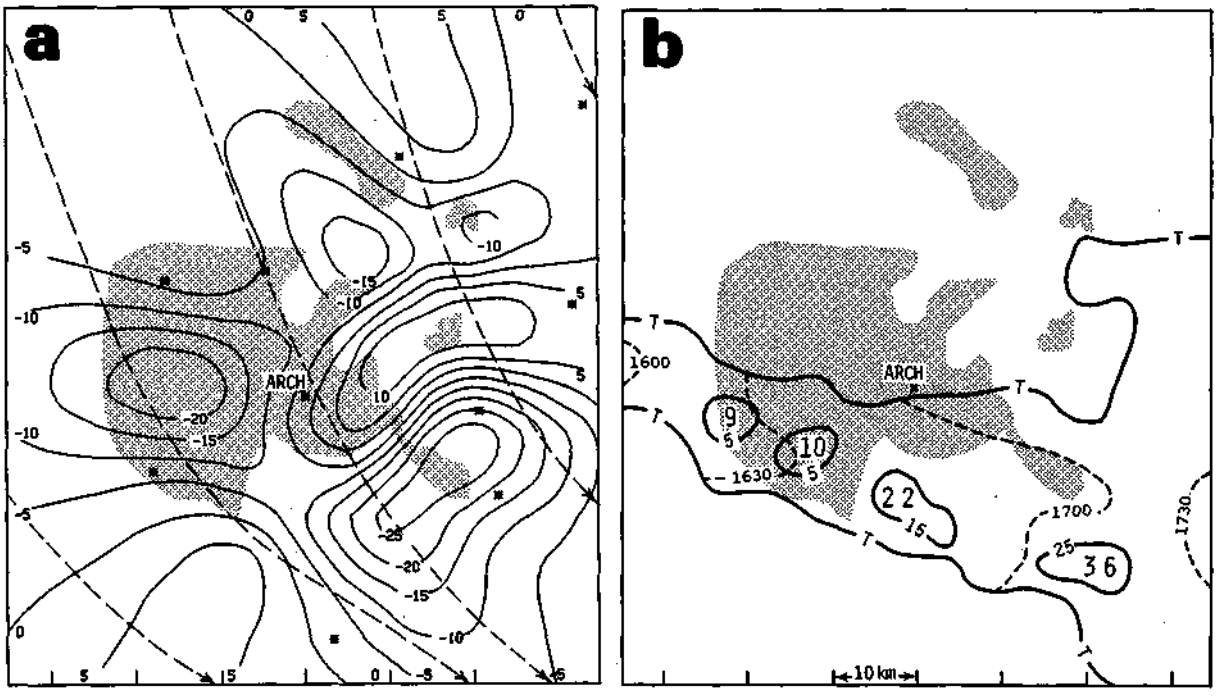

Figure C-43. Streamlines and divergence (10^{-5} s^{-1}) at 1600 CDT on 14 July (a) and rain accumulations from late afternoon rainstorm on 14 July (b) [In (b) heavy lines enclose heaviest rain cores (in mm); dashed lines are isochrones (time CDT) of leading edge of rain area; large numbers give maximum point rainfall (mm)]

The disturbance over the area produced zones of convergence and divergence which, in individual cases, reached 5 X 10^{-4} s^{-1}. The metropolitan area of St. Louis was on the average, a region of convergence throughout the afternoon and throughout the subcloud layer, both for fair weather and for pre-rain conditions. This was a consistent feature for all of the wind fields within 4 hours of the onset of rain in the METROMEX network, but there was considerable variation from day-to-day and, under certain conditions, from early to late afternoon on fair days.

To some extent this variability was related to the direction and speed of the wind. When the area was dominated by synoptic scale divergence and the PBL winds were from NE or SE, the flow (over a good portion of the metropolitan area) was divergent in the late morning and early afternoon, becoming convergent later in the afternoon. With winds from the NW and SW, flow over the metropolitan area was convergent from noon through 1600 CDT with an increase in magnitude in mid afternoon. The flow over the rural areas upwind of the metropolitan area tended to be convergent at noon but later in the afternoon was most often divergent. The flows downwind of the metropolitan area were highly variable, more so than in other sections of the region, sometimes convergent and sometimes divergent.

The pattern of the divergence field was on the average more sensitive to wind direction than wind speed. However, the intensity of the field, i.e., the magnitudes of the divergence and convergence, was more sensitive to wind speed, with the larger values of divergence and convergence occurring with the stronger winds.

The average perturbation approximated a direct urban circulation, particularly in mid and late afternoon, with air flowing into the metropolitan area in the lower PBL, rising, and flowing outward at the upper levels. The depth of the afternoon converging flow over the metropolitan area increased with time from a few hundred meters to over 1 km, and more than doubled in

strength. This was associated with a deepening PBL. The depth of the circulation was greater over the metropolitan area than in other sections.

The thermal stratification of an air column moving into the metropolitan area will be modified because of vertical stretching associated with the convergence, so that the lapse rate will approach the dry adiabatic. This could explain, at least in part, the differences between the observed urban and rural temperature profiles. The shallow unstable layer close to the surface over the country would stabilize as a consequence of the stretching, while the conditionally unstable layer in the middle and upper PBL would become less stable. This would act to produce a more neutral stratification in the city over a deeper layer, as was observed.

This is not to imply that increased mixing due to mechanical or thermal eddies does not play an important role in the modification of the thermal stratification, but only that there is an important interaction between the mesoscale dynamics over the region and the micro-meteorological processes associated with surface roughness and heating. Although the stabilization of the lower layers may decrease the free convection off the surface, the increase in roughness over the city enhances forced convection, so that there may be no loss in upward flux in the surface layer. The destabilization in the upper part of the PBL is the more critical factor, for it permits deeper penetration of eddies and thermals and therefore causes increased flux of surface heat and other effluents into the free atmosphere above the PBL.

What effect might the urban perturbation in wind field and the urban modification of the thermal characteristics of the PBL have on precipitation? The convergence and ascending air over the city means that the upper PBL (and cloud layer if one develops) would be provided with a continual supply of warm surface air from the urban surface, and from the nearby rural surroundings with sensible heat enhanced in passage over the urban surface. Moreover, the less stable lapse rate in the upper PBL increases the probability that thermal and mechanical eddies originating in lower levels would reach cloud base. Thus it might be expected that clouds originating or passing over the city would have greater initial updraft velocities at cloud base, although not necessarily warmer temperatures because of elevated cloud bases.

Sustained updrafts are favorable for the development of deep moist convection and for the intensification of clouds passing over the area. Although the vapor density below cloud base may be less over the city than over the country, recent theoretical work (Koenig et al., 1978) indicates that sensible heat is a more critical factor for cloud initiation than is latent heat. The enhanced source of low level air provided by the convergence will offset partially or entirely the reduction in vapor density in the lower levels. The increased area from which low level source air is drawn and the vertical motion associated with the convergence may also result in enhanced vertical transport of condensation or ice nuclei which would be favorable for rain enhancement also. Thus directly and indirectly the modification of the structure of the PBL could favorably influence the production of rain in the near vicinity of the urban area.

REFERENCES IN PART C

Ackerman, B. 1971a. *Argonne airflow studies in METROMEX. In* 1971 Operational Report for METROMEX. S. A. Changnon, Jr., editor. Contract AEC-1199, NSF GA-28189X, pp. 14-23.

Ackerman, B. 1971b. *A field program to study the urban wind field, METROMEX 1971.* Annual Report Part III. Argonne National Laboratory, ANL-7860, pp. 162-182.

Ackerman, B. 1972. *Winds in the Ekman layer over St. Louis.* Preprints, Conference on Urban Environment and Second Conference on Biometeorology, AMS, Boston, pp. 22-27.

Ackerman, B. 1973a. *The airflow program in METROMEX. In* Summary Report of METROMEX Studies, F. A. Huff, editor, Illinois State Water Survey Report of Investigation 74, pp. 113-125.

Ackerman, B. 1973b. *Airflow over the metropolitan area of St. Louis.* 66th Annual Meeting of the Air Pollution Control Association, 31 pp.

Ackerman, B. 1974a. *METROMEX: Wind fields over St. Louis in undisturbed weather.* Bulletin American Meteorological Society, v. 55:93-94.

Ackerman, B. 1974b. *Wind fields over the St. Louis metropolitan area.* Journal Air Pollution Control Association v. 24(3):232-236.

Ackerman, B. 1974c. *Wind profiles and their variability in the planetary boundary layer.* Preprint Symposium on Atmospheric Diffusion and Air Pollution, AMS, Boston, pp. 19-22.

Ackerman, B. 1974d. *Spatial variability of the wind velocity in the lowest 500 meters.* Preprints Conference on Aerospace and Aeronautical Meteorology, AMS, Boston, pp. 325-328.

Ackerman, B. 1975a. *Thermodynamic structure across a city on days with convective rains.* 55th Annual AMS Meeting, Denver.

Ackerman, B. 1975b. *Observational studies of the mesoscale wind field over an urbanized region.* First Conference on Regional and Mesoscale Modeling, Analysis, and Prediction, AMS, Boston.

Ackerman, B. 1977. *Mesoscale wind fields over St. Louis.* Preprint, 6th Conference on Weather Modification, AMS, Boston.

Ackerman, B., G. Achtemeier, S. A. Changnon, Jr., P. T. Schickedanz, and R. G. Semonin. 1978. *Illinois precipitation enhancement program and design and evaluation techniques for high plains experiment.* Final Report. Appendix B. Bureau of Reclamation Contract 14-06-D-7197.

Ackerman, B., and H. Appleman. 1974. *Boundary layer program. In* Interim Report of METROMEX Studies, 1971-1973, F. A. Huff, editor, NSF Grant GI-38317, pp. 121-146.

Ackerman, B., and B. Wormington. 1971. *Some features of the urban heat island.* Argonne National Laboratory Annual Report ANL7860 Part III, pp. 183-192.

Angell, J. K., D. H. Pack, C. R. Dickson, and W. H. Hoecker. 1971. *Urban influences on night time airflow estimated from tetroon flights.* Journal Applied Meteorology v. 10:194-204.

Atwater, M. A. 1975. *Thermal changes induced by urbanization and pollutants.* Journal Applied Meteorology v. 14(6): 1061-1071.

Auer, A. H., Jr. 1965. *The vertical distribution of Aitken nuclei in the vicinity of Fort Collins, Colorado.* Technical Paper No. 68, Department Atmospheric Sciences, Colorado State University, Ft. Collins, 29 p.

Auer, A. H., Jr. 1975. *The production of cloud and Aitken nuclei by the St. Louis metropolitan area (Project METROMEX).* Journal de Recherches Atmospheriques v. 9:11-22.

Auer, A. H., Jr., and R. A. Dirks. 1974. *Contributions to an urban meteorological study: METROMEX.* Bulletin American Meteorological Society v. 55:106-110.

Barnes, S. L. 1964. *A technique for maximizing details in numerical weather map analysis.* Journal Applied Meteorology v. 3:396-409.

Bornstein, R D. 1975. *The two-dimensional URBMET urban boundary layer model.* Journal Applied Meteorology v. 14:1459-1477.

Braham, R. R., Jr. 1974. *Cloud physics of urban weather modification — a preliminary report.* Bulletin American Meteorological Society v. 55(2):100-106.

Braham, R. R., Jr. 1977. *Overview of urban climate.* Proceedings Conference on Metropolitan Physical Environment, U.S. Forest Service General Technical Report NE-25, pp. 3-17.

Cataneo, R. 1973. *Aircraft measurements and observations. In* Summary Report of METROMEX Studies, 1971-1972, F. A. Huff, editor, Illinois State Water Survey Report of Investigation 74, pp. 153-162.

Chandler, T. J. 1976. *Urban climatology and its relevance to urban design.* World Meteorological Organization Technical Note 149.

Changnon, S. A., and R. G. Semonin. 1975. *Studies of selected precipitation cases from METROMEX.* Illinois State Water Survey Report of Investigation 81, 329 p.

Changnon, S. A., Jr., F. A. Huff, P. T. Schickedanz, and J. L. Vogel. 1977. *Summary of METROMEX, Volume 1: Weather anomalies and impacts.* Illinois State Water Survey Bulletin 62, 260 p.

Czys, R. R. 1977. *University of Chicago measurements of ice-forming nuclei from METROMEX.* Preprint 6th Conference on Planned and Inadvertent Weather Modification, AMS, Boston, pp. 29-32.

Dirks, R. A. 1974. *Urban atmosphere: Warm dry envelope over St. Louis.* Journal Geophysical Research V. 79 : 3473-3475.

Dixon, W. J., editor. 1975. *BMDP biomedical computer programs.* University of California Press, Berkeley, 792 pp.

Dytch, H. E. 1974. *Observations of natural CCN and large aerosol over St. Louis.* Preprint Conference on Cloud Physics, AMS, Boston, pp. 5-8.

Fitzgerald, J. W., and P. A. Spyers-Duran. 1973. *Changes in cloud nucleus concentration and cloud droplet size distribution associated with pollution from St. Louis.* Journal Applied Meteorology v. 12(4):511-516.

Flocchini, R. G., T. A. Cahill, D. J. Shadoan, S. J. Lange, R. A. Eldred, P. J. Feeney, and G. W. Wolfe. 1976. *Monitoring California's aerosols by size and elemental composition.* Environmental Science & Technology v. 10:76-82.

Flocchini, R. G., P. J. Feeney, R. J. Sommerville, and T. A. Cahill. 1972. *Sensitivity versus target backings for elemental analysis by alpha-excited X-ray emission.* Nuclear Instruments and Methods v. 100:379-402.

Friedlander, S. K. 1973. *Chemical element balances and identification of air pollution sources.* Environmental Science & Technology v. l(3):235-240.

Garenstroom, P. D., S. P. Perone, and J. S. Moyers. 1977. *Application of pattern recognition and factor analysis for characterization of atmospheric particulate composition in southwest desert atmosphere.* Environmental Science & Technology v. 11:795-800.

Gatz, D. F. 1974. *METROMEX: Air and rain chemistry analyses.* Bulletin American Meteorological Society v. 55(2):92-93.

Gatz, D. F. 1975. *Relative contributions of different sources of urban aerosols: Application of a new estimation method to multiple sites in Chicago.* Atmospheric Environment v. 9:1-18.

Gatz, D. F. 1976. *The chemical composition of precipitation and aerosols at St. Louis.* Proceedings, Symposium on Man's Impact on Atmospheric Compositions and Processes, American Chemical Society, Northeast Regional Meeting, Albany, NY.

George, J.J. 1960. *Weather forecasting for aeronautics.* Academic Press, New York and London, 673 p.

Grosh, R. C, and R. G. Semonin. 1973. *Moisture budgets and wind fields of thunderstorms passing over an urban area in the Midwest.* Preprint 8th Conference on Severe Local Storms, AMS, Boston, pp. 130-137.

Hall, F. P., Jr., C. E. Duchon, L. G. Lee, and R. R. Hogan. 1973. *Long range transport of air pollution: A case study.* Monthly Weather Review v. 101:404-411.

Harman, H. H. 1967. *Modern factor analysis.* 2nd edition, University of Chicago Press.

Hopke, P. K., E. S. Gladney, G. E. Gordon, W. H. Zoller, and A. G. Jones. 1976. *The use of multivariate analysis to identify sources of selected elements in the Boston urban aerosol.* Atmospheric Environment v. 10:1015-1025.

Huff, F. A. 1977. *Diurnal distribution of summer rainfall. In* Summary of METROMEX, Volume 1: Weather Anomalies and Impacts, by S. A. Changnon, F. A. Huff, P. T. Schickedanz, and J. L. Vogel, Illinois State Water Survey Bulletin 62, p. 42.

Huff, F. A., and J. L. Vogel. 1977. *Comparison of urban and topographic effects in selected network areas. In* Summary of METROMEX, Volume 1: Weather Anomalies and Impacts, by S. A. Changnon, F. A. Huff, P. T. Schickedanz, and J. L. Vogel, Illinois State Water Survey Bulletin 62, pp. 53-60.

Huschke, R. E., Editor. 1959. *Glossary of meteorology.* AMS, Boston, 638 p.

Kocmond, W. C, and E. J. Mack. 1972. *The vertical distribution of cloud and Aitken nuclei downwind of urban pollution sources.* Journal Applied Meteorology v. 11:141-148.

Koenig, L. R., F. W. Murray, and P. M. Tag. 1978. *Differences in atmospheric convection caused by waste energy rejected in the forms of sensible and latent heats.* Atmospheric Environment v. 12.

Langer, G., and J. Rodgers. 1975. *An experimental study of the detection of ice nuclei on membrane filters and other substrata.* Journal Applied Meteorology v. 14:560-570.

Mayrsohn, H., and J. H. Crabtree. 1976. *Source reconciliation of atmospheric hydrocarbons.* Atmospheric Environment v. 10:137-143.

Miller, R. C. 1967. *Notes on analysis and severe-storm forecasting procedures of the military weather warning center.* Air Weather Service Technical Report 200.

Murray, F. W., L. R. Koenig, and P. M. Tag. 1978. *Numerical simulation of an industrial cumulus and comparison with observations.* Journal Applied Meteorology v. 17(5):655-668.

Ochs, H. T., III. 1974. *Cloud modeling in METROMEX.* Preprint 4th Conference on Weather Modification, AMS, Boston, pp. 396-400.

Ochs, H. T., III, and R. G. Semonin. 1976. *Microphysical computations in urban and rural clouds.* Preprint International Conference on Cloud Physics, AMS, Boston, pp. 22-26.

Ochs, H. T., III, and R. G. Semonin. 1977. *The sensitivity of cloud microphysics to an urban environment.* Preprint 6th Conference on Inadvertent and Planned Weather Modification, AMS, Boston, pp. 41-44.

Oke, T. R. 1974. *Review of urban climatology, 1968-1973.* World Meteorological Organization Technical Note 134, WMO No. 383, 132 p.

Oke, T. R. 1977. *Review of urban climatology, 1973-1976.* University of British Columbia.

Rummel, R. J. 1970. *Applied factor analysis.* Northwestern University Press, Evanston, IL., 617 p.

Semonin, R. G. 1974. *Urban induced weather modification.* 1974 Earth Environment and Resources Conference Digest, U.S. Environment and Resource Council, Bowie, Maryland, pp. 40-41.

Semonin, R. G. 1975. *Isolated storm of 14 July 1973. In* Studies of Selected Precipitation Cases from METROMEX, S. A. Changnon and R. G. Semonin, editors, Illinois State Water Survey Report of Investigation 81, pp. 68-89.

Semonin, R. G. 1976. *The variability of pH in convective storms.* Journal of Water, Air, & Soil Pollution v. 6:395-406.

Semonin, R. G., and S. A. Changnon. 1972. *Illinois State Water Survey in METROMEX. In* 1972 Operational Report for METROMEX, W. P. Lowry, editor, pp. 43-61.

Semonin, R. G., and S. A. Changnon. 1974. *METROMEX: Summary of 1971-1972 results.* Bulletin American Meteorological Society v. 55(2):95-100.

Showalter, A. K. 1953. *A stability index for thunderstorm forecasting.* Bulletin American Meteorological Society v. 34:250-252.

Spurny, K. R., and J. P. Lodge. 1972. *Collection efficiency tables for membrane filters used in sampling and analysis of aerosols and hydrqsols.* National Center for Atmospheric Research Technical Note, NCAR-TN/STR-77.

Staff, Atmospheric Sciences Section, ISWS. 1973. *Projects of the Illinois State Water Survey. In* 1973 Operational Report for METROMEX. W. P. Lowry, editor, pp. 33-44.

Staff, Atmospheric Sciences Section, ISWS. 1974. *Projects of the Illinois State Water Survey. In* 1974 Operational Report for METROMEX. R. R. Braham, Jr., editor. pp. 11-19.

Staff, Atmospheric Sciences Section, ISWS. 1975. *Projects of the Illinois State Water Survey. In* 1975 Operational Report for METROMEX. A. H. Auer, editor. pp. 13-25.

U. S. Environmental Protection Agency. 1975. *Scientific and technical assessment report on manganese.* National Environmental Research Center, Research Triangle Park, N.C., USEPA Office of Research and Development, Washington, D.C., EPA-600/6-74-002.

Vogel, J. L. 1977. *Synoptic weather relations. In* Summary of METROMEX, Volume 1: Weather Anomalies and Impacts, by S. A. Changnon, F. A. Huff, P. T. Schickedanz, and J. L. Vogel, Illinois State Water Survey Bulletin 62, p. 85.

Vulkovich, F. M., J. W. Dunn, III, and B. W. Crissman. 1976. *A theoretical study of the St. Louis heat island: The wind and temperature distribution.* Journal of Applied Meteorology v. 15(5):417-440.

Winchester, J. W. 1977. Personal communication.

Winston, J. S. 1956. *Forecasting tornadoes and severe thunderstorms.* U. S. Weather Bureau Forecasting Guide No. 1, 34 p.

Wuerch, D. E., A. J. Courtois, C. Ewald, and G. Ernst. 1972. *A preliminary transport wind and mixing height climatology, St. Louis, Missouri.* NOAA Technical Memorandum NWS CR-49, 13 p.

PART D CONTENTS

PART D CONTENTS (CONCLUDED)

Part D. Cloud and Precipitation Processes

STUDIES OF ANOMALOUS CUMULUS CLOUDS

Ronald C. Grosh

Introduction

An interesting finding from the analyses of the 1975 satellite cloud photographs was the diurnal variations in the locations of the cloud occurrence maxima (see following section). The morning data showed maximum cloudiness over the hills to the west of St. Louis, but later in the day St. Louis, and still later Alton, also became relatively cloudy. A negative feedback mechanism may be acting which involves existing clouds reflecting energy and suppressing further convective development relative to surrounding areas which were originally less cloudy. This mechanism would act in a manner similar to that described by Purdom and Gurka (1974).

One goal of the METROMEX cloud analysis was to determine where the clouds, which grow into rainstorms near St. Louis, initiate and how the rain clouds grow. Furthermore, if altered urban energetics play the dominate role in the formation of the precipitation anomaly (relative to enhanced coalescence effects), then determining the source region of clouds which yield precipitation in the anomaly zone will help to delineate the causes of the urban precipitation anomaly.

The St. Louis urban area is a source of anomalously frequent radar precipitation echo initiations (Braham and Dungey, 1976). Consequently, echo merging is more frequent over the urban area, and urban echoes are larger and produce more rain than rural echoes (Changnon, 1976, and page 310 in this report). A key question to answer therefore is, "What causes the frequent echo initiations?" It is possible that more clouds produce precipitation echoes over the urban area than do those over rural areas. This would be taken as strong evidence that the urban area was . altering the coalescence process by supplying anomalously large particles to cloud updrafts. However, the analyses of the satellite cloud photographs (next section) show that cloud occurrence frequencies are not spatially uniform. The location of the first echo maximum (which is based mainly on afternoon data) occurs where the afternoon cloud occurrence maxima exist. Therefore, it seems probable that dynamic alterations of cloud energetics are important in the precipitation anomaly.

The anomalous cloud frequencies observed in the satellite photographs were determined by noting the presence or absence of cloud anywhere (or everywhere) in 9.7 X 9.7 km squares, and thus they do not necessarily correspond to individual clouds. However, the first echo results correspond to individual entities often on scales of a few hundred meters across. It is therefore not possible to directly compare the satellite-derived cloud frequencies with the echo frequencies so as to determine if the cloud anomaly is sufficient to account for the first echo anomaly. At this point it would appear reasonable to assume that the urban area produces more clouds and that urban clouds have a higher fraction of echo initiations within them. It is therefore important to obtain ground truth (as well as satellite-based) cloud information relevant to the urban precipitation anomaly.

An all sky (hemispheric) cloud camera was operated during the summers of 1971-1975 at St. Louis University (SLU), which is near the center of St. Louis, to monitor cloud activity.

In response to many field observations of frequent initial cumulus forming near the Wood River refinery complex, plus the fact that one part of the precipitation anomaly was located just to the southeast of Alton, a second all sky camera was operated at the Alton Civic Memorial Airport (ALN) in 1975. A third cloud camera was operated at Pere Marquette State Park (PMQ) during 1971-1973.

The cloud data derived from the film of the three cameras were examined to determine if there were regions where cumulus clouds initiated with anomalous frequency. The photographs from the ALN camera were also examined with the intention of discovering evidence of other unusual cloud formations which might be forming in response to urban-industrial forcing. Anomalous activity involving isolated clouds in this area had been reported frequently (e.g., Auer, 1976). It was desired to thoroughly document the possible type and frequency of industrial cumulus developments. Reports of similar industrial clouds forming at many other locations have been made by Stout (1961), Stinson (1977), Stinson and Brown (1977), Barber et al. (1974), Aoki and Yabuki (1975), Changhon and Henderson (1974), Culkowski (1962), Hobbs et al. (1970), Kramer et al. (1976), and Bibby (1976). Satellite observations of industrial clouds have been reported by Brown and Karn (1976) and Detwiler (1974).

Data

The all sky cloud camera system used at SLU and ALN consists of a 16-mm camera mounted in an inverted fashion over a reflecting hemisphere 18 cm in diameter. A clock and date indicator are included in the field of view. Photographs were timed for once every 5 minutes during daylight hours within chosen operational periods. Data were obtained with the SLU camera during August 1971, June-August 1972, June-August 1973, July-August 1974, and July-August 1975. Data were obtained in the June-August periods of 1971-1973 at PMQ. Photographs were obtained with a pointing 35-mm camera which photographed a 120° sector that included E, SE, and S. Photographs were made once every 5 minutes. Data were obtained with the ALN camera in July-August 1975. Due to various maintenance and equipment problems not all days during these periods yielded data of usable quality.

The first cumulus (Cu) which formed early in the day after morning cloud layers or fog had cleared were studied to develop a census of cumulus initiations. Only the first 5 to 10 Cu that formed during each day were considered. The average time of the appearance of the first Cu was 1115 CDT and the first 10 Cu normally formed within the subsequent 20 to 30 minutes. Only periods when individual Cu could be identified with reasonable certainty were included. Periods with simultaneous occurrences of altocumulus and cirrocumulus were avoided. This approach was applied to all 5 years; the data of the earlier study of Schickedanz (1974a) for the first three years (1971-1973) were re-examined and only those cases with clear Cu formation were utilized with the 1974-1975 data.

Surface cloud observations at nearby weather stations were checked to assure proper identification of cloud types. Questionable cases were dropped. SLU camera data from 40 days during the summers of 1971-1975 met the data selection requirements. Data on 28 August days were used along with one June day and 11 July days. The data used from the ALN camera were obtained on 11 days in August 1975 and 10 days in July 1975.

These data selection procedures were chosen to assure measurement of only low-level cumulus clouds which were likely to have been affected by local boundary layer processes. This approach limited the days studied to those in rather clear periods. Thus, the data are biased toward rather clear summer days when non-frontal weather conditions were present. However, on

25 percent of the days included for study (at all camera sites), rain developed in the network after the initial Cu formations. All periods.in which Cu could be identified were used from the 3-year PMQ camera data, which are not directly comparable with data from the other two sites.

Analytical Procedures

For each period of cumulus initiations meeting the selection criteria, the locations of the first cloud, the first 5 clouds, and the first 10 cumulus clouds to initiate were determined. The determination was made by projecting the film data on a screen and then overlaying the screen with a circle divided into sectors. The distance of clouds from the SLU camera was also determined by use of two assumptions: 1) that the lens-mirror system was azimuthally equidistant (Holle and MacKay, 1972), and 2) that cloud bases were at 1.2 km (the local summer average). The azimuthally equidistant assumption means that the relation between zenith angle and distance of the image point from the picture center is linear. The location data were then partitioned into clouds ≤4.8 km and those >4.8 km from the camera center. The resolution of the lens-mirror system when 16-mm film is employed makes it extremely difficult to obtain quantitative distance beyond 4.8 km.

The cloud locations determined from the SLU film were then partitioned into eight sectors of the circle corresponding to 337.5 to 22.5° (N), 22.5 to 67.5° (NE), 67.5 to 112.5° (E), etc. The location data from the ALN camera were partitioned into only six sectors of 60°. This was done so that the refinery area would be completely within one sector. The cloud locations at PMQ were sorted according to 40° sectors (E, SE, S) and counted.

Regional Cloud Initiation Frequencies at St. Louis Site

The cumulus initiation frequencies at SLU are. shown in table D-l. If initiations were evenly distributed, each sector would have 12.5%. The NW and W sectors show the most noticeable differences from chance occurrence (12.5%) for all stratifications, but particularly for the first cumuli where the observed W value (26.9%) is more than twice the expected value. When only Cu initiations at locations less than or equal to 4.8 km from the camera site are considered, the N sector also has evidence of anomalously high initiation frequencies. Values to the SW, and E are all less than expected. The western sector values dominate the Cu initiation frequencies, but when more than just the first Cu are considered, there is also a tendency for unusually large frequencies in the NW sector and, to a lesser extent, the northern sector.

First cumulus initiations in the W and NW sectors occurred, on the average, 49 minutes earlier than the initiations in the other sectors (1102 vs 1151 CDT). A t-test revealed that the probability of this difference occurring by chance was about 0.002. The average Cu initiation time for all sectors was 1133 CDT with a maximum range of nearly 9 hours (0835 to 1720 CDT).

The 1975 data were investigated for those cases in which the first Cu was in the W sector, and those in which the first 10 Cu were largely in the W sector. These days were studied to determine if the approach of cloud systems with a westerly motion was causing an apparent anomaly in the W sector. Synoptic weather charts and satellite photographs for the 6-hour period centered on the cloud initiation time were examined on these days to determine if cloud system movement from the west toward St. Louis appeared likely.

There were seven days in 1975 with first cumuli in the W sector, and five of these (71%) were judged to have been free from cloud system motion from the west. On only one day did

Table D-1. St. Louis Summer Cumulus Initiation Frequencies from 40 Days in 1971-1975

	Percent of total in each sector								
	N	*NW*	*W*	*SW*	*S*	*SE*	*E*	*NE*	*Number of cumuli**
First 10 Cu	13.5	17.9	21.9	9.0	9.0	10.6	8.8	9.4	480
First 5 Cu	13.0	17.2	24.4	9.5	7.3	12.6	6.9	9.2	262
First Cu	11.9	14.9	26.9	9.0	4.5	10.4	7.5	14.9	67
First 10 Cu within 4.8 km of camera	15.3	14.7	23.7	10.7	10.7	9.7	7.0	8.3	300

*** The numbers of cumuli include multiple clouds on individual photographs and, therefore, are greater than the simple expected numbers of 40, 200, and 400**

westward motion appear likely, and on the seventh day results were indeterminate. There were nine days when the W sector cloud occurrence frequency was the largest observed or equal to the largest among the first 10 cumuli initiations. Six of these days (67%) were judged to be free of cloud system motion from the west. The three other days were classified as indeterminate. In summary, about 70% of the days with W sector dominance in cumulus initiations were unaffected by the motion of cloud systems, and only one day appeared to have distinct evidence for cloud system motion from the west.

The influence of cloud system motion from the west was conservatively determined by completely deleting the data from those days judged as having cloud system advection from the west or as uncertain. The resulting frequencies (table D-2) show that the first cumuli frequencies are altered only slightly. The locational frequencies of the first 10 initiations are also altered by only a few percent. In this case, the alteration is enough to lower the W sector frequency (for this year) to a level equal to that of the NW sector. Both of these sectors were high in all the stratifications of the 1975 SLU data. Therefore, the effect of cloud system motion, as seen in the W sector frequency reductions due to the very conservative correction procedure, is not viewed as significant. This suggests an area of preferred cloud initiation over the western and northwestern portions of the St. Louis metropolitan area.

Table D-2. Cumulus Cloud Initiation Data at St. Louis Based on Days without Cloud System Motion from the West, 1975

	Percent of total in each sector								
	N	*NW*	*W*	*SW*	*S*	*SE*	*E*	*NE*	*Number of cumuli*
First Cu	8.3	19.4	22.2	8.3	5.6	13.9	8.3	13.9	36
	(7.9)*	(18.4)	(26.3)	(7.9)	(5.3)	(13.2)	(7.9)	(13.2)	(38)
First 10 Cu	10.3	21.4	21.4	8.5	8.5	12.0	10.7	7.3	234
	(10.0)	(19.3)	(24.5)	(9.7)	(8.6)	(10.4)	(10.0)	(7.4)	(269)

• **Values in parentheses are the 1975 frequencies with all clouds**

Comparison of Results with Previous Analyses

A previous analysis of the SLU cloud camera data for the years 1971-1973 was performed by Schickedanz (1974a). That analysis differed from the present one in that initiations of all clouds were counted rather than only initiations of cumulus, the clouds considered most likely to be affected by local influences. It is of interest to compare the present results with the previous analysis.

The main difference between the two analyses (table D-3) occurs in the N sector where the earlier analysis has a maximum frequency of 19%. The 1971-1975 cumulus analysis has its maximum frequencies in the W and NW sectors (table D-l). Since the results of the present analysis of the 1971-1973 data (table D-3) are in a good agreement with the all cloud results (Schickedanz, 1974a), it is clear that sampling variations are the main cause of the difference between the two analyses.

Maps of the surface winds at the hour closest to the time of the appearance of the first cumulus were plotted for the 9 days in 1975 when the cloud frequency in the W sector (from the SLU camera site) dominated among the first 10 cumuli. This analysis was based on data from all wind networks with a total of 20 stations. Frequently, the St. Louis urban area experienced convergent flow but there was also upslope flow in the W sector. The spatial resolution of the observations was not sufficient to isolate which of these mechanisms was mainly responsible for the cumulus initiations nor which sector was most strongly influenced by them. In general, however, the dominance of the W sector appears real.

Atmospheric Stability when First Cumulus Formed in the West Sector

The synoptic weather types for the periods in 1975 during which first Cu were forming were determined from 3-hourly weather maps. These data revealed that 5 (71%) of the 7 cases with first Cu in the W sector were air mass type periods. The other cases were cold and stationary frontal types. The 13 cases when the initial Cu formed in another sector were only slightly different. Eleven (85%) of these cases were classified as air mass types and 2 were classified as stationary fronts. The difference is too small to be significant.

In 3 of the 7 cases with the first Cu occurring in the western sector, rainfall subsequently developed in the area. In 7 of the other 13 cases rainfall followed. The frequency difference (3 of 7 vs 7 of 13) is small and it appears that synoptic conditions on days when the first Cu appeared in the W were not noticeably more (or less) stable than those on days when cumulus began in other sectors.

Table D-3. Comparison of the 1971-1973 Results from Two Cloud Initiation Frequency Analyses

	Percent of total in each sector							
	N	*NW*	*W*	*SW*	*S*	*SE*	*E*	*NE*
First 10 clouds *(Schickedanz, 1974a)*	19.0	14.0	18.0	9.0	13.0	8.0	7.0	12.0
First 10 cumuli *(Present analysis)*	22.5	9.2	16.7	5.0	12.5	10.0	10.0	13.3

Surface Meteorological Conditions

Surface meteorological observations from the nearby National Weather Service first order station at Lambert Field (STL) were studied to see if conditions in periods with first Cu in the W and NW sectors were different from those when first Cu were observed in the other six sectors (table D-4). These observations are taken as an approximation of regional conditions at SLU. The 1100 CDT observation time was chosen because this was the hour closest to the average first Cu initiation time (1115 CDT).

The differences between 1100 CDT conditions on the days when the first Cu were in the W and NW sectors, and those on all other days were compared with a t-test. Relative humidity and temperature values were significantly different. The t-test results are limited since the data are probably not independent nor normally distributed. On the anomalous W and NW formation days temperatures were 1.2° C lower which would favor cloud formation in the W and NW sectors if enhanced surface heating took place there, such as might be associated with insolation on a slope or an urban heat island in central St. Louis. Higher humidities (resulting from the lower temperature) on these days would also make cloud formation easier since the LCL is lower. Thus, anomalous convective clouds may have been favored by higher relative humidities and relatively unstable local conditions in the W and NW sectors.

The cloud base heights calculated from T and T_d were lower than the value assumed in the data reduction procedure (1.0 km vs 1.2 km). Thus, on the average, the observed clouds are closer (by about 1 km) to the camera site than estimated. This difference does not affect the results substantially.

Cloud Initiation Frequencies at Pere Marquette Site

The initiation locales of the first 10 cumulus clouds of the day at this rural site 48 km NW of St. Louis were investigated by sorting the cloud locations according to three 40° sectors (75-115° or E, 116-155° or SE, and 156-195° or S). The results showed that the south sector had 32% of the clouds, 1% less than if they were evenly distributed. The SE sector, which included a view of the St. Louis metropolitan area, had 30% of the total. The east sector had 38% of the initiations, 5% more than expected with a normal distribution. The differences of the observed and expected frequencies were not statistically significant.

Most of the cloud initiations photographed are believed to have been within 24 km of the camera. Haze frequently limited visibility to less than 16 km at PMQ, and on several days, field

Table D-4. Surface Observations at 1100 CDT at STL on Days with Cumulus Initiations Observed at SLU

First Cu in sector	*N (days)*	*Relative humidity %*	*Visibility (km)*	*Sea level pressure (mb)*	*T (°C)*	*T_d (°C)*	*Wind direction (deg)*	*Wind speed (knots)*	*Cloud base height (km)*
W and NW	18	64.5	12.2	1018.2	28.2	20.6	200	6.8	0.91
Others	22	60.8	13.3	1018.8	29.4	21.0	180	6.5	1.03
W and NW—others		3.7*	-1.1	-0.6	-1.2*	-0.4	20	0.3	-0.12
Average	40	62.4	12.75	1018.6	28.9	20.8	189	6.6	0.98

* Indicates difference appears to be statistically significant at the 0.1 to 0.05 level

Note. The cloud base heights (CBH) have been computed with the equation CBH = 0.0671 ($T - T_d$) using the average values of T and T_d

personnel located the exact placement of the initial Cu viewed at PMQ. Thus, the area viewed, or studied, was essentially the bottomlands to the S and SE, and the river bluffs and higher rural country to the E. Within this 24-km range, the only potentially significant man-made influence on clouds was a major power plant located 19 km to the ESE (in the E sector of this analysis). On several occasions, initial Cu were formed in the plume from the stacks of this plant. On certain days clouds also generated along the sharp river bluff (oriented WNW-ESE) in the E sector. Thus, the topographic influence and the power plant effluents occasionally affected cumulus initiations, leading to the slightly higher than expected frequency to the E.

Regional Cloud Initiation Frequencies at Alton Site

The cumulus initiation frequencies observed in the six sectors surrounding the Alton (ALN) dome camera are shown in table D-5. The W and SW sectors, which include the Alton urban area and the Wood River refinery (WRR) area were 150% of the expected frequency (16.7%) in both the first 5 and first 10 cumuli categories. The other four sectors were below the expected frequency. However, when only the first cumulus cloud of each day is considered the SW sector (refinery) is the only one above the expected value, being 47.5%, or three times the expected value.

To further examine this finding, the number (percent) of the days that a sector was involved in a first Cu observation was determined. This procedure reduces the importance of multiple Cu appearances in one sector on a first Cu frame. The last line in table D-5 shows that the frequency for the SE sector (19.4%) is also greater than the expected value. The SE does not have any values in the other stratifications that are greater than the expected value and, since this one exception is of rather modest size, not much significance is attached to it. It is more important, however, to note that there is little difference between the bottom two rows, indicating that multiple Cu appearances in the SW sector on a few first Cu frames were not important in producing the anomaly, but that this industrial sector was where the first Cu initiated on many days. This important result confirms many visual observations of solitary cumulus over the refinery area. It suggests that the large amounts of heat and moisture released to the atmosphere by the refineries may be playing a role in the early formation of cumulus clouds (Auer, 1976).

It may be that the high frequencies in the W sector for the first 5 and 10 cumuli are related to advection of some sort from the refinery sector. However, actual cloud advection is very doubtful as the large majority of cumuli observed were short-lived, and cloud motion and wind direction were considered during the data reductions. It is more likely that the Alton urban-industrial area also acts to initiate cumulus earlier than in rural areas.

First cumulus occurred earlier in the SW (refinery) sector than in the other five sectors. On the 13 days during which the first cumulus to form initiated in the SW sector, they began, on

Table D-5. Frequency of Cumulus Initiation at Alton

	Percent per 60-degree sector						
	W (Alton)	*SW (WRR)*	*SE*	*E*	*NE*	*NW*	*Number of cumuli*
First 10 Cu	22.9	22.9	13.7	12.9	13.7	14.0	271
First 5 Cu	21.7	24.8	13.7	14.3	12.4	13.0	161
First Cu	12.5	47.5	15.0	12.5	5.0	7.5	40
Sector involved in first Cu episode (%)	9.7	41.9	19.4	12.9	6.5	9.7	31 cases

the average, at 1057 CDT with a range between 0918 and 1350 CDT. On the 8 days when the first cumulus initiated in other sectors, the average initial occurrence was 37 minutes later, at 1134 (range 1008 to 1353). A t-test indicated that the probability of this 37-minute difference occurring by chance is about 0.2. Therefore, it is of marginal significance. The average initiation time for all ALN sectors was 1111 CDT.

The hourly wind observations at ALN were examined for the periods when first cumulus formed in the refinery (SW) sector to determine if upslope winds could be playing a role in the cumulus initiations. The wind direction at ALN had a southerly component on 8 of the 13 days with the first cumulus in the refinery sector. In four cases the wind had a northerly component, and one day was calm. Wind speeds on all but one day were less than 8 mph. The wind speed and direction data tend to favor little cross sector motion by the forming clouds during the 5 minutes between observations. It therefore seems probable that most of the clouds did not form in other sectors and move into the refinery sector during the 5 minutes between the photographic exposures. However, the predominance of southerly wind components indicates that the possibility of upslope flow contributing to cumulus initiation cannot be ignored.

The time periods on the 13 days when the first cumulus to form occurred in the oil refinery (SW) sector were studied to discern whether or not the Cu initiations were the result of the motion of larger scale cloud systems toward the camera site from the SW. Clouds forming in advance of such a system could appear to be local initiations when they really were more closely associated with the destabilization of a moving dynamic system. The 3-hour synoptic weather maps were examined in conjunction with the associated satellite photographs. These data indicated that clouds probably approached from the south on only one of the 13 days. The other 12 days showed no detectable evidence of cloud systems approaching Alton from the south. It is concluded that cloud systems moving toward the camera site from the south probably played a very small role in the initiation maximum in the refinery sector.

The localized first Cu source regions found by the two cameras (mainly SW of ALN airport and mainly W and NW of SLU) are not at the same azimuth and this is taken as further strong evidence that advection of large cloud systems into the initiating sector played a minor role in the findings.

Atmospheric Stability when First Cumulus Formed in the Refinery Area

The 13 periods when first Cu formed in the refinery sector were characterized by weak synoptic forcing. None of them occurred on rain days in the network. Synoptic weather types were mostly of the air mass variety (9 cases, or 69%). Stationary (3 cases) and warm frontal situations (1 case) existed during the other periods. Six of the 8 cases when cumulus initiated in other sectors were also air mass types, and the other 2 periods were characterized by squall zone conditions. Five of these 8 days were marked by the development, of rain. The frequency of weather conditions present when initial Cu were observed to form in the refinery sector and those when Cu formed in the other sectors was not much different. Most cases were rather weak air mass situations with high surface dew points. However, the differences in the subsequent development of rainfall suggests that on days when the first Cu developed in the refinery sector weather conditions were probably more stable throughout the region than on the other days. This emphasizes the potency of the cumulus generation mechanism acting in the refinery sector.

Surface Meteorological Conditions for ALN Site

The 1000 CDT surface meteorological observations from nearby STL and BLV stations were checked to see if periods with first Cu in the refinery sector were different from those when first Cu were observed in the other sectors. It should be remembered that local conditions at ALN may differ from those at STL and BLV and that these observations serve as an approximation of regional conditions.

Table D-6 shows the average values of the surface observations for days with the first Cu in: the refinery (SW) sector, all other sectors, the difference between these two groups and, finally, the average for all six sectors combined. Only the temperature difference, as observed at STL, was significant at the 0.1 level, although differences in several other variables approached significance (wind direction and visibility). However, the relative humidity, a variable known to strongly affect the clouds forming cooling tower plumes (Barber et al., 1974) varied by less than 2%. Only the temperature difference approached significance based on the Belleville data. Thus, the days with anomalous cumulus forming in the refinery sector were cooler by about 2°C than the other days, but humidity differences did not appear to play an important role. The effect of humidity on the length of cooling tower plume clouds is most noticeable when the humidity is very high (≥ 75%, Barber et al., 1974). Only one day with cumulus observed by the ALN camera was this moist.

Statistical Evaluation of Sector Cu Initiation Frequencies at SLU and ALN

A Chi-square test was used to determine the probability of the observed sector distributions of the initiations (tables D-l and D-5) occurring by chance in a sample from a uniform distribution. The probabilities that the observed distributions occurred as a result of sampling variations are shown in table D-7. All the distributions had a 3% or less probability of happening by chance, and over half the distributions found had less than a 0.01% probability of chance occurrence. The first cumulus distribution at Alton was the most unlikely to occur by chance,

Table D-6. Surface Observations at 1100 CDT on Days with Cumulus Initiations Observed at ALN

First Cu in sector	*N (days)*	*Relative humidity (%)*	*Visibility (km)*	*Sea level pressure (mb)*	*T (°C)*	*T_d (°C)*	*Wind direction (deg)*	*Wind speed (knots)*	*Cloud base height (km)*
St. Louis (Lambert Field, STL)									
SW (refinery)	13	65.8	12.4	1019.5	27.7	20.6	174	7.6	0.85
Others	8	64.0	9.7	1017.9	29.6	22.0	235	6.5	0.91
WRR—others		1.8	2.7	1.6	-1.9*	-1.4	-51	1.1	-0.06
Average	21	65.1	11.05	1018.9	28.4	21.1	197	6.9	0.88
Belleville (Scott AFB, BLV)									
WRR	13	60.2	10.1		28.7	20.1	194	4.4	1.03
Others	8	59.1	9.5		29.9	20.9	181	4.6	1.09
WRR—others		1.1	0.6		-1.2	0.8	13	-0.2	-0.06
Average	21	59.8	9.8		29.1	20.4	189	4.5	1.05

* Difference significant at the 0.1 level

Table C-7. Probability that Cumulus Initiation Distributions Occurred by Chance

	Probability based on Cbi-square test
SLU Site	
First 10 Cu	<<0.0001
First 5 Cu	<<0.0001
First Cu	≐0.02
First 10 Cu within 4.8 km	<<0.0001
ALN Site	
First 10 Cu	≐0.03
First 5 Cu	≐0.02
First Cu	≐0.0001*
% of days involved in first Cu	≐0.02*

• Includes Yates correction for small expected values

but at St. Louis University the first 5 to 10 cumuli distributions were the most unlikely to occur by chance. It appears that there are different mechanisms acting to initiate cumulus early at the two sites. Urban-induced convergence aided by topography probably affect cumulus development at SLU. However, the topographic influence at ALN is less, and the refinery effluents dominate early convection.

Comparison of Results from the St. Louis and Alton Sites

Comparison of Initiation Frequencies. The frequencies in the sectors of greatest interest at both sites were divided by the expected value frequency for each site (12.5% at SLU and 16.7% at ALN) to obtain a ratio which makes it possible to compare their magnitudes (table D-8). This was done because the analysis involved a different number of sectors at each site.

When the first 10 cumuli are considered, the ratio shows that the sectors to the W and NW of SLU were relatively more frequent places for initiations than were the W (Alton) and SW (refinery) sectors from ALN. However, when only the first Cu are considered, the refinery sector at ALN exceeds the W sector at SLU.

Initiation Sequence. It is interesting to compare the temporal variations of cumulus initiations at the two sites. At SLU the strongest sector for first Cu initiations was the west, but as more clouds formed, the adjacent sectors to the north (the NW and to a much less extent the N sector) increased in frequency. After the first 10 Cu had formed, the frequency in the NW sector was very similar to that in the W sector. At ALN this clockwise shift was also evident. The first Cu initiation frequency in the SW (refinery) sector was very dramatic, but by the time 10 Cu had formed, the adjacent sector to the W had an equal initiation frequency.

Table D-8. Ratios of Cumulus Initiation Frequencies for High Frequency Sectors*

	Sector W	*Sector SW*
First 10 Cu at ALN	1.37	1.37
First 10 Cu at SLU	1.75	1.43
First Cu at ALN		2.84
First Cu at SLU	2.15	

• Observed frequency (%) + expected sector frequency (%)

Thus the area of cloud generation tended to shift northward in a systematic fashion. This is not cloud motion but an actual change in location of where clouds initiated. This shift is comparable to the apparent northward shift of the afternoon urban heat island circulation (see Ackerman, page 180 of this report) and the urban cloud frequency maxima observed by satellite (see next section). The cause of this motion is not known. If the role of particulates in the cloud formation process is discounted (because sufficient condensation nuclei are normally present for clouds to develop), the timing of the cloud initiations and maximizations must be related to the development of local and urban circulation patterns caused by kinetic and thermal energy alterations which must also develop in a south to north pattern. The reason these circulations develop regionally is also not known. However, the prevailing low-level wind direction at St. Louis has a strong southerly component.

Insolation and Slope Orientation. Since the local interaction of insolation and slope orientation may affect the early generation of cumulus, the relationship of the sun to major topographic features may be important. All morning the sun heats the east side of the major N-S ridge at the W edge of St. Louis. These conditions appear to be favorable for cumulus initiations in these western sectors from SLU but not elsewhere. Interaction between insolation and slope orientation are also possible at ALN, although they appear less likely to play a role in the initiation anomaly. More detailed investigations are required to determine the relationship between cloud occurrence and slope heating at either site.

Comparison of Cumulus Initiation Anomaly Areas with Satellite-Observed Cloud Anomalies. Most (300 or 62.5%) of the 480 cumulus initiations measured at the SLU camera likely developed within about 4.8 km of the site. Further, it appears likely that most of the 480 Cu initiated within about 6.0 km of the camera since this radius (r) encloses a circle with an area, A, satisfying the relationship

$$(300/480) = 0.625 = [\Pi(4.8)^2 / A] = [(4.8)^2 / r^2]$$

Thus, the initiation anomaly areas observed in this study are likely limited to within about 6 km from the camera sites. However, these results depend on the azimuth equidistant assumption and the cloud base height assumption. It seems probable that the center of the 1000 CDT cloudiness, as observed by satellite, may be just beyond the observing range of the surface cameras.

The center of the 1000 CDT cloud occurrence maximum observed in the 1975 satellite photographs is in the WNW direction from SLU and about 16 km beyond the site. This cloud occurrence maximum is located directly over the highest point in the topography and is oriented parallel to the topographic ridge on the W edge of the city. It also extends eastward to ALN. The cumulus initiations observed to the W and NW of the SLU site are partially related to topographic effects and to urban effects. Some of the cumulus developments at ALN may also be topographically induced by the slopes on that side of the river.

Comparison of Initiation Times. A comparison of the average times at which the first Cu were observed from ALN and SLU reveals that on the average cumulus formed earlier by about 22 minutes at ALN (1011 vs 1133 CDT). This difference is too small to be significant. It would occur by chance 35% of the time. If data for only the four rural sectors at ALN are considered, the average cumulus initiation is 8 minutes later than at the urban SLU site, in agreement with the difference suggested by Auer and Eaton (1976). The 10 days of lidar observations of Auer and Eaton show that the urban boundary layer develops 30 to 45 minutes sooner than the rural boundary layer. However, it must be remembered that urban cumulus bases tend to be 0.3 to 0.6 km higher than rural cumulus bases and this tends to reduce the time lag. Thus, the observed difference is not statistically significant. The time required for the first 10 cumuli to

form was shorter at the SLU site by about 5 minutes than at the Alton site (23 minutes vs 28 minutes). Thus, the rate of cumulus formation at SLU was actually faster than that at Alton. However, the difference between the mean durations is too small to be statistically significant.

Comparison of Cumulus Raincell Initiation Anomalies. The pattern of precipitation initiations during the summers of 1971-1975 show an anomalous frequency to the SW of ALN, the region observed to have frequent cumulus initiations in July-August 1975. However, the region to the W and NW of SLU, where the St. Louis cumulus initiation anomaly was observed, is not the most frequent precipitation initiation area around that site. Areas to the NE and S of this camera had more rain initiations. Thus, one of the Cu initiation anomalies is located within a precipitation initiation anomaly while the other is slightly upwind of one. This suggests the clouds near Alton may develop precipitation faster than those to the W of SLU.

Cumulus Growth Patterns Observed at Alton Site

The July-August 1975 photographs from the Alton site were examined to discern clouds that were obviously being affected by the refinery industrial regions. All periods with clouds were studied, not just those with initial convection. Nine days on which unusual cumulus growth apparently related to local man-made effects were found in the 46-day sample. These days and the clouds observed are described in table D-9.

In general, two types of industrial cloud episodes were found. The most obvious industrial-related clouds were those which were observed to remain semistationary over, or to repeatedly arise from, particular locations near the horizon in the industrial SW and W sectors. This type of episode was frequently observed (8 days) and is referred to as the 'anchored' type. These events frequently consisted of one or more small chains of Cu, but at some times the resulting Cu were larger. These episodes were sometimes isolated events with few or no other Cu present, similar to the spectacular example described by Auer (1976). On the other occasions, scattered Cu were present in other sectors. The other type was labeled the 'growth' type.

On one day (17 July) early cumulus observed to the W and SSE grew into two very large congestus clouds while remaining in the same sectors. This type of cloud development (the 'growth' type) was apparently anchored to surface sources, but is distinguished from the other group because of the remarkable vertical development which took place. It is not possible to be certain that the cloud's growth was strongly affected by urban influences, but the case was a quite impressive example of local development.

The five cases which appeared to be the most clear examples of urban-industrial influences are described in more detail. These five days are 17 July and 2, 7, 19, and 26 August 1975. Cloud photographs taken by the GOES satellites, surface weather maps, and other supplemental data were examined for each of these days. It should be emphasized that the 'anchored' clouds are not necessarily closely related to initial Cu developments. In fact, only half of the 'anchored' cases in table D-9 occurred during the period when the first 10 Cu were forming.

However, 7 August was such a day. The first 10 Cu to form on 7 August all formed in the SW sector near the refinery area, between 0950 and 1055 CDT. The clouds were quite small. Anchoring after the initial 10 Cu formed was not particularly strong on this day. In the satellite photo for 1000 CDT St. Louis and most of Illinois appeared clear. Since this was the time the first 10 industrial Cu were forming over Wood River, it is apparent that they were too small to be detected by the satellite. They were also isolated from other significant convection. Weak cumulus convection was apparent in eastern Illinois by 1300 CDT. Even weaker convection extended in diffuse bands to the E of St. Louis and then into SE Missouri. The same appeared to be the case

Table D-9. Days when Unusual Cumulus Growth Patterns Were Observed at Alton Airport

Date	*Time (CDT)*	*Comments*
16 July	1600-1900	Repeated small Cu formed to SSW followed by movement to W; no other Cu present; warm air mass type; RH = 42%
17 July*	1220-1300	Two of the initial Cu grew rapidly into congestus (to SSE and W), and were anchored; funnel cloud reported SW at 1530 CDT by pilot; no surface fronts nearby, but a low at 500 mb (which persisted from previous day) was in the area; a squall line developed by 1300 CDT; RH = 57%
27 July	1400-1800	Small cloud persisted near SSE; same size and position was maintained; STL had scattered or 'a few' Cu for much of this period; other clouds, including CiCu were present; a marginal case; warm air mass type; RH = 52%
2 August*	1825-1945	Small cloud group remained over same spot to S after rain passed; other clouds appeared at varied location at this time; bright cumuli; late anchoring; front nearby; squall zone type; RH = 74%
7 August*	0950-1055	Early anchoring; initial Cu formed to SSW only; after 1100 a general outbreak of Cu followed but some Cu were still anchored after outbreak; wind SE; all 10 first Cu were in WRR sector; persistent ridging at surface and aloft; cold air mass type; RH = 68%
	Also ~ 1600	Marginal; cold air mass type; RH = 47%
8 August	1030-1100	Initial Cu formed in S and W about 30 minutes before forming elsewhere; marginal case; Cu are more scattered than on the 7 August; cold air mass type; RH = 60%
19 August*	1220-1825	S and SW sectors appeared to be persistent cloud sources and locations; though other Cu were frequently present, these two areas were almost always active in about the same spot (in mid-afternoon there was a shift farther into the S sector and then back); some of the anchored Cu were large; stationary front was nearby in Central Illinois, but warm air mass type prevailed near St. Louis; RH = 64%
26 August*	1550-1930 (WRR) 1630-1930 (Alton)	Best example; anchored Cu in both the WRR and Alton sectors; Alton Cu could be from Portage Des Sioux power plant; few (1-3) small Cu were grouped and present in same spot; a few other Cu were present; scattered Cu were present previously; some network rain and Ci were present at this time; both cases lasted until sunset (late anchoring); stationary front nearby; RH = 63%
27 August	1400-1930	Area of persistent clouds to S; other clouds were present; frequently saw small group of Cu which appeared in about the same place to SSW; all clouds appeared to move fast; anchored Cu lasted until sunset; stationary front type; RH = 65%

* These five days were the most obvious cases

at 1600 CDT but convection did not appear near St. Louis. The St. Louis area was near an area of ridging in the weather pattern for this day, and the GOES photographs confirmed its very stable nature.

Anchoring appeared more obvious on three other 'anchored' days (2, 19, and 26 August) partially as a result of longer anchoring durations. Although none of these three cases occurred during the first 10 Cu period, one case (19 August) occurred immediately afterwards.

The 19 August case was accompanied by other Cu and the anchored Cu were frequently large. The 1000 CDT satellite photo showed very few clouds near St. Louis, but there was a very weak and small cloud band extending southward from NE Missouri to near the network. A large cloud mass existed in eastern Iowa, Wisconsin, and Minnesota behind the surface location of a stationery front. By 1300 CDT, the cloud line near St. Louis extended westward and split into two lines. At about this time the 'industrial Cu' began to appear (1220-1825 CDT). By 1600 CDT the eastern end of the southern cloud line had apparently become a dominate weather feature in Illinois with large cumulonimbus extending from 60 km NE of St. Louis eastward into Indiana.

The line showed no major activity to the west. Examination of the Water Survey radar data indicated that echoes existed to the NW before they approached the network. This was a day when great instability was present near St. Louis, although no rain was observed in the rain-gage network.

The most obvious cases of anchoring occurred on days when cumulus plumes or chains of clouds appeared to continuously persist for several hours above the same location. Two of these days are described. Both of these cases occurred after initial cumuli had dissipated.

On 26 August cumulus plumes existed over ALN during two intervals (separated by about 30 minutes) during the 3 hours before sunset. During this same period, as well as in the previous 90 minutes, very clear cloud anchoring was also occurring in the refinery sector. This twin display was the most dramatic industrial cloud episode observed in July-August 1975. There was a cirrus overcast. Sky photographs taken elsewhere of the Portage Des Sioux power plant reveal it was generating Cu plumes on 26 and 27 August. A close-up photograph of the refinery cloud on 26 August showed one moderate sized rather flat cumulus with a white top and yellow bottom above a dark layer of surface air. A few small pannus clouds were also present. The surface weather maps for the period showed a stationary front through south-central Illinois and within 80 to 130 km north of St. Louis. The front remained in the area through the next day (27 August) when a similar plume was observed at Wood River. The front was diffuse and may have ocsillated back and forth over St. Louis during the 26th, though the official NWS analysis maintained it to the N over Quincy in spite of wind direction changes at STL. Dew point temperatures at St. Louis remained about 18° C throughout the 2-day period. The GOES photographs on the 26th showed much cloudiness in the area, most of it Ci bands oriented SW to NE. The Ci makes it hard to determine the orientation of any lower Cu bands. It was not possible to tell if cloud system motion was playing a role in the interesting cloud behavior. This appears very unlikely since two plumes of different orientation were observed in two different sectors. It is clear, however, that the local stability was probably not great due to the presence of the front.

On 2 August a single Cu plume was observed in the refinery sector during very bright and clear conditions around 1830 CDT. The St. Louis area was in a broad area with lines of small cumuli located in the southerly flow ahead of a rapidly moving cold front. The bands became organized into two distinct cloud lines by 1600 CDT. The frontal band was in eastern Iowa, and the other band (which was probably associated with the 'convective layer' which frequently generates pre-frontal squall lines) was over St. Louis. By 1915 CDT, St. Louis was between the two

main cloud bands and only weak convection was active there. The satellite photograph was rather dark at that time, but the cloud pattern seems to be clear and agrees with the dome camera observation of a general clearing coincident with the first observation of the industrial-derived clouds at 1825 CDT. Obviously, some instability was present at St. Louis but it was decreasing.

The 'growth' case on 17 July was impressive. Network rainfall on this day was locally heavy with three maxima of about 40 mm, one located near the Spirit of St. Louis airport, one in western St. Louis, and one 8 km SW of Edwardsville. The satellite photographs supported a case for local effects on this day. A Cb cloud mass was isolated near St. Louis. The bluffs near Alton and those of the Illinois River also seemed to be playing an important role in cloud development on this day. No fronts were near Illinois, although there was a 500 mb low in the vicinity, so that if low-level convection became intense enough, convection might be supported aloft.

Weather Conditions on Days with Anchored Cumuli. Five of the eight cases of anchored Cu were associated with air mass synoptic weather types, two were associated with stationary fronts, and one with a squall zone. Network rain fell before and during the 2 August episode, but on no other day with anchored Cu. Thus, the anchored outbreaks appear to have occurred when the atmosphere was rather stable. However, during three of the air mass cases surface fronts or upper troughs were also nearby (over Illinois, but not in the immediate vicintiy of St. Louis). Thus, only two of the cases occurred during very stable conditions associated with strong ridging. Therefore, it is evident that the anchoring effect was observed during a wide variety of weather conditions.

Aoki and Yabuki (1975) have stated that during summer in the coastal region near Sakai, Osaka, Japan, small industrial clouds were observed above chimneys in the morning and evening; and in winter they formed during the afternoon as well. Conditions favorable to industrial Cu formation were stated to be those in which cloud parcels rising from chimney effluents would be hotter and more unstable relative to surrounding air. However, it appears that there must be some limit on the instability present in order that summer industrial clouds may be recognizable from background cloud. The present data tend to support the notion that some instability is important for industrial Cu formation since surface fronts or upper troughs were nearby in 6 of the 8 anchored cases. Local effects may either go unnoticed on the photographs or be relatively insignificant when very unstable and cloudier conditions prevail.

Conclusions

1. There are cloud initiation anomalies in the St. Louis urban-industrial area. When the first 10 cumuli to initiate are considered, the areas within a few kilometers and to the W and NW of St. Louis University, and those SW and W of the Alton Airport have anomalously high initiation frequencies. The probability of the observed areal initiation distributions occurring by chance was <0.03. These anomalies do not appear to be the result of the motion of cloud systems or fronts. The unusual growth patterns of cumulus observed to repeatedly form in about the same location near the refinery complex SW of Alton also indicate the veracity of the cloud anomaly. Other convincing evidence of these anomalies comes from the analyses of satellite cloud photographs. These showed morning cloud occurrence maxima over west-central St. Louis and Alton, areas where the anomalies were observed by the dome camera. By mid afternoon another satellite-observed cloud anomaly was between the two cameras.

When the first 10 cumuli to initiate are considered, areas to the east of the rural PMQ site had slightly higher initiation frequencies than expected. Cu initiations were affected by power plant effluents and topographic features (river bluffs).

2. Particularly noteworthy is the frequency of first cumulus which formed near the refineries. The first cumulus formed there with a frequency three times the expected frequency. Chi-square testing of the first Cu distribution at Alton indicates that the probability that this initiation anomaly occurred by chance is about 0.0001. The periods when first Cu were anomalously forming in the refinery sector were more stable and cooler on a regional basis than when first Cu formed in the other sectors. However, local surface heating may have created anomalous instability in the Wood River sector. Unusual cumuliform behavior was also frequently noticed over the refinery hours after the initial cumulus formed. There appear to be quite strong local influences acting to generate and sustain Cu in this region.

3. The areal distribution of the first 5 and first 10 Cu to form around the St. Louis site was also very unlikely to have occurred by chance (probabilities « 0.0001).

4. When the normalized frequencies (ratios) of the first 5 and 10 Cu to appear in the two most frequent sectors at SLU (W and NW) are compared with their counterparts in the two key sectors at ALN (SW and W), it was found that the SLU frequencies were 22% more predominant.

When only the ratio frequencies of first Cu to form are considered, the SW sector at Alton was much more impressive (70% greater) than the dominant W sector at SLU. Apparently, different localized cloud initiation mechanisms are active at the two sites.

5. The timing of first Cu initiations observed over rural areas may be delayed relative to urban sites. If only the four non-industrial sectors at ALN are considered, the first Cu initiations average 8 minutes later than at SLU and agree partially with the lag suggested by the urban and rural lidar observations of Auer and Eaton (1976). Apparently, the 30- to 40-minute earlier development of the urban boundary layer is partially compensated by the 0.3 to 0.6 km higher urban cloud base heights.

6. The anomalous cumulus initiation areas noted at Alton and St. Louis are located within or near precipitation initiation anomalies. The fact that the cumulus and precipitation initiation areas are in close proximity suggests that the higher precipitation initiation frequency is related to the cloud initiation mechanisms. This mechanism is believed to have a dynamical rather than a microphysical (enhanced coalescence) nature. It is also implied that the development of precipitation from cumulus may frequently take place relatively rapidly near Alton. This is consistent with the observation that raincells near Alton are more intense than those near St. Louis, since the anomalous cloud and precipitation initiation and intensification all appear to be related to enhanced updraft strength.

7. The conditions during which the anomalous Cu initiations were observed tended to be relatively stable. Air mass synoptic weather conditions prevailed during about 75% of all the observed localized initiation periods. On days with strong synoptic phenomena present, it was frequently impossible to distinguish new clouds from old clouds and most such days had to be discarded from the study. Thus, the clouds examined in this study occurred on days with a very definite bias toward weak convection in the first place. Obviously, this does not change the fact that the first Cu tended to be observed during rather stable conditions. It may be that the refinery influences are also active on the more cloudy days which have hot been as well observed in this study. The unusual anchored clouds near the refineries largely occurred when destabilizing influences (fronts) were nearby. It seems reasonable to conclude that some atmospheric instability is required for industrial or urban-induced cumulus to form. However, if conditions are too unstable, other clouds may interfere with the detection of possible industrial effects.

8. The cause of the cloud initiation anomalies can only be speculated upon. The possibility that two or more mechanisms were acting should not be discounted. Point number 4 above supports this possibility as does the finding that anomalous first Cu at SLU are accompanied by cool

moist conditions but at ALN they are accompanied with a 50% smaller relative humidity difference. Wind analyses indicate some upslope flow at both sites during periods with anomalous Cu initiations, and satellite observations have confirmed the influence of topography on local cloud occurrence. However, at the SLU site there was frequent evidence of low-level convergence related to the urban area at these times and insolation on slopes may also have played an important role in the generation of the anomalies.

The sensible and latent heat released by the refineries is believed to play a major role in triggering the remarkably frequent first Cu and also the later unusual anchored clouds SW of the Alton site. The available data are not adequate to determine the relative importance of the potentially causative mechanisms at either site. However, the morning cloud occurrence maxima observed in the hills to the W of St. Louis in satellite photos indicate that the hills or slopes play an important role in early cumulus formation and suggest that urban-industrial influences and topographic energetics are probably more important than microphysical (coalescence) influences in the generation of the urban cloud anomaly.

9. The Cu initiation anomaly W and NW of SLU occurred when conditions were relatively cold and moist. The colder air overlying SLU would be expected to yield a more unstable atmosphere over a localized heat source (urban or solar-topographic). The higher relative humidities on anomalous cloud days (implying a lower cumulus base height) would also be expected to hasten the formation of cumulus. However, these conditions might be expected to result in more rapid cloud growth anywhere in the region surrounding the cameras. Whatever caused the cumulus initiation anomaly in the N and NW sectors (center of St. Louis) overrules this expectation. It may be that the local triggering in the anomalous sectors is unnoticeable in the initial cumulus frequencies except when conditions are most favorable (cool). On other occasions, buoyant impulses rising and attempting to form initial cumuli in the anomalous sectors are not more successful than those in the other sectors. Thus, regional weather conditions exert some control over the initial cumuli anomaly observed to the W and NW of SLU.

It is interesting to note that weather conditions play a lesser role in the first cumulus anomaly observed over the oil refineries. Only the temperature was significantly different on the days with first Cu. No other weather variables showed significant differences between days with first Cu in the refinery sector and the other sectors.

The important surface weather difference between the SLU and ALN first Cu anomalies is in relative humidity. The refineries in the anomaly sector from ALN are known to be a significant local source of moisture as well as heat. No localized moisture source is known of in the region just W and NW of SLU. The refineries are a very localized moisture and heat source compared with regional and urban scale variations (and therefore are not detected at STL or BLV). Thus, the case for local influences on cumulus initiations may be strengthened. The moisture and heat sources in the refinery area diminish the need for temperature and humidity conditions favorable to cumulus initiation. Therefore, it is not surprising that weather conditions play a role in Cu initiation W of SLU but do not appear as important at the much different Wood River site.

SATELLITE-OBSERVED URBAN CLOUD DISTRIBUTIONS

Ronald C. Grosh

Introduction

METROMEX observations have confirmed the presence of precipitation and severe weather anomalies. Interest has focused on the questions of where the clouds that contributed to the precipitation alterations formed, and when and how they grew and combined to become rainstorms. This section focuses on the cloud issues. The effect of clouds on the urban energy budget is also commented upon since clouds greatly influence incoming and outgoing short and long wave radiation and may thereby affect their own growth.

The availability of the two GOES satellites in 1975 made it possible to analyze cloud distributions near the St. Louis urban-industrial area. Previous estimates of urban effects on cloudiness showed urban changes of ± 5 to ± 10%, but these were based on very sparse surface observations. This statistical application of satellite observations to the question of urban influences on cloudiness is not affected by the limited spatial resolution of surface observations. The present study differs from many previous satellite cloud studies in that a small area is under study and precise gridding is required. A photographic data format was chosen and a subjective technique was employed to determine the cloud threshold. Photographs were aligned by means of an optical device (Zoom Transfer Scope) which could magnify the satellite image and stretch it in any direction to facilitate alignment. A description of the technical problems encountered in the analyses of satellite data is not included.

Cloud photographs from the two GOES satellites were analyzed for cloud occurrence frequency (COF) near St. Louis during the summer of 1975 for the hours of 1000, 1300, 1600, and 1900 CDT. Photographs to be included in the analysis had to be taken within ± 30 minutes of the hour. The total number of photographs used at each hour (out of a possible 92) are 82, 74, 67, and 38, respectively. Photographs of the type used were not always produced during the required periods. This problem was most frequent during dry conditions; 78% of all 1975 rain periods were represented in the photo sample compared to 68% of all dry periods. Noticeably fewer photographs at 1900 CDT resulted because landmarks used to grid these photographs were frequently obscured by darkness and cloud shadows. Thus, the 1900 CDT analyses are possibly less valid than those for other hours. The photographs are derived from visible channel data with about 1.6 km resolution. Alignment of the cloud photographs with the base map is estimated to be accurate to within 10 km.

A grid of 81 squares, each covering 93 km^2 , was centered on the St. Louis area for the purpose of determining cloud frequencies. The isolines on the resulting frequency maps are labeled with percentages based on the number of times any cloudiness was observed in a grid square, divided by the number of available photographs at that hour. The data shown on these maps include observations of all cloud types. Intervals between isolines on all maps shown correspond to ± 1 up to ± 3 standard deviations (SD) from the map mean value.

Cloud frequency maps were also analyzed for stratifications of the data based on the surface wind speed and direction, day of the week, rainfall, synoptic type, and the occurrence of stagnant conditions (smoke, haze, or fog).

Cloud Occurrence Frequencies

Cloud frequencies for each period are shown in table D-10. The area mean frequencies increase markedly between 1000 and 1300 and decrease greatly between 1600 and 1900 CDT. This reveals the dominant influence of cumuliform clouds and their typical cycle on the results. The ranges and deviations of the afternoon values are the largest indicating that local effects are stronger after solar heating has proceeded for sometime, and that the magnitude of local effects can be expected to show diurnal variations. However, the deviation at 1600 is also noticeably smaller than at 1300 and 1900, indicating more widespread cloudiness at 1600 CDT. This reduction is most noticeable on rain days and is associated with cirrus anvils and other heavy cloudiness on these convectively active days when coverage was frequently 100%.

Clouds at 1000 CDT. There are two main features to the 1000 CDT pattern (figure D-la). A small area of very high frequencies (>2 SD above the mean) is located in NW St. Louis where the peak is 50%. This is in the area where surface cloud camera studies during 1971-1975 indicated anomalous cumuli initiations. High frequencies are also observed throughout the hilly region west and southwest of St. Louis and also in the Alton area. The other important feature is a large area of low cloudiness south of and over St. Louis where clouds were present less than 40% of the time. The range of values among the 82 areal values at 1000 CDT was small (15%), but the pattern is reasonable and in agreement with an analysis of five years of surface camera results. There is no obvious indication of an urban enhancement or decrease of clouds at 1000 CDT.

On the basis of the 1000 CDT analyses, it appears that most of the urban area received more solar radiation than did the areas SW, W, and NW of St. Louis. However, temperature (T) and dew point (T_d) maps for all 82 days with satellite photographs at 1000 CDT reveal that areas with high cloud frequency tended to have high T and T_d, whereas those with low COFs generally had lower T and T_d. The strong (>2 SD) frequency maximum in the warm moist NW area is quite distinct when winds are from the southeast (figure D-2). Thus, the high T and T_d in this area apparently are the result of convective motions aided by slope heating, local convergence, and perhaps by the upwind urban area as well. The reason that the areas in the southern part of the region and over St. Louis, which have low frequencies and apparently greater susceptibility to solar heating, have not become the warmest areas on the map is not known. It may be that these areas had heavier nocturnal clouds, pollutant layers, or fog to burn off. Also, these areas may heat more slowly due to surface characteristics. In the city this is strongly suspected. An area with concrete streets and buildings will have high heat conductivity and capacity. Urban surface temperatures might also be depressed because of reflection and/or absorption throughout the subcloud layer by enhanced aerosols. The cloudy hill area has greater local relief, and for morning sun angles probably is conducive to enhanced local heating and the development of thermally driven circulations.

Table D-10. Cloud Percentage Occurrence Characteristics at St. Louis, Summer 1975

Hour (CDT)	N (days)	Mean	Standard deviation	Area values		
				Minimum	Maximum	Range
1000	82	42.6	2.8	35	50	15
1300	74	75.9	5.2	65	86	21
1600	67	77.5	3.5	67	88	21
1900	38	49.2	5.2	39	61	22

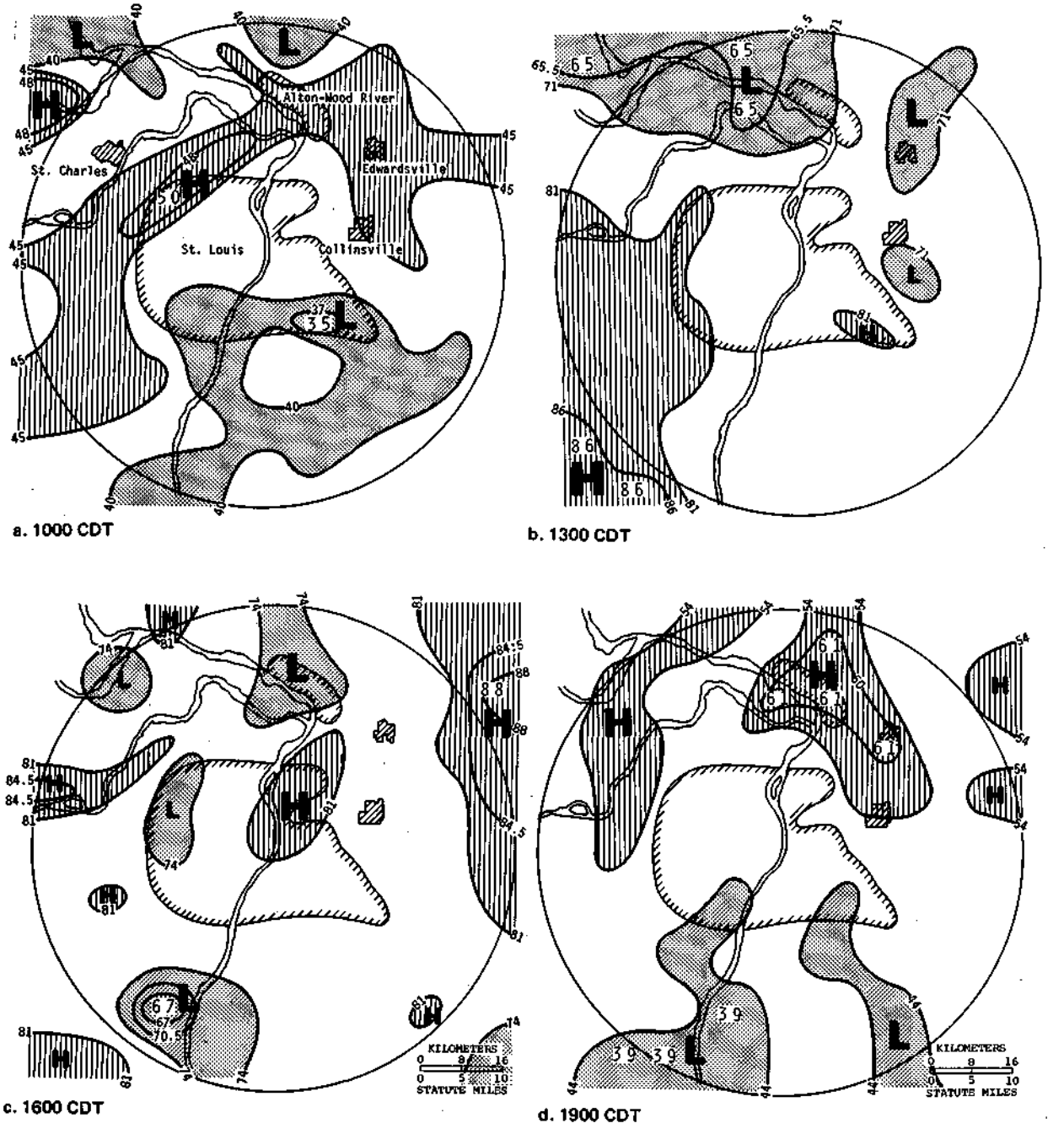

Figure D-1. Normalized cloud frequencies at 1000,1300,1600, and 1900 CDT

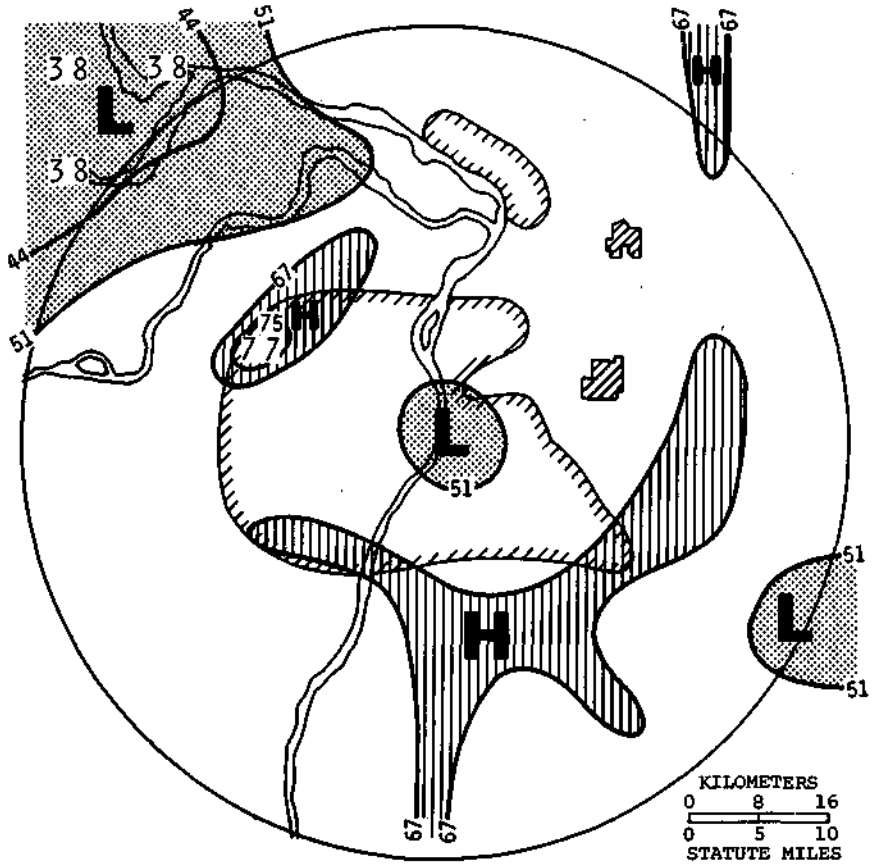

Figure D-2. Normalized cloud frequencies at 1000 CDT with SE winds

Clouds at 1300 CDT. The cloud pattern at noon (figure D-lb) shows that the hills to the west of St. Louis are still relatively cloudy. The area in the SE part of the metropolitan area where a minimum had been at 1000 CDT has changed to an isolated high. The main area of low frequency is in the north part of the area and near the river bottomlands. Relative temperature and dew point patterns at noon change only slightly from those at 1000 CDT. Basically, cloud frequencies at noon correspond to high temperatures and moderate to high dew point temperatures.

Clouds at 1600 CDT. In mid afternoon (figure D-lc) there is an area with very high values (> 3 SD) on the northeast and east edge of the network, an area where frequencies had been below average at noon. Another cloudy area is found to the west, a possible result of valley effects. A third high frequency area is the central St. Louis industrial area. It may be a result of urban effects and coincides with the area where anomalously frequent precipitation initiation was observed by radars.

At 1600 CDT an urban heat island appears to be present (on sampled days) as shown in figure D-3a. This pattern is associated with a moist ring which surrounds St. Louis and is most distinct to the north and south where T_d >20° C (figure D-3b). The urban cloud frequency maximum coincides with the urban heat island and high dew point values in northeast St. Louis. The juxtaposition of moisture and temperature perturbations in this region implies low level enhancement of convection. The high cloud frequencies in the east may relate to the nearby high temperatures and dew points.

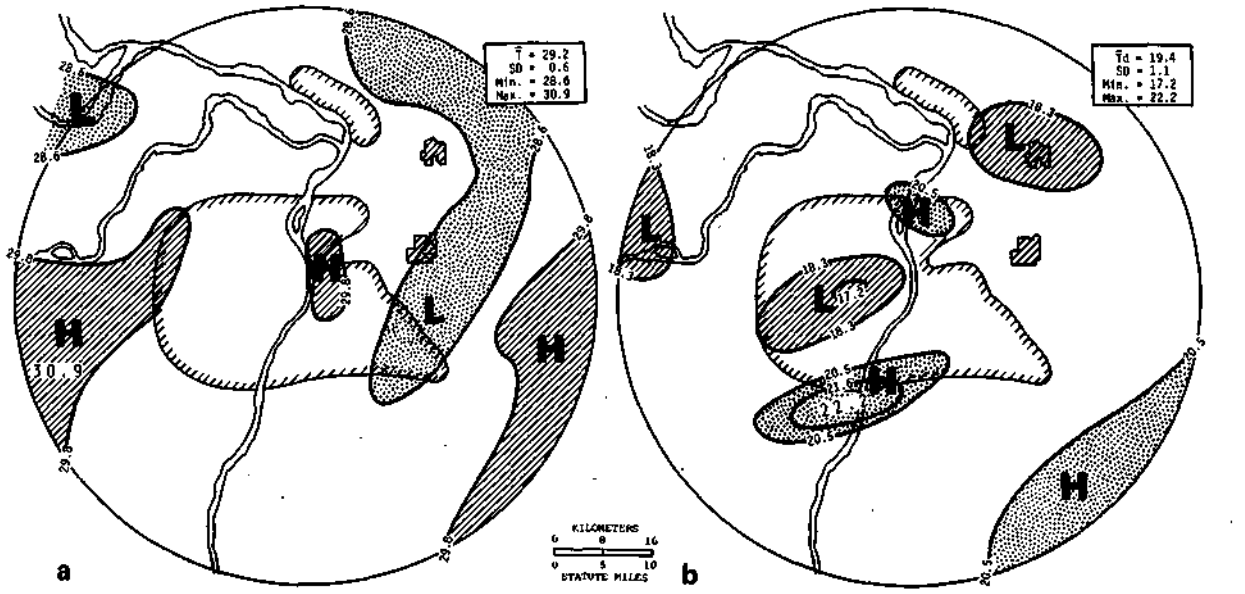

Figure D-3. Surface temperatures and dew points (° C) at 1600 CDT

The urban cloud maximum over St. Louis at 1600 CDT was most pronounced when winds were from the southwest and also during stagnant periods (figure D-4). Other stratifications of the cloud data based on rainfall, synoptic type, winds, and day of the week did not reveal conditions which selectively enhanced this maximum. There were 36 days in the sample shown in figure D-4. This urban maximum was carefully examined to ensure that clouds were present and that smoke, haze, or fog were not mistaken for cloud. Surface cloud observations from three weather observing sites and two cloud cameras near the urban maximum confirmed that clouds were present during these 36 days. The maximum appears to be the result of clouds which developed during weak wind conditions when urban-industrial pollutants could build up to levels noticeable from the ground. Thus, low wind or stagnant conditions favor the development of urban clouds in late afternoon.

Clouds at 1900 CDT. At 1900 CDT the main high frequency area was centered over Alton and Edwardsville with peak values >2 SD above the network mean (figure D-ld). Other lesser areas of high frequencies were also located close to regions where distinct maxima existed at 1600 CDT, suggesting a shift to the northeast. The southern part of the region was characterized by generally low frequencies. In many respects the 1900 CDT pattern suggests a return to that at 1000 CDT. The relationships between the T, T_d, and cloud fields are more complex than when the sun was higher and are not discussed.

The relationship between cloud frequencies and rainfall was complex at all hours. At 1900 CDT most of the clouds associated with the maximum at Alton were very inefficient as little or no rain was recorded near Alton between 1800 and 2000 CDT on the days with data. This complexity results because most clouds do not produce rain and only a small sample of rain events is available for comparison. However, if more rain events had been included, the frequencies (figure D-ld) probably would not have changed greatly.

A similar analysis of data based only on the 24 days when cloud photographs were available for all four time periods did not produce any major differences in the results. However,

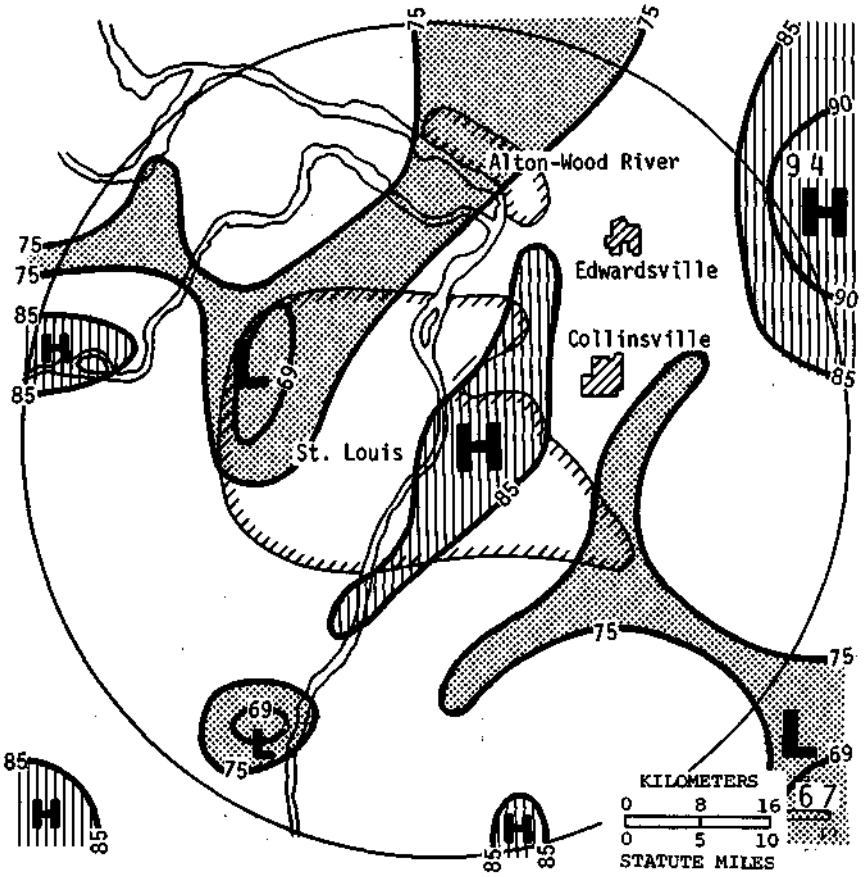

Figure D-4. Normalized cloud frequencies at 1600 CDT with stagnant conditions

cloud frequencies in the SE were slightly higher at 1000 and 1300 CDT and lower at 1600 than shown in figure D-l. Thus, the SE cloud frequencies were more susceptible to changes than was originally thought.

Summary

These 1975 cloud data indicate that there are important temporal variations in the meso-scale distributions of cloud frequencies. Of particular interest is the sequence suggesting relative clear conditions over the urban area at 1000 and 1300 followed by cloud development in St. Louis at 1600 and then shifting on to Alton and Edwardsville at 1900 CDT. These are the regions where the urban precipitation maximum is observed. St. Louis and the area to its southeast have low frequencies at 1000 CDT. At 1300 a small maximum appears on the southeast edge of St. Louis. A larger urban maximum exists a few miles farther to the north at 1600, and by a very impressive apparent urban generated maximum even farther north at 1900 CDT.

Other local temporal variations indicate that clouds regulate their own growth by controlling insolation. For example, the clearest area at 1000 CDT, to the southeast St. Louis, had a maximum just three hours later. The area of intermediate to high values at 1000 CDT in the rural northeast of the area takes 6 hours to produce another maximum. The Alton area, which was frequently

cloudy at 1000, does not produce another relative maximum until 9 hours later. However, the whole network did not follow a simple cycle of low values changing to high values and then down again. For example, the hills in the west remained relatively cloudy throughout the day, although the relative maxima were most pronounced early in the day.

Other results show that frequency maxima appeared downwind from St. Louis for all wind directions at 1600 and 1900 CDT, but only for some directions at earlier hours. Weekends had much higher frequencies than weekdays. However, the 1900 CDT urban maximum at Alton occurred only on weekdays. Very low frequencies were observed near Alton on weekends. At 1600 CDT higher winds ($\geq$ 5m s^{-1}) resulted in urban frequencies being highest at St. Louis and low at Edwardsville. For winds <5 m s^{-1}, a strong high occurred over Edwardsville.

Thus, interactions between winds, topography, sun angle, surface characteristics, stability, urban emissions, and feedback from clouds themselves control the local distribution of summer clouds and dictate the degree of urban influence on cloud activity.

CLOUD CHARACTERISTICS

Richard G. Semonin

Cloud Base Characteristics

The routine measurements of cloud base heights were obtained during the course of all aircraft flights for the Survey effort, when clouds were present. Results for 1971-1972 data were reported by Semonin and Changnon (1974). All the observations indicated cloud bases over the St. Louis metropolitan area were, on the average, 600 m greater than those of similar clouds over rural areas. This difference is supported by the findings of Auer and Dirks (1973) in that the magnitude of temperature and moisture field anomalies can clearly account for the observed rural-urban variation of convective cloud bases.

Cloud Base Updrafts

The primary objective of the METROMEX cloud base flights in 1972 and 1973 was to release unique tracer materials (lithium chloride and indium) into updrafts of convective clouds (Gatz, 1974) to study scavenging processes. This objective required that measurements of the updraft speed be obtained prior to release of the material. The measurements which were logged by the on-board meteorologists were obtained from an instantaneous vertical speed indicator (IVSI). Measurements from the IVSI system require that the power settings and aircraft attitude be maintained for level flight. Information was not entered into the notes or logs unless proper aircraft attitude was being maintained for a particular measurement; therefore, the updraft data collected should be of good quality.

The cloud base data analyzed herein were derived from 15 cloud flights on 13 days during 1972 and 1973. Sixty-nine cloud base updraft velocity measurements were obtained from cumulonimbus clouds.

The analysis of the data focused upon the location of the updraft relative to the direction of movement of the FPS-18 radar echoes and, of course, the speed of the updraft. The results of the analysis are presented in table D-ll. Sevently percent of the 51 known-position updrafts occurred on the front of the echoes, and most of those were located on the right front. Their average speed was 2.3 m s^{-1} and their median speed was 1.7 m s^{-1}. The speeds were higher (average 3.4 and median 3.6 m s^{-1}) for the 'unknown' category. The unknown category refers to updrafts that were measured but could not be located relative to the radar echo because the radar echoes were obscured by ground clutter. When all of the updrafts were considered, the average and median speeds were 2.5 m s^{-1}.

Table D-l1 also includes a distribution of various updraft speeds relative to radar echo position. Fifty-eight percent (22 of the 38) 'front-located' updrafts were less than 2.5 m s^{-1}, and only about 20% were greater than 5.1 m s^{-1}. The updrafts with 'unknown' positions were stronger, on the average, than the known ones. This is reflected in their distribution of updraft speeds. More than 50% of the unknown updrafts were $\geq$ 3.8m s^{-1}. This result may occur because the storms involved were more complex and stronger; hence, the echo position could not be determined satisfactorily. When all the updrafts are considered, approximately 50% of the 69 updrafts were $\leq$2.5 m s^{-1}, and about 75% were $\leq$3.8 m s^{-1}.

The flight crew, who were experienced in updraft and cloud flying (Henderson and Duckering, 1973), noted that:

1) Most inflow areas are of small diameter and short duration
2) Weak thunderstorms or dissipating cloud systems provide no identifiable base inflow areas
3) The base inflow areas are identifiable in large cumulus clouds with durations ≥ 30 minutes

The cloud base updrafts were often difficult to find from the aircraft because of multi-cloud visibility problems, and the conditions often required radar direction to help locate potential updraft areas.

Liquid Water Content of Clouds

Many small cumulus and cumulus congestus clouds were penetrated in the course of the Survey's flight program and the liquid water content (LWC) was measured. The clouds were stratified to separate out those subject to direct urban influence. The LWC values for the remaining natural or unaffected clouds were measured and averaged for each penetration. These values were used to calculate means for each altitude. Data from more than 175 clouds on 26 days in 1971-1975 were included in the final sample.

The cloud dimensions in the vertical were estimated by the flight crews to range between 1.7 and 3.7 km in depth with cloud bases between 1 and 2 km. A composite cloud was developed by normalizing the total cloud depth to 100 units and then noting the normalized altitude of aircraft penetration and measurement. The average LWC was calculated for 10 units thickness of the normalized altitude. Table D-12 shows the distribution of LWC with height in the composite unaffected natural cloud.

The obvious feature shown in the table is the increase of LWC upward through the convective clouds. Through the mid-section of the clouds (40 to 70%), the values are consistently near 1 g m^{-3} and in the upper 30% of the cloud depth the values are near 1.5 g m^{-3}. There were insufficient penetrations by the aircraft at lower levels to provide enough measurements to get a representative average.

The values shown in table D-12 are qualitatively in agreement with values reported by Dytch (1977) at the lower levels. Although the data he presented were not stratified in the same manner as those obtained here, the normalized average LWC for cumulus congestus cases show between 0.41 and 0.74 g m^{-3} for penetrations between 57 and 36% of the cloud depth. The

Table D-11. Cloud Base Updraft Data of Illinois Thunderstorms Stratified of Their Position Relative to the Radar Echo Movement

	Left front	*Right front*	*Left rear*	*Right rear*	*Unknown*	*All*
Number of updrafts	14	24	6	7	18	69
Average speed, m s^{-1}	2.5	2.3	2.3	2.0	3.4	2.5
Median speed, m s^{-1}	2.5	1.7	2.5	1.3	3.6	2.5
Maximum speed, m s^{-1}	6.1	5.5	3.1	3.1	7.1	7.1
Number of updrafts ≤1.5 m s^{-1}	6	12	0	4	3	25
Number of updrafts 1.5–2.5 m s^{-1}	0	4	2	0	3	9
Number of updrafts 2.5–3.8 m s^{-1}	5	3	4	3	2	17
Number of updrafts 3.8–5.1 m s^{-1}	0	1	0	0	5	6
Number of updrafts ≥5.1 m s^{-1}	3	4	0	0	5	12

Table D-12. Average Liquid Water Content as a Function of Height in Natural Clouds Observed in METROMEX

Penetration altitude (% of cloud depth)	*Liquid water content ($g\ m^{-3}$)*
90-100	1.61
80-89	1.48
70-79	1.50
60-69	1.01
50-59	1.07
40-49	1.02
30-39	
20-29	0.59
10-19	
0-9	

Table D-13. The Median Condensation Nuclei and Liquid Water Content in Unaffected and Urban-Affected Clouds

	Median CN (cm^{-3})	*Median LWC ($g\ m^{-3}$)*
Unaffected clouds	1500	0.98
Affected clouds	3750	1.10

upper level values correspond to the LWC measurements reported by Ackerman (1974a) and Carrera (1975) for clouds of similar dimensions to those reported here. However, those measured by Ackerman were classified as 'vigorous' convective clouds. Carrera (1975) also reported that the clouds observed downwind consistently possessed greater LWC than upwind clouds.

These results, while not elucidating a causal factor of the precipitation anomaly, are useful for validating cloud models developed to assess urban effects on microphysical processes such as that described by Ochs and Semonin (1976). The LWC values observed during METROMEX, in conjunction with the detailed measurements of cloud droplet spectra (Dytch, 1975; Carrera, 1975) and the water partitioning (Ackerman, 1974a), are all cloud parameters which must be simulated faithfully to be useful in the transferral of the St. Louis results to other urban areas.

In-Cloud Measurements of CN

One of the priorities for the aircraft operations in our METROMEX effort involved penetration of cumulus and cumulus congestus clouds at altitudes 200 m below cloud top to measure condensation nuclei (CN) and LWC. Both urban-affected and rural clouds were sampled on the same day during each summer from 1971 through 1975, but because this was not a high priority assignment, measurements were gathered on only 14 days. On these 14 days, 127 clouds were penetrated, and the locations were categorized into those unaffected or those affected by the St. Louis urban environment. This categorization took into consideration the cloud locales, the surface wind direction, and the wind at cloud level as determining factors. There were 74 unaffected clouds and 53 affected by the urban-perturbed boundary layer. The median values of CN and LWC for both types are shown in table D-13.

The CN inside of clouds subject to urban influences was 2.5 times greater than that in clouds which were apparently free from the St. Louis-related aerosol plume, and this difference was statistically significant at the 0.05 level. The LWC increased 12% in the affected clouds, but this figure is not statistically significant because of the variability of this parameter.

Measurement of free-air CN immediately prior to and after cloud penetration showed a uniform ratio of inside/outside CN concentration. The ratio was 2 for unaffected clouds and 1.3 for affected clouds. This in-cloud increase of CN for both cloud types is quite small compared with the values observed by Auer (1976) in an industrial cumulus where the ratio was reported as high as 10.

CLOUD MODELING

H. T. Ochs, III

USE OF MODELING

Research Goals

The original METROMEX research plan outlined the important roles that numerical modeling should pursue (Changnon et al., 1971). Mesoscale boundary layer modeling of the St. Louis urban complex has been performed at the University of Wyoming (Auer and Dirks, 1974). The purpose of this section is to discuss the Water Survey cloud modeling effort and to present research results from one of two numerical cloud modeling studies by the Water Survey under NSF support. The studies have investigated urban-related dynamic and microphysical effects on development and subsequent growth of cumulus clouds.

METROMEX has provided an excellent opportunity to compare model results with field observations. This process allows both model and observation deficiencies to be illuminated and to guide future urban-weather research. Through this interaction with the data collection effect of METROMEX, the Survey's modeling effort; addressed four goals: .

1) To help determine the urban factors critical to observed cloud and precipitation alterations and establish the relative contribution of each to the total change in precipitation
2) To use models tested against available field data to discern needs for additional field measurement
3) To aid in determining the minimum critical field measurements that would detect the potential for, or existence of, urban-induced precipitation anomalies in areas other than St. Louis
4) To aid in transferring METROMEX results to other urban complexes

Two areas were investigated through the use of numerical models. First, a 2-dimensional time-dependent model of a vertical slice of the atmosphere was developed for application to the St. Louis urban area. This study was designed to determine if surface conditions could play a significant role in preferentially initiating cumulus clouds on certain days.

The second interest area involved warm rain microphysical processes which were suspected of playing an important role in the modification of rainfall by urban areas. Under a subcontract to the Illinois State Water Survey, Dr. R. L. Reinhardt of Sierra Nevada Corporation supplied his earlier work in condensation and collection computations (Berry and Reinhardt, 1974). He aided in combining the programs into a single parcel model of condensation, collection, and breakup. He also aided in the improvement of the condensational growth algorithm. Incompatabilities between the finite differencing schemes employed for condensation and collection necessitated developing a new scheme to eliminate the problem (Ochs and Yao, 1978; Ochs, 1978). This model was used to test the hypothesis that giant cloud condensation nuclei (CCN) were in part responsible for observed anomalies in the St. Louis urban area.

Modeling Evolution

A 2-dimensional time-dependent cloud model of cumulus initiation in a vertical plain was developed for study of local effects in the St. Louis urban area (Ochs, 1975). The model domain was 76.8 km wide and 2.41 km high and had a 150-m grid interval. The model was applied

to conditions on two days during which cumulus convection occurred and neither strong winds nor vigorous frontal activity were present. Diurnal trends of surface temperature and mixing ratios along several rural-urban-rural cross sections were imposed at the lower boundary of the model. Observed upper air rawinsonde data were used to specify the initial horizontally stratified distributions of temperature, mixing ratios, and winds at 1 to 2 hours before reported development of initial cumulus activity.

The modeled results agreed favorably with the approximate time and location of the initial sightings of cumulus activity in the vicinity of St. Louis. These findings and subsequent results obtained by artificially modifying the surface temperature and moisture fields suggested that on the days modeled, the surface temperature distribution was more important than the surface moisture pattern in determining the location of initial cumulus activity. On one of the two cases studied, the location of initial cumulus activity coincided with a subsequent isolated storm.

The results of this first phase of the numerical modeling effort helped lead us into a more intense study of surface conditions and rainfall initiation. They also provided a strong rationale for increasing the density of the temperature-moisture network in St. Louis.

On the basis of initial findings, certain METROMEX scientists hypothesized that the presence and importance of increased concentrations of giant cloud condensation nuclei (CCN) in the urban-affected air to explain the apparent increase in efficiency with which clouds over the urban area produce precipitation. This speculation was based on radar and cloud base operations that indicated reduced distances between cloud base and first echoes in urban clouds and on observations of increased concentrations of small CCN in urban-affected air. Observations also indicated increased concentrations of cloud droplets in urban and downwind clouds. A parcel model that incorporates an adaption of highly accurate numerical techniques was developed to test this hypothesis (the subject of the remaining portions of this section). New methods of computing condensation and collection on an Eulerian radius domain were developed to prevent numerical errors from leading to erroneous conclusions. Observations of small CCN and giant particle concentrations were used to initialize a population of saturated solution droplets in subsaturated air. The development of the precipitation spectrum and radar reflectivity factor was studied during prescribed ascents. The model suggests that variations in concentrations of all CCN-size ranges over the extremes in observed data produce little effect on the evolution of precipitation. Variations in chemical composition and partial solubility also do not appear to account for observations. The model and other observations suggest that, if increased cloud base heights over the urban area lead to less rapidly developing updrafts, the observations can be explained in terms of this dynamic effect.

The microphysical modeling has resulted in a reassessment of the potential influence of anthoropogenic giant CCN in modifying urban weather. An alternative hypothesis suggested by the modeling results, coupled with field observations, has been developed to explain the differences between cloud bases and first echo bases in the St. Louis-East St. Louis area and those in the surrounding rural areas. Future research involving cloud modeling and a re-examination of some aspects of the radar data have been suggested as a next step toward verifying or refuting the new hypothesis.

Although unanticipated, the results of both aspects of the cloud modeling effort point to dynamic related causes of the urban anomalies on precipitation. Anthropogenic variations in CCN concentrations do not appear as important as once believed. Future research in other urban areas should probably de-emphasize microphysical studies and concentrate more on dynamic related factors.

MODELING INTERPRETATIONS OF CLOUD DATA

METROMEX results show the existence of local rainfall and severe weather anomalies in the proximity of St. Louis (Changnon et al., 1971). A second METROMEX study area concerned efforts to obtain and interpret data that would illuminate the physical processes that contribute to these anomalies. Project aircraft probed clouds that had ingested urban modified air, as well as those unaffected by the St. Louis urban complex, to gather contrasting data. Other flights were conducted in storm updraft areas to seek data on microphysical and mesoscale alterations related to urban perturbations. These measurements included cloud condensation nuclei (CCN), cloud microphysical structure, and the 3-dimensional subcloud thermodynamic structure; Fitzgerald and Spyers-Duran (1973) reported observations of fair-weather cumulus microstructure in areas upwind and downwind of the urban-industrial complex that indicated a definite alteration toward greater droplet concentrations and more narrow distributions in the urban and downwind clouds as opposed to upwind clouds.

These observations led Braham (1974) and Semonin and Changnon (1974) to hypothesize the existence of giant condensation nuclei to justify a lower formation of radar echoes and the distinct change in the surface drop-size spectra (Semonin and Changnon, 1974). Cloud base observations of cloud droplet spectra in urban and downwind clouds are suggestive of a deterrent to precipitation formation by the coalescence process. The radar first echo statistics, however, indicate an enhanced development of precipitation particles below the freezing level.

This section reports on the study of the many facets of these various atmospheric observations, and the hypothesis of giant nuclei, carried out with a sophisticated numerical model of cloud microphysics. The goal of this modeling research was to seek coherent explanations of the many physical observations to help test the hypothesis, and to point the way for future research on urban effects at other cities.

A microphysical parcel model was used to investigate the evolution of precipitation sized drops. The essential features of the model are here described and its applicability to the problem and assumptions are discussed. After the methods of model initialization are presented, the effects of CCN concentration, CCN composition, and CCN solubility are discussed. Variations in the evolution of radar reflectivity caused by changes in parcel ascent rates are also presented. The results for computed drop distributions then follow, reflecting the effort to gain physical interpretations of the results and to assess the degree that drop sedimentation might alter these results. Finally, some relevant METROMEX observations are discussed in light of the model computations, and the possible role of observed and hypothetical urban induced CCN variations is discussed.

The Model

The numerical simulations depict the evolution of the droplet spectra in a rising parcel of air from an initial population of CCN and include the effects of condensation (or evaporation), coalescence, and breakup'. The ascent rate is prescribed and there is no interaction with the parcel environment. The model and numerical techniques employed are completely described in Ochs and Yao (1978) and Ochs (1978) and only a brief description of the important aspects of the model are presented here.

A small parcel of air is lifted at a chosen rate at the onset of the computation. Changes in the parcel temperature, relative humidity, and density are computed as a function of the ascent rate and latent heat processes. The ascent is assumed adiabatic, and thus there is no mixing of heat or moisture with the environment. In addition, the sedimentation of large drops from the volume and the fall of drops into the parcel from above are not considered.

As the ascending parcel expands and cools, the relative humidity increases. As saturation is approached and exceeded, condensation on the CCN occurs. The droplets grow in a Eulerian framework in which the mass doubles every second category. The droplet mass of category J is given by

$$X(J) = X_o \exp[(J-1)/J_o)] \quad (1)$$

where J_o is 2/ln2. Equation 1 is only used to specify the mass at the center of each category. A linear mass coordinate is chosen within each category such that the category end points meet and the ratio of adjacent slopes is constant (Ochs and Yao, 1978). An Eulerian framework is chosen so that the microphysical simulation is compatible with a cloud simulation in an Eulerian spatial domain at a later time.

An adaptation of Egan and Mahoney's (1972) numerical technique is used for the condensation, coalescence, and breakup calculations (Ochs and Yao, 1978). This scheme has some important advantages when applied to this problem. First, the transport scheme employed strongly reduces numerical spreading of the droplet spectrum which, if present, would lead to premature development of large drops. Also, when used in conjunction with the piecewise linear mass co ordinate previously discussed, the mass of the liquid water and CCN material is conserved to within computer truncation error (Ochs and Yao, 1978).

Objectively chosen variable timesteps are used in all aspects of these computations. As droplets grow rapidly in the activation stage, short condensation timesteps are used, but collection has little effect on the development of the distribution at this time allowing a long coalescence timestep. Later, the drops grow very slowly by condensation allowing the long timestep method of Clark (1973) to be used. When collection processes begin to dominate the changes in the distribution shape, shorter collection timesteps are adopted to preserve accuracy.

The equation for the condensational growth of droplets is given by Fukuta and Walters (1970). The equation is used under the assumption that the droplets are in thermal equilibrium with their environment. In addition, the density, osmotic coefficient, and surface tension of the solution droplets are computed as functions of the mass ratio of solute to water.

The collection process is treated stochastically. The kernel employed is derived from the linear collision efficiencies, Y_c, given by Jonas (1972), Klett and Davis (1973), Shafrir and Gal-Chen (1971), and Beard and Grover (1974). The terminal velocities are computed as functions of height by use of the methods of Beard (1976, 1977).

Two schemes for large drop breakup are used simultaneously in the model. The first is that developed by Srivastava (1971) which treats the aerodynamic disintegration of large drops. Brazier-Smith et al. (1972,1973) developed the second scheme in which drops undergoing off-center collisions separate, producing satellites if the rotational energy generated by the collision exceeds the binding energy due to surface tension. Both of these methods have been tested by Young (1975) who states that the second scheme (collisional breakup) is more important than the first in determining the final drop distribution shape.

In this model the parcel is assumed to represent a rising volume in the center of a developing cumulus cloud. A radar reflectivity of 20 dbZ is the approximate detectability limit of the METROMEX weather radars that operated in the St. Louis area. The crucial assumption is that the sedimentation of larger drops out of the parcel is not significant and that the drops that do fall out are replaced by similar drops from above. It is not the purpose of these calculations to predict the actual height at which a first radar echo develops, but to investigate the relative effects from changes in CCN concentration or composition on the initial development of precipitation.

Model Initialization

The smaller size CCN in the initialized distribution were measured in the St. Louis area by other METROMEX participants (Fitzgerald and Spyers-Duran, 1973; Braham, 1974). Samples of air gathered during aircraft flights were analyzed in a diffusion cloud chamber immediately upon landing. Sedimentation of the larger particles and the inability to use very low supersaturations preclude the use of this technique for the measurement of giant CCN. The spectra measured are present in the form

$$N = C\,S^{k} \qquad (2)$$

where N is the total number of CCN activated at a supersaturation, S, and C and k are constants. The values of C and k were evaluated by varying S between 0.17 and 1.0% and applying a best-fit analysis to the data.

Since no data exist for giant CCN in the St. Louis urban area, an approximation to the tail of the CCN distribution was made. As a starting point, the distribution of equation 2 was extended until it intersected the total aerosol distribution. The total aerosol distribution, given by $4 \times 10^{-12}\ r^{-3}$ particles $cm^{-3}\ (\ln r)^{-1}$ where r is the dry radius of the particle, was followed beyond the intersection. For particles >40 *μm* radius an exponent of r of -6.5 was employed (Noll and Pilat, 1971). In each case the initial distribution is truncated at a dry CCN radius of 80 μm. Test calculations showed that the results are insensitive to this truncation value since there are too few nuclei of greater size to affect the processes considered. All of the particles in the entire CCN distribution were assumed to be composed of ammonium sulfate. This hybrid distribution formed the reference against which various changes in chemical makeup, solubility, and concentration were assessed.

The total aerosol distribution is initialized by converting the dry CCN into saturated solution particles which provide the initial droplet concentrations in each category. The initialization of the segment of the distribution governed by equation 2 is slightly more complicated. Equation 2 is used differentially in conjunction with the growth equation to determine the number density distribution in terms of the nuclei mass. The growth equation determines the activation supersaturation as a function of solution droplet physical properties. The nuclei material is then assumed to be in a saturated solution and the number density distribution for the categories determined by equation 1 can be evaluated. The effect of differences in the hygroscopic nature of the CCN was investigated by employing sodium chloride instead of ammonium sulfate CCN in some computations.

To facilitate an accurate match to the data represented by equation 1, the CCN smaller than the point at which the cloud chamber data intersects the total aerosol curve are always assumed to be composed of soluble material of a single compound. Fitzgerald (1974) investigated the effects of populations of CCN with varying properties and found the resulting cloud droplet spectrum insensitive to these changes in the chemical makeup and partial solubilities of the CCN aerosol.

The initial temperature and pressure for all computations was 16.7°C and 886 mb. The parcel relative humidity was 83% and the mixing ratio was about 11.2 g kg^{-1}. These initial conditions produce saturation at about 850 mb and 13.1°C which are typical conditions for summer cloud bases in St. Louis. Various parcel ascent rates and accelerations with height were used.

Effects of Variations in CCN Concentrations

Figure D-5 presents the initial CCN distributions used for the calculations that are derived, in part, from the observations of Braham (1974) near St. Louis. The designation UW71 stands for the mean 'upwind 1971' and DW 72 indicates the mean 'downwind 1972' distribution, and so forth. The extreme values shown were derived from scatter diagrams of all data collected. The

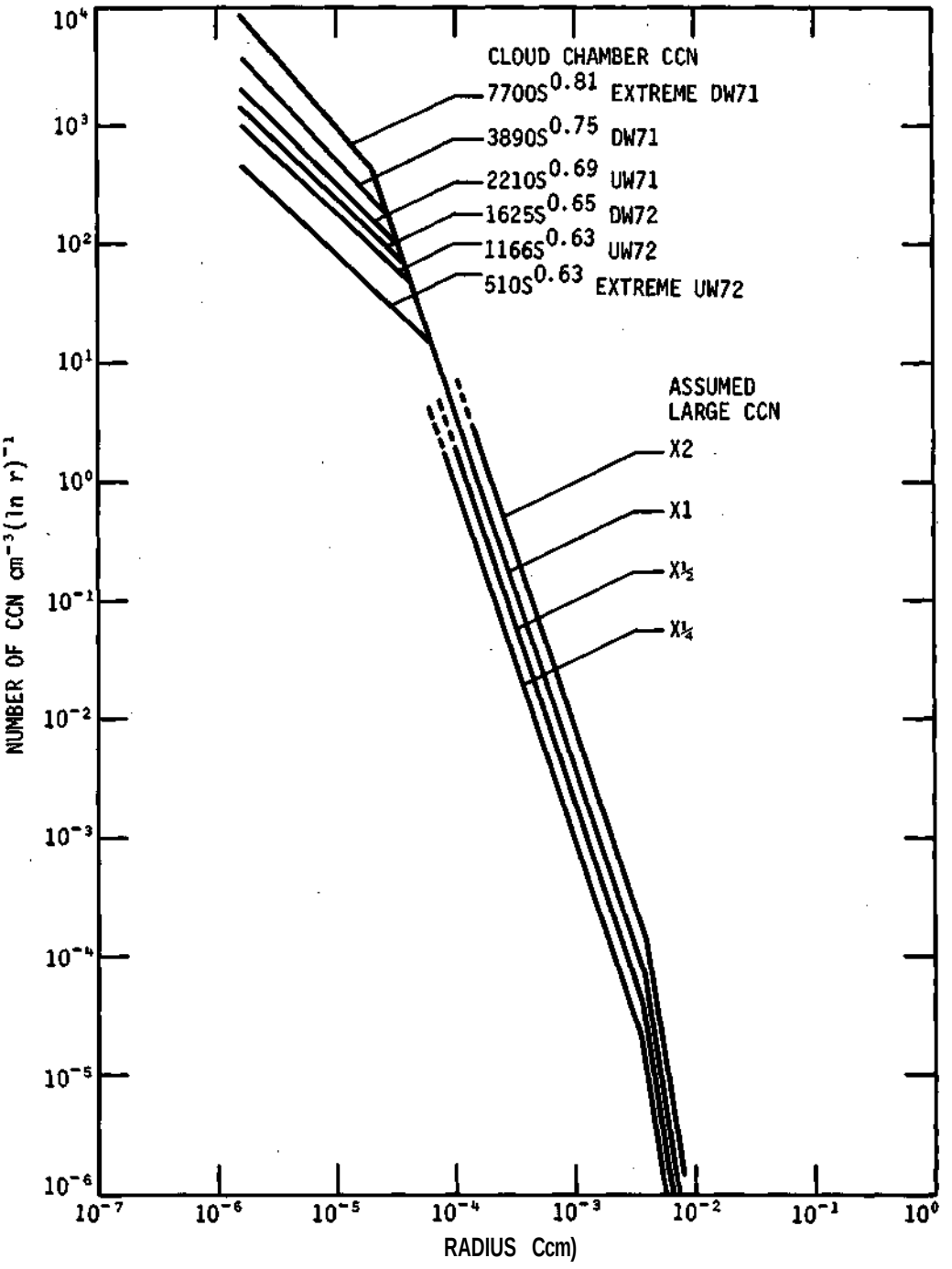

Figure D-5. Initial dry CCN radius (Any of the observed cloud chamber CCN could be paired with one of the four assumed CCN distribution tails)

CCN distribution labeled 'extreme DW71' contained the greatest number concentration that was measured during the two summers, and similarly, the distribution labeled 'extreme UW72' represents the least number concentration.

The total aerosol distribution used for CCN of greater than about 1.0 μm diameter is labeled X1 in figure D-5. Those distributions labeled X2, *X1/2,* and X1/4 are the X1 distribution multiplied by powers of two.

Figure D-6 depicts the results obtained for a constant ascent rate of 1.0 m s^{-1}. The radar reflectivity factor is plotted as a function of time for the six cloud chamber distributions with the X1 CCN distribution tail (the complete plot is given in only one case). For these cases all of the CCN were assumed to be completely soluble ammonium sulfate particles. Square brackets delineate the number of cloud droplets activated in each case. The most striking aspect of figure D-6 is that in spite of the wide range in the number of activated cloud droplets (a difference of a factor of 5.6) all six parcels achieved a reflectivity of 20 dbZ within 150 s of each other.

Two compensating effects account for this result. First, higher concentrations of cloud droplets lead to smaller mean droplet sizes since the population of cloud droplets share approximately equally in the water vapor that becomes available for condensation in the ascending parcel. Thus the collision efficiencies between the cloud droplets and larger collector drops is reduced because of the reduced size of the cloud droplets. The transport of mass to larger drop sizes is thus inhibited leading to a retardation in the production rate of precipitation sized drops.

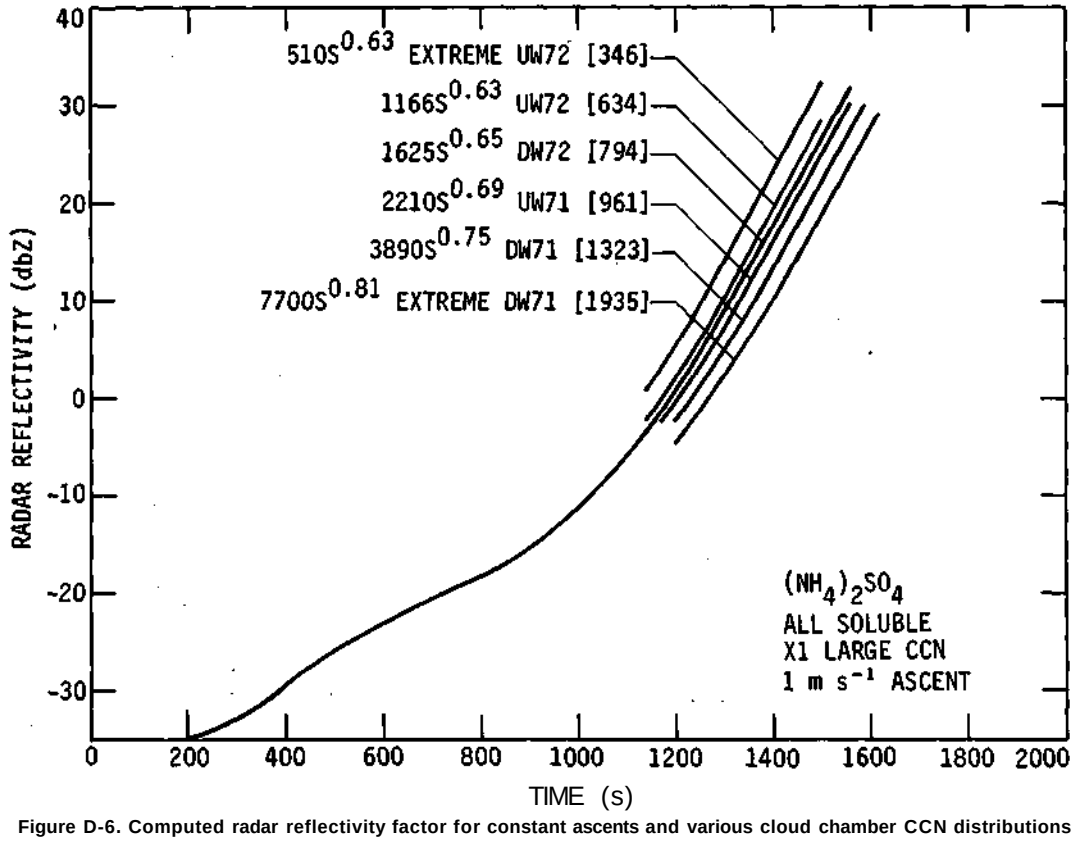

Figure D-6. Computed radar reflectivity factor for constant ascents and various cloud chamber CCN distributions

The second compensating effect results from the increased probability that collections will occur between the higher concentrations of cloud droplets and larger collector drops leading to an increase in the rate of precipitation production. Figure D-6 indicates that these effects almost cancel each other with the first slightly dominating the second.

If significant differences in drop distributions exist at equivalent radar reflectivities, then sedimentation effects might significantly affect the results of figure D-6. If one distribution contained larger drops than another at the same radar reflectivity, then a simulation that included sedimentation effects might show much different time intervals in equivalent reflectivity values.

Figure D-7 shows the distributions of drops greater than about 0.1 mm radius from the extreme UW72 and DW71 cases presented in figure D-6. Straight line segments are used to connect the calculated data points. The computed reflectivities for the distributions shown differed by only 0.014%. As can be seen, there is a slight tendency for the extreme DW71 CCN distribution to produce more of the largest drops at equivalent radar reflectivities. Recalling that this CCN distribution produced 5.6 times more active cloud droplets than the extreme UW72 distribution makes the distribution differences depicted in figure D-7 understandable.

The more concentrated cloud droplet population results in a significantly lower supersaturation over the duration of the ascent. The amount of vapor condensed in both parcels must be approximately equal as they ascend through the same elevations at the same vertical speeds. The growth rate of the cloud droplets, which are responsible for most of the condensation, must be lower in the parcel with the largest number of cloud drops. Therefore, the supersaturation in this parcel must be significantly lower.

The few larger droplets present in this parcel at cloud base do not grow as much by condensation because of the lower supersaturation, resulting in a slight reduction in the concentration

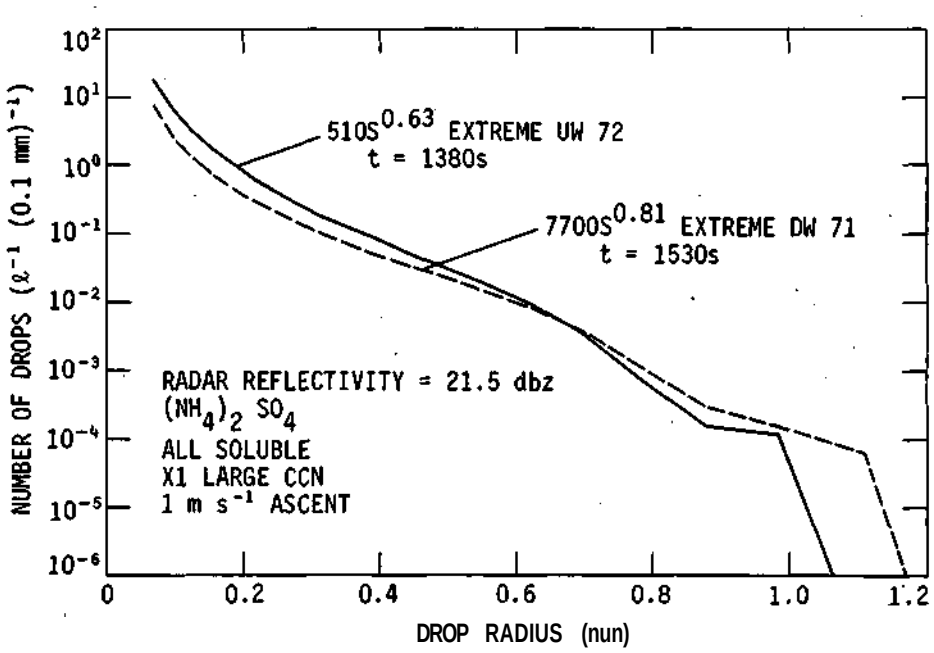

Figure D-7. Computed precipitation distributions at constant radar refelctivity for two simulations from figure D-6

of the smaller drop sizes shown in figure D-7. The collection process has to make up for this deficiency by producing more of the larger drops shown in figure D-7. A longer time is required for the collection process to produce more of the larger drops. This longer time also allows collisions between similar sized drops to spread the distribution to a slightly greater maximum size in the parcel with the more concentrated cloud drops. The general tendency in figure D-7 would probably lead to a slight lowering of the development of this reflectivity in the extreme DW71 case with respect to the extreme DW72 case if sedimentation effects were considered in the model.

Figure D-8 presents results obtained by varying the total aerosol portion of the CCN distribution with the DW72 cloud chamber distribution always used for the smaller CCN. With the constant 1.0 m s^{-1} ascent, a factor of 8 difference in the larger CCN concentration results in only a 115 s difference in the time to achieve a radar reflectivity of 20 dbZ. There is a slight tendency (similar to that depicted in figure D-7) for the *XV1/4* case to produce a longer large drop distribution tail than the X2 distribution for an equivalent computed radar reflectivity. This is consistent with the reasoning used to explain figure D-7. The *XV1/4* distribution activates slightly more cloud droplets and thus this case has a slightly lower super saturation than the X2 case. This effect is probably small since differences in the numbers of activated cloud droplets in the cases presented in figure D-8 are significantly less than those for the figure D-7 cases. The fact that the *XV** case starts with fewer large droplets at cloud base also contributes to the effect since the accretion of cloud droplets by the *XV1/4* distribution tail would proceed at a slower rate.

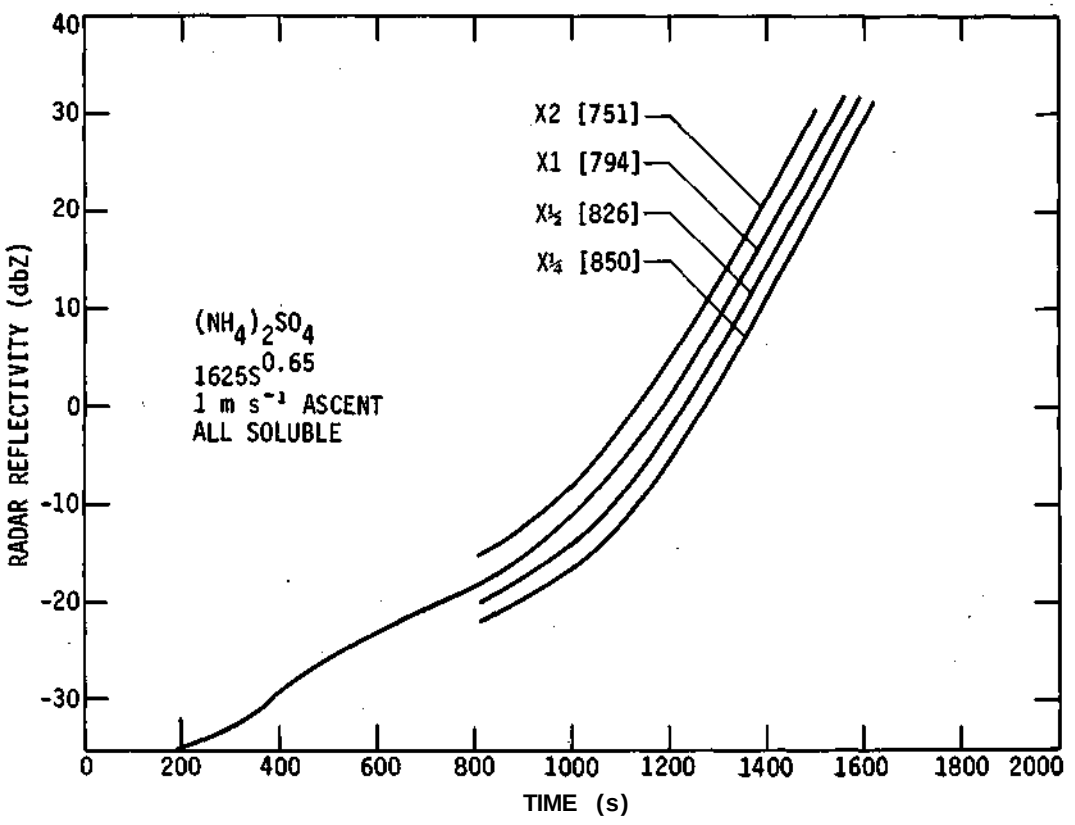

Figure D-8. Computed radar reflectivity factor for constant ascents and various CCN distribution tails

Additional computations have been made to compare possible upwind and downwind concentration differences. This series of computations was designed to assess the only available large particle concentration measurements in the St. Louis urban area. Johnson (1976) presents average distributions upwind and downwind of St. Louis for sizes between 5 and 55 μm diameter. These observations indicate that the average downwind distribution particle volume contains 1.8 times that of the average upwind distribution. His summary of 18 cases indicates a maximum volume ratio of 4.4 and a minimum of 1.15.

Figure D-9 shows the initial distributions for this series of computations. Johnson's (1976) data are extrapolated to smaller sizes until the UW72 and DW72 distributions are intercepted. The UW72 cloud chamber CCN spectrum with the X1 tail truncated at 26.5 /um radius is included for comparison. Note that a large difference between this distribution and those including Johnson's data exists near particles of about 1.0 μm diameter.

Figure D-10 shows very little difference between any of the calculated radar reflectivities in these cases. In fact, there is no difference at the 20 dbZ level between the downwind cloud chamber CCN coupled with Johnson's downwind large particle spectrum which activated about 200 more drops than the upwind case.

The truncated X1 distribution has similar end points to the upwind small CCN coupled to Johnson's downwind giant particle spectrum. However, the center area between about 10^{-5} and 5 X 10"* cm radius differs by a factor greater than 10. The results show that the case involving the X1 tail activated 33 more drops and produced a reflectivity of 20 dbZ at about 10 s earlier than the case with the UW72 small CCN with Johnson's downwind tail. Thus, the concentration of intermediate sized CCN has little effect on the evolution of radar reflectivity.

It is difficult to assess the exact reasons for the slight differences in large drop distribution shapes for drop sizes less than about 0.5 mm shown in figure D-l1 since the different cases contain different numbers of cloud drops and start with different distribution shapes for the larger CCN (see figure D-9). However, the important point is that figure D-l1 does not indicate large differences in the production of the largest drops.

Effects of Variations in CCN Chemical Composition

The effect of the chemical properties of the CCN on the initial development of precipitation is studied by repeating a calculation with more hygroscopic sodium chloride CCN. This is achieved in the calculations by changing the physical properties of the CCN material as well as the functions that represent the solution properties of the drops. The sodium chloride computations are initialized at a relative humidity of 80% as opposed to 83% for the ammonium sulfate and on the same dry adiabat as the computations with ammonium sulfate CCN.

The DW72 cloud chamber CCN spectrum with the X1 tail is adopted for this test and the method of initialization remains the same as in the previous cases. Thus the tail of the distributions is identical for both chemical compositions since the number concentration of particles is specified by the total aerosol distribution. In the region where the diffusion cloud chamber data are used to specify the CCN distribution, the initial number concentrations are slightly different. To activate the same number of particles at a given supersaturation and thus approximate the same cloud chamber distribution, there must be fewer sodium chloride than ammonium sulfate particles in a given size interval. Since sodium chloride is more hygroscopic than ammonium sulfate, a smaller sodium chloride particle would activate at a given supersaturation. For the chosen distribution there are 16% more ammonium sulfate than sodium chloride particles per radius interval centered at 0.1 μm.

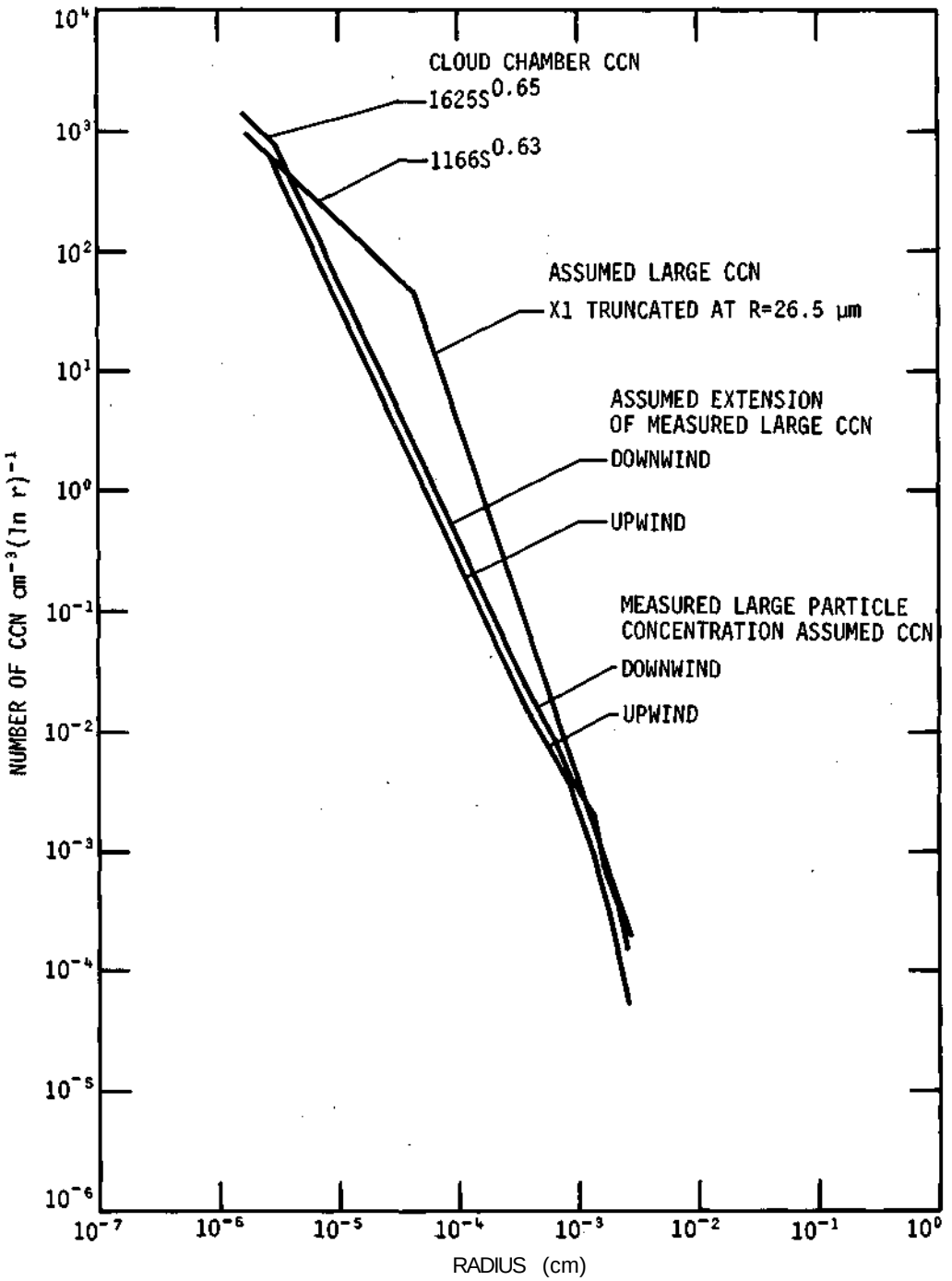

Figure D-9. Initial CCN distributions including measured ultra giant particle concentrations

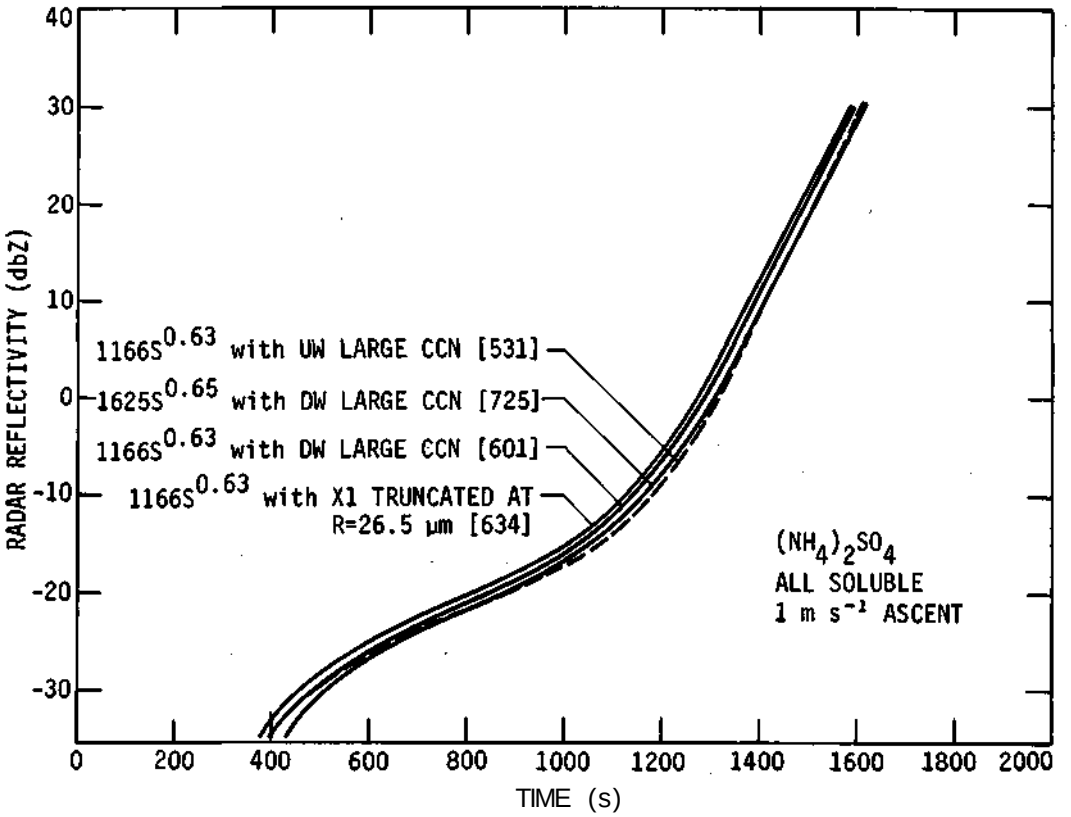

Figure D-10. Computed radar reflectivity factor for the CCN distributions in figure D-9

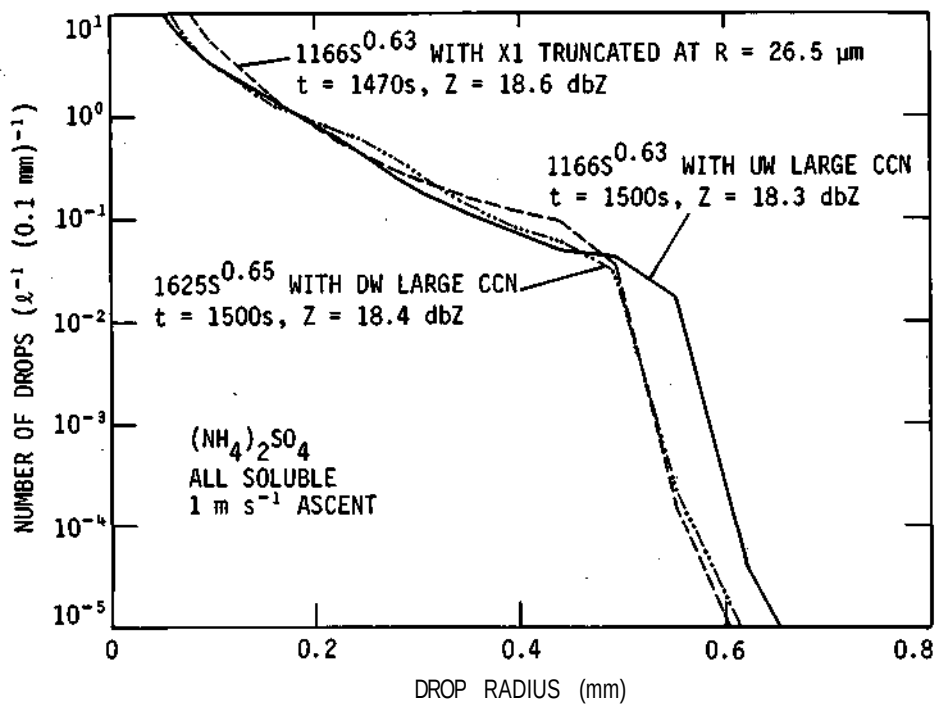

Figure D-11. Computed precipitation distributions at nearly constant radar reflectivity for three cases in figure D-10

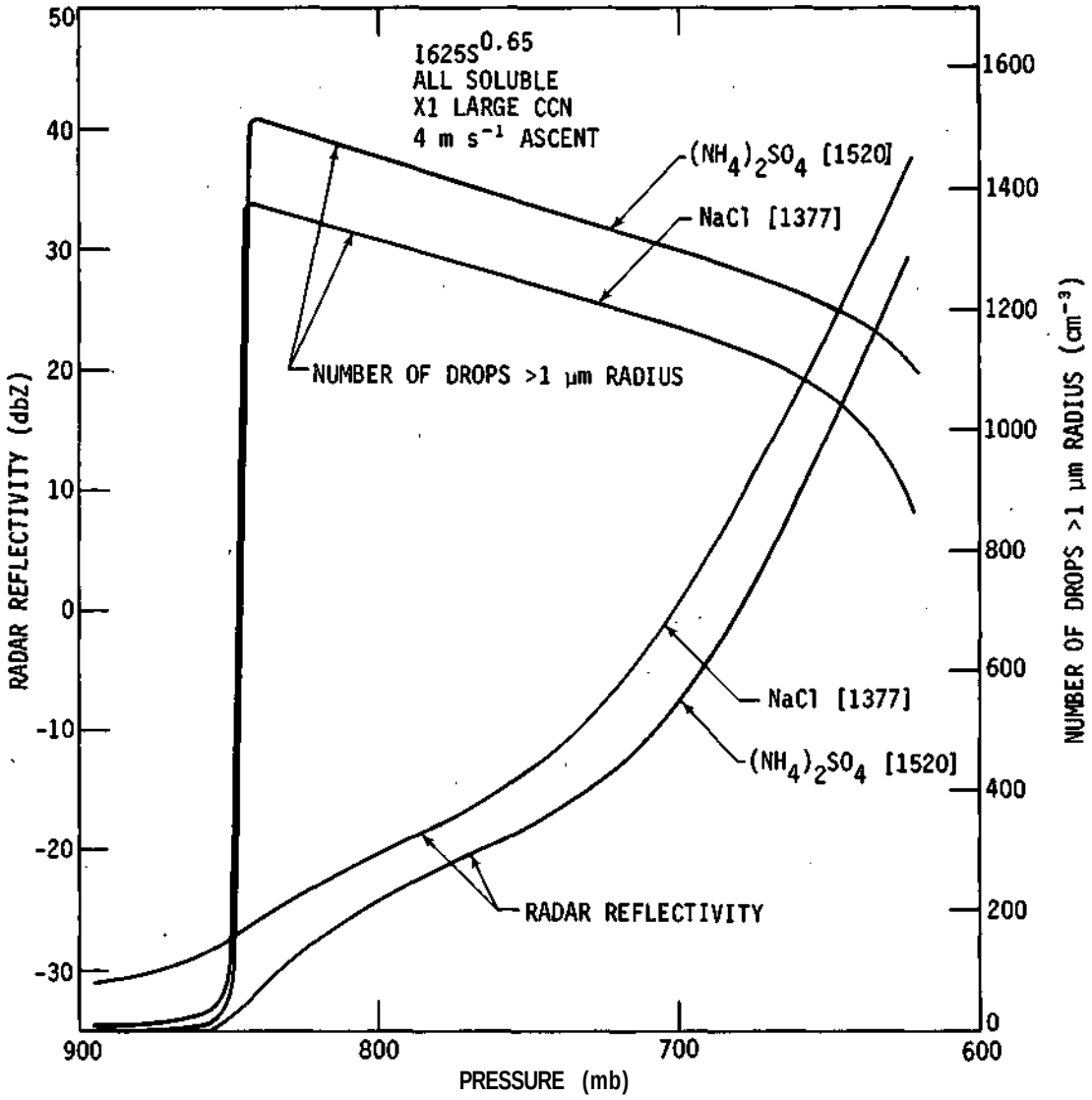

Figure D-12. Computed radar reflectivity factor and number of drops greater than 1.0 μm radius for equivalent CCN distribution concentrations and different chemical compositions

Figure D-12 shows the results of two computations which indicate that the sodium chloride distribution achieves a radar reflectivity of 20 dbZ at about 200 m lower than the ammonium sulfate case. The initial parcels were lifted at a constant 4 m s^{-1} and the numbers in square brackets indicate the number of activated drops in each case. This result confirms the findings of Fitzgerald (1974) who showed that the cloud droplet distributions are not sensitive to the chemical composition of the soluble material in the CCN. Therefore, with nearly identical cloud droplet distributions one would expect a similar evolution of radar reflectivity. A comparison of the evolving large drop distributions showed no tendency for one case to develop the largest drops faster than the other.

Effects of Variations in CCN Solubility

Several computations were performed with specified portions of the total aerosol segment of the initial CCN distribution assumed to be composed of insoluble particles that contain a very small amount of soluble material. These particles are simulated by initializing a chosen portion of the distribution tail with pure water drops that are not permitted to evaporate while the parcel is subsaturated. When the parcel becomes supersaturated the water drops can grow by condensation without solution effects. The growth of the pure water drops simulates the rapid dilution and subsequent growth of an insoluble particle with a vanishingly small amount of soluble material on its surface (Junge and McLaren, 1971). In fact, in a condensation and collection simulation this approximation might cause a slightly slower evolution of the drop spectra than if the partial solubility were more precisely modeled. When small solution droplets are collected by the larger water drops, the effects of the solute on the condensation process is terminated since the combined drop will contain a very dilute solution. If a large insoluble core were present in the collector drop, the solution at the drop surface would remain more concentrated. Therefore, the computations with the simulated insoluble nuclei represent a slight overestimation of the effect of these particles.

The CCN distribution is initialized as before except insoluble particles are used beyond a preselected drop category. The number concentration for both soluble and insoluble CCN is determined by the same total aerosol curve. Since the soluble ammonium sulfate particles are initialized as saturated solution droplets in an 83% relative humidity parcel, and water drops with the same radius as the dry insoluble CCN are used beyond a given category, there is a discontinuity in the initial number density distribution of droplets.

Figure D-l 3 presents results obtained by varying the point at which the insoluble distribution begins. The DW72 cloud chamber CCN distribution with the X1 large CCN tail and a 4.0 m s^{-1} ascent rate are employed. There is little effect of the physical property of the distribution tail for sizes $\geq$ 68 μm radius. This is likely a result of too few particles larger than this size to significantly affect the calculation. On the other hand, reducing the critical size below 12 *μm* has a negligible effect on the evolution of radar reflectivity. This result is easily understood. The cloud droplets distribution achieves a mean radius of about 5 μm shortly after activation, and there is a small relative fall velocity between 12 μm droplets and the 5 μm cloud droplets. Thus there are insufficient collection events for droplet pairs below 12 μm radius to affect the calculations. The data presented on figure D-l 3 also indicate the insensitivity of the number of activated cloud drops to the properties of the CCN in the distribution tail, but the computations show that the solubility of particles in the range between about 15 and 50 μm radius can affect the evolution of radar reflectivity.

Two effects contribute to the variations of calculated reflectivity depicted in figure D-l3. First, there is the reduced size of the initial drops that represent the insoluble particles. If these particles had been soluble they would have been initialized as larger saturated solution drops. Second, the essentially pure water drops are not permitted to grow below the point where saturation is achieved and they grow very slowly in the slightly supersaturated parcel. On the other hand, droplets formed from pure ammonium sulfate CCN in the distribution tail lag far behind their equilibrium radius and thus can condense significant amounts of water vapor both before and after saturation is reached.

In order to assess the relative importance of these two factors an additional computation was made. The number density distribution for the all soluble case shown on figure D-l 3 was employed with pure water drops making up the spectrum beyond 1.5 μm radius. In this hypothetical case, the CCN are assumed to achieve the same initial increase in size that would occur if they were

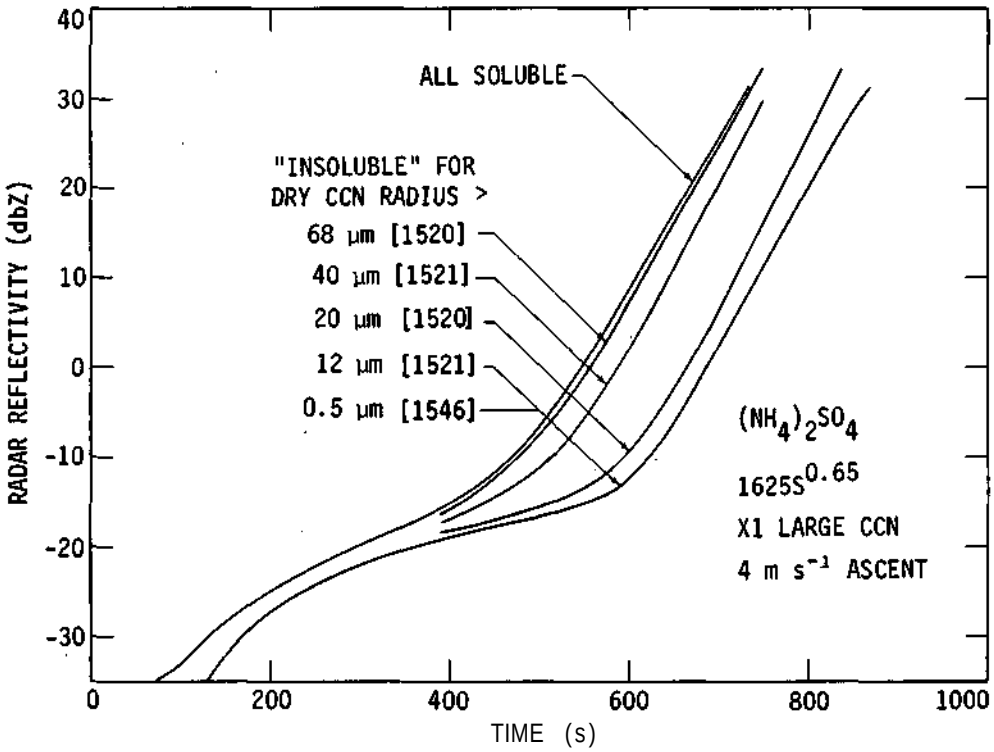

Figure D-13. Computed radar reflectivity factor for a CCN distribution in which particles greater than a chosen size were assumed to be insoluble with a very thin coating of soluble material

composed of ammonium sulfate; however, they are not permitted the subsequent benefit in growth rate from the solute. The results indicate that the development of radar reflectivities is retarded by about 45 s from the case in which pure ammonium sulfate CCN were used throughout the distribution. The corresponding case in which the insoluble CCN were initialized at their dry radius was delayed from the soluble case by 135 s. Therefore both the initial size change for the pure ammonium sulfate CCN and the solution effects on condensational growth are significant in assessing the reasons for the delayed radar reflectivity in the cases with insoluble CCN.

The DW71 distribution was chosen to illustrate the combined effects of solubility and number concentrations in the distribution tail. Figure D-14 shows the evolution of radar reflectivity for initial CCN containing pure ammonium sulfate with the X1 and *XV1/2* distribution tails. The curves marked 'insoluble' large CCN have insoluble particles initialized beyond 5 μm radius. Both the X1 and X1/2 tails were employed here also. The results show a significantly greater dependence on extreme differences in solubility than on the factor of two changes in CCN concentrations in the distribution tail. Identical sets of calculations were performed for the other three average summer cloud chamber CCN distributions with the same results. The relative times between the achievement of a threshold radar reflectivity on figure **D-14** are approximately the same for the calculations with the other distributions.

Since the number of droplets activated in the corresponding soluble and insoluble cases presented in figure **D-14** are almost identical, the supersaturation during the time that the radar echo develops is also nearly identical. However, as has been discussed, there are significant differences in the ability of the CCN beyond 5 μm radius to grow by condensation. Also, initial size differences between soluble and insoluble cases resulting from the deliquescences of the soluble

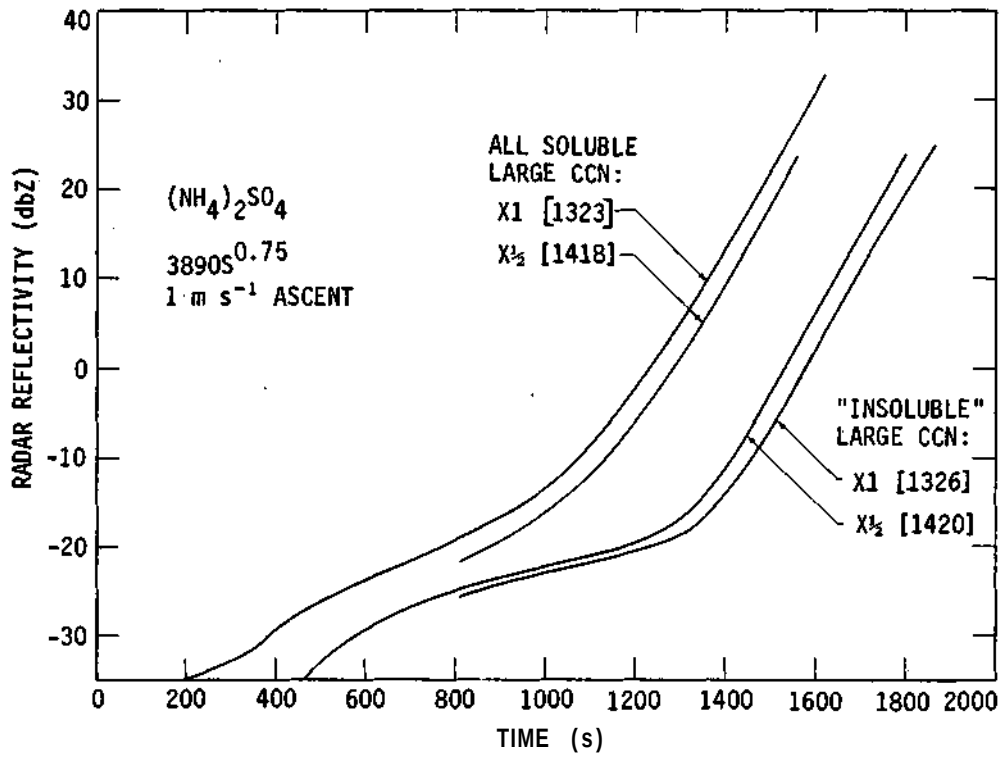

Figure D-14. Computed radar reflectivity for different CCN distribution tails and solubilities

CCN, have been shown to contribute to the computed differences in the evolving radar reflectivity. With arguments similar to those previously presented, there must be more of the largest drops or the distribution must extend to larger sizes for the insoluble cases at corresponding values of radar reflectivity. Since the 'insoluble' cases require a longer time to achieve the same radar reflectivity, the distribution spreads to larger sizes. In fact, the condensational growth for CCN greater than 5 μm is so severely retarded in the insoluble case that large differences in the drop distributions for the two X1 cases of figure D-14 can be seen in figure D-15. The neglected sedimentation effects would act-to reduce time differences in the radar reflectivities of figure D-14. It would therefore be improper to draw conclusions about vertical displacements of equivalent radar reflectivities from these calculations.

In order to more completely assess the effects of partial solubility on the evolution of precipitation, several computations were performed with the CCN mass in the distribution tail composed of soluble and insoluble fractions. The insoluble fraction was assumed to have a density of 2.0 g cm^{-3} and, as in previous calculations, all masses were conserved to computer truncation error. The soluble portion of the CCN is assumed to be ammonium sulfate. When the droplets are initialized in the parcel the soluble fraction of the nuclei mass is assumed to be in a saturated solution that completely surrounds the insoluble portion of the CCN particle. In the cases presented in figure D-16 all CCN beyond about 0.5 μm radius are assumed to have some insoluble material. A few categories just beyond 0.5 μm are used as a transition region where the fraction of soluble material varies smoothly between 100% and a selected value. All categories for initial droplets with masses greater than those in the transition region have the same ratio of soluble to

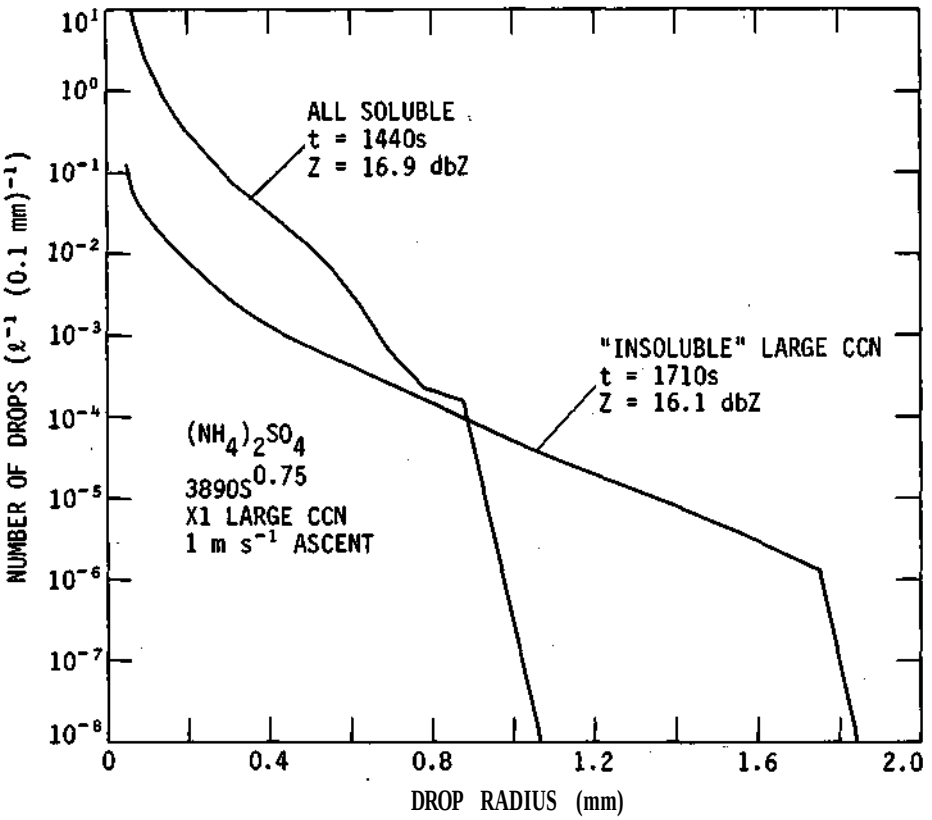

Figure D-15. Computed precipitation distributions at nearly constant radar reflectivities for two cases from figure D-14

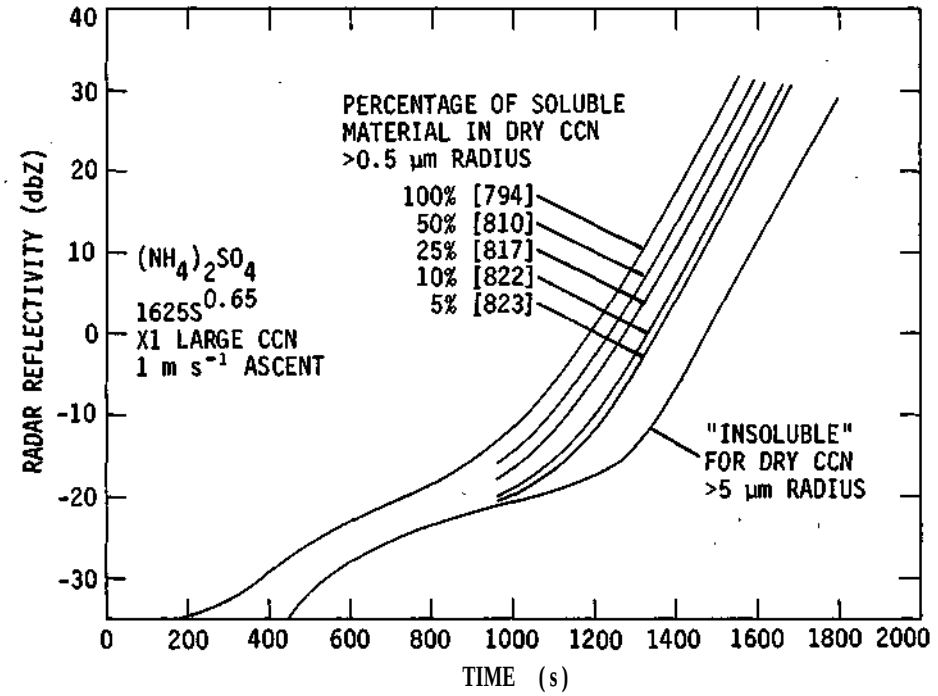

Figure D-16. Computed radar reflectivity factors for a CCN distribution in which the largest CCN were assumed to have constant partial solubilities ranging from 100 to 0%

insoluble material. The results shown in figure D-l3 indicate that the details of this transition region should have little effect on the evolution of the radar refelctivity. The DW72 cloud chamber CCN coupled with the X1 tail was used for the results of figure D-l6 and the corresponding case is presented in which CCN greater than 5 μm were almost entirely insoluble. The results indicate that over a wide range of partial solubilities the retardation of precipitation formation from the 100% soluble case is significantly less than for the insoluble case.

In each case presented in figure D-l6 the initial distributions of dry CCN sizes are identical. Thus the variations depicted in figure D-l6 can be attributed to essentially two interacting factors. First, the CCN with larger fractions of insoluble material become larger solution droplets when they deliquesce at the onset of the calculation. Second, the droplets with smaller fractions of insoluble material dilute faster as condensation proceeds thus reducing the subsequent condensation rate. The net effect is that CCN with small fraction of soluble material start as smaller droplets and do not grow as large by condensation, thus retarding the collection process. These effects are at their maximum in the insoluble case of figure D-16.

The differences in resulting drop distributions at nearly equivalent radar reflectivities can now be anticipated. The retarded condensational growth (leading to a slower development of the collection process) for the CCN distributions with smaller soluble fractions should lead to reduced drop concentration sizes near 100 μm radius. This reduction in number coupled with increased times required to achieve an equivalent radar reflectivity should result in a longer drop tail. The drop distributions for the cases depicted in figure D-16 are present in figure D-l7. Both figures D-16 and D-l7 indicate that even a small (5%) fraction of soluble material in the CCN will allow enough condensational growth to significantly reduce the retardation of radar reflectivities

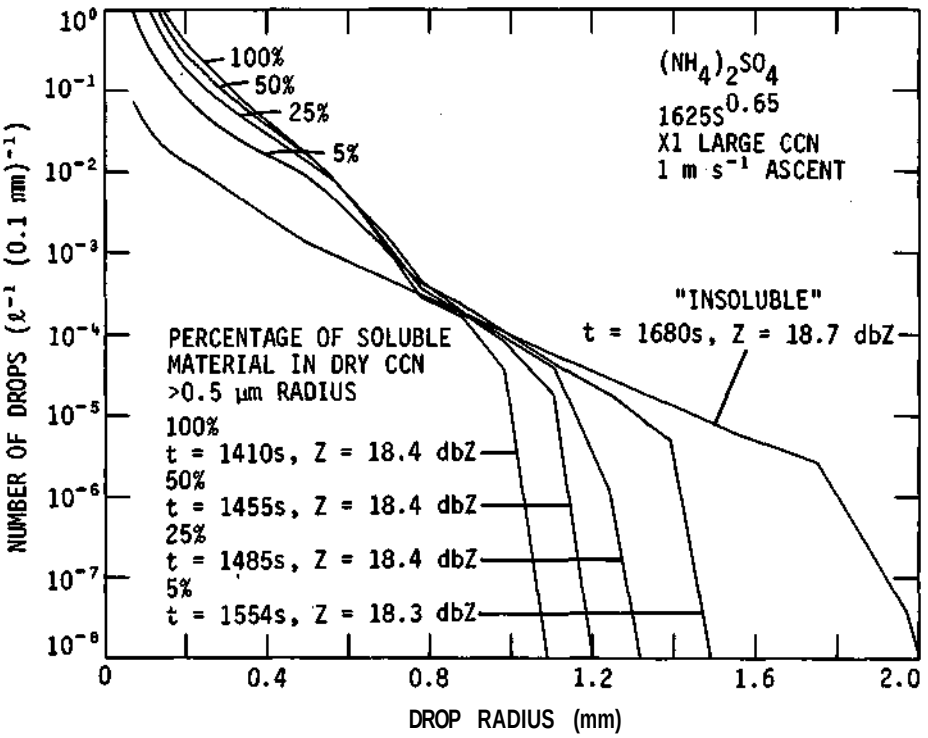

Figure D-17. Computed precipitation distributions at nearly constant radar reflectivity for the cases from figure D-16

from the extreme effect of the almost completely insoluble CCN. The large differences in concentrations of the largest drops between the 100% soluble and the insoluble cases are also not present for a substantial range of partial solubilities.

Effects of Variations in Vertical Speed

The model computations show that variations in updraft speed cause large differences in the elevation at which significant numbers of precipitation sized drops form. Figure D-18 depicts

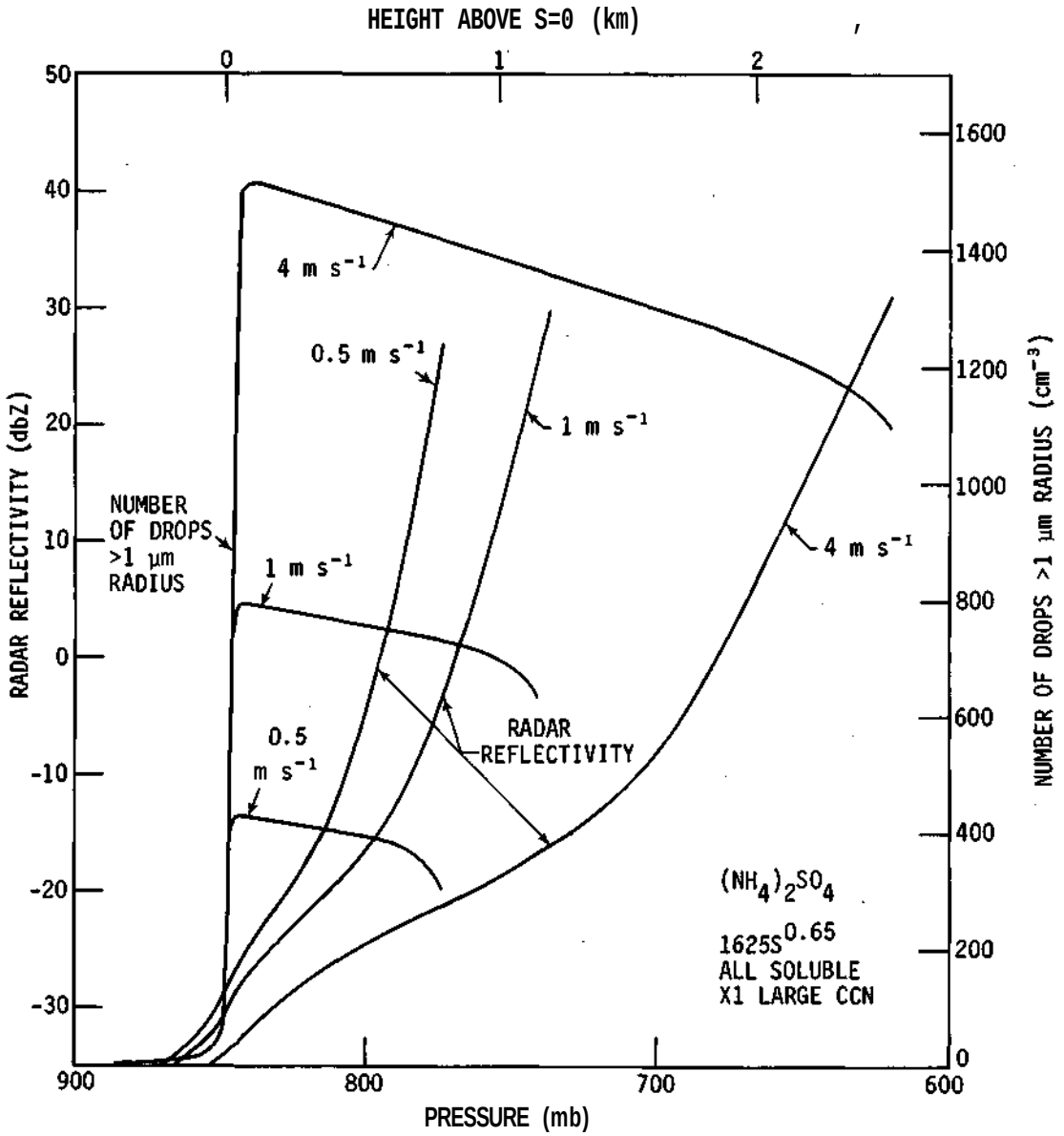

Figure D-18. Computed redar reflectivity factor and number of drops greater than 1.0 µm radius for various constant ascent rates

results obtained with the DW72 cloud chamber CCN distribution and the X1 tail at three parcel ascent rates. All CCN were assumed to be pure ammonium sulfate.

Figure D-18 indicates that high vertical speeds through cloud base result in larger concentrations of cloud droplets. These results show that, at a constant ascent rate, more activated drops result in a smaller mean size for the cloud droplets, resulting in reduced collision efficiencies with larger drops. This effect is partially compensated for by the increased opportunities for collisions resulting from the higher concentrations of cloud droplets. The development of precipitation is only slightly retarded by the presence of more cloud droplets.

Figure D-18 shows that, if three identical parcels are lifted through cloud base at different vertical speeds, different numbers of activated cloud droplets result. If the three parcels then ascend at equivalent rates above the activation region, the results on radar reflectivity can be anticipated. The results presented in figure D-6 indicated that the parcels would arrive at 20 dbZ in almost the same duration of equivalent ascent rates. For different assumed updrafts in figure D-18, the parcel with the higher updraft speed would have reduced time at each pressure level for collisions within the parcel to occur and thus the results of figure D-18 would be expected. The reduced time at each level is partially compensated for by the increased size of the condensing cloud droplets at each succeeding elevation. However, given the results of figure D-6, this effect is felt only after the precipitation has been delayed. If identical numbers of cloud droplets are activated, the cloud droplets in parcels with greater updraft speeds would survive to higher levels and thus larger sizes before being swept out by larger droplets.

Figure D-19 shows the predicted drop distributions for the cases shown in figure D-18 at a radar reflectivity near 15.7 dbZ. At this point, the peak of the cloud droplet spectrum for the 0.5, 1.0, and 4.0 m s^{-1} cases was at 8.5, 8.5, and 9.0 μm radius, respectively. The larger, more numerous cloud droplets produced in the 4.0 m^{-1} case would allow more efficient accretion of cloud droplets by the larger drops. Figure D-19 indicates that the 4.0 m s^{-1} case has not had sufficient time for the collection process to spread the distribution to the same largest drop sizes of the 0.5 and 1.0 m s^{-1} cases. In any event, the smaller maximum precipitation drop size in the 4.0 m s^{-1} case would only serve to increase the difference in the elevation of equivalent radar reflectivities between this and the other two simulations if sedimentation effects were included. The factors influencing the shape of the large drop end of the distribution, such as the rate of growth of the cloud drops, their concentrations, and the time for the spread of the distribution to larger drops, all combine to result in little difference in the 0.5 and 1.0 m s^{-1} maximum drop size at 15.7 dbZ.

In order to better model the effect of variations in cloud updrafts, several computations were made with a vertical speed that increased at the rate of 2.0 m s^{-1} km^{-1} after saturation was achieved with a constant vertical ascent rate of 1.0 m s^{-1} in subsaturated conditions. The UW72 cloud chamber CCN distribution with ammonium sulfate as the soluble portion of the CCN was used in these calculations. The results are shown in figure D-20. The tail of the CCN distribution was varied to include the completely soluble X1 and *X1/2* tail, a X1 tail with the CCN mass only 5% soluble beyond 5 *μm*, and an 'insoluble' X1 tail beyond 5 *μm*. The 'insoluble' CCN are active CCN that are primarily composed of insoluble compounds with a very thin coating of soluble material. These results when compared with previous results show that the distance between the levels at which a given value of radar reflectivity is achieved, increases from the corresponding constant 1.0 m s^{-1} case. The parcels achieve vertical speeds of between 4.6 and 6.4 m s^{-1} at the 20 dbZ level. There is about 900 m separating the extreme cases with variable vertical speeds as compared with 300 m for a constant 1.0 m s^{-1} ascent.

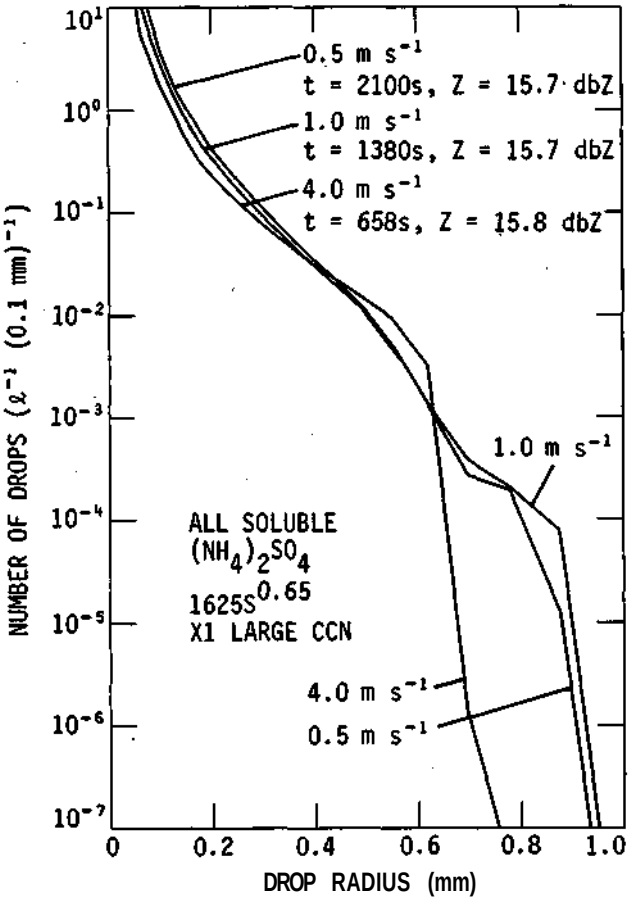

Figure D-19. Computed precipitation distributions at nearly constant radar reflectivities for the cases from figure D-18

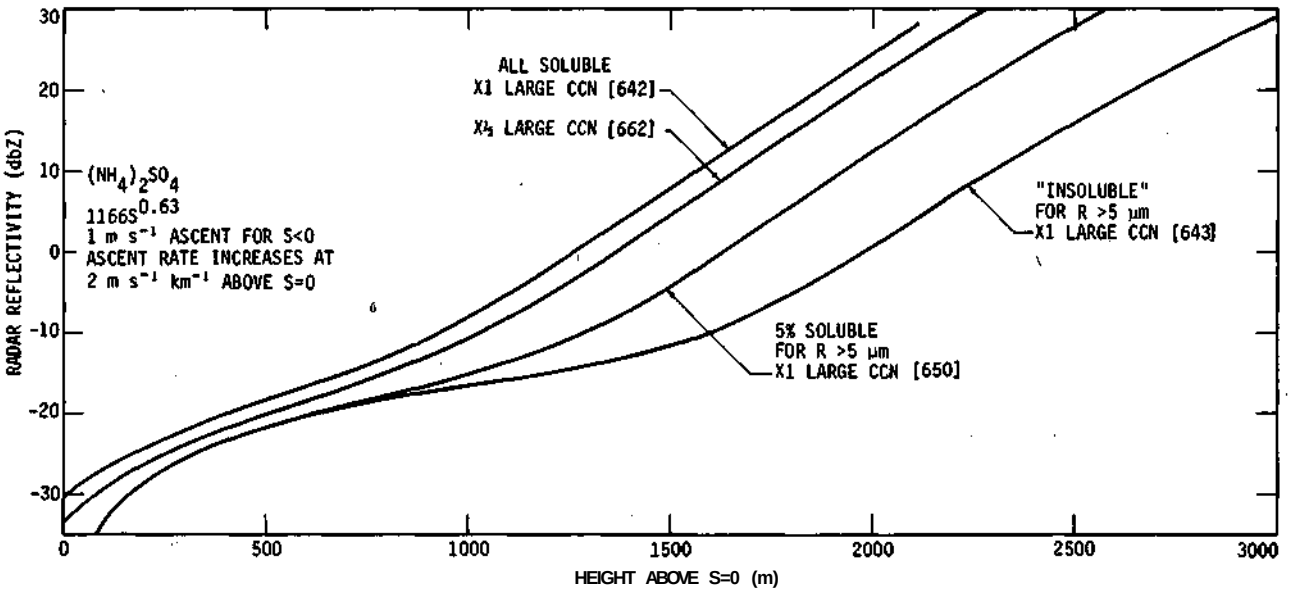

Figure D-20. Computed radar reflectivity factor for an accelerating ascent rate above the point at which the parcel achieves saturation

Three calculations were made to investigate the effect of varying the rate of increase in updraft speed above the region where activation occurs. The results are presented in figure D-21. A hypothetical cloud chamber CCN distribution of 1000 $S^{0.7}$ was coupled with the X1 large CCN distribution for these calculations. The ascent rate was held constant at 3.0 m s^{-1} until a liquid water content of 0.1 g m^{-3} was achieved. At this point the activation stage was completed and each parcel contained 939 cloud droplets. Beyond this point the vertical speed of the parcels was increased at 1.0 and 2.0 m s^{-1} km^{-1}. The radar reflectivity of 20 dbZ was achieved in 567 and 523 s beyond the 0.2 g m^{-3} point, as opposed to 621 s for the constant 3.0 m s^{-1} case. The corresponding difference in elevation for the extreme cases at 20 dbZ was about 900 m.

An examination of the predicted precipitation distributions for these cases showed essentially identical distributions at equivalent radar reflectivities. The saturation mixing ratios and liquid water contents are different since the elevations of these equivalent reflectivities are significantly different. Recalling that the drop distributions were identical at a liquid water content of O.lgm^3, the parcels that attain a greater elevation at a given value of radar reflectivity should contain larger cloud drops. For example, at 15 dbZ the parcel with a constant ascent rate contained cloud droplets with a mean size of 9.8 µ rn while the parcel with the 2.0 m s^{-1} km^{-1} increasing ascent rate contained droplets with a 10.9 µ m mean size. However, the constant updraft parcel required 90 s longer to achieve the 15 dbZ level. Thus, the constant updraft parcel had a longer time for collections to spread the spectrum to larger sizes, but it had slightly smaller cloud droplets which would inhibit transfer of liquid water to the precipitation distribution. These compensating effects lead to an almost identical largest size drop at a given value of radar reflectivity for the cases presented in figure D-21. This does not mean, however, that sedimentation effects would not significantly alter the elevation difference between equivalent reflectivities in these situations. The higher vertical velocities attained in the cases that develop detectable radar reflectivities at greater elevations means that these parcels would be more likely to carry precipitation aloft than the lower, slower moving parcels. For example, at the 20 dbZ level the 0.0, 1.0, and 2.0 m s^{-1} km^{-1} cases achieved vertical speeds of 3.0, 5.3, and 8.5 m s^{-1}, respectively. Thus, sedimentation effects would tend to further separate the vertical locations of detectable radar reflectivities in these cases.

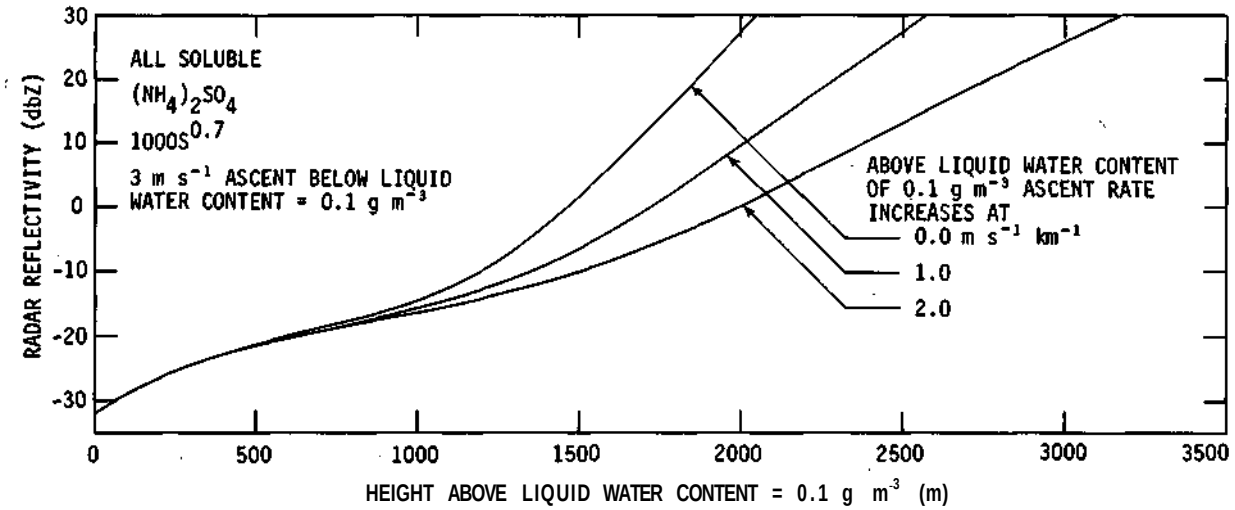

Figure D-21. Computed radar reflectivity factor for various lapse rates of parcel velocity above the point at which a liquid water content of 0.1 g m^{-3} is achieved

Review of Some Relevant Observed Data

. Fitzgerald and Spyers-Duran (1973) and Braham (1974) found increased concentrations of CCN in air samples gathered downwind of the St. Louis urban-industrial complex compared with similarly obtained upwind samples. Their measurement techniques, however, preclude use of these data for determination of giant CCN concentrations. These researchers also reported measurements of cloud base droplet distributions over and around St. Louis. These measurements indicated that urban and downwind cloud base droplet distributions contained a greater concentration of droplets than upwind distributions. For example, Fitzgerald and Spyers-Duran (1973) reported average cloud droplet concentration increases in downwind clouds of 1.7 and 1.5 times similar upwind clouds during two days in August of 1971. They also pointed out that the cloud droplet concentration increases were consistent with the increased average CCN concentration in the air ingested by these clouds. This consistency was demonstrated with Twomey's (1959) equation.

Radar observations of first echoes in the St. Louis area have been reported by Braham (1974) and Dungey(1977). Braham (1974) reported that urban-rural differences in the temperature of first echo tops typically ranged between 2 and 5° C depending on the temperature at the echo top. He also indicated that about 65% of urban and 50% of rural first echo tops occurred at altitudes below the –4° C level indicating a high probability that warm rain processes are important to first echo development in the St. Louis area. Dungey (1977) used a more extensive data set from 1972 through 1975 and determined that the average urban first echo base height was 335 m lower than the average rural echo base. The average difference in first echo top heights was 60 m. The Water Survey results in this volume show echo base differences of 500 m (urban lower) and top differences of 100 m (urban higher), as shown in table D-15 (page 276). The urban echoes in both analyses were defined as those occurring directly over the St. Louis-Alton-Wood River area.

Semonin and Changnon (1974) presented average cloud base observations from the summer of 1972. These data indicated that cloud bases in an area approximately encompassing St. Louis and East St. Louis had bases that averaged 300 to 600 m higher than clouds in rural areas. Other data support this average difference. Ackerman and Appleman (1974) presented average pre-rain soundings in the center of the city at the St. Louis Arch and 22 km east . These data indicated approximately 600 m greater elevation for the convective condensation level at the Arch. Further support is derived from the numerous surface and aircraft data which indicated that the boundary layer was warmer and drier in the urban area (see, for example, Sisterson, 1975).

The increased cloud droplet concentrations and the lesser distance between cloud base and the first echo base found in urban clouds led Braham (1974) and Semonin and Changnon (1974) to hypothesize the presence of increased concentrations of giant CCN to explain the apparent increase in efficiency with which urban clouds produce first echoes. In fact, Johnson (1976) measured increased concentrations of large particles in urban air compared with air over the rural surroundings. He indicated that particles in both urban and rural samples appear to be insoluble with a thin coating of soluble material (personal communication). There are no direct measurements of the partial solubility of these large particles in the St. Louis area. However, Ochs and Gatz (1978) have measured the average solubility of all particles greater than 5µ m diameter during a 2-week period in the summer of 1977 in Champaign, Illinois. The average percentage of soluble material was found to be 30%.

From these observations we conclude that the cloud base to first echo base distance averages between 650 and 1100 m less in urban clouds (those occurring over St. Louis and East St. Louis) than in surrounding rural clouds.

Discussion of Model Results and Further Speculation

This section has concerned the investigation of the effects of various CCN properties on the development of precipitation in the St. Louis urban area. Concentrations of giant CCN have been set forth as a potential contributing factor in explaining the urban effect on precipitation. In order to isolate the effect of CCN properties on precipitation development, a closed parcel model was employed. No mixing or entrainment was allowed and sedimentation effects were neglected. The implications of these approximations on the results were discussed. An important point is that no attempt has been made to attach any great significance to the predicted elevations of particular values of computed radar reflectivities. Results of one calculation were always compared with another with the idea that a relatively large effect was being sought.

Variations in CCN concentrations in the small, large, and giant size ranges cannot be used to explain the METROMEX observations. Variations in concentrations were made which met or exceeded the maximum spread in the field observations. This result is in agreement with the predictions of Hindman et al. (1977).

A point of peripheral interest is that computations with the model used do not indicate that the giant nuclei are important to the precipitation process. Figure D-22 shows the results of systematically eliminating CCN whose size exceeds given values. For the distribution of soluble CCN employed in these computations, particles greater than 40 μm in radius have little effect on the time of development of a given radar reflectivity. This occurs because their initial concentrations are too low to be effective. On the other hand, if CCN greater than 5 or 10 μm are eliminated, the development of precipitation is retarded significantly. Thus, the model only suggests that variations in giant CCN concentrations of the magnitudes observed in the St. Louis area do not appear to account for the echo and cloud observations.

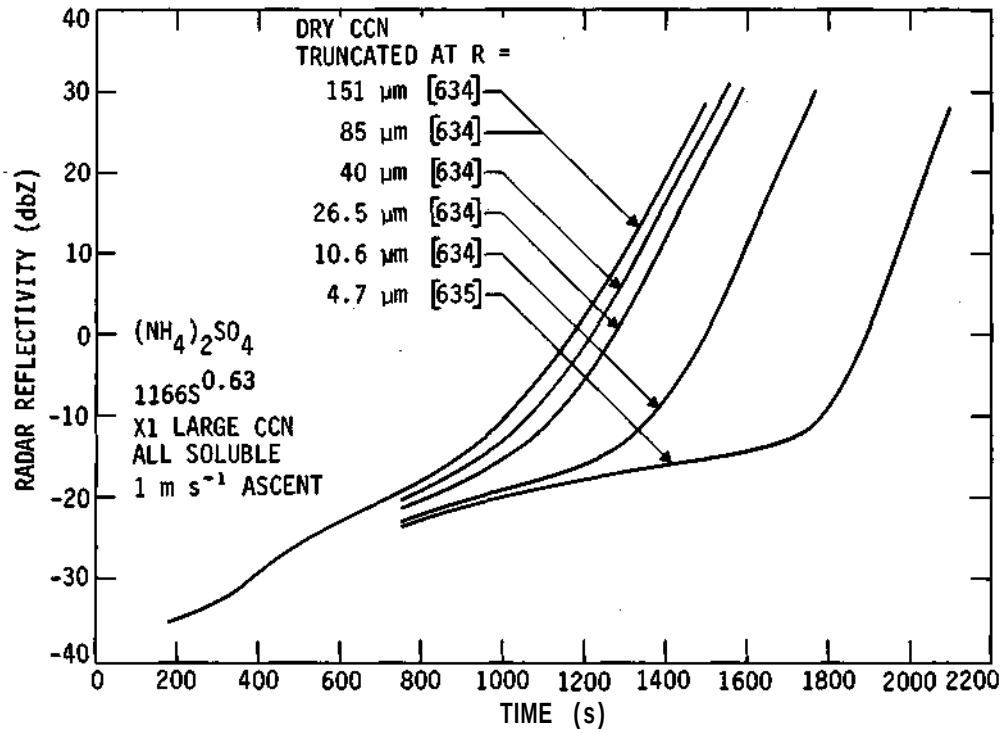

Figure D-22. Computed radar reflectivity for parcels with CCN distributions truncated at various dry CCN radii

Effects of variations in the chemical or physical makeup of CCN and their effects on precipitation evolution were also studied. One could hypothesize that more hygroscopic anthropogenic CCN in the urban area contribute to the observed effects. The results, however, suggest that differences similar to those between sodium chloride and ammonium sulfate are insufficient to explain the field observations. Therefore, if one were to use the hygroscopic nature of the CCN as the explanation for the observed differences in urban-rural cloud base to first echo distances, one would have to argue that the St. Louis-East St. Louis area produces extremely hygroscopic CCN that are not present elsewhere. However, the model results show that these highly hygroscopic CCN would probably lead to a reduction in the number of activated cloud droplets. Since this tendency is contrary to the observed increases in cloud base droplet concentrations in urban clouds, the hypothesized explanation of the observations based on hygroscopic CCN seems invalid.

The modeling results, as well as the available observational evidence, suggest that the partial solubility of the largest CCN is probably not the explanation of the field observations. Results suggest that large differences in the giant CCN partial solubility would be required to explain the observations. However, there is some qualitative observational evidence that the required large difference in urban-rural giant CCN partial solubility does not exist (D. B. Johnson, personal communication).

Results of this modeling research suggest that dynamic effects could easily account for the cloud-echo observations. There are increases in average cloud base heights above the St. Louis-East St. Louis area. Urban and rural soundings show a drier and warmer subcloud layer over St. Louis than over eastern rural areas. These data also show that the average pre-rain soundings were very similar above the cloud base predicted by the convective condensation level over St. Louis. Since new convective clouds over St. Louis have higher cloud bases, they would develop along moist adiabats with lower equivalent potential temperatures than similar rural clouds. The cooler temperatures in the St. Louis clouds would result in less buoyancy and thus reduce updraft speeds in similar above cloud base environments. This reasoning suggests that the dynamic effects of reduced updraft speeds in clouds developing over St. Louis could explain the observations.

Dungey (1977) reports a 240 m reduction in first echo heights for clouds located downwind by 1, 2, and 3 hours when compared with rural echoes. The downwind regions were defined by determining a first echo steering wind derived from first echo movements and projecting the city area in the appropriate direction for 1, 2, and 3 hour periods. Semonin and Changnon's (1974) cloud base data indicate that the cloud bases in these downwind areas are probably similar to those in the surrounding rural area. The small difference in cloud base to first echo heights between the clouds in these downwind areas and rural areas are probably explainable in terms of differences in CCN concentrations or physical properties.

Future research should test the hypothesis presented here for explaining the observed cloud base to first echo distances. A time-dependent cloud model which incorporates a detailed simulation of cloud microphysics could be used for this purpose. Current models with Eulerian grid spacings should be sufficient to assess the observed difference between average cloud base and first echoes over the city and rural areas. These differences of ~ 1000 m should be detectable in models with grid spacings of about 100 m providing that sufficiently accurate numerical techniques are employed. Ackerman and Appleman's (1974) pre-rain soundings could be used. Much smaller distances might be difficult to assess since results could be susceptible to numerical errors. Another aspect of this topic worth pursuing would be to subdivide Dungey's (1977) city area to determine if there are any significant differences between first echoes occurring over the St. Louis-East St. Louis area and the Alton-Wood River area. This might be possible if a large enough data set is available.

RADAR ANALYSES OF URBAN EFFECTS ON RAINFALL

F. A. Huff

Processed radar echo data for the FPS-18 (10-cm) system were analyzed for 35 storm periods during the summers of 1972-1975. These storms were selected because of the high quality of both radar and rainfall data. They include a representative sample of convective storms of varying intensity, duration, volume, and synoptic type. Analysis was made of the spatial distribution of the initiation of radar echoes (convective entities) with primary emphasis on comparison of initiations in potential urban-effect, hill-effect, and rural regions of the experimental area. Mergers of radar echo systems, which frequently precede intensification of surface rainfall, were investigated and assessed with respect to urban effects and hill effects on their occurrence. Statistical summaries were made of the movement, duration, and other definitive parameters of the echo characteristics, with stratifications according to urban, non-urban, and topographic exposures in their development and/or movement. All echo values discussed herein are based on near surface measurements.

During 1971-1974, the radar system consisted of an FPS-18 with peak power output of one megawatt operating with a 12-foot diameter antenna which scanned at a fixed elevation angle of 0.5 to 1 degree (Brunkow and Morgan, 1973). Digitization of the radar output was accomplished in the field, and the digitized data were fed into an electronic integrator for initial processing. The data were archived on standard digital computer tapes through use of a video processor. In 1975, the system was modified through installation of a new 20-foot diameter antenna (narrower beam), a new digital video integrating processor with magnetic tape recording, and a mini-computer (TI-980) to control the radar operations and data recording. The 1975 modifications made the radar system adaptable to 3-dimensional analysis of radar echoes in the experimental area.

The FPS-18 was operated with a minimum detection level of 27 db in 1972, 32-42 db in 1973, 32 db in 1974, and 25 db in 1975. This inconsistency has limited the direct comparison of analytical results to some extent, but much useful information relative to the urban rainfall effect was obtained from the radar echo records. In the various analyses, it was decided to employ a grid system with unit areas of 23 km^2 which are approximately equivalent to the area represented by each raingage in the METROMEX network. The FPS-18 was located at the Pere Marquette Headquarters (PMQ) which was too close to the extreme NW portion of the raingage network for reliable echo analysis in that region. Consequently, the area within a 26-km radius from PMQ (figure D-23) was not used in the network echo studies. This eliminated 30 of the grid squares (690 km^2) in the NW part of the research circle of 40-km radius. In some analyses, four of these smaller grid squares were combined to provide averages over 92 km^2. This was done where the sample size was relatively small, or where a broader areal division appeared desirable.

Radar Echo Initiations

Initially, all echo intensity centers (reflectivity centers) for each minimum reflectivity level were examined separately by plotting the locations on the grid base map. An echo intensity center was defined as a closed center (gain step) of maximum reflectivity associated with a radar echo system. The system could contain one or several intensity centers. In a multicellular echo

system, each separate intensity center was counted in tabulating the echo initiations. For each season, a rainfall map was also constructed for the period in which the echoes were recorded on the integrator. Because of the size of the radar sample, it was decided to combine the data for the four summers despite variations in the minimum detection level. This provided a much larger sample which permitted more precise definition of echo initiation areas through use of the 23-km^2 grid. Despite the change of detection level with time, all parts of the network were exposed to the same situation, so that the total 4-summer pattern should provide a satisfactory first estimate of the near surface echo initiation distribution on the METROMEX network.

Figure D-23 shows the total number of occurrences of echo initiations in the sample of 35 storms involving 1550 initiations in the summers of 1972-1975. A total of 29 initiations in the 23-km^2 grid just south of Wood River was outstanding within the network. Oil refineries and other industries in this area provide heat, moisture, and aerosols for potential cloud nuclei. Since there are no significant topographic features in this major initiation area, it appears that initiation

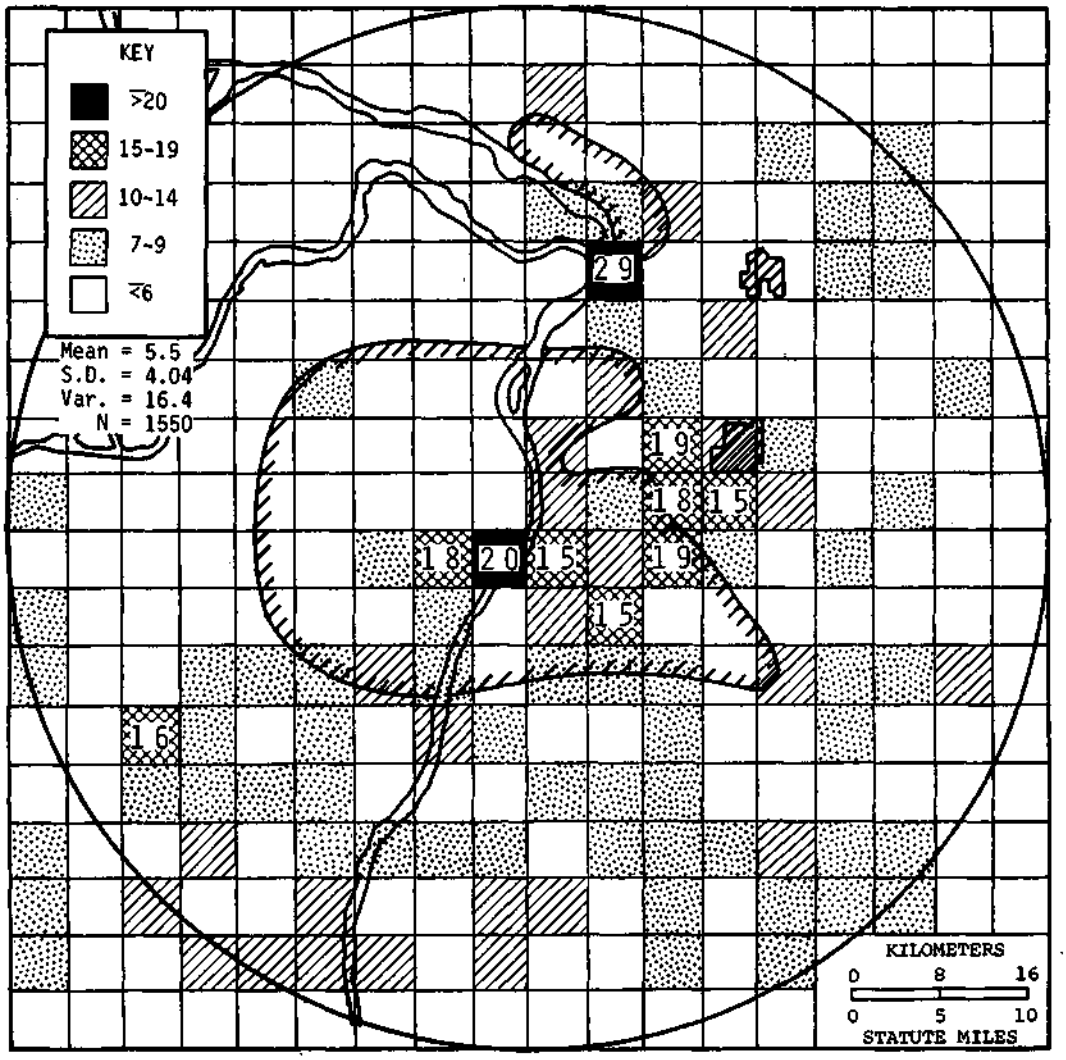

Figure D-23. Radar intensity center initiations in 23 km^2 grids, 1972-1975

and/or intensification of convective clouds are favored in this particular region because of urban-industrial effects.

Other outstanding areas of high frequency were located in and just east of St. Louis. In general, these initiation highs were over or just downwind (NE, E, SE) of regions of heavy industry and dense urban structures. Another high exists in the Ozark foothills SW of St. Louis. The mean grid square frequency for the 23-km^2 grids was 5.5 for the 35 storms with a standard deviation of 4.0. Thus, the 29 occurrences near Wood River was over five times the network mean, and those in south St. Louis (18, 20 in figure D-23) were over three times the network mean. These statistics indicate a pronounced preference for echo initiation in certain locations in potential urban-effect regions. Approximately 26% of the grid squares had 2 or less initiations, and only 13% had more than 10 occurrences. Of 35 grid areas exceeding 10 occurrences, 63% (22) were in or near the urban-industrial regions of St. Louis and Alton-Wood River.

Figure D-24 provides a broader scale description of the distribution pattern of echo initiations. Here, the frequency in 92-km^2 grids is shown for the 35 storms. The maximum frequency

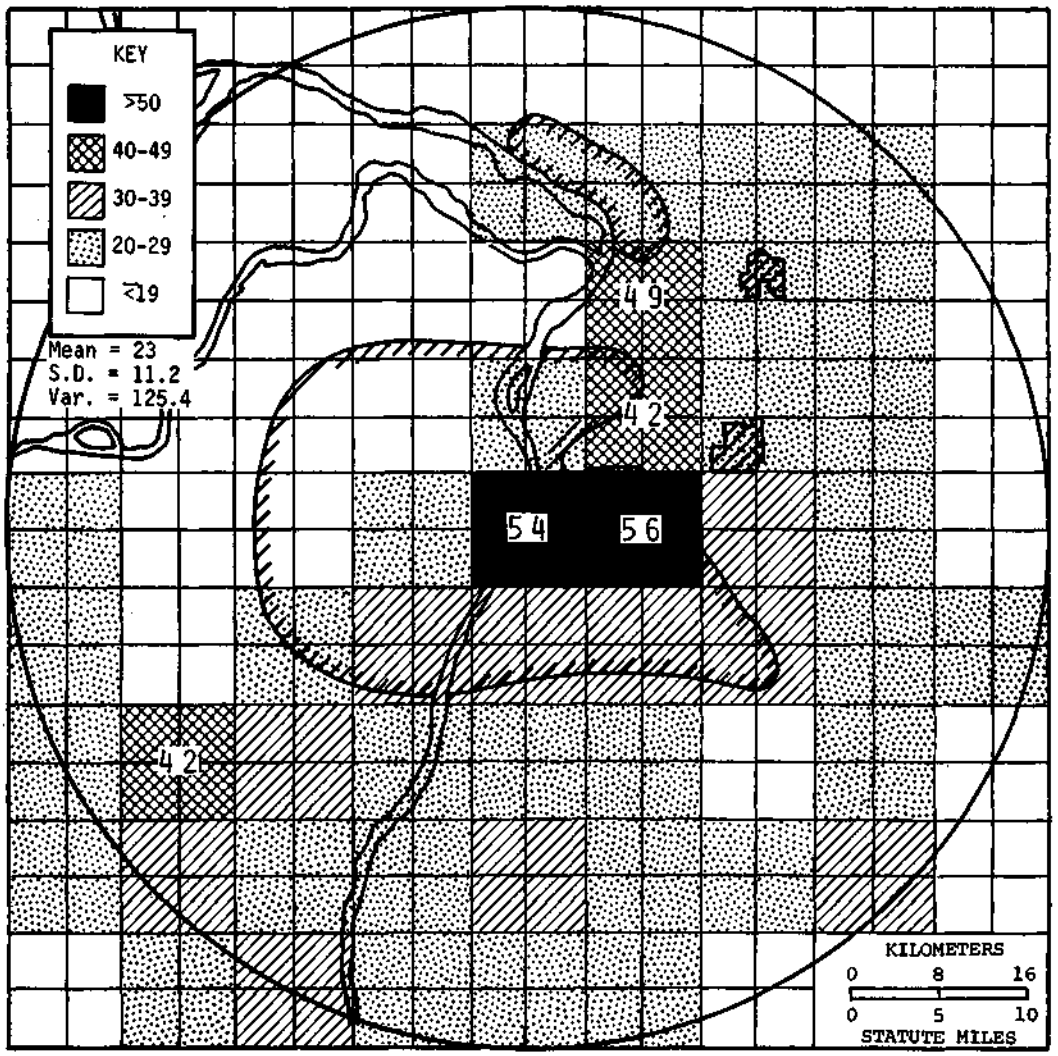

Figure D-24. Radar intensity center initiations in 92 km^2 grids, 1972-1975

occurred in the major urban-industrial region across East St. Louis and then northward to Granite City and Wood River. Another smaller region of high frequency occurred in the Ozark foothills, SW of St. Louis.

Figure D-25 shows the total rainfall occurring during the period in which radar echoes were recorded in the 35-storm sample. In general, correspondence between the rainfall and echo initiation patterns was fair. High echo frequencies and heavy rainfall amounts closely coincided in the East St. Louis-Collinsville-Belleville area, and a secondary high in both patterns was located east of Edwardsville. West of the St. Louis urban region, there were lows in both the rainfall and echo initiation patterns. However, association between the two patterns was poor in the Ozark foothills southwest of St. Louis where high initiation frequencies occurred in areas of relatively light rainfall. Apparently, the initiations over the Ozarks resulted in lighter rainfalls, on the average, than those in the urban-effect regions. Indirectly, this indicates a stronger enhancement mechanism in the urban region.

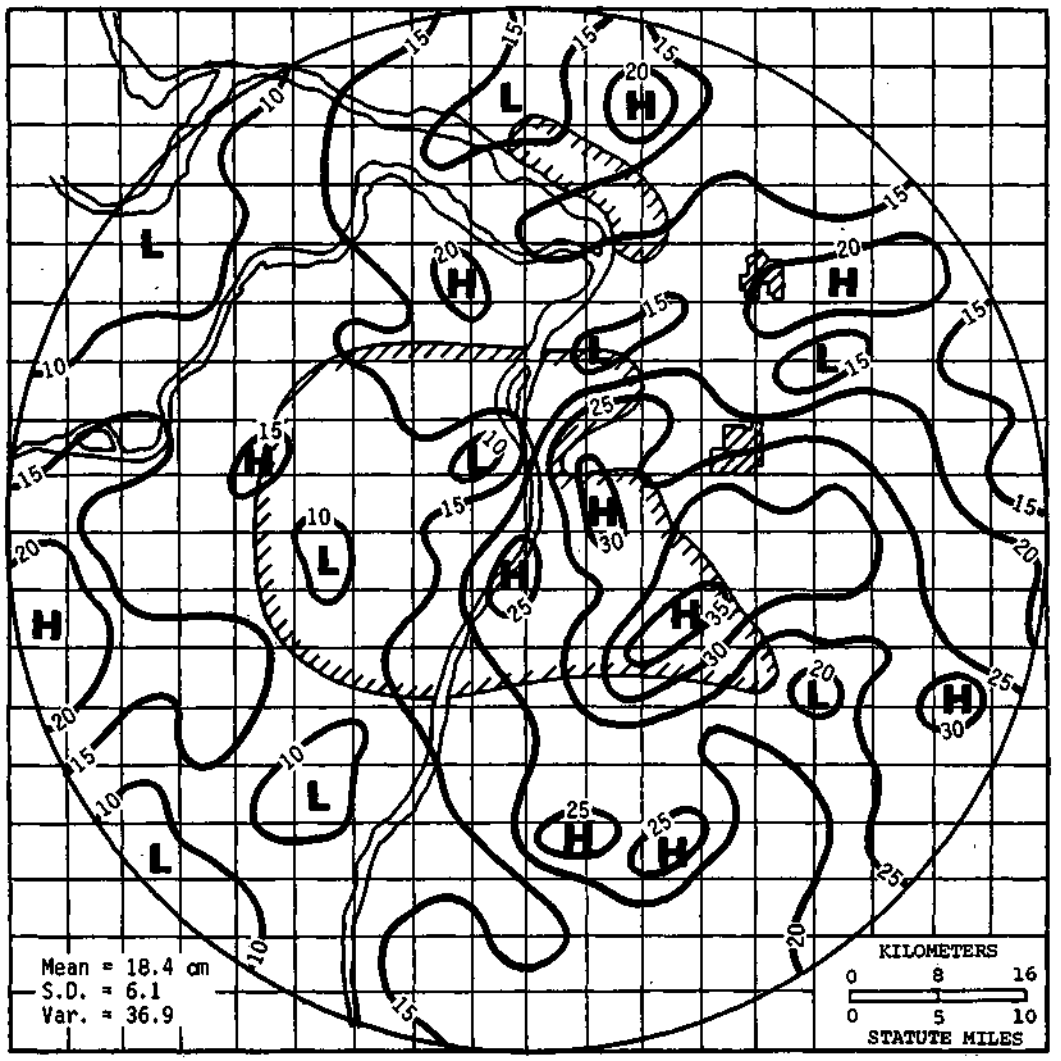

Figure D-25. Rainfall (cm) in 35-storm sample of radar echoes, 1972-1975

Normalization of Echo Initiation Distribution

A simple normalization procedure was used to minimize the rainfall effect on the echo frequency pattern. In doing this, an average rainfall (R) was determined for each grid square. Then, the number of initiations (I) in each grid square was divided by the number of echo initiations per inch (25 mm) of rainfall. This normalized pattern is shown in figure D-26.

Figure D-26 shows that the two highest area frequencies in the normalized pattern are just south of Wood River and in the Ozark foothills southwest of St. Louis. The value of 4.03 at Wood River is over four times the network mean of 0.91, and the Ozark high of 3.20 is over three times the areal average.

The normalized pattern shows a large area of high frequencies in the SW part of the network which is in the Ozark foothills. In fact, 7 of the 12 highest ratios were located in this region. This indicates that the Ozark foothills are a favorable region for the development and/or intensification of convective activity, and consequently, raincells. Since these hills are recognized as a

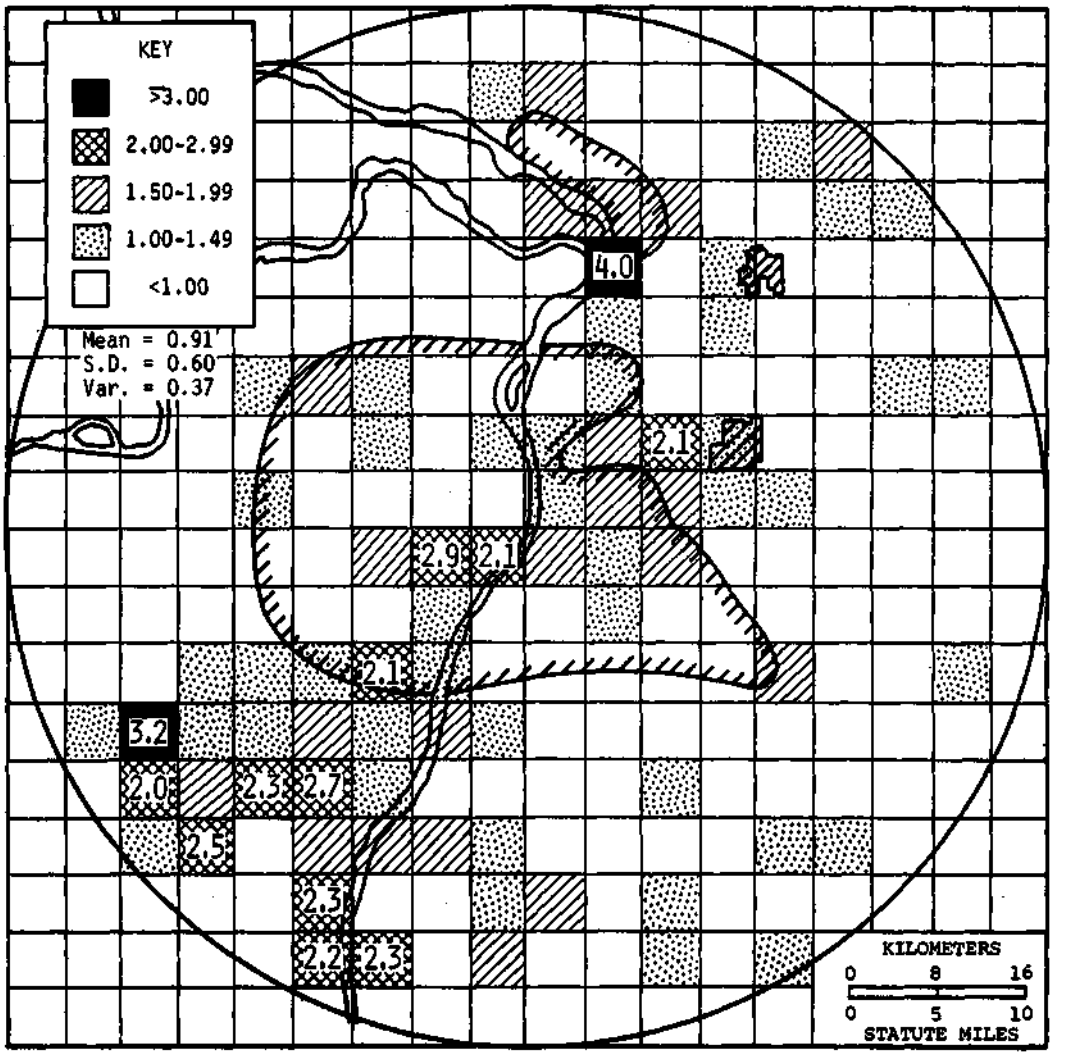

Figure D-26. Echo initiations per 25 mm of rainfall during 1972-1975

region where convective activity is likely to be stimulated, the finding is not surprising. In fact, it is reassuring, since it provides evidence that our 35-storm sample may be reasonably representative of average conditions. The satellite cloud results also show that the hill area was one of frequent cloudiness.

Assuming the distribution in figures D-23 and D-26 are reasonable approximations of the average distribution, one would conclude that raincells are most likely to develop and/or intensify near Wood River, across the south-central and eastern portions of the urban-industrial area of St. Louis, and in the Ozark foothills. Overall, the greatest frequencies occurred in and downwind of the urban-industrial areas and in the SW hills. Thus, the radar analysis has provided support for the presence of urban and hill enhancement of convective activity in the METROMEX area through more frequent development of convective entities in these regions.

Radar Echo Mergers

Since mergers of convective clouds and rain systems have been shown to be associated frequently with rain intensification (Huff, 1967; Simpson et al., 1972), the 35-storm sample was used to investigate echo mergers as depicted on the near-surface echo data. Merging was counted only for echo joining between distinct echo systems. A radar echo system was defined as an echo entity separated in space from all other echoes, and the system could (and often did) consist of one or several intensity centers within its enveloping isoecho. This is analogous to the surface raincell definition used in the METROMEX studies (see page 280).

A total of 138 mergers was identified in the 35-storm sample. This corresponds to an average of approximately 4 per storm in the experimental area. These mergers were summarized and plotted on a 92-km^2 grid on the METROMEX network (figure D-27). Because of the relativel small sample size, results cannot be considered conclusive. However, evidence was found that mergers are favored in urban and hill areas.

The grid squares with the most occurrences (8, 11) were on the east edge of the St. Louis urban-industrial area. The network average per grid square was only 2.1. Approximately 36% of the mergers were within the region bounded by St. Louis, Belleville, and Collinsville, which is frequently within the potential urban-effect region. Comparison of figures D-25 and D-27 shows the heaviest rainfall in and east (downwind) of the region where it is closely aligned with the region of most frequent mergers. In fact the maximum of 11 mergers in figure D-27 coincides with the peak of 35 cm in the rainfall map of figure D-25.

Properties of Echo Intensity Centers

The intense centers of echoes in the 35 selected storms were analyzed for several properties Analyses of the echo centers were made of duration, maximum intensity (dbZ), path length, speed and direction of movement. The echo intensity centers were stratified into the following groups: urban effect, potential urban effect, no effect or control, and hill effect centers. There was an inadequate sample of centers from the bottomlands to study. Centers crossing the hill-urban area or the bottomlands-urban area were also eliminated from the analyses because of very few occurrences.

An urban-effect center was defined as one that developed within the urban-industrial area or passed over this area during its lifetime. A potential urban-effect center was defined as one first detected 1) within 8 km downwind of St. Louis or Alton-Wood River, or 2) within 20 minutes travel time from either the St. Louis or the Alton-Wood River urban-industrial areas, based upon the existing steering winds.

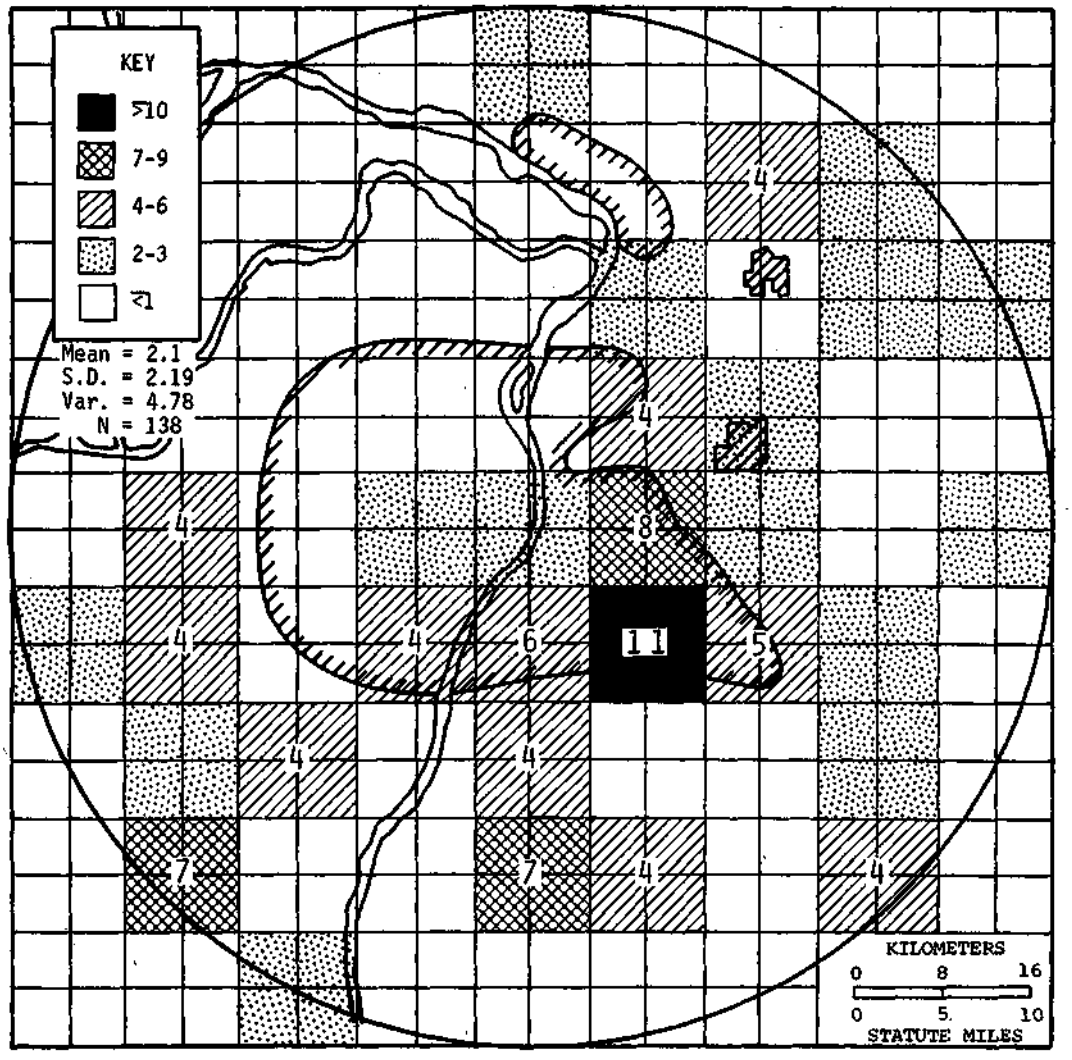

Figure D-27. Radar echo system mergers, 1972-1975

Table D-14 provides a summary of the mean values for moving and quasi-stationary centers for each of the land use-topography stratifications. Duration, path length, and maximum intensity provide a measure of the size and intensity of the echo centers. Comparisons of urban-effect and no-effect moving center echoes show the urban centers have considerably longer durations (+45%) and path lengths (+75%), and higher maximum intensity (+10%). No significant difference was noted in the mean speed of the urban and non-urban echo centers. Except for shorter path length, hill-effect centers were similar to urban-effect storms. The most frequent direction of motion was from 241 to 260° for both urban and no-effect moving centers.

The quasi-stationary center means in table D-14 show a substantially longer duration (+67%) for the urban centers compared with the no-effect centers, and a slightly higher maximum intensity (+8%). The urban quasi-stationary centers are also considerably longer in duration (+50%), on the average, than the hill-effect centers. The statistics in table D-14 provide further substantiation of

Table D-14. Statistical Summary of FPS-18 Echo Center Properties

Echo type	N	Duration (minutes)	Maximum intensity (dbz)	Path length (km)	Speed (knots)
Means for moving centers					
Urban effect	221	29	43	14	20
Potential urban effect	145	22	42	11	21
No effect	359	20	39	8	21
Hill effect	178	28	43	10	19
Means for quasi-stationary centers					
Urban effect	123	15	40		
Potential urban effect	77	9	36		
No effect	227	9	37		
Hill effect	96	10	38		

both an urban and hill enhancement of convective entities, and indicate the urban influences exceed the hill effects on precipitation processes.

The means of duration, path length, and maximum intensity for the moving centers in the potential urban-effect class in table D-14 were between the urban-effect and no-effect values. These statistics suggest that echo intensity centers developing downwind of the urban-industrial areas may experience enhancement, but of a lesser degree than those developing directly over the urban-industrial areas.

As shown earlier, the most frequent region of echo initiation in the 35-storm sample was in the Alton-Wood River refinery area. Observations of METROMEX personnel and cloud cameras have indicated the development of convective clouds and rainfall over this area with little or no movement of the convective entity. Radar analyses showed 47% of the Alton-Wood River echoes were quasi-stationary compared with 32% at St. Louis. It is likely that the lack of apparent movement results from the dissipation of the urban-generated system as it moves away from its generation source. A good example of this was in the early stages of a very heavy storm during the evening of 25 July 1973 (Changnon and Huff, 1975) when radar echoes appeared to be quasi-stationary in the above region for approximately 90 minutes before moving northeastward and intensifying.

Summary and Conclusions

Analyses were made of near-surface (PPI) echo observations from 35 storms sampled with the 10-cm, FPS-18 radar during 1972-1975. Major emphasis was placed upon preferred areas of echo initiation and echo mergers in the METROMEX network of 5200 km^2. There were 1551 initiations and 138 mergers identified in the 35-storm sample within the experimental area. Results of the echo initiation analyses indicated a strong trend for echo initiations to occur most frequently in the vicinity of Wood River, in south St. Louis, and in the Ozark foothills SW of St. Louis. Overall, a relatively high frequency of echo initiations occurred in the urban-industrial regions of St. Louis and Wood River and E and NE of St. Louis in the Edwardsville-Collinsville-Belleville region, where downwind effects would most frequently occur because of the pronounced trend for storms to move across the METROMEX network with a westerly component.

Analysis of the most frequent location of echo mergers, which are frequently associated with the intensification of surface rainfall, indicated a preference for the area extending east from St. Louis. This is a portion of the network that is frequently exposed to potential urban effects. Another preferred merger area was found in the Ozark Hills which is a favored breeding area for convective activity.

Comparison of average properties of urban and non-urban echoes showed that those intensity centers exposed to urban effects had longer durations and path lengths, and higher maximum intensity than the unaffected echo centers.

In general, radar analyses have provided evidence of an urban effect on rainfall in the St. Louis metropolitan area, and have contributed substantially to our knowledge on the subject. The radar has been valuable in defining regions where the urban effect is most pronounced, and also in evaluating topographic effects upon rainfall in the experimental region.

VERTICAL CHARACTERISTICS AND BEHAVIOR OF RADAR ECHOES

Stanley A. Changnon, Jr.

The operation of a TPS-10 (3-cm wavelength) radar with a RHI (range-height indicator) capability by the Water Survey at the Pere Marquette site 50 km NW of St. Louis provided an interesting set of data to investigate certain characteristics of precipitation entities, displayed in the vertical. A semisystematic operation of this system in the July-August 1973 period provided a set of data for two studies designed to gain information about urban effects on the vertical dimensions of radar echoes.

One study was aimed at an investigation of first echoes (FE), that part of a cloud where radar detectable precipitation droplets first form. First echoes provide information useful for interpreting the processes involved in precipitation development. In particular, comparison of first echo statistics from different land use areas can indicate the presence of any local influences. This research, although based on data from only one summer, was considered a useful adjunct to the more extensive first echo study conducted by the University of Chicago (Braham and Dungey, 1978). They used data from an identical radar at a site 130 km east of the PMQ site. Thus, the PMQ data in this study provide echo results for an area west of the area sampled by the Chicago radar.

The other study investigated the effects of the urban area on the behavior of the tops of individual echoes throughout their lifetimes. This was accomplished by studying and comparing the echo top histories of echoes sorted by urban vs non-urban classes, and also by merger vs non-merger classes. Echo top behavior was chosen for study for two reasons. First, echo tops reflect the convective strength and behavior of summer showers and thunderstorms. Second, since vertical radar data were available only with a 3-cm radar, potential analyses of echo volumes and reflectivities would be undesirable and biased by attenuation problems. Such is not the case with tops which are largely unaffected by signal attenuation. Furthermore, echo tops are generally indicative of the extent of precipitation development and of echo volume.

Data and Analysis

The TPS-10 (3-cm wavelength) radar has an RHI capability so that it displays 2-dimensional (height-distance) aspects of echoes. Photographs were taken each second of the RHI display for a 2 beam width. Two-dimensional echo descriptions were developed from these data. Data collected in July-August 1973 between 0800 and 2400 CDT were used. Most of the echoes occurred in a 115^{o} sector centered on St. Louis (located 50 km SE of the radar) and in a range span (ring) of 16 to 88 km from the radar (figure D-28). Since this radar is subject to attenuation problems, the only echoes studied were those considered to have little or no effects from intervening echoes.

Data were from 19 discrete rain periods, most of which represented all the echoes on a given day. The sampling period in 1973 was one of near-average summer rainfall throughout much of the echo study area, being greatest east of St. Louis and least west.

Data were collected on the bases and tops of 811 first echoes. These included 385 classed as isolated, which came largely with synoptic weather conditions classed as air mass, squall zones, and warm or stationary fronts. The other 426 first echoes were classed as being with organized systems, and most came with squall lines and cold fronts. The first echoes (FE) were investigated on the basis of their being with organized systems or isolated systems and also on a regional basis.

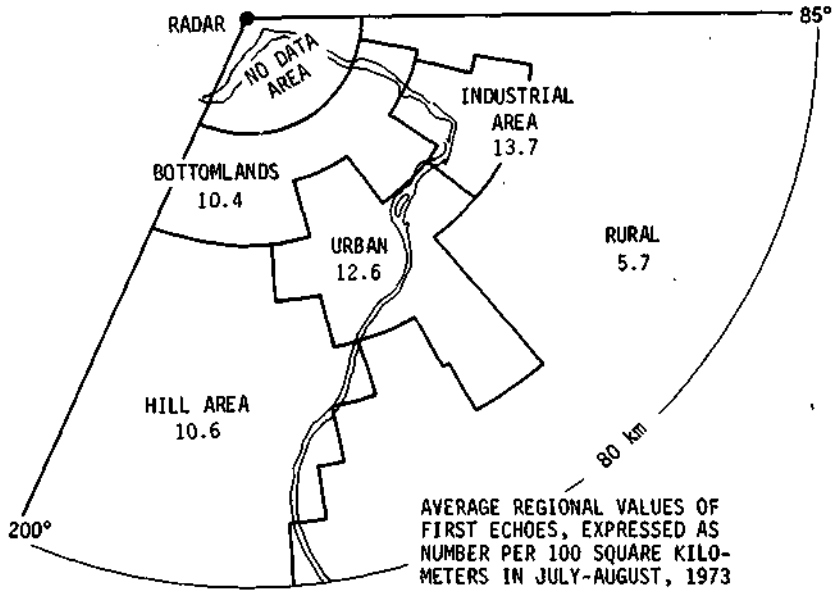

Figure D-28. First echo frequencies in different land use-physiographic areas

The four general regions of classification were 1) the Ozark Hills (called hill area), 2) the major 2-river bottomlands NW of St. Louis, 3) the urban-industrial area (St. Louis plus Alton), and 4) the rural area (all other areas located S, E, and NE of St. Louis). In certain instances, the data for St. Louis and Alton areas were analyzed separately. These five areas are shown in figure D-28.

Data were also collected on the tops of 702 echoes whose entire lifetime could be followed. There were no reduced-gain data available from the radar, and all echo definition was based on the minimum detectable reflectivity which was 27 dbZ. An echo was the entity defined by its first echo and was considered an 'echo' until it dissipated even though it may have embraced one or more nearby echoes that grew up alongside it with less than 4 km separating them. The range resolution of the radar data was 0.8 km. If two echoes that had existed at least 10 minutes and had been more than 8 km apart moved together such that they meshed to form one or more cells for at least 5 minutes, the time of union was considered a 'merger.' The subsequent behavior of the top of the merged echo was recorded for both of the original separate echoes until the two tops could not be distinguished.

Data recorded for each echo included the time, height, and its locale as noted every 1 to 3 minutes during its lifetime. From these records, summaries were derived for each echo, including its 1) initiation time, 2) duration, 3) top heights at initiation and dissipation, 4) maximum growth in any 5-minute period, 5) maximum height and the stage of echo duration when it occurred, and 6) average heights determined for the four stages of echo duration. Each stage was simply one-fourth (1st, 2nd, 3rd, and 4th) of the duration.

If an echo crossed above either the St. Louis and/or Alton-Wood River urban area (figure D-28), the information recorded included 1) the stage(s) of echo duration when it was over the urban area, 2) its duration over the urban area, 3) echo top height 5-10 minutes prior to reaching the urban boundary, 4) the echo height 10 or 20 minutes after entering the urban area, 5) the maximum height at any time over the city, 6) echo height at departure from the urban area, and 7) whether it initiated or dissipated over the city. An echo was classified as 'urban' by its presence

within a volume formed by the vertical extension of the metropolitan boundaries. Other informatio on the data and analysis procedures is available elsewhere (Changnon, 1976).

First Echo Results

The average tops, bases, and total echo heights for each area and both echo organizational groups are shown in table D-15. The results for the echoes in organized systems show that those over the urban area, bottomlands, and hill area were much the same, although the urban first echo had a slightly lower base and taller top. The base of the urban FE was much lower (500 m) than the rural echo.

The 385 FE that formed in generally isolated random fashion also displayed regional differences. The average urban FE had a much lower base than those of any other area, but with all echo tops being similar. In general, the urban FE had a depth about 600 m greater than those of the other areas. Inspection of the averages of all 385 isolated FE (table D-15) shows these to be much lower than those associated with the organized systems. The typical isolated FE also has much less depth (3500 m vs 2800 m).

The results for all echoes (table D-15) reveal that bases of urban FE were 400 to 500 m lower than those of all other FE. The tops of hill area and bottomland FE were 300 to 450 m higher than the urban and rural FE. In general, the urban FE are distinctly different from those of any other region. The FE of the bottomlands and hill areas are identical, and they differ (deeper with higher tops) from the typical rural FE. Thus, rural FE differ from all other FE. The results on FE dimensions strongly indicate that local land use and topography both affect, on the average, the vertical position where precipitation develops inside clouds. Urban-industrial influences induce precipitation at lower levels than it occurs in clouds over other areas.

Table D-15. Average Heights (thousands of meters) of First Echo Tops and Bases in July-August 1973 Based on Degree of Organization of Rain Echoes and on Land Use-Physiographic Regions

	Hill	*Bottomland*	*Urban*	*Rural*	*All*
Organized Systems *					
Frequency of echoes	241	36	54	95	426
Tops	6.4	6.5	6.6	6.7	6.5
Bases	2.9	2.8	2.7	3.2	3.0
Vertical extent	3.5	3.7	3.9	3.5	3.5
Isolated Echoes **					
Frequency of echoes	113	16	75	181	385
Tops	4.8	4.7	4.9	4.8	4.9
Bases	2.1	2.1	1.7	2.2	2.1
Vertical extent	2.7	2.6	3.2	2.6	2.8
All Echoes					
Frequency of echoes	354	52	129	276	811
Tops	5.9	5.9	5.6	5.5	5.7
Bases	2.6	2.6	2.1	2.6	2.5
Vertical extent	3.3	3.3	3.5	2.9	3.2

* Cold front and squall lines
** Air mass and squall zones

The 1973 areal distribution of first echoes was also determined for the five study areas. The frequencies were normalized to 100 km^2 frequencies, and the resulting regional values appear in figure D-28. The Alton (41 FE) and St. Louis (88 FE) areas were calculated separately. The St. Louis value (12.6 FE/100 km^2) was 19% above the hill value (table D-16) and 121% above the rural values. The Alton value was slightly higher than the St. Louis value, but together they envelop a local FE maximum defined by Braham and Dungey (1978) based on 1971-1975 radar data.

The sizeably lower rural value (table D-16 and figure D-28) was recomputed on the basis of rural area data for FE at ranges comparable to those of the two urban and industrial areas. This was done to correct for range-square sampling problems that might result in sampling of fewer FE at greater ranges (>60 km). This rural adjustment yielded a rural value of 8.7 FE/100 km^2 . The St. Louis urban area frequency (12.6) was still much greater (45%, table D-16) and the Alton industrial value was 57% greater.

Echo Top Behavior

Echo-top histories for 702 echoes from 19 rain periods in the 1973 summer were analyzed to perceive whether urban-related echoes and merged echoes behaved differently from non-urban echoes or non-merged echoes. The major findings from an exhaustive study (Changnon, 1976) are presented here.

The 190 echoes that merged during their lifetime represented 27% of the total. Merging occurred most often in the first and second stages (growth periods) of echo lifetimes. All merged echoes grew vertically and 93% had durations exceeding 30 minutes. Conversely, only 60% of all 702 echoes grew vertically and 47% lasted 30 minutes or more. The merged echoes were most prevalent in the 1800-2100 CDT period, 3 hours later than the maximum for the other echo classes, and they lasted longer (94 minutes) than all of the other echoes (43 minutes). This was a period of obvious urban effects on precipitation.

The average height of merged echoes in all four stages was from 1500-2700 m higher than all other echo classes except the urban echoes which were the highest. The average maximum 5-minute growth of merged echoes was higher than those of all echo classes except the urban. Hence, the typical urban echo had a faster growth rate and achieved higher tops than the typical merged echo, but the merged echo lasted longer than the urban echo and was bigger than all other classes of non-urban echoes.

Echo growth after merger was sizeable. The change 10 minutes after the mergers was an average increase of 1500 m, and 74% of the merged echoes had grown. Twenty minutes after merger, the average echo height was 1200 m higher than that at the merger.

Table D-16. Comparison of St. Louis and Alton Industrial Frequencies of FE with Those of Other Areas

Area	*St. Louis area value (%)*	*Alton area value (%)*
Rural	121	140
Hill	19	29
Bottomland	21	32
Rural Adjusted *	45	57

* Rural area within 60 km of radar

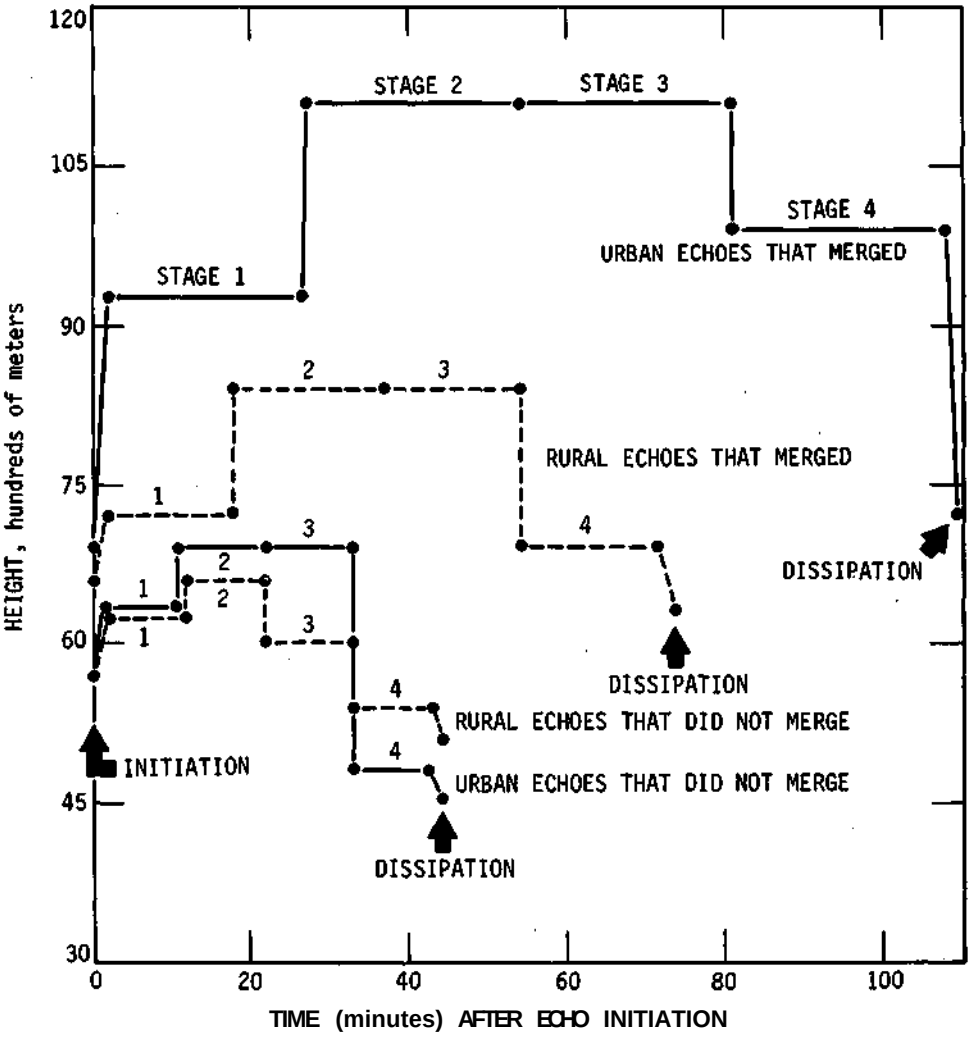

Figure D-29. Time-height profiles for urban and rural echoes

The 137 echoes that developed or passed over the two urban industrial areas were classed as potentially urban affected. Analyses of their characteristics revealed that the 61 merged echoes in the urban class were truly major echoes in duration (110 minutes), heights (typically 50% higher than the non-merger urban echoes), and growth rates (110% higher). The characteristics of the 61 urban merger echoes were compared with those of the 76 urban non-merged echoes (figure D-29), and their durations differed greatly, 110 minutes for the merger vs 44 minutes for the non-merger group. The merged echo was over the urban area 50% longer, and only 10% of those that merged dissipated over the urban area, compared with the dissipation of 34% of the non-merged echoes. Heights of these two subclasses of urban echoes differed greatly with the merger class averaging 4800 m higher at 10 minutes after entering the urban area and 5900 m higher when they exited the urban area.

Comparisons of urban echoes with rural echoes on any given day revealed that 65 to 75% of the urban echoes were taller at all stages of life, and 84% had maximum 5-minute growth rates

Table D-17. Summary of Urban and Non-Urban Echo Differences

	Urban class	*Non-urban class*
Percent of class total with		
Vertical growth	84	53
>30 minutes duration	75	40
Mergers	44	23
Selected merger echo characteristics		
Duration, *min*	110	73
Average height change 20 minutes after merger, *m*	2,100	900
Average maximum height in lifetime, *m*	14,100	10,200
Average of maximum 5 minutes of growth, *m*	4,800	2,400

that exceeded those of the rural echoes. The average duration of the urban echoes was 219% greater than the average of the non-urban echoes.

Table D-17 summarizes some other key differences between urban and non-urban storms. Clearly, the urban echoes were much more often vigorous storms (in growth and longevity) than those in the non-urban sample. Almost twice as many urban echoes merged, a condition to be expected since 1) the typical urban echo was taller (larger) and longer lasting, and 2) the FE studies show the urban areas to have a greater frequency of echo initation than occurs in any comparable sized area in the surrounding rural area.

Table D-17 also presents the most significant differences between selected characteristics of the urban echoes that merged and non-urban merged echoes. The urban merged echoes were 40 to 130% greater in the four characteristics dictating urban inducement or more vigorous convection. The heights of the 137 urban echoes (mergers and non-mergers) had a bi-modal (high and low) distribution in all stages, and since all other echo classes had only a single height mode, this suggests that the effects of the urban area resulted in two classes of convection. Furthermore, the urban non-merged echoes were not different from rural non-merged echoes (figure D-29). Thus, the key finding of this study relating to the influence of urban conditions on convective rain processes is the considerable urban enhancement of the vertical growth, height (dimensions), and longevity of echoes that passed over the cities and merged over or beyond (generally east) the two urban areas. Merging of precipitation cells has long been noted to enhance convective activity, to result in heavier rain rates, and on occasion to produce other forms of severe weather. It appears that the urban conditions affected about 45% of the echoes leading to sufficient growth and duration to result in merging.

SURFACE RAINCELL ANALYSES

Paul T. Schickedanz*

One of many approaches used to understand and evaluate the effect of the urban-industrial complex on precipitation in METROMEX has been the analysis of surface raincells (Schickedanz, 1972). The data for surface rain cell analysis have been obtained from the basic research circle of recording raingages which has an area of 5500 km^2 and a density of 24.2 km^2 per gage. The resulting raincell analysis was used to identify the precipitation characteristics that are altered by the urban-industrial complex.

The altered characteristics were determined by delineating individual raincells (patterns of rain usually produced by a single convective shower or thunderstorm) and describing each cell's history in terms of initiation, movement, maximization, duration, size, and total rain production. The chief advantages of this technique are that it yields:

1) the spatial portrayal of a cell, the smallest definable rain-producing entity from the surface rain network
2) the description of several cell parameters to provide the means to infer how in-cloud physical processes have been changed by urban influences

A semi-objective raincell definition and several analytical procedures for describing the cells were developed in order to minimize subjectivity for cell delineation (Schickedanz, 1972, 1973, 1974b, 1974c). In addition, a large portion of the analysis was computerized (Schickedanz and Busch, 1975) thereby reducing the effort involved in handling the vast quantity of data.

In this section, the characteristics of surface raincells are used 1) as a descriptive tool for demonstrating the magnitude, structure, and characteristics of the urban-industrial influence on rainfall, and 2) as an investigative tool for exposing and explaining causes of the altered precipitation pattern.

THE RAINCELL APPROACH

Rationale

Under favorable conditions, individual updraft areas within a thunderstorm develop into units of convective circulation. These units can be detected on a radar scope and are defined as regions of localization of convective activity within the thunderstorm (Byers and Braham, 1949). There often is more than one cell during a storm period, each of which may be either independent or dependent of dynamic influences of surrounding cells in the storm. During the storm period, each cell may be in different stages of development at any one time. The stages of development for a cell are 1) the cumulus stage, characterized by updrafts in the cell; 2) the mature stage, characterized by both updrafts and downdrafts in the cell; and 3) the dissipating stage, characterized by weak downdrafts throughout the cell (Byers and Braham, 1949).

In the Thunderstorm Project (Byers and Braham, 1949), it was found that the surface rainfall pattern under a thunderstorm follows closely the arrangement of cells and reflects, to a considerable extent, the various stages of cell development. In METROMEX, *surface raincells* are

**All of this section contributed by P. T. Schickedanz except "Raincell Mergers," page 302.*

designated as small isolated precipitation areas in the surface rainfall patterns which are characterized by closed isohyets of high intensity gradients and which generally reflect conditions within the cells aloft. Thus, the cells investigated were those from rain showers as well as those from thunderstorms. The underlying assumption of the METROMEX raincell analysis was that *statistically significant changes which occur in the surface raincell parameters in the vicinity of urban-industrial areas are broadly indicative of urban-industrial induced changes in the clouds aloft.* Thus, the analysis of surface raincells in the vicinity of urban-industrial complexes can yield insight into the physical processes involved.

Analytical Procedure

A raincell was defined in the following manner: *a raincell in a multicellular system is a closed isohyetal entity within the overall enveloping isohyet of the rain-producing system; that is, it defines an isolated area of significantly greater rainfall intensity than the system-enveloping isohyet. When raincells develop apart from a multicellular storm system, the system-enveloping isohyet will not be present, and the single cell is uniquely defined by the separation between rain and no rain.*

The delineation of these cells required several steps. First, the precipitation data were digitized directly from the raingage charts (weighing bucket gages) and entered on magnetic tape through the use of a Model 3400 X-Y digitizer (Autotrol). The digitized amounts were then processed by the IBM 360 computer so that a 5-minute printout of rainfall rates was obtained. The 5-minute rates were then plotted by the computer at predetermined contour intervals.

From the 5-minute isohyetal maps, a determination of which rainfall entities constitute a raincell had to be made. This was accomplished through the application of the cell definition; however, a size restriction on the area, an intensity restriction on the rainfall rate, and a time restriction on the interval between initiation and dissipation of a cell were necessary. These restrictions included: 1) a cell could not envelop more than one-third of the underlying isohyet of the storm; 2) a cell could be delineated by rainfall rate when the difference between its smallest point value and the base isohyet equaled or exceeded a rate of 1.9 cm hr^{-1}; and 3) in order for a cell to quality for initiation, it had to be present for longer than 5 minutes. These definitions and procedures provided a semi-objective method of cell delineation. It should be noted that these definitions were developed after much inspection of the rain data and many trial and error attempts to define a large volume of different rain types.

Once the raincells were defined on the 5-minute maps, various cell parameters were determined for each cell. These parameters included rainfall volume, mean rainfall, area, duration, maximum rain per 5-minute period, maximum area per 5-minute period, mean path length, mean path velocity, maximum point rainfall, minimum point rainfall, as well as an isohyetal representation of the total rainfall pattern resulting from each cell. Further details concerning the computer procedures and techniques employed are given by Schickedanz and Busch (1975).

The raincells as defined in this manner represented the rainfall intensity cores on 5-minute maps. In the multicellular system, the cores were usually much smaller than the total rain area. These cores were imbedded in the surrounding background rainfall and did not represent the total storm rainfall produced by the storm system during a 5-minute period. The restrictions on area, size, and duration were designed to separate these cores from their surrounding isohyets (background isohyets) so that alterations in their characteristics (volume, area, mean, duration, etc.) could be evaluated in relation to urban and industrial areas where they developed and/or passed. This definition of cells implies that most of the urban rainfall effect would be exhibited within these rainfall cores as opposed to the general background rainfall.

The background isohyet could vary from one 5-minute period to the next in order to permit the delineation of the raincell (rain core) according to definition. This was required because the background rainfall was constantly increasing and decreasing in intensity and a constant background isohyet would not permit the tracing of cells from one 5-minute period to the next. However, the definition provided a high degree of consistency from map to map, because the same spacing of isohyets was used for every 5-minute period (Schickedanz, 1972; Schickedanz and Busch, 1975).

Statistical and Design Considerations

The chief problem in evaluating inadvertent rain changes on raincells is that the 'treatment' (urban) effect is not assigned at random to the experimental unit. Even if the problem of randomization is disregarded, there is a difficulty in that the treatment effect is uncontrollable, and the factors which cause the treatment effect are either unknown, or the degree to which they are present is unknown (Changnon and Schickedanz, 1971). These considerations eliminated the usual treatment vs non-treatment (seeded vs non-seeded) comparisons that are so useful in planned weather modification where the non-treatment data serve as the control.

Another consideration in evaluating inadvertent modification is that the target or effect area for the precipitation change is unknown. In planned weather modification, the location of the treatment is known, so the target area is better defined. Also, since the seeding is often assigned at random, the most valid and useful comparison is seeded vs non-seeded data (the exact boundary of the target area is not as critical as when the comparison must be based on a target vs non-target basis). Therefore, assumptions had to be made with regard to how the urban complex acts as a treatment agent (roughness of terrain, increased CN and IN, and added heat or moisture) in order to delineate apparent target (effect) and control (no-effect) regions.

Since the lack of randomization is unavoidable in inadvertent rain modification evaluation, the approach was that of 'data analysis' (Flueck, 1971). *In the data analysis approach, the final proof and acceptance of inadvertent modification of precipitation does not and cannot rest entirely upon statistical evidence and results from tests of hypothesis, The test statistic is treated as an informative summary statistic and is to be clearly distinguished from the concept of the test statistic as a strict accept-reject rule.* Thus, the flexibility of attack and the willingness to study things as they are, rather than as they, hopefully, should be, were stressed.

In applying the concept of data analysis to non-randomized comparisons, we were guided by the general concept of data analysis as described by Tukey (1962), who indicated that much of data analysis must be a matter of judgment. 'Theory,' whether statistical or non-statistical, must guide, not command. Tukey (1962) states: "Data analysis must progress by approximate answers, at best, since its knowledge of what the problem really is will at best be approximate. It would be a mistake not to face up to this fact, for denying it, we would deny ourselves the use of a great body of approximate knowledge. . . . "

Thus, the METROMEX raincell analysis proceeded with the knowledge that the treatment effect was not assigned at random. Therefore, the definition of target (effect) and control (no-effect) areas in the analysis and ensuing text could not be completely rigorous. However, because of the well-designed field instrumentation program (Changnon et al., 1971), there was a great wealth of 'approximate' knowledge available from the analysis of METROMEX raincell data. This knowledge yielded invaluable information which could be used as a broad basis for establishing the causes, effects, and reality of inadvertent precipitation modification.

Delineation of Effect and No-Effect Cells

An inherent problem in this study was how to classify, on any basis, cells as potentially affected by any (or all) urban factors and those not affected by any (or all) urban factors. Any delineation of urban-affected and not urban-affected cells was complicated by the uncertainty of the source of 'treatment agents' and by the locale, involving the manner in which these are transported to cells aloft. Three-dimensional continuous monitoring of all treatment agents (strength and locale at a given time) was impossible over a prolonged period of several months. However, detailed 3-dimensional monitoring of all possible treatment agents was available for certain 'case study' storms and cloud systems of 1971-1973. Since this type of information was not available for all rain periods and since the agents were not always known, some general stratification methods were required which could only approximate the true 'effect' and 'no-effect' cells. However, by defining and then studying a variety of stratifications, speculation could be made concerning the most likely sources, and their potential contributions could be explored.

In this report two general types of stratifications were used to delineate effect and no-effect cells. After much thought, a rather simple stratification was chosen according to the source regions where the cells initiated and/or through which they passed during their life history. Because of the possible bias introduced by the location of the source regions (Schickedanz, 1973, 1974c), another form of general stratification was employed. This involved an effort to classify the storms as either effect or no-effect storms according to the factor approach, thereby providing a double stratification of effect and no-effect cells according to both space (source regions) and time (storms). This latter stratification is referred to as the 'factor stratification.'

Basic Stratification

From a survey performed by Venezia and Ozolins (1966) and from information provided by METROMEX personnel, St. Louis area industries were plotted on a base map. For convenience, a simplified boundary was drawn around the contiguous urban-industrial area of St. Louis, and it was designated as the L area (figure D-30). This area was considered to be a potential source of vertical motions, heat, cloud and ice nuclei, and moisture (all potential treatment agents) to the atmosphere. Certainly, not all point sources of treatment agents were included within this boundary; however, the maximum concentration was enclosed and, importantly, it served as a basis for stratifying the raincells into potential 'effect' and 'no-effect' cells.

Aircraft observations of temperature, aerosols, and other atmospheric conditions during 1971-1972 (Semonin and Changnon, 1974; Auer and Dirks, 1974; Braham, 1974) supported the concepts that 1) a temperature perturbation exists over the highly urbanized area of St. Louis, and 2) the city serves as a source of CCN. They did not support the concept that the city is a moisture source. In addition, airflow measurements during 1971-1973 (Ackerman, 1974) have shown that the city disturbs the circulation, often producing convergence over and downwind of the city in the low atmosphere. This would tend to concentrate aerosols and potential CCN and ice nuclei for cloud base ingestion.

Somewhat removed from St. Louis is the contiguous area of Wood River and Alton. This area has a concentration of heavy industries including three petroleum refineries, iron and steel foundries, and coke plants. For convenience, a simplified boundary was drawn around this area and it was designated the Wood River (W) area as shown on figure D-30. The W area is a nuclei source (CCN and ice) not unlike St. Louis in its volume (Semonin and Changnon, 1974; Auer and Dirks, 1974; and Braham, 1974), but it has a much smaller, though concentrated, thermal perturbation than does St. Louis. There is also some evidence that the effluents of the major cooling towers in the W area may result in a localized increase in moisture.

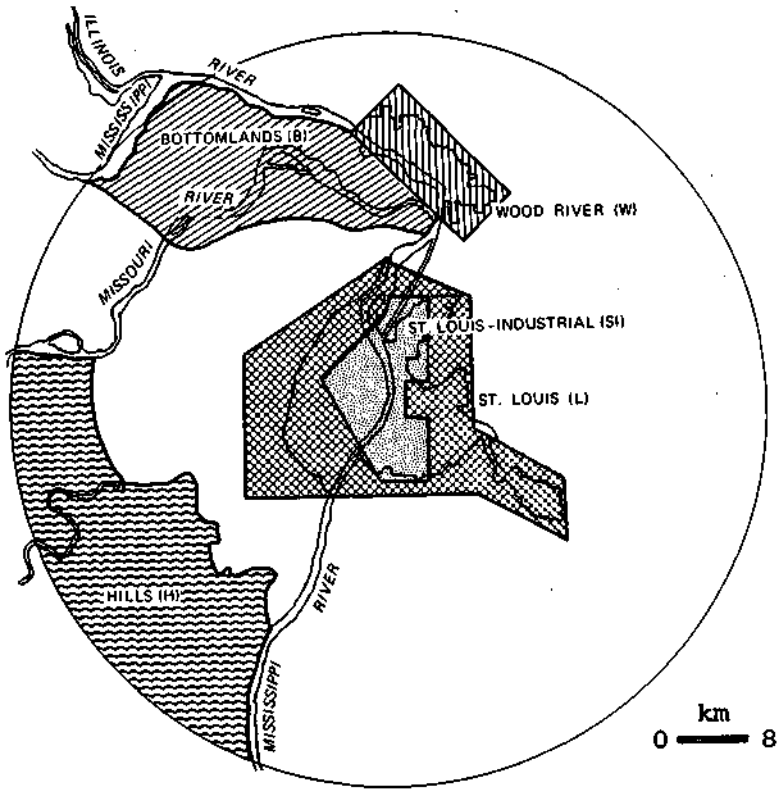

Figure D-30. Hypothesized regions of potential treatment agents

In addition, there are two non-urban areas which were considered potential places with localized effects due to topography and additions of moisture. These are 1) the major river bottomlands NE of St. Charles in the northwestern part of the network between the Missouri and Mississippi Rivers, and 2) the forested foothills of the Ozark Plateau in the southwestern part of the network. The area between the two rivers and the surrounding marshy land was designated as the 'bottomlands' (B) as shown on figure D-30. Likewise, from the topographical maps, the prominent area of surface roughness and higher elevation was designated as the 'hills' (H), also shown on figure D-30. These areal stratifications were made to separate some possible topographical land use influences from the control sample.

All cells which occurred (i.e., cells that developed and/or passed) within a given source area, but never in any of the other four areas (L, W, H, B), were designated as 'effect' cells. Cells that never occurred in any of the four areas (L, H, W, B) were considered to be control (C) or 'no-effect' cells. In addition, cells which were in both L and H only, and in W and B only, were considered as two more classes of effect cells. Also, a subarea was selected from the L area as being representative of major heat and nuclei sources within the L area. This subarea (labeled St. Louis-industrial) had large CN production rates and was the center of the afternoon heat island. All cells which occurred in this St. Louis-industrial area (SI), but never in the H, W, or B areas, were designated as SI effect cells.

To summarize, the effect and no-effect areas were designated as follows:

L = St. Louis total urban-industrial effect area
SI = St. Louis-industrial (subarea of L) effect area
W = Alton-Wood River industrial effect area
H = Hills, topographic effect area
B = Bottomlands, topographic effect area
C = Control or no-effect area

Factor Stratification

The factor statistical approach was used in this study to determine potential areas of effect from the storm rainfall patterns and to determine in which storms the effect was present. For this purpose, the effect was considered to be present when there was a rainfall anomaly in the vicinity of or immediately downwind from St. Louis, Granite City, or Wood River. The factor approach was used to determine 1) the presence of the anomaly, 2) the location of the anomaly, and 3) the storms in which the anomaly occurred. This provided a means of stratifying the cells according to effect and no-effect storms as well as by area. This stratification permitted an investigation of the cell parameters according to the effect conditions (i.e., the presence of the rainfall anomaly) or no-effect conditions (i.e., the absence of the effect anomaly) with regard to the various source regions. An opportunity was also provided to investigate the question of bias due to location since the bias should be present under both the effect and no-effect conditions.

The factor approach was applied to the mean areal rainfall over each of the 10 X 10 km radar sampling areas (100 km^2) shown on figure D-31. The mean areal rainfall values for the 64 sampling areas (variables) were determined for each storm (observation) of the 5-year period.

The mean areal values from the 64 areas were used to form a m x n (m = 330 storms, n = 64 areas) matrix X. The matrix was then subjected to an R-type factor analysis. This analysis was performed by first standardizing each of the columns (areas of the X matrix) by their respective means and variances so that a m X n matrix Z of standardized variates was obtained. The correlation matrix R, which is a matrix of correlation coefficients between the columns (areas) of Z, was then determined. From the R matrix, a set of new variables was constructed such that the new variables were exact mathematical transformations of the original data. This transformation was accomplished by determining the characteristic scalar roots (eigenvalues) and the non-zero vectors (eigenvectors) of R which simultaneously satisfy the equation:

$$RE = XE \quad (1)$$

where E is the n X n matrix consisting of a set of orthonormal eigenvectors of R as the columns, and λ represents the eigenvalues (characteristic scalar roots) of R. Equation 1 can be rewritten in the form:

$$(R - \lambda I_n)E = 0 \quad (2)$$

where I_n is the identity matrix of order n x n. The solution of the scalars λ and the eigenvectors E is the classical Characteristic Value Problem of matrix theory (Hohn, 1960).

The magnitude of the eigenvalues represents the variance of the observations in the Z matrix explained by each eigenvector. The eigenvectors are then ordered so that the first diagonal element of λI_n represents the largest eigenvalue, and the second the next largest, etc. The eigenvectors are also scaled by multiplying each orthonormal eigenvector by the square root of its eigenvalue to obtain the 'principal components loading matrix':

$$A = ED^{1/2} \quad (3)$$

where $D = \lambda I_n$, the n x n diagonal matrix of the eigenvalues of R. The columns of the A matrix are called factors and are independent of each other. This extraction of factors results in a principal component solution (i.e., an exact mathematical transformation without assumptions), and the factors are designated as defined factors (Kim, 1975). If the diagonal elements of the R matrix are replaced with initial estimates of communalities (i.e., the squared multiple correlation between each variable and all

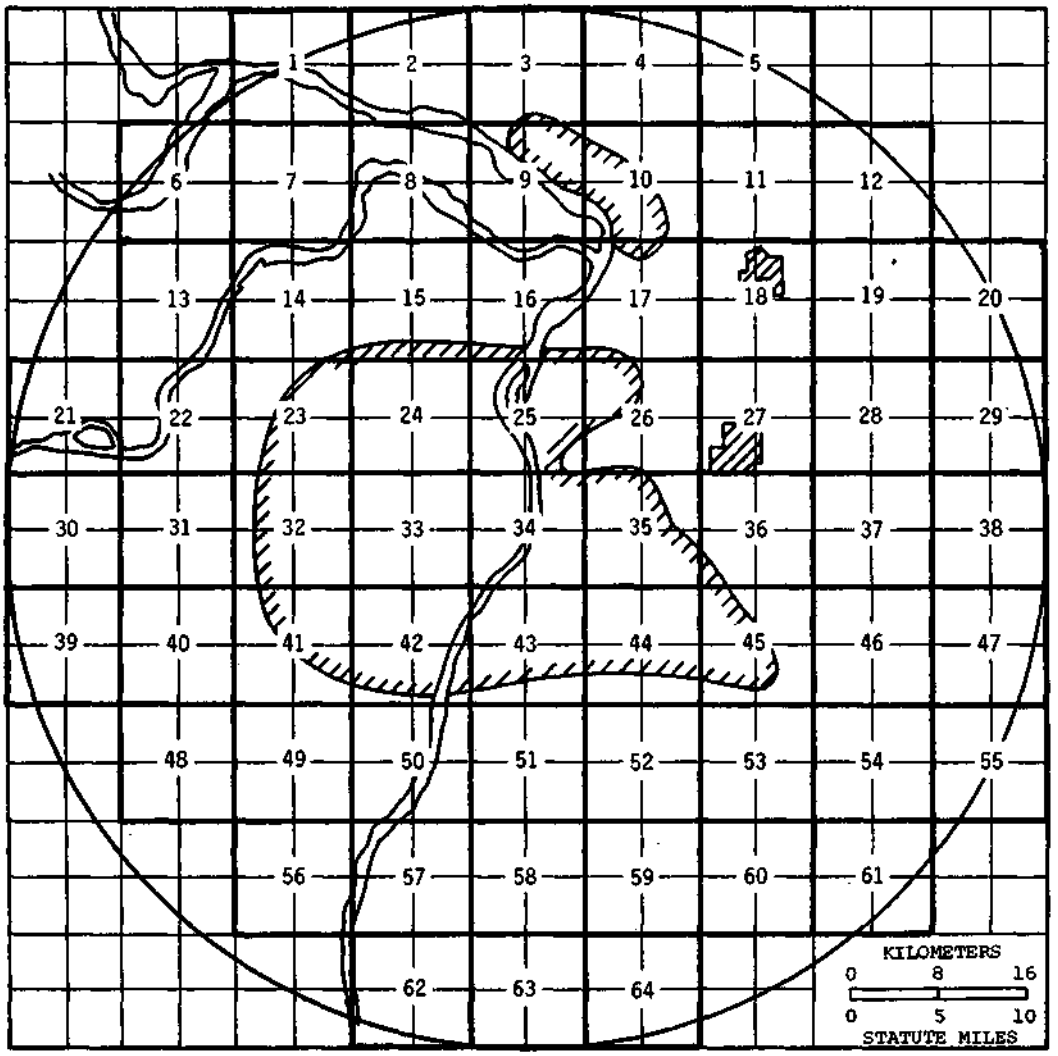

Figure D-31. The basic sampling squares used in the factor analyses

others in the set) prior to factoring, the result is the principal factor solution (Kim, 1975). In this case, the matrix is defined to be the 'principal factors loading matrix,' and the factors are called inferred factors (i.e., assumptions about the variance in common have been imposed). Whether the factors be defined or inferred, the first factor explains the largest amount of the combined variance of the observations in the Z matrix; the second factor explains the second largest amount of variance, and so on.

The exact configuration of the factor (eigenvector) structure is not unique; one factor solution can be transformed into another without violating the assumptions or mathematical properties of a given solution (Kim, 1975). Since some factor structures are more meaningful than others (i.e., some are more simple, some are more informative, some are more revealing), it is often desirable to rotate the factors to a terminal solution that satisfies both the practical and theoretical needs of the research problem. Occasionally, the initial factor structure satisfies these needs and can be used for the terminal solution.

The factors of the A matrix are spatial functions which are linear combinations of the various areas, and each area possesses a certain amount of the variance contained within a particular eigenvector. For

example, the areas enclosed by the 0.4 isoline contain a high amount of variance (large positive values of the sixth eigenvector). The areas within the 0.6 isoline contain an even higher amount of the variance of the sixth eigenvector. Thus, it can be stated that the areas within the 0.6 isoline are loaded heavily on the sixth eigenvector. Because of the proximity of the high variance region (value ≥ 0.4) of this eigenvector to St. Louis, it was designated as the St. Louis (L) factor.

However, in order for the St. Louis factor or any other 'effect factor' to be meaningful, it is necessary to determine the corresponding principal components (principal factors). The matrix A is a transformation matrix which can be used to transform the matrix into a set of principal components (or principal factors).

$$F = Z(AT)^{-1} \quad (4)$$

where F is the principal components (or principal factors) matrix of order m X n. The scaled eigenvectors (factors) of the A matrix are orthogonal (uncorrelated) functions of space and the principal components of the F matrix are orthogonal (uncorrelated) functions of time.

The temporal plot of the sixth principal component (St. Louis principal component) for the storms during 1971-1975 is shown on figure D-32. The large positive (up) values of the series represent the storms in which there was a rainfall maximum within the 0.4 isoline of the sixth eigenvector shown on figure D-32. For example, the large positive loadings in August 1972 and 1973 indicated that in these two years, the rainfall highs in the St. Louis area were the strongest in August. In contrast, the highs were distributed quite evenly between the three months in 1975.

The temporal series on figure D-32 was used to classify the storms which produced the storm rainfall pattern 'type' of figure D-46b as St. Louis effect storms. Similarly, the factors for other potential source regions (Edwardsville, Granite City, Wood River, etc.) and the corresponding effect storms for these factors were also selected.

This permitted a double stratification of the raincells for each factor in that the raincells passing through any of the potential source regions could be classified according to whether or not the effect was present (effect or no-effect storms). The similar classification of the control cells into effect and no-effect storm cells provided a powerful tool for investigating 1) the influence of the various source regions on the rainfall parameters and 2) the possibility of bias in the basic stratifications.

RESULTS FROM BASIC STRATIFICATION OF RAINCELLS

Total Rain Production of Cells

Cell rain volume was studied extensively because rain volume is the single most important parameter insofar as the ultimate benefit of enhancement or suppression of rainfall is concerned. This parameter represents the total water output by the cell and is an integrated measure of all other cell parameters and of the various atmospheric conditions which produced the cell. However, before considering this cell parameter, it is informative to first consider the number of cells available for analysis.

Many of the cells were not completely contained within the network. The analyses that follow were restricted to complete cells, that is, the 7889 cells which had gone through their complete life histories within the boundaries of the raingage network. The sample sizes of complete cells for each of the basic stratifications are listed in table D-18. For the 1971-1975 period, the control stratification had the largest number of cells, and the St. Louis stratification had the second largest number. The differences in sample sizes among the various stratifications are largely

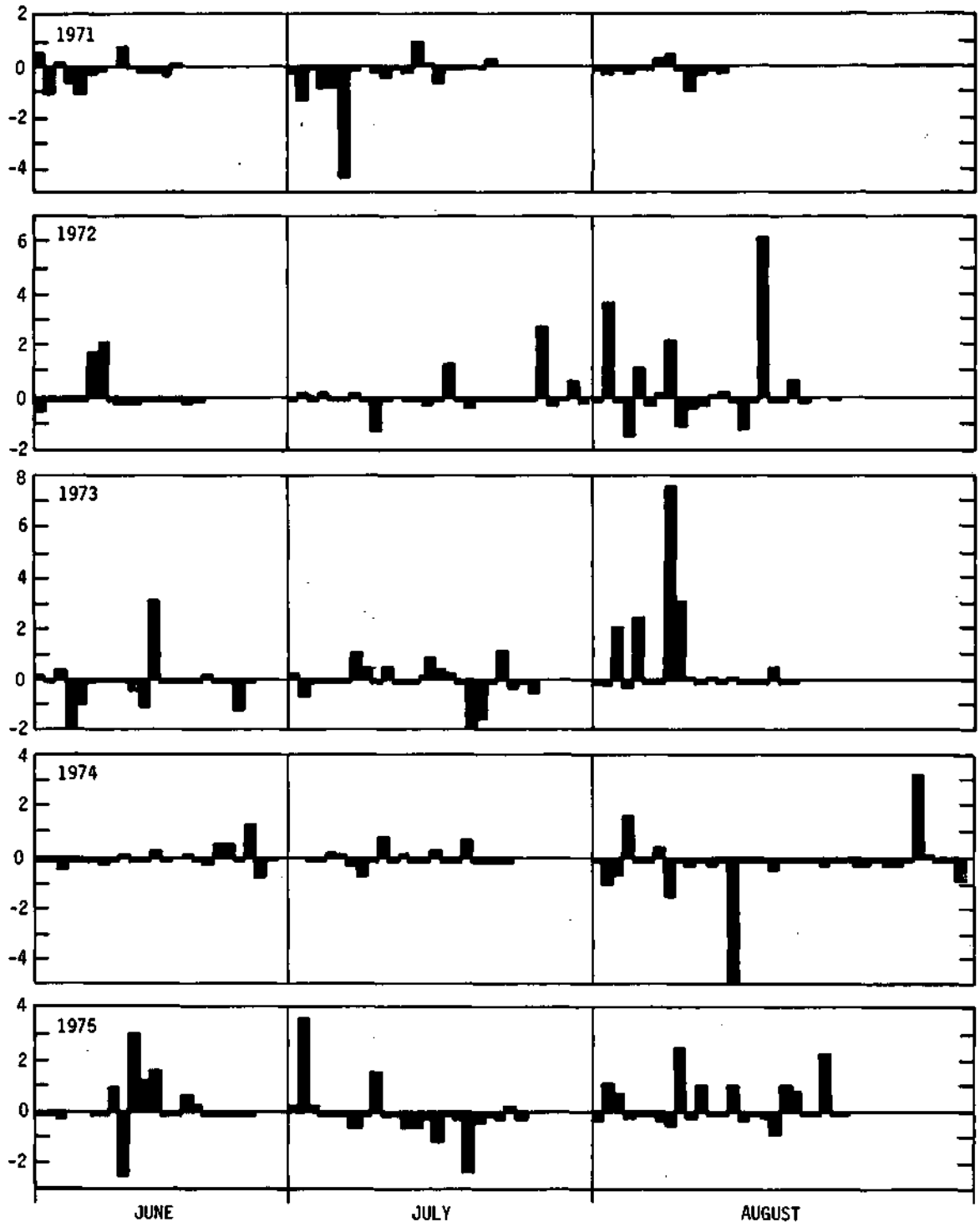

Figure D-32. Temporal plot of the sixth principal component for the St. Louis effect area

Table D-18. Comparison of Sample Size from Effect and No-Effect Raincells (Complete Cells)

	L	SI	W	H	B	C
1971	119	37	30	29	56	285
1972	206	74	40	46	74	585
1973	274	94	66	66	85	726
1974	599	188	175	124	202	1738
1975	548	166	138	110	173	1395
1971-1975	1746	559	449	375	590	4729

due to the differences in areal sizes (in km^2 St. Louis 775, St. Louis-industrial 170, Wood River 170, hills 436, bottomlands 363, and control 3576). There were 3160 effect cells and 4729 no-effect cells for a total of 7889 complete cells (SI cells are excluded from these samples because they are a subsample of L). Results from the comparison of the volumes of 3160 effect cells and 4729 no-effect cells are listed in table D-19.

Since all effect values were compared with the control values, the validity of the control values was important. Thus, a comparison was made of these mean control (natural) values with those obtained in earlier studies of unmodified raincells. In the Thunderstorm Project in Ohio, Braham (1952) obtained a mean value of 1.24×10^8 kg or approximately 100 acre-feet (12.34 hectare-meters) for the total rain volume. Huff and Schickedanz (1970) obtained a median value of 110 acre-feet (13.57 hectare-meters) for raincells on a dense rural network in extreme southern Illinois. When we consider that different techniques were used to delineate the raincells, the agreement of the 5-year control value of 11.0 hectare-meters with these previous values is quite good.

The volume data for all cells (1971-1975) in table D-19 indicates that cells occurring in the urban-industrial areas produced the largest percentage differences. The percent differences of cells are 125% for St. Louis (L), 211% for St. Louis-industrial (SI), 77% for Wood River (W), 75% for the hills (H), and only 12% for the bottomlands (B). The percentage increase in the SI cells was approximately three times that of the H cells; the percentage increase in the L cells was approximately 1.7 times that of the H cells; and the percentage increase in the W cells was nearly the same as the H cells. The largest increase in the hill cells occurred in 1973, which was the wettest year. This agrees with the findings of Jones et al. (1974) who concluded that the effect of small hills on rainfall in southern Illinois was the greatest during the heaviest rains, particularly those totaling more than 2 inches (5.08 cm) during the warm season of the year.

The above findings illustrate one of the basic difficulties involved in evaluating weather modification experiments. Large increases are often obtained in single cloud experiments, but the increase over an entire region is often quite small and difficult to evaluate. In this instance, dramatic increases apparently occur in rain entities (i.e., raincells), but the maximum increase in the rainfall pattern for 1971-1975 was on the order of 50%.

One reason that the raincells have a greater percentage increase (211%) than the apparent increase that occurs within certain regions of the research circle (e.g., the Edwardsville increase of 49%) is the nature of the derived cullular rainfall. Overall, the cellular rainfall (rain cores) from *complete* cells during 1972-1975 represented only 21% of the total summer rainfall pattern (see figure D-50c), and the incomplete cells plus the non-cellular rainfall (background) represented 79%. The percentage values for rainfall from complete cells were 39% for L, 42% for SI, 30% for W, 22% for H, 28% for B, and 28% for C.

Table D-19. Comparison of Average Volume from Effect and No-Effect Cells Stratified According to Path Length

	L	*SI*	*W*	*H*	*B*	*C*
			≤6.4 km			
1971	8.5(25)	10.9(60)	11.3(66)	13.7(101)	3.5(-49)	6.8
1972	14.2(92)	17.7(139)	11.7(58)	7.7(4)	12.8(73)	7.4
1973	15.8(74)	18.4(102)	16.9(86)	11.7(29)	9.6(5)	9.1
1974	6.0(5)	7.8(37)	5.8(2)	7.4(30)	5.4(-5)	5.7
1975	9.2(33)	11.2(62)	7.9(14)	5.5(-20)	8.3(20)	6.9
1971-1975	9.4(38)	11.7(72)	8.8(29)	8.1(19)	7.5(10)	6.8
			≤12.8 km			
1971	16.5(60)	23.3(126)	17.5(70)	19.9(93)	8.2(-20)	10.3
1972	18.8(70)	18.1(63)	12.2(10)	12.9(16)	16.2(46)	11.1
1973	27.0(125)	30.8(157)	19.7(64)	16.8(40)	14.6(22)	12.0
1974	9.1(26)	11.8(64)	6.7(-7)	9.2(28)	7.5(4)	7.2
1975	14.2(58)	16.1(79)	10.7(19)	9.7(8)	10.5(17)	9.0
1971-1975	15.0(65)	17.7(95)	10.9(20)	12.0(32)	10.6(16)	9.1
			≤19.3 km			
1971	21.2(88)	30.2(167)	35.9(218)	19.4(72)	13.2(17)	11.3
1972	31.7(142)	37.8(189)	14.8(13)	13.2(1)	18.5(41)	13.1
1973	30.4(134)	39.7(205)	23.2(78)	25.3(95)	15.0(15)	13.0
1974	11.2(40)	14.2(78)	8.0(0)	10.9(36)	7.9(-1)	8.0
1975	18.6(82)	23.2(127)	13.1(28)	14.7(44)	11.0(8)	10.2
1971-1975	19.5(91)	25.0(145)	14.2(39)	15.4(51)	11.7(15)	10.2
			All cells			
1971	26.5(114)	40.8(229)	50.5(307)	23.6(90)	13.2(6)	12.4
1972	46.2(216)	63.7(336)	51.3(251)	22.1(51)	18.8(29)	14.6
1973	37.6(163)	50.5(253)	27.1(90)	30.8(115)	15.3(7)	14.3
1974	13.4(56)	18.3(113)	8.0(-7)	11.1(29)	8.4(-2)	8.6
1975	22.3(114)	28.3(172)	14.6(40)	18.8(81)	12.1(16)	10.4
1971-1975	24.8(125)	34.2(211)	19.5(77)	19.1(74)	12.3(12)	11.0

Note: Volume is measured in hectare-meters; effect-control difference is given in parentheses expressed as % of control

When incomplete cells (cells not completely contained in the network) were included with the complete cells, the total cellular rainfall represented 39% of the total storm rainfall and the non-cellular rainfall represented 61%. The percentage values for total cellular rainfall were then 40% for L, 44% for SI, 38% for W, 39% for H, 38% for B, and 40% for C. If rainfall modification is most effective in cellular (convective) rainfall (rain intensity centers), as opposed to non-cellular rainfall, these results imply that the rainfall increase over a region will necessarily be small even with large increases in individual convective rain entities. However, the cellular rainfall generally described the overall rainfall pattern in 1972-1975. Within some of the major rainfall highs, percentage values were as high as 49%. For example, in the L area during 1972-1975, point percentage values within the Granite City high reached 49%.

One of the problems inherent in the raincell analysis is the evaluation of cells not completely contained in the network. The analyses were restricted to cells completely contained within the network. Such a restriction to complete cells may cause the data to be biased toward the effect cells. This bias may occur because St. Louis is located in the center of the research circle and, therefore, has the greatest opportunity to sample the heavier, longer-moving raincells.

Also, there is a problem of positively skewed rainfall distributions. In fact, the volume data are well fitted by the normal distributions, which clearly indicates that these are postively skewed distributions. There is the possibility that, with these distributions, a few large raincells may dominate the sample to the extent that the difference between an effect and control sample may be solely attributed to these large cells. These cells may frequent one particular area instead of another simply by chance, and this could lead to erroneous conclusions. To address these difficulties, raincells were partitioned according to path lengths of ≤6.4, ≤12.8, and ≤19.3 km. This stratification allows the inspection of the data in the absence of heavy cells with path lengths >19.3 km. Certainly, cells of shorter path lengths have a greater opportunity to be equally sampled in the research area shown on figure D-30. Results of comparisons of effect and no-effect cells stratified according to path length are listed in table D-19. For the ≤6.4 km stratification, the magnitude of the percentage increases for 1971-1975 in the several areas ranked in the same order as in all cells. That is, the SI cells had the largest percentage increases, the L cells had the second largest percentage increases, the W cells had the third largest percentage increases, and so on. This helps to demonstrate that an effect not resulting from sampling bias is present in the L, SI, W, and H stratifications.

In the ≤ 19.3 km category, the magnitudes of the increases were ordered somewhat differently (H cells were greater than the W cells), but the percentage increases in the effect cells are still present (table D-19) although the percentage increases are not as large as in the 'all-cell' category. In the ≤19.3 km category, however, the precent increases remained 145% in the SI cells and 91% in the L cells. *This indicates that the major portion of the increases in rainfall volume can be attributed to factors other than biased urban sampling of heavy and long moving cells.*

Associated Meteorological and Temporal Conditions

Synoptic Types. The raincells were partitioned according to synoptic types as defined by Vogel (1974). This partitioning reduced the sample size such that only the squall zone, squall line, air mass, cold front, and static front classifications had a sufficient number of raincells to make comparisons between effect and no-effect cells. A comparison of cell volume from effect and no-effect cells according to synoptic type for the combined summers of 1971-1975 is presented in table D-20.

In the control sample, the squall line and cold front cells were the heaviest rain producers. In L, the largest percentage increases occurred with cells from squall lines, squall zones, and cold fronts, respectively. The largest percentage increases in W occurred with cells from squall lines, cold fronts, and static fronts, respectively. In the SI cells, the largest percentage increases occurred with squall zones, squall lines, and air masses, respectively. For the H and B cells, the largest percentage increases occurred with static fronts. In general, it would appear that the largest urban increases occurred with fronts and organized convective activity, with the exception of air masses in the SI cells. [However, note that the sample size is only 9 for air mass storms.] In contrast, the hills and bottomland cells have their largest percentage increases in the stationary frontal activity.

Diurnal Distribution. The diurnal distribution of cell rainfall for the summers of 1971-1975 was investigated by dividing the cells according to occurrence in four periods: 0001-0600, 0601-1200, 1201-1800, and 1801-2400 (CDT). The purpose of this division was to determine if the four areas representing potentially different treatments produced different effects during certain periods of the day. If so, this might provide indirect indications of the relative importance of various urban inputs to the enhancement of rainfall.

Table D-20.Comparison of Average Rainfall Volume
from Effect and No-Effect Cells According to Synoptic Type
for Summer 1971-1975

	L	*SI*	*W*	*H*	*B*	*C*
Volume (hectare-meters)						
Squall zone	17.4(93)	28.8(220)	11.7(30)	18.0(100)	10.6(18)	9.0
Squall line	33.3(107)	51.5(220)	37.2(131)	26.3(63)	16.3(1)	16.1
Air mass	11.4(34)	27.1(219)	13.5(59)	9.8(15)	12.3(45)	8.5
Cold front	21.8(86)	29.0(148)	20.7(77)	20.4(74)	11.6(-1)	11.7
Static front	7.9(55)	10.4(104)	8.9(75)	10.7(110)	8.4(65)	5.1
Sample size						
Squall zone	516	150	163	108	217	1530
Squall line	584	205	117	119	171	1382
Air mass	64	9	19	27	37	237
Cold front	254	69	65	43	76	647
Static front	196	70	51	43	45	538

Note: Effect-control differences are expressed as % of control in parentheses

Table D-21.Comparison of Average Rainfall Volume
from Effect and No-Effect Cells According to Time of Day
for Summer 1971-1975*

	L	*SI*	*W*	*H*	*B*	*C*
0001-0600	15.1(97)	20.1(161)	11.4(49)	12.0(57)	8.1(5)	7.7
0601-1200	13.0(52)	14.5(69)	12.3(43)	13.9(62)	8.8(2)	8.6
1201-1800	40.4(171)	59.5(299)	27.4(84)	28.1(89)	16.9(14)	14.9
1801-2400	22.8(89)	33.8(180)	23.7(96)	22.1(84)	14.4(19)	12.0

*** Volume (hectare-meters)**
Note: Effect-control differences are expressed as % of control in parentheses

The mean rainfall volumes for each area are listed in table D-21. The control data reveal that the heaviest rainfall occurred during the maximum heating period, 1201-1800, and that the lightest rainfall occurred during the minimum temperature period, 0001-0600. This was also true for cells in the B area, but this was not true for the urban-industrial cells in the L and SI areas. In these areas the rainfall also was heaviest during the maximum heating period, 1201-1800, but the minimum rainfall occurred later during the period 0601-1200.

The percent differences for the L and SI cells reveal some interesting departures from the diurnal trend of the W, H, and B cells. For cells in St. Louis, the increase is 1) 97% for the period 0001-0600, which is larger than increases for the other three areas during the same period, 2) greatest during the 1201-1800 period, and 3) least during the 0601-1200 period. This is also true for the St. Louis-industrial cells, which have percentage increases nearly twice the size of those for St. Louis alone. Inspection of yearly data revealed that the percent increases in the SI cells during the 0001-0600 CDT period was present in 4 of the 5 years 1971-1975. Moreover, the percent increase in the L cells during the 0001-0600 period was present in 3 of the 5 years. This consistency indicates that the differences are not the result of bias from a given year.

It would appear that a major enhancement of the rainfall occurs in the St. Louis cells and the subset of St. Louis-industrial cells during the maximum heating period (1201-1800). There is also a localized increase during this period in the W and H cells, but it is much smaller and its magnitude is similar to that of the increase noted at 1801-2400.

For cells in the Wood River area, the largest percentage increases occur in the late evening hours (1801-2400) and during the maximum heating period (1201-1800). However, in the early morning hours, the percent increase is not as large in the W cells as it is in the L cells. METROMEX temperature data indicate a weak heat island in the vicinity of the W area, but it is not as intense nor as large in areal extent as the one in the L area. Therefore, it is possible that the normal early morning inversions are not destroyed or penetrated as frequently over the W area as over the L area. Thus, the effluents from the W area would not reach the cloud base as often as in the L area, and would not contribute as much to an early morning rainfall increase.

Weekday versus Weekend Patterns. If industries in the St. Louis area operate differently on weekends than on weekdays, or if the temperature (or moisture) of the city on weekdays is different from that on weekends, then it is conceivable that rain production might be different on weekdays than on weekends. This concept was tested by partitioning the cells in each of the source regions according to weekdays and weekends. The average cell volumes for the weekends and weekdays are listed in table D-22. For control cells, the mean volume for weekdays is approximately 1.3 times that of weekends, or 30% greater than for weekends. On the other hand, it is noted that the very similar percentage increases are also present in all source regions. Even more important, the percentage increase in each of the areas is nearly the same on weekdays as it is on weekends. This indicates that the increase in each area is the same regardless of whether the cells occur on weekdays or on weekends. Accordingly, it is concluded that no evidence supports a difference in rain production on weekdays compared with weekends.

This conclusion is further supported by a comparison of weekday temperature patterns with weekend temperature patterns. This comparison was made by first determining the temperature on the clock hour prior to the start of each storm during 1972-1975. [These determinations were made from 25 temperature stations in the METROMEX network.] The mean temperature for each site was used to estimate any missing values for the site. Although this is a coarse estimate of the missing value, it does provide one with a conservative estimate of the value insofar as the mean network temperature pattern from several storms is concerned.

The average temperature pattern prior to the start of the storm was determined for all weekdays and is shown on figure D-33a. [Subsequent references to temperature patterns are to those existing prior to the start of the storm.] This pattern is indicative of the general temperature regime within the research circle whose dominating feature is a large urban heat island over the city with an extension to the west. The weekend pattern, which is clearly very similar to the weekday pattern, is shown on figure D-33c. In order to pinpoint regions of differences between weekday

Table D-22.Comparison of Average Rainfall Volume from Effect and No-Effect Cells According to Weekdays and Weekends for Summer 1971-1975*

	L	*SI*	*W*	*H*	*B*	*C*
Weekday	26.9(110)	37.4(192)	21.7(70)	19.3(51)	13.9(9)	12.8
Weekend	19.8(104)	26.9(177)	16.1(66)	16.6(71)	9.5(-2)	9.7
Weekday-weekend ratio	1.36(3)	1.39(5)	1.35(2)	1.16(-12)	1.46(11)	1.32

* Volume (hectare-meters)
Note: Effect-control differences are expressed as % of control in parentheses

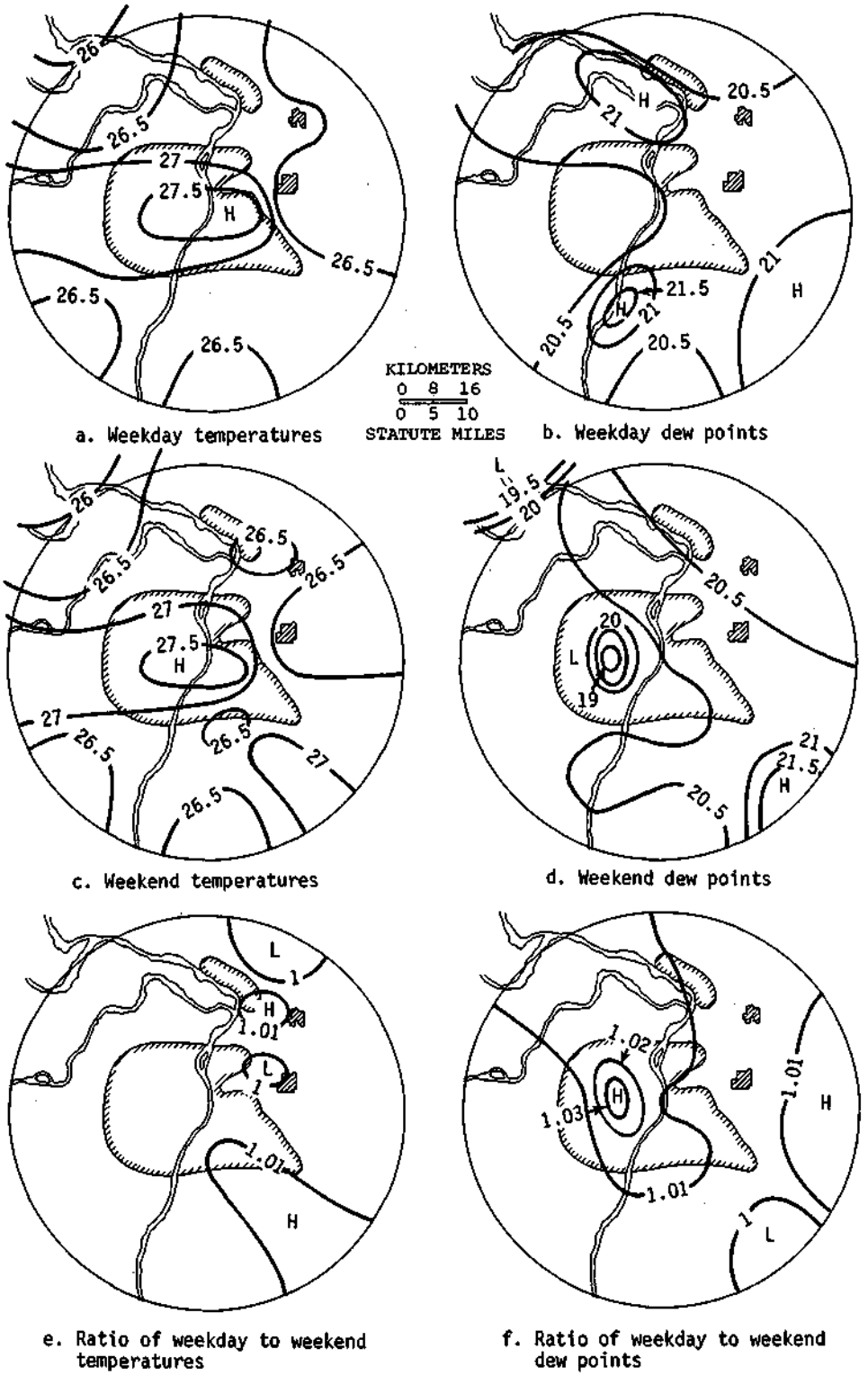

Figure D-33. Comparison of average temperature and dew point (° C) patterns on weekdays and weekends

and weekend patterns, the ratio comparison pattern of the weekday to the weekend temperatures was determined and is shown on figure D-3 3e. Little difference exists between the weekday and weekend patterns. The ratio value of 1 extends over most of the research circle with the exceptions of an area with ratio values slightly less than 1 in the extreme northern part of the circle and in a small area between Granite City and Collinsville. There are also two areas with ratios slightly greater than 1, one in the vicinity of Wood River and the other in the southeastern part of the circle. The ratios never fall below 0.99 and never exceed 1.01, so point differences between weekday and weekend patterns are <1%. Hence, differences in precipitation would not be expected between weekdays and weekends if the urban heat island is a major cause of the rainfall anomalies.

A comparison was also made of the weekday and weekend dew point patterns prior to the start of a storm since this is also a possible cause of the rainfall anomalies. These comparisons are shown on figures D-33b, d, and f. The weekday pattern is typical of general moisture conditions prior to rainfall in the research area. It is characterized by a dry area in the city which extends to the west. This broad, relatively dry area generally coincides with the relatively warm area shown on figure D-33a. Another characteristic of the moisture pattern is the more moist area located east of the Mississippi River and the more moist area extending from Granite City northwestward into the bottomlands area between the Missouri and Mississippi Rivers. The weekend pattern basically contains the same pattern features found in the weekday pattern.

The ratio comparison pattern of weekday dew points to weekend dew points (figure D-33f) shows the weekday pattern is more moist than the weekend pattern in the region enclosed by the 1.01 isoline. This broad area includes the city and the area extending northwestward into and through the bottomlands area. There is also a more moist area in the eastern portion of the circle and a small area drier on weekdays than on weekends (ratio values <1) in the southeastern part of the research circle. Thus, any difference in rain production by cells caused by differences between weekday and weekend moisture conditions would be expected to be the greatest in the bottomlands cells and/or in the St. Louis cells.

The differences in moisture supply, on the order of 1 to 3% are quite small. However, an inspection of table D-22 indicates that the greatest ratio difference between weekday and weekend cells occurs in the bottomlands area (ratio 1.46). The average volume for weekend cells in the bottomlands is very similar to that of the control cells, and even though the weekday volume is somewhat greater than the control, it is certainly not as great as the volumes in the other areas for weekday cells. Essentially, there is no difference between weekday and weekend dew points values. Therefore, differences in precipitation would not be expected between weekdays and weekends if the surface moisture field is a major cause of the rainfall anomalies.

Distribution by Months. Since the synoptic conditions and/or the circulation patterns may be different from month to month during the summer, another useful stratification to make is one by months. Thus, the raincell data were stratified according to month of occurrence (June, July, and August), and the resulting rainfall volumes are listed in table D-23. For the control data, the rainfall volume was the heaviest during July, whereas the volumes for June and August were lower and nearly identical. In the St. Louis-industrial (SI) and St. Louis (L) cells, the volumes are considerably heavier during July and August than during June. This is also true for the H cells, whereas the W and B cells have the heaviest rainfall volumes during June.

With regard to effect-control percent differences, the largest percentage increase occurs in August for the St. Louis cells and in July for the St. Louis-industrial cells, although the percentage increase in August is nearly as large as in July for the St. Louis-industrial cells. In the W and B cells, the highest percentage increase occurs in June though the percent increase is

Table D-23. Comparison of Average Rainfall Volume from Effect and No-Effect Cells According to Month for Summer 1971-1975*

	L	SI	W	H	B	C
June	21.5(103)	28.1(166)	25.0(137)	14.3(35)	14.1(34)	10.6
July	25.5(118)	43.3(271)	23.2(99)	21.2(81)	11.6(-0)	11.7
August	26.1(143)	37.4(248)	13.0(21)	19.9(85)	11.4(6)	10.7

• Volume (hectare-meters)
Note: Effect-control differences are expressed as % of control in parentheses

relatively small when compared with the percent increase in the other categories. Thus, the results of this comparison indicate that effects on rain volumes in the source regions vary according to month. Additional analyses concerning these findings are discussed in later sections.

Comparisons by Cell Parameters

Before determining the structure of the rainfall increase, it must first be established whether the test comparisons between the two sets of cells are significant. In this study, discriminant analysis was used 1) as a method for testing whether a test comparison is significant when all parameters are jointly considered, and 2) to determine the cell parameters which contribute the most in determining the difference between the two sets of cells. The Chi-square approximation was then employed to obtain Chi-square values for assessing the discriminating power of the test battery. In this multivariate procedure, only one test statistic is obtained for all cell parameters. In the typical univariate procedure, several test statistics are obtained and often the importance of a single test parameter will be overestimated.

The Chi-square values are useful in assessing which test comparisons have the greatest differences between potentially affected and control cells, but they are not used as a strict accept-reject rule. The major reason for this is that the test statistic is applied to a total population of cells and not to a random sample from a population. Nevertheless, it is of interest to consider those values of Chi-square required for significance at the 10% level if these were random samples. Hence, the probability of the Chi-square statistic for random sampling conditions is given. However, these probabilities are given only for those comparisons in which the values are ≤ 0.10.

Once it has been determined that a difference exists, the standardized discriminant coefficients are used to establish which cell parameters are the most important. These parameters are listed in tables D-24 through D-28 whenever the corresponding discriminant weights are ≥ 0.50.

Table D-24 presents the results obtained from the application of discriminant analysis to the indicated test comparisons for stratifications based on the path length of the cells. Assuming that the test comparisons with probabilities <0.01 are significant, then the 'all cells' category is significant for all test comparisons. Significant differences exist between the L and control cells, and between SI and control cells for all stratifications of path lengths. Further inspection of the L vs C and the SI vs C test comparisons reveals that the most important parameter in these comparisons for all stratifications is area. In addition, for the category of path lengths ≤ 6.4 km, the volume is important in both test comparisons, while the mean rainfall is important in the L comparison and the maximum rainfall is important in the SI comparison.

For the 'all cells' category, all comparisons are significant. However, the comparisons appear to have different characteristics. For example, whereas the L vs C and the SI vs C comparisons

Table D-24. Multivariate Discriminant Test and the Most Important Cell Parameters for Selected Test Comparisons According to Path Length

Test comparison	*≤6.4 km*	*≤12.8 km*	*≤19.3 km*	*All cells*
L vs C	VO,M,A(<.01)	M,A(<.01)	A(<.01)	A(<.01)
SI vs C	VO,A,MXR (<.01)	A(<.01)	A(<.01)	A(<.01)
W vs C	IN	IN	IN	VO(<.01)
H vs C	IN	VO,M,MXA,PL, MIN(=.02)	MXA,PL(<.01)	PL(<.01)
B vs C	IN	IN	IN	VO,M,MXA (<.01)
L vs W	IN	A(=.04)	VO,M,A(=.03)	VO,A(<.01)
L vs H	IN	IN	A,MXA,PL (=.05)	A,MXA,PL(<.01)

Note: Chi-square probabilities are given in parentheses; cell parameters are listed only when standardized discriminant weights are ≥ ±.5
Legend: A=area; Duration; IN=insignificant; M=mean rainfall; MIN=minimum rainfall; MXA=maximum area/ 5 min; MXR=maximum rainfall/5 min; PL=path length; VE=velocity; and VO=volume

Table D-25. Multivariate Discriminant Test and the Most Important Cell Parameters for Selected Test Comparisons According to Years*

Test comparison	*1971*	*1972*	*1973*	*1974*	*1975*
L vs C	A(<.01)	A(<.01)	A(<.01)	A(<.01)	PL(<.01)
SI vs C	A(<.01)	A(<.01)	none(<.01)	A(<.01)	MXR,PL(<.01)
W vs C	VO,M,A,MXR, MXA(<.01)	A(<.01)	IN	IN	VO,MXR,MXA, PL,MIN(=.06)
H vs C	M,MXA,MIN (=.02)	IN	A,MXR,MXA, PL,MIN(<.01)	M,MXR,PL (<.01)	PL(<.01)
B vs C	IN	IN	IN	IN	IN
L vs W	VO,M,A,MXR, VE(=.03)	IN	IN	IN	IN
L vs H	IN	IN	IN	IN	IN

*** Chi-square probabilities are given in parentheses**
Note: See table D-24 for legend

are dominated by the area parameter, the W vs C comparison is dominated by the volume parameter and the H vs C comparison is dominated by the path length parameter. However, the B vs C, L vs W, and L vs H comparisons are dominated by a mixture of all parameters (volume, mean, maximum rain/5 min, area, and path length). Furthermore, in the ≤19.3 km and ≤12.8 km test comparisons, a mixture of cell parameters (the area parameter is generally most important) is the rule.

Table D-25 gives a breakdown of significant comparisons by years. The L vs C and SI vs C comparisons are significant in all 5 years, whereas the W vs C comparison is significant in 3 of 5 years and the H vs C comparison is significant in 4 of 5 years. In the W vs C and H vs C comparisons, a mixture of the most important cell parameters has a tendency to occur, whereas the L vs C and SI vs C comparisons typically have only one outstanding parameter. Although area is often one of the important parameters in the W vs C and H vs C comparisons, a mixture of parameters that contribute to differences between cells often occurs.

Table D-26. Multivariate Discriminant Test and the Most Important Cell Parameters for Selected Test Comparisons According to Synoptic Classification of the Storm*

Test comparison	*Air mass*	*Squall line*	*Squall zone*	*Cold front*	*Static front*
L vs C	VO,A(=.04)	A(<.01)	A(<.01)	A,MXR(<.01)	A(<.01)
SI vs C	VO,M,A,MXA (<.01)	A(<.01)	A(<.01)	M-,A-(<.01)	A(<.01)
W vs C	VO,M,MXR, MXA(=.08)	VO,PL(<.01)	IN	IN	IN
H vs C	M,A,MXA,PL, MIN(=.07)	PL(<.01)	MXR,MIN (<.01)	PL(=.07)	M,A,MXR,VO (=.04)
B vs C	A,PL,VE(=.01)	IN	MXR,VE (=.06)	IN	IN
L vs W	IN	IN	IN	IN	M,A,MXR,MIN (=.04)
L vs H	IN	A,PL(=.08)	A,VE,MIN (=.06)	IN	IN

*** Chi-square probabilities are given in parentheses**
Note: See table D-24 for legend

Table D-27. Multivariate Discriminant Test and the Most Important Cell Parameters for Selected Test Comparisons According to Time of Day*

Test comparison	*0000-0600*	*0600-1200*	*1200-1800*	*1800-2400*
L vs C	MXR(<.01)	A,PL(<.01)	A(<.01)	A,PL(<.01)
SI vs C	PL(<.01)	A(<.01)	A(<.01)	A(<.01)
W vs C	M,A,MXR,PL, MIN(<.01)	VO,M,A,MXR, MXA(=.02)	VO,M,A,MXR, PL(=.01)	MXR,PL(<.01)
H vs C	VO,PL(=.09)	IN	M,PL(<.01)	VO,A,MXA,PL (<.01)
B vs C	IN	IN	VO,M,A,MXR, VE(=.07)	IN
L vs W	A,MXR,PL, MIN(=.03)	VO,M,A,MXA, PL(=.04)	VO,MXR,PL (<.01)	IN
L vs H	IN	M,A,PL,(=.07)	IN	IN

*** Chi-square probabilities are given in parentheses**
Note: See table D-24 for legend

It is also noted that 1971 is the only year in which a significant difference occurred between L and W cells.

The results given in the table imply that W and H cells are different from the associated control cells by parameters other than those of L and SI cells. However, a direct comparison of L and W cells produces significance in only one year.

The multivariate test of selected comparisons according to synoptic classification of the storms is shown on table D-26. The L vs C and SI vs C comparisons are significant in all of the synoptic classifications. Overall, the most important cell parameter is area. A mixture of parameters contributes to the difference between cells with respect to the various synoptic types.

Table D-27 includes comparisons of cells during 6-hour periods of the day. The L vs C and SI vs C comparisons are significant for all 6-hour periods. Area generally seems to be the most important parameter, although maximum rain and path length are important for the L vs C and the

Table D-28. Multivariate Discriminant Test and the Most Important Cell Parameters for Selected Test Comparisons According to Months*

Test comparison	*June*	*July*	*August*
L vs C	A(<.01)	A(<.01)	A(<.01)
SI vs C	A(<.01)	A(<.01)	A(<.01)
W vs C	VO,PL(<.01)	VO,MXR(<.01)	D,MXR,MXA, PL(=.06)
H vs C	IN	MXR,PL(<.01)	M,A,MXA,PL (<.01)
B vs C	IN	IN	IN
L vs W	IN	VO,MXR,PL (=.03)	VO,M,A,(<.01)
L vs H	IN	IN	IN

*** Chi-square probabilities are given in parentheses**
Note: See table D-24 for legend

SI vs C comparisons, respectively, during the 0000-0600 period. A mixture of cell parameters are important in the W vs C and H vs C comparisons, but the maximum rain and maximum area are important parameters for all 6-hour periods. These parameters are also important in the L vs W comparisons, and this implies that an important difference between L and W cells may involve the maximum rainfall parameter (related to rainfall intensity).

Table D-28 gives the most important cell parameters for test comparisons according to months (June, July, and August). It illustrates that area is the most important parameter for L vs C and SI vs C comparisons in all months. However, in the W vs C comparison, a mixture of parameters contribute to the difference between cells (maximum rain and maximum area are two of the parameters). It is also evident that more significant differences occur in July and August than in June. However, the L vs C, SI vs C, and W vs C comparisons are significant in all three months.

The overall results would imply that area is the single most important parameter in the St. Louis (L) and St. Louis-industrial (SI) cells. It is also generally present in the other areal stratifications of cells. This may have physical meaning, or it may simply mean that the cells are biased according to area, since St. Louis is located such that it has a greater opportunity to sample the longer-moving and longer-duration cells. However, the comparisons involving path length (table D-24) would auger against this, since area is important in all four of the path length stratifications. Also, it was previously demonstrated that a percent increase in volume existed even in the short cells (path length $\leq$6.4 km).

From these comparisons, maximum rain seems to be more important in the Wood River cells, and this may be the major difference between Wood River and St. Louis cells. These differences could be related to greater dynamic effects in the St. Louis area that lead to raincells with larger areas. Since the differences between Wood River cells and control cells are most often characterized by parameters relating to intensity (maximum rain and maximum area), a different physical process appears to be operative in these cells.

The fact that cells from all areas are significantly different in some of the stratifications implies that all non-control cells are somewhat different from the control cells. However, as noted in table D-19, the differences are ordered such that the largest difference is found in the SI cells followed by L, W, H, and B cells. Thus, the urban-industrial cells have the largest differences.

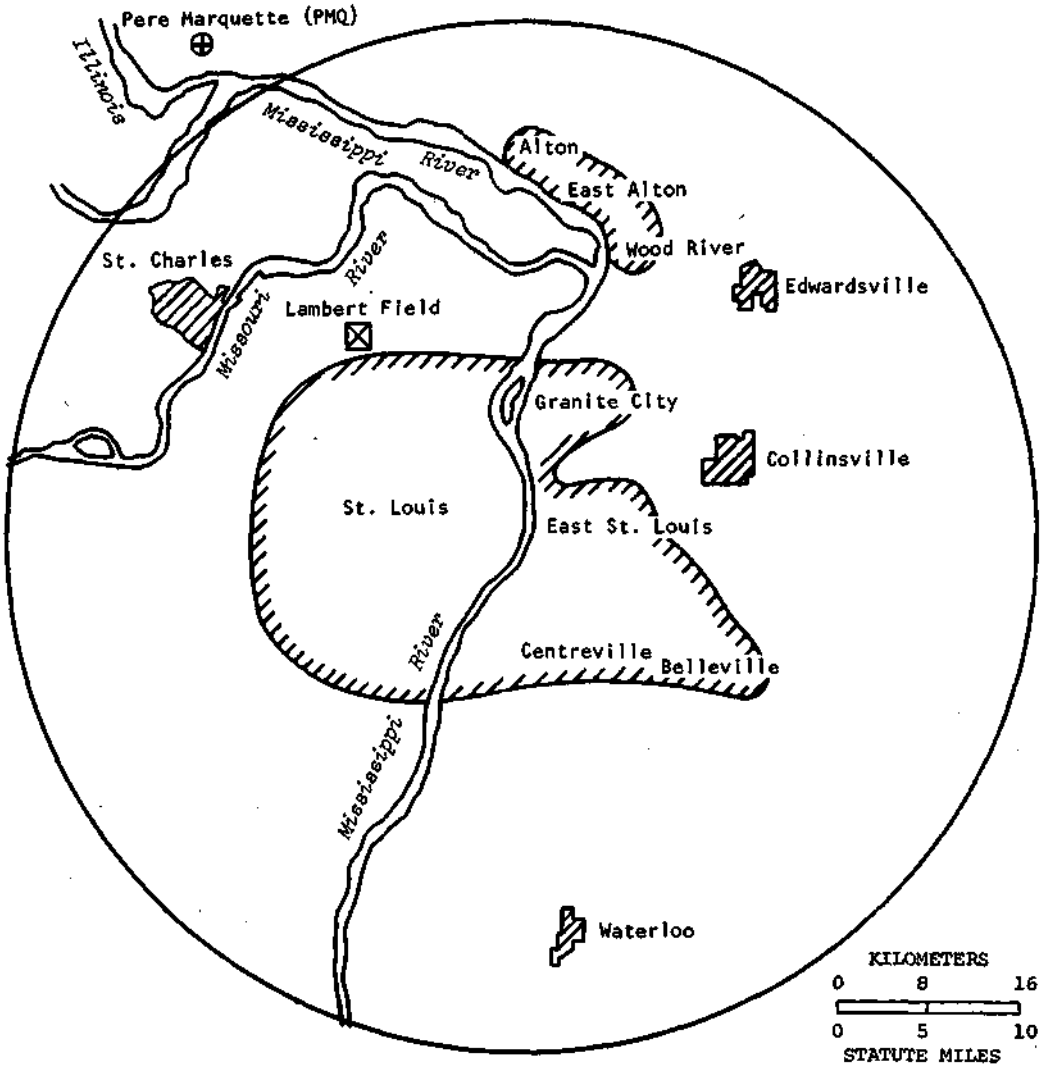

Figure D-34. Location of cities and other points of interest within the research circle

Raincell Initiations

Locations of cities and other points of interest referred to in the following sections are shown in figure D-34. The June 1971-1975 raincell initiation pattern (figure D-35a) has two primary areas of maximum initiation: 1) an area including Edwardsville, Wood River, and Granite City, and 2) an area extending from the Mississippi River across East St. Louis. Other secondary raincell initiation maximums were indicated.

The maximum cell initiation (30) region during June occurred at Edwardsville. Other large initiation values occurred directly north of Granite City, directly east of East St. Louis, and northeast of Belleville.

Four primary regions of raincell initiation are found on the July 1971-1975 pattern (figure D-35b): 1) the Wood River-Edwardsville region, 2) the northwest bottomlands, 3) south St. Louis, and 4) the region directly south of East St. Louis-Centreville and Belleville.

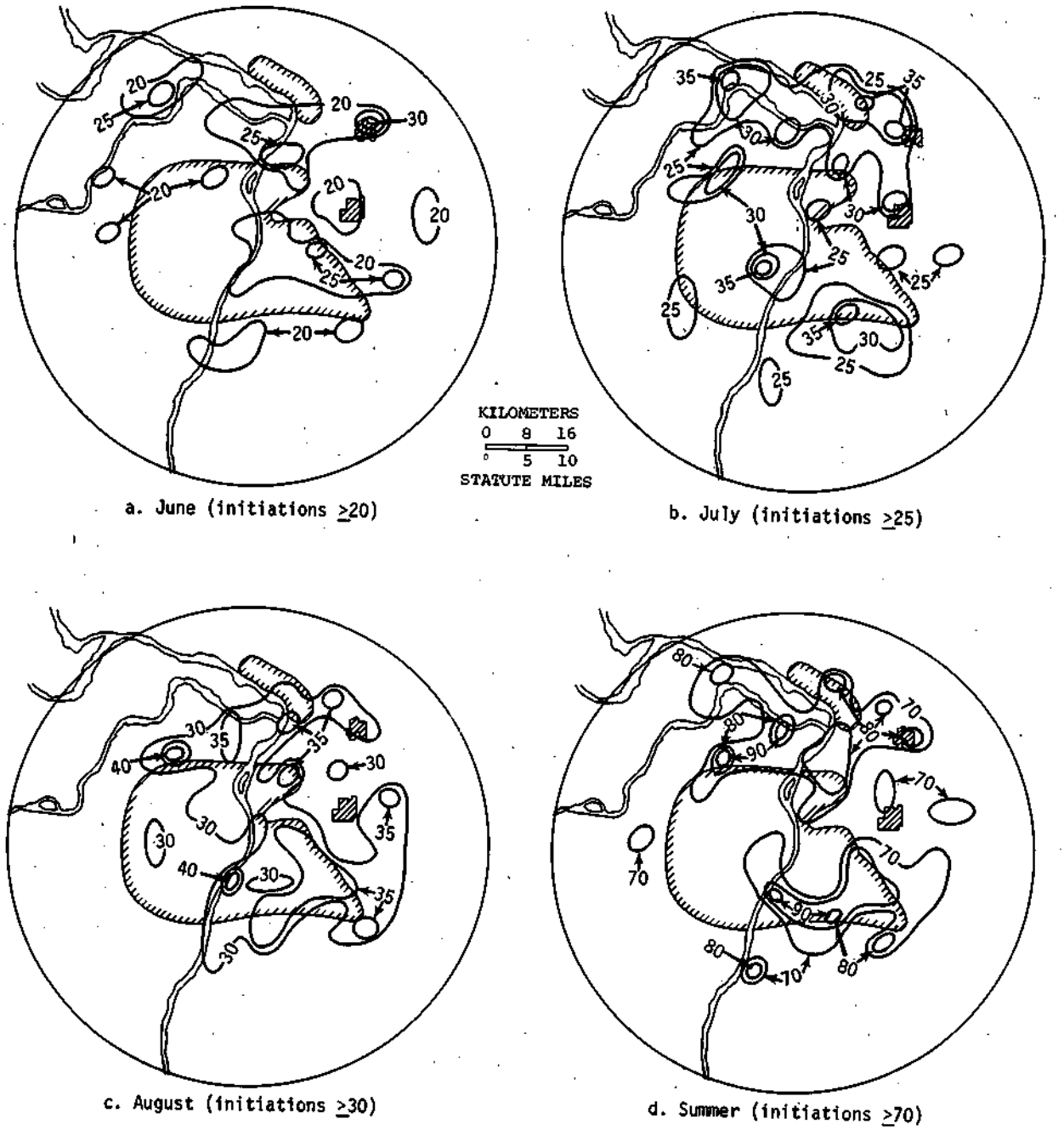

Figure D-35. Monthly and seasonal patterns of complete raincell initiation

Comparison of the June and July initiation patterns indicates three major differences: 1) the appearance of the strong Wood River-Edwardsville initiation maximum in July —the June maximum located between Wood River and Granite City apparently shifted northward, 2) the appearance of the south St. Louis initiation maximum in July —this region seems to be a new development rather than a shift of a maximum from the June pattern, and 3) the maximum located across East St. Louis in June seems to have shifted to directly south of the city, and a minimum initiation area is centered over East St. Louis in July.

Similarities of the June and July initiation patterns include the existence of initiation maximums in the bottomlands and around Collinsville.

The maximum raincell initiation region for August 1971-1975 (figure D-35c) extended from the east side of East St. Louis to Belleville. A general initiation maximum occurs along a line from Alton to directly south of East St. Louis, and isolated areas of peak initiation activity occur elsewhere. The greatest number of cell initiations (>40) occurred in the vicinity of Lambert Field.

Comparison of the August initiation pattern with those for June and July shows two major differences: 1) no cell initiation maximum occurs in the northwest bottomlands in August —such a maximum existed in both the June and July patterns, and 2) no pronounced initiation maximum occurred over south St. Louis in August —such a maximum existed in July but not in June. Similarities of the July and August patterns include the initiation maximums near Lambert Field and southeast of Centreville.

The June, July, and August patterns were combined to give the total raincell initiation pattern for summer 1971-1975 (figure D-35d). Two principal regions of maximum raincell initiation are evident: 1) a region extending from the northwest bottomlands and Lambert Field east to Edwardsville, and 2) a region that meanders from the southern portion of St. Louis southeastward to Belleville.

It is important to note that, in general, the maximums in all initiations did not occur within the city of St. Louis. In fact, it seemed that initiation maximums were most likely to be located along the boundaries of the city on the north, northeast, south, or southeast sides. Thus, the instability of the temperature gradient along the boundaries of the urban heat island may be influencing the initiation of raincells.

Raincell Mergers*

Analyses were made of the characteristics of raincell mergers in the METROMEX network during 1971-1975. A limited sample of radar data (see section on radar analysis, page 265) had indicated that radar echo mergers tend to occur more frequently in the St. Louis-Collinsvilie-Belleville area where the urban effect is strong. Mergers of convective clouds and rain systems have been shown to be associated with rain intensification (Huff, 1967; Simpson et al., 1972). Mergers would likely be favored in a region of urban rainfall enhancement, since the major cause of enhancement appears to be growth in raincell sizes:in the St. Louis area (Huff, 1977b) related to more first echoes in the area.

Therefore, it was considered pertinent to pursue evaluation of the merger phenomena further through use of the large sample of surface raincell data. Particular attention has been given to the comparative frequency of mergers between urban-effect, topographic-effect, and no-effect regions within the network. The enhancement of rainfall following mergers has been

**'Contributed by Floyd A. Huff; the work was performed jointly under the Metromex program and NSF Grant ENV74-2435 7 entitled "Assessment of Weather Modification in Alleviating Agricultural Water Shortages during Droughts."*

studied during relatively dry, wet, and near-normal periods to determine whether mergers, and, consequently, rainfall enhancement are more frequent in regions of topographic and urban effects during dry periods. If so, this is useful background information both for evaluating the potential of weather modification to alleviate droughts, and for planning modification operations, if deemed desirable.

A merger was defined as the joining of two surface raincells which had been at least 8 km apart initially, and had existed for at least 10 minutes prior to merger. Qualification also dictated that the merged entity exist for at least 10 minutes following merger. In order to eliminate numerous mergers of very tight raincells which contribute insignificantly to storm totals, it was required that the maximum intensity in one of the two merging cells (or both) must be 6 mm hr^{-1} (0.25 in hr^{-1}) or more prior to merger. This limited the sample to those convective entities which could contribute significantly to urban and topographic anomalies, and to rain entities of significance from the standpoint of planned weather modification. The above definitive criteria yielded a sample of 325 mergers during the five summers.

Initially, a problem arose in assignment of cell area within a complex storm system where the individual cells were not isolated from surrounding precipitation. It was decided to define cell area as the area included in closed isohyets directly asociated with a particular cell. This procedure separated the cell rainfall (rain intensity center) from the lighter background rainfall of the parent storm system.

Analyses were performed for each storm day to determine the number of mergers meeting the definitive criteria, their location in the network, changes in cell intensity and area following merger, and duration of cells prior to and following merger. The merger was assigned to the raingage nearest to which it occurred. This provided a convenient means for comparison of frequency of mergers in different parts of the network. The merger data were then summed over monthly and seasonal periods, and were stratified also into three monthly groups classified as below normal, near normal, and above normal. The separation by normality of rainfall was made to investigate differential effects, and thus to help evaluate the urban and topographic effects and the potential for planned weather modification. Mergers were also stratified according to synoptic type, storm mean rainfall, and diurnal occurrence.

Monthly and Seasonal Spatial Distributions of Mergers

1971. Summer 1971 was the driest in the 1971-1975 period. The network averaged 54% of normal in June. This increased to 115% in July and dropped to only 21% of normal in August. The 3-month period was 63% of normal. Mergers were concentrated downwind of St. Louis in the Granite City-Collinsville area (figure D-36a) and along the Missouri River and the Merrimac River which is downwind of the Ozark foothills. This pattern suggests that the mergers were stimulated by environmental influences, including river bottomlands (heat-moisture source), the St. Louis urban area, and possibly the SW hills. The greatest number of mergers was in the NE quadrant of the network where the seasonal rainfall was heaviest (Huff, 1977a, figure B-2) and all were in the vicinity or downwind of urban-industrial areas at St. Louis and Alton-Wood River.

1972. Summer rainfall averaged *69%* of normal with a range from 32% of normal in June to 80% in July and 104% in August. The most mergers occurred in the SE quadrant (figure D-36b) where 36% of the total occurred. This quadrant is subject to both urban and hill effects, depending upon storm movement and low-level winds. Figure D-36b shows a concentration E of St. Louis which was likely urban-related, and others S to SE of the city where both topographic and urban effects could have been involved. Summer rainfall was heaviest in the SE and NE quadrants (Huff, 1977a, figure B-3).

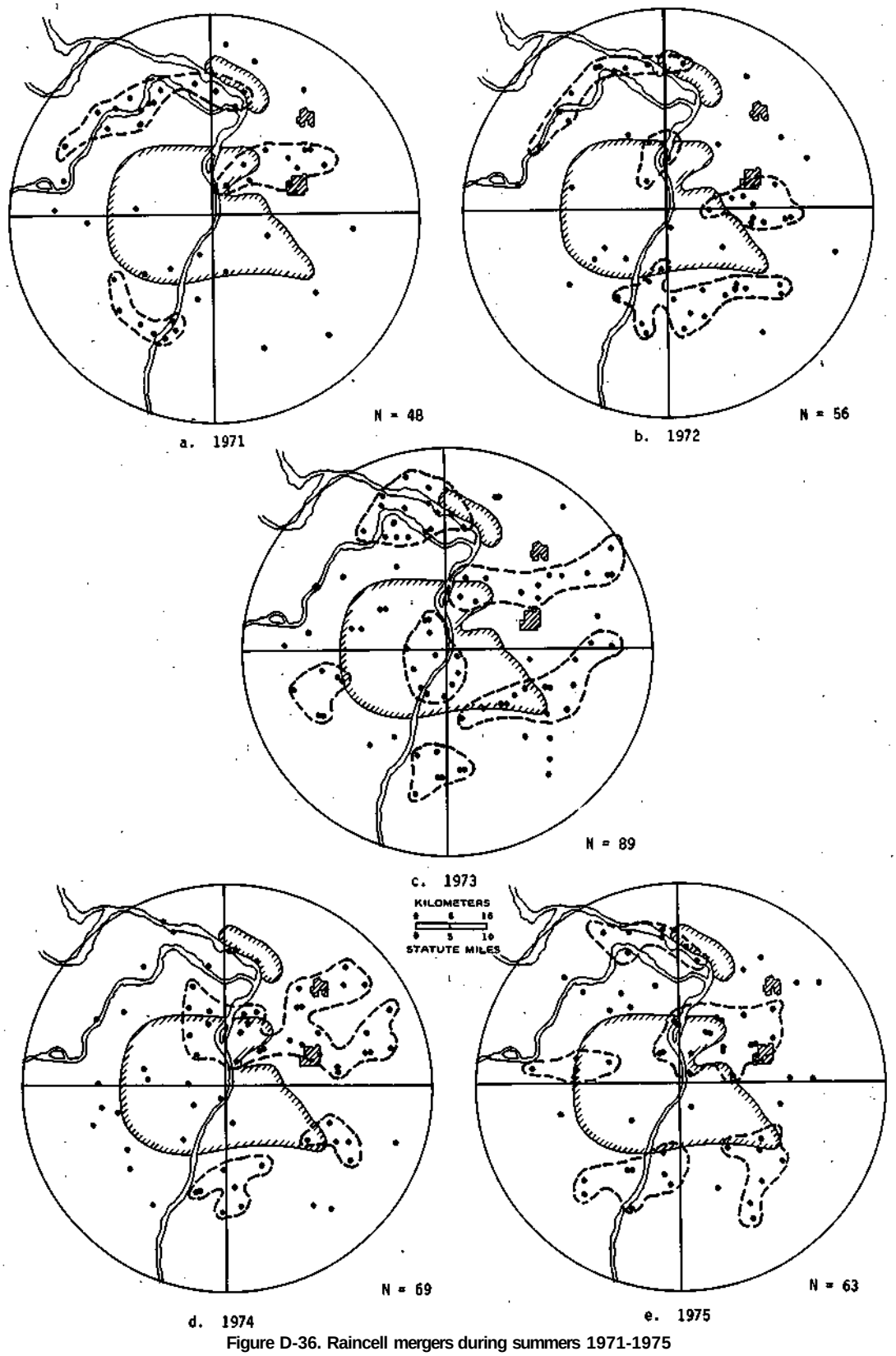

Figure D-36. Raincell mergers during summers 1971-1975

1973. Average rainfall was slightly above normal (103%) for the summer with a large positive departure of 125% of normal in June followed by 101% in July and 78% in August. Heaviest rainfall was in the Granite City area (Huff, 1977a, figure B-4): Approximately 50% of the mergers (figure D-36c) occurred within or a few miles downwind of the urban-industrial areas in this nearly normal summer. A preferential area was indicated also in the bottomlands in the NW quadrant. A total of 89 mergers were identified compared with 48 and 56 in the dry summers of 1971 and 1972.

1974. This was a moderately below-normal summer (81%) with 61% of normal in June, 31% in July, but a heavy 156% in August. The greatest concentration of mergers was in the NE quadrant with 41% of the network total (figure D-36d). These were all in locations where they could have been urban-related. There was no particular concentration along the river valleys, NW bottomlands, or hills. Of the *69* mergers, 22% were in the immediate urban area of St. Louis and Alton-Wood River, and 19% were downwind (E or NE) of the urban-industrial areas.

1975. Summer rainfall was near normal (101%), and ranged from 68% of normal in June to 109% in July, and a heavy 139% in August. Again, the most obvious concentration of mergers was in the urban-industrial areas or within a few miles downwind of them (figure D-36e). Of 63 mergers, 48% were within or downwind of the urban-industrial areas, particularly in the St. Louis-Collinsville-Edwardsville area. There were slight indications of preferential regions associated with bottomlands and hills. The cluster of mergers in the NE quadrant correlates well with the region of relatively heavy rainfall extending from Granite City to Edwardsville (Huff, 1977a, figure B-6).

June 1971-1975. Figure D-37 shows plots of echo locations for each month for all five summers combined. The June plots indicated three regions of concentration —in the bottomlands of the NW quadrant, in the immediate urban area of St. Louis, and S and SE of St. Louis in regions subject to both topographic and urban influences. Below-normal rainfall was experienced in 4 of the 5 Junes. Only 25% of the 325 mergers sampled during 1971-1975 occurred in June. The concentration of mergers in the areas of potential urban and topographic effects in this relatively dry group of months has implications relative to planned weather modification activities, since mergers are frequently associated with rain intensification. The merger clusters in figure D-37a correspond to highs in the June rainfall pattern (Huff, 1977a, figure B-7).

July 1971-1975. Figure D-37b shows the distribution of mergers during July. Again, there were concentrations in the bottomlands, and this concentration extended SW along the Missouri River valley. Another concentration was over and east of St. Louis, and a third occurred in the SE quadrant. In general, there was good agreement in the location of major merger areas in the relatively dry June pattern and the July distribution when 3 of the 5 months had above-normal rainfall. Merger clusters tended to occur in or near regions of relatively heavy rainfall for July 1971-1975.

August 1971-1975. There were three above-normal months in the five summers, and two were much above normal (139% and 156%). Major concentrations occurred NE, E, and SE of St. Louis in regions subject to possible urban effects (figure D-37c). Secondary concentrations occurred in the NW quadrant and in the vicinity of the Ozark foothills. Thus, in all three months there were concentrations in regions that are frequently downwind of the St. Louis urban-industrial region. A strong correlation between August rainfall and merger clusters was indicated.

Summer 1971-1975. Figure D-38 shows the spatial distribution of all 325 mergers during the 5-summer period. For easier interpretation, totals are shown for grid squares of 92 km^2 which is the same grid pattern used in the radar echo study discussed elsewhere in this report (see page 265).

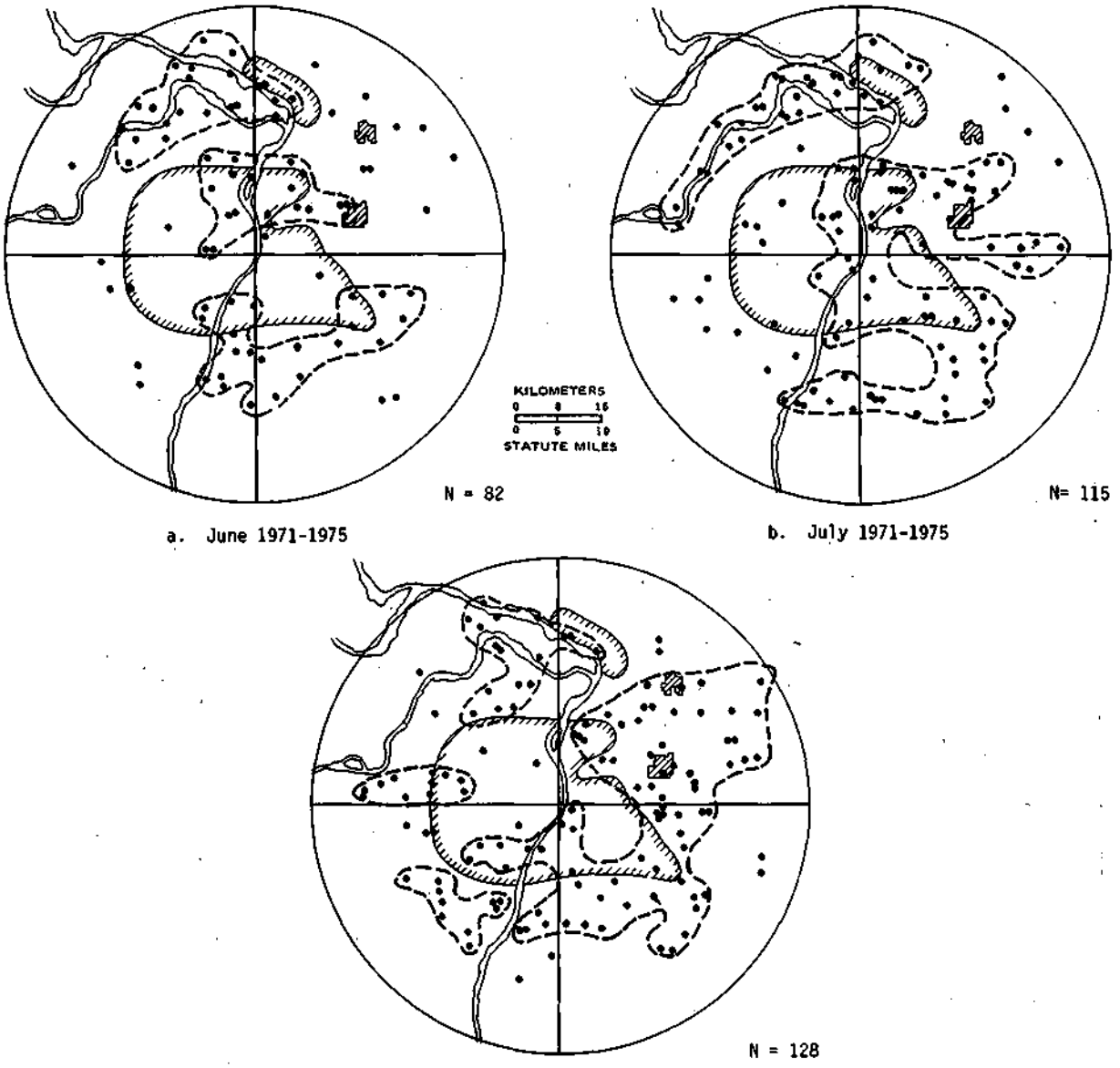

a. June 1971-1975

b. July 1971-1975

c. August 1971-1975

Figure D-37. Raincell mergers during June, July, and August 1971-1975

The average frequency was 6 with a standard deviation of 4. Mergers occurred most frequently in the Granite City-Collinsville region and in the bottomlands of the NW quadrant of the network. Frequencies in these areas were 2 to 3 times the network mean and over 2 standard deviations above the mean. Thus, the greatest frequencies were in areas subject to urban and topographic effects. Above-average frequencies also occurred in the southern part of the network where storms may be affected by movement across the Ozark foothills and the river bluffs. Frequencies over the western suburbs were below average, and this is a region of minimum urban effect.

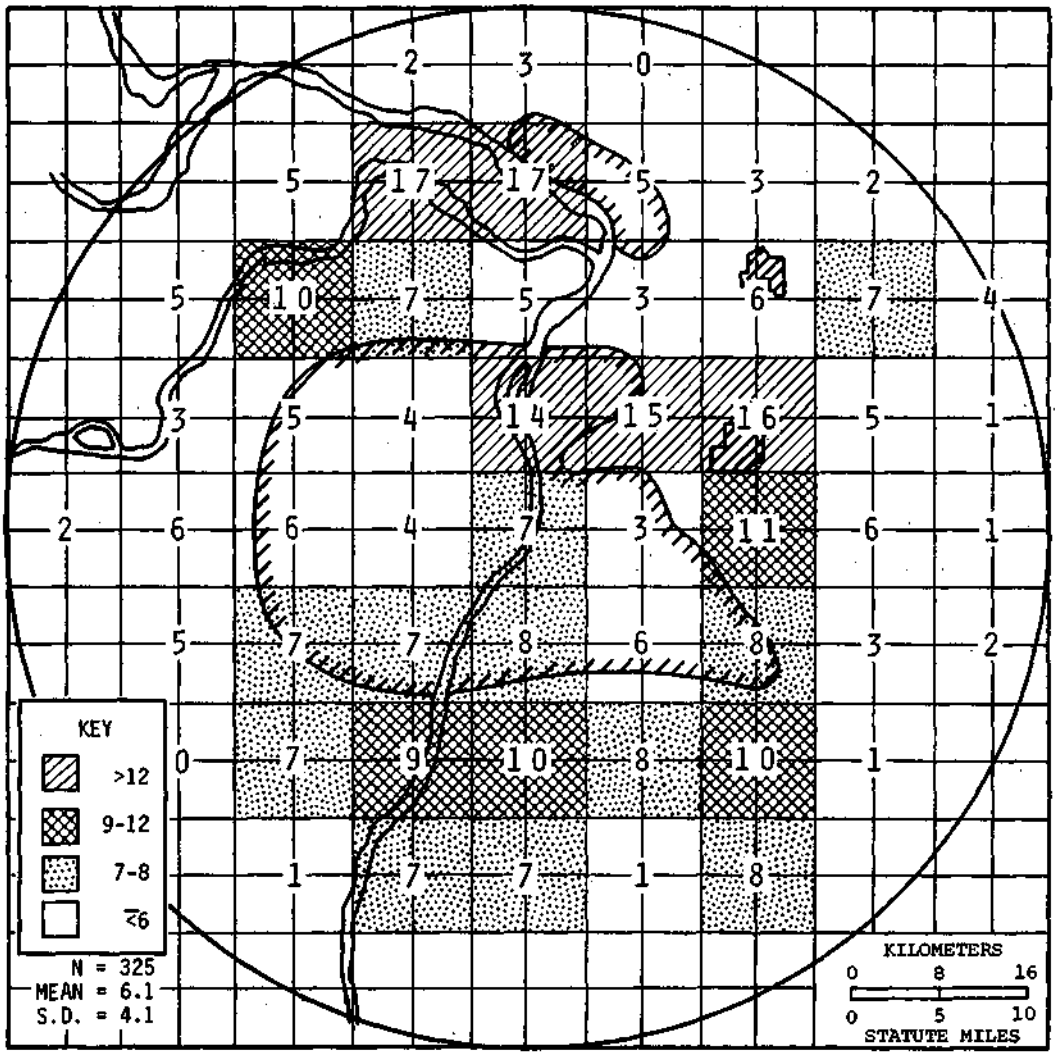

Figure D-38. Spatial distribution of all raincell mergers 1971-1975

In general, there appears to have been a tendency for mergers to occur most frequently in a major urban-effect area E and NE of St. Louis and in regions under topographic influences. Thus, figure D-38 provides support for other analyses which indicate that convective entities tend to develop more frequently or become enhanced over the urban-industrial region, which then leads to mergers and rain intensification downwind of the city (usually NE, E, or SE of the urban area). The bottomlands are believed to be a favored region of convective development in which topographic features and some urban input are involved, and this too should favor merger or consolidation of clouds.

Comparison was made of the raincell mergers in figure D-38 and the merger of radar echo systems in figure D-28 (section on radar analyses). There is general agreement between the relatively small radar echo sample (138 mergers in 35 storms) and the much larger raincell sample. Both show maximum frequencies in the region east of the urban-industrial area and in the vicinity of the Ozark foothills. Merger of radar echoes could not be determined in the NW bottomlands because this area was in the radar ground pattern.

Diurnal Distribution of Mergers

The frequency of raincell mergers at 3-hour intervals was calculated for summers 1971-1975 to determine whether mergers occurred more often during the daytime. It will be shown later that cell initiation and cell rainfall maximize in the period 1200-1500. These statistical results indicate the availability of more individual cells with greater rainfall available for merger at a later time. Since other analyses had shown that total rainfall maximized in the period from 1500 to 1800 CDT, it seemed reasonable to expect mergers to maximize at approximately the same time. Sample size was not adequate to group diurnal mergers further by individual month and year.

As expected, analyses indicated that 77 (24%) of the mergers occurred from 1500 to 1800, when approximately 20% of the network summer rainfall occurred. As shown in figure D-39b, the mergers tended to cluster in the late afternoon over and east of St. Louis. This is a logical sequence of urban initiation and enhancement of convective entities over the urban-industrial areas which would promote mergers (more and larger raincells) over and downwind of the city. That is, the mergers are clustering where expected in consideration of urban enhancement processes, storm motions, and maximizing of rainfall in late afternoon. The pattern of total rainfall for 1500-1800 (Huff, 1977a, figure B-23) closely resembled the merger pattern in the 1500-1800 period.

Figures D-39a and c show the distribution of mergers at 1200-1500 and 1800-2100 which ranked next to 1500-1800 in merger occurrences. During 1200-1500, nearly 20% of all mergers occurred, and 58 (18%) were recorded at 1800-2100. The earlier pattern at 1200-1500, preceding the network maximum, shows major clusters extending eastward from St. Louis and along the Missouri River valley into the bottomlands at the confluence of the Missouri and Mississippi. Reference to total rainfall patterns during this period does not show the strong correlation between mergers and rainfall that is apparent in the late afternoon patterns. These topographic-related convective entities apparently do not become as intense, on the average, as the urban-related entities.

The early evening pattern (1800-2100) in figure D-39c shows a major merger cluster ESE of the city in the Belleville area. The total rainfall pattern at that time also indicated a high in the Belleville region. The maximizing of rainfall and mergers farther downwind of the city is reasonable considering most frequent storm movements (W-E). Storms forming in the peak rain period of 1500-1800 would often be centered farther eastward, but still in the network in the early part of the 1800-2100 period.

Mergers were least frequent from 0000 to 0600 when only 39 (12%) of the total were recorded. Approximately 16% occurred in the 0600-1200 period, 43% from 1200 to 1800, and 29% from 1800 to 2400.

Distribution of Mergers by Synoptic Storm Type

The 325 mergers identified in the summers of 1971-1975 were classified by the synoptic storms types used by Vogel (1977). Analyses showed that approximately 72% of the mergers occurred in squall systems (squall lines and squall zones). Only 3% of the total occurred in non-frontal air mass storms. These frequencies agree well with the total rainfall distribution, in that a majority of the summer rainfall occurred with squall activity and very little with air mass situations. Since so many mergers were associated with squall systems, the spatial distribution of their occurrences was similar to the total distribution pattern of figure D-38. Thus, not unexpectedly, mergers are most likely to occur with organized, relatively large convective storm systems.

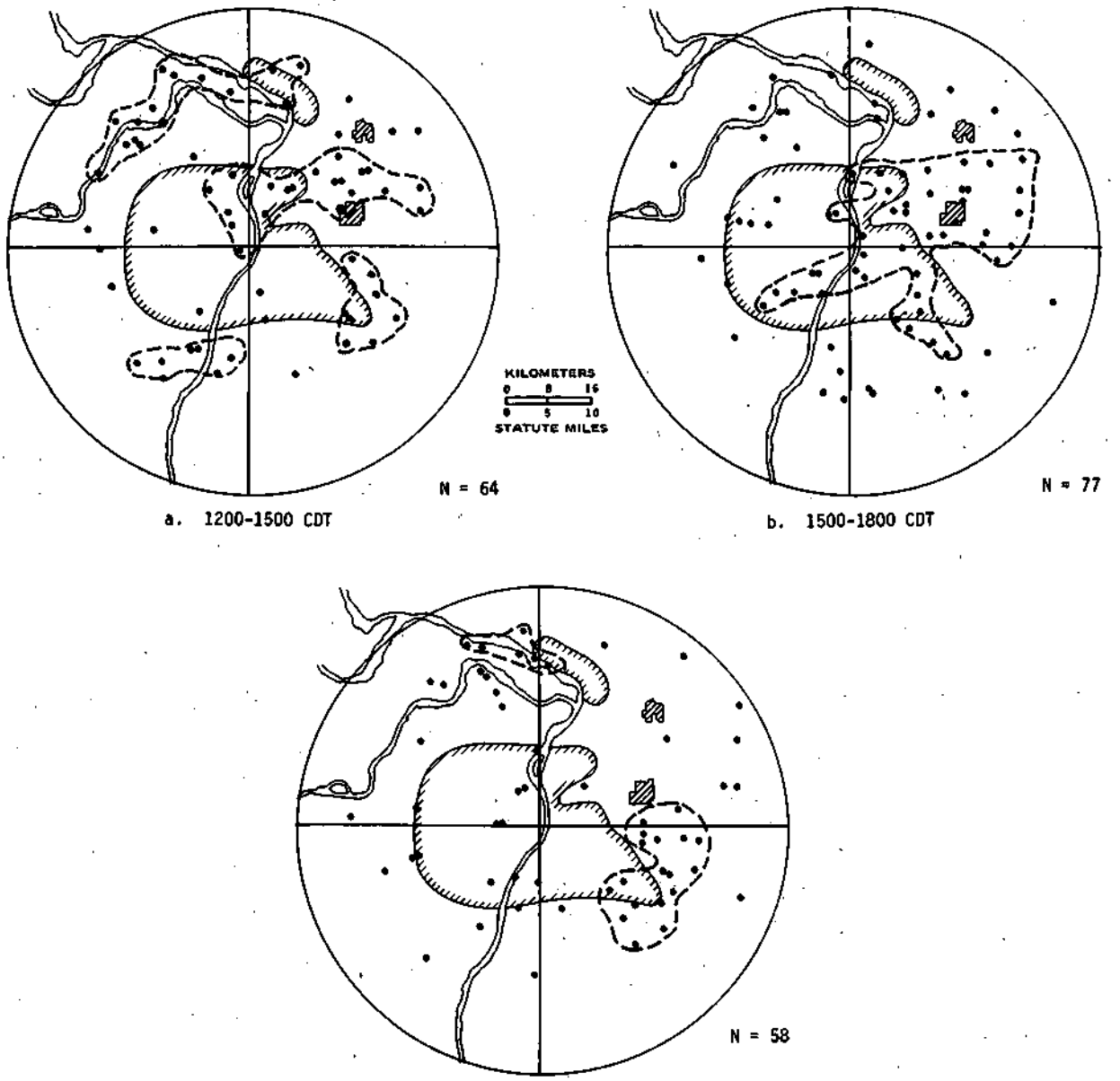

a. 1200-1500 CDT

b. 1500-1800 CDT

c. 1800-2100 CDT

Figure D-39. Diurnal distribution of raincell mergers 1971-1975

Distribution of Mergers by Storm Mean Rainfall

The sample of 325 mergers was grouped according to storm mean rainfall to determine how the frequency of mergers was related to storm magnitude (intensity) and whether there were differences in the mean rainfall relation within the network. Storms were divided into four classes in which network mean rainfall was a trace, 0.25 to 2.30 mm, 2.31-12.45 mm, and ≥ 12.45 mm. Approximately 4, 20, 52, and 24%, respectively, fell into the above groups. Nothing of significance was discerned in this analysis. For example, the area E of St. Louis and the NW bottomlands had the greatest frequencies in all three classes having significant rainfall amounts.

Spatial Patterns in Wet and Dry Periods

The spatial pattern of mergers was investigated for differences in relatively wet and dry periods. For this purpose, the 15-month sample was divided into six relatively dry, three near-normal, and six relatively wet months. The dry months had rainfall ranging from 31 to 68% of normal. The near-normal months varied from 80 to 101% of normal, and the wet months from 104 to 156% of normal.

Spatial patterns for the three groups are shown in figure D-40. The dry pattern of figure D-40 shows the greatest frequency of mergers just east of St. Louis in the Granite City-Collinsville area. Other areas with above-average frequency lie along the river valleys of the Mississippi and Missouri including the NW bottomlands, and in the Ozark foothills. Only 26% of the total mergers occurred in the six relatively dry months compared with 48% in the six wet months.

The wet month pattern of figure D-40 shows relatively high areas east of St. Louis in the regions of Granite City-Collinsville and Edwardsville-Collinsville-Belleville, and in the confluence of the Missouri and Mississippi Rivers in the NW bottomlands. Relatively high frequencies are also indicated again along the Missouri River, portions of the Mississippi, and the Ozark foothills. In general, the near-normal pattern of figure D-40 has relatively high areas in the same regions as the wet and dry months. Overall, there is a definite indication that mergers are favored downwind of urban-industrial areas, in river valleys, and hill regions.

Effects of Mergers on Raincell Characteristics

If mergers of convective entities tend to intensify the rain production processes as indicated by. several investigators (Huff, 1967; Simpson et al., 1972), then the rain intensity and/or areal extent of the rain-producing entities should tend to increase following mergers. Therefore, analyses were made to determine the characteristics of raincells prior to and following mergers. A general summary of the changes observed in the METROMEX sample of 325 mergers during 110 storm days in presented in table D-29.

Table D-29 shows that most mergers were followed by an increase in both area and rain intensity. Thus, 78% of the mergers were followed by an intensity increase and 82% by an area increase. Conversely, only 14 and 10%, respectively, were followed by a decrease in intensity and area. This helps verify previous observations that the merger of convective entities tends to increase the total rain production from the raincells involved.

The duration statistics in table D-29 show that the merged cells had a median duration of 33 minutes following merger, and this exceeds the duration of either cell prior to the merger. Among the 325 mergers, the median of the maximum intensity change after merger was an increase of 27 mm hr^{-1}, a relatively intense rate in itself. Similarly, the median of the maximum area change following merger was an increase of 90 km^2 , and this also is a substantial change.

Figure D-41 provides a more detailed description of the distribution of maximum intensity and area increases following mergers. The frequency curve derived from the intensity data shows

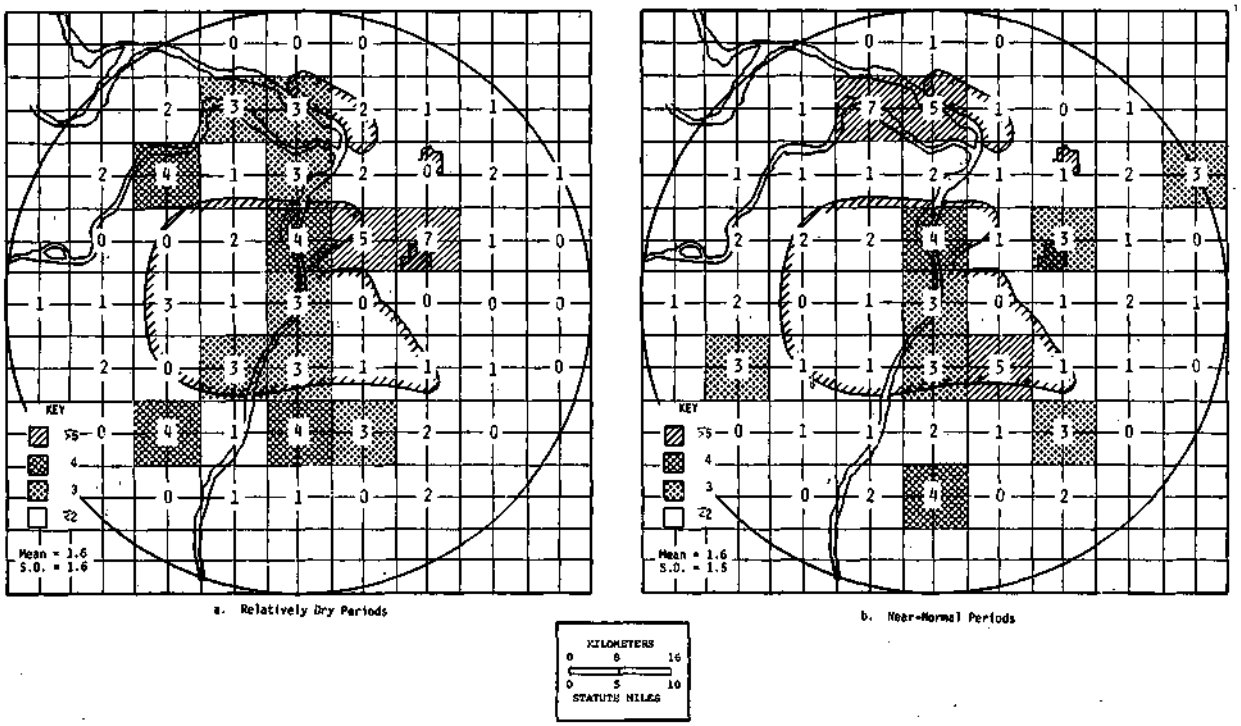

Figure D-40. Distribution of raincell mergers in wet and dry periods

Table D-29. Statistics of Rainfall Mergers for Summers of 1971-1975

Number and percent of mergers with intensity increase	254	(78)
Number and percent of mergers with no change in intensity	25	(8)
Number and percent of mergers followed by intensity decrease	46	(14)
Number and percent of mergers followed by area increase	266	(82)
Number and percent of mergers followed by no area change	25	(8)
Number and percent of mergers followed by area decrease	34	(10)
Median duration of merger-involved cells		
Oldest cell prior to merger *(min)*	26	
Newest cell prior to merger *(min)*	13	
Merged cell *(min)*	33	
Median of maximum intensity change after merger, $mm\ hr^{-1}$ and %	27	(57)
Median of maximum area change after merger, km^2 and %	90	(37)
Maximum intensity change among all cases, $mm\ hr^{-1}$	190	
Maximum area change among all cases, km^2	1119	

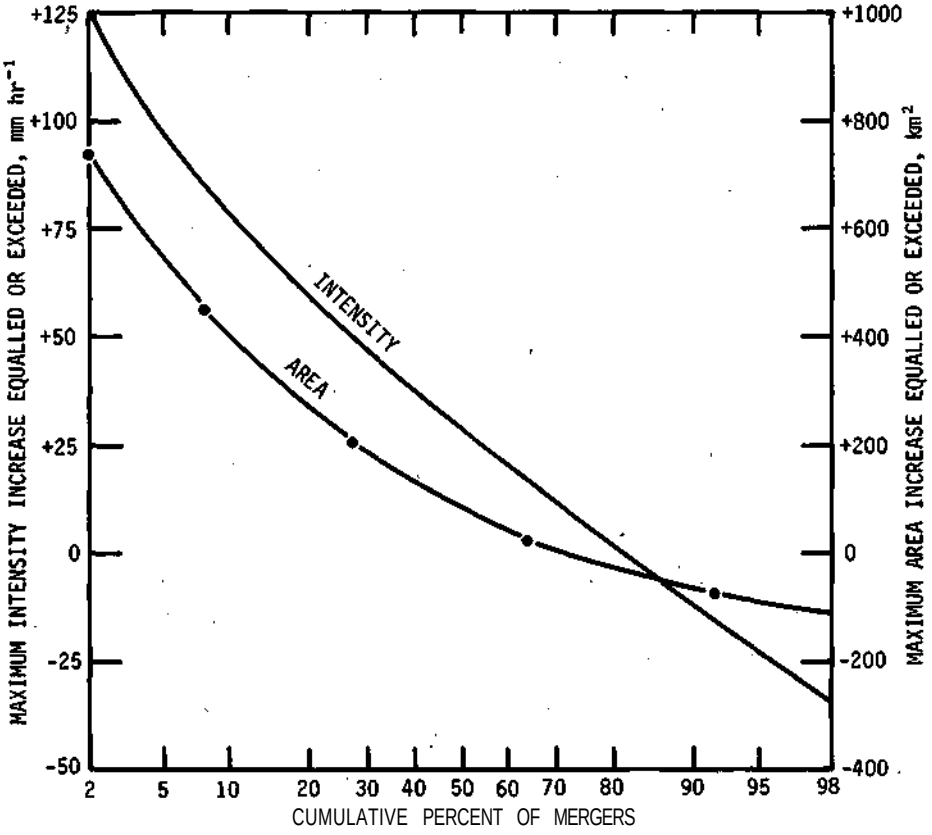

Figure D-41. Frequency distribution of maximum increase in intensity and area following surface raincell mergers, summers, 1971-1975

maximum increases ranging from 125 mm hr^{-1} for the upper *2%* of the mergers, and a gradual decrease to a negative 35 mm hr^{-1} at the lower *2%*. Area shows a range from a positive 740 km^2 at the upper 2% to a negative 100 km^2 at the lower 2%. Examination of other frequency distributions computed for months having relatively dry, near-normal, and above-normal rainfall conditions did not indicate any significant trend for the intensity to vary with changing degrees of wetness and dryness. However, a slight trend was indicated in area change. Thus, the medians of the maximum intensity increases for the six dry, three near-normal, and six wet months used previously in the merger analyses were 25, 29, and 27 mm hr^{-1}, respectively. However, medians for the same three groups for area change increased gradually from 73 to 90 to 98 km^2 for the dry, near-normal, and wet months.

Figures D-42 and D-43 show further comparisons of the changes that occur in intensity and area when mergers of relatively intense raincells take place. Figure D-42 shows the frequency distribution curves derived for 1) maximum rainfall intensity following mergers, 2) the most intense of the two merging cells 5 minutes prior to merger, and 3) the less intense of the merging cells. These distributions provide a measure of the peak intensities of the merged entities, and the intensity characteristics of the cells responsible for the merger.

Figure D-43 shows the frequency distributions derived from area measurements prior to and following cell mergers. The upper curve shows the distribution of maximum areas associated with the merged entities, and the lower curve shows a similar distribution for the total area included in the two cells producing the merger. The upper curve indicates that approximately 5% of the merged entities have areas of 1300 km^2 or more. This reduces gradually to 1000 km^2 at the 10% level, 650 km^2 at the 25% level, 390 km^2 at the 50% level, and 240 km^2 at the 75% level.

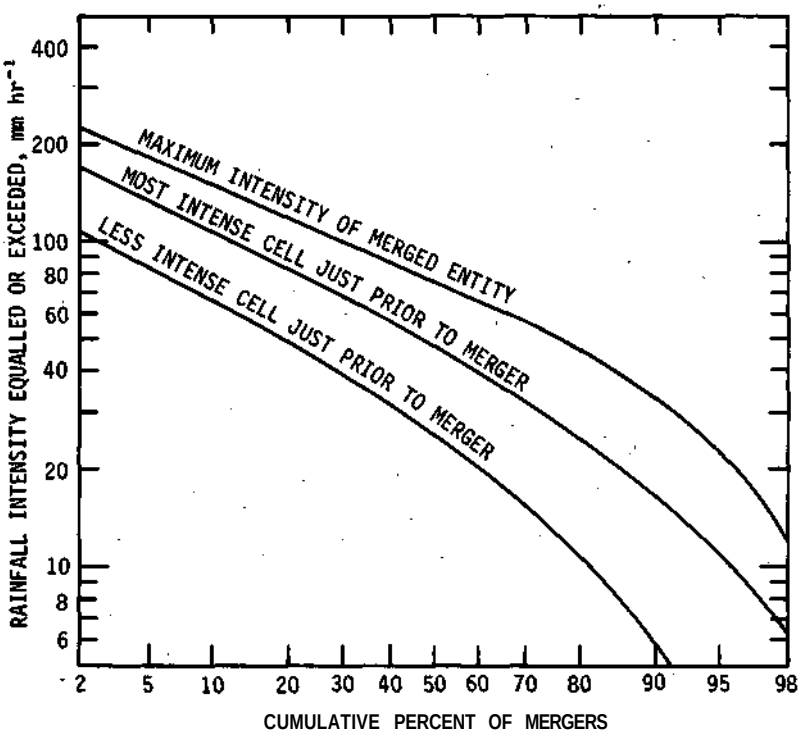

Figure D-42. Frequency distribution of rain intensity prior to and following mergers

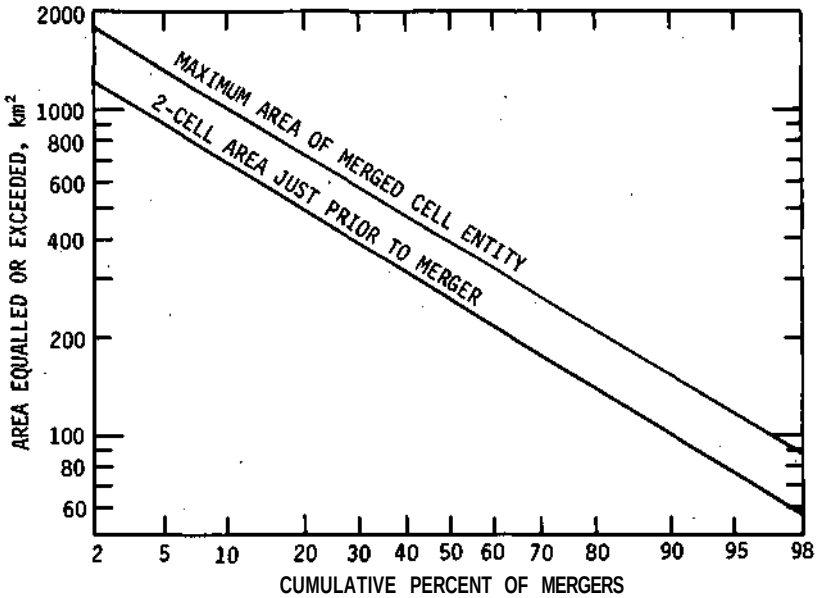

Figure D-43. Frequency distribution of raincell areas prior to and following mergers

The reader should remember that the above curves are derived from ranking the data for each type of cell; therefore, intensity or area increases cannot be read by subtracting between curves in figures D-42 and D43. Actual changes as pairs of cells merge into a single entity are provided in figure D-41. Figures D-42 and D-43 are shown to provide a description of the relative sizes and intensity of cells involved in the mergers analyzed from the 1971-1975 data, and these include only mergers when one or more of the merging cells had a rate of 6 mm hr^{-1} or more just prior to merger.

A typical frequency distribution of the cell duration derived from the 1971-1975 data is provided in figure D-44. This figure indicates that approximately 5% of the merged cells last 90 minutes, 15% continue for 60 minutes or more, and 80% last 20 minutes or longer.

RESULTS FROM FACTOR ANALYSIS APPROACH

Classification of Effect Zones of Influence

The factor approach was applied to the storm mean areal rainfall during the summers of 1971-1975 over each of the 10 X 10 km (100 km^2) radar sampling areas shown on figure D-31. The results of the R-mode factor analysis with a varimax rotation are shown on figures D-45 and D-46. Eight major storm rainfall types were delineated by the factor approach; each explains 1.4 to 21.7% of the total rainfall variance. The first four factors appear to be characteristic of non-urban industrial rainfall when classified according to the areas in which the maximum rainfall occurred (figure D-45).

Factor 1 is associated with storms that maximize in the bottomlands and northwest portion of the research circle, while factor 2 is a pattern type associated with storms that maximize

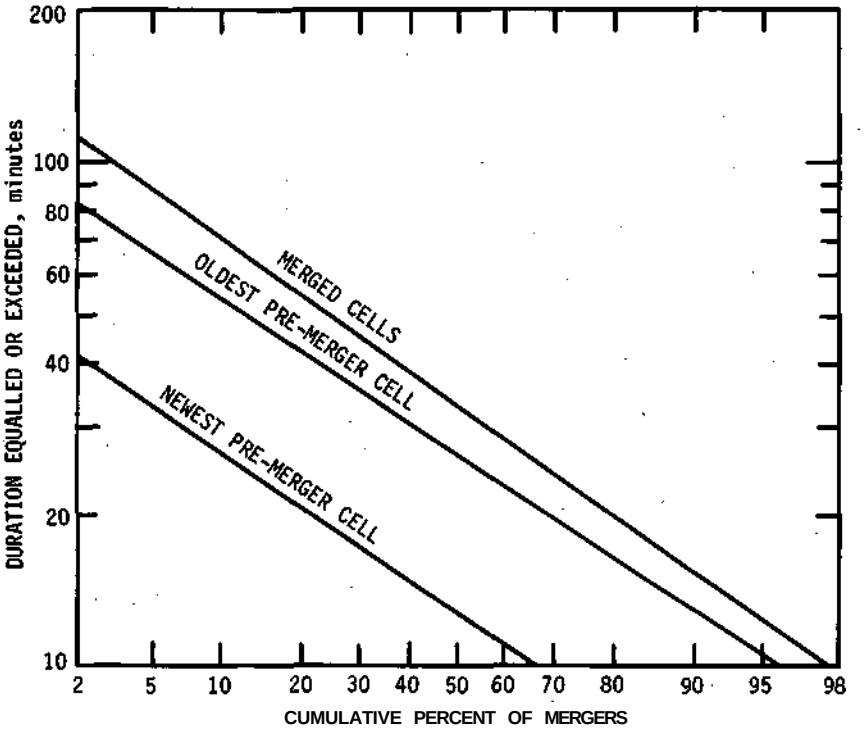

Figure D-44. Frequency distribution of raincell duration prior to and following mergers

on the eastern side of the network. Factor 3 is associated with storms that maximize in the southern part of the network, and factor 4 is associated with storms that maximize in the western part of the research circle. The specific area of storm maxima in each of the four factors is broadly characterized by the areas enclosed within the 0.4 and 0.6 isolines. The positive values of the principal components associated with each factor can be used to select those storms which maximized within the 0.4 and 0.6 isolines on figures D-45a and d.

In contrast, factors 5 through 8 (figure D-46) appear to be characteristic of urban-industrial related rainfall when classified according to the area in which the maximum rainfall occurred. Factor 5 is a pattern type associated with storms in the Edwardsville area, factor 6 is associated with storms in the St. Louis area, and factors 7 and 8 are associated with storms which maximize in more than one area. For example, factor 7 is positively loaded in the Wood River and south St. Louis region and is negatively loaded in the Granite City area and eastward as well as in the extreme western area of the network. The interpretation of this pattern is that when storm rainfall tends to maximize in the Wood River and south St. Louis areas, it is low in Granite City and in the western portion of the network. Conversely, when the rainfall is high within the negative regions of Granite City and in the western side of the network, it is low in the Wood River and south St. Louis area. Again, an inspection of the positive values of the associated principal components will indicate the storms in which rainfall maximized in the positive areas, and the negative values of the principal components will indicate the storms in which rainfall maximized in the negative areas. Factor 8 is a pattern type for storms that maximized in the Collinsville area and eastward, and in the Meramec River valley and southward.

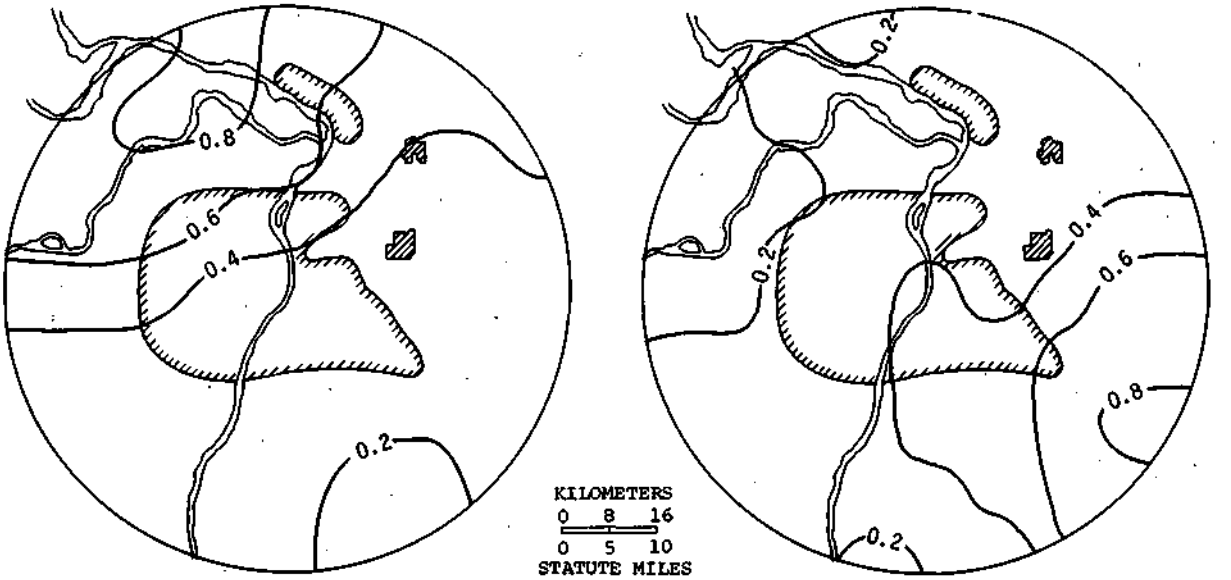

a. Factor 1, the bottomlands factor (21.7% of variance explained)

b. Factor 2, the east side factor (15.8% of variance explained)

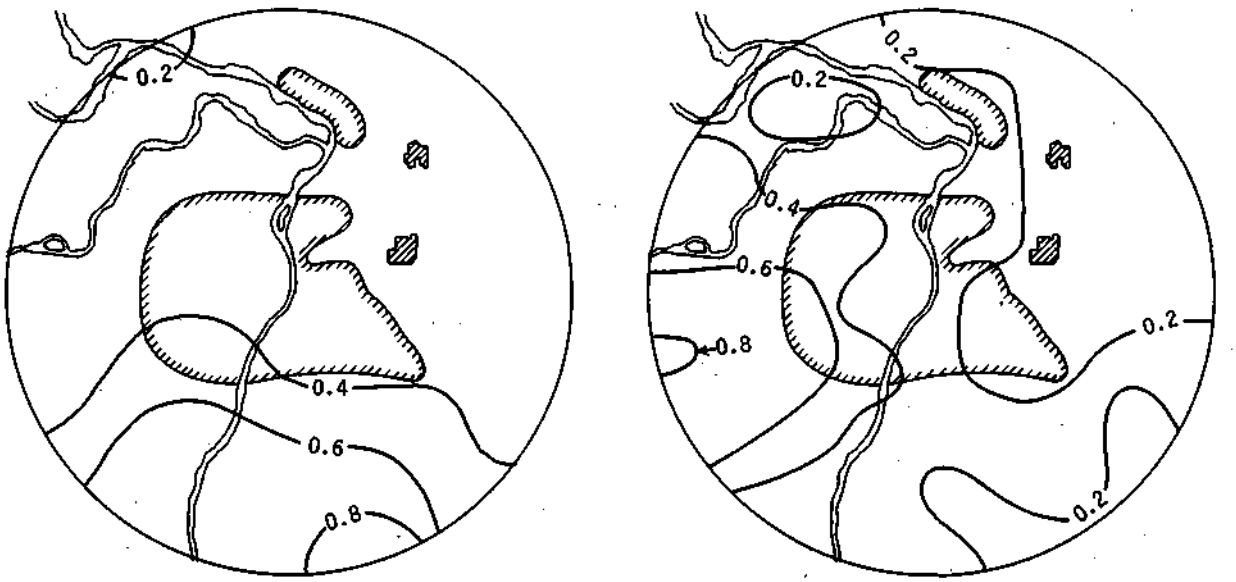

c. Factor 3, the south side factor (15.7% of variance explained)

d. Factor 4, the west side factor (12.4% of variance explained)

Figure D-45. Spatial pattern types for storm rainfalls during summer 1971-1975 as indicated by factors 1-4

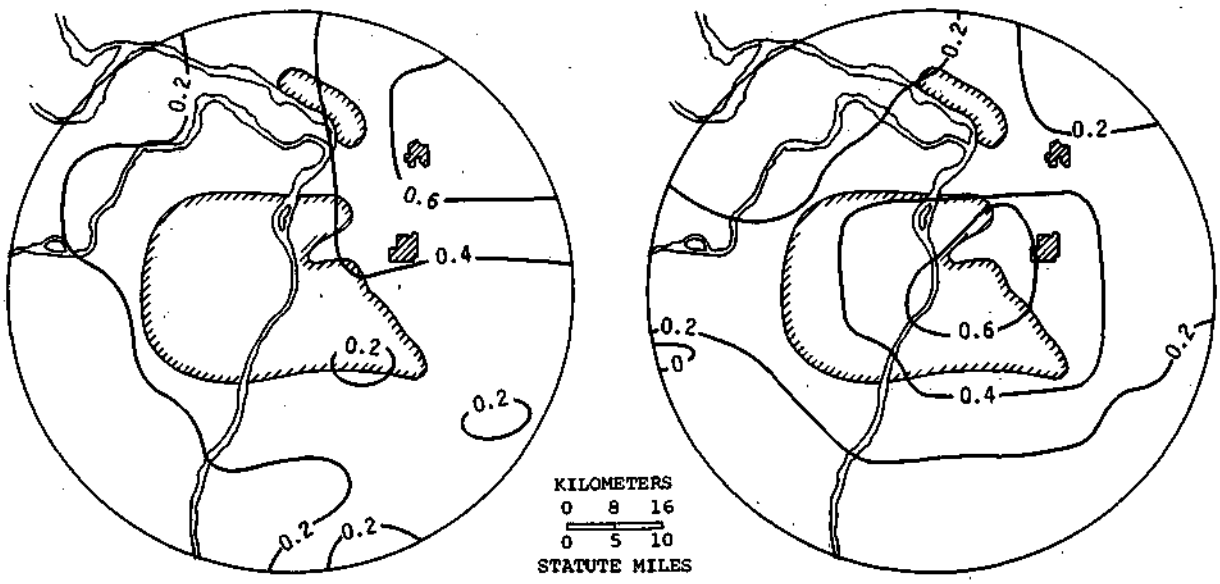

a. Factor 5, the Edwardsville factor (12.0% of variance explained)

b. Factor 6, the St. Louis factor (9.5% of variance explained)

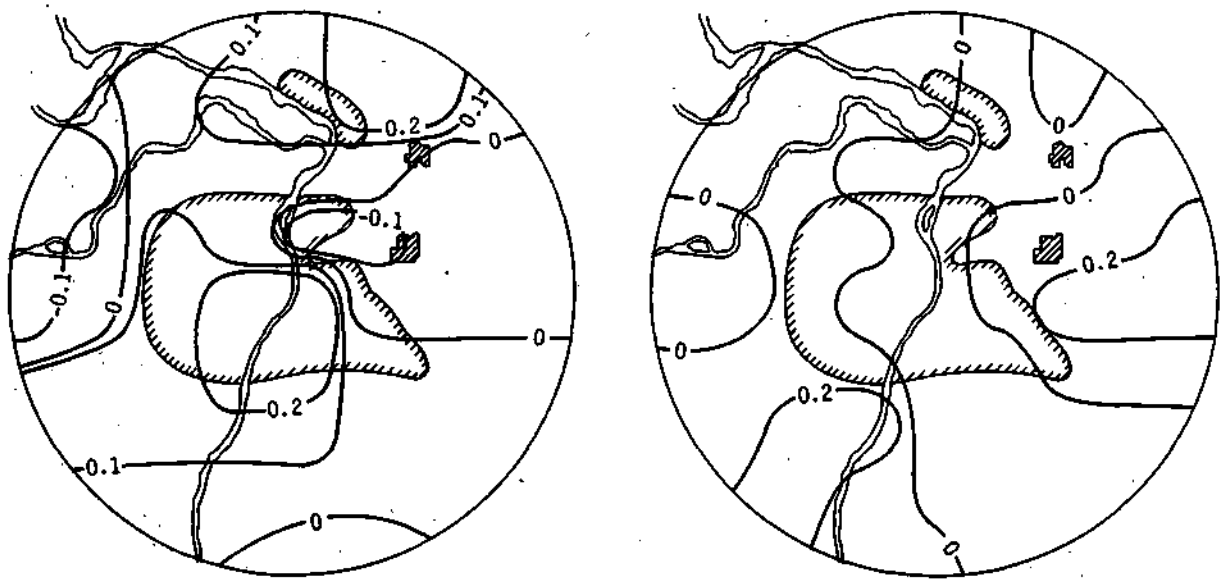

c. Factor 7, the Wood River-South St. Louis-Granite City factor (1.5% of variance explained)

d. Factor 8, the Collinsville factor (1.4% of variance explained)

Figure D-46. Spatial pattern types for storm rainfalls during summer 1971-1975 as indicated by factors 5-8

As indicated previously, the temporal plots of the various principal components are useful for determining the storms associated with the various spatial patterns of figures D-45 and D-46. The temporal plot of the first principal component (bottomlands) for the storms during 1971-1975 is shown on figure D-47. The utility of the figure is noted by the largest principal components to occur during the 5-year period. For example, the principal component associated with the storm on 27 August 1974 has a value approximately equal to +9. This value indicates that a very intense storm took place in the bottomlands region at this time. Similarly, the storms on 10 August 1974 and 23 July 1973 (principal components equal to approximately +7 and +6, respectively) were also very intense storms that occurred in the bottomlands area.

It is also easy to determine the months in which the most intense storms occurred within the bottomlands area. For example, during 1971 a relatively large number of storms maximized in July as comapred with June and August in the bottomlands area (i.e., six storms had principal components greater than 1). An interesting example with respect to years is that only a few light storms occurred in the bottomlands area during June of 1971, 1972, and 1974. In June 1973, however, an intense storm occurred there (18 June), and in June 1975, three intense storms occurred in this region (16,17, and 25 June).

Temporal plots for the other principal components were also indicative of storm rainfall patterns during the 5-year period. These plots are not shown, but their use clearly identifies the strength of the storm pattern according to the factors shown on figures D-45 and D-46.

The use of principal components allows one to elect storms that maximized in the various factor patterns shown on figures D-45 and D-46. The storms with principal component values ≥ 0.0 for a particular factor pattern were designated as effect storms, because they were most likely to be affected by the area of interest. The storms with principal component values ≤ 0.0 were considered to be no-effect storms since they did not produce their maximums within the factor patterns shown on figures D-45 and D-46.

The effect and no-effect storms were then determined for each of the factor patterns, and the rainfalls were summed to obtain the overall storm patterns for the effect storms. These overall patterns were similar to the overall factor patterns and, therefore, are not shown.

The raincells associated with each of the effect storms were then analyzed. In particular, the raincell parameters for each of the cell stratification areas (L, W, H, B, and C) were partitioned according to effect and no-effect storms. Thus, a double stratification of the raincells was available. This permitted, for example, the comparison of the target-to-control raincells for both effect and no-effect storms.

Also, the comparison of control cells in effect storms with those in the no-effect storms and the comparison of effect cells in effect storms with those in no-effect storms provides a method of testing for the areal bias due to positioning of the areas within the research circle.

For each of the cell stratifications listed in table D-30, the effect and no-effect storms for the nearest factor pattern were chosen to adjust the areal bias of the cells. First, the average cell volumes for the source areas and control areas were determined for the effect and no-effect areas.

The assumption was then made that the difference between the cell volumes in the source area and the control area in the no-effect storms is the areal bias and results from location within the network. The areal bias was expressed as a percentage of the control cell volume. The percent bias figure was then multiplied by the cell volumes of the control cells in the effect storms to obtain the amount of bias adjustment for the source area cells. The amount of bias was then added or subtracted from the source area cells to obtain an adjusted effect volume. The adjusted effect volume and the control volume were used to obtain the adjusted percent effect.

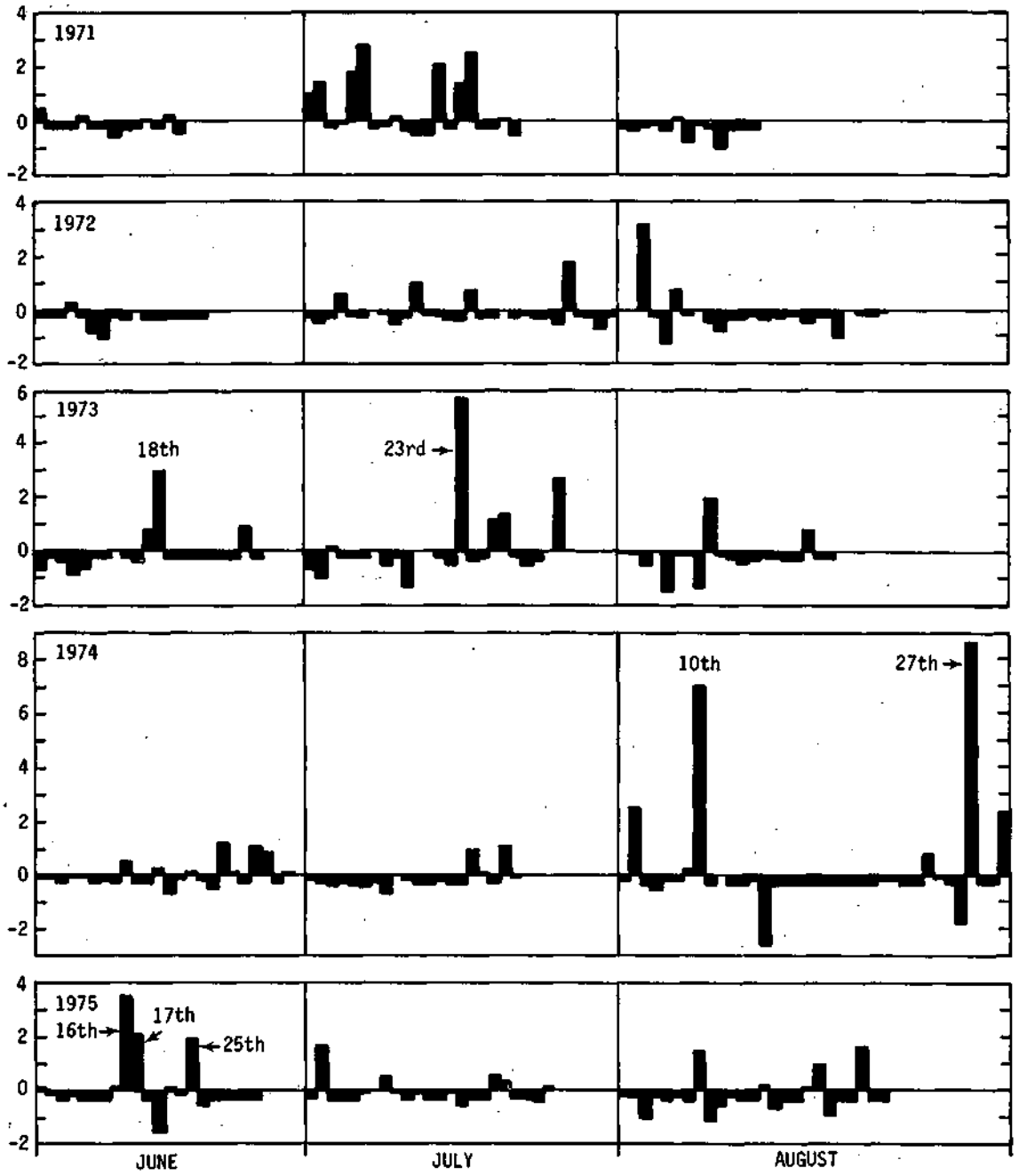

Figure D-47. Temporal plot of the principal component for the bottomlands effect area

Table D-30. The Adjustment of Raincell Volumes for the Areal Bias by Use of the Factor Method

No-effect storms		Effect storms		Adjustment for effect storms				Adjustment for all storms			
Source area	Control area	Source area	Control area	% areal bias	Amt. of bias	Adj. effect	Adj. % effect	Amt. of bias	Adj. effect	Adj. % effect	Unadj. % effect
B cells (Bottomlands factor 1)											
10.41	11.95	12.95	10.07	-13	-1.31	14.26	42	-1.43	13.73	25	12
H cells (West side factor 4)											
13.83	10.19	24.11	12.11	36	4.36	19.75	63	3.96	15.14	38	74
W cells (Edwardsville factor 8)											
11.74	10.39	23.00	11.50	13	1.50	21.50	87	1.43	18.07	64	77
L cells (St. Louis factor 3)											
13.75	9.20	32.08	12.69	49	6.22	25.86	104	5.39	19.41	76	125
SI cells (St. Louis factor 3)											
18.86	9.20	47.18	12.69	105	13.32	33.86	167	11.55	22.65	106	211

Note: Volumes are measured in hectare-meters

The percent areal bias, along with the control and source volumes from table D-19, was also used to obtain the percent of bias in all storms. The amount of bias was used to obtain the adjusted effect volume and the adjusted percent effect. The unadjusted percent effect from table D-19 was then compared with the adjusted percent effect (table D-30).

The results suggest the presence of some bias due to location of the areas. All percent increases, with the exception of the bottomlands, have been decreased from their original estimates. The bottomlands figure has been increased, suggesting that the bottomlands sampled a greater portion of the cells with shorter path lengths and shorter durations. The percent effect of other cells has been decreased, but the most important finding is that the largest percent increases still occur in the urban and industrial cells. Although it is not possible to completely adjust for bias, the application of the two schemes for adjustment (factor approach and cell stratifications by path length) suggests that an effect on the urban and industrial cells is indeed present, and that the percentage effect is the largest in these cells compared with the other categories of cells.

Relationship between Total Cell Patterns, Storm Patterns, and Raincell Characteristics

In this section, raincell patterns stratified by month, year, and time of day are investigated. In order to study the characteristics of those cells which relate to the storm rainfall patterns, the following approach was selected.

For the area of rainfall maximum, the corresponding factor pattern for storms which maximized in that same area was determined. For all storms within the factor pattern, the principal components were stratified according to cell movement, surface airflow, 850 mb airflow, and 700 mb airflow. In this manner, the general characteristics, or model, of a given month, year, or time period could be determined by averaging the principal components within the cell movement, surface airflow, etc., categories. These average values than represent the characteristics of the most intense storms.

For example, assume that the cell movement, as determined from the average value of the principal components, is toward the SE in August for a given area of interest. It can then be deduced that the storms that contributed the most to that pattern had cell movements toward the SE. It is conceivable that a greater number of storms may have cell movements to some direction besides SE, but they did not contribute as much to the patterns within the area of interest.

Total Raincell Pattern by Months

First, the total raincell pattern for June 1972-1975 is shown (figure D-48a). [All raincell patterns are for the period 1972-1975 since the raincell patterns were not determined for 1971.] A rainfall maximum in and extending to the NE of Edwardsville is the distinctive feature of this pattern. In order to elicit more information concerning the raincell maximum, the cell stratifications according to principal components are shown on figure D-48b. The area of storm maximization during June is shown, as is the relative magnitudes of the average principal components within the various cell movement categories. The primary cell movement of the major rain-producing storms was toward the ENE with secondary cell movements noted to the ESE and NE. Thus, cells in the area of the maximum moved from the direction of the Alton-Wood River and St. Louis areas. The surface airflow was from the SE, and the 850 and 700 mb winds were from the SW and SSW. As a result, the raincell maximum is located in a position to frequently sample effluents from the urban-industrial area or to have cells develop in the urban-industrial areas.

The July total raincell pattern of figure D-49a is strikingly different from the June pattern. The most obvious change is that the major high is located over the Alton-Granite City region, and a secondary maximum is located to the SE. The Edwardsville factor pattern (figure D-49b) shows preferred major cell movements to the SE and a secondary component to the NE for storms maximizing in the Edwardsville area. The associated 850 mb wind flow is also from the NW, indicating a possible steering of the cells. Furthermore, the St. Louis factor pattern (not shown) indicated

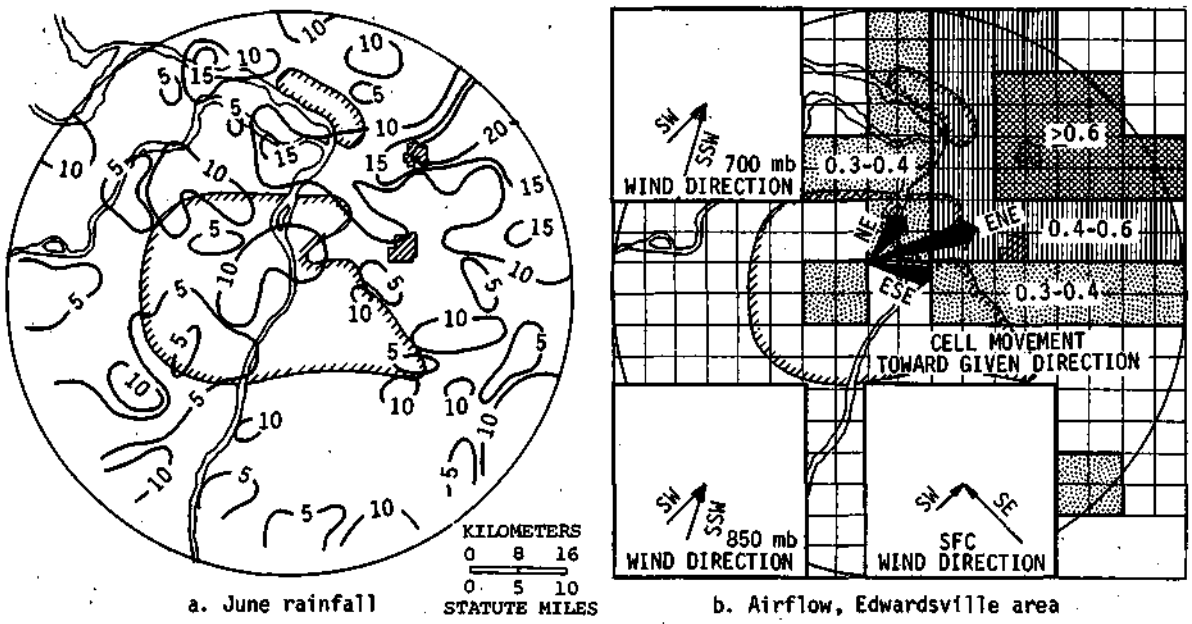

Figure D-48. Total raincell rainfall (cm) for June 1972-1975 and storm-airflow relations in the Edwardsville area during June

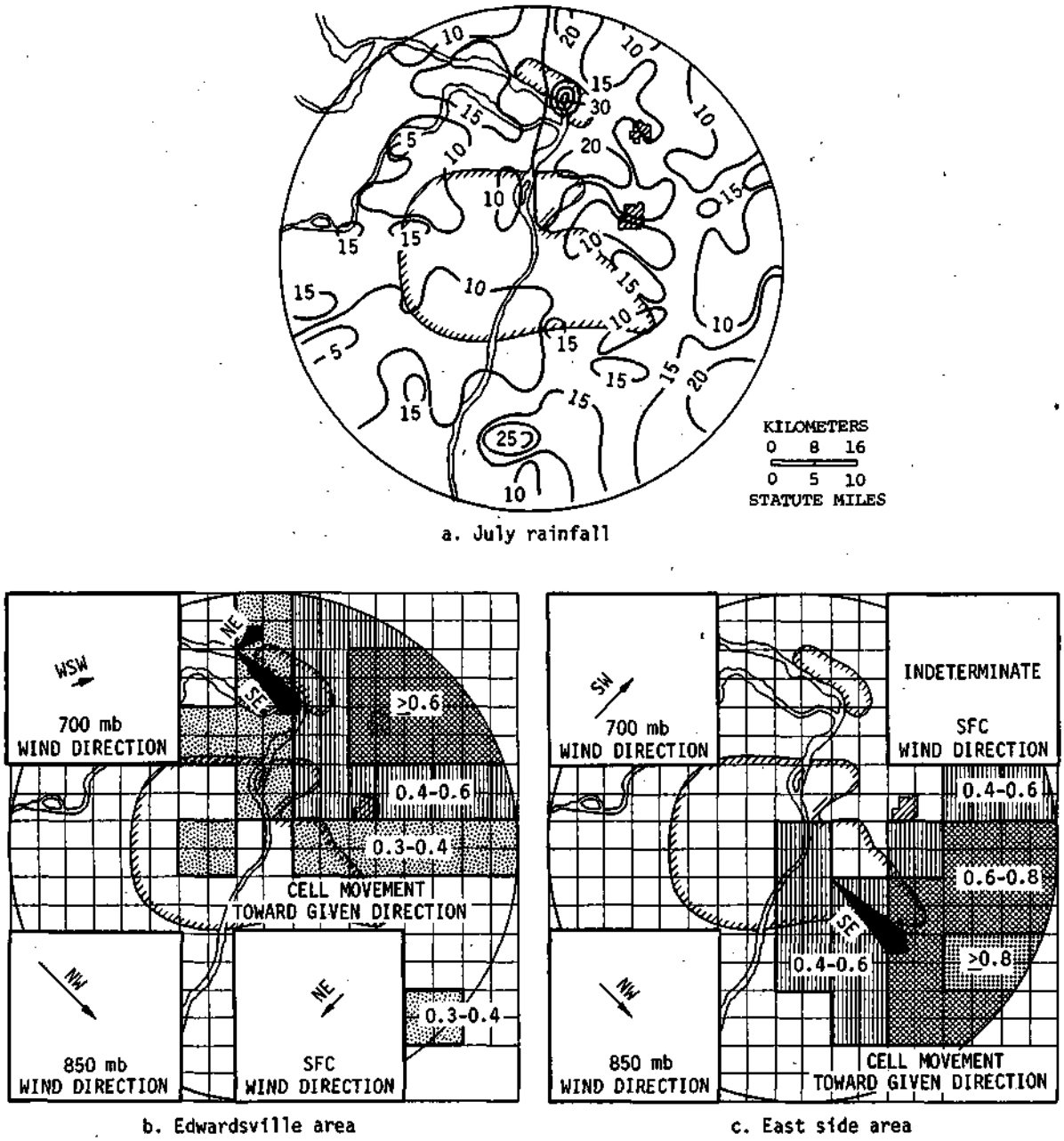

Figure D-49. Total raincell rainfall (cm) pattern for July 1972-1975 and storm-airflow relations In the Edwardsville and east side areas during July

a NNE movement of cells into the area coincident with a high in the cell rainfall pattern. However, this NNE movement of cells involved only three storms, so this result is not as reliable as results obtained from the other stratifications.

Other July raincell maximums occurred in 1) the area east of the Mississippi River in the southern part of the network and 2) the area along the southwest edge of the network. This latter

maximum occurs in the vicinity of the east side factor (factor 2); therefore, the cell movement-airflow stratifications are shown for this factor during July on figure D-49c. The preferred cell movement is to the SE from St. Louis, the 850 mb wind flow is from the NW, and the 700 mb wind flow is from the SW. The surface wind components were so small that the directions were indeterminable. However, the 850 mb flow illustrates that the area of rainfall maximum also has the opportunity to sample effluents from the urban-industrial area. Thus, the raincell maximums seem to be associated with the St. Louis region through cell movements and airflow.

The Edwardsville high is present in the total raincell pattern during August (figure D-50a), but the largest rainfall maximum occurs in the Granite City-Collinsville-Belleville area. The factor pattern for the St. Louis factor in August (figure D-50b) shows that the primary cell movement is toward the SE, the 850 mb airflow is from the WSW, and the 700 mb flow is from the NW. Thus, both the 700 mb flow and the cell movements suggest that the raincell maximum in August is located in such a position as to have been from cells influenced by passage over the St. Louis urban-industrial complex.

This conclusion was further strengthened by the factor pattern for storms that maximized in the Edwardsville area (not shown). Maximum cell movements were toward the ENE for this factor. Thus, the Edwardsville maximum in the August raincell patterns was also situated in a position to benefit from cells moving out of the St. Louis region.

The overall implication of the monthly raincell patterns is that the raincell maximum shifts from month to month in accordance with its position in relation to the urban-industrial sources and the prevailing cell movement and airflow patterns. The monthly stratification was therefore considered to be very informative and was used in the analysis of extra area effects (Changnon et al., 1977).

The total raincell pattern for the three summer months combined is shown on figure D-50c. This pattern indicates that the maximum cell rainfall occurs to the east of the Mississippi River with major maximums located in 1) the region extending from St. Louis to Edwardsville, 2) the Belleville region, and 3) the region along the southeastern part of the network. The primary air-flow and cell movements for the three summer months would suggest that urban-industrial effects might be expected to materialize in these regions.

Total Raincell Pattern by Years

An examination of the total raincell pattern over the entire METROMEX network for 1972 shows that maximums in raincell precipitation occurred in Edwardsville, Collinsville, and the area southeast of East St. Louis (figure D-51a). In 1972, raincells that maximized in the Edwardsville region tended to move in an east-southeasterly direction (figure D-51b). This would suggest that the rainfall maximum noted around Edwardsville might be associated with raincells moving from the Wood River industrial area. Raincells that maximized in the St. Louis region primarily moved either to the east-northeast or to the southeast (figure D-51c). The rainfall maximum around Collinsville could be associated with ENE-mpving raincells that had passed over the metropolitan St. Louis area, and the rainfall maximum southeast of East St. Louis could be associated with those cells that moved to the SE from the metropolitan St. Louis area.

The 1973 total raincell pattern (figure D-52a) was quite dissimilar to the 1972 pattern. The maximum raincell precipitation area was centered on Granite City, where amounts ranged from 15 to 20 cm. In general, the area of maximum precipitation shifted westward in 1973, which suggests that the predominant upper airflow pattern over the METROMEX network in 1973 was quite different from the pattern that prevailed the year before. Raincells that maximized in the St. Louis region (figure D-52b) generally moved to the SE during the summer of 1973; unlike

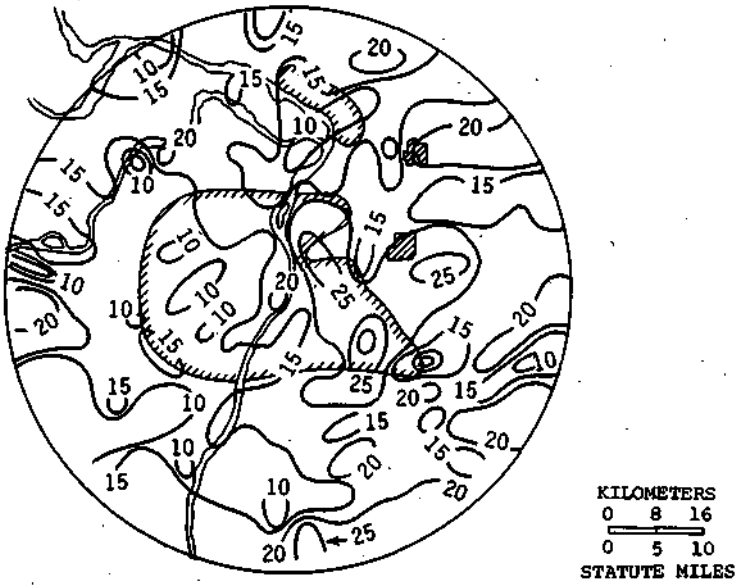

a. August rainfall

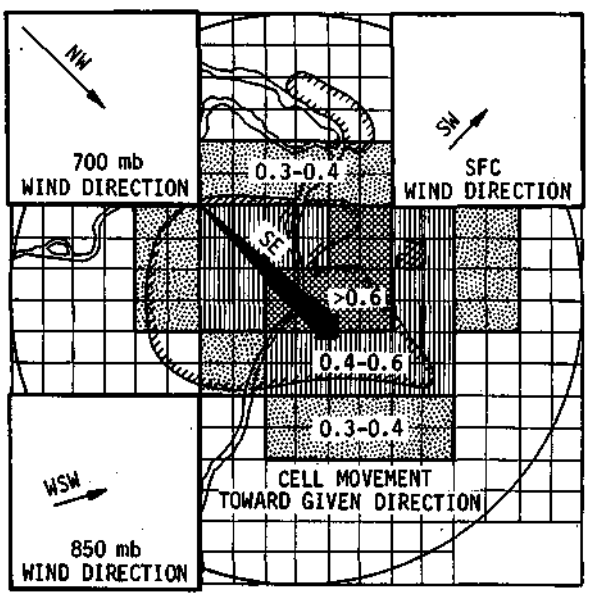

b. St. Louis area

c. Summer rainfall

Figure D-50. Total raincell rainfall (cm) pattern for August and summers 1972-1975, and storm-airflow relations in the St. Louis area during August

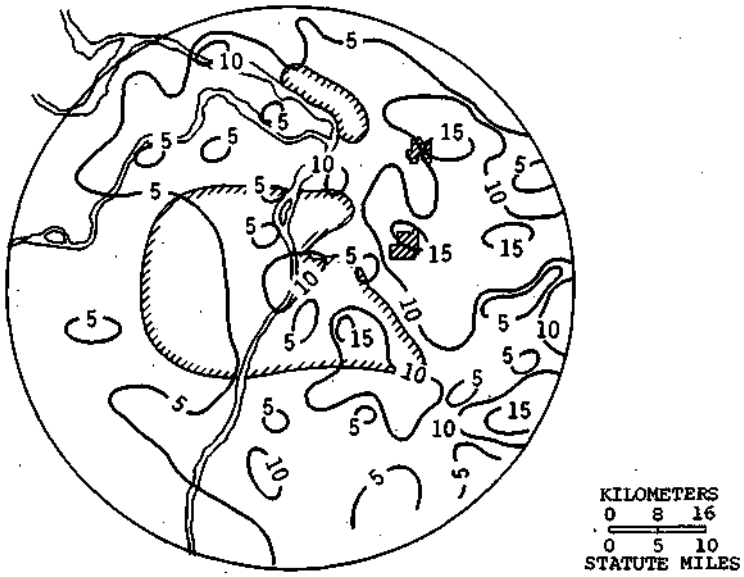

a. 1972 rainfall

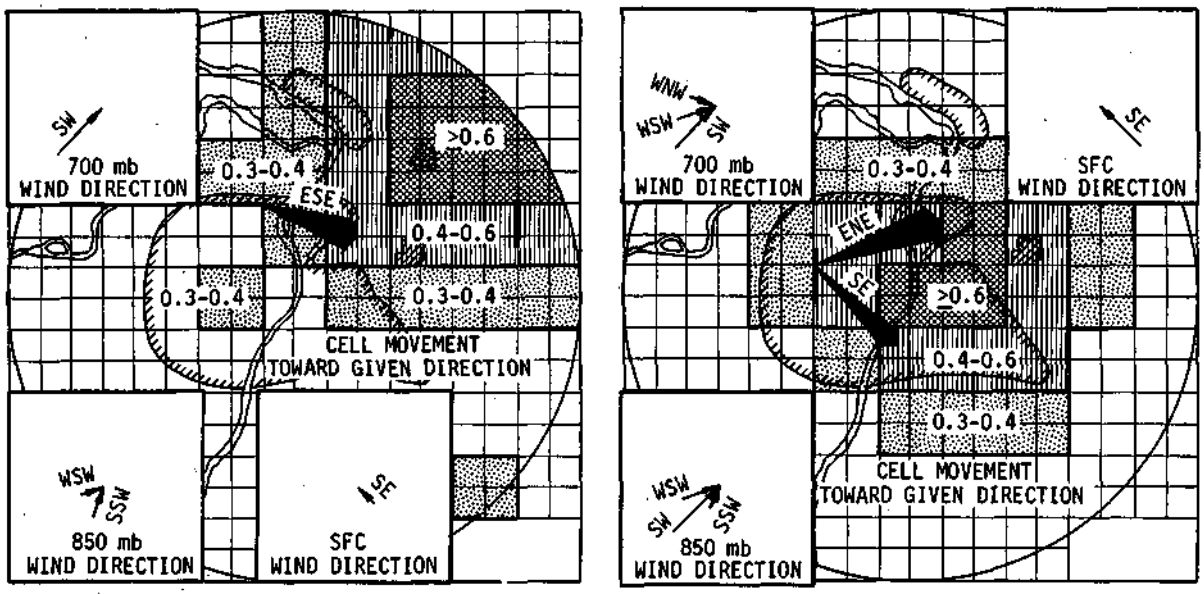

b. Edwardsville area

c. St. Louis area

Figure D-51. Total raincell rainfall (cm) pattern for 1972 and storm-airflow relations" in the Edwardsville and St. Louis areas during 1972

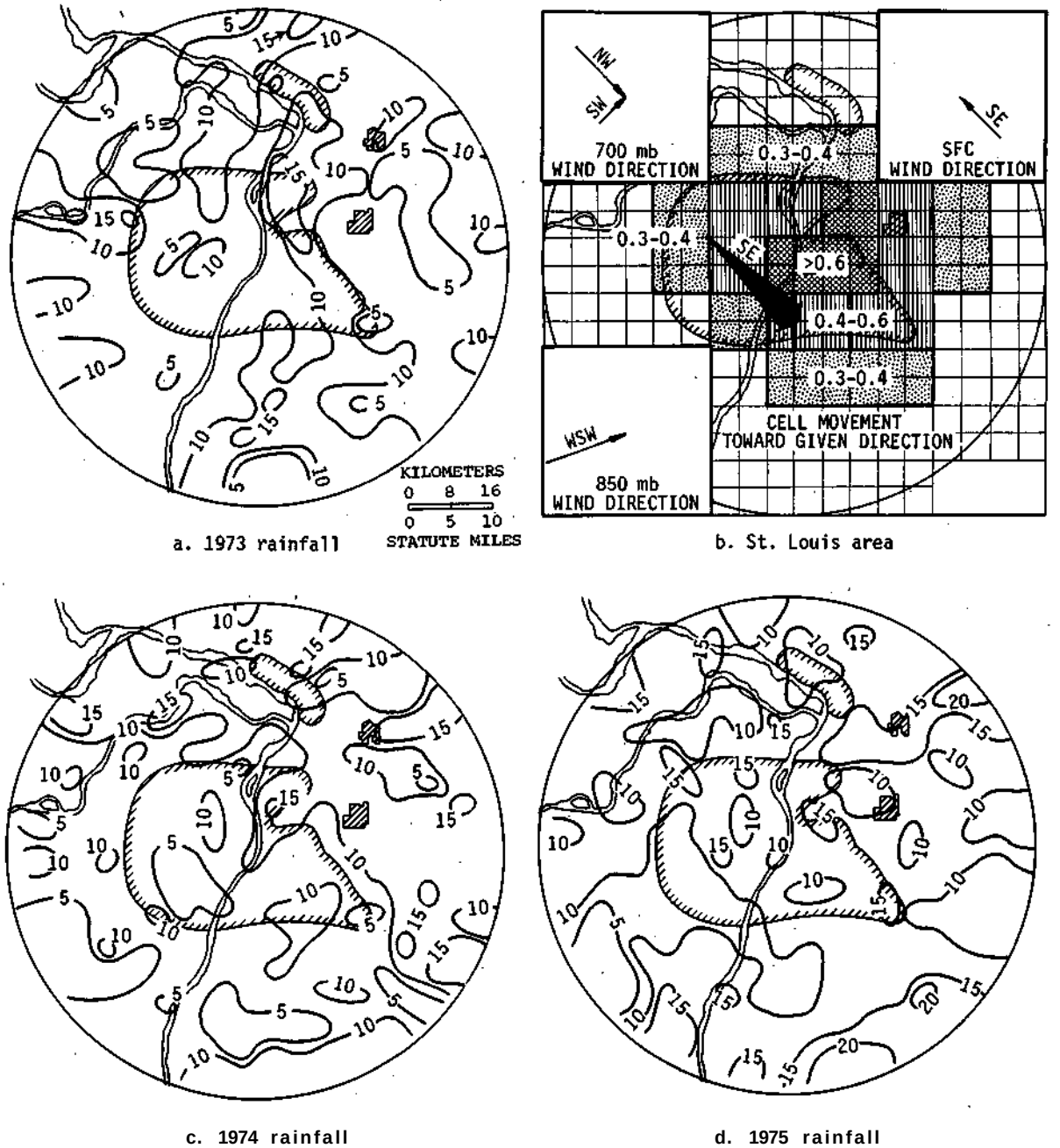

Figure D-52. Total raincell rainfall (cm) patterns for 1973-1975 and storm-airflow relations in the St. Louis area during 1973

1972, no significant cell movement to the ENE or NE was noted. At the 700 mb level, a NW-to-SE wind flow dominated during 1973, whereas a SW-to-NE wind flow was the rule during 1972. The fact that the upper air patterns and cell movements were so different for these two years may explain the shift in maximum raincell precipitation during 1973.

The most prominent feature of the 1974 total raincell pattern (figure D-52c) is that the most significant rainfall amounts occurred in the northern and eastern sections of the METROMEX circle. Excluding isolated areas of maximum rainfall, only the maximum raincell precipitation located at and to the ENE of Edwardsville was noteworthy. Raincells that maximized in the Wood River-Edwardsville area generally moved to the ENE (not-shown), and the airflow at 700 mb was from WSW to ENE. Furthermore, the raincells in the St. Louis area also moved to the ENE (not shown). Thus, the large general area of precipitation was located downwind and 'down movement' from the St. Louis and Edwardsville areas.

The total raincell pattern for 1975 yielded two distinct rainfall peaks: 1) the area between Wood River and Granite City extending through and to the NE of Edwardsville, and 2) the area along the SE edge of the METROMEX circle (figure D-52d). The first area of maximum rainfall appears to be related to the dominant cell movements in Edwardsville and St. Louis. Raincells that maximized in the St. Louis region moved to either the NE or SE, while raincells that maximized in the Wood River-Edwardsville region primarily moved to the SE. This area of maximum rainfall was positioned such that it was 'down movement' from both Wood River and St. Louis.

The 850 mb flow was chiefly from the NW for the Edwardsville region, and from both the SW and NW for the St. Louis region. Thus, the 850 mb flow also places the rainfall maximum downwind of Wood River and St. Louis. It is unlikely that the second maximum (located along the SE edge of the circle) is related to the St. Louis area. Although one of the general directions of cell movements was to the SE, the distance between St. Louis and the second maximum is most likely too great to suggest a linkage between the two.

Overall, a relationship seems to exist between the cell movements and wind directions and the location of the St. Louis, Edwardsville, and Wood River areas. This relationship is reflected by the positioning of the rainfall maximums in relation to the possible source areas from year to year. However, this relationship does not appear to be as strong as it was with the monthly raincell data. In either case, monthly or yearly, considerable evidence exists for an urban-industrial influence on raincells.

In the original stratifications, the cells were classified by hypothesized regions and the influence of the urban-industrial areas was explored by investigating the cell parameters. With the factor approach, the area of raincell maxima was studied with regard to cell movements and wind directions to determine if the area of the raincell maximum could be traced back to the urban-industrial areas. This concept is pursued further with the diurnal stratifications.

Diurnal Raincell Initiation and Rainfall Patterns

0000-0300 CDT. The raincell initiation pattern for the storms during 1972-1975 that initiated during the 0000-0300 CDT period and the total rainfall pattern from these cells are presented in figure D-53. The primary initiation region is located over the north-central portion of the network. Cell rainfall for the period was generally light (less than 5 cm per gage), with the greatest rainfall amounts occurring over the bottomlands and the area north and east of Alton-Wood River (figure D-53d).

The average temperature and dew point patterns that prevailed during the hour before cell initiation are also shown (figure D-53a and b). A well-defined heat island existed over the St. Louis metropolitan area and another region of warm surface air was situated over the southeast

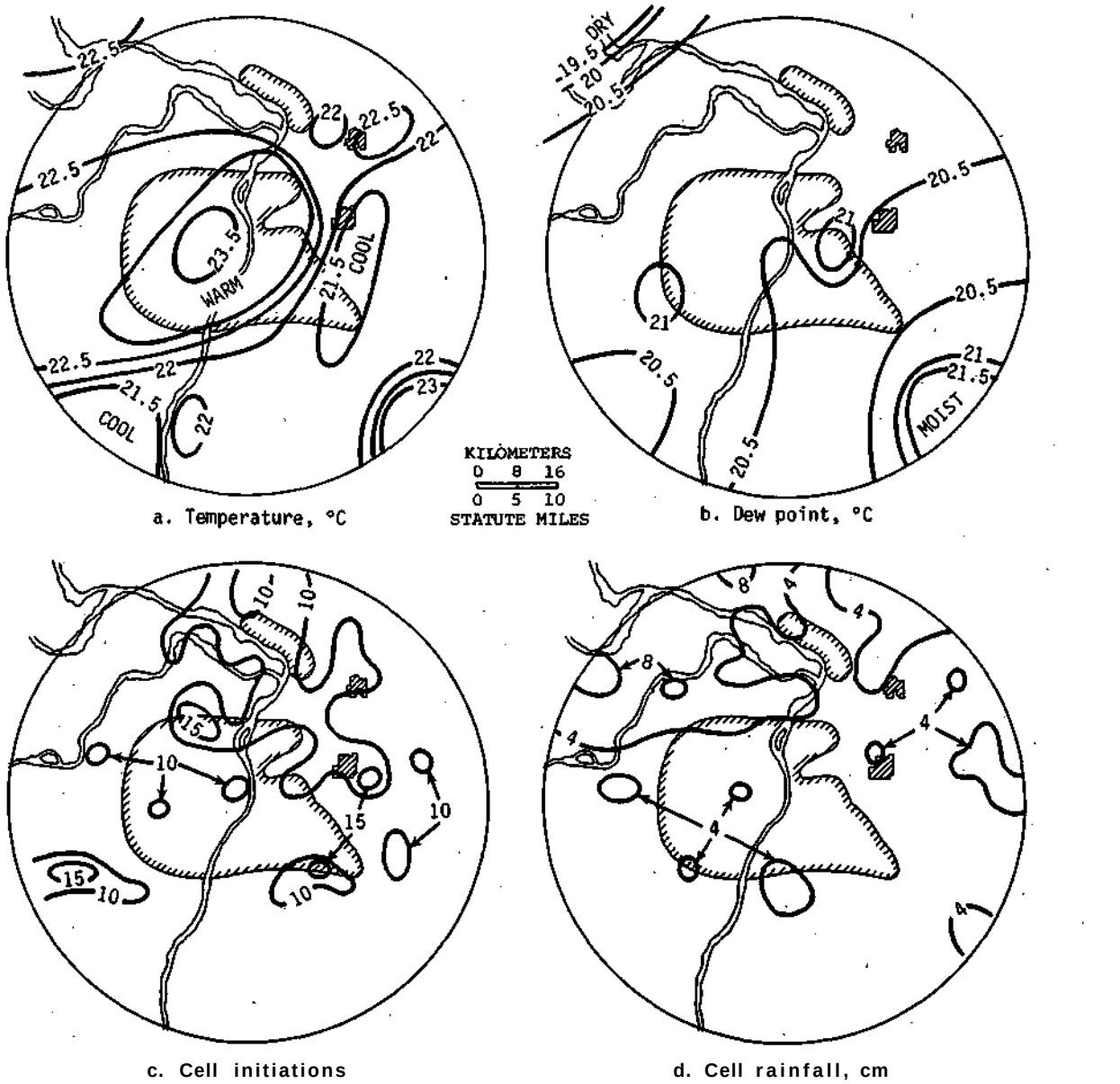

Figure D-53. Temperatures and dew points prior to cell initiations and cell rainfall for 0000-0300 CDT

portion of the circle. Highest dew point values (21.5° C) were also found along the southeast portion of the circle. There is no suggestion that cell initiations or rainfall in this period were related to surface temperature or moisture anomalies. However, as noted earlier, nocturnal raincells over the urban-industrial areas were significantly larger than control cells.

0300-0600 CDT. No large cell initiation region was noted for the storms that initiated during 0300-0600 CDT (figure D-54c), although more initiations occurred over the northern half of the circle. Cell initiations were near their lowest frequencies for the day. Maximum initiation values were only in the range of 10 to 12, and the average number of initiations per gage was less

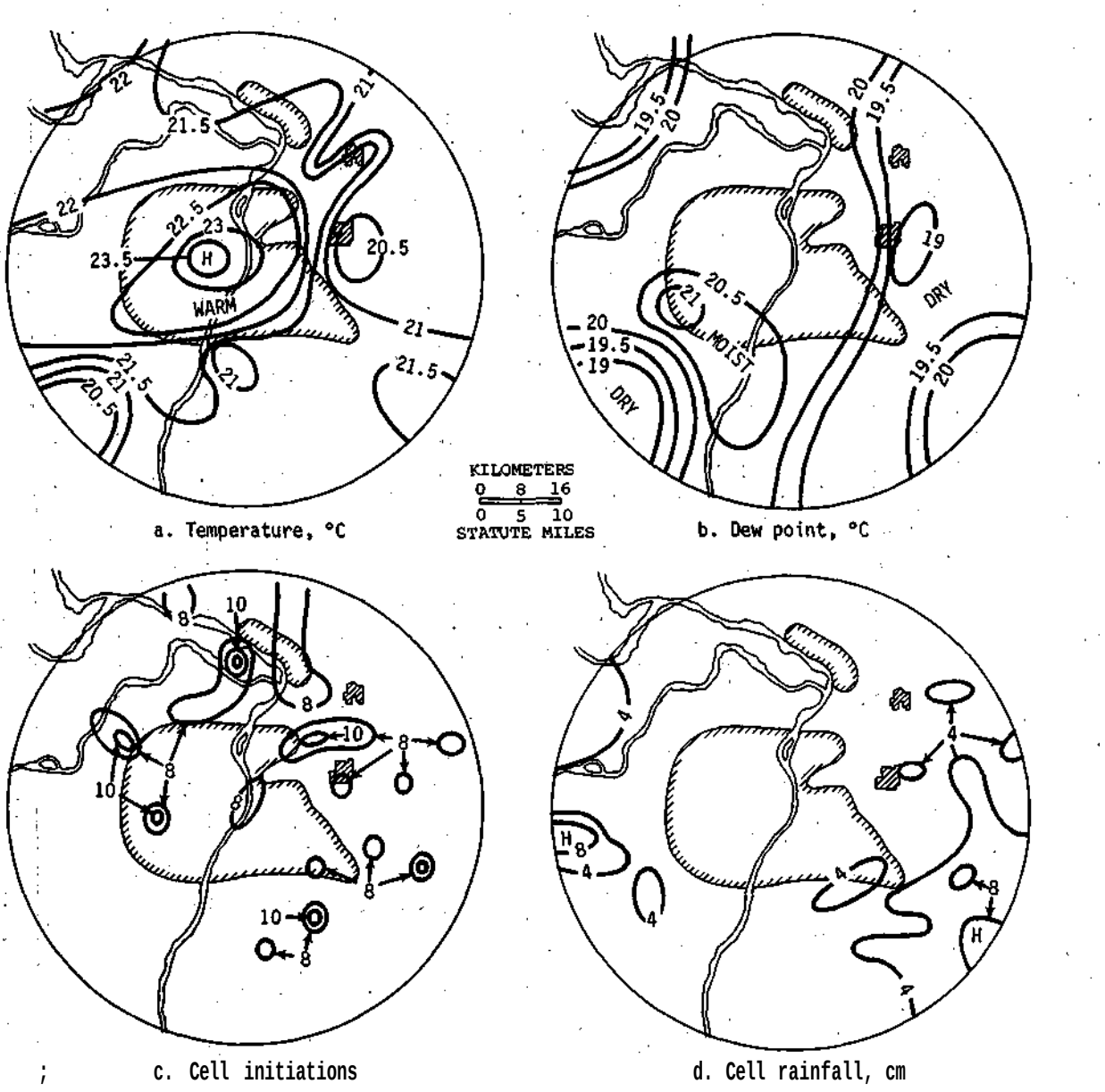

Figure D-54. Temperatures and dew points prior to cell initiations and cell rainfall for 0300-0600 COT

than 8. Cell rainfall for the period was also quite light, with the greatest rainfall amounts occurring away from the city (figure D-54d).

The heat island remained strong over the St. Louis metropolitan area during this period, as did the pocket of warm air over the southeast portion of the east side (figure D-54a). Highest dew point values (20.5 to 21.0° C) were found south and west of St. Louis, directly NE of the hills region (figure D-54b).

Cells associated with storms that maximized in the east side high region (figure D-55) moved to the SE during this period, and thus could have been influenced by the St. Louis urban-industrial area.

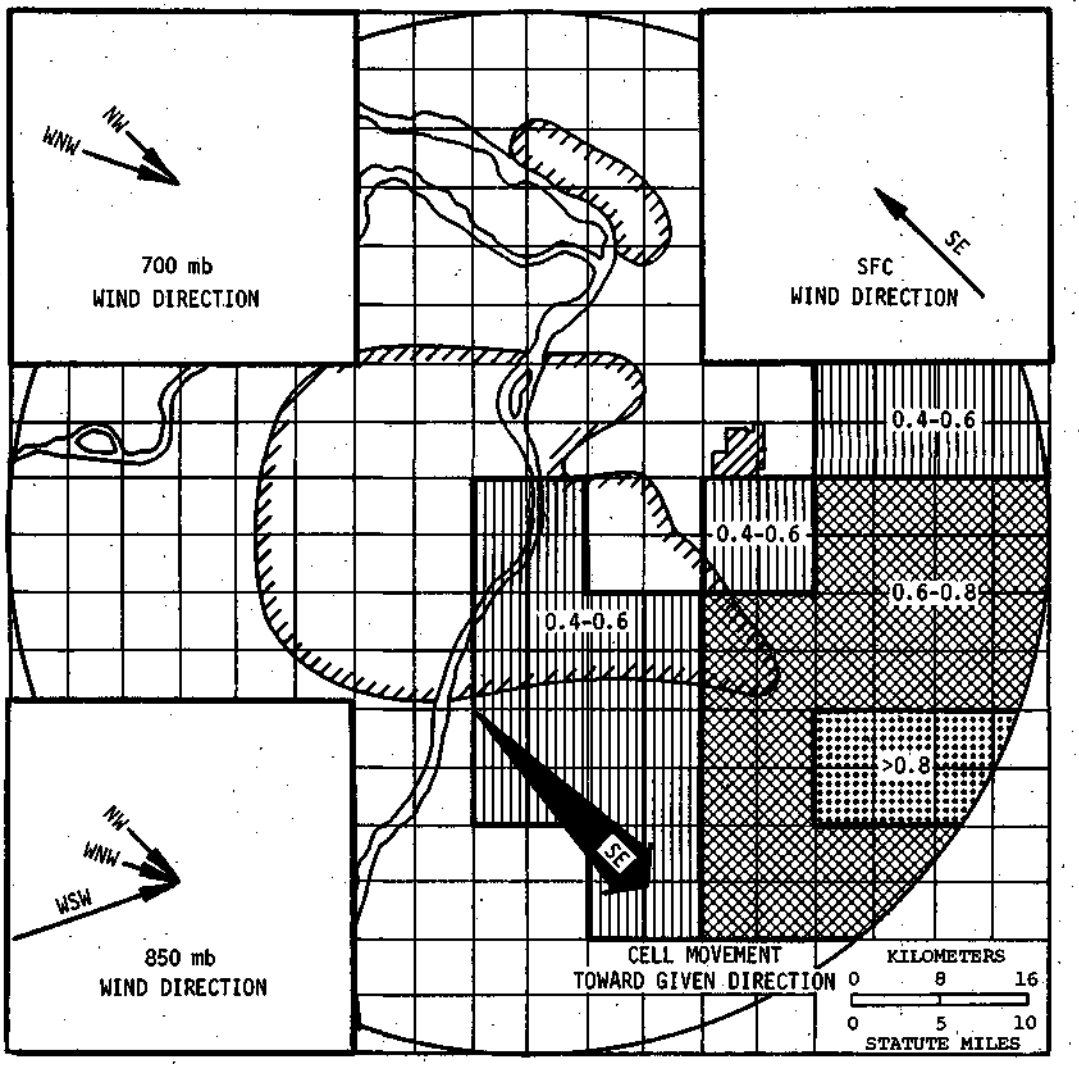

Figure D-55. Storm-airflow relations in the east side area for 0300-0600 CDT

0600-0900 CDT. The raincell initiation pattern for the storms that initiated during 0600-0900 CDT was quite variable (figure D-56c). Of the eight 3-hour periods, the fewest cells initiated during this period. Maximum initiations per gage were on the order of 8 to 10, but the average number of initiations per gage was much lower. Cell rainfall for the period was somewhat more intense than during the previous two 3-hour periods (figure D-56d). Maximum rainfall occurred south and east of St. Louis, but secondary maximums occurred over the city and in the hills.

The warmest surface temperatures (22.5°C) remained over the St. Louis metropolitan area, but the pocket of warm air over the southeast from 0000-0600 did not appear from 0600-0900 (figure D-56a). Highest dew point values (20°C) were noted over the St. Louis urban area and over the west hills (figure D-56b).

Cell initiations tended to occur in warm and cool regions as well as in moist and dry areas. However, there was a strong tendency for the cell rainfall to occur in the moist regions (dew points $\geq$ 19°C).

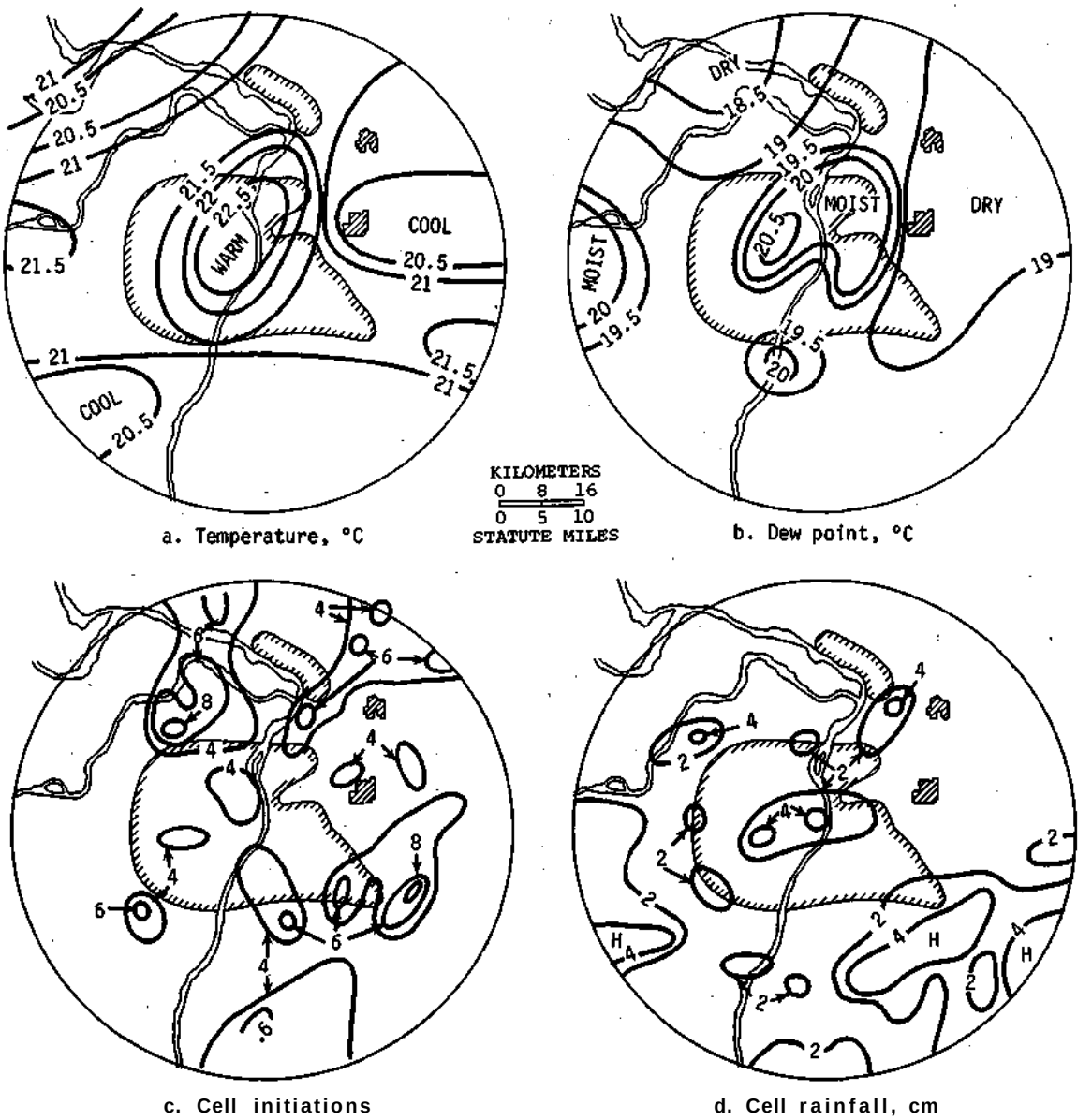

Figure D-56. Temperatures and dew points prior to cell initiations and cell rainfall for 0600-0900 CDT

Cells associated with storms that maximized over the east side in **0600-0900** generally moved in an ENE direction (not shown), so these cells were more likely to be associated with the initiation area over the southern part of the circle rather than over the urban area. A rainfall maximum occurred in the moist area over the urban-industrial area. The upper airflow and the surface wind direction correlation values were insignificant for the period 0600-0900, although surface winds were generally light southeasterly and upper winds were generally from the west or southwest.

0900-1200 CDT. More organized regions of cell development occurred with the cells that initiated during **0900-1200 CDT** (figure D-57c). The primary initiation area was centered on

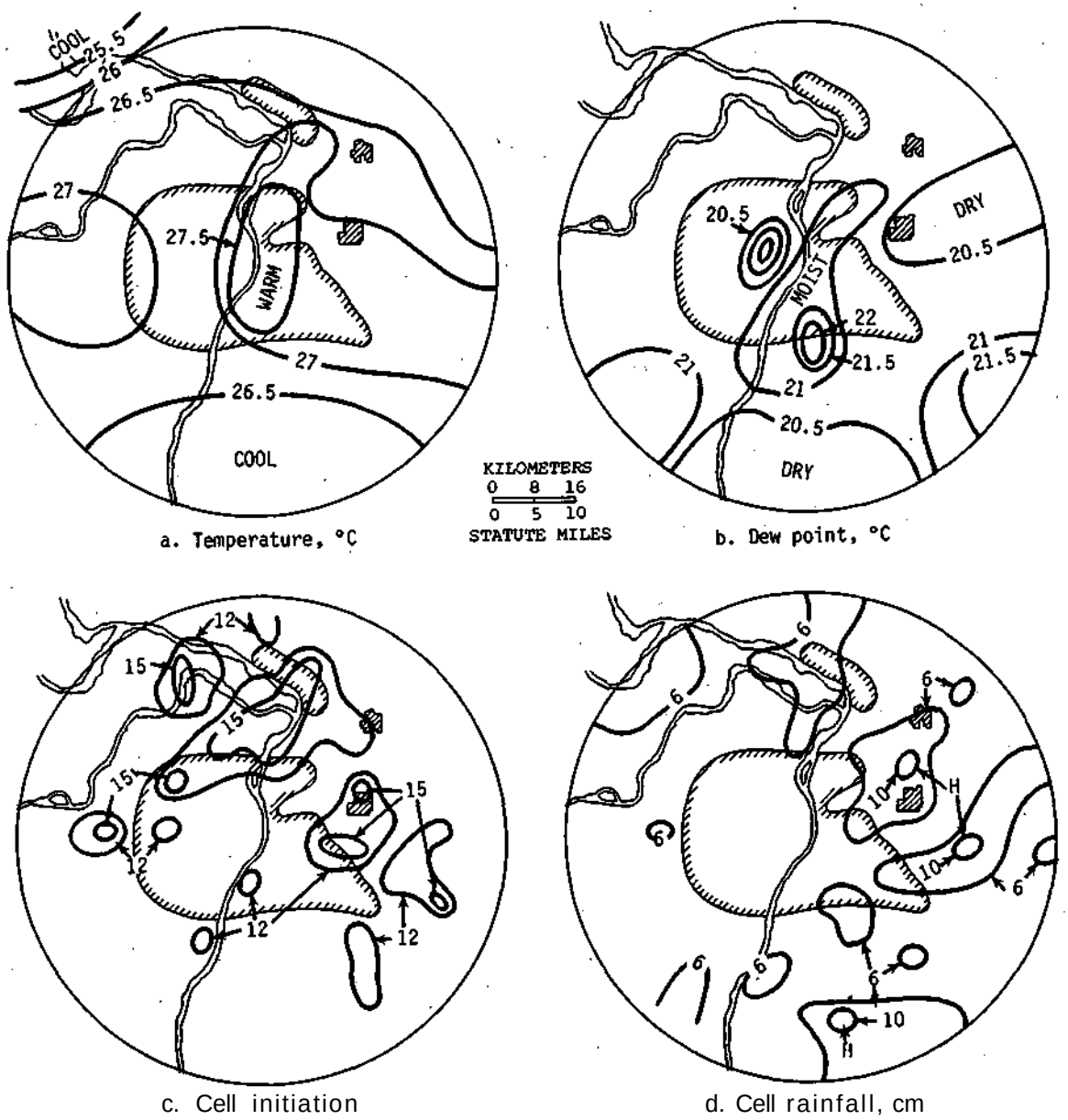

Figure D-57. Temperatures and dew points prior to cell initiations and cell rainfall for 0900-1200 CDT

the north-central region of the network (Alton to north St. Louis), and secondary maximums occurred directly east of St. Louis. Maximum initiation values were on the order of 15 to 18, a marked increase over the previous 3-hour period. Cell rainfall increased significantly during this period (figure D-57d). Maximum rainfall regions were located primarily north and east of the St. Louis metropolitan area, but one region existed in the southern part.

The warmest surface temperatures (27° C) occurred over the St. Louis metropolitan area and eastward to the edge of the circle as well as over the western part of the circle (figure D-57a). The highest dew point values (21.0 to 21.5° C) were noted over the center of the network, the southwest hills, and the SE portion of the circle (figure D-57b).

The most significant regions of cell initiation were along the boundary of, but not directly over, the urban heat island. Little or no direct areal correlation seems to exist between raincell initiation maximums and the location of more moist surface regions.

Cells associated with storms that maximized over the east side and over St. Louis generally moved to the SE, while cells associated with storms that maximized over Edwardsville and Collinsville moved to the NE and ENE, respectively. This indicates that the maximums east of St. Louis are generally 'down movement' from the St. Louis urban area, and suggests that the maximums may be due in part to the presence of the St. Louis urban area. It appeared that the 850 mb wind flow was a more accurate indicator of cell movement for this time period than the 700 mb wind flow.

1200-1500 CDT. A striking pattern in the region of maximum cell development occurred during 1200-1500 GDT (figure D-58c). The region of maximum initiation extended from the Wood River-Edwardsville area southwestward to the southernmost sector of St. Louis and followed generally the same path as the Mississippi River. This closely agrees with the first echo maximum. In this area, more than 25 initiations per gage were common. This was an interesting shift from the initiation pattern of 0900-1200 CDT, and more cells initiated during this period than in any other period. Cell rainfall also maximized during the 1200-1500 CDT period (figure D-58d). The most notable feature on the rainfall map was the large area in and east of St. Louis. One raingage in Granite City received over 30 cm of rain during this period. This position of the heaviest 3-hour rainfall was unique to the 1200-1500 CDT period.

The warmest surface temperatures (30.5° C) occurred over 1) the St. Louis metropolitan area, 2) the hill area southwest of St. Louis, 3) the southern river bottomlands, and 4) a small area to the southeast (figure D-58a). Dew points maximized over the eastern section of the circle and over the northwest bottomlands (21.5° C). They were slightly lower over the St. Louis metropolitan area.

It is important to note that both cell initiation and cell rainfall values reached maximum levels during this period. Also, the temperature pattern had become quite uniform over the greater part of the network (i.e., the urban heat island had weakened), but the dew point pattern had shifted such that the eastern half of the network was more moist. A weak relationship exists between the more moist eastern half of the network and the region of maximum cell rainfall. Raincell initiations maximize in a relatively warm region with a strong dew point gradient (moist to the east, dry to the west). There is a suggestion that surface conditions relate to the initiation frequency.

The most common movement exhibited by cells associated with storms that maximized over St. Louis, over Wood River, and over Edwardsville was to the SE (figure D-59). This movement of strong raincells supports the rainfall maximum over East St. Louis, Granite City, and western Belleville. But not all cells moved to the SE; some cell movement to the ENE and NE was exhibited by cells maximizing over the St. Louis, Collinsville, and Wood River-Edwardsville areas. The rainfall maximums around Edwardsville and Alton-Wood River are probably due in part to these NE and ENE-moving cells. For the St. Louis, Collinsville, and Wood River-Edwardsville areas, the 700 mb wind flow is a strong indicator of cell movement, but the 850 mb flow most resembles cell movement for the east side area.

1500-1800 CDT. The most pronounced raincell initiation area.for the storms that initiated during 1500-1800 CDT was found in and northwest of St. Louis (bottomlands), although other significant initiation areas were found south and east of St. Louis (figure D-60c). The pattern was quite different from the previous 3-hour period, and the number of initiations per gage dropped markedly (maximum initiation values fell to 12 to 14). In short, both the pattern of maximum

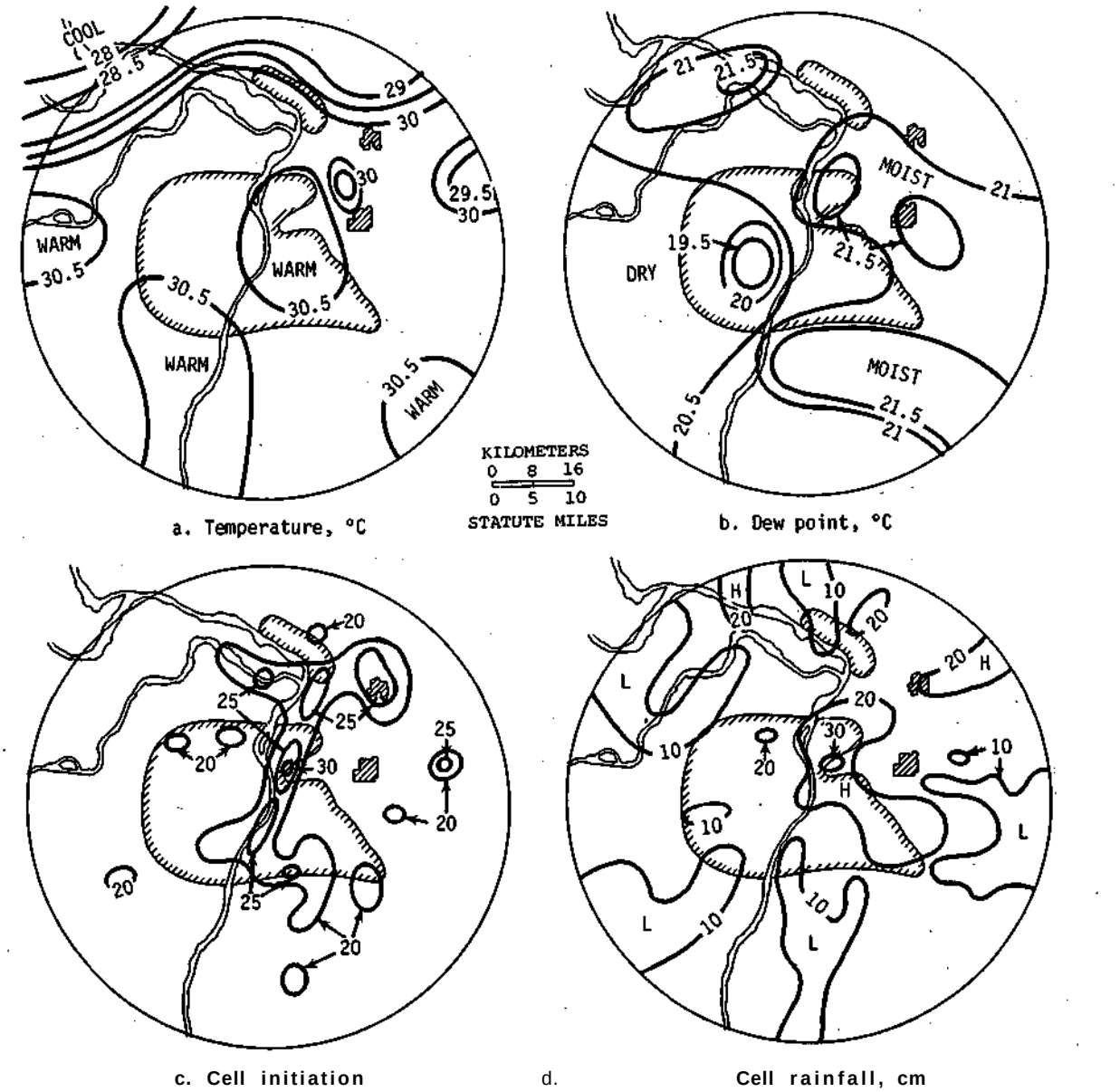

a. Temperature, °C

b. Dew point, °C

c. Cell initiation

d. Cell rainfall, cm

Figure D-58. Temperatures and dew points prior to cell initiations and cell rainfall for 1200-1500 CDT

initiation areas and the number of initiations per gage were significantly altered from the period 1200-1500. Cell rainfall for the period was generally lighter and the rainfall pattern was different from that in the previous period (figure D-60d). The large maximum rainfall area which was situated over East St. Louis from 1200-1500 did not persist, but a new extensive area of maximum rainfall existed to the east of the city, suggesting propagation. This new raincell rainfall maximum area had lower maximum rainfall values (on the order of 6 to 14 cm per gage).

It was warm over the entire network (average temperature 30° C), but temperatures were slightly cooler over the eastern third of the network where most of the cell rainfall was occurring (figure D-60a). Highest dew point values were found mostly in the southeast, and lowest dew point values were over and to the west of St. Louis (figure D-60b).

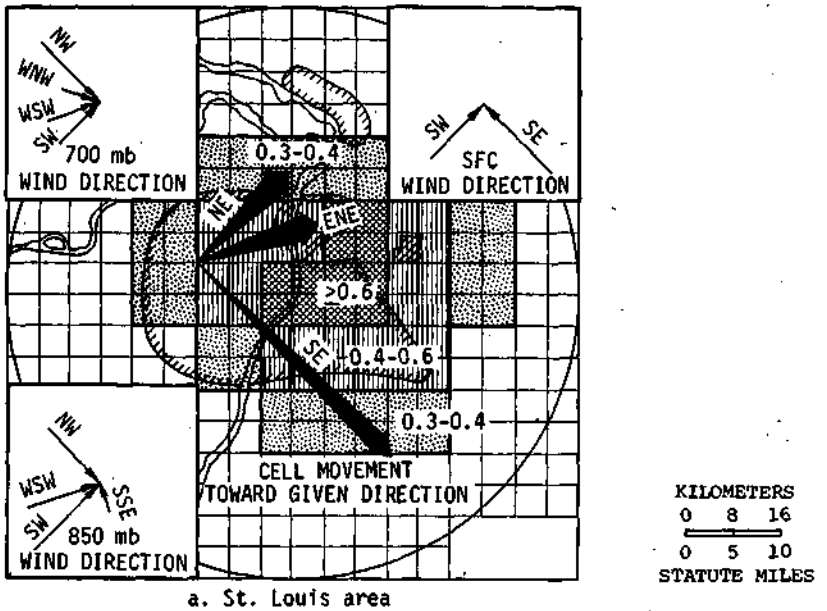

a. St. Louis area

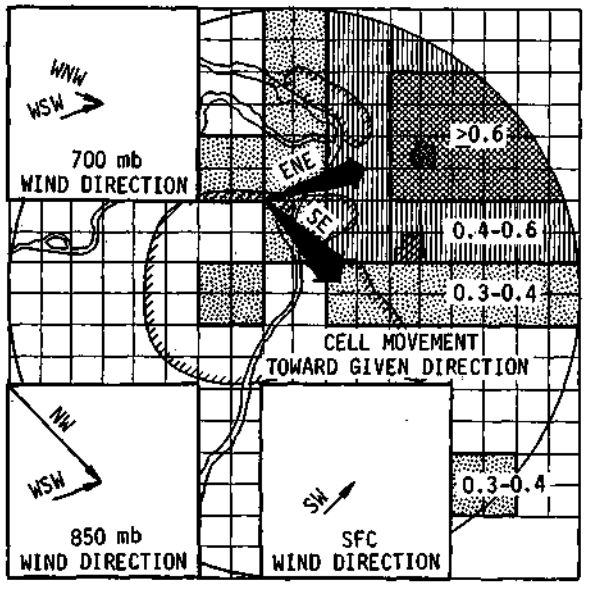

b. Edwardsville area

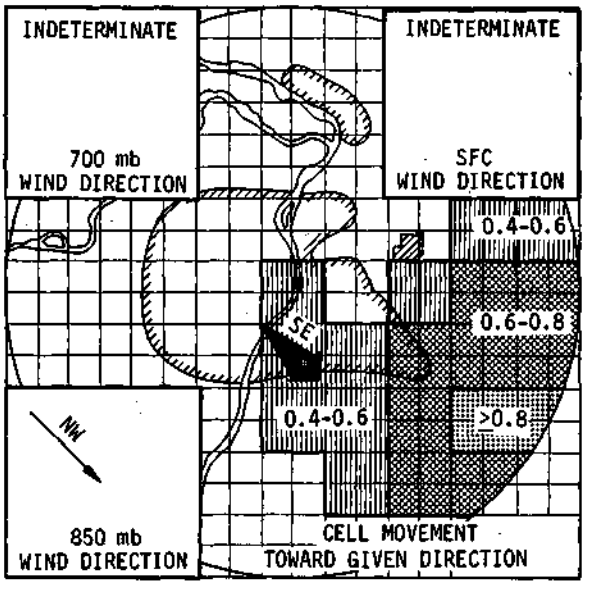

c. East side area

Figure 0-59. Storm-airflow relations for the St. Louis, Edwardsville, and east side areas for 1200-1500 CDT

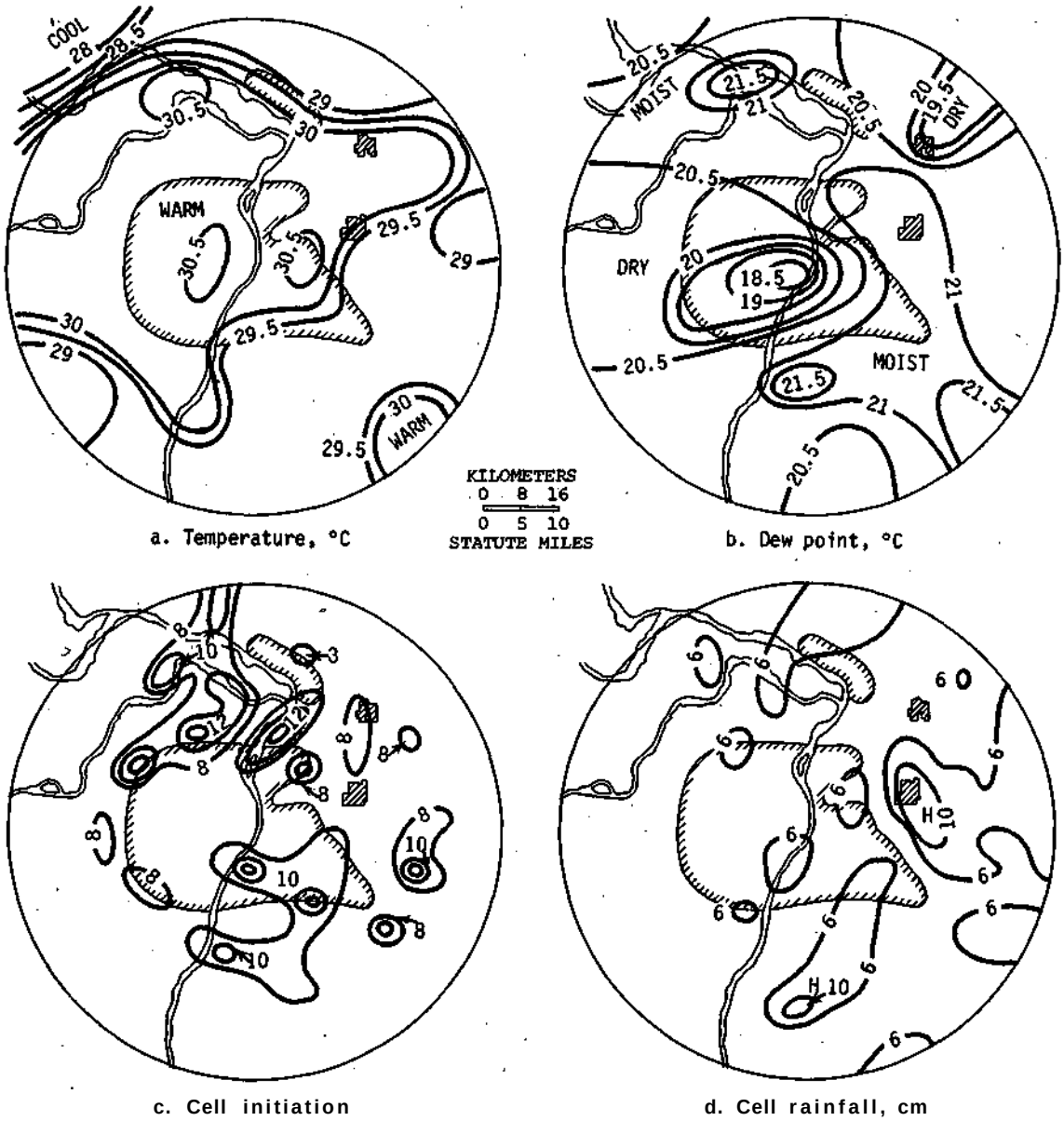

Figure D-60. Temperatures and dew points to cell initiations and cell rainfall for 1500-1800 CDT

Cell initiations tended to occur in most moist regions and did not occur in the well-defined area with dew points ≤20°C. The eastward shift of maximum cell rainfall may have occurred because 1) the area of heavy cellular rainfall at 1200-1500 CDT propagated to the east, and 2) drier air existed over the St. Louis area. The area of maximum cell rainfall for 1500-1800 occurred in a region that was moist before the rain.

Cells associated with storms that maximized over the St. Louis and Collinsville areas tended to move to the SE, and a significant number of cells associated with storms that maximized over the east area moved to the SE, also (figure D-61). The fact that these SE-moving cells might have been intensified due to their proximity to the urban area helps to explain the rainfall maximums

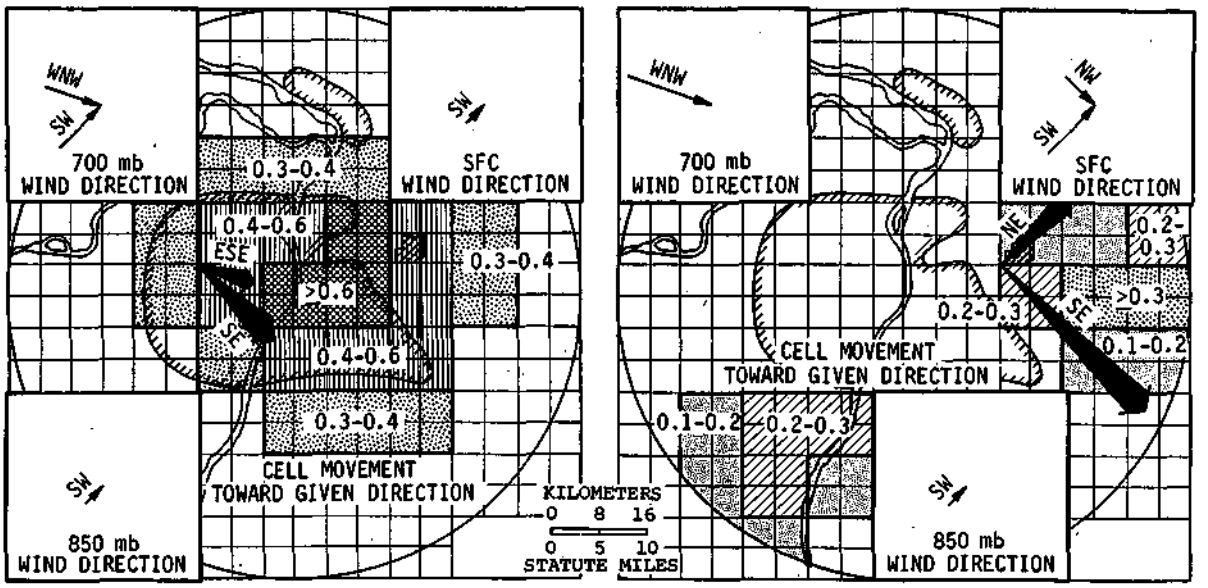

a. St. Louis area

b. Collinsville area

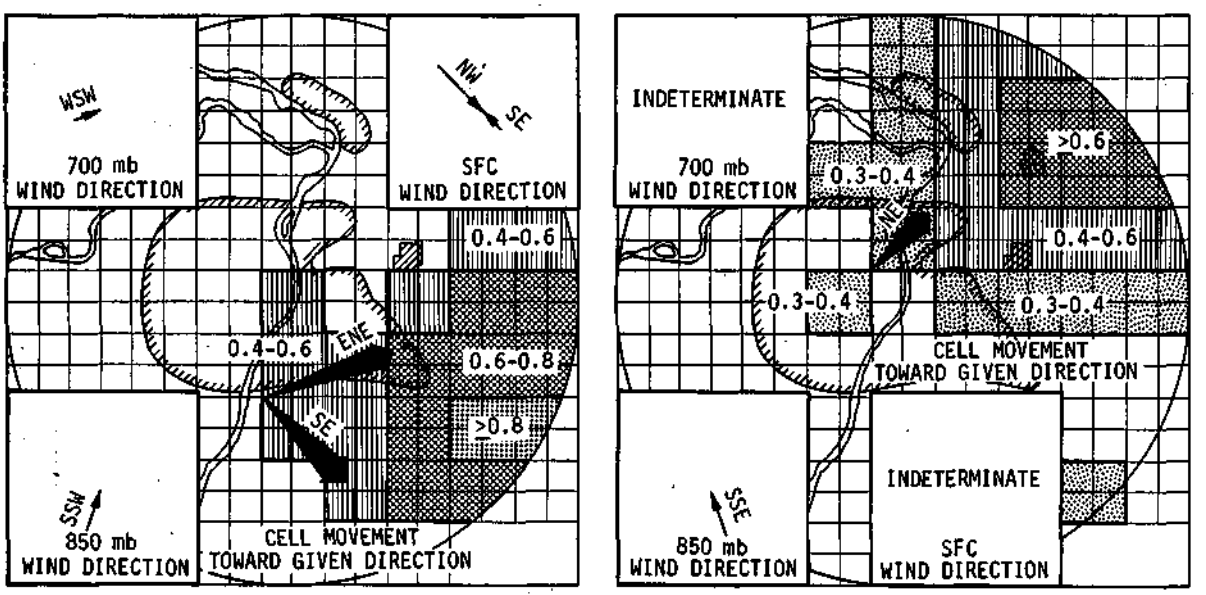

c. East side area .

d. Edwardsville area

Figure D-61. Storm-airflow relations for the St. Louis, Collinsville, east side, and Edwardsville areas for 1500-1800 CDT

Figure D-62. Temperatures and dew points prior to cell initiations and cell rainfall for 1800-2100 CDT

southeast of Belleville and south of East St. Louis. Cells that maximized over the Wood River-Edwardsville region generally moved in a NE direction (figure D-61d), so these cells maximized 'down movement' from the St. Louis urban area. This may help to explain the rainfall maximum north of Alton-Wood River. Some cells that maximized over Collinsville moved to the NE, and the majority of cells that maximized over the east side moved to the ENE. These cells help to explain the large rainfall maximum extending from Collinsville to the east edge of the network.

1800-2100 CDT. The raincell initiation maximum was located just south in the eastern portions of St. Louis for storms that initiated during the 1800-2100 CDT period (figure D-62c). [The maximums for 1500-1800 were located here and north of the city.] Maximum initiation

values were on the order of 12 to 14 per gage, not significantly different from the prior 3-hour period, but these large values were less frequent during 1800-2100 CDT. The average number of initiations per gage was significantly lower during this period. Cell rainfall was much lighter and the areas of maximum rainfall were more scattered than was the case during 1500-1800 (figure D-62d). The only rainfall maximum of consequence was located on a west-to-east line extending from directly south of Wood River through Edwardsville to the edge of the network. Only three raingages received more than 8 cm of rain; all three were located north and east of Edwardsville.

The urban heat island was becoming more evident at this time, with 29° C noted at two gages within St. Louis (figure D-62a). Highest dew point values were located east and south of the St. Louis metropolitan area, while lowest values occurred over the Edwardsville area and across the northern hills into the west side of St. Louis (figure D-62b).

Cell initiations tended to occur in the warmer and more moist regions of the network. However, no apparent relationship exists between heavier rainfall areas and more moist areas of the network. Although more cells initiated to the south and east of St. Louis than to the NE and around Edwardsville, it is interesting to note the low cell rainfall values across the SE quadrant.

Cells associated with storms that maximized over the Wood River-Edwardsville and Collinsville areas generally moved in a ENE direction, although some Wood River-Edwardsville cells moved to the NE and some Collinsville cells moved to the SE (figure D-63). The NE-moving raincells from both areas maximize 'down movement' from the urban region and therefore may help to explain the rainfall maximum that occurs in and around Edwardsville. The SE-moving raincells from the Collinsville area support the rainfall maximums that occur east and southeast of Belleville. Both Wood River-Edwardsville and Collinsville area cells were driven by SSW winds at 850 mb and SW or NW winds at 700 mb (figure D-63).

2100-2400 CDT. A scattered cell initiation pattern prevailed for storms that initiated at this time (figure D-64c). Although over 20 initiations occurred at one isolated gage S of St. Louis, only about 25 gages experienced 15 or more initiations. Of these, 20 were on the Illinois side of the Mississippi River and most were in and around St. Louis. An increase in the average cell initiations per gage was noted during this period. Cell rainfall for the period was somewhat more intense than for the 1800-2100 period or the 0000-0300 period (figure D-64d). Maximum rainfall amounts were located in the south-central region of the circle.

The urban heat island was very well developed by this time, as represented by the fact that the highest temperature values (26.5° C) occurred over downtown St. Louis (figure D-64a). Highest dew point values occurred across the south-central region of the network (2.15 to 22.0° C), while lowest dew point values occurred over the northwest corner of the network (figure D-64b).

The more moist region coincided quite well with the region of maximum rainfall (over the southern part of the network), but cell initiation maximums existed in regions of relatively high and low dew point values. The cell initiation maximums tended not to occur over the urban heat island but did occur along its outer perimeter.

Cells associated with storms that maximized over the Wood River-Edwardsville region generally moved in a NE direction, while the cells that maximized over the Collinsville region generally moved in an ENE direction. Both the NE and the ENE-moving cells support the 6-cm rainfall maximum at and to the east of Edwardsville. A strong correlation existed between cell movement and the 700 mb wind flow during this period, but sample sizes were too small to place much emphasis on this correlation.

To summarize, raincell initiations and cell rainfall both maximized, and seemed to be the most directly affected by the St. Louis urban area, during the 1200-1500 CDT period, the period of maximum heating. The cell initiation and rainfall patterns for storms that initiated during the

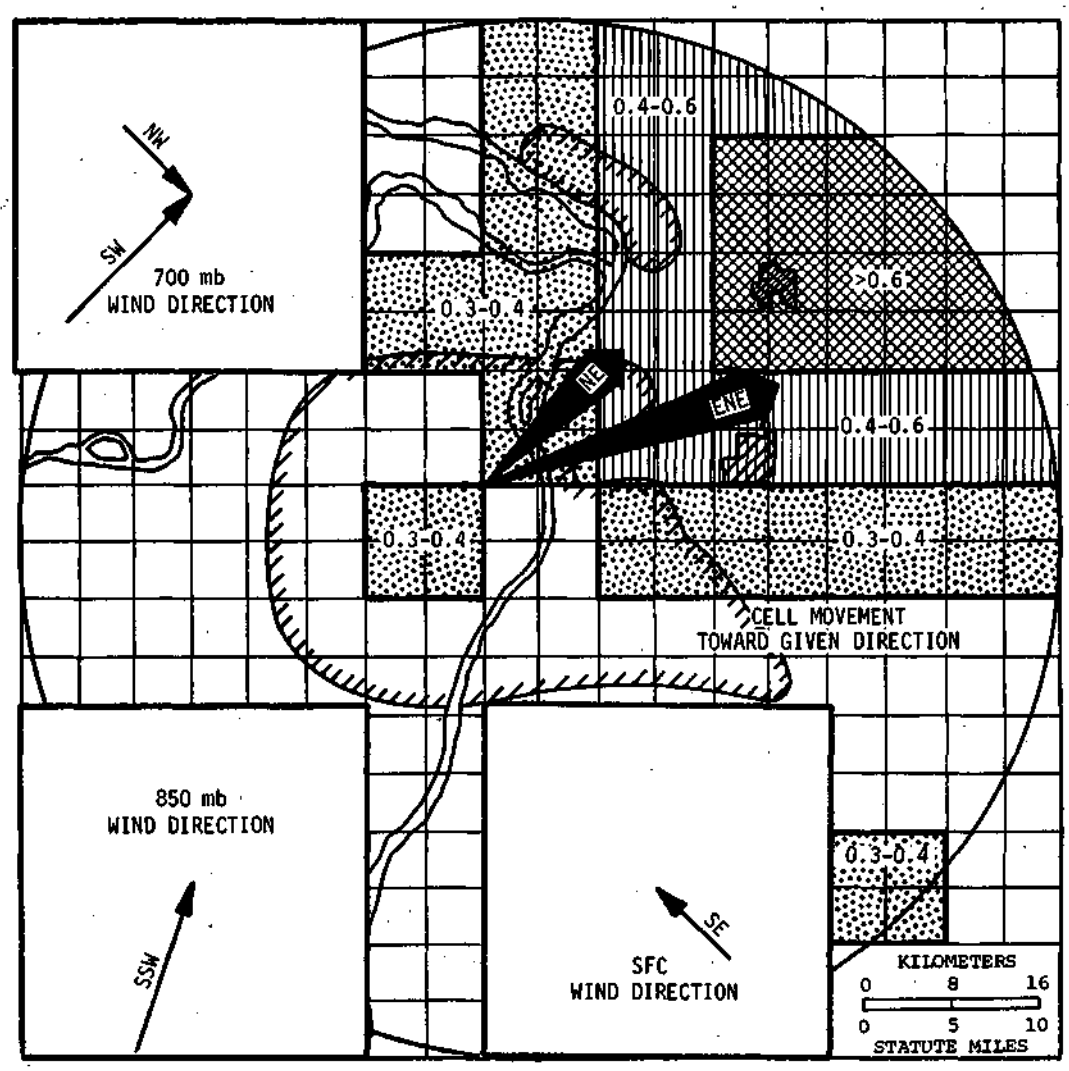

Figure D-63. Storm-airflow relations for the Edwardsville area for 1800-2100 CDT

1500-1800 and 1800-2100 periods also seemed to be affected by the urban area. Cell initiations and cell rainfall were affected to a lesser degree by the urban area with respect to storms that initiated during all other 3-hour periods. Only weak evidence exists for relationships between surface temperature and dew point patterns that occurred the clock hour before storms began and the cell initiation and associated rainfall patterns. It could *not* be said that raincells tended to initiate or tended to produce more rainfall in regions of high dew point values.

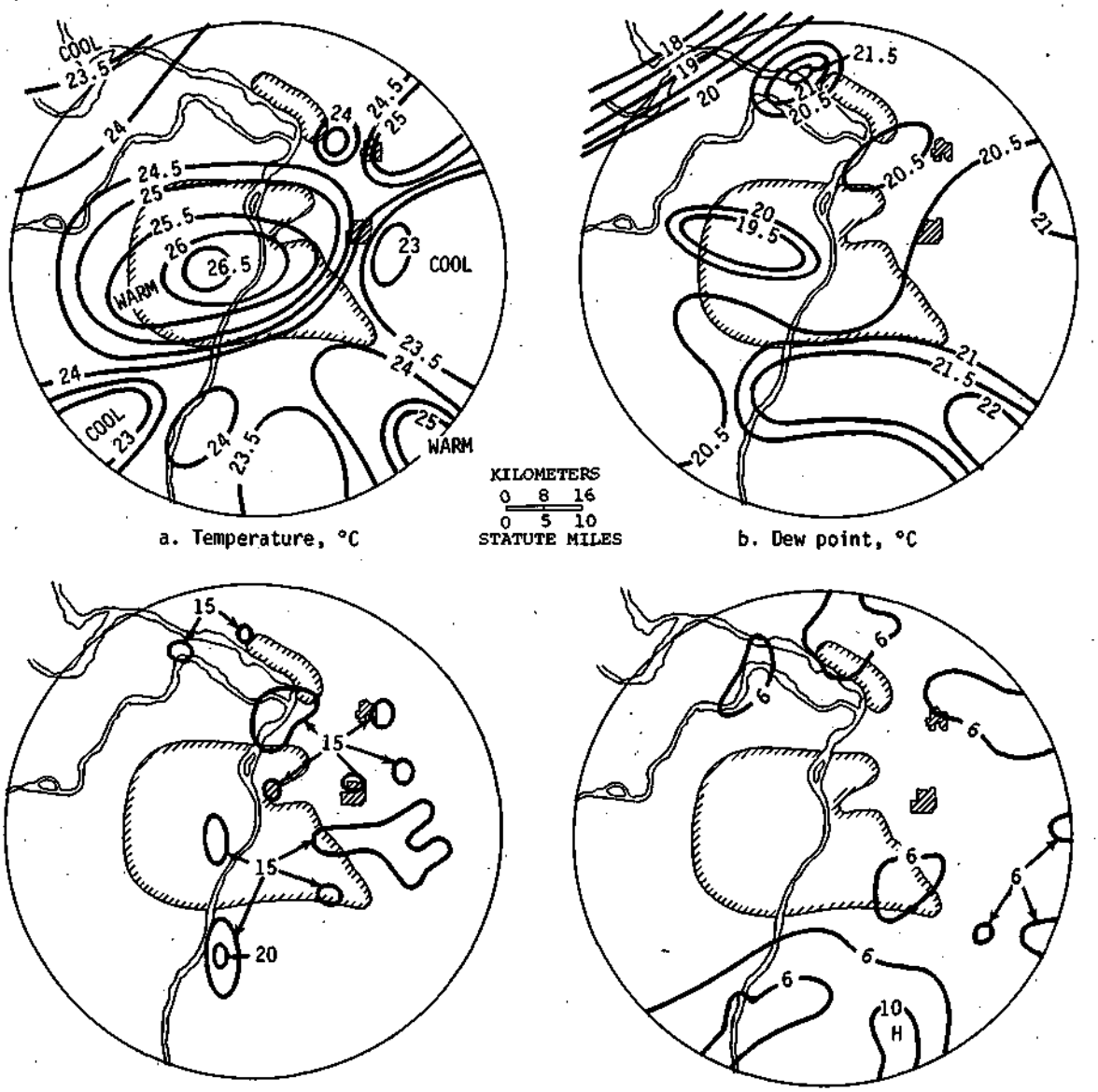

a. Temperature, °C

b. Dew point, °C

c. Cell intiation

d. Cell rainfall, cm

Figure D-64. Temperatures and dew points prior to call initiations and cell rainfall for 2100-2400 CDT

SUMMARY AND CONCLUSIONS

Raincells were used to obtain information concerning the essence of the rainfall increase and to demonstrate the magnitude of the effect. Raincells occuring over six areas defined on the basis of urban, industrial, and rural land use, which was further subdivided according to physiographic divisions (hills and bottomlands), were compared with those in flat rural areas labeled as the control area. The key results are as follows:

1) The largest percentage increase in cell volume, 211% above the control, occurred in cells that developed and/or passed over the St. Louis industrial area. The next largest percentage increase in cell volume, 125%, occurred in cells associated with the overall urban area of St. Louis. Other percentage increases in cell volume were 77% in the Wood River area, 74% in the hills region, and 12% in the bottomlands. All these areas had cells bigger than in the control areas.

2) A stratification by path length indicated that the effect is still present, even in cells with short path lengths. This indicated that the major portion of the increases in rainfall volume can be attributed to factors other than to some biased sampling of heavy and long-moving raincells.

3) In the St. Louis-industrial area, the largest (percentage) increases in raincell volume occurred with squall zones and squall lines. In the Wood River industrial area, the largest (percentage) increases in raincell volume occurred with squall line and cold front storms. In the hills and bottomlands, the largest percentage increase in raincell volume occurred with stationary front storms.

4) For the control and bottomlands cells, the heaviest cell rainfall occurred during the maximum heating period, 1201-1800 CDT, and the lightest rainfall occurred during the minimum heating period, 0001-0600. In urban-industrial cells, the heaviest rainfall occurred during the maximum heating period, 1201-1800 CDT, and the minimum rainfall occurred during the 0601-1200 period.

5) The percentage increase in cells is the same on both weekends and weekdays. Surface temperature patterns and moisture patterns on weekdays and weekends are nearly the same, so the conclusion is that no difference exists on weekend and weekday cells.

6) Stratifications of cells according to months indicate that differences exist between the cells in the different source regions. The largest percentage increases occur a) for the Wood River area in June, b) for the St. Louis-industrial area in July, and c) for the St. Louis urban area in August. The percentage increase in August is nearly as large as the percentage increase in July for the St. Louis-industrial cells. In general, urban influences are greater in July and August.

7) For the St. Louis and St. Louis-industrial cells, differences are significant for all stratifications according to path length, year, synoptic type, period of the day, and month. Wood River cells are significant only in the 'all cells' category in 3 of 5 years, and in air mass and squall lines in the synoptic classifications. However, these cells are significant in all diurnal periods and in all three monthly periods.

8) Maximum rain rarely appears as an important cell parameter in the St. Louis-industrial and St. Louis cells, but often appears in the Wood River cells. Also, mixtures of cell parameters rarely appear in the St. Louis and St. Louis-industrial cells, but often appear in the Wood River cells. This implies that physical processes may be different

for cells in the St. Louis-industrial areas than for cells in the Wood River area. These differences may be due to greater dynamic effects in the St. Louis area.

9) Analyses of the characteristics of raincell mergers indicated a relatively strong tendency for mergers to occur most frequently in a major urban-effect area E and NE of St. Louis, along river valleys, and to a lesser extent in the more hilly regions of the experimental area. In general, there was strong association between the spatial distribution of mergers and total monthly and seasonal rainfall. There was also generally good agreement between the spatial distribution of surface raincell mergers and the smaller sample of radar echo mergers discussed in a previous section of this report.

10) Diurnally, the greatest frequency of mergers occurred in mid to late afternoon (1500-1800 CDT), and the greatest concentration of mergers at that time was over and E of St. Louis where mergers are favored by the urban enhancement of convective activity. The pattern of total rainfall for 1500-1800 closely resembled the merger pattern and 25 to 35% of the total summer rainfall occurred in this 3-hour period in the region where the concentration of mergers was greatest. Comparison of rainfall in regions of greatest merger concentrations indicated that the urban-related mergers tend to intensify the ongoing rainfall processes more than topographic-related mergers.

11) Synoptically, 72% of the surface raincell mergers were associated with squall systems (lines and zones), and only 3% with air mass storms. Thus, the merger process is much more likely to occur with organized storm systems generally because more cells exist. It is interesting to note that approximately 75% of the total summer rainfall in 1971-1975 was associated with squall systems and only 2% with air mass storms. This is another indication of the strong relationship between mergers and rain production at the surface.

12) Analyses indicated that 78% of the mergers were followed by an increase in intensity and 82% by an area increase, whereas only 14% and 10%, respectively, were followed by decreases in intensity and area. This is in agreement with echo top findings following mergers. This further verifies the important role of mergers in stimulation of the total rain production from convective cells.

13) Analyses of mergers in relatively dry, near-normal, and wet periods indicated similar merger trends in the three groups. That is, mergers tended to be concentrated over and downwind of St. Louis, along river valleys, and in the more hilly regions of the network. In dry months, 32% of the total mergers occurred in a N-S line over St. Louis and to the E in the region from Granite City to Collinsville, whereas 25% occurred in this region in the near-normal months and 27% in the wet months. Thus, the merger processes which are closely related to the rain enhancement processes are equally active in dry and wet months and are apparently stimulated by inadvertent weather mechanisms. This is a favorable finding from the standpoint of planned weather modification; that is, there is an indication that weather modification has potential to stimulate rain production under some conditions during dry periods when water shortages exist.

14) Factor analysis was used to adjust cell volumes for possible bias due to area. The adjustment for bias indicated that a) the 211% increase in cell volume for St. Louis-industrial cells should be reduced to 106%, b) the 125% increase in cell volume for St. Louis cells should be reduced to 76%, c) the 77% increase in cell volume for Wood River cells should be reduced to 64%, d) the 74% increase in cell volume for hills

cells should be reduced to 38%, and e) the 12% increase in cell volume for bottomland cells should be increased to 25%. This represents a severe attempt at adjustment, but, even so, the effect on the cells is still present.

15) The use of factor analysis to relate cell movement and wind direction to the areas in which storms maximized indicated that the maximums in the raincell patterns tend to be located downwind from and with movement from the urban and industrial sources. This shifting in location of the raincell maximums in relation to the cell movement and wind direction is strongest on a monthly basis, but is also present to a certain extent in the yearly data. These formed convincing models of urban influences on raincells.

16) Maximums in cell initiations for summer occurred a) in the region extending from the bottomlands east to Edwardsville, and b) a region extending from the southern portion of St. Louis through Belleville. The two areas essentially cover the northern and southern portions of St. Louis and indicate that the number of initiations was lower in the central portion of the city.

17) A diurnal stratification was performed to obtain 3-hour cell initiation and cell rainfall patterns. Maximums in both cell initiations and cell rainfall occurred during the maximum heating period, 1200-1500 CDT. Since the two parameters maximized over and slightly downwind of the St. Louis urban-industrial area during this 3-hour period, and since the patterns were quite anomalous when compared with the other 3-hour patterns, it seems likely that both parameters were influenced by the presence of the St. Louis urban-industrial region. Other weaker relationships between the urban area and cell initiation and rainfall patterns were evident during the other 3-hour periods, especially during 1500-1800. It seems evident that the urban area plays a significant role in the rainfall pattern over the St. Louis area, since most of the rain received over the area falls during 1200-2400. Only weak evidence exists for relationships between surface temperature and dew point patterns that occurred the clock hour before storms began and regions of maximum cell initiation and cell rainfall during 3-hour periods of the day.

DEPOSITION OF AEROSOLS

D. F. Gatz, R. G. Semonin, arid M. E. Peden

A major purpose of the METROMEX research was to describe the distribution of rainfall in the St. Louis metropolitan area during the summer months. This section describes the deposition of certain chemical elements in portions of the same area. Deposition of materials by rain (wet deposition) and dry deposits in the rain samplers (dry deposition) were both measured. The purposes of these measurements were:

1) To measure the amount of deposition and its spatial variability for elements with strong natural (soil) and anthropogenic sources
2) To facilitate comparison of rainfall and chemical deposition, for purposes of a) assessing the role of the rainfall anomaly on aerosol deposition, and b) testing hypotheses regarding the role of urban aerosols in precipitation modification
3) To document the deposition of special tracer materials introduced into precipitation systems to study aerosol and hydrometeor trajectories and scavenging efficiencies

Thus, these measurements were designed to help us find the causes of the urban precipitation anomaly and its effects, and to give us information about the transport and deposition of urban aerosols in precipitation systems. This research adds to our understanding of the effects of cities on the weather and environmental quality of surrounding areas.

The field sampling effort required for these measurements was unprecedented. A recent survey of North American sampling networks for precipitation analysis (Miller and Wisniewski, 1978) showed only one network with more sites, and no large networks performing daily sampling with a comparable density of collectors. Samplers were operated for periods of 6 to 8 weeks during the summers of 1972-1975.

Results reported here are largely related to purpose (1), the measurement of deposition and its spatial variability. Data analyses to fulfill purposes (2) and (3) are still in progress.

EXPERIMENTAL METHODS

Methods to be described include field procedures used in collecting samples, laboratory sample handling and chemical analysis techniques, and statistical methods used in analysis.

Field Methods

Two different rain sampling networks were used, the first from 1972-1974, and the second in 1975. Both are shown in figure D-65. The 1972-1974 network was rectangular. It extended eastward from St. Louis, contained 80 samplers and covered approximately 1900 km^2 The 1975 grid was irregular in shape. It was oriented NE-SW, centered roughly on the Alton-Wood River area, and covered 2200 km^2 . In both networks, stations were placed about 5 km apart in approximately a square grid. Of the 85 sites in the 1975 network, 19 were also used in the earlier network.

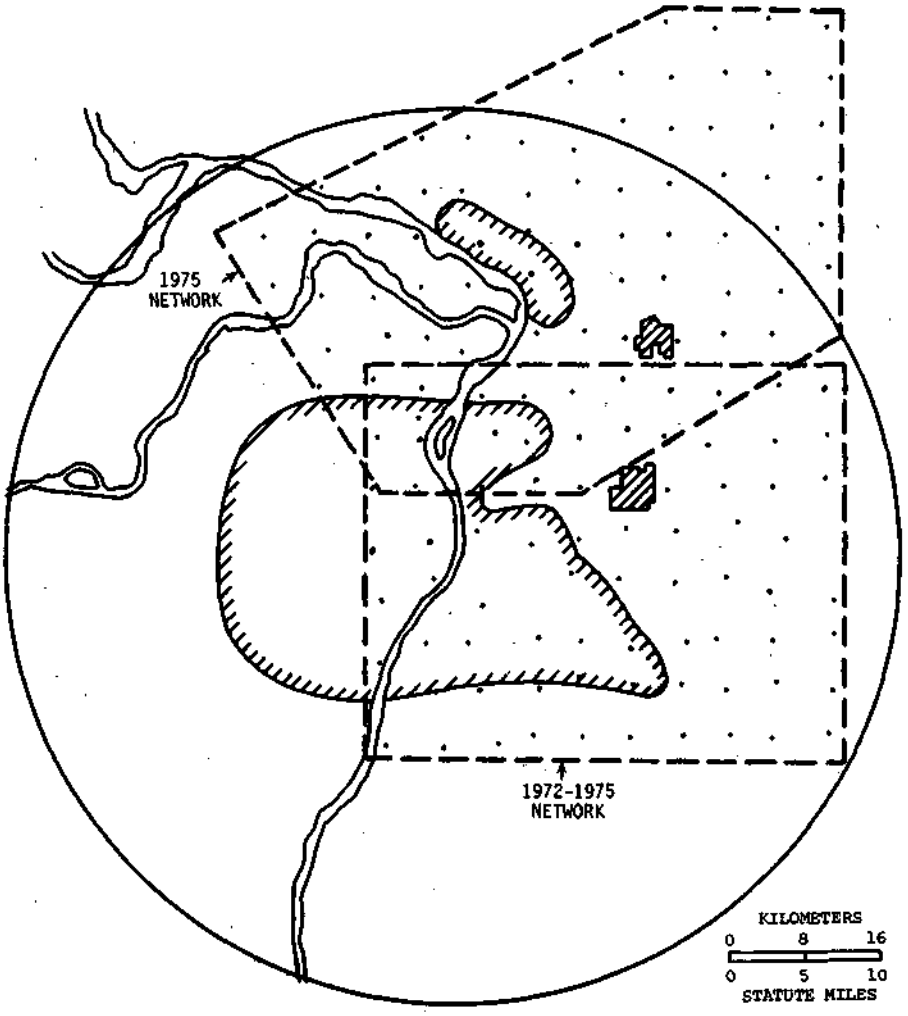

Figure D-6S. Precipitation chemistry sampling networks

Samplers were installed at raingage sites. This provided a standard measure of rainfall at each site. Unfortunately, many sites were subject to contamination, usually by road dust and auto exhaust from adjacent roads. Specific sampler locations were generally chosen so as to minimize the influence of local dust sources for prevailing surface winds in summer (SE to SW) while still providing convenient and rapid access for field technicians, so as to minimize the time required to change samplers across the network.

In 1972 and 1973 samples were collected in wide mouth (8.7 cm diameter) bottles of linear polyethylene, used only once. The same bottles were used in 1974 and 1975, but in those years they were lined with bags of conventional polyethylene because a shortage of raw materials caused by the oil embargo made it impossible to get new bottles. Liners were also used only once. All samplers, whether lined or unlined, received a precleaning consisting of three deionized water rinses, after tests showed that such cleaning was both necessary and sufficient to remove contaminants of the elements being measured.

Samplers were mounted 1.5 m above ground on metal fence posts in such a way that contamination by splash from the posts was very unlikely.

Criteria for determining which days to expose samplers varied over the four summers of sample collection. From 1972 through 1974 samplers were distributed on days when morning forecasts indicated a 30% or greater chance of rain. In 1975 field technicians worked on a schedule of five days on, one day off, which resulted in the collection of four separate sets of daily samples in each six day cycle.

Oh days designated for sampling, a team of field technicians in automobiles distributed bottles to network locations. They labeled each bottle with experiment number, site number, data, and time, and left it exposed with cap off. Samplers ordinarily remained in the field for about 24 hours. However, on a few occasions bottles were retrieved following rain on the same day they were put out, and on rare occasions bottles remained in the field for 48 or 72 hours.

After the sample bottles were retrieved from the field, they were brought to field headquarters and then transported to our laboratory in Champaign. Samples normally arrived in Champaign within three days of their collection in the field, and laboratory personnel ordinarily completed initial processing (pH and conductivity measurements, and filtration) within ah additional 72 hours. Sample sets were ordinarily processed in order of their collection in the field, but sets containing rain samples had priority over those having only dry collections.

Much emphasis was placed on care and cleanliness on the part of the field technicians, to minimize contamination. As a test of the success of these contamination control efforts, and of the overall reproducibility of the sampling and analysis procedures, six samplers were exposed at Civic Memorial Airport (site 22) during the 1975 sampling season. As shown in the diagram of the site (figure D-66) three of the samplers were lined with polyethylene bags and three were unlined, to test the reproducibility of both types of samplers. The samples from this site were treated identically to those from all other sites in the network.

Laboratory Procedures

Water samples were first weighed in the sample bottles. The empty bottles were later reweighed so that net sample mass could be determined and converted to volume.

Conductivity and pH measurements were made on unfiltered samples to insure accuracy (Rainwater and Thatcher, 1960). Measurements were performed on aliquots withdrawn from the sample, to avoid contamination. Conductivity measurements were made on 3-ml aliquots in an inverted glass conductance cell connected to a manually balanced AC bridge. The measured values were multiplied by the cell constant to obtain conductance in units of micromohs cm^{-1}. Care was taken to insure a uniform temperature for both pH and conductivity measurements.

The pH measurements were made on 1-ml aliquots in polystyrene vials, with a micro-combination electrode. Care was taken to keep the samples away from acid or ammonia fumes that might have changed the pH of a sample if absorbed.

Conductivity and pH measurements were omitted on samples of less than 25 ml. Samples less than 50 ml were diluted by addition of 50 ml of distilled deionized water, to provide enough sample volume for all subsequent analyses. The next step in processing was filtration.

Samples were filtered through 0.45 µ m pore diameter membrane filters, usually millipore type HA, after leaching the filters and rinsing the apparatus with 100 ml of deionized water. This procedure proved effective in avoiding contamination of the water soluble fraction of the samples for Li, Na, Mg, K, Ca, Mn, Fe, Cu, Cd, In, Cs, andPb.

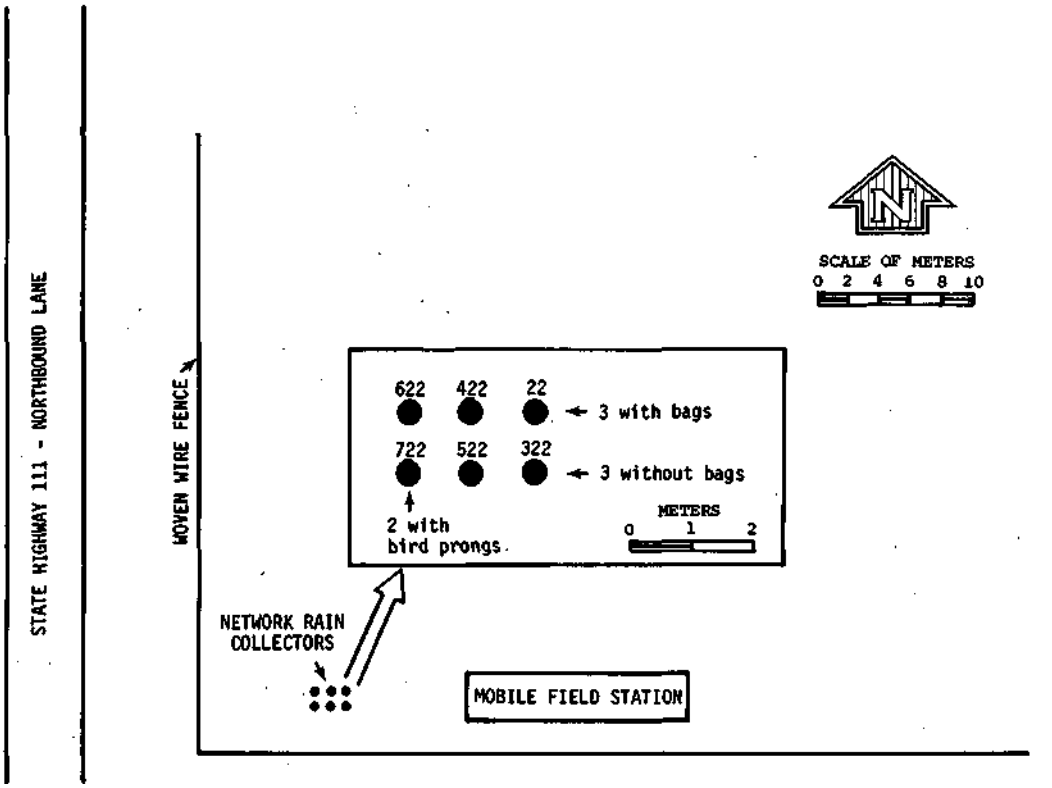

Figure D-66. Arrangement of samples at site 22, 1975

The filters were dried, folded to contain the insoluble materials, and stored in plastic vials The filtrate was acidified to approximately pH 2 and stored in polyethylene bottles until analysis.

Samples from the 1972-1974 network were analyzed for soluble Li, Na, Mg, K, Ca, and Zn by standard flame methods on an Instrumentation Laboratory Model 353 atomic absorption spectrophotometer. Samples from 1975 were routinely analyzed for soluble Li, Mg, K, Ca, and Zn, and insoluble Li, K, Fe, and Zn, by standard flame or flameless methods. Occasionally samples were also analyzed for soluble Fe, Cd, and Pb, and insoluble Mg, Ca, and Pb.

Data Processing

Element concentrations in rain samples received extensive editing and computer data processing to insure a valid data set for study and interpretation. Figure D-67 shows the sequence of steps in this procedure.

Measurements recorded initially on laboratory data sheets were punched on cards and verified. These cards were then used as input to a computer program that corrected for blanks, dilutions, and known systematic errors, and punched a new set of data. At this point, experiments having fewer than 5 wet samples (i.e., with rain in the bottle) were selected as 'dry' experiments.

For these dry experiments, dry deposition rates (mass cm^{-2} hr^{-1}) were computed for each site without rain. These data were edited to remove extreme outliers, such as samples known to have been contaminated. For example, samples containing bird droppings were identified from field and laboratory notes on sample condition, or by their simultaneously high concentrations of

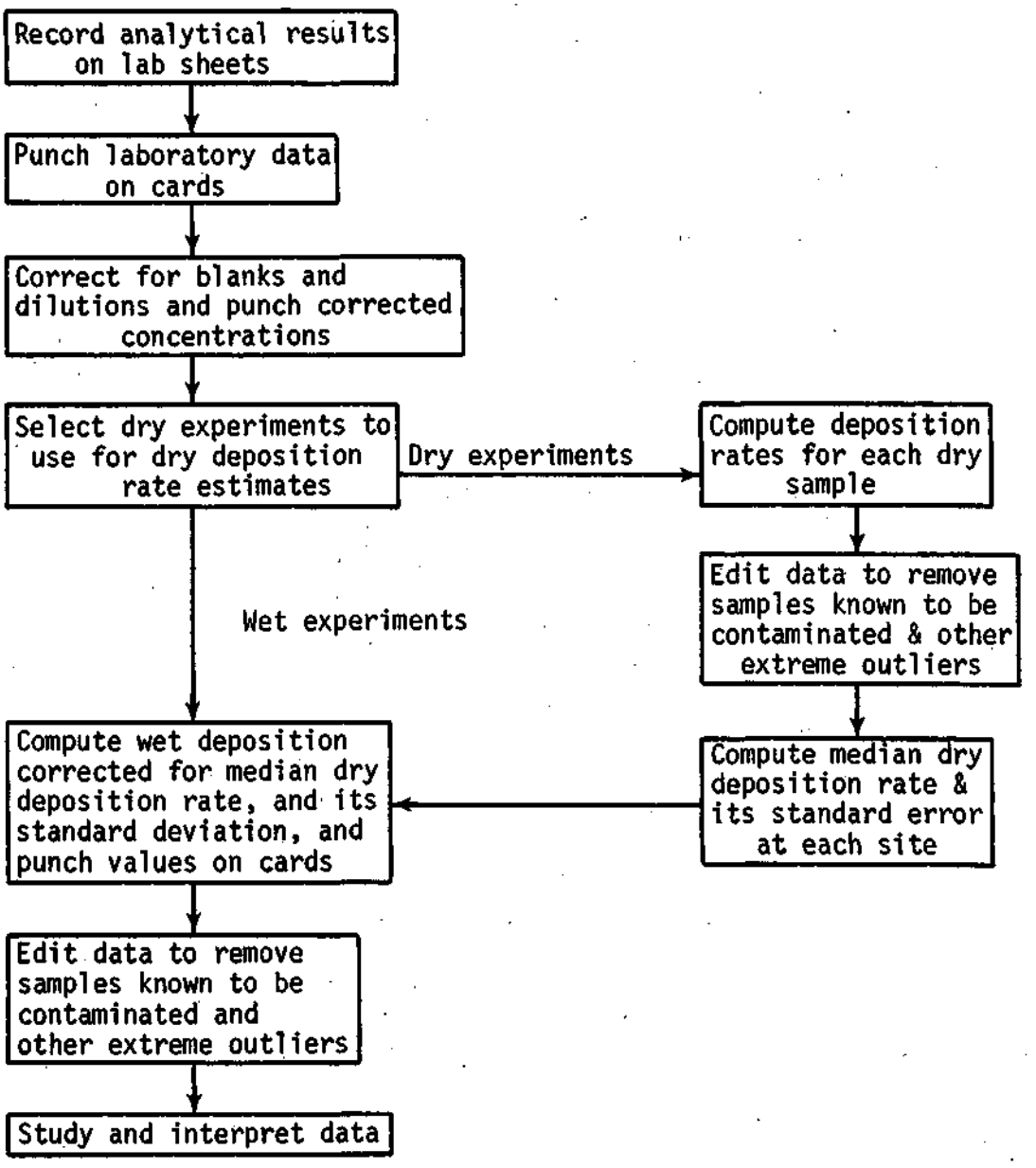

Figure D-67. Schematic of data processing procedures

Mg and K, and alkaline pH values. In cases where no obvious contaminants were observed, and only a single element had an unusually high value, the decision to keep or discard the value was a subjective one, based upon extensive familiarity with the data, with the location of the sampler, and with collection procedures. Some sites were known to be located near sources of contaminants such as dust from limestone gravel roads. The philosophy followed with respect to obvious road dust contamination was generally to keep the data, since the dry deposition rates were intended to correct wet samples for local dry deposition into the sample bottles. However, single high values, more than 10 times the next lower value on other days at that site and well in excess of values at

surrounding sites in the same experiment, were ordinarily discarded. In any case, the presence or absence of a single high value ordinarily had little effect on the median dry deposition rate, which was the value used to correct wet samples.

The median dry deposition rate and its standard error (SE) were evaluated with the BMDP package of statistical programs (Dixon, 1975), which uses the equation

$$SE = (x_i - x_j)/2\sqrt{3}$$

where i is the integer part of $\frac{1}{2}(n+\sqrt{3}n) + 1$, j is the integer part of $\frac{1}{2}(n-\sqrt{3}n) + 1$, and n is the number of observations. The median dry deposition rate at each site was used to correct the measured deposition in rain samples from the same site, and its standard error was used in the calculation of the uncertainty of each wet deposition measurement.

The calculation to correct measurements on rain samples for the contribution of dry deposition was performed next. The corrected deposition, D (μ g cm^{-2}),is given by the equation

$$D = (kVC/A)\text{-}dT \qquad (1)$$

where k is the measured (uncorrected) concentration in the sample (μ m ml^{-1}), V is the sample volume (ml), C is a conversion constant (10^3 ng ng^{-1}, d is the dry deposition rate (ng cm^{-2} hr^{-1}), T is the time of sampler exposure (hr), and A is the area of the sample bottles (59.45 cm^2).

This assumes that the average dry deposition rate on rain days is equal to the median rate measured on dry days. One might argue that the dry deposition decreases once rain has wet soil surfaces and washed the near-surface air clean of aerosols. On the other hand, summer convective storms may raise considerable soil aerosols along the leading edge of their downdraft gust front, leading to very high dry deposition rates in open collectors for short periods of time. In any event, this method is only an estimate of the dry deposition contribution to total measured deposition.

Ideally, one should use collectors that open only during rain. Such collectors are now commercially available. They were not available when this study began, but the cost of 80 of them would have been prohibitive in any case.

By substitution of the constants, equation 1 becomes

$$D = 16.82kV\text{-}dT \qquad (2)$$

For any given sample, V and T will be constants, so that equation 2 has the general form

$$c = ax — by$$

where the constants are a = 16.28V and b = T. The rules for propagation of error for such a subtraction of one parameter from another leads to the following approximate expression for the variance of the result (Bevington, 1969)

$$s_c^2 = a^2 s_x^2 + b^2 s_y^2$$

By substituting the expressions for the constants we obtain the expression for the variance of the net wet deposition,

$$s_D^2 = 283V^2 s_k^2 - T^2 s_d^2 \qquad (3)$$

Evaluation of this expression for a given measurement requires numerical values for s_k^2 and s_d^2, in addition to the measured values of V and T. Since the median dry deposition rate at each site is used in the dry deposition correction, it is proper to use the square of the standard error of the median for s_d^2. The variance s_k^2 of an individual (uncorrected) element concentration was evaluated for each element from the multiple samples collected at site 22. Concentrations

were found to fit the lognormal distribution more closely, than the normal distribution. Thus, the variance is given by

$$s_k^2 = k^2 s_l^2 \qquad (4)$$

where s_l^2 is the variance of the natural logarithms of the concentrations, and k is concentration in rain as defined earlier. The values of s_l^2 evaluated from replicate samples at site 22 are given later in table D-32.

The uncertainties reported in this paper refer only to the soluble fraction of the rain samples. That is, both s_d^2 and s_k^2 were evaluated specifically from analysis of soluble materials, and of course, were evaluated separately for each element.

The corrections program also punched a set of cards containing D values to be used for further analyses. These data were also edited to remove data for samples known to be contaminated and other extreme outliers. In the case of wet samples, these outliers were identified semi-objectively by two methods.

One method used a computer-generated plot of deposition vs rainfall for each experiment. This permitted a rapid identification of samples in which deposition was greatly in excess of what occurred at other sites with similar rainfall in the same experiment. The other method used computer-generated plots of element ratios to Na. Na was chosen as the index element because at an inland location such as St. Louis its only significant source appears to be soil. This is not true of other soil elements such as Ca or Mg, which occurred in limestone dust from quarries, gravel roads, or agricultural liming. Thus, the Ca/Na ratio can be used to indicate the presence of excess road dust not accounted for by the median dry deposition rate. Such contamination would also give Ca in excess of that expected only from rainfall, so such a sample would emerge as an outlier with both methods. Elemental depositions that appeared as extreme outliers (in excess of about 10 times the mean of other samples) in *both* tests were discarded. If two elements in the same sample were discarded, the entire sample was declared invalid.

RESULTS

Reproducibility Experiment

Six samplers, half with polyethylene liners and half without, were operated at site 22. There were two main purposes of the experiment. The first main purpose was to measure and compare dry deposition rates in lined and unlined samplers. If dry deposition rates for lined and unlined samplers were not significantly different, a single dry deposition rate for each element could be determined from dry experiments from all years and applied to all rain samples. On the other hand, if significant differences were found, dry deposition rates would have to be determined separately for years with and without liners. In any case, rates had to be determined separately for 1975, since a different network was used.

The second main purpose was to measure the variability of element concentrations in replicate rain samples. Such information is needed to estimate the uncertainty in an individual concentration measurement. As shown earlier, the uncertainty in the measured concentration before correction for dry deposition is needed in the evaluation of the overall uncertainty in the corrected concentration.

Dry Deposition Comparison. Two-way analyses of variance were performed for each element on dry deposition rates measured on five days in 1975. The raw data and a standard

Table D-31. Soluble Mg Dry Deposition Rates

(In ng cm^{-2} hr^{-1})

	Sampler number	Day 1	2	3	4	5
Lined	22	1.10	0.61	3.62	0.40	1.43
	422	1.42	0.82	5.53	0.45	1.75
	622	3.46	0.42	1.69	0.36	2.36
Unlined	322	1.17	0.87	1.20	0.90	7.37
	522	1.55	0.68	5.77	0.92	8.19
	722	5.61	0.82	2.83	0.87	8.30

Anova table for In transformed data

Source of variation	DF	SS	MS	F	P
Days	4	16.9693	4.2423	4.2423/0.2372 = 17.88	0.00001
Days-liners interaction	4	2.4336	0.6084	0.6084/0.2372 = 2.56	0.0784
Days-samplers interaction	16	3.7952	0.2372		
Liners	1	2.0845	2.0845	2.0845/0.1934 = 10.78	0.0304
Samplers (error)	4	0.7735	0.1934		
Total	29	26.0561			

table of results for soluble Mg are shown in table D-31 to illustrate the method. The table shows an F value of 17.88 for variation from one day to another, with a corresponding probability of 0.00001 of obtaining such a result if in fact there were no differences between days. The F value for differences between lined and unlined samplers is 10.78, with a corresponding probability of 0.0304. Thus, the difference in the dry deposition rate of soluble Mg between lined and unlined samplers is significant at the 5% level, but not at the 1% level. The interaction between days and liners is not significant at either the 1% or 5% levels. Soluble Mg was chosen for illustration because it was the only element for which a significant difference in dry deposition rate (at the 5% level) was observed between lined and unlined samplers. The nature of the variation in the dry deposition rate of soluble Mg is further illustrated in figure D-68, where the mean values for the three lined and three unlined samplers are plotted against days. Untranformed values have been plotted for simplicity.

The figure shows relatively large differences from day to day, compared with the differences between lined and unlined samplers. An analysis of variance on data from days 1 to 4 only confirmed that the large difference between lined and unlined samplers on day 5 accounts for the 5% significance level that was achieved overall for such differences. The same large difference on day 5 also accounts for the nearly significant (5% level) F value for day-liner interaction. Without day 5, neither F value approached the 5% significance level.

The fact that Mg was the only element to show significant differences at the 5% level, and that this result was caused by data from a single day, suggests that dry deposition rates into lined and unlined samplers are not significantly different. In any case the error made by using the median of the two rates on any given day is likely to be small compared with that incurred by ignoring day-to-day differences, as we do by using a long-term median value. Finally, as shown later, the change in net deposition caused by changing the dry deposition correction by a factor of 2 amounts to only 10% for samples larger than 20 ml (0.34 cm of rain) and the uncertainty in the concentration measurement is usually much larger than that.

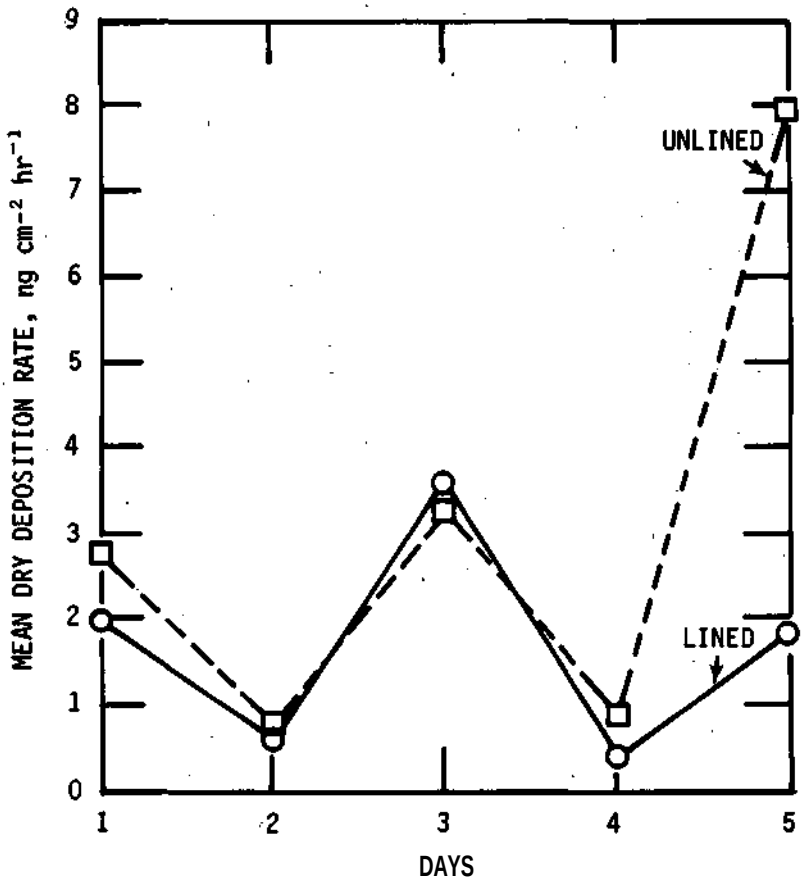

Figure D-68. Variation in soluble Mg dry deposition rate

Thus, a single median dry deposition rate was determined for each element at each site, with data from all years, and this rate was then used to correct wet samples from all years.

Concentrations in Rain. The uncertainty in an individual measured concentration in rain (uncorrected for dry deposition) is needed to evaluate the uncertainty in the corrected concentrations (equation 3). These uncertainties were evaluated from analyses of replicate samples collected in six collectors (half lined, half unlined) at site 22 in 1975. Ten separate rains were sampled, but the small volumes of some samples precluded analysis of all samples for all elements. Thus, for some elements, results for fewer than 10 events are available.

Because concentrations in rain generally follow the lognormal distribution (Gatz, 1976), the appropriate measure of variability is the variance of the natural log transform of the concentration, which is related to the variance of the concentration by equation 4. A separate variance was computed for the concentration from the three lined samplers and three unlined samplers in each event. These variances were then pooled; that is, average variances were computed for lined and unlined samplers. The results are shown in table D-32. Note that in four cases, the individual variances used to compute the pooled variance were not homogeneous (5% level). In strict terms this means that the samples were not drawn from the same population and the pooled variances are invalid, but they are still included for each of these as the best available estimate of the true variance.

Table D-32. Measurements of Pooled Variances of Log Concentrations at Site 22,1975

	Soluble		Insoluble	
	Lined	*Unlined*	*Lined*	*Unlined*
Li	0.460*(9)	0.482(9)	1.272(8)	1.395(8)
Mg	0.219(10)	0.194(10)		
K	0.595(10)	1.024(10)	0.508(8)	0.110(8)
Ca	0.395(9)	0.510(9)	0.198(2)	0.554(2)
Fe			0.417(8)	0.468*(8)
Zn	0.304*(9)	0.609(9)	1.84(5)	0.756(5)
Cd	0.731(3)	0.497*(3)		
Pb	0.067(1)	0.083(1)	0.062(2)	0.126(2)

* Computed from variances shown to be non-homogeneous at the 0.05 significance level using Cochran's test (Winer, 1962)

Note. Blanks indicate no measurements; values in parentheses are the number of events analyzed

Table D-33. Mean Value of Variances of Log Concentrations at Site 22 and the Water Survey Roof

	Site 22		Water Survey roof
	Soluble	*Insoluble*	*Soluble*
Li	0.471(9)	1.33(3)	
Na			0.0421(8)
Mg	0.206(10)	0.206*	0.0047(8)
Cl			0.0432(8)
K	0.810(10)	0.309(8)	0.0519(8)
Ca	0.452(9)	0.376(2)	0.0082(8)
Fe		0.442(8)	
Zn	0.456(9)	1.30(5)	
Cd	0.614(3)		
Pb	0.075(1)	0.094(2)	
NH_4+			0.0013(8)
NO_3^-			0.0089(8)
$SO_4=$			0.0014(8)

* Not measured; assumed equal to the value for soluble Mg

Note. The number of events averaged is given in parentheses

Differences between the pooled variances of lined and unlined samplers (table D-32) were found not significantly different (at the 5% level) with a t-test. Thus, mean values were computed, and are shown in table D-33. These values were used in equations 3 and 4 to compute the uncertainty in corrected concentrations. Also shown in table D-33 are the results of a parallel reproducibility study on samples collected on the roof of the Water Survey building in Champaign. Two, three, or four samplers (the same open polyethylene bottles used in METROMEX) collected replicate samples from eight separate precipitation events. The samplers were exposed immediately prior to the precipitation, and the samples were collected and filtered by laboratory personnel within a few hours after the precipitation ended. Thus, this set of samples received more careful handling, plus prompt filtration and a minimum exposure to dry-deposited materials, than was possible for the METROMEX field samples.

The results show striking differences from the two replicate sampling programs. Even - though only 3 elements were common to both studies, it is clear that the samples collected on the Water Survey roof exhibited much less variability. This difference apparently resulted from the extra care taken in sampling and sample handling. For example, it is now known (Peden and Skowron, 1978) that gradual dissolution of insoluble materials in rain can cause rapid increases in soluble Ca and Mg concentrations if samples are not filtered or centrifuged within 24 hours of the rain. The field samples, while handled with all practical speed, would not have been filtered so quickly and differing amounts of insoluble material in the samples, whether blown into the samplers dry or collected by the falling rain, could have dissolved to some extent, yielding unusually variable concentrations.

Ca and Mg are very abundant in soils; thus windblown.soil material is a likely source of insoluble material in the samples. However, the finding of high variability in the non-soil elements Zn and Cd suggests that the large variability found in the field samples has other causes as well.

Figure D-69 shows the uncertainty (as the standard deviation) of an individual measurement for each element as a function of uncorrected concentration, over the typical range of concentrations. It shows many standard deviations in the range of 50% to over 100% of the measured concentrations. Thus, there is also a large uncertainty in an individual deposition value derived from the measured concentration. The uncertainty in the net deposition is virtually all due to the uncertainty in the measured (uncorrected) concentration. The contribution of the dry deposition rate uncertainty is almost always less than 1%.

With approximate rules for propagation of error (Bevington, 1969) and the assumption of a standard deviation of 100% of each measured concentration, the standard error of the network mean deposition for one event is approximately 10 to 15%.

The net deposition is in most cases not very sensitive to the value of the dry deposition rate used in equation 2. Figure D-70 shows that for sample volumes of 20 ml (0.34 cm of rain) or more, the error caused by varying the dry deposition rate by a factor of 2 is less than 10%.

Dry Deposition Rates

Dry deposition rates were measured mainly to provide values for use in correcting rain samples for dry deposition into the open collectors. The relationship between dry deposition to plastic bottles and to natural surfaces is not clear, and it may be useless to carry data interpretation beyond the calculation of the rates needed to correct rain samples. Yet, measurements of dry deposition in 80 to 85 collectors over 1900 to 2200 km^2 in 20 to 30 events are a unique data set, which should be fully explored and reported even if their application is somewhat uncertain.

Rates of deposition into exposed sample bottles were measured for 32 days in the 1972-1974 period and 5 days in 1975. Not all elements were determined in every sample set, however, and at each site some results were discarded because of contamination or the occurrence of light rainfall. Thus, the number of individual observations used to determine the median at each site varies from element to element and site to site for each network. Summaries of the numbers of observations used to determine the various median rates are given in figures D-71, D-72, and D-73. In the 1972-1974 period only the soluble components of the dry deposition rate were determined. The median number of observations used in those determinations varied from 13 for Na, Mg, and Ca, to 26 for Li. At no site were fewer than 5 samples used for any determination of a median.

In 1975 (figure D-72 and D-73), only 5 events were available from which to determine median rates. However, over 90% of the sites had useful data for all 5 events.

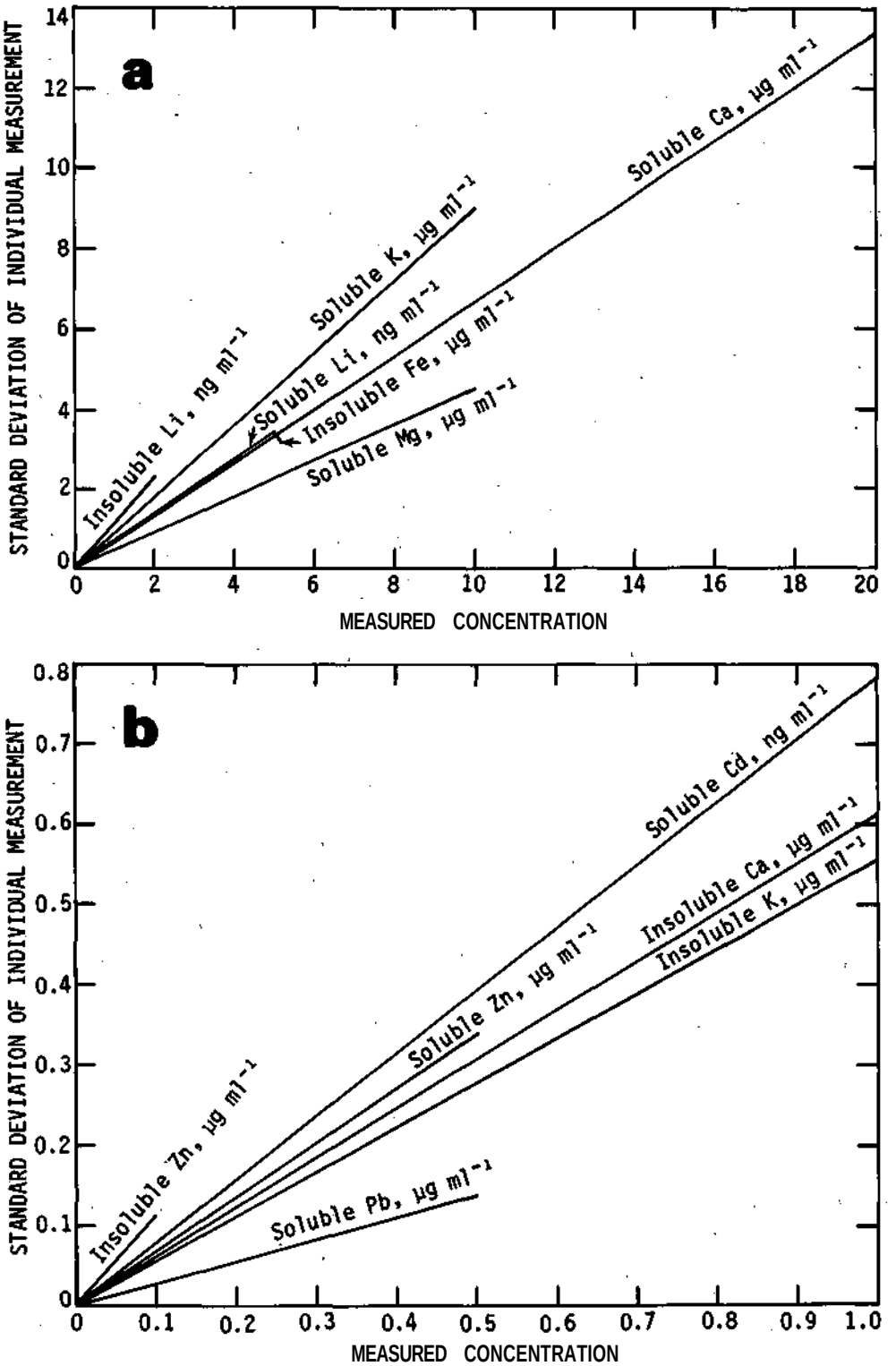

Figure D-69. Variation of uncertainty with measured concentration (Length of line shows typical concentration range)

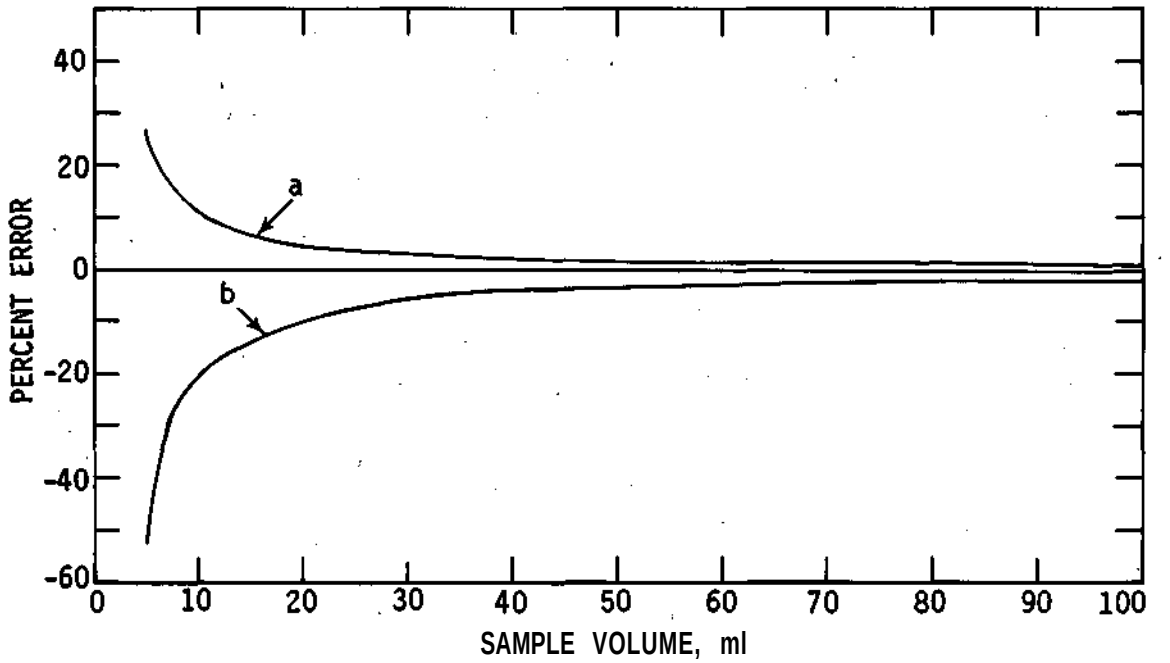

Figure D-70. Examples of error in corrected deposition (equation 2) caused by using dry deposition rates of one-half (line a) and twice (line b) that measured, as a function of sample volume (k = 1.0. µg ml^{-1}, d = 1.2 ng cm^{-3} hr^{-1})

Maps of median dry deposition rates for six elements (only soluble portions were measured during the 1972-1974 period) during the 1972-1974 period are given in figure D-71. Large areas of relatively large deposition rates occurred pver urban and industrial areas (St. Louis, East St. Louis, Granite City).for Li, Mg, Ca, and Zn. For Ca and Mg, smaller areas of comparable rates also occurred in rural areas. Na and K deposition rates were highly variable, with maxima of comparable magnitudes and areas occurring in both rural and urban areas. Except for isolated 'hot spots' the overall patterns of Ca and Mg dry deposition rates are quite similar, perhaps reflecting common sources.

It is important to note that measured dry deposition rates apply to deposition in collectors of a particular size, shape, and location, on dry summer days. The median value for any given site cannot necessarily be taken as representative of the surrounding area or of natural surfaces. Yet, the broad scale patterns, where similar rates are found at 5 to 10 or more contiguous collectors, appear to signify some real differences between rates in rural and urban areas. The higher rates in urban areas found for Li, Mg, Ca, and Zn also agree with patterns of concentrations of the same elements in air (Gatz, 1977); however, the same relationship did not occur with Na and K.

Maps of median dry deposition rates in the 1975 network are shown in figures D-72 (soluble portions) and D-73 (insoluble portions). Note that the 1975 data are medians from 5 daily samples, whereas the 1972-1974 data are medians of usually 3 times that many.

Comparison of measured dry deposition rates was made in the overlapping portion of the two networks of interest as an indication of how well measurements on 5 days (in 1975) represent mean conditions measured over many more days (1972-1974). Deposition in the 19 collectors in the overlapping portion of the two networks was compared in two ways for each of four elements. The first is the ratio of mean deposition rates in 1975 and 1972-1974. The second is the correla-

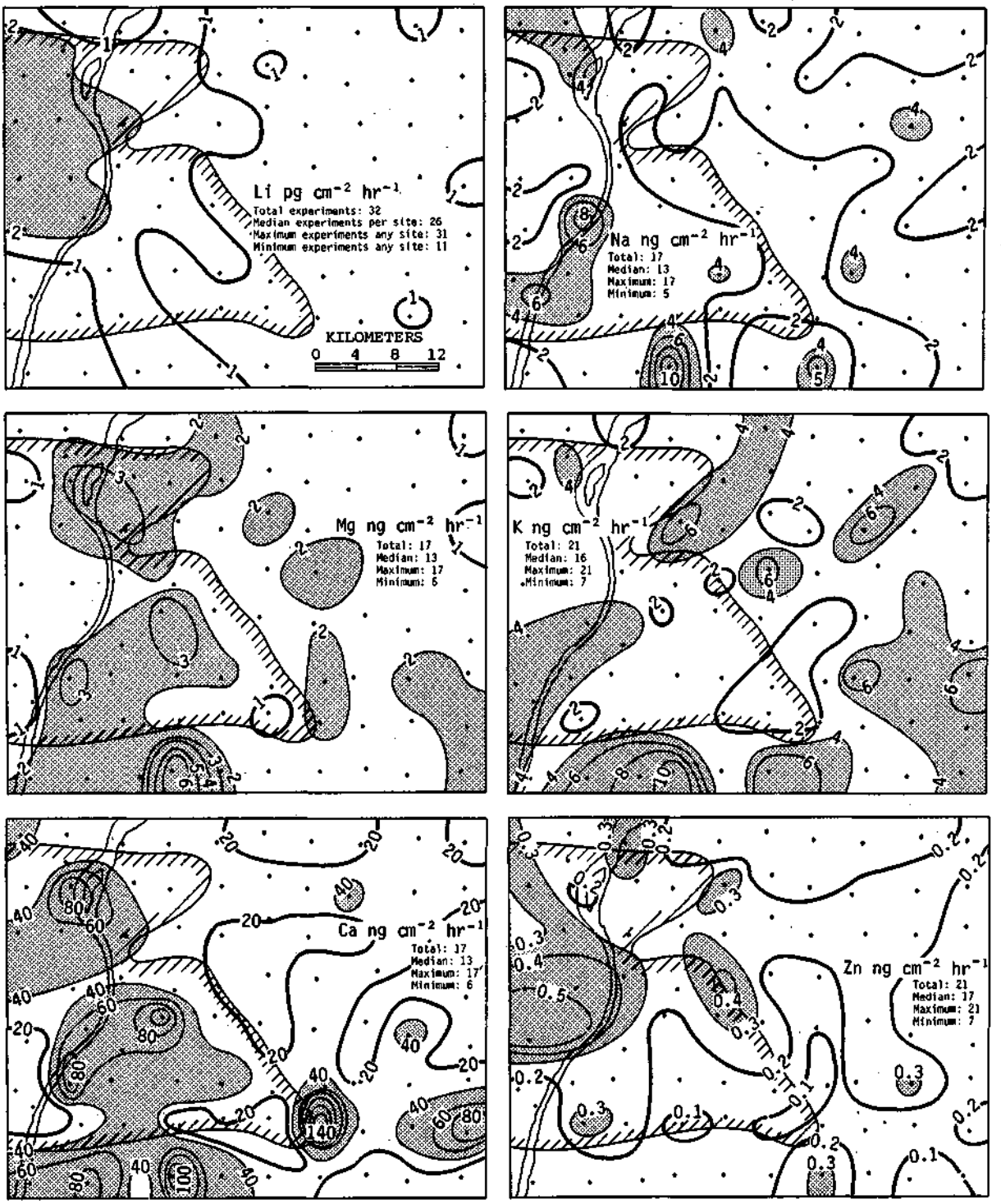

Figure D-71. Distribution of median dry deposition rates in 1972-1974 network (Higher rates are shaded for emphasis)

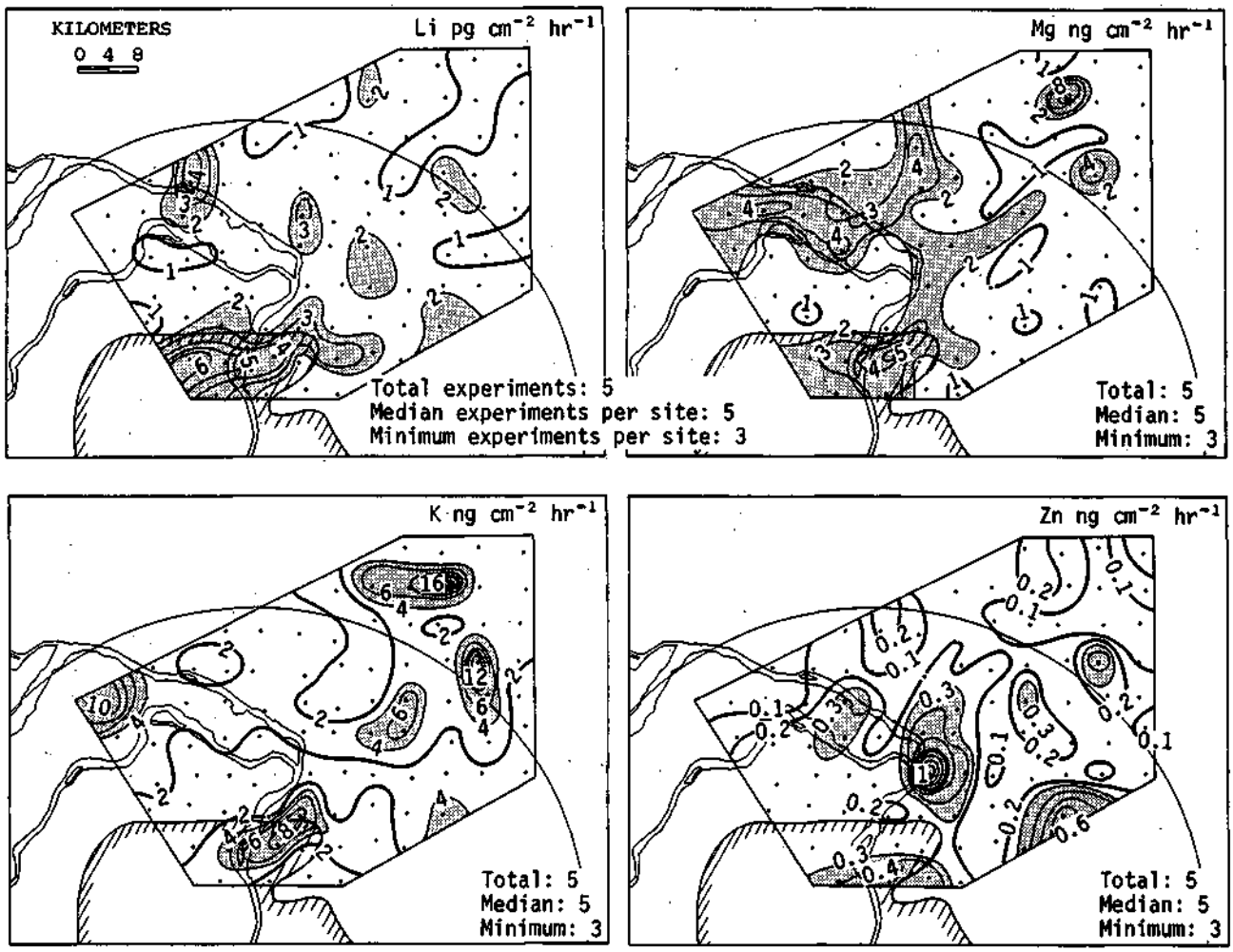

Figure D-72. Distribution of median dry deposition rates for soluble portions in 1975 network (Higher rates are shaded for emphasis)

tion coefficient. Calculated values of these parameters are shown in table D-34. Mean deposition rates in 1975 ranged from 84% greater for Li to 16% lower for K, compared with the 1972-1974 mean rates. Correlation medians at the respective sites between years were not strong, the largest value being 0.58 for Mg.

Another comparison of interest involves the relative patterns and magnitudes of soluble and insoluble dry deposition rates. This can be done for Li, K, and Zn over the entire 1975 network from figures D-72 and D-73 and table D-35. Soluble and insoluble Li show little correlation ($r = 0.06$); K shows a somewhat higher correlation ($r = 0.37$) mostly because of a few sites suspected of local contamination. Zn shows corresponding maxima in the Granite City and Wood River areas, but overall a rather small correlation ($r = 0.25$).

In terms of magnitudes of soluble and insoluble dry deposition rates, insoluble exceeds soluble Li by a factor of about 4 to 6 (table D-35). On the other hand, the deposition rate of soluble K is comparable or slightly larger than insoluble K, and the rate for soluble Zn is almost double that of insoluble Zn, based on 5 experiments in 1975.

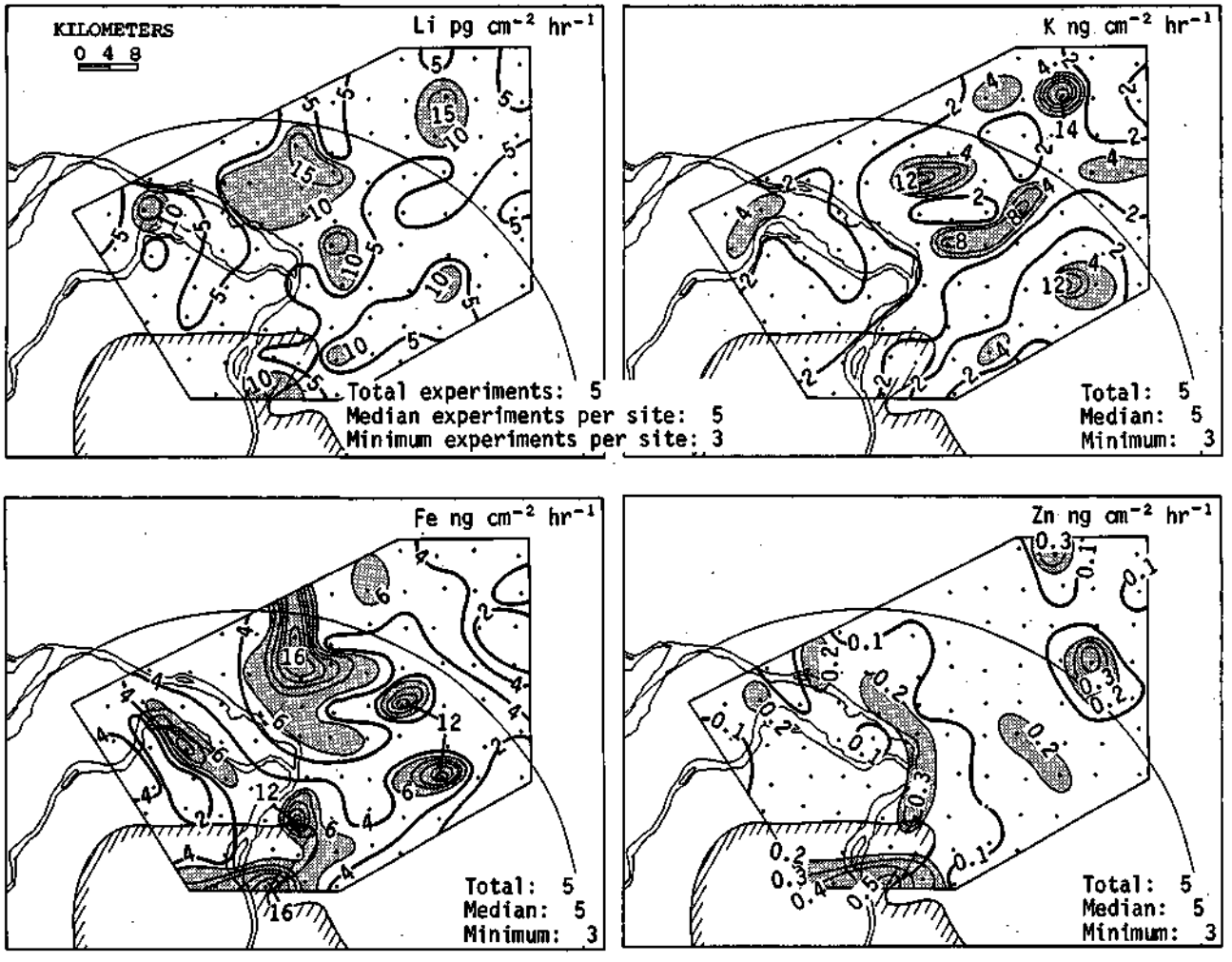

Figure D-73. Distribution of median dry deposition rates for insoluble portions in 1975 network (Higher rates are shaded for emphasis)

The question of the adequacy of 5 events for estimating average deposition over a network of 80 to 85 sites now becomes important. Can we depend on the comparison of soluble and insoluble deposition rates based on just 5 days?

An answer is suggested by comparing mean deposition rates from 5 days in the 1975 network with those obtained from many more events in the 1972-1974 network (table D-35). Comparisons between the two networks may be made for soluble Li, Mg, K, Ca, and Zn. The agreement is remarkably good. Differences between network means ranged from about 5% of their mean for Zn and Mg to 44% for Li, while Ca and K had intermediate values of 7 and 17%, respectively. This suggests that the 1975 average depositions are valid and thus permit valid comparisons of soluble and insoluble deposition rates.

It is possible to calculate deposition velocity, V_d, by the use of the results in table D-35 and airborne concentrations measured in the same area and reported elsewhere (Gatz, 1977). The deposition velocity is defined as

$$V_d = (d/_X)$$

Table D-34. Comparison of Dry Desposition Rates for Soluble Portions of Elements in the 19-Collector Overlapping Portion of the 1975 and 1972-1974 Networks

	Li	*Mg*	*K*	*Zn*
1975/1972-1974	1.84	1.12	0.84	1.30
r	0.48	0.58	0.18	-0.16

Table D-35. Measured Dry Deposition Rates at St. Louis*

*Network mean** dry deposition rate (g hectare' mo')*

	Soluble		*Insoluble*
	1972-1974	*1975*	*1975*
Li	0.080 ± 0.005	0.125 ± 0.008	0.495 ± 0.031
Na	193 ± 14		
Mg	140 ± 7	147 ± 10	
K	272 ± 16	230 ± 23	220 ± 22
Ca	2730 ± 230	2540 ± 240	
Fe			394 ± 38
Zn	16 ± 0.8	17 ±	9.5 ± 0.9

*** With the assumption that collections in polyethylene bottles may be applied to natural surfaces**

*** * Mean of the median rates at individual sites; uncertainties shown are standard errors of the mean**

where d is dry deposition rate (mass cm^{-2} s^{-1}) and x is concentration in air (mass cm^{-3}). Thus, V_d is a derived parameter having dimensions of velocity (cm s^{-1}). In this case the reference height for x is 1 to 2 m.

Results with various assumptions are shown in table D-36. These results are preliminary, and should be considered mean summer values over approximately 1900 km^2 for periods of a month or more. Despite their preliminary nature, the agreement of the V_d values for K and Zn between the 1972-1974 and the 1975 networks is striking, and suggests that the values are credible. The range of values observed is in general agreement with measurements of dry deposition on filter papers in the United Kingdom (Cawse, 1976) and there is a crude trend toward increasing values with increasing particle diameter, as observed by Cawse (1974,1975, 1976). For example, Zn is generally found on small particles (<1 μm diameter) and Ca on large (>2 µ m diameter).

Until now we have been comparing primarily mean values of various parameters between networks. In the following section we examine the variability of dry deposition rates within networks.

Areal Variability. The coefficient of variation (CV) is an index of the variability of the dry deposition rate over a network of samplers, and is defined by

CV = (standard deviation/mean) 100

Thus, it gives the deviation from the mean that should encompass about 68% of the observations from a normally distributed population. A summary of results for each element is shown in table D-37 for the 1972-1974 network, and table D-38 for the 1975 network. Means generally ranged from 100 to 150% in the 1972-1974 network, and 90 to 200% in the 1975 network. Minimums were generally between 50 and 60% in the 1972-1974 network, and somewhat higher in 1975. Maximum values were higher for the 1972-1974 network, with the highest value being 557% for Na.

Tables D-37 and D-38 show that variability over the network decreases sharply when median values over several events are considered, rather than single events. Comparison of the two tables

Table D-36. Summary of Mean Deposition Velocities

	Deposition velocity,* cm s^{-1}		
	1972-1974	1975	United Kingdom, 1975**
Li	1.69†		
Na	2.86‡		0.20–1.3
Mg	2.58‡		0.59–>3
K	4.07†	4.11	0.58–>2
Ca	5.25§	3.55	0.38–1.4
Zn	0.93†	1.14	0.28–0.99

* Concentrations in air were estimated from measurements of Gatz (1977)
** Range of values observed at inland stations by Cawse (1976), with filter paper as a collection substrate for dry depositon
† Assumes same ratio of total/soluble dry deposition as found in 1975 network
† Assumes aerosol is 65% soluble .
§ Assumes aerosol is 90% soluble

Table D-37. Summary of Coefficients of Variation (%) of the Dry Deposition Rate, 1972-1974 (Soluble Fractions)

	Li	Na	Mg	K	Ca	Zn
Number of cases	32	17	17	21	17	21
Individual cases						
Minimum	44	51	46	64	57	47
Median	120	106	88	126	114	99
Mean	135	148	107	139	109	130
Maximum	487	557	313	298	163	397
All cases	53	62	45	51	74	46

Table D-38. Summary of Coefficients of Variation (%) of the Dry Deposition Rate, 1975

	Li		Mg	K		Ca	Fe	Zn	
	S*	I*	S	S	I	S	I	S	I
Number of cases	5	5	5	5	5	5	5	5	5
Individual cases									
Minimum	72	64	64	182	107	97	91	89	118
Median	81	115	69	184	136	110	122	117	165
Mean	87	105	95	197	140	111	123	116	175
Maximum	102	138	178	220	170	134	150	163	265
All cases	62	58	65	94	93	88	88	67	86

* S = soluble fraction; I = insoluble fraction

shows considerable improvement over individual events even for medians from only 5 events, and even further improvement for 17 to 32 events.

The coefficient of variation of the dry depositon rate for a single experiment is a way of expressing the relative error to be expected if the deposition at a single collector were used as an estimate of the deposition over the whole network. It is also of interest to determine what errors would be expected from using more than one collector (but fewer than 80) to estimate the mean dry deposition rate over the network.

Results for 1-day sampling periods are shown in table D-39 in terms of the root mean square deviations (RMSD) divided by their respective mean dry deposition rates for the 1972-

Table D-39. RMS Deviations for 1-Day Sampling Periods, as Percent of 80-Collector Mean Dry Deposition Rates*

	Number of days	*Number of collectors in subnetwork* 40	20	10	5
Li	32	39	19	85	94
Na	17	132	386	118	132
Mg	17	29	17	102	66
K	21	65	117	68	169
Ca	17	16	19	45	90
Zn	21	22	19	115	141

• **Rates given in table D-35**

1974 network, as given table D-35. The RMSD is defined as

$$RMSD=[d_{80i}-d_{Xi})^2/N]^1/2$$

where d_{80i} is the mean dry deposition rate on day *i* from the 80-collector network, d_{Xi} is the mean dry deposition rate on day *i* from a smaller subnetwork, x = 40, 20, 10, or 5 collectors, and N is the number of days of sampling. The subnetworks used are shown in figure D-74.

The RMS deviations in table D-39 generally increase as the number of collectors decreases, but there are numerous exceptions where a smaller number of collectors gave better agreement

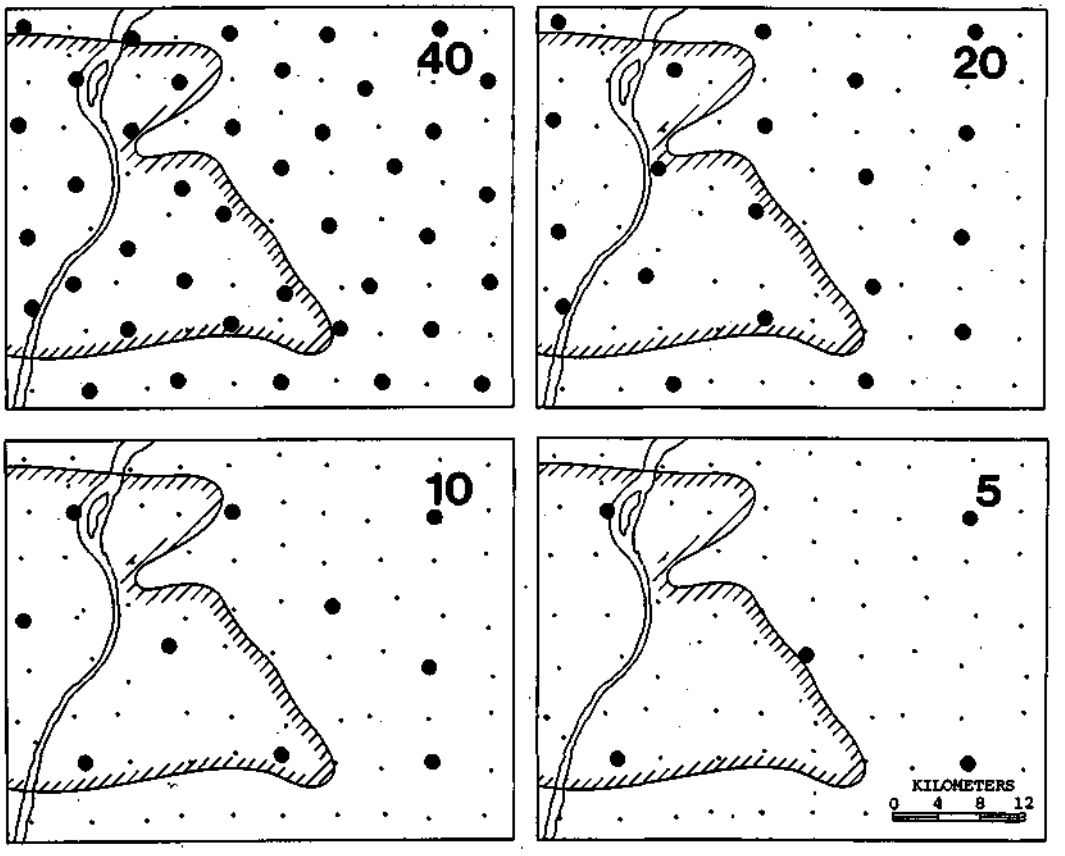

Figure D-74. Subnetworks used to compute results shown in figure D-78

Table D-40. Observed Deviations from 80-Collector Mean for Medians of All Data, as Percent of 80-Collector Mean Dry Deposition Rates*

	Number of collectors in subnetwork			
	40	*20*	*10*	*5*
Li	2.3	4.9	9.0	1.0
Na	3.2	2.4	5.3	9.5
Mg	4.9	1.3	13.2	10.1
K	3.7	2.8	8.5	2.1
Ca	8.4	7.9	30.5	13.0
Zn	5.0	2.3	10.9	7.7

*** Rates given in table D-35**

with the 80-collector mean than a larger number. This illustrates the extremely variable character of dry deposition rates on a daily basis, and shows the difficulty of measuring a daily areal mean value even with a dense network.

Measuring an areal mean over approximately a month can be done with considerably more accuracy, as indicated by the results in table D-40. To obtain these values, median dry deposition rates were determined for each site in the network with data for all available days, as given in table D-39. Network means of these medians were then determined for 80, 4.0, 20, 10, and 5 collectors, with the same subnetworks as before (figure D-74). The values in table D-40 are relative deviations from the 80-collector mean for each of the subnetworks.

Again, accuracy generally decreases as the number of collectors decreases, but again there are many exceptions. However, the observed deviations are with one exception all less than 15% which suggests that monthly mean dry deposition rates over approximately 1900 km^2 may be determined quite accurately with not more than 20 collectors, while daily areal means, even with 80 collectors, would be somewhat uncertain.

Wet Deposition

Information on deposition of elements in rain is presented in two ways. The distributions of median wet deposition values (mass cm^{-2}), are shown in figure D-75, while the same results normalized to the network means of each element are shown in figure D-76 along with normalized rainfall data.

In figure D-75, all six elements show major deposition maxima in or near urban areas. For most of the six, high deposition values also appear at rural locations. For some elements these maxima occur mostly at single sites, suggesting local sources, but large rural areas of high deposition are seen for K and Ca. Five of the six (Li, Na, K, Ca, and Zn) also had large areas of very low values over the city of St. Louis.

The relative amounts of the several elements deposited in rain is clearly seen by comparing their respective network mean depositions (figure D-75). Of the six elements shown, Ca deposition was by far the greatest, about 10 times that of K, the next highest element. K and Na depositions were about equal, and about twice that of Mg, which was about 15 times the Zn deposition. Zn, in turn, was about 70 times the Li deposition.

Maps of median element deposition, normalized to network means, appear in figure D-76, together with maps of normalized rainfall. Three different rainfall maps appear in the figure, each matching the elements accompanying it with respect to the days included in the analysis.

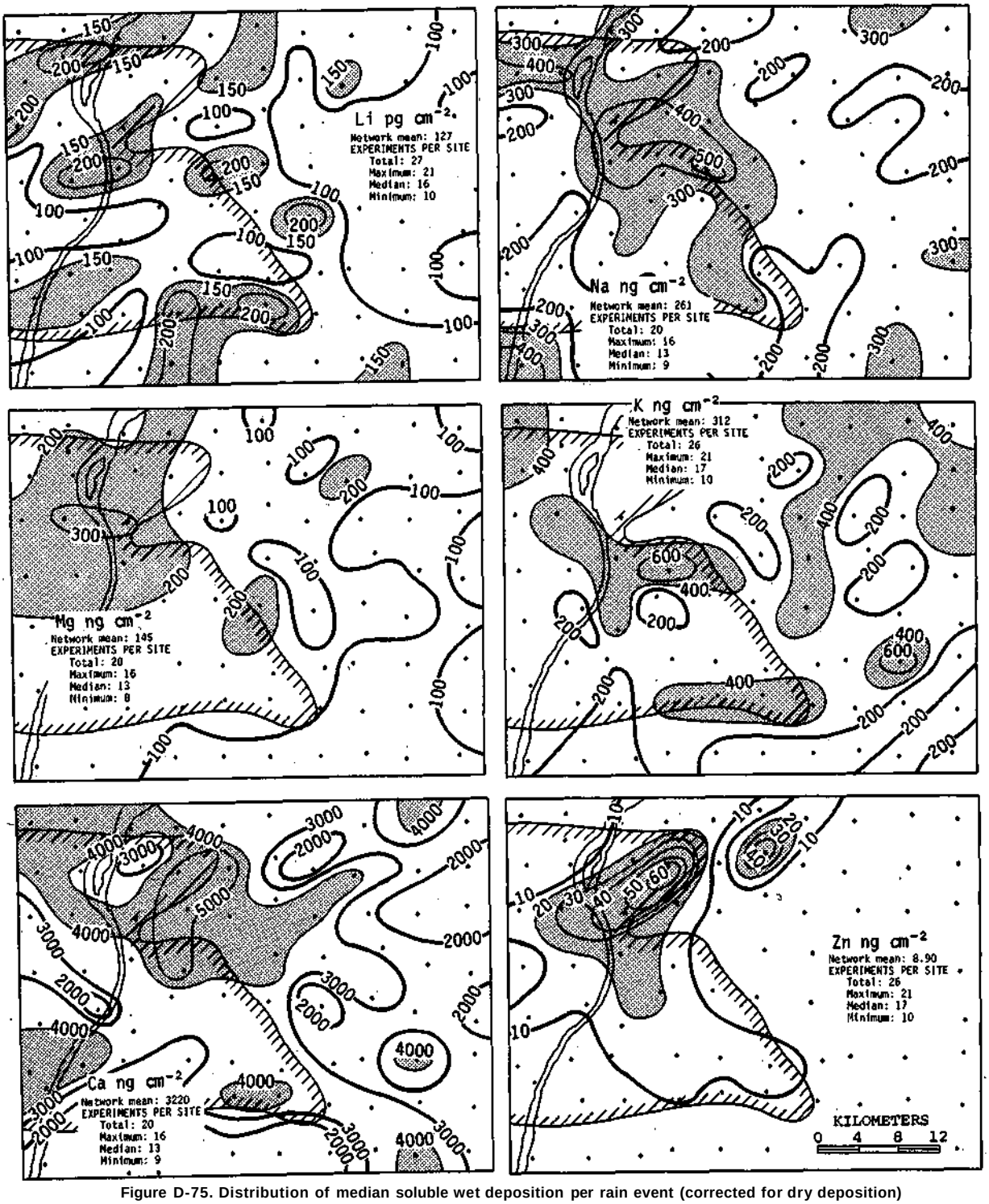

Figure D-75. Distribution of median soluble wet deposition per rain event (corrected for dry deposition) in the 1972-1974 network (Higher values are shaded for emphasis)

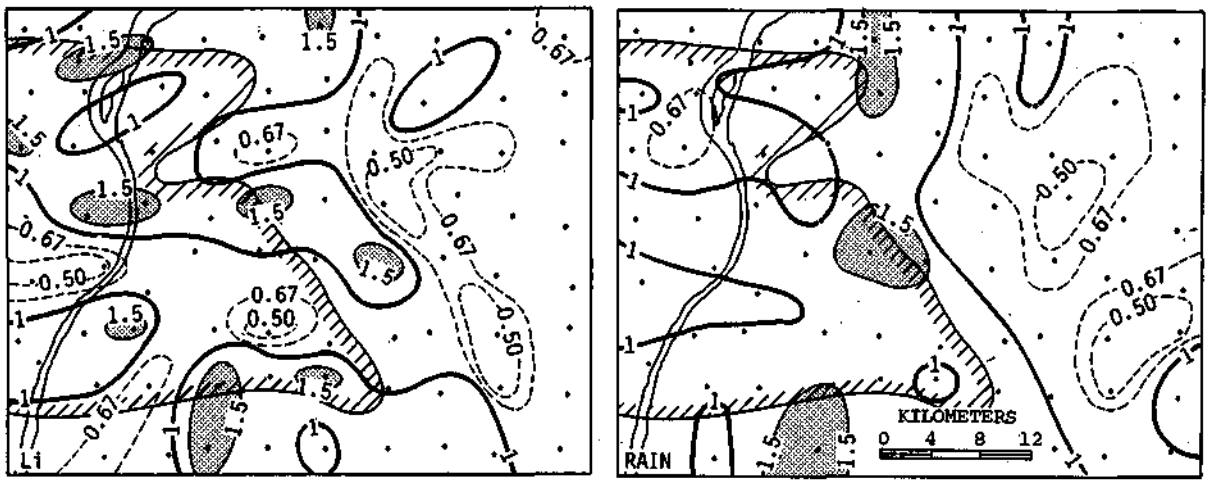

a. NON-TRACER Li DEPOSITION AND RAINFALL FOR THE SAME EVENTS

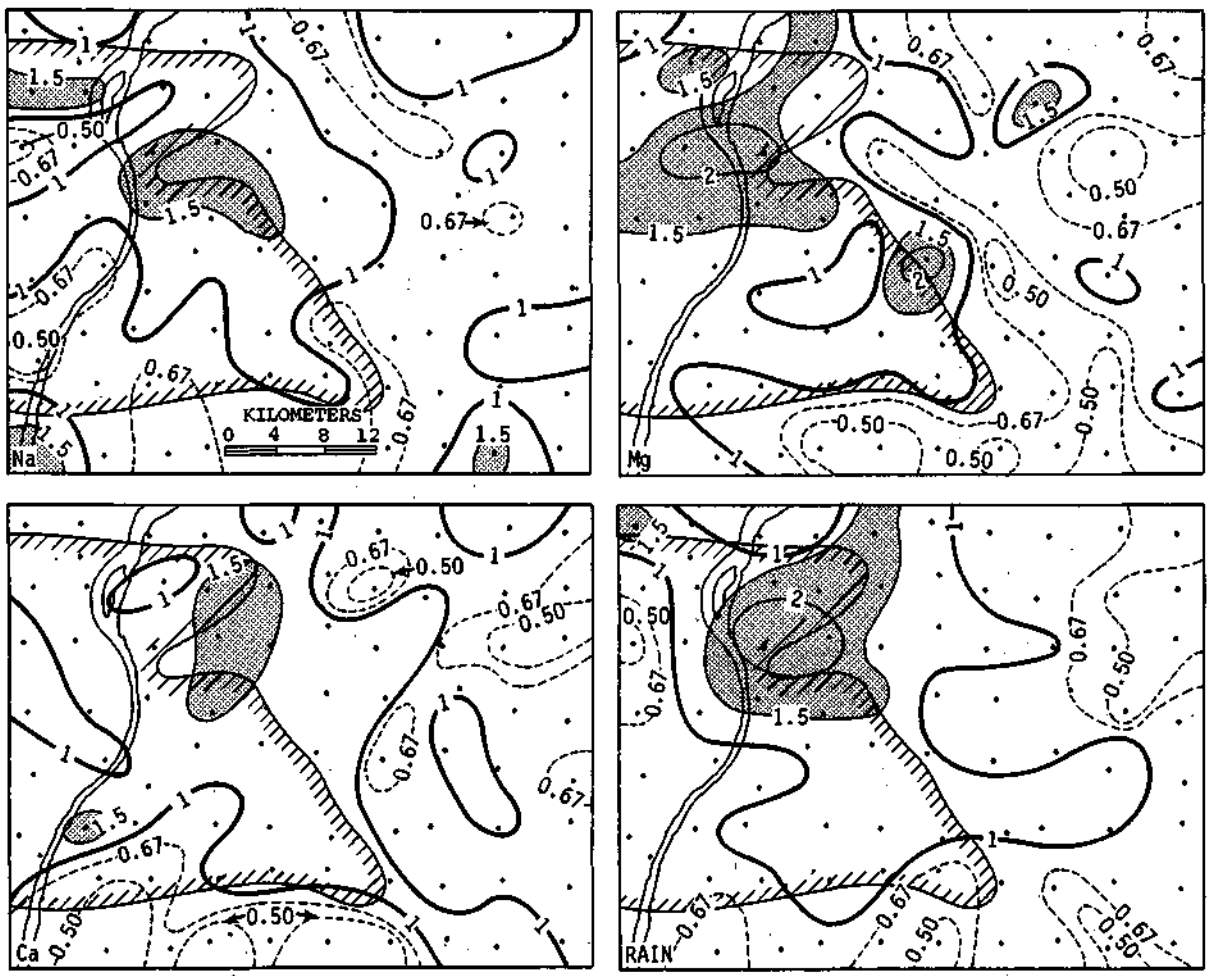

b. Na, Mg, Ca DEPOSITION AND RAINFALL FOR THE SAME EVENTS

Figure D-76. Same data as figure D-75, except each element has been normalized to its network mean value (Values above 1.5 are shaded for emphasis)

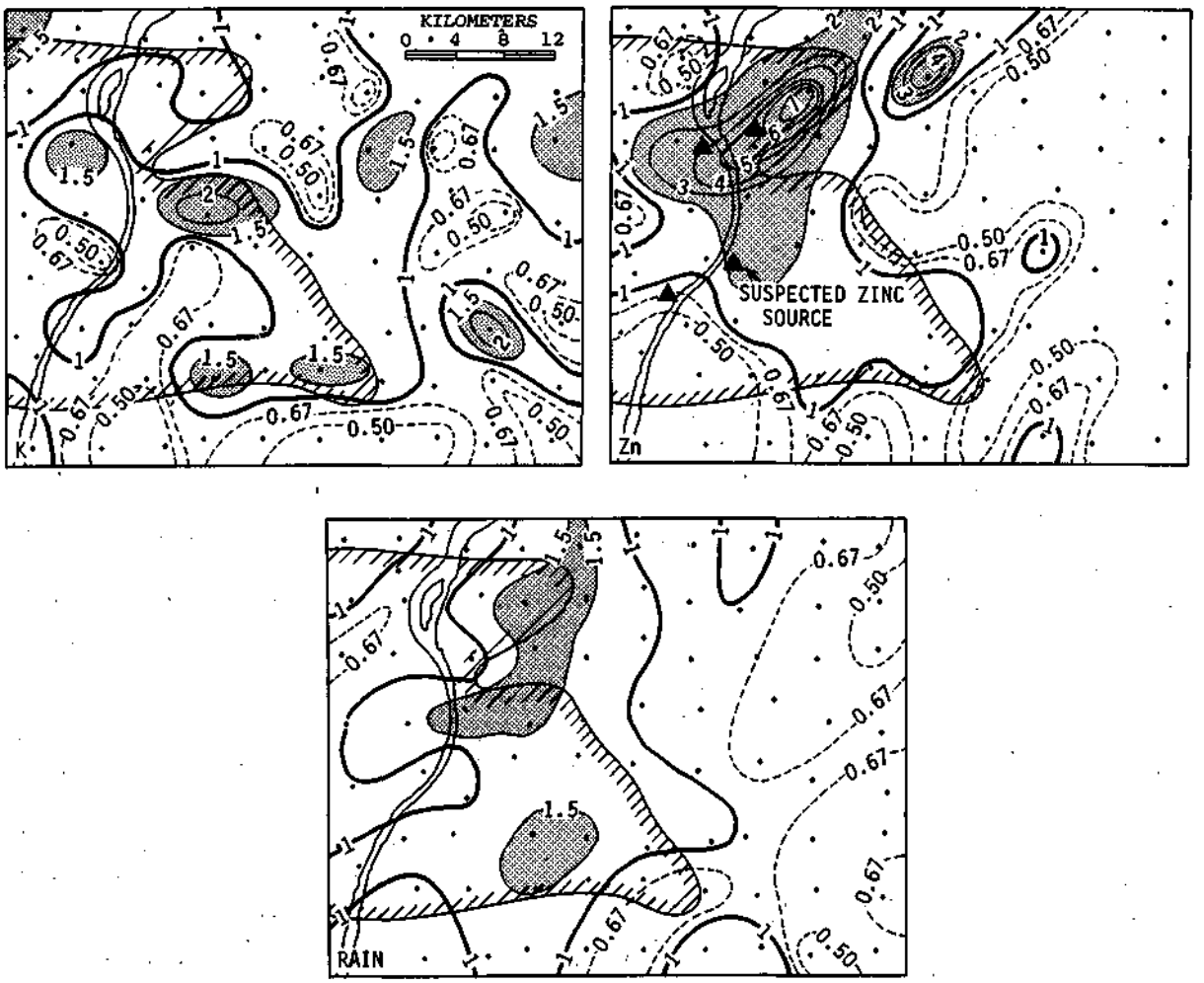

c. K, Zn DEPOSITION AND RAINFALL FOR THE SAME EVENTS

Figure D-76. Concluded

For example, the normalized rain map in figure D-76b was constructed from rainfall data from the same rain events analyzed for Na, Mg, and Ca.

Since element deposition is the product of element concentration in rain and rainfall amount, element deposition should be strongly influenced by rainfall. Thus, element deposition should always be considered in relation to rainfall. The best way to do this is to normalize element deposition and rainfall to network means, so that the maps to be compared will have identical units. Non-normalized data would have dissimilar units and the isopleths chosen for analysis could not be identical, except in rare cases.

Figure D-76a compares normalized depositions of Li and rain for non-tracer events. Values over 1 generally occurred in the western half of the network for both parameters. Also for both, values at several sites exceeded 1.5, but none exceeded 2.0. This suggests that mean deposition of background Li over many events (in this case, 27) depends primarily on rainfall; no strong local sources are indicated.

Figure D-76b compares rainfall with Na, Mg, and Ca deposition for 20 events, again on a normalized basis. Speaking generally, values greater than 1.0 occurred in the northwest quadrant of the network, and values less than 1.0 occurred along the southern and eastern borders, on all four maps. Maxima of Ca and Na deposition (values > 1.5) occurred in the same area near Granite City as the maximum rainfall deposition. The area of maximum Mg deposition was near, but enough westward of the rainfall maximum, to suggest the possibility of a local Mg source. The size of the Mg deposition maximum, and its location over urban and industrial areas, suggests that such a source would be dispersed throughout the urban area, rather than a single point source.

Figure D-76c compares normalized K, Zn, and rain deposition in 26 events. Three totally different patterns occurred. The rainfall maximum extended along a north-south axis parallel to, and east of, the Mississippi River. A very irregular pattern of K deposition was observed, with high values throughout the network, mostly covering only single sites. This pattern is consistent with a widely distributed source of K such as soil and fertilizer.

Zn, on the other hand, shows a strong deposition maximum over the Granite City industrial area, and a secondary maximum several km to the east. This strongly suggests local sources, and several are known to be present in the East St. Louis industrial area, as shown in the Zn deposition map.

Soluble Ca and Mg depositions are expected to be affected to some extent by partial dissolution of insoluble materials prior to filtration (Peden and Skowron, 1978), but the magnitude of this effect on these samples is not known.

The relationship between rainfall and element deposition is explored further in figure D-77, which shows the total mass of element deposited during an event, plotted against the total rain deposited. For each element there is a considerable scatter in the points, but always a definite trend of increasing deposition with increasing rainfall. The straight lines drawn on each graph are the least squares linear regression lines. Each is labeled with the correlation coefficient between rain deposition and element deposition.

The graph for Li shows results from tracer experiments and results from rains when no tracer was released. Both groups show considerable scatter, particularly the tracer experiment data. Separate least squares regression lines are shown for both groups. The line for the tracer experiment data would at first glance suggest a greater deposition of Li during tracer experiments than in non-tracer rains. Three tracer experiments in particular deposited considerably more Li in relation to their total rainfall than the other experiments. These experiments are labeled 120, 130, and 135. One is immediately tempted to attribute the higher Li deposition in these storms to the extra Li released as tracer, but a brief consideration of the relative masses shows that this cannot be the entire reason. The mass of tracer released in each experiment is shown by the length of the bar plotted next to each point. The amounts released in all three cases were less than 1 kg, whereas the difference between the observed deposition and that expected in a comparable non-tracer rain is much more than 1 kg in each case.

Perhaps a comparison with the deposition of other elements in the same experiments will give a clue to the unusually strong source of Li in these experiments. The points corresponding to these three experiments have been labeled on the graphs of the other elements in figure D-77 to permit comparison. The points for experiments 120 and 135 are to the right of the regression line for Na, Mg, K, and Ca, which shows unusually high deposition for the observed rainfall for all of these elements.

In experiment 120, 60% more Li was deposited than 'expected' where the expected value is taken from the regression line for non-tracer rains at the observed rainfall. Mg and Ca

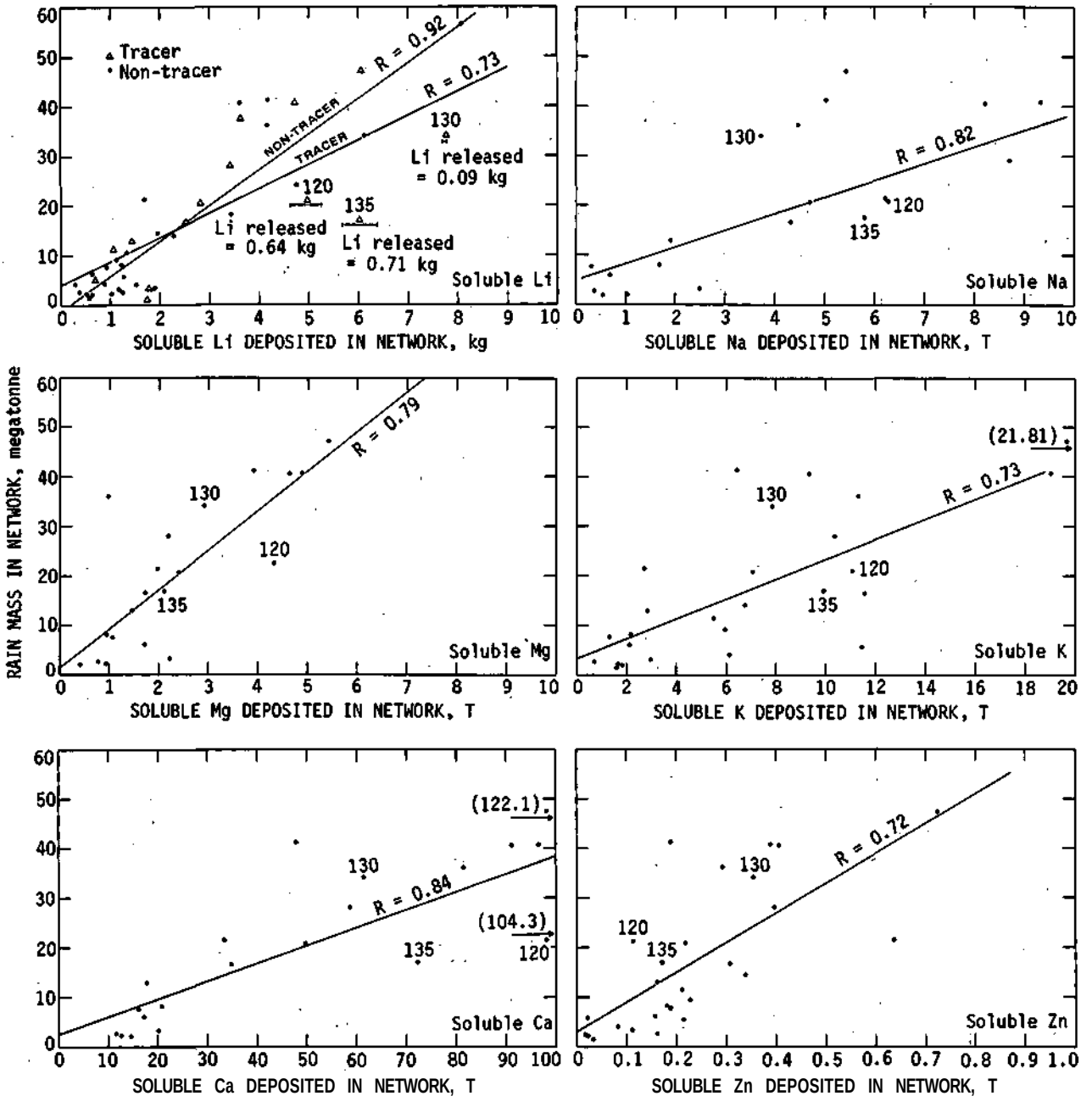

Figure D-77. Total network rainfall deposition vs total network element deposition

excess depositions in experiment 120 were even larger, at *66%* and 100%, respectively. In experiment 135, 136% more Li was deposited than expected. No other element was deposited in such a large excess over its expected value in that experiment, but Ca had the highest excess, at 78%. Thus, the source of the unusual Li deposition in experiments 120 and 135 may be linked to that of Ca, and perhaps Mg. Cement plants, limestone quarries, gravel roads, and soil dust are prominent sources of Ca and Mg. These are apparently not the Li source in experiment 130, however.

Areal Variability. The variability of elemental wet deposition and the accompanying rainfall may be expressed in several different ways. We begin our discussion of areal variability in terms of the coefficient of variation (CV). Results for 1972-1974 are shown in table D-41. Mean values of daily network medians range between 90 and 150, except for soluble Zn at 195. Similar mean values of the CV were also observed for dry deposition rate (tables D-37 and D-38). Maximum values for the various elements on any day ranged generally from 160 to about 280, except for Zn, which again was higher. Similar maximums were observed for dry deposition in the 1972-1974 network, although the 1975 maximums were slightly smaller (table D-38). Wet deposition minimum CV's were generally between 30 and 60, which is in good agreement with those for dry deposition in the same network. Minimums for rainfall and Zn were lower and higher, respectively, than this range.

Coefficients of variations for rainfall are consistently smaller than those for the element wet deposition (table D-41). The maximum value for rainfall CV, 148%, was smaller than all the maximum values for the elements. The mean CV for rainfall is also smaller than any of the element means.

Here again, the coefficients of variation based on long-term median elemental deposition values at each site (14-27 rain events) are sharply lower than the values for individual days. This shows that the accuracy with which the areal mean wet deposition may be estimated by a single site increases as the time period of the estimate (or the number of rain events) increases.

For single events, a single site would be in error by about 100 to 150% in estimating an areal mean over 1900 km^2 about 68% of the time. On the other hand, a single site would estimate the areal mean elemental deposition over 14 to 27 events in the summer within about 50% (except for Zn) about 68% of the time. The Zn estimate would be within 125% about 68% of the time.

Errors in estimates of network wet deposition from subnetworks of 40, 20, 10, and 5 collectors are given in figure D-78a for individual days and in figure D-78b for medians of all available days.

The results in figure D-78a show a generally increasing error as the number of collectors used in the estimate decreases. Except for 1) the tracer Li cases, 2) Zn, and 3) rainfall, the results

Table D-41. Summary of Coefficients of Variation (%) for Soluble Wet Deposition, 1972-1974

		Li						
	Rainfall	*Non-tracer*	*Tracer*	*Na*	*Mg*	*K*	*Ca*	*Zn*
Number of days	41	27	14	20	20	26	20	26
Individual days								
Minimum	17	37	30	56	58	54	50	105
Median	89	101	94	84	92	126	88	176
Mean	88	112	125	98	100	147	92	195
Maximum	148	224	279	193	222	281	160	494
All days	31	38	43	32	44	46	35	125

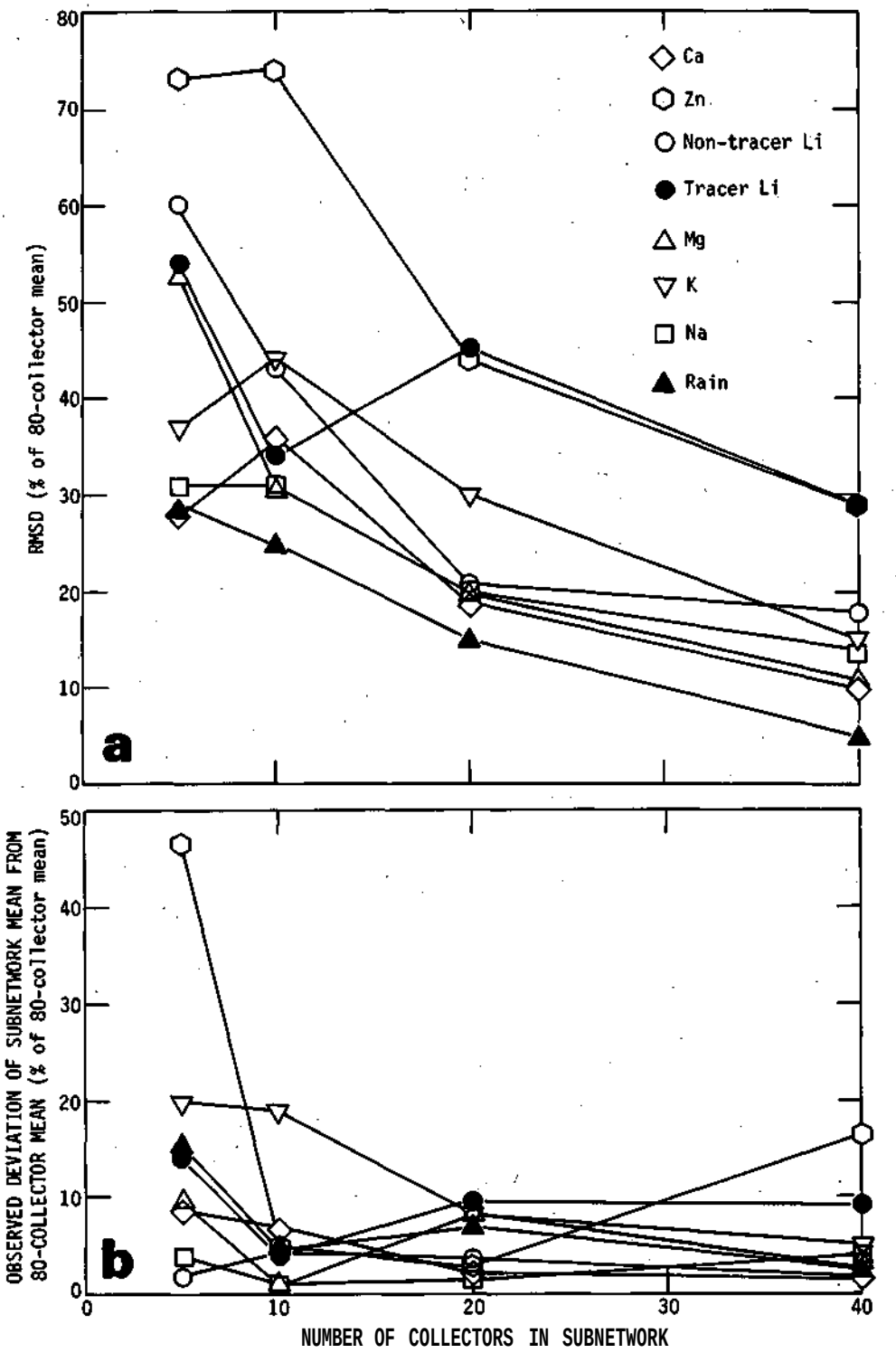

Figure D-78. Deviations of mean wet deposition from 80-collector mean for subnetworks [a) RMS deviations for individual days, b) observed deviations, for medians of all available data]

are quite uniform, showing a RMSD uncertainty (relative to the 80-collector total) between 10 and 20% for 40 collectors, rising to 15 to 30% for 20 collectors, to 25 to 45% at 10 collectors, and to 30 to 55% for 5 collectors. Daily rainfall may be estimated with generally more accuracy than element deposition for a given number of gages. However, deposition of an element with known local sources (Zn) is estimated more poorly than those with more uniformly distributed sources. Li deposition in tracer experiments was also estimated with greater uncertainty than most other elements. It is consistent with the Zn results to suspect that this may have been caused by deposition of tracer over limited local areas, but proof is lacking.

Figure D-78b shows deviations from the mean 80-collector deposition computed from the median wet deposition maps (figure D-75) for the same sets of 40, 20, 10, and 5 collectors. As expected, the deviations were generally smaller, element for element, for the long-term medians than for individual days (figure D-78a). As before, Zn exhibited relatively large deviations, especially for 40 and 5 collectors. However, rainfall was not any better estimated than element deposition by the reduced-density networks.

Comparison of Soluble Wet and Dry Depositions

Network mean dry deposition rates for soluble fractions of elements in the 1972-1974 network were presented in table D-35 in units of g hectare^{-1} mo^{-1}. It is possible to estimate approximate rates of wet deposition in the same units to compare the relative importance of wet and dry deposition in the 1972-1974 precipitation chemistry network. Huff (1977a) gave the mean 5-year summer (June to August) rainfall in the research circle as 121 cm. This is equivalent to 24.2 cm per summer.

In the precipitation chemistry network we observed a mean rainfall of 1.04 cm per rain day. Dividing this figure into the mean summer rainfall we get 23 rain days for summer, or about 8 rain days per month.

Network mean wet soluble depositions per rain day for the six elements were given in figure D-75. These values were multiplied by 8 to get approximate monthly depositions and the units were converted to g hectare^{-1} mo^{-1} to be the same as the dry deposition rates. The comparison is given in table D-42. Absolute deposition rates varied markedly, reflecting differences in concentrations of the airborne materials; however, the relative rates of wet and dry deposition are remarkably constant. Dry deposition accounts for 44 to *69%* of the total.

Table D-42. Comparison of Monthly Mean Wet and Dry Deposition for Soluble Fractions of Six Elements, 1972-1974

Deposition rate (g hectare' mo')

	Dry	Wet	% Dry
Li	0.080	0.10	44
Na	190	210	48
Mg	140	120	54
K	270	250	53
Ca	2700	2600	51
Zn	16	7.1	69

DISCUSSION

Dry Deposition

The main purpose for collecting and analyzing dry samples was to obtain values of dry deposition rate at each sampling site for use in correcting precipitation samples. Replicate samples were collected in lined and unlined collection bottles to test for differences in dry deposition rates to the sampler configurations used in different years. No significant differences between collectors were found, but the results (figure D-68) show that large day-to-day variations occur. This large variability extends to comparisons of mean deposition rate in the overlapping portion of the 1972-1974 and 1975 networks, but network mean dry deposition rates for the soluble portions of four elements on 5 days in 1975 agreed very well with those from the 1972-1974 network.

Net wet deposition was found to be relatively insensitive to variations in dry deposition rate. Thus, median dry deposition rates, calculated from 13 to 26 dry days in the 1972-1974 network, and from 5 days in the 1975 network, were used to correct wet samples.

Many sampling sites were subject to occasional contamination from local dust sources, usually roads. Yet, the patterns of median dry deposition rate suggest that observed differences between urban and rural locations are indeed real, because many areas of relatively high or low deposition rates include several collection sites.

High urban dry deposition rates for most elements are consistent with observations of higher concentrations of the same elements in urban air. High deposition rates of Ca, Mg, Na, and K were also measured in rural areas, but the high rural rates were often confined to smaller areas.

Soluble and insoluble portions of dry-deposited Li, K, and Zn were always found to have dissimilar deposition patterns, suggesting distinctly different sources for soluble materials, as opposed to insoluble. Li was about 80% insoluble, Zn was about 65% soluble, and K was about evenly divided between soluble and insoluble.

Even though the relationship between dry deposition to plastic bottles and to natural surfaces is not known, it is of some interest to extrapolate the measured dry deposition rates on the assumption that the two are approximately the same or related in some simple way. Even if these assumptions are not true, useful results may still be obtained in a relative sense, i.e., for one element relative to another, as long as their particle size distributions are similar. Mean dry deposition rates in the two networks were found to agree quite closely. Furthermore, computed deposition velocities for the two networks agreed well with each other and reasonably well with those measured in the United Kingdom where the dry deposit was collected on filter papers shielded from precipitation.

If dry deposition measurements in wide mouth plastic bottles are useful measurements of dry deposition, it is well to examine the relationship between measurements over an 80-collector network, and those at a single site, or at some larger fraction of the 80 sites.

For a single site, the coefficient of variation gives the percent difference from the 80-collector mean deposition rate that should not be exceeded 68% of the time. Table D-37 and D-38 showed that median values of the coefficient of variation on individual days range from 100 to 200%, while values for 5 days combined (1975 network) drop further to 45 to 74%. Thus, the error in estimating the mean deposition rate in an 80-collector network from a single measurement decreases as the number of events increases. In the same way, estimate of the 80-collector mean generally improved for any given number of events as the number of collectors increased from 5 to 40. Occasionally, however, the 5-collector or 10-collector estimate of the 80-collector mean was better than those from 20 to 40 collectors. This reflects the highly variable nature of

the dry deposition rate field and the particular choice of collectors used for the estimate. Obviously, a different choice of collectors would have given somewhat different results. Nevertheless, the sites chosen represented a reasonable distribution of collectors over the area of the network, and the results indicate the degree of variability that occurred.

Wet Deposition

Wet deposition samples were collected and analyzed to measure the mass of various elements deposited, and their distribution, over a 1900 km^2 network near an urban area. To evaluate the accuracy with which deposition over the area can be measured for a single event or a combination of many events, it is necessary to know the uncertainty of an individual measurement.

This was evaluated by collecting and analyzing replicate samples at a single site. Both lined and unlined collectors were evaluated. Pooled variances were found not significantly different between the two types of collectors.

However, variances were found to be surprisingly large under field conditions compared with a similar experiment under more controlled conditions on the roof of the Water Survey building. This shows that the reproducibility of an individual observation should always be evaluated under typical field conditions so results can be properly interpreted. It is not sufficient to do the experiment under conditions not representative of actual field conditions.

Even with the observed large uncertainty of an individual measurement, the standard error of the mean network wet deposition for a daily sample is 10 to 15%.

Evaluation of maps of median wet deposition per day showed that for most elements maximum deposition occurred near urban or industrial areas, which also happened to be the location of the maximum rainfall. Deposition of these elements, all of which have widely distributed sources, appeared to be generally proportional to rainfall. Another pattern was found in the case of Zn, however. A local maximum, clearly in excess of that expected from rainfall alone, was found near known Zn sources.

Further investigation of the relationship between element deposition and rainfall, both integrated over the entire network for each storm separately, also shows network deposition generally increasing with network rainfall, but with a considerable scatter in the points. Evidently the airborne concentration of the element and meteorological conditions vary enough from day to day that the relationship between network rainfall and deposition is not a simple proportionality.

For soluble Li, the regression line relating total rainfall and total deposition in the network was slightly different on days when tracer was released from the line on days when no tracer was released. The difference in linear regression lines was caused principally by three days on which Li deposition was far in excess of that expected on non-tracer days for the same rainfall. The excess mass deposited was more than could be accounted for by the released tracer material. Similarities in deposition of Li and Ca on two of the three unusual days suggests that perhaps some insoluble Li dissolved in the samples prior to analysis. This seems feasible because Li was found to be 80% insoluble in dry deposition samples.

The areal variability of wet deposition is somewhat less than that of dry deposition rates. From the calculated coefficients of variation in individual experiments, use of a single site to estimate the network mean deposition would result in errors of up to 150% for most elements, and up to 200% for Zn, about 68% of the time. A single site would estimate the netwo'rk mean over 14 to 27 days within 45% (except for Zn) about 68% of the time. Mean network rainfall estimates would be somewhat better than element deposition estimates for single days, but not for long periods.

Smaller errors would be made if more than one site was used. On individual experiments, 5 collectors produce errors of less than about 30 to 55% about 68% of the time for most elements, and 10 collectors reduce the same errors to 25 to 45%. From 20 collectors the same errors are reduced still further, 15 to 30%, and for 40 collectors even further, to 10 to 20%. Elements that have local sources, such as Zn, have greater errors, and rainfall has smaller errors, for individual days.

Errors (relative to the 80-collector mean) in estimates of mean deposition over multiple events made by using 5,10, 20, or 40 collectors were considerably less than for individual events. The errors made (at 68% confidence) ranged generally from 10 to 30% for 5 collectors, dropped to less than 25% for 10 collectors, dropped to less than 5% for 20 collectors, and to almost 0 for 40 collectors. Zn still exhibited generally larger errors, but rainfall was not estimated any better than element deposition over multiple events.

If dry deposition in rain collectors can be taken as representative of natural surfaces for the elements studied, and if certain assumptions are valid, dry deposition represents 44 to 69% of the total deposition in the 1972-1974 network.

SUMMARY AND CONCLUSIONS

Wet and dry deposition of elements having natural and anthropogenic sources were measured over the St. Louis area. This section has reported and compared mean values and the areal variability of wet and dry deposition over the sampling networks. Areal variability was interpreted in terms of the deviations from the mean depositions measured from all 80 collectors, for subnetworks of 40, 20,10, and 5 arbitrarily chosen collectors. In addition, the error in estimating a network mean value to be expected from using a single collector chosen at random was evaluated.

Dry deposition rates were the same in lined and unlined collectors.

Large day-to-day and site-to-site variability in dry deposition rate was observed, but network mean values for 5 days in 1975 agreed very well with those from many more days in the 1972-1974 network.

Soluble and insoluble portions of dry-deposited materials have very dissimilar deposition patterns, suggesting different sources. Although the relationship between deposition to natural surfaces and to plastic bottles is not known, deposition velocities with plastic bottle collectors at St. Louis were found to be somewhat larger than, but still in reasonable agreement with, those measured on filter papers in the United Kingdom.

Use of a single site to estimate the 80-collector mean dry deposition rate resulted in an error that decreases as the time period of the estimate increases. For a single day, errors of 100 to 200% occurred about 68% of time. For deposition integrated over approximately 1 summer month, observed deviations from the 80-collector mean ranged from 45 to 75%.

Increasing the number of collectors to estimate the 80-collector mean also gave better results. For a single day, errors of less than 65 to 170% occurred 68% of the time with 5 collectors. This range dropped to 16 to 132% for 40 collectors. For a time period approximating a summer month, 5 collectors were able to approximate the mean of 80 collectors within about 10% and 40 collectors were mostly within 5%.

Evaluation of the uncertainty of an individual wet deposition observation must be done under realistic field conditions. Such an evaluation in this work showed relatively large uncertainties for individual samples; still, network mean values were known within 10 to 15% (68% confidence) based on 80 collectors.

Maximum deposition of both elements and rain occurred near urban-industrial areas. For most elements overall deposition was proportional to rainfall. However, Zn deposition was much greater than expected from rainfall in a local area northeast of a number of Zn sources.

As with dry deposition, single-site estimates of 80-site mean wet deposition improved as the time period of the estimate increased.

For single days, the 68% confidence errors were as large as 150% (200% for Zn), but over 14 to 27 days the same error was about 50%. Better estimates were obtained when more collectors were used. On individual days, 5 collectors yielded errors (68% confidence) of 30 to 55%, while for 40 collectors the same error was 10 to 20%. For a time period approximating the summer season, 5 collectors were within 10 to 30% of the 80-collector mean, while the deviation for 40 collectors was less than 1%.

A preliminary comparison of overall mean rates of dry and wet deposition in the St. Louis area during the summer suggests that dry deposition accounts for 44 to 69% of the total deposition of the elements studied.

The results reported here took considerable time and effort, and yet represent only the , summer (convective rainfall) season at a midwestern U. S. location. Information is also needed for other seasons (precipitation types), for other locations, for larger areas, and for other constituents, so that the uncertainties associated with atmospheric deposition over areas of various sizes can be better understood.

REFERENCES IN PART D

Ackerman, B. 1974a. *The partition of liquid water near the freezing level.* Preprint Conference on Cloud Physics, Tucson, AMS Boston, pp. 300-304.

Ackerman, B. 1974b. *METROMEX: Wind fields over St. Louis in undistrubed weather.* Bulletin American Meteorological Society v. 55:93-95.

'Ackerman, B., and H. Appleman. 1974. *Boundary layer program. In* Interim Report of METROMEX Studies: 1971-1973, F. A. Huff, editor, NSF Grant Gi-38317, pp. 121-142.

Aoki, M., and K. Yabuki. 1975. *Artificial clouds induced by combustion.* Weather, pp. 182-188.

Auer, A. H., Jr. 1976. *Observations of an industrial cumulus.* Journal Applied Meteorology, v. 15(4):406-413.

Auer, A. H., Jr., and R. A. Dirks. 197.3. *Interim progress report project METROMEX.* Report to Environmental Protection Agency, Grant R-800875, 68 p.

Auer, A. H., Jr., and R. A. Dirks. 1974. *Contributions to an urban meteorological study: METROMEX.* Bulletin American Meteorological Society v. 55:106-110.

Auer, A. H., Jr. and F. D. Eaton. 1976. Final Report to the National Science Foundation, Research Applied Directorate Weather Modification Association Grant AEN-76-00898. Department of Atmospheric Science, College of Engineering, University of Wyoming, Laramie, 39 p.

Barber, R. R., A. Martin, J. G. Shepard, and G. Spurr. 1974. *The persistence of plumes from natural draft cooling towers.* Atmospheric Environment v. 8:407-418.

Beard, K. V. 1976. *Terminal velocity and shape of cloud and precipitation drops aloft.* Journal Atmospheric Sciences v. 33:851-864.

Beard, K. V. 1977. *Terminal velocity adjustment for cloud and precipitation drops aloft.* Journal Atmospheric Sciences v. 34:1293-1298.

Beard, K. V.,.and S. N. Grover. 1974. *Numerical collision efficiencies of small raindrops colliding with micron size particles.* Journal Atmospheric Sciences v. 31:543-550.

Berry, E. X., and R. L. Reinhardt. 1974. *An analysis of cloud drop growth by collection: Part III-IY.* Journal Atmospheric Sciences v. 31:2118-2135.

. Bevington, P. R. 1969. *Data reduction and error analysis for the physical sciences.* McGraw-Hill Book Co., New York, 336 p, Chapter 5.

Bibby, N. M. 1976. Cover photograph. Weather v. 35(5).

Braham, R. R., Jr. 1952. *The water and energy budgets of the thunderstorm and their relation to thunderstorm development.* Journal of Meteorology v. 9(4).

. Braham, R. R., Jr. 1974. *Cloud physics of urban weather modification — a preliminary report.* Bulletin American Meteorological Society v. 55(2):100-106.

Braham, R. R., Jr., and M. Dungey. 1976. *Effects of a large city upon convective clouds and coalescence rain.* Preprints International Conference on Cloud Physics, Boulder, AMS, Boston, pp. 275-278.

Braham, R. R., Jr., and M. J. Dungey. 1978. *A study of urban effect on radar first echoes.* Journal Applied Meteorology v. 17(5).

Brazier-Smith, P. R., S. G. Jennings, and J. Latham. 1972. *The interaction of falling water drops: coalescence.* Proceedings Royal Society London Series A v. 326:393-408.

Brazier-Smith, P. R., S. G. Jennings, and J. Latham. 1973. *Raindrop interactions and rainfall rates within clouds.* Quarterly Journal Royal Meteorological Society v. 99:260-272.

Brown, F. R., and F. S. Karn. 1976. *Air pollution from the Ohio River and Monongahela River Valleys.* ERTS-1 A New Window on our Planet, U. S. Geological Survey Professional Paper 929, pp. 261-265.

Brunkow, David, and G. M. Morgan, Jr. 1973. *METROMEX radar studies. In* Summary of METROMEX Studies, 1971-1972, F. A. Huff, editor, Illinois State Water Survey Report of Investigation 74, pp. 103-111.

Byers, H. R., and R. R. Braham, Jr. 1949. *The thunderstorm.* U.S. Weather Bureau, Government Printing Office, Washington, D.C., 287 p.

Carrera, N. J. 1975. *Urban influences on cloud microstructure downwind from St. Louis, Missouri: Upper level observations.* Journal de Recherches Atmospheriques v. 9(4):157-165.

Cawse, P. A. 1974. *A survey of atmospheric trace elements in the U.K. (1972-73).* Report, United Kingdom Atomic Energy Authority, Harwell, Oxfordshire, AERE-R7669.

Cawse, P. A. 1975. *A survey of atmospheric trace elements in the U.K.: Results for 1974.* Report, United Kingdom Atomic Energy Authority, Harwell, Oxfordshire AERE-R8038.

Cawse, P. A. 1976. *A survey of atmospheric trace elements in the U.K.: Results for 1975.* Report, United Kingdom Atomic Energy Authority, Harwell, Oxfordshire, AERE-R8398.

Changnon, S. A., Jr. 1976. *Effects of urban areas and echo merging on radar echo behavior.* Journal Applied Meteorology v. 15:561-570.

Changnon, S. A., Jr., and T. J. Henderson. 1974. Cover Photograph. Bulletin American Meteorological Society v. 55(2).

Changnon, S. A., Jr., and F. A. Huff. 1975. *Squall zone storms on 25-26 July 1973. In* Studies of Selected Precipitation Cases from METROMEX, S. A. Changnon and R. G. Semonin, editors, Illinois State Water Survey Report of Investigation 81, 329 p.

Changnon, S. A., Jr., and P. T. Schickedanz. 1971. *Statistical studies of inadvertent weather modification of precipitation.* Preprints International Symposium on Probability and Statistics in the Atmospheric Sciences, Honolulu, AMS, Boston.

Changnon, S. A., Jr., F. A. Huff, and R. G. Semonin. 1971. *METROMEX: An investigation of inadvertent weather modification.* Bulletin American Meteorological Society v. 52(10):958-967. ;

Changnon, S. A., Jr., F. A. Huff, P. T. Schickedanz, and J. L. Vogel. 1977. *Summary of METROMEX, Volume 1: Weather anomalies and impacts.* Illinois State Water Survey Bulletin 62, 260 p.

Changnon, S. A., Jr., R. G. Semonin, and F. A. Huff. 1976. *A hypothesis for urban rainfall anomalies.* Journal Applied Meteorology v. 15:544-560.

Clark, T. L. 1973. *Numerical modeling of the dynamic's and microphysics of warm cumulus convection.* Journal Atmospheric Sciences v. 30:857-877.

Culkowski, W. M. 1962. *An anomalous snow at Oak Ridge, Tennessee.* Monthly Weather Review v. 90(5):194-196.

Detwiler, A. 1974. *Urban influence on cumulus formation.* Bulletin American Meteorological Society v. 55:1240-**41.**

Dixon, W. J., Editor. 1975. *BMDP biomedical computer programs.* University of California Press, Berkeley, 792 p.

Dungey, M. 1977. *The effects of St. Louis on first echo frequencies.* Proceedings 6th Conference on Planned and Inadvertent Weather Modification, Champaign, AMS, Boston, pp 49-52.

Dytch, H. E. 1975. *Urban influences on cloud microstructure downwind from St. Louis, Missouri: Lower level observations.* Journal de Recherches Atmospheriques v. 9(4): 145-156.

Dytch, H. E. 1977. *Urban influences on cloud microstructure downwind from St. Louis, Missouri.* Cloud Physics Laboratory Technical Note No. 51, University of Chicago, 119 p.

Egan, B. A., and J. R. Mahoney. 1972. *Numerical modeling of advection and diffusion of urban area source pollutants.* Journal Applied Meteorology v. 11:312-322.

Fitzgerald, J. W. 1974. *Effect of aerosol composition on cloud droplet size distribution: A numerical study. .* Journal Atmospheric Sciences v. 31:1358-1367.

Fitzgerald, J. W., and P. A. Spyers-Duran. 1973. ***Changes in cloud nucleus concentration and cloud droplet size distribution associated with pollution from St. Louis.*** **Journal Applied Meteorology v. 12:511-516.**

Flueck, John A. 1971. ***Statistical analyses of the ground level precipitation data.*** **Final Report, Part IV, NSF** Grant GA-20470, University of Chicago, 294 p.

Fukuta, N., and L. A. Walters. 1970. ***Kinetics of hydrometeor growth from a vapor-spherical model.*** **Journal** Atmospheric Sciences v. 27:1160-1172.

Gatz, D. F. 1974. *METROMEX: Air and rain chemistry analyses.* Bulletin American Meteorological Society v. 55(2):92-93.

Gatz, D. F. 1976. ***The chemical composition of precipitation and aerosols at St. Louis.*** **Proceedings, Symposium** on Man's Impact on Atmospheric Compositions and Processes, American Chemical Society, Northeast Regional Meetingi Albany, N.Y.

Gatz, D. F. 1977. ***Airborne elements: Their concentration distributions at St. Louis. In*** **Study of Air Pollution** Scavenging, by R. G. Semonin et al., Fifteenth Progress Report to Energy Research and Development Adminstration, Contract No. EY-76-S-02-1199, Illinois State Water Survey, Urbana, C00-1199-58.

Henderson, T. J., and D. Duckering. 1973. *METROMEX 1973.* Atmospherics Incorporated, Fresno, California, 51 p.

Hindman, E. E., P. M. Tag, B. A. Silverman, and P. V. Hobbs. 1977. *Cloud condensation nuclei from a paper* ***mill, Part II: Calculated effects on rainfall.*** **Journal Applied Meteorology v. 16:753-755.**

Hobbs, P. V., L. F. Radke, and S. E. Shumway. 1970. ***Cloud condensation nuclei from industrial sources and their apparent influence on precipitation in Washington state.*** **Journal Atmospheric Sciences v. 27:81-89.**

Hohn, F. E. 1960. *Elementary matrix algebra.* The Macmillan Company, New York, 305 p.

Holle, R. L., and S. A. MacKay. 1972. ***Tropical cloud cover seen by all sky cameras on Barbados and adjacent*** *Atlantic Ocean during two summers.* NOAA Technical Memorandum ERL OD-10, Boulder, Colorado, 47 p.

Huff, F. A. 1967. *Mesoscale structure of a severe rainstorm.* Preprints 5th Conference on Severe Local Storms, St. Louis, AMS, Boston, pp. 211-218.

Huff, F. A. 1977a. *1971-1975 rainfall pattern comparisons. In* Summary of METROMEX Volume 1: Weather Anomalies and Impacts, by S. A. Changnon, F. A. Huff, P. T. Schickedanz, and J. L. Vogel, Illinois State Water Survey Bulletin 62, pp. 13-29. . .

Huff, F. A. 1977b. *Distribution of heavy raincells. In* Summary of METROMEX, Volume 1: Weather Anomalies and Impacts, by S. A. Changnon, F. A. Huff, P. T. Schickedanz, and J. L. Vogel, Illinois State Water Survey Bulletin 62, pp. 182-192. .

Huff, F. A., and P. T. Schickedanz. 1970. *Rainfall evaluation studies.* Final Report, Part II, NSF Grant GA-1360, Illinois State Water Survey, Urbana, 224 p.

Johnson, D. B. 1976. *Ultragiant urban aerosol particles.* Science v. 194:941-942.

Jonas, P. R. 1972. *The collision efficiency of small drops.* Quarterly Journal Royal Meteorological Society v. 98:681-683.

Jones, D. M. A., F. A. Huff, and S. A. Changnon, Jr. 1974. *Causes for precipitation increases in the bills of southern Illinois.* Illinois State Water Survey Report of Investigation 75, 36 p.

Jones, D. M. A., and P. T. Schickedanz. 1974. ***Surface temperature, moisture, and wind studies. In*** **Interim** Report of Metromex Studies: 1971-1973, F. A. Huff, editor, NSF Grant GI-38317, pp. 98-120.

Junge, C, and E. McLaren. 1971. ***Relationship of cloud nuclei spectra to aerosol size distribution and composition.*** Journal Atmospheric Sciences v. 28:382-390.

Kim, J. 1975. *Factor analysis. In* Statistical Package for the Social Sciences, by N. N. Nie, C. H. Hull, J. G. Jenkins, K. Steninbrenner, and D. H. Bent, Second Edition, McGraw-Hill Book Co., New York, pp. 469-515.

Klett, J. D., and M. H. Davis. 1973. ***Theoretical collision efficiencies of small cloud droplets at small Reynolds number.*** Journal Atmospheric Sciences v. 30:107-117.

Kramer, M. L., D. E. Seymour, M. E. Smith, R. W. Reeves, and T. T. Frankenberg. 1976. *Snowfall observations* ***from natural-draft cooling tower plumes.*** **Science v. 193-1239-1241.**

Miller, J. M., and J. Wisniewski. 1978. ***A review of precipitation chemistry studies —North America and adjacent areas.*** Unpublished manuscript.

Noll, K. E., and M. J. Pilat. 1971. *Size distribution of atmospheric giant particles.* Atmospheric Environment v. 5:527-540.

Ochs, H. T., III. 1975. *Modeling of cumulus initiation in METROMEX.* Journal Applied Meteorology v. 14(5):873-882.

Ochs, H. T. 1978. ***Moment conserving techniques for microphysical computations, Part II: Model testing and results.*** Journal Atmospheric Sciences, paper submitted.

Ochs, H. T., III, and D. F. Gatz. 1978. *Water solubility of atmospheric aerosols.* Atmospheric Environment, paper submitted.

Ochs, H. T., III, and R. G. Semonin. 1976. ***Microphysical computations in urban and rural clouds.*** **Preprints** International Conference on Cloud Physics, Boulder, AMS, Boston, pp. 22-26.

Ochs, H. T., III, and C. S. Yao. 1978. ***Moment conserving techniques for microphysical computations, Part I: Numerical techniques.*** Journal Atmospheric Sciences, paper submitted.

Peden, M. E., and L. M. Skowron. 1978. *Ionic stability of precipitation samples.* Atmospheric Environment, paper submitted.

Purdom, J. F. W., and J. J. Gurka. 1974. ***The effect of early morning cloud cover on afternoon thunderstorm development.*** Preprints 5th Conference on Weather Analysis and Forecasting, AMS, Boston, pp. 58-60.

Rainwater, F. H., and L. L. Thatcher. 1960. *Methods for collection and analysis of water samples.* U.S. Geological Survey Water Supply Paper 1454, U.S. Government Printing Office, Washington, D. C.

Schickedanz, P. T. 1972. ***The raincell approach to the evaluation of rain modification experiments.*** **Preprints** 3rd Conference on Weather Modification, Rapid City, S. D., AMS, Boston, 336 p.

Schickedanz, P. T. 1973. ***A statistical approach to computerized rainfall patterns.*** **Preprints 3rd Conference on** Probability and Statistics in Atmospheric Science, Boulder, AMS, Boston.

Schickedanz, P. T. 1974a. *METROMEX cloud camera studies for 1971-73. In* Interim Report of METROMEX Studies: 1971-1973, F. A. Huff, editor, NSF Grant GI-38317, pp. 143-146.

Schickedanz, P. T. 1974b. *Climatological assessment of extra-area seeding effects.* Journal of Weather Modification v. 6:92-108.

Schickedanz, P. T. 1974c. ***Inadvertent weather modification as indicated by surface raincells.*** **Journal Applied** Meteorology v. 13:891-900.

Schickedanz, P. T., and M. B. Busch. 1975. ***Data processing and analytical procedures for urban precipitation studies.*** Proceedings National Symposium on Precipitation Analysis for Hydrologic Modeling, Davis, California, sponsored by American Geophysical Union, pp. 101-110.

Schickedanz, P. T., and S. A. Changnon, Jr. 1977. *Extended area rainfall findings. In* Summary of METROMEX, Volume 1: Weather Anomalies and Impacts, by S. A. Changnon, F. A. Huff, P. T. Schickedanz, and J. L. Vogel, Illinois State Water Survey Bulletin 62, pp. 67-84.

Semonin, R. G., and S. A. Changnon, Jr. 1974. *METROMEX: Summary of 1971-1972 results.* Bulletin American Meteorological Society v. 55(2):95-100.

Shafrir, U., and T. Gal-Chen. 1971. ***A numerical study of collision efficiencies and coalescence parameters for*** *droplet pairs with radii up to 300 microns.* Journal Atmospheric Sciences v. 28:741-751.

Simpson, J., W. L. Woodley, and R. M. White. 1972. ***Joint federal-state cumulus seeding program for mitigation*** *of 1971 south Florida drought.* Bulletin American Meteorological Society v. 53:334-343.

Sisterson, D. L. 1975. *Studies on the urban moisture budget.* Report AS114, Department of Atmospheric Science, College of Engineering, University of Wyoming, Laramie, 141 p.

Srivastava, R. C. 1971. ***Size distribution of raindrops generated by their breakup and coalescence.*** **Journal Atmospheric** Sciences v. 28:410-415.

Stinson, J. R. 1977. ***Cloud and precipitation formation by refinery emissions.*** **Journal Weather Modification** v. 9:38-40.

Stinson, J. R., and C. D, Brown. 1977. ***Cloud and precipitation formation and modification by refineries and power plants. Journal Weather Modification v. 9:32-37.***

Stout, G. E. 1961. ***Some observations of cloud initiation in industrial areas. In*** **Air over Cities, Symposium,** Division of Air Pollution, U.S. Department of Health, Education, and Welfare, pp. 147-154.

Tukey, John W. 1962. *The future of data analysis.* Annals of Mathematical Statistics v. 33(1).

Twomey, S. 1959. ***The nuclei of natural cloud formation, II: The supersaturation in natural clouds and the variation of cloud droplet concentrations.*** **Geofisica Pura E Applicata 43:243-249.**

Venezia, R., and G. Ozolins. 1966. *Air pollutant emission inventory.* Interstate Air Pollution Study, Phase II Project Report, U.S. Department of Health, Education, and Welfare, Cincinnati, Ohio, 50 p.

Vogel, J.L. 1974. *Synoptic studies. In* Interim Report of Metromex Studies: 1971-1973, S. A. Changnon and F. A. Huff, editors, NSF Grant GI-38317, pp. 6-16.

Vogel, J.L. 1977. *Synoptic weather relations. In* Summary of METROMEX, Volume 1: Weather anomalies and impacts, by S. A. Changnon, F. A. Huff, P. T. Schickedanz, and J. L. Vogel, Illinois State Water Survey Bulletin 62, pp. 85-110.

Winer, B. J. 1962. *Statistical principles in experimental design.* McGraw-Hill Book Co., New York, p. 94.

Young, K. C. 1975. ***The evolution of drop spectra due to condensation, coalescence, and breakup.*** **Journal** Atmospheric Sciences v. 32:965-973.

Part E. Recapitulation and Outlook

Richard G. Semonin, Bernice Ackerman, Stanley A. Changnon, Jr.

Summary of Volume 2

The results obtained from the 4-year (1972-1975) sample of surface temperatures, moisture, and winds, indicate that the derived means are representative of the longer-term conditions in the St. Louis metropolitan and surrounding rural areas.

The urban heat island is greatest at night, averaging from 3 to 5° C above rural areas depending on cloud cover and wind speed. A weak heat island is observed, on the average, throughout the day. During the afternoon the heat island is minimal, but positive, with an urban-rural temperature difference of about 0.5° C when there is 0.3 sky cover or more. Hence, St. Louis is a relative source of sensible heat during most daytime periods as well as at night.

Comparison of the patterns of surface temperatures and precipitation quantities for the afternoon and evening hours suggests a weak relationship that disappears with time. The areas with relatively high temperatures at 1200 to 1500 CDT are in the city, west of St. Louis, and in the bottomlands. These are locations where rainfall initiates during these hours and where relatively heavy rains occur during the 1500-1800 CDT period. However, after 1800 CDT an inverse relationship exists for surface temperature and rainfall patterns.

The surface mositure patterns over the city show a marked diurnal variation. The city is relatively moist from midnight to 0700. During the daytime and evening the city surface is slightly drier than the rural areas. The bottomland area west of Alton is a relatively moist area throughout the day and thus a potential local moisture source.

In an effort to evaluate the joint effects of temperature and moisture, the surface equivalent potential temperature patterns were examined. Average patterns based on the prestorm conditions of 45 typical rainstorms showed that EPT values tended to be lower over most of the city, with variable high and low values throughout the rural areas. If a relationship exists between surface EPT values and precipitation quantity, it was not obvious in these analyses.

The study of surface wind conditions reveals a very distinct urban influence on the surface wind structure. Surface wind speeds are influenced out to 50 km beyond the city with a relative maximum in surface wind speeds over the center of the city. The degree of urban influence on rural winds is dependent upon the direction of the winds and their strength. A composite upwind to downwind cross section of wind speeds through the city suggests convergence from about 16 to 9 km upwind of the city center, divergence over the city itself, then convergence to about 16 to 17 km downwind, suggesting a 'convergence donut' around the city.

Low-level mean patterns of condensation and ice nuclei reveal maximum concentrations closely associated in position with the industrial corridor along the Mississippi River from south St. Louis northward to Alton-Wood River. The zones of high CN and IN

concentrations are close to the maxima found for radar echo and raincell initiations. The patterns of CN also suggest a relationship to the isohyetal patterns for air mass showers and for precipitation in the drier months, suggesting that locally derived CN may play a role in the precipitation process under these conditions. The local CN possibly produce an effect on precipitation in relatively dry conditions that is different from that during heavier rainfall conditions with their typically more organized migrating cloud systems. Some of the results suggest that the chemistry of the aerosols could be important factors in their effectiveness as CN and IN.

Analyses of the thermodynamic structure of the planetary boundary layer reveal that the mixing height is greater over the city than over the rural areas, indicating that the potential exists for urban effluents to be transported to relatively higher levels of the atmosphere. The existence of a deeper layer of neutral stability and constant mixing ratio indicates that this potential is probably realized. Although the EPT in the lowest 500 to 1000 m was lower over the city than over the country, these studies indicated that the EPT aloft in the upper PBL was, on the average, higher over the city than over the country. The heat and moisture transported to higher levels (1 to 2 km above the surface) may in some conditions remain aloft during the evening and thus influence nocturnal convective storms. Thermodynamic analyses suggest that cloud bases over the city should be higher than over rural areas, which is supported by actual cloud-base measurements.

Studies of the kinematics of the PBL wind fields during the afternoon revealed that St. Louis affects the winds in all types of weather conditions, producing zones of convergence and divergence, with their magnitude and location dependent on the ambient wind conditions. In general, the metropolitan area is found to be a zone of convergence, particularly in the late afternoon. An urban circulation was found superimposed on the ambient flow most of the time. The results suggest that updraft speeds at cloud bases might be stronger over the city because of the more favorable lapse rate in the upper PBL and that updrafts would tend to be sustained by virtue of the convergence. Measurements of cloud updrafts support this, with higher updraft speeds and larger updrafts in urban clouds than in rural clouds.

Studies of cloud behavior and frequencies provided interesting clues as to the local influences on convection. Surface cloud photographs largely from isolated 'air mass' type days revealed two local areas of preferred cloud initiations; the central part of St. Louis and the Alton-Wood River industrial complex. The relatively high frequencies of cumulus initiations in these two areas were statistically significant. The initiation of cumulus clouds in rural areas typically began 10 to 30 minutes later than those over the city. Apparently two mechanisms are effective in producing these local cumulus initiation anomalies. In the St. Louis area the maximum appears to occur in the preferred zone of convergence in the boundary layer, whereas the initiations in the Alton-Wood River area were directly over sensible heat sources.

Satellite cloud measurements were used to define the areal frequency of clouds during daylight hours. These patterns reveal that much of the St. Louis area is typically relatively clear in the morning and early afternoon, allowing for greater heating. Increased local cloudiness over the eastern area of the city is observed by 1600 which spreads into the Alton-Wood River area by 1900 CDT. The hill area southwest of St. Louis is relatively cloudy throughout the day, and the relatively moist bottomlands and Alton areas are cloudy zones early in the day (1000 CDT). In essence, the

cloud studies indicate urban-industrial influences on the initiation of cumulus clouds and on their local distribution, but the degree of influence is a function of a number of other factors.

Studies of cloud characteristics in the region reveals that the typical urban cumulus cloud has a higher base (by 300 to 600 m) than the rural cloud and also has updrafts that are greater. The condensation nuclei concentrations found inside urban cumulus clouds are generally 2.5 times greater than those found in rural cumulus, and the liquid water content in the urban clouds is about 10% greater than in rural clouds, although this difference is not statistically significant. In a word, the inside of urban clouds is dirtier and wetter than the inside of rural clouds.

Cloud modeling was employed to help discern local effects on the cloud and precipitation processes. On days of weak convection, typical of non-frontal or air mass conditions, it was found that local surface temperature influences help initiate cumulus clouds, and that local heating effects were of greater importance for cloud development than the availability of local moisture. In general, it is of interest to note that the center of the urban heat island is at, or near, the location where the cloud photographs showed the highest frequency of cumulus initiation, which suggests that this 'anomaly' may be partially due to the local release of sensible heat as well as to convergence.

Numerical calculations suggest that the development of the droplet spectrum is insensitive to changes in CCN size, their concentrations, or their chemical composition. One result suggests that reduced updraft speeds in urban clouds could explain the urban versus rural differences noted in the height of first echoes. In the net, certain results of this microphysical modeling do not appear reasonable in light of the measurements of updrafts and other cloud parameters, indicating that certain assumptions made relating to sedimentation and the lack of consideration of the ice process limit the validity of the results.

The analyses were presented in this report in an order that relates generally to a sequence of potential physical events leading to precipitation, ranging from the surface condition upward through the PBL and on into observed cloud effects. Next to be considered was detectable precipitation inside clouds, as measured by weather radars.

Investigations of the initiation of precipitation inside cumulus clouds based on 3-dimensional radar measurements reveal that the 'first echoes' of storms developing over the city had similar depth and height as those pver rural areas for organized precipitation systems. However, for isolated showers and unorganized convection, the first echoes over the urban area had markedly lower bases than did the first echoes over the surrounding rural areas. Further, the first echoes with isolated conditions typically had less depth and lower bases than those with organized systems, regardless of the location of their development. The areal frequencies of first echoes aloft show a marked, 20 to 50%, increase over the city and the Alton-Wood River area. The tops of urban precipitation echoes also increased in height much more frequently than did tops of non-urban echoes, and of the echoes that grew, the urban echoes grew faster and reached greater heights than did the rural echoes. This study also revealed that urban echoes merged with another echo at least twice as often as did rural echoes.

Further radar echo studies were based on echoes measured near the surface, which is closely related to the precipitation as it reaches the ground. These data indicated a preference

for precipitation echoes to first appear over the Alton-Wood River and St. Louis metropolitan areas, and the hill area southwest of St. Louis. A zone of frequent echo mergers was found in and just east of St. Louis as well as in the hill area. Studies of echo intensity cores revealed that those that developed or passed over St. Louis lasted longer, traveled further, and were more intense than the intensity cores of echoes over the rural area.

Further information on the sequence of precipitation development was obtained for individual clouds and storms from surface raincell patterns, as measured by raingages. The volume of rainfall from these cells indicated that the greatest effect occurred from those that developed or passed over the St. Louis industrial area (an increase of 211%), but increases were also found in the Alton-Wood River industrial area (+77%), and in the hills region and the bottomland. Synoptically, the greatest effects in both urban-industrial areas occurred in squall line storm conditions, but influences were found also in other organized precipitation systems. Analyses of the characteristics of raincell mergers indicated a relatively strong tendency for mergers to occur most frequently in a major urban-effect area east and northeast of St. Louis, along river valleys, and to a lesser extent in the more hilly regions. In general, there was strong association between the spatial distribution of mergers and total monthly and seasonal rainfall.

The raincell analyses revealed that urban-induced influences appeared' during the afternoon and continued until the early morning hours. Comparison of raincell characteristics influenced by the St. Louis metropolitan area and by the Alton-Wood River industrial area reveal differences, particularly in the high rainfall rate. This suggests that local processes affecting precipitation in these two areas differed.

One of the impacts of the modification of the precipitation is the scavenging of suspended materials, cleansing the atmosphere but possibly contaminating the surface. The day-to-day and site-to-site variability in chemical deposition, both wet (in rainfall) and dry, is considerable. The results suggest the need for relatively dense networks to sample various trace metals and other pollutants. For the elements studied, results suggest that dry depositon accounts for 44 to *69%* of the total deposition of pollutants. In other words, the precipitation in the effect area accounts for 31 to 56% of the depositio of various chemical compounds.

METROMEX Inadvertent Weather Modification Hypotheses

The summary of the key findings contains several suggested pathways between an urban-modified atmosphere and altered cloud and precipitation properties. Even so, many of the data are presented as climatological sets which, by their very cumulative nature, may mask more direct evidence of causative factors. The statistical treatment of the observations, however, leads to the development by physical reasoning of one or more hypotheses connecting urbanization and weather modification. Precise knowledge of the natural production of precipitation is limited, and certainly the identification of those factors critical to inadvertent modification of the processes is also necessarily limited.

The findings presented in this volume begin with the surface and extend upward eventually leading to clouds and precipitation. The hypotheses developed here are an attempt to explain the initiation of small clouds and the observed precipitation patterns by using the measured physical parameters in a consistent chain of reasoning.

There are three stages of development of precipitation to be considered when examining the potential effects of an urban-industrial complex on the atmosphere. The first of these is the development of small convective clouds without the ensuing development of precipitation. The study of this cloud development can provide information on preferred areas for the cloud initiation or enhancement. Admittedly, the conditions under which the large scale atmosphere produces scattered convective clouds may also provide unique circumstances and emphasize cloud development over a particular area that may not be representative during synoptic scale pre-storm situations.

The second stage of cloud development to be considered is that of convective clouds that extend beyond the planetary boundary layer but do not produce organized precipitation, that is, cumulus congestus. More frequently than not, these clouds are observed as precursors to the development of precipitation or precede migratory precipitation systems as the atmosphere destabilizes. The observations required to ascertain urban effects on such clouds would include cloud base height and cloud top height as well as microphysical parameters such as the droplet size spectrum.

Finally, the urban area is suspected of influencing those clouds which either are about to precipitate or are already producing rainfall across or in proximity to the urban center. The direct influence of the metropolitan area on such clouds is difficult to ascertain because the increased rainfall arises from initiation of new showers or the enhancement of an existing, moving system. To quantitatively separate and study the contribution from these two possible mechanisms requires more sophisticated analyses than straight-forward rainfall observation.

Synoptic Situation Characterization. The summer synoptic conditions that precede these three stages are those conducive to scattered cumulus activity. They generally include the presence of a high pressure system centered to the east or southeast of Illinois providing southerly component flow across the state. On the west side of such a high, a capping inversion is frequently observed inhibiting vertical development of convective clouds. With time, the high pressure migrates eastward and is replaced by a more disturbed atmosphere usually associated with a migratory frontal system approaching from the west. The capping inversion is gradually dissipated and the lower troposphere becomes less stable throughout, with continuous influx of moisture at low levels preparing the atmosphere for more active convection. The atmosphere is now suitable for the development of scattered convective showers which are free to develop to great heights. Unless this condition is associated with a surface disturbance or a passing upper air trough, the showers will remain scattered and disorganized. With the approach of a synoptic scale disturbance (front, upper trough) the convective activity becomes more organized resulting in either frontally associated precipitation or a squall line (or both).

Boundary Layer Characterization. Under any of these synoptic situations, there are three ways in which an urbanized area may affect clouds and precipitation: 1) through the point and area sources of effluents as a consequence of man's activities, that is, aerosols (CCN, IN), water vapor, and heat; 2) increased upward flux of heat, moisture, and effluents on the turbulence or thermal scales; and 3) mesoscale mechanical deformation of airflow resulting in converging flow in the lower layers.

There is evidence that all three exist, at least in part, in St. Louis. Direct measurements of the aerosols and of the droplet spectra near cloud base indicate that the city tends to increase the number concentration of cloud condensation nuclei, thus increasing the continental character of the clouds originating or passing over the urban area. Evidence concerning ice nuclei is much less definite. Although there is evidence of low-level sources, measurements in the troposphere indicate there may not be increased activity of this kind.

Although water vapor is produced in many of man's urban-industrial activities, this source is much smaller during the summer than that due to evapotranspiration from rural vegetation. Consequently, the urban surface represents a reduced rather than an enhanced source of moisture, and the vapor content of the surface boundary layer is generally lower than that in the country.

The very complicated group of processes involved in the heat balance at the urban surface does not necessarily predict uniformly warmer temperatures in the city during midday. However, there is evidence that in the lower boundary layer, a midday positive temperature differential does exist, particularly in cloudy weather. The urban-rural temperature difference has been found to exist throughout much of the depth of the planetary boundary layer.

First Cloud Initiation Hypothesis. The nocturnal inversion is observed to be stronger in rural areas than in the urban center where the heat island maximizes at night. In the early morning, the solar radiation on a relatively clear city (as evidenced from satellite cloud studies) begins to dissipate the inversion at the surface. The inversion is weakest in the urban center, and the morning heating allows surface air to reach the lifting condensation level earlier than in a rural area where a much stronger inversion must be overcome. The urban surface by virtue of its roughness characteristics and its slightly warmer temperature produces an increased flux of heat and water vapor through mechanical mixing or through enhanced thermal transport. Further, the boundary layer airflow is perturbed by the urban structure inducing convergence over the city throughout much of the PBL. The depth of the convergence increases during the day as the PBL increases in depth.

These features of the evolving boundary layer prepare the atmosphere for the appearance of the first clouds. The dissipation of the nocturnal inversion by solar heating, in conjunction with the city-related mesoscale convergence, allows mixing of near-surface properties throughout the lower levels of the boundary layer. This process results in the formation of the first clouds of the day over the urban areas with bases coinciding with LCL. Continued mixing of the lowest atmospheric layers produces cloud bases more nearly at the convective condensation level by early and mid-afternoon. The observed convective condensation level is higher over the urban center because the city is warmer and somewhat drier than the surrounding rural countryside resulting in higher cloud bases.

Isolated Shower Initiation Hypothesis. The development of air mass showers may follow the cloud initiation hypothesis for fair weather cumulus, but in a general atmospheric environment conducive to deeper convection. These clouds are commonly quasi-stationary and consequently are more responsive to localized perturbations in their immediate environment. For example, the qualitative relationship between condensation nuclei observations at a level in the mid-planetary boundary layer and the air mass precipitation suggests that there may be a physical relationship between them.

In addition, neutral stratification extends through a much deeper layer over the city than over the rural area. The country exhibits a superadiabatic lapse rate in the surface boundary layer and lower PBL, and a conditional instability in the upper half of the PBL. Both of these are destroyed in the city stratification, possibly indicating either thorough mixing or possibly mesoscale dynamic effects. Regardless, this rural-urban difference means that mechanical and thermal eddies rise through greater depth in proximity to the city. Because these clouds are either stationary or very slowly moving, a source of condensation nuclei will be available for transport by the subcloud base kinematic flow leading to ingestion by the cloud and possible modification of the microphysics. Equally accessible to the cloud is the sensible heat released from the urban area if the clouds are situated in proximity to the heat island.

Since cloud bases are higher in city-affected regions, and since the tempratures in the middle troposphere are observed to be very little different over city and country surfaces, initial lower parcel

buoyancy is expected, possibly resulting in lower urban vertical velocities. This expectation, however, is partially offset by the urban-produced mesoscale convergence which provides a more continuous and extensive source of low level moisture and sensible heat.

These features of the altered urban atmosphere suggest that cloud modification should occur in simple, unorganized air mass shower situations. In other words, isolated shower activity (often including the defined squall zone classification) should be more readily related to the disturbed boundary layer and the urban effects more easily identified than they should be with migratory, organized precipitation systems. However, the five-year precipitation sample does not indicate that the major inadvertent influence on the precipitation pattern occurs in air mass conditions, although the urban influence on air mass showers is apparent in summer dry periods.

Organized Storm Enhancement Hypothesis. The next resulting question is, do these urban influences exist in organized convective systems? The organized synoptic scale precipitation systems, squall lines and fronts, represent another aspect of atmospheric instability. The atmospheric baroclinicity, or degree of atmospheric stratification, is altered significantly in proximity to fronts and upper-level troughs. The horizontal boundary between air masses is a region where the atmosphere is very unstable since it is striving to achieve equilibrium. These boundaries provide a mechanism for cloud and precipitation development which would produce precipitation in a reasonably organized fashion over the METROMEX area irrespective of the presence of the St. Louis metropolitan region.

We are then faced with one of two choices (or both) as contributing causes of the observed anomalous precipitation pattern. The first of these follows from the previous discussion of air mass showers whereby the showers develop in response to urban effects, and are rooted in the urban area. These showers are then in existence and available to merger with an approaching migratory system. In this sequence of events, no enhancement in precipitation would occur until the migratory cells join with the urban-related cells somewhere in proximity to the Mississippi River to be followed by increased precipitation somewhere to the east.

The second possibility is that in the absence of urban-developed air mass showers, the urban area in some way directly modifies either the dynamics or cloud microphysics of the clouds composing the storm.

Since other evidence from all over the Midwest shows that such migratory storms are not a steady-state system, but rather undergo continuous growth and decay of the individual cells, it seems more logical to consider in greater detail the first of these alternatives as the connecting link between urban effects and precipitation from moving systems.

It is known that any deep convection tends to deform the airflow around it, and that new cloud cells, or newly developing clouds areas, occur preferentially in one or two quadrants around the cloud. The quadrant in which the new cloud formation occurs is more closely related to the direction of the wind shear in the cloud layer than to the direction of the wind. Thus in some cases the storm may be continually generated on the upwind side (so called back feeder cells) and in other cases on the downwind side of the storm (front feeder cells). The urban effect will depend on the location and character of these feeder clouds in the migratory system.

The major precipitation anomaly has been found to the east and most particularly to the northeast of St. Louis. The winds above the PBL in the summer are most commonly from the WSW through the NW. Thus this particular area is downwind (east) from the main St. Louis metropolitan area, from the heavily industrialized Granite City, and from the Alton-Wood River

refinery and industrial area. In addition, the anomaly also extends downwind from a major moisture source over the Missouri-Mississippi River bottoms. Since the effect that is seen over Edwardsville is apparently due to a relatively few major rainstorms, and those primarily classified as squall lines, it is obvious that the pattern is due to an enhancement of previously existing, migratory systems.

In summary, there is a great deal of evidence available from previous studies of squall lines and lines of thunderstorms, to show that these lines frequently propagate new lines ahead of it. The metropolitan area, with its observed urban to downwind convergence zone and other features conducive to cloud and precipitation development, is a preferred region for either development of a new line or intensification of an existing line. Thus, the modification of a line attributed to the urban area might not result from direct effects on the original migratory system, but possibly is due to either the greater likelihood of additional rain through pre-line initiations or through strengthening the existing line by mergers with urban-affected cells.

Unresolved Questions and Recommendations

The hypotheses set forth in the above section follow from the key findings presented in the summary, and the following questions arise from the hypotheses.

1) Can the initial cloud development be related to various land use patterns?
2) What is the evolution behavior of the PBL with increasing atmospheric instability and passage of a synoptic scale system?
3) What is the role of the PBL in cloud and precipitation development?
4) What is the effect of antecedent conditions in urban and rural areas on cloud and precipitation morphology?
5) Where are the cloud initiations corresponding to individual first echoes?
6) Where are the first echo initiations corresponding to individual raincells?
7) Does the urban area act to enhance the strength and/or duration of convection in existing and developing cells?
8) Do urban-generated CN, CCN, and IN measurably modify the precipitation process?
9) Is there an increased urban-related dynamic effect leading to enhancement of feeder cells around pre-existing large storms in organized systems?
10) What is the urban effect apt to be during and between a series of rain events (separation of less than three hours), i.e., does the city 'look' more rural or uniquely different with a wetted surface?
11) What is the recovery time for the city to return to the pre-rain atmospheric state following a rain event?
12) Why are precipitation cell mergers further east in wet months than in relatively dry or near-normal periods?
13) What is the mechanism for increased rainfall after merger?

This list of significant unresolved questions is not meant to be all encompassing, but is representative of the more important problems remaining after our five-year field research. Certain of these questions can be answered from the available data, whereas some will require limited additional field measurements. The major recommendations, then, are simply to:

- Undertake a series of detailed case studies, being careful to select from the data bank those cases with the most comprehensive sets of measurements
- Initiate appropriate modeling efforts for transferability of results to other cities

- Carefully design a future field measurement program to address specific remaining questions

The fulfillment of the first recommendation may require considerable effort since much of the focus to date has, of necessity, been on the climatological approach. Other findings, developed in great detail, have not yet been adequately interrelated to other detailed results. The case studies will require a careful blending of the measurements to answer questions concerning mesoscale cloud events as opposed to focused data subsets. The enormity of such efforts, elapsed time, and support have limited the attention that could be given to case study investigations.

The outcome from such studies will direct attention to gaps in the data bank requiring additional field experimentation and will provide initialization and verification data for future modeling efforts. Hopefully, the variables to be measured will be limited and the synoptic conditions to be sampled carefully specified.

PROJECT PUBLICATIONS

Ackerman, Bernice. 1972. *Winds in the Ekman layer over St. Louis.* Preprints, Conference on Urban Environment, AMS, Boston, pp. 22-27.

Ackerman, Bernice. 1973. *Airflow over the metropolitan area of St. Louis.* Reprint 73-26, 66th Annual Meeting of the Air Pollution Control Association, June 24-28, 31 pp.

Ackerman, Bernice. 1974. *METROMEX: Wind fields over St. Louis in undisturbed.weather.* Bulletin American Meteorological Society v. 55(2):89-100.

Ackerman, Bernice. 1974. *Wind fields over the St. Louis metropolitan area'.* Journal of Air Pollution Control Association v. 24:232-236.

Ackerman, Bernice. 1974. *Wind profiles and their variability in the planetary boundary layer.* Preprints, Symposium on Atmospheric Diffusion and Air Pollution, Santa Barbara, AMS, pp. 19-22.

Ackerman, Bernice. 1974. *Spatial variability of the wind velocity in the lowest 500 meters.* Preprints, Sixth Conference on Aerospace and Aeronautical Meteorology, El Paso, AMS, Boston, pp. 325-328.

Ackerman, Bernice. 1975. *Vertical fluxes and exchange coefficients over St. Louis.* Field Program 1975. Final Report to U. S. Environmental Protection Agency under Grant R803-682-01-1. 61 p.

Ackerman, Bernice. 1977. *Mesoscale wind fields over St. Louis.* Preprints, Sixth Conference on Weather Modification, Champaign, AMS, Boston.

Adam, John R., Robert Cataneo, Donald F. Gatz, and Richard G. Semonin. 1973. *Study of rainout of radioactivity in Illinois.* Eleventh Progress Report to U.S. Atomic Energy Commission. Contract AT(11-1)-1199, 157 p.

Auer, August H., Jr. 1975. *1975 Operational report for METROMEX.* University of Wyoming, 47 p.

Braham, Roscoe R., Jr. 1974. *1975 Operational report for METROMEX.* University of Chicago, 39 p.

Cataneo, Robert. 1974. *Operational aspects of project METROMEX - an inadvertent weather modification study.* Preprints, Fourth Conference on Weather Modification, Ft. Lauderdale, AMS, Boston, pp. 379-318.

Changnon, Stanley A., Jr. 1971. *The 1971 Operational report for METROMEX.* Illinois State Water Survey, Urbana, 93 p.

Changnon, Stanley A., Jr., Floyd A. Huff, and Richard G. Semonin. 1971. *METROMEX: An investigation of inadvertent weather modification.* Bulletin American Meteorological Society v. 52:958-967.

Changnon, S. A., Jr., R. G. Semonin, and W. P. Lowry. 1972. *Results from METROMEX.* Preprint, Conference on Urban Environment and Second Conference on Biometeorology, Philadelphia, AMS, pp. 191-197.

Changnon, S. A., Jr., and R. G. Semonin, editors. 1975. *Studies of selected precipitation cases from METROMEX.* Illinois State Water Survey Report of Investigation 81, Urbana, 329 p.

Changnon, S. A., Jr., R. G. Semonin, and F. A. Huff. 1976. *A hypothesis for urban rainfall anomalies.* Journal of Applied Meteorology v. 15(6):544-560.

Gatz, D. F. 1972. *Washout ratios in urban and non-urban areas.* Preprint, Conference on Urban Environment and Second Conference on Biometeorology, Philadelphia, AMS, pp. 124-128.

Gatz, D. F. 1974. *METROMEX: Air and rain chemistry analysis.* Bulletin American Meteorological Society, v. 55(2):89-100.

Gatz, D. F. 1974. *St. Louis air pollution: Estimates of aerosol source coefficients and elemental emission rates.* Preprint, Symposium on Atmospheric Diffusion and Air Pollution, Santa Barbara, AMS, pp. 109-114.

Gatz, D. F. 1975. *Relative contributions of different sources of urban aerosols: Application of a new estimation method to multiple sites in Chicago.* Atmospheric Environment v. 9:1-18.

Gatz, D. F. 1976. Comment on 'Acid precipitation in the northeastern United States,' by Charles V. Cogbill and G. E. Likens. Water Resources Research, 12(3):569-570.

Gatz, D. F. 1977. ***A review of chemical tracer experiments on precipitation systems.*** **'Atmospheric Environment,** v. 11:945-953.

Gatz, D. F. 1978. ***Identification of aerosol sources in the St. Louis area using factor analysis.*** **Reprint, 4th** Joint Conference on Sensing of Environmental Pollutants, American Chemical Society.

Grosh, R. C, and R. G. Semonin. 1973. ***Moisture budgets and wind fields of thunderstorms passing over an urban area in the Midwest.*** Preprint, Eighth Conference on Severe Local Storms, Denver, AMS, pp. 130-137.

Henderson, T. J., and D. W. Duckering. 1972. ***Final report METROMEX 1972: A summary of operations conducted by Atmospherics Incorporated during the period 5 July through 15 August. 1972.*** **34 p.**

Henderson, T. J. and D. W. Duckering. 1973. ***Final report METROMEX 1973: A summary of operations conducted by Atmospherics Incorporated during the period 7 July through 19 August 1973.*** **51 p.**

Henderson, T. J. and D. W. Duckering. 1975. ***Final report METROMEX 1974: A summary of operations conducted by Atmospherics Incorporated during the period 7 July through 17 August 1974.*** **48 p.**

Henderson, T. J. and D. W. Duckering. 1976. *METROMEX 1975: A summary report.* 53 p.

Huff, F. A., Editor. 1973. *Summary report of METROMEX studies, 1971-1972.* Illinois State Water Survey Report of Investigation 74, Urbana, 169 p.

Lowry, W. P. 1973. *1973 Operation report for METROMEX.* Illinois State Water Survey, Urbana, 63 p.

Mansell, Joel W. 1976. Comments on 'The Effect of Tropospheric Temperature Lapse Rates on the Ascent Rates of Pilot Balloons. Journal of Applied Meteorology, v. 15(7):799-801.

Mansell, Joel W. 1977. *Reply.* Journal of Applied Meteorology, v. 16(1):115.

Ochs, Harry T. 1974. *A numerical cloud model in an urban environment.* Proceedings, of the Fifth Modeling and Simulation Conference, Pittsburgh, Pennsylvania.

Ochs, Harry T. 1974. *Cloud modeling in METROMEX.* Proceedings of the Fourth Conference on Weather Modification, Ft. Lauderdale, Florida.

Ochs, Harry T. 1975. *Modeling of cumulus initiation in METROMEX.* Journal of Applied Meteorology, v. 14:873-882.

Ochs, Harry T., and R. G. Semonin. 1976. ***Microphysical computations in urban and rural clouds.*** **Proceedings** of the International Conference on Cloud Physics, Boulder, Colorado.

Ochs, Harry T., and R. G. Semonin. 1977. ***The sensitivity of cloud microphysics to an urban environment.*** Proceedings of the Sixth Conference on Planned and Inadvertent Weather Modification, Champaign, Illinois.

Ochs, Harry T. 1978. ***Moment conserving techniques for microphysical computations, Part II: Model testing and results.*** Journal of Atmospheric Sciences, paper submitted.

Ochs, Harry T., and C. S. Yao. 1978. ***Moment conserving techniques for microphysical computations, Part I: Numerical techniques.*** Journal of Atmospheric Sciences, paper submitted.

Peden, Mark E. 1976. ***Flameless atomic absorption determinations of Cd, Pb, and Mn in particle size fractionated aerosols.*** Paper, Published in Methods and Standards for Environmental Measurement, Special Publication 464, National Bureau of Standards, November.

Peden, Mark E., and Loretta M. Skowron: 1978. *Ionic stability of precipitation samples.* Atmospheric Environment, accepted for publication.

Rattonetti, A. 1974. ***Determination of soluble cadmium, lead, silver, and indium in rainwater and stream water with the use of flameless atomic absorption.*** **Analytical Chemistry, v. 46:739-742.**

Rattonetti, A. 1976. ***Stability of metal ions in aqueous environmental samples.*** **Proceedings, Seventh IMR** Symposium: Gaithersburg, Maryland, pp. 633-648.

Semonin, Richard G. 1971. *Study of rainout of radioactivity in Illinois.* Tenth progress report, AEC contract . AT(11-1)-1199, 39 p.

Semonin, Richard G. 1972. *Tracer chemical experiments in Midwest convective clouds.* Proceedings, Third Conference Weather Modification, Rapid City, South Dakota, pp. 83-87.

Semonin, Richard G. 1972. *The use of chemical and biological tracers in cloud physics.* International Conference on Cloud Physics, London.

Semonin, Richard G. 1972. *Study of rainout of radioactivity in Illinois.* Interim Eleventh Progress Report to U.S. Atomic Energy Commission, Contract AT(11-1)-l199, 12 p.

Semonin, Richard G. 1974. *Urban-induced weather modification.* 1974 Earth Environment and Resources Conference Digest of Technical Papers, pp. 40-41.

Semonin, Richard G., and Stanley A. Changnon, Jr. 1974. *METROMEX: Lessons for precipitation enhancement in the Midwest.* Preprint, Fourth Conference on Weather Modification, AMS, Boston, pp. 353-357.

Semonin, Richard G., and Stanley A. Changnon, Jr. 1974. *METROMEX: Lessons for precipitation enhancement in the Midwest.* Preprint, Fourth Conference on Weather Modification, Ft. Lauderdale, AMS, pp. 353-357.

Semonin, Richard G., and Stanley A. Changnon, Jr. 1974. *METROMEX: Summary of 1971-1972 results.* Bulletin American Meteorological Society, v. 55(2):95-100.

Semonin, Richard G., and Donald F. Gatz. 1974. *Study of rainout of radioactivity in Illinois.* Twelth Progress Report to U.S. Atomic Energy Commission, Contract AT(11-1)-1199, 21 p.

Semonin, Richard G. 1975. *Study of rainout of radioactivity in Illinois.* Thirteenth Progress Report to U.S. Atomic Energy Commission, Contract AT(11-1)-1199, 24 p.

Semonin, Richard G. 1976. *The variability of pH in convective storms.* Journal of Water, Air, Soil Pollution, v. 6:395-406.

Semonin, Richard G. 1976. *The variability of pH in convective storms.* Proceedings, First International Symposium on Acid Precipitation and Forest Ecosystem, USDA Forest Service General Technical Report NE-23, pp. 349-361.

Semonin, Richard G. 1976. *Study of air pollution scavenging.* Fourteenth Progress Report to the Energy Research and Development Administration, Contract AE (11-1)-1199, 23 p.

Semonin, Richard G. 1977. *Temporal and spatial variability of rainfall pH.* Proceedings, Conference on Metropolitan Physical Environment, USDA Forest Service General Technical Report NE-25, pp. 53-61.

Semonin, Richard G., and Gary J. Stensland. 1977. *A search for inadvertent modification of precipitation chemistry using data from single events.* Preprint, Sixth Conference on Inadvertent and Planned Weather Modification, pp. 65-68.

Semonin, Richard G., B. Ackerman, D. F. Gatz, S. D. Hilberg, M. E. Peden, R. K. Stahlhut and G. J. Stensland. 1977. *Study of air pollution scavenging.* Fifteenth Progress Report to the Energy Research and Development Administration, Contract AE (ll-l)-l199.

Staff. 1974. *METROMEX: An overview o.f Illinois State Water Survey projects.* Bulletin American Meteorological Society, v. 55:89-100.

Vogel, John L. 1975. *Effects of surface factors on thunderstorms.* Preprint, Ninth Severe Local Storms Conference, Norman, AMS, pp. 113-119.

METROMEX INSTRUMENT SITES

ALN	Alton Civic Memorial Airport, IL
ARC	St. Louis Memorial Arch, MO
BCC	Belleville Community College, IL
BHN	Brighton, IL
BHS	Bunker Hill High School, Bunker Hill, IL
BLL	Belleville, IL
BLV	Scott Air Force Base, IL
BVK	Beavercreek Field Site, IL
BWM	Brentwood, MO
CAH	Cahokia Airport, IL
CLV	Collinsville, IL
CKM	Cahokia Mounds, IL
CMB	Columbia, IL
CRV	Centreville, IL
DRR	Doerr Field Site, IL
EDW	Edwardsville, IL
ELV	Ellisville, MO
ESL	East St. Louis, IL
FLO	Florissant, MO
FNG	Fernridge, MO
FRB	Freeburg, IL
FRM	SIU Experimental Farm, IL
FSB	Fosterburg, IL
FTP	Forest Park (in St. Louis)
GDF	Godfrey, IL
GRC	Granite City, IL
GTS	Green Trails School, MO
GVR	Grover Field Site, MO
HES	Hamel Field Site, IL
IMS	Imb's Station Field Site, IL
KMM	Kimm's Farm Field Site, IL
KMX	KMOX Field Site, IL
LVT	Livingston, IL
MCH	Machens Field Site, MO
MDT	Millstadt, IL
MRN	Marine Field Site, IL
MRV	Maryville, IL
MTA	Mascoutah, IL
MVM	Mehlville, MO
NDS	New Douglas Field Site, IL
NGL	Nagel's Farm Field Site, IL
NWB	Newburg Field Site, MO
OFN	O'Fallon, IL
OKV	Okawville, IL
PMQ	Pere Marquette State Park, IL
PTB	Pontoon Beach, IL
RCK	Rock Creek, MO
RXS	South Roxana, IL
SCH	St. Charles, MO
SIE	Southern Illinois University-Edwardsville, IL
SJB	St. Jacobs, IL
SLU	St. Louis University Field Site, MO
SRX	South Roxana, IL
SSH	State School, Bellfontaine Neighbors, MO
STL	Lambert Field, MO
SUS	Spirit of St. Louis Airport, MO
TYV	Tyson Valley, MO
VLM	Valmeyer, IL
WBH	Weber Hill, MO
WLO	Waterloo, IL
WSP	Weiss Airport Field Site, MO
WDR	Wood River, IL

ABBREVIATIONS AND ACRONYMS

above ground level	AGL
Air Pollution Control District	APCD
Atomic Energy Commission	AEC
centimeter(s)	cm
centimeter(s) per hour	cm hr^{-1}
Central Daylight Time	CDT
Chicago Area Program	CAP
cirrus	Ci
cirrocumulus	CiCu
cloud condensation nuclei	CCN
cloud occurrence frequency	COF
coefficient of variation	CV
condensation nuclei	CN
convective condensation level	CCL
cubic meter(s)	m^3
cumulonimbus	Cb
cumulus	Cu
decibel(s)	db, dbZ
degree(s) Celsius	° C
degree(s) Fahrenheit	° F
degree(s) Kelvin	° K
degrees of freedom	DF
Department of Energy	DOE
dew point temperature	T_d
Energy Research and Development Administration	ERDA
Environmental support units	EMSU
equivalent potential temperature	EPT
first echo(es)	FE
Geostationary Operational Environmental Satellite	GOES
gram(s)	g
gram(s) per kilogram	g kg^{-1}
horsepower	hp
ice nuclei	IN
Illinois Environmental Protection Agency	IEPA
Illinois State Water Survey	ISWS
instantaneous vertical speed indicator	IVSI
kilometer(s)	km
lifting condensation level	LCL
liquid water content	LWC
Local Standard Time	LST
mean sea level	MSL
mean squares	MS
meter(s)	m
meter(s) per second	m s^{-1}
metric ton(s)	T
Metropolitan Meteorological Experiment	METRO-MEX
microgram(s)	µg
micrometer(s)	µm
miles(s)	mi
mile(s) per hour	mph
millibar(s)	mb
milliliter(s)	ml
millimeter(s)	mm
nanogram(s)	ng
National Center for Atmospheric Research	NCAR
National Oceanic and Atmospheric Administration	NOAA
National Science Foundation	NSF
National Weather Service	NWS
picogram(s)	pg
planetary boundary layer	PBL
plan position indicator	PPI
precipitable water	PW
probability	P
range-height indicator	RHI
Regional Air Pollution Study	RAPS
relative humidity	RH
root mean square deviation	RMSD
second(s)	s
square centimeter(s)	cm^2
square kilometer(s)	km^2
square meter(s)	m^2
standard deviation	SD
sums of squares	SS
surface	SFC
temperature	T
U.S. Environmental Protection Agency	USEPA

Chemicals	
aluminum	Al
bromine	Br
cadmium	Cd
calcium	Ca
cesium	Cs
copper	Cu
indium	In
iron	Fe
lead	Pb
lithium	Li
magnesium	Mg
manganese	Mn
mercury	Hg
potassium	K
silica	Si
sodium	Na
sulfur	S
sulfer dioxide	SO2
titanium	Ti
zinc	Zn